SECTION 1
CONE PENETROMETER TESTING AT THE MIXED OXIDE FUEL FABRICATION FACILITY

INTRODUCTION

Applied Research Associates, Inc. (ARA) under contract to Duke, Cogema, Stone & Webster, LLC, conducted Electric Cone Penetration Tests with seismic soundings (S-CPT) at the Mixed Oxide Fuel Fabrication Facility (MFFF), Savannah River Site, South Carolina. This report documents ARA's site investigation efforts, test techniques, and analysis of the data for fieldwork conducted May 31 through July 24, 2000. Presented in this report is the field testing methods, data analysis techniques, and a brief discussion of the results.

TEST LOCATIONS

Sixty-four cone penetrometer test locations were conducted at the MFFF site. All penetrations measured tip stress, sleeve stress, and penetration pore pressure. Twenty of the penetrations included resistivity data in addition to the above measurements. At fifteen of the locations, seismic shear and compressional wave measurements were recorded on five foot intervals. Pore pressure dissipations were conducted as directed by the Stone and Webster field representative. In addition to CPT soundings, twenty soil samples were collected and five dilatometer tests were performed.

Table 1 lists the penetrations conducted and relevant information about each location. All locations were grouted upon retraction of the rod string or using a standard tremie grout method.

Table 1. Summary of CPT Testing at The MFFF site.

Test ID	ARA Filename	Type of Test	Date of Test	Maximum Depth (ft)	Dissipation Depth (ft)	Northing (ft)	Easting (ft)	Elevation (ft)	G.W.T. Depth (ft)
CPT-01S	409u008	S/P-CPT	6/9/00	104.4	104.4	80784.9	55554.0	258.2	73.4
CPT-02R	414u003	R/P-CPT	6/14/00	112.8	65.3, 101.6	80635.0	55616.4	257.8	57.3
CPT-03S	408u007	S/P-CPT	6/8/00	109.7	64.1, 74.1	80551.4	55700.8	253.2	57.8
CPT-04R	417u002B	R/P-CPT	6/17/00	135.5	80.0, 135.5	80465.4	55320.8	272.6	73.6
CPT-05S	408u004	S/P-CPT	6/8/00	124.8	71.7, 108.5	80499.7	55478.5	264.5	61.9
CPT-06R	415u002	R/P-CPT	6/15/00	103.2	64.8, 78.6	80470.7	55633.2	256.9	58.0
CPT-07R	419u001	R/P-CPT	6/19/00	114.3	78.7, 87.5, 98.1	80438.0	55228.2	280.2	79.6
CPT-08S	402u004	S/P-CPT	6/2/00	140.0	111.4, 140.1	80393.7	55329.1	273.0	74.6
CPT-09R	420u005	R/P-CPT	6/20/00	126.5	50.6, 80.7, 88.1, 112.3	80394.0	55445.7	266.2	67.0
CPT-10R	420u001	R/P-CPT	6/20/00	142.5	45.6, 85.3, 104.9	80406.7	55527.1	261.9	67.0
CPT-11S	402u001	S/P-CPT	6/2/00	106.4	78.0, 106.4	80394.0	55624.1	258.5	62.4
CPT-12R	323u003	R/P-CPT	6/23/00	102.9	67.4, 86.0	80373.1	55747.5	254.5	61.0
CPT-13S	405u005	S/P-CPT	6/5/00	166.5	135.5	80262.2	55233.6	296.7	100.0
CPT-14R	419u008	R/P-CPT	6/19/00	123.7	68.9, 85.9, 123.7	80292.7	55330.8	276.0	75.0
CPT-15R	322u001	R/P-CPT	6/22/00	130.0	79.0, 114.9	80295.0	55462.7	269.1	68.5
CPT-16S	408u001	S/P-CPT	6/8/00	122.1	84.7, 116.1	80281.0	55628.6	260.5	79.0
CPT-17	410u001	P-CPT	6/10/00	106.5	80.1	80259.4	55747.7	255.9	62.0
CPT-18R	322u005	R/P-CPT	6/22/00	120.3	82.9, 97.2	80192.1	55405.9	277.0	73.8
CPT-19S	403u002	S/P-CPT	6/3/00	118.0	98.0, 106.1	80177.3	55467.5	274.8	75.4
CPT-20R	322u003	R/P-CPT	6/22/00	107.0	76.0	80211.3	55570.4	266.9	65.8
CPT-21	412u004	P-CPT	6/12/00	138.7	110.1	80148.4	55060.1	295.4	97.0
CPT-22	412u007	P-CPT	6/12/00	152.6	104.4, 114.6	80143.8	55221.9	297.3	100.0
CPT-23S	406u003	S/P-CPT	6/6/00	123.8	92.9, 104.6	80088.9	55379.4	277.3	69.4
CPT-24	410u003B	P-CPT	6/10/00	63.4	--	80115.0	55548.5	272.6	78.8
CPT-24A	410u005	P-CPT	6/10/00	143.1	102.0	80115.0	55548.5	272.6	78.8
CPT-25	412u001	P-CPT	6/12/00	84.5	76.4	80104.7	55621.7	268.9	68.8
CPT-26S	406u001	S/P-CPT	6/6/00	127.1	85.1, 112.7	80116.2	55726.7	261.9	65.5
CPT-27R	322u008	R/P-CPT	6/22/00	128.6	86.0, 104.5	80001.4	55254.2	277.5	72.0
CPT-28S	431y006	S/P-CPT	5/31/00	150.0	107.0	80001.8	55332.0	279.2	76.5
CPT-29R	413u009	R/P-CPT	6/13/00	119.2	66.8, 89.1	79985.8	55422.4	276.4	68.5
CPT-30R	414u001	R/P-CPT	6/14/00	141.0	60.8, 79.3, 125.3	79973.4	55538.3	274.2	71.0
CPT-31S	401u002	S/P-CPT	6/1/00	126.3	126.1	79977.3	55610.3	271.7	67.0
CPT-32R	324u001	R/P-CPT	6/24/00	130.3	78.0, 82.6	80005.4	55755.6	264.7	63.8
CPT-33R	413u003	R/P-CPT	6/13/00	142.1	81.0, 116.2,	79842.0	54922.7	274.6	71.6
CPT-34S	407u001	S/P-CPT	6/7/00	146.0	111.8, 118.2	79826.9	55323.2	270.8	72.0
CPT-35S	403u005	S/P-CPT	6/3/00	109.4	24.8, 94.9, 141.0	79888.6	55389.0	272.6	71.8
CPT-36R	413u007	R/P-CPT	6/13/00	127.2	84.5,. 97.9, 119.9	79898.9	55478.3	273.4	69.5
CPT-37S	405u001	S/P-CPT	6/5/00	135.5	66.6, 124.0	79886.1	55629.4	268.4	67.0
CPT-38R	323u001	R/P-CPT	6/23/00	133.9	81.7, 93.5, 121.8	79899.9	55568.6	271.3	67.4
CPT-39R	324u005	R/P-CPT	6/24/00	120.4	56.2, 82.1, 99.1	80206.6	55646.9	262.1	64.0
CPT-40R	324u007	R/P-CPT	6/24/00	113.2	91.0	79941.1	55448.0	275.0	72.3
CPT-42	408L001	P-CPT	7/8/00	126.0	87.1	80169.8	55591.7	267.5	69.9
CPT-43	315L055	P-CPT	7/15/00	116.6	--	80257.7	55585.0	264.0	76.0
CPT-44	320L005	P-CPT	7/20/00	118.0	85.2, 95.3	80530.3	55109.3	284.7	85.8
CPT-45	321L001	P-CPT	7/21/00	142.6	94.0, 130.0	80531.1	55194.0	280.5	82.5
CPT-46	320L003	P-CPT	7/20/00	147.3	83.1, 129.1	80482.0	55032.8	284.5	74.0
CPT-47	320L007	P-CPT	7/20/00	116.0	116.0	80456.7	55146.5	284.1	86.1
CPT-48	322L005	P-CPT	7/22/00	110.5	96.5	80463.6	54964.1	281.2	82.4
CPT-49	319L003	P-CPT	7/19/00	123.1	105.8	80332.7	54931.1	292.4	91.5
CPT-50	319L001	P-CPT	7/19/00	134.1	102.5, 108.6, 127.6	80370.9	55140.0	294.4	107.8

est ID	ARA Filename	Type of Test	Date of Test	Maximum Depth (ft)	Dissipation Depth (ft)	Northing (ft)	Easting (ft)	Elevation (ft)	G.W.T. Depth (ft)
CPT-51	318L008	P-CPT	7/18/00	138.7	95.3, 104.1	80318.7	55198.3	295.5	95.0
CPT-52	319L005	P-CPT	7/19/00	119.9	114.2, 119.1	80277.0	54867.3	293.4	94.7
CPT-53	315L022	P-CPT	7/15/00	124.8	89.0, 106.4	80309.5	55059.9	292.8	90.2
CPT-54	320L001	P-CPT	7/20/00	123.1	96.4, 104.2	80243.1	54940.0	293.7	92.9
CPT-55	318L005	P-CPT	7/18/00	136.5	96.3, 113.0	80259.6	55141.9	294.4	94.1
CPT-56	318L001	P-CPT	7/18/00	120.1	103.5	80207.0	54866.7	294.2	92.5
CPT-57	318L003	P-CPT	7/18/00	128.8	101.2, 115.1	80229.2	55058.2	293.6	91.8
CPT-58	317L004	P-CPT	7/17/00	121.8	103.0, 114.1	80135.1	54866.9	295.1	88.0
CPT-59	415L005	P-CPT	7/15/00	126.0	99.1	80152.7	54956.9	295.5	75.7
CPT-60	415L003	P-CPT	7/15/00	141.0	99.4	80142.2	55140.6	295.7	66.6
CPT-61	321L003	P-CPT	7/21/00	114.6	90.5, 97.1	80037.6	54869.6	279.3	76.3
CPT-62	322L001	P-CPT	7/22/00	115.7	70.8, 95.6	80055.6	54956.3	278.5	75.9
CPT-63	322L003	P-CPT	7/22/00	118.6	104.5	80066.0	55055.5	279.4	90.0
CPT-64	415L001	P-CPT	7/15/00	141.0	--	80034.9	55165.3	279.8	66.6
DIL-10	--	DMT	7/7/00	88.0	--	80398.5	55537.5	261.8	--
DIL-15	--	DMT	6/30/00	103.0	--	80291.5	55466.0	269.1	--
DIL-23	--	DMT	7/6/00	108.0	--	80088.4	55382.8	277.2	--
DIL-25	--	DMT	7/1/00	83.0	--	80108.4	55620.2	268.4	--
DIL-29	--	DMT	6/29/00	95.0	--	79975.5	55420.4	276.2	--
SS-05	--	SS	6/27/00	117.0	--	80499.8	55473.5	264.5	--
SS-10	--	SS	6/28/00	75.0	--	80411.5	55529.9	261.8	--
	--	SS	6/28/00	115.0	--	--	--	--	--
SS-14	--	SS	6/28/00	67.0	--	80292.7	55330.8	276.0	--
	--	SS	6/28/00	94.0	--	--	--	--	--
SS-22	--	SS	6/26/00	130.0	--	80153.0	55221.7	297.0	--
SS-24	--	SS	6/27/00	125.0	--	80112.8	55547.7	272.8	--
SS-26	--	SS	6/27/00	112.0	--	80116.2	55726.7	261.9	--
SS-29	--	SS	6/26/00	70.0	--	79982.6	55417.0	276.6	--
	--	SS	6/26/00	100.0	--	--	--	--	--
SS-36	--	SS	6/26/00	62.0	--	79902.7	55477.0	273.3	--
	--	SS	6/27/00	121.8	--	--	--	--	--
SS-37	--	SS	6/28/00	60.0	--	79882.3	55625.6	268.8	--
	--	SS	6/28/00	69.0	--	--	--	--	--
	--	SS	6/28/00	90.0	--	--	--	--	--
	--	SS	6/28/00	115.0	--	--	--	--	--
SS-39	--	SS	6/27/00	104.0	--	80208.8	55650.3	261.7	--
SS-46	--	SS	7/24/00	114.8	--	80487.6	55036.0	284.2	--
	--	SS	7/24/00	133.0	--	--	--	--	--
	--	SS	7/24/00	142.0	--	--	--	--	--

REPORT OUTLINE

This report is organized into 4 Sections and 4 Appendices. Section 2 discusses the CPT equipment, field procedures, and daily calibrations. Section 3 describes the methods used to interpret the CPT results as well as a discussion of a typical CPT Profile from the MFFF site. Section 4 lists references. Appendix A presents the piezocone data. Appendix B has been intentionally left blank. Seismic test wave histories and velocities are located in Appendix C. Appendix D contains pore pressure dissipation data. Dilatometer data is found in Appendix E.

SECTION 2
TESTING EQUIPMENT AND PROCEDURES

INTRODUCTION

The electric cone penetrometer test (CPT) was originally developed for use in soft soil. Over the years, cone and push system designs have evolved to the point where they can now be used in strong cemented soils and even soft rock. ARA's penetrometer consists of an instrumented probe that is forced into the ground using a hydraulic load frame mounted on a heavy truck with the weight of the truck providing the necessary reaction mass. The probe has a conical tip and a friction sleeve that independently measures vertical resistance beneath the tip as well as frictional resistance on the side of the probe as a function of depth. A schematic view of ARA's penetrometer probe is shown in Figure 2.1. A pressure transducer in the cone is used to measure the pore water pressure as the probe is pushed into the ground (P-CPT).

A resistivity module is attached directly behind the cone to measure the electrical resistance of the subsurface. This probe also includes three geophones aligned along the X, Y, and Z-axis for measuring shear and compressional waves.

PIEZO-ELECTRIC CONE PENETROMETER EQUIPMENT AND TEST

The cone penetrometer tests were conducted using the ARA penetrometer truck. The penetrometer equipment is mounted inside a van body attached to a ten-wheel truck chassis with a diesel engine. Ballast in the form of weights is added to the truck to achieve an overall push capacity of 60,000 lbs. Penetration force is supplied by a pair of large hydraulic cylinders bolted to the truck frame.

A 15-cm^2 penetrometer probe (which has 1.75-inch diameter, 60° conical tip, and a 1.75-inch diameter by 6.5-inch long friction sleeve) was used on this project. This probe size is in conformance with ASTM D 5778 (Ref. 1). The shoulder between the base of the tip and the porous filter is 0.08 inch long as shown in Figure 2.1. The penetrometer is advanced vertically into the soil at a constant rate of 48 inches/minute (2cm/second), although this rate must sometimes be reduced as hard layers are encountered. The electric cone penetrometer test is conducted in accordance with ASTM D 5778 (Ref. 1).

Inside the probe, two load cells independently measure the vertical resistance against the conical tip and the side friction along the sleeve. Each load cell is a cylinder of uniform cross section instrumented with four strain gages in a full-bridge circuit. The forces are sensed by the load cells and the data are transmitted from the probe assembly via a cable running through the push tubes. The analog data are digitized, recorded, and plotted by computer in the penetrometer truck. A set of data is normally recorded each second, for a minimum resolution of about one data point every 0.8 inch of cone advance. The depth of penetration is measured using a string potentiometer mounted on the push frame.

Electronic data acquisition equipment for the cone penetrometer consists of a computer with a graphics monitor and a rack of eight signal conditioners. Analog signals are transmitted from the probe to the signal conditioners where the CPT data are amplified and filtered at 1 Hz. Once amplified, the analog signals are transmitted to a high-speed analog-to-digital converter board, where the signals are digitized; usually at the rate of one sample per second for the penetration data. The digital data are then read into memory and written to the internal hard disk for future processing. Upon completion of the test the penetration data are plotted. The digital data are brought to ARA's New England Division in South Royalton, Vermont, for analysis and preparation of report plots.

Saturation of the Piezo-Cone

Penetration pore pressures are measured with a pressure transducer located behind the tip in the lower end of the probe. Water pressures in the soil are sensed through a 250 micro-inch porous polyethylene filter that is 0.25-inch high and 0.202-inch thick. The pressure transducer is connected to the porous filter through a pressure port as shown in Figure 2.1. The pressure port and the filter are filled with high viscosity silicone oil.

In order for the pressure transducer to respond rapidly and correctly to changing pore pressures during the penetration, the filter and pressure port must be saturated with oil upon assembly of the probe. A vacuum pump is used to de-air the silicone oil before use and also to saturate the porous filters with oil. The probe is assembled with the pressure transducer facing upwards and the cavity above the pressure transducer is filled with de-aired oil. A previously saturated filter is then placed on a tip and oil is poured over the threads. When the cone tip is screwed into place. excess oil is ejected through the pressure port and filter, thereby forcing out

any trapped air. The high viscosity of the silicone oil coupled with the small pore space in the filter prevents the loss of saturation as the cone is pushed through dry soils. Saturation of the cone can be verified with a calibration check at the completion of the penetration. Extensive field experience has proven the reliability of this technique.

Field Calibrations

Many factors can effectively change the calibration factors used to convert the raw instrument readouts, measured in volts, to units of force or pressure. As a quality control measure, as well as a check for instrument damage, the load cells and the pressure transducer are routinely calibrated in the field. Calibrations are completed with the probe ready to insert into the ground so that any factor affecting any component of the instrumentation system will be included and detected during the calibration.

The tip and sleeve load cells are calibrated with the conical tip and friction sleeve in place on the probe. For each calibration, the probe is placed in the push frame and loaded onto a precision reference load cell. The reference load cell is periodically calibrated in ARA's laboratory against instruments traceable to NIST standards. To calibrate the pore pressure transducer, the saturated probe is inserted into a pressure chamber with air pressure supplied by the compressor on the truck. The reference transducer in the pressure chamber is also periodically calibrated against an NIST traceable instrument in ARA's laboratory. Additionally, the linear displacement transducer used to measure the depth of penetration, is periodically checked against a tape measure. All records of device and load cell calibrations are located at ARA's New England Division.

Each instrument is calibrated using a specially developed computer code that displays the output from the reference device and the probe instrument in graphical form. During the calibration procedure, the operator checks for linearity and repeatability in the instrument output. At the completion of each calibration, this code computes the needed calibration factors using a linear regression algorithm. At a minimum, each probe instrument is calibrated at the beginning of each day of field testing. Furthermore, the pressure transducer is recalibrated each time the porous filter is changed and the cone re-saturated. Calibrations are also performed to verify the operation of any instrument if any damage is suspected.

Penetration Data Format

Figure 2.2 presents a typical CPT profile from the MFFF site investigation. This plot presents tip stress, sleeve friction, friction ratio and penetration pore pressure. As shown in Figure 2.1, the piezo-cone probe senses the pore pressure immediately behind the tip. Currently, there is no accepted standard for the location of the sensing element. ARA chose to locate the sensing element behind the tip since the filter is protected from the direct thrust of the penetrometer and the measured pore pressure can be used to correct the tip resistance data as recommended in Reference 2. The magnitude of the penetration pore pressure is a function of the soil compressibility and, most importantly, permeability. In freely draining soil layers, the measured pore pressures will be very close to the hydrostatic pressure computed from the elevation of the water table. When low permeability soil layers are encountered, excess pore pressures generated by the penetration process cannot dissipate rapidly and this results in measured pore pressures, which are significantly higher than the hydrostatic pressures. Whenever the penetrometer is stopped to add another section of push pipe, or when a pore pressure dissipation test is run, the excess pore pressure may begin to dissipate. When the penetration is resumed, the pore pressure quickly rises to the level measured before the penetrometer was stopped. This process causes some of the spikes that appear in the penetration pore pressure data.

Pore Pressure Correction of Tip Stress

Cone penetrometers, by necessity, must have a joint between the tip and sleeve. Pore pressure acting behind the tip decreases the total tip resistance that would be measured if the penetrometer was without joints. The influence of pore pressure in these joints is compensated for by using the net area concept (Ref. 2). The corrected tip resistance is given by:

$$q_T = q_c + u\left[1 - A_n/A_T\right] \qquad \textbf{(2.1)}$$

where:
- q_T = corrected tip resistance (psi)
- q_c = measured tip resistance (psi)
- u = penetration pore pressure measured behind the tip (psi)
- A_n = net area behind the tip not subjected to the pore pressure (1.95 in^2)
- A_T = projected area of the tip (2.405 in^2).

Hence, for the ARA cone design, the tip resistance is corrected as:

$$q_T = q_c + u(.2054) \tag{2.2}$$

Laboratory calibrations have verified Equation 2.2 for ARA's piezo-cone design.

A joint also exists behind the top of the sleeve (see Figure 2.1). However, since the sleeve is designed to have the same cross sectional area on both ends, the pore pressures acting on the sleeve cancel out. Laboratory tests have verified that the sleeve is not subjected to unequal end area effects. Thus, no correction for pore pressure is needed for the sleeve friction data.

The net effect of applying the pore pressure correction is to increase the tip resistance. Generally, this correction is only significant when the measured tip resistance is very low.

Numerical Editing of the Penetration Data

Any time that the cone penetrometer is stopped or pulled back during a test, misleading data can result. For instance, when the probe is stopped to add the next push rod section, or when a pore pressure dissipation test is run, the excess pore pressures will dissipate towards the hydrostatic pore pressure. When the penetration is resumed, the pore pressure rises very quickly to the pressures experienced prior to the pause in the test. In addition, the probe is sometimes pulled back and cycled up and down at intervals in deep holes to reduce soil friction on the push tubes. This results in erroneous tip stress data when the cone is advanced in the previously penetrated hole.

To eliminate this misleading data from the penetration profile, the data is numerically edited before it is plotted or used in further analysis. Each time the penetrometer stops or backs up, as apparent from the depth data, the penetration data is not plotted. Plotting of successive data is resumed only after the tip is fully re-engaged in the soil by one tip length of new penetration. In addition, each time the probe stops, the previous 0.5 inch of penetration data is filtered out. This filter is required to remove data that was recorded while the operator was in the process of stopping the probe. This algorithm also eliminates any data acquired at the ground surface before the tip has been completely inserted into the ground. The sleeve data is similarly treated and this results in the first data point not occurring at the ground surface, as can be seen in the tip and sleeve profiles in Figure 2.2. These procedures ensure that all of the penetration data

that is plotted and used for analysis was acquired with the probe advancing fully into undisturbed soil.

RESISTIVITY TESTING

Resistivity, one of the oldest geophysical exploration techniques, was originally developed to locate mineral and oil deposits and ground water supplies. The measurements principal exploited by resistivity surveying is that an electrical contrast exists between different geological materials and that this electrical contrast can be used to identify and locate geologic materials. Resistivity surveys are being increasingly used in contaminated site investigation programs to delineate the extent and degree of contamination at a site. These surveys rely on the electric contrasts that typically exist between contaminated soils and uncontaminated soils. For example, leachate from a landfill will contain a higher concentration of dissolved solids, which will decrease the resistivity of the groundwater (Ref. 3). Soils contaminated with hydrocarbons (fuel oils, cleaning solvents, etc.) will typically have higher resistivity than uncontaminated soils as the hydrocarbon can act as an insulator.

The Resistivity-CPT (R-CPT) is an adaptation of conventional borehole tools. The R-CPT probe is in intimate contact with the soil and pore fluid which eliminates two problems associated with borehole resistivity surveys; 1) intrusion of drilling fluids into borehole walls which changes the resistivity of the media and 2) the requirement that any casing materials be non-conducting.

Figure 2.1 is a schematic of ARA's R-CPT probe. The probe consists of 4 electrodes separated by high strength plastic reinforced insulators. The outer two electrodes induce an electric current into the soil and the inner two electrodes measure the potential drop, which is proportional to the resistivity of the soil. To avoid polarization effects, the four electrode array is operated at a frequency of 40 HZ. Electronics in the CPT vehicle are used to modulate and demodulate the current and potential measurement signals to and from the probe. The probe is calibrated in a large water solution in which the conductivity is varied. The data from the calibration tests is used to determine the probe calibration factor, which is dependent on the probe geometry.

SEISMIC CONE PENETROMETER EQUIPMENT AND TEST

The seismic cone penetrometer test was developed in the early 1980s and is gaining rapid acceptance in the geotechnical community. As with the conventional electric cone penetrometer test, initial development work has concentrated in weak materials. ARA's seismic cone equipment and field procedures were developed specifically for both weak soils and strong, dry, cemented soils. The seismic cone penetrometer test utilizes three geophones (Geospace Model GS-14-L9 velocity gages) mounted inside the penetrometer probe to detect the arrival at depth of seismic waves generated on the surface. Two horizontal transducers monitor shear wave (S-wave) traces from which the shear wave velocity can be determined. A third geophone, mounted vertically, is used to measure the compression wave (P-wave) traces and to subsequently derive the compressional velocity.

In the Seismic-Electric Cone Penetrometer Test (S-CPT), the cone is stopped at prescribed depth intervals, and S- and P-waves are generated on the ground surface near the push tubes. Both average downhole velocities and velocities between the depth intervals can be computed from the arrival time or time of peak data. The 2.0-inch diameter expander behind the sleeve minimizes coupling between the ground and the push tubes, mitigating problems with wave propagation down the push tubes.

High-energy shear waves are generated by an automated shear wave source in the front pad of the CPT rig (Figure 2.3). This system consists of a double-acting hydraulic cylinder used to horizontally move a large hammer. The hammer impacts either end of the front lifting pad of the penetrometer truck and induces a horizontal shear wave. By striking the pad on either end, polarized shear waves can be generated. This pad is 1 ft wide and about 8 ft long and oriented parallel to the axles of the truck. The point of impact of the shear hammers is 36 inches horizontally from the penetrometer push rod. Typical seismic traces are shown in Figure 2.4, where time of first peak shear wave motions are indicated. The first major shear wave is used to select the shear time of peak as denoted by the arrows. The use of polarized shear waves clarifies this time of peak.

In a similar fashion, compressive waves are generated by hitting a pile cap with an automated P-wave hammer or a sledge hammer. The point of impact is 72 inches horizontally away from the push rod.

Typical compressional wave traces are shown in Figure 2.5. Determining arrival time of the compressional wave (P-wave) is relatively more difficult. However, the time of first peak can usually be determined with consistency.

PORE PRESSURE DISSIPATION RESULTS

At selected depths, the penetrometer is stopped and the dissipation of excess pore pressure is observed. Pore pressures, as sensed by the pressure transducer, are recorded at regular time intervals (typically 1 second, but the sample rate can be adjusted for local site conditions) and plotted on the graphics monitor. Dissipation tests are usually run until at least 50 percent of the excess pore pressure has dissipated. This length of time, t_{50}, can be used to determine the lateral coefficient of consolidation and permeability in the given soil layer. Depending on site conditions, t_{50} can range from a few minutes to several hours. These tests are sometime run to complete dissipation to measure the hydrostatic pore pressure. During the dissipation test, the penetrometer is stationary with no downward force applied by the penetrometer truck.

A classic dissipation profile in a clay soil is shown in Figure 2.6. Total pore pressure is presented on a semi-log plot versus time. The classic dissipation curve will show a dissipation rate that decreases with time. If the dissipation test is allowed to run long enough, the static pore pressure will eventually be reached. The value of P_n at the top of Figure 2.6 is the average of the last ten pore pressure measurements. If the dissipation test is sufficiently long, P_n will be equal to the static pore pressure. This value can also be determined from the water table elevation at some sites. Knowing the static pore pressure (u_o), as well as the peak pressure observed during the test (u_p), the pore pressure at 50 percent of dissipation (u_{50}) can be determined. Time to 50% dissipation (t_{50}) can then be read directly from the dissipation profile.

Many of the penetration profiles from the work at the MFFF site exhibit the classic shape as depicted in Figure 2.6. At some locations, the dissipations start with a vacuum condition due to dilatation occurring during the penetration. From this condition the pore pressures increase as presented in Figure 2.7. This curve shape does not permit the traditional dissipation analysis algorithms to be used to determine hydraulic conductivity. For this reason only the plots of the dissipations as a function of time are presented in the appendix and not analysis tables.

SOIL SAMPLE COLLECTION

ARA has developed its own soil sampler based on extensive field experience with other types of samplers, and has created a more robust sampler (Figure 2.8) that can be deployed with the heaviest CPT rigs. The assembled soil sampler is deployed to the desired depth where a tip release tool is then lowered down the rod string to unlock the sampler tip. Once released, the rods and sampler are advanced and the soils are forced into a stainless steel sleeve or split spoons through the core catcher. The probe is then retracted, bringing the sample to the surface. The sampler collects a sample 1.4 inches in diameter and up to 21 inches in length.

DILATOMETER TESTS (DMT)

Marchetti Dilatometer Tests are conducted to estimate the lateral earth pressures and soil compressibilities. Material properties derived from the DMTs can be used to evaluate settlement, lateral earch pressures and ECR. The dilatometer consists of a flat-plate penetrometer, which is instrumented with a flexible, circular diaphragm mounted on one face of the blade. The test is operated from a console in the penetrometer truck which is used to push the blade into the ground. The dimensions and geometry of the blade are shown in Figure 2.9. A detailed, recommended procedure for conducting the test has been presented by Schmertmann (Ref. 4) and will be summarized briefly here.

Immediately after the blade is forced into the ground to a desired test depth, using the penetrometer truck, the flexible diaphragm is expanded with compressed gas. As gas pressure is slowly increased and the membrane starts to move outward against the soil, an electric signal ("A" reading) identifies the pressure required to lift the diaphragm off the plan of the blade. As diaphragm expansion continues, a second electric signal ("B" reading) denotes when a central diaphragm displacement of 1mm is reached. A third pressure ("C" reading) is read when the diaphragm is deflated back to the plane of the blade.

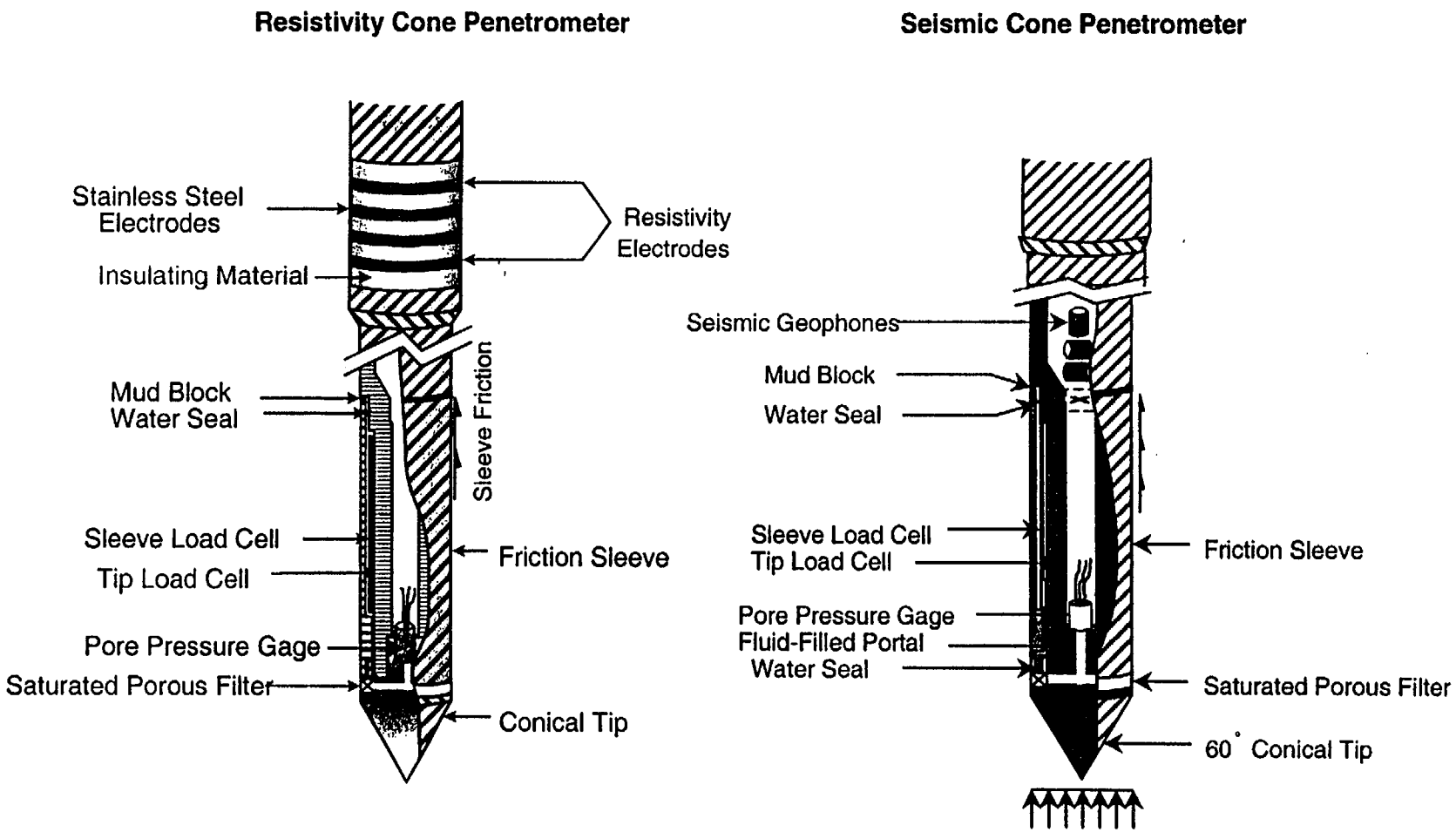

Figure 2.1 Schematic of ARA's Resistivity and Seismic cone penetrometers

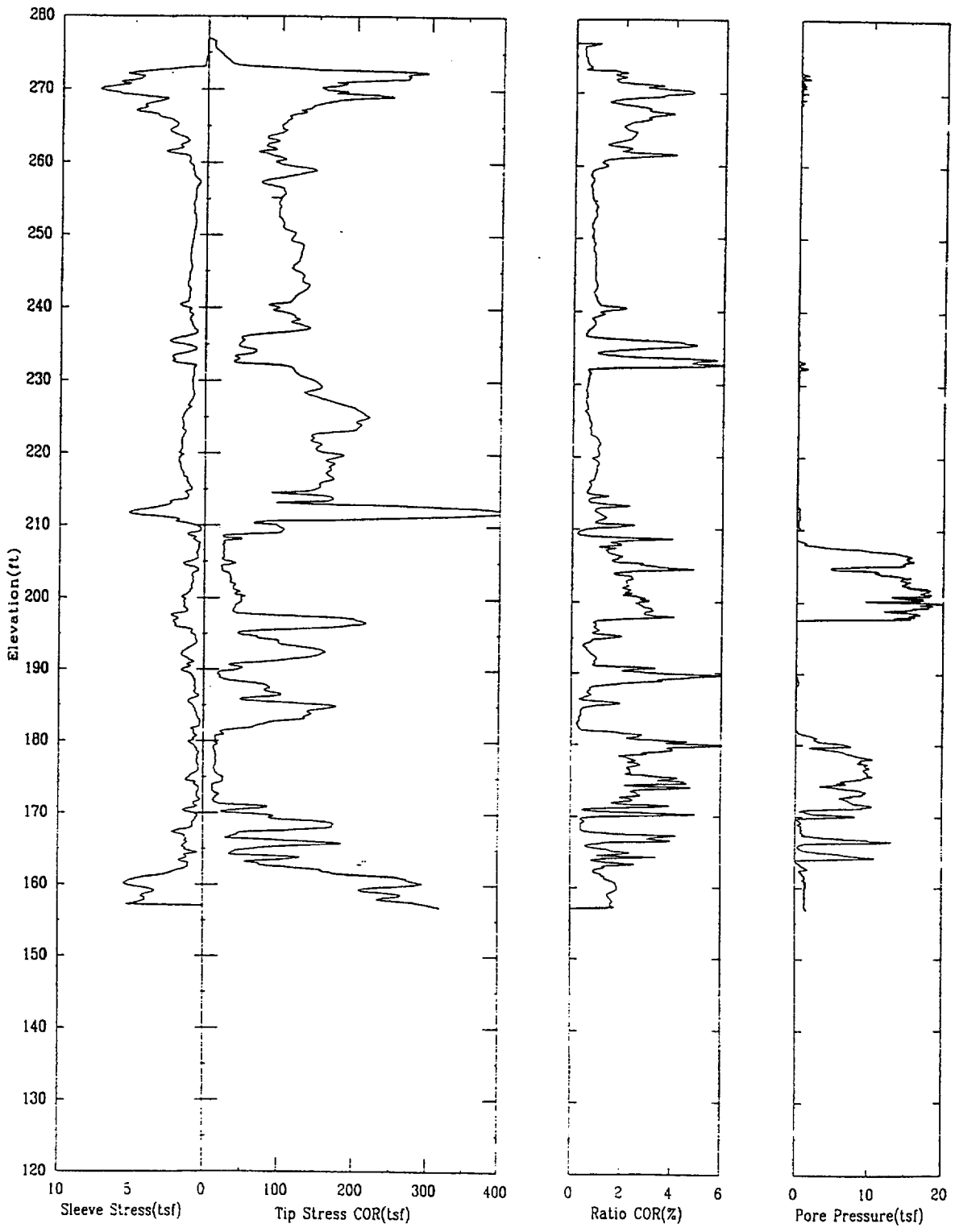

Figure 2.2 Typical CPT profile from the MFFF

File 322u005.ECP

CPT-18R APPLIED RESEARCH ASSOCIATES, INC. 06/22/00
North 80192.1 East 55405.9 Elevation 277.0

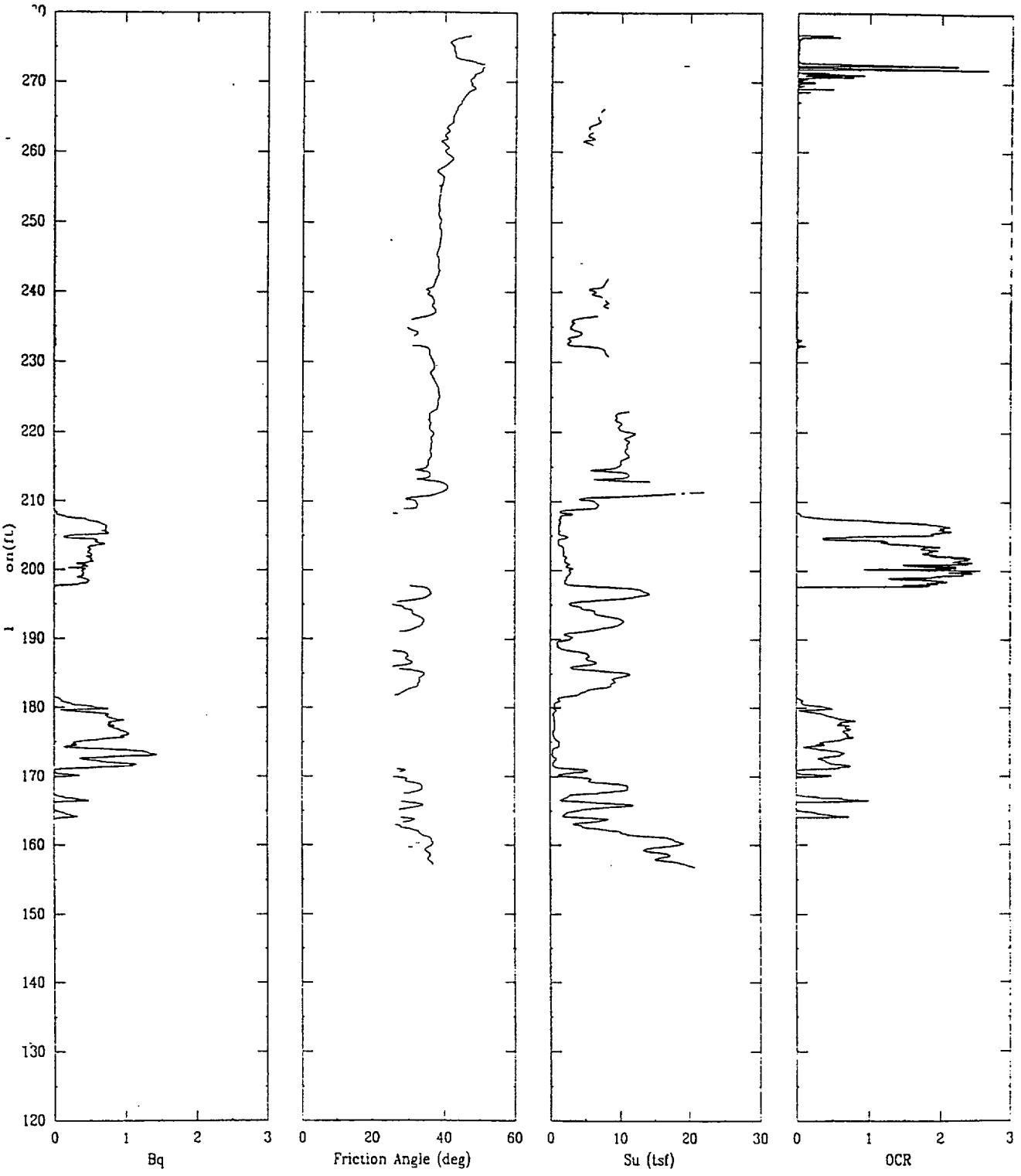

File 322u005.ECP

Figure 2.2 Typical CPT profile from the MFFF (continued)

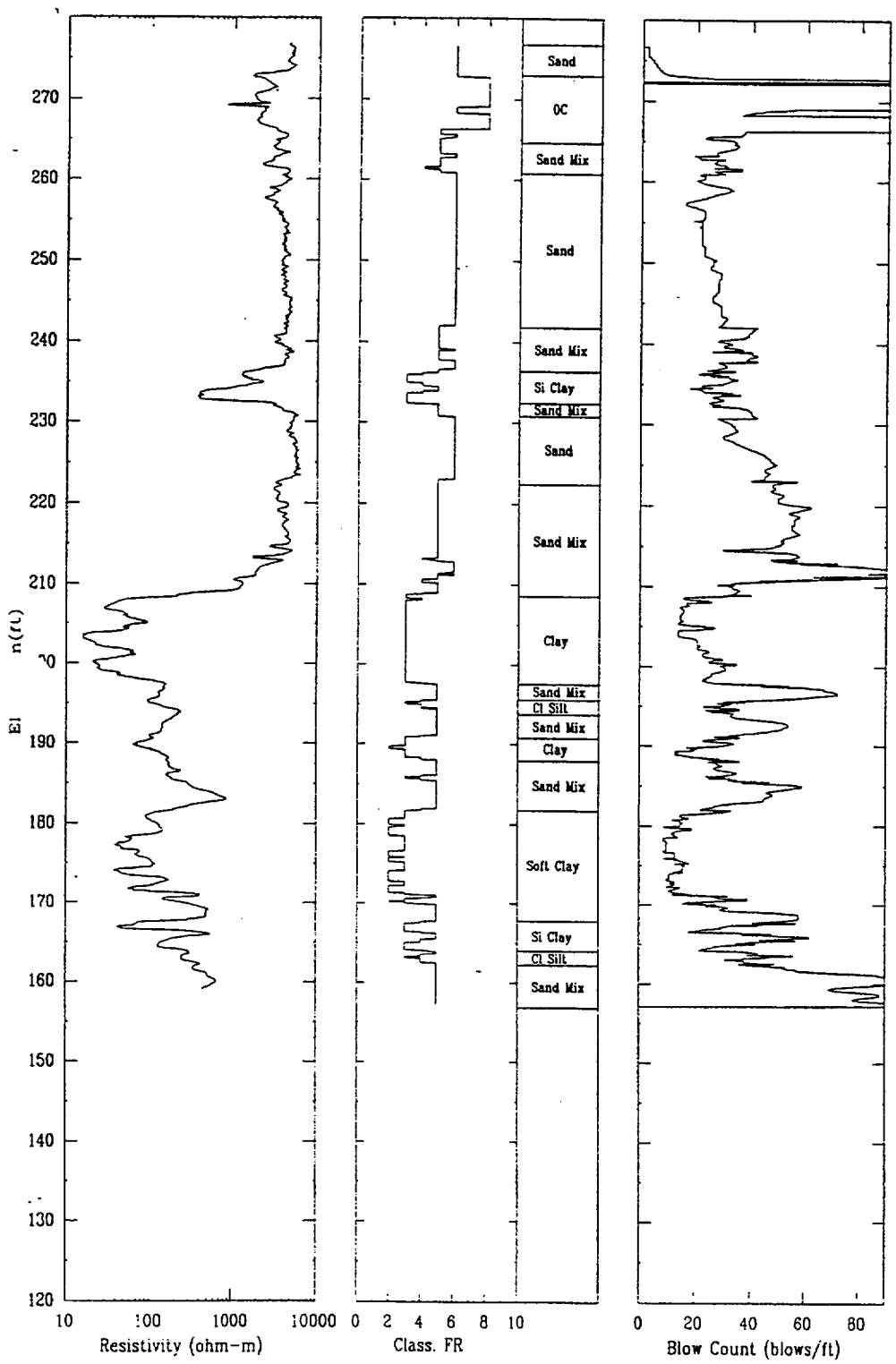

File 322u005.ECP

Figure 2.2 Typical CPT profile from the MFFF (concluded)

Seismic Shear Wave Hammer

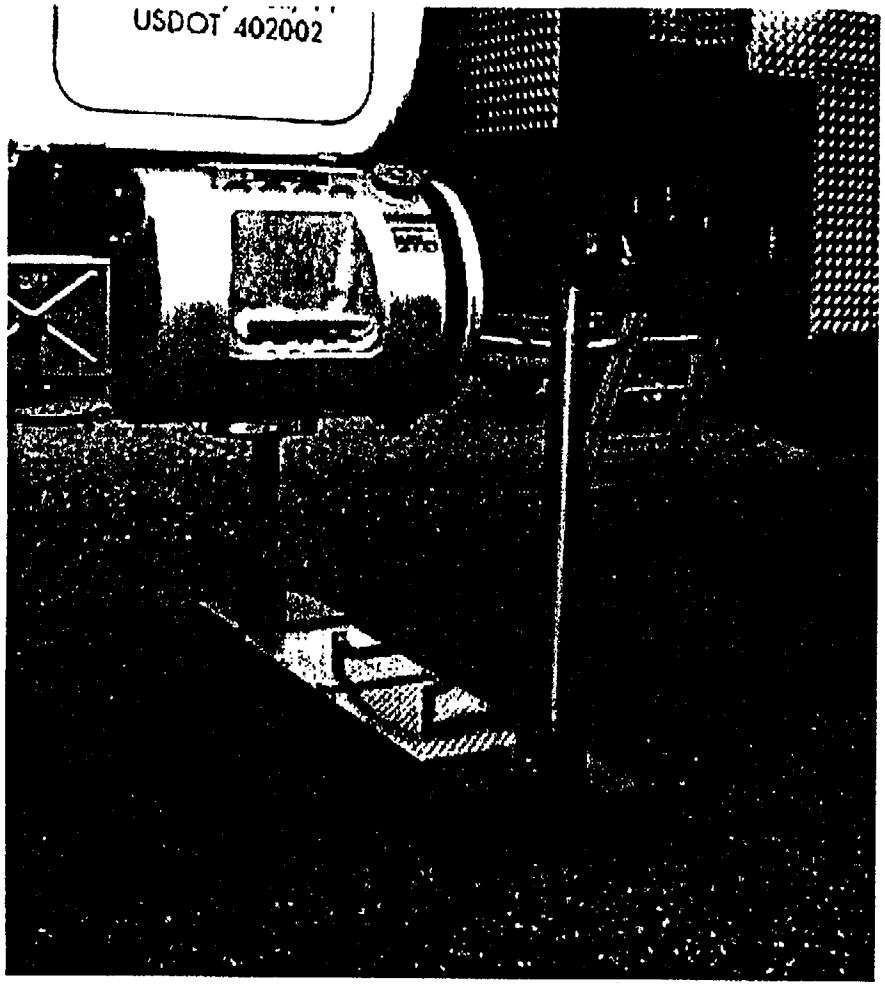

Figure 2.3 High energy seismic shear wave hammer

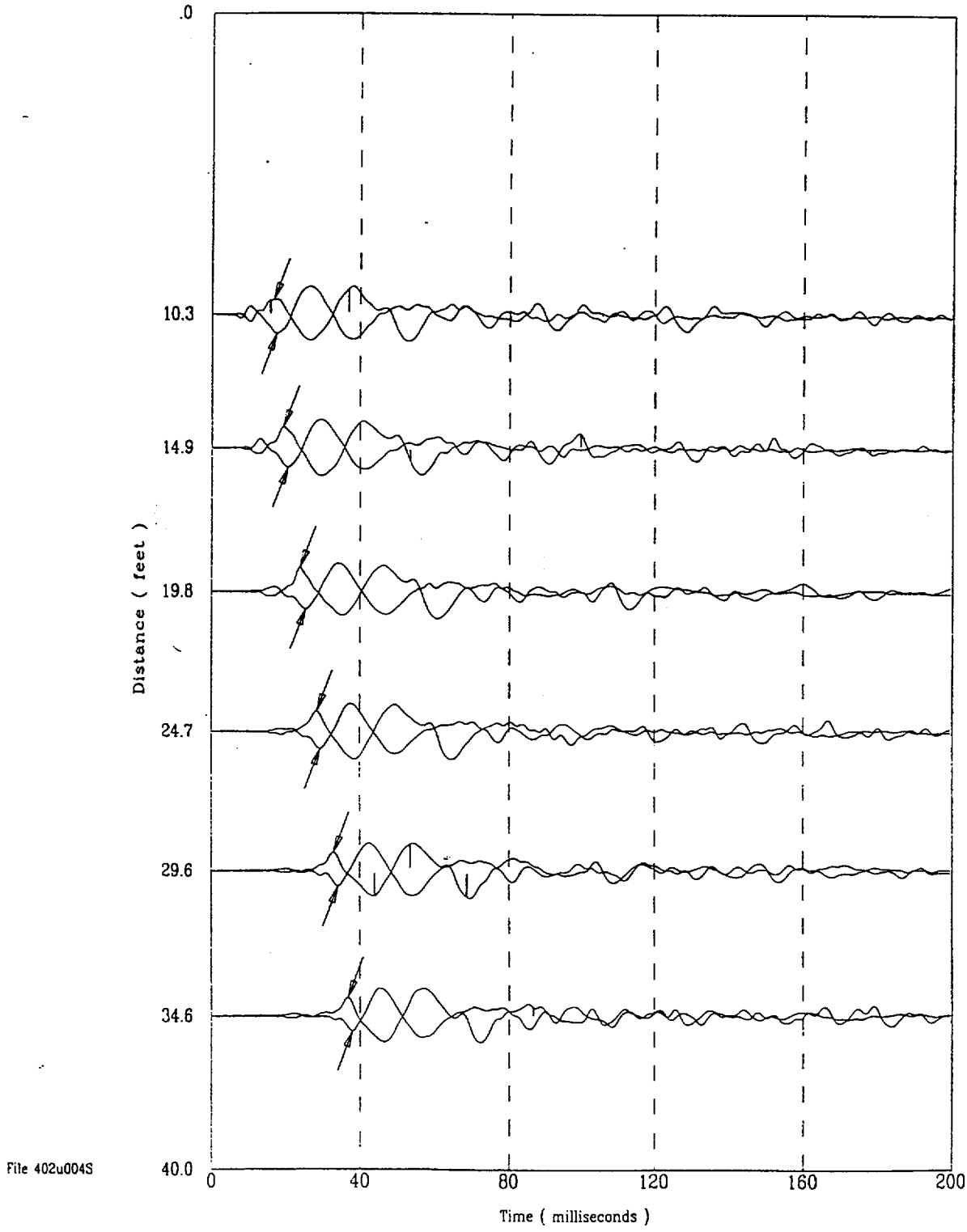

Figure 2.4 Typical shear wave traces

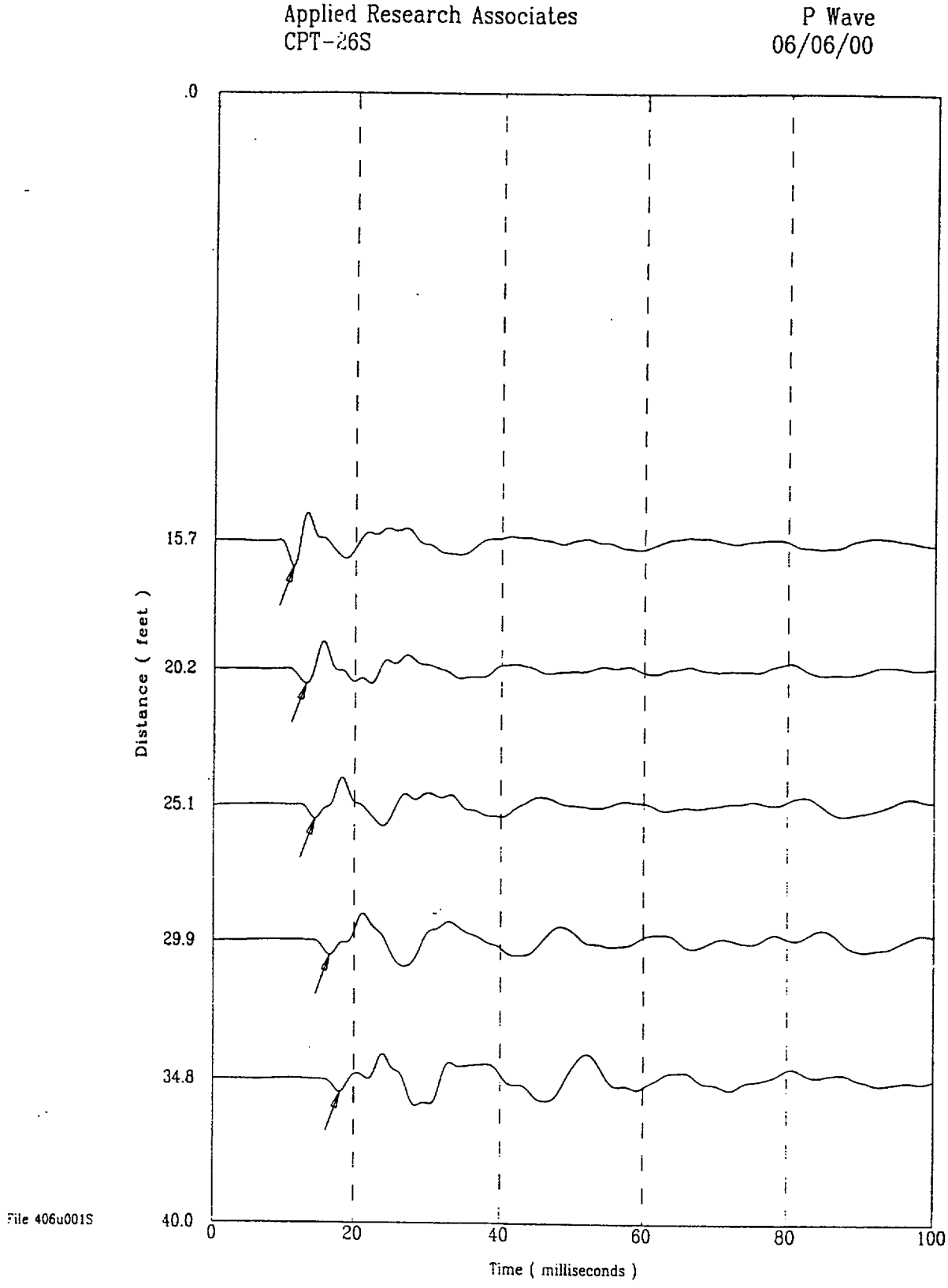

Figure 2.5 Typical compression wave traces

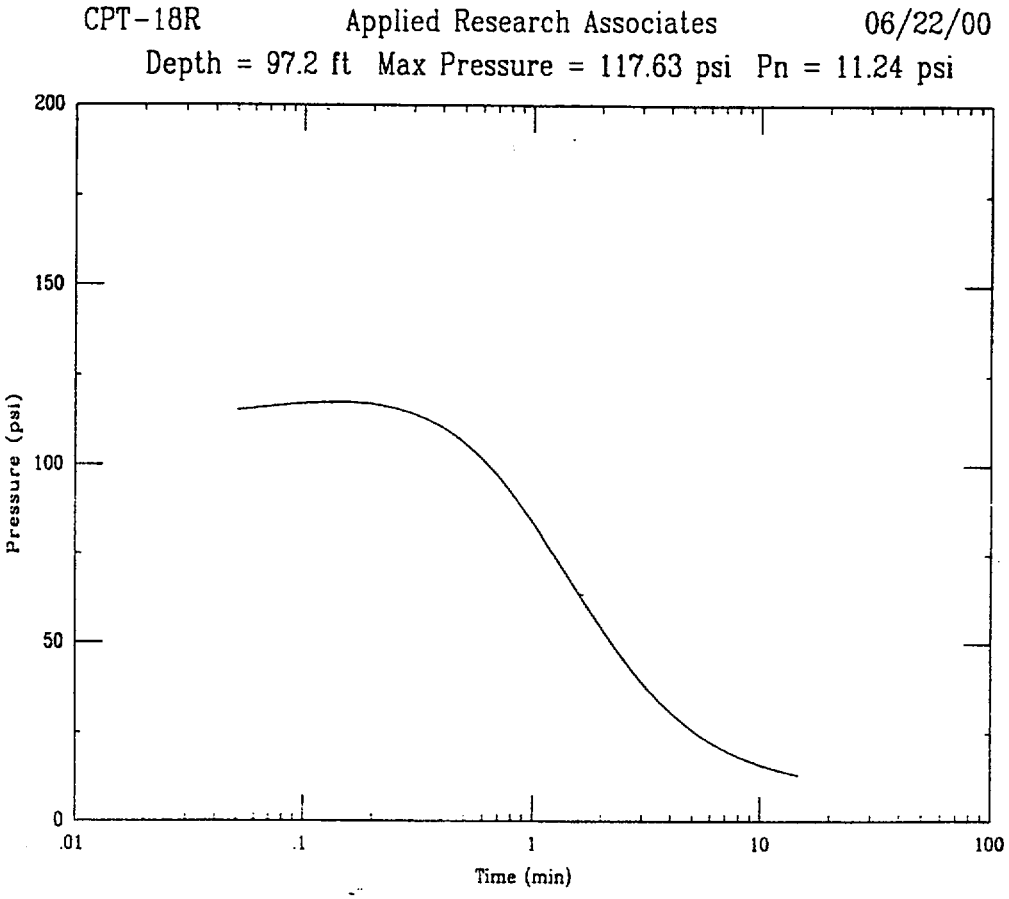

Figure 2.6 Classic dissipation profile from MFFF project

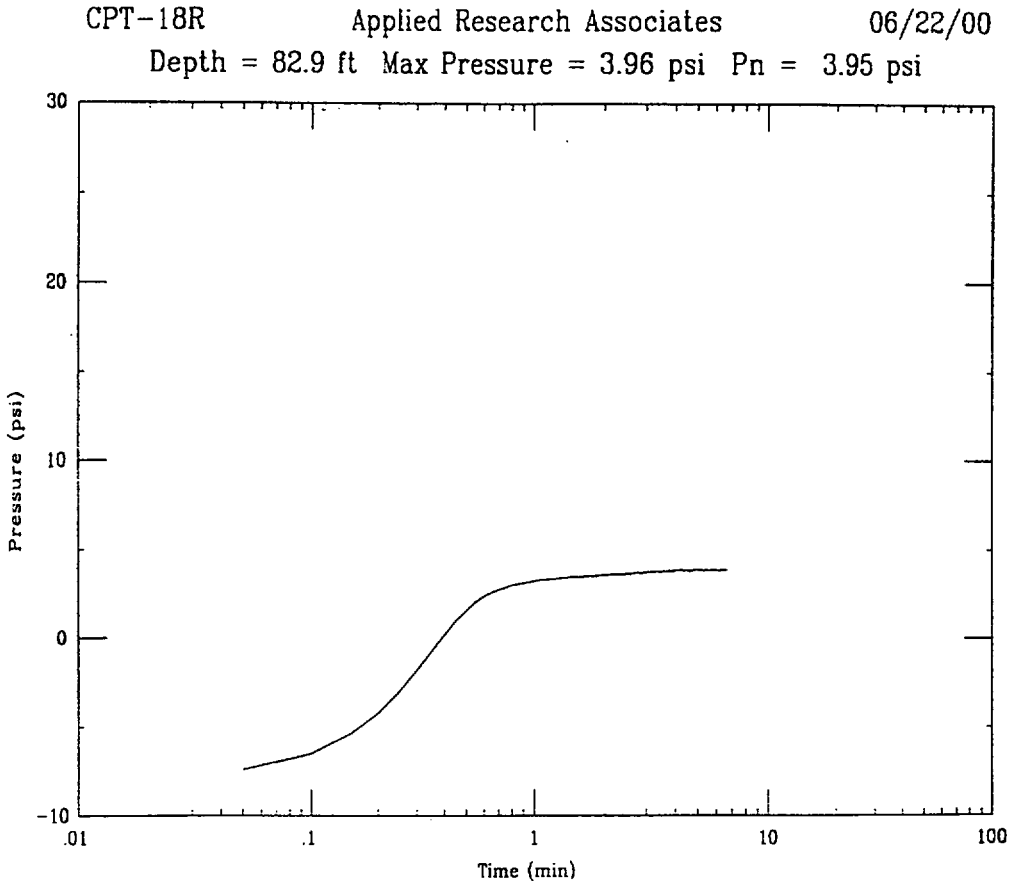

Figure 2.7 Dissipation test showing dilating condition

Soil Sampler
(Patent No. 5211249)

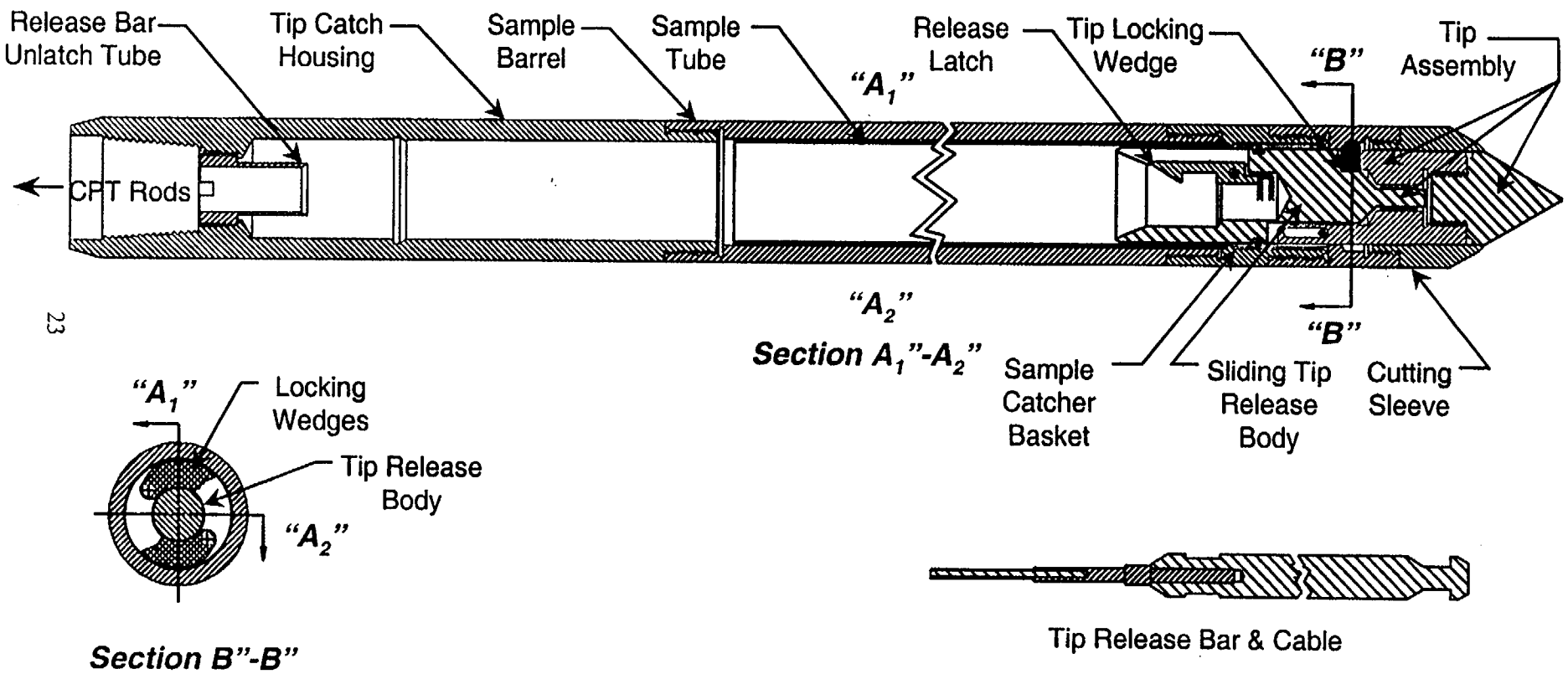

Figure 2.8. Soil Sampler schematic

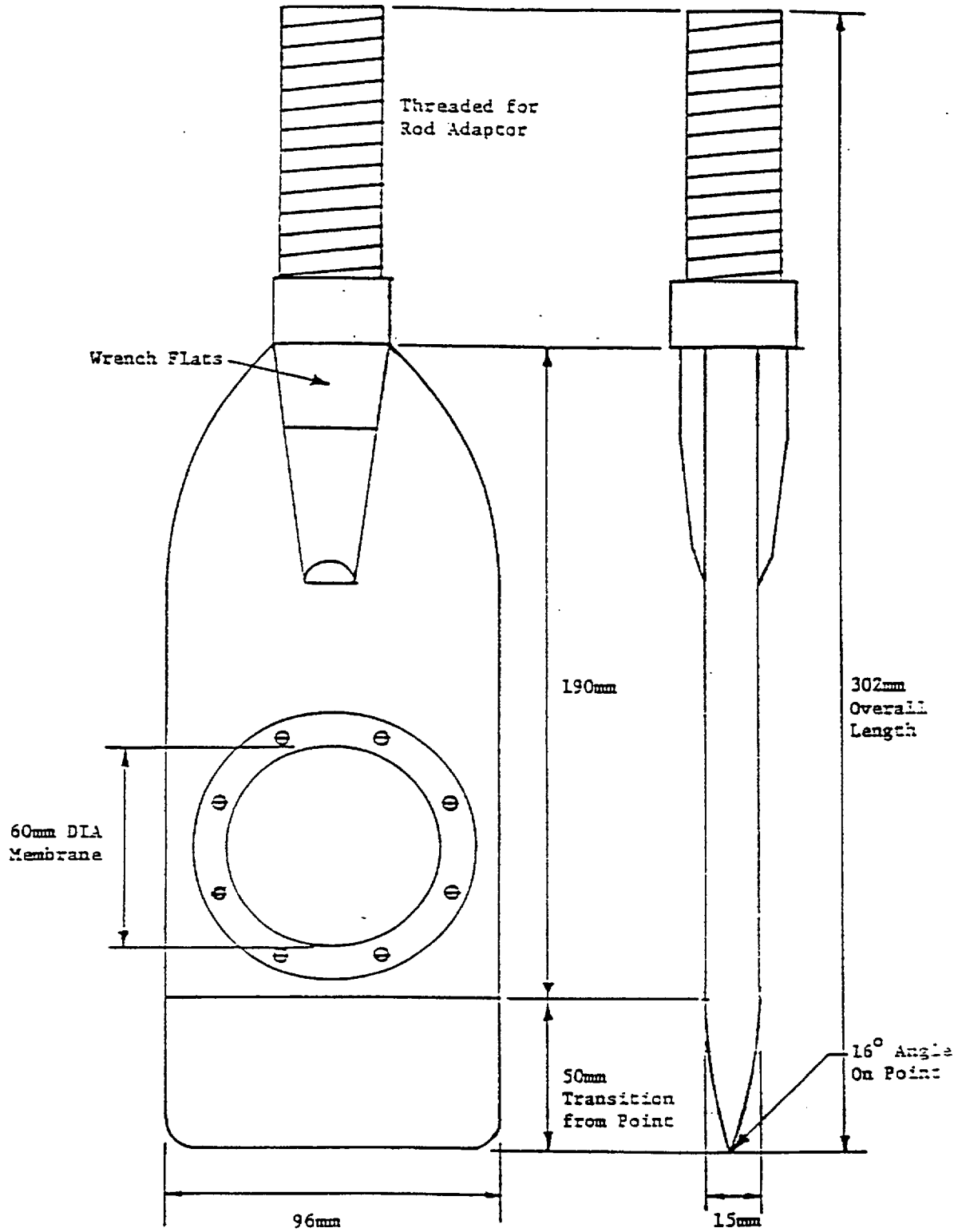

Figure 2.9 Schematic of dilatometer used at the MFFF site

SECTION 3

DATA ANALYSIS TECHNIQUES

OVERVIEW

Presented in this section is a description of analysis techniques used to determine engineering parameters. The methods used to determine the soil type information from the CPT are also discussed. The second portion of this section discusses typical piezo-resistivity and seismic cone penetrometer tests.

LOCATION OF THE SITE WATER TABLE

Generally, the static water table at a given site can be identified from the penetration pore pressures, since it will be equal to the hydrostatic pore pressure in freely draining soil layers. When no such layers are present, pore pressure dissipation tests can be performed to determine hydrostatic pressures. This information was used in the soil classification routines for the calculation of effective stress of the soil materials. A saturated unit weight of 120 pounds per cubic foot is assumed for all calculations.

SOIL BEHAVIOR TYPE

The tip resistance, friction ratio, and pore pressure values from CPT profiles can be used to determine a soil stratigraphy profile. Plots of normalized tip resistance versus friction ratio and normalized tip resistance versus penetration pore pressure can be used to determine Soil Behavior Type, SBT, as a function of depth. Both methods of soil description are based on empirical charts developed by Robertson (Ref. 2). The friction ratio based routines were selected for this project, since this approach is more robust than the pore pressure approach. The friction ratio SBT is determined from the chart in Figure 3.1 using the normalized corrected tip stress and the normalized friction ratio of f_{SN}.

The normalized tip resistance is defined as:

$$q_{NT} = \frac{q_T - \sigma_{vo}}{\sigma'_{vo}} \tag{3.1}$$

The normalized friction ratio is defined as:

$$f_{SN} = \frac{f_s}{q_T - \sigma_{vo}} x\,100 \qquad (3.2)$$

where: fs = sleeve friction

q_T = corrected tip resistance

σ_{vo} = total overburden stress

σ'_{vo} = effective overburden stress

The intersection point of the q_T and f_{SN} values normally falls in a classification zone. The zone number corresponds to a soil behavior type (SBT) as shown in Figure 3.1. At some depths, the CPT data will fall outside of the range of the chart. When this occurs, no data is plotted and a break is seen in the SBT profile. This occasionally occurs at the top of a penetration as the effective vertical stress is very small and produces normalized cone resistances greater than 1000.

The classification profiles are very detailed due to the high sampling rate of one sample every 2 cm (0.8 in) for CPT profiles. Frequently significant variability in soil types over small changes in elevation can be observed in the profiles. To provide a simplified soil stratigraphy for comparison to standard boring logs, a layering and generalized classification system was implemented. Layer thicknesses are determined based on the variability of the SBT profile. The layer sequence is begun at the ground surface and layer thicknesses are determined based upon changes in the standard deviation of the SBT number. Whenever an additional 6-inch increment deviates from the previous increment, a new layer is started, otherwise, this material is added to the layer above and the next 6-inch section is evaluated. The soil type for the layer is determined by the mean value for the complete layer.

Although not presented on the CPT profiles, the electronic .ecp files contain the pore pressure classification values based on pore pressure ratio. This method uses the normalized corrected tip stress in bars and the pore pressure ration B_q.

$$B_q = \frac{u_{meas} - u_o}{q_t - \sigma_{vo}} \qquad (3.3)$$

where: u_{meas} = measured penetration pore pressure

u_o = static pore pressure, determined from the water table elevation

q_T = corrected tip resistance

σ_{vo} = total overburden stress

The intersection point of the q_T and B_q or f_{SN} values normally falls in a SBT zone. The SBT zone number corresponds to a soil type as shown in the figure. At some depths, the CPT data will fall outside of the range of the chart. When this occurs, no data is plotted and a break is seen in the SBT profile. Close analysis of this chart indicates that as the SBT numbers vary, so does the soil grain size. What is missing in these charts are mixed soils, such as sandy clays or clayey sands. This type of mixed soil represents special cases and may be misclassified as silts.

STANDARD PENETRATION TEST

Correlations between the cone penetrometer tip stress measurements, q_c, and standard penetration test blow count (N) data have been made by a number of researchers. Robertson and Campanella (Ref. 2) have summarized many of these studies and presented a relationship between q_c, N, and soil type. The blow count corresponding to 60 percent of the energy transferred to the sampler can be estimated from a ratio based on the soil type. For this project, the ratios used to compute the N value were as follows:

Soil Classification Number (SCN)	q/N ratio
less than 1.5	2.0
1.5 to 7.5	SCN/1.5
greater than 7.5	1.5

This relationship shows that as the materials increase in grain size up to an overconsolidated or cemented material (SCN = 7.5 or more) the q_c/N ratio increases. The correlation between q_c and N_{60} should be considered an estimate only, due to the rapid fluctuations in tip stress that can result in large changes in the calculated blow count. Also, the techniques used in performing the SPT test in any geographical area need to be considered. If the energy level normally transferred to the sampler is not nearly 60 percent of the theoretical maximum, the local correlation will be either higher or lower than the data presented in this report.

FRICTION ANGLE (ϕ)

The effective stress friction angle in granular soils can be estimated from the tip resistance data using an empirical correlation derived between laboratory triaxial tests on sands and penetration tests through prepared sands in large calibration chambers. The triaxial tests were performed at confining stresses equal to the horizontal effective stress in the calibration chamber. The tip stress data were then correlated with peak effective friction angle as (Ref. 2):

$$\tan \phi' = .38 \log_{10} \frac{q_c}{\sigma'_{vo}} + 0.1 \qquad \textbf{(3.4)}$$

where: ϕ' = effective internal friction angle (deg)
q_c = total measured tip stress
σ'_{vo} = effective overburden stress.

UNDRAINED SHEAR STRENGTH (S_u)

Estimates of the undrained shear strength in fine grained saturated soils can be made using the empirical relationship (Ref.2):

$$S_u = \frac{q_c - \sigma_{vo}}{N_k} \qquad \textbf{(3.5)}$$

where: S_u = undrained shear strength
q_c = total measured tip stress
σ_{vo} = total overburden stress
N_k = cone factor

The cone factor, N_k falls between 11 and 19 with an average of 15. In the absence of field vane shear data, sa is the case for the MFFF site, Robertson and Campanella (Ref. 2) recommend assuming N_k to be 15. If N_k is 19 for a given material, using N_k of 15 overestimates the undrained shear strength by 27%; and if N_k is 11, the strength is underestimated by 27%.

PRESENTATION OF ϕ AND S_u VALUES

Conventional engineering considers only friction angles (ϕ) to be appropriate in granular soil deposits such as sands. Similarly, undrained shear strength (Su) values are used in saturated,

low permeability layers such as clays. The distinction between which parameter is appropriate at a given depth is based on the soil type. When the average SBT number is greater than 4.0, the granular material is assumed to dominate and the friction angle is plotted. Conversely, if the SBT number is less than or equal to 5, the fine grained material is assumed to dominate and the undrained shear strength is plotted. These SBT numbers are found in the electronic files supplied with this report. Both values are plotted for SBT values of 4 and 5. When the data does not fall within the range of the classification system, neither ϕ' or S_u values are presented.

ESTIMATES OF OVERCONSOLIDATION RATIO (OCR)

A soil is termed normally consolidated if the current stress is the maximum to which the material has ever been subjected. The overconsolidation ratio (OCR) is defined as:

$$OCR = \frac{(\sigma_{v'o})_{max.past}}{(\sigma_{v'o})_{present}} \qquad (3.6)$$

where: $(\sigma'_{vo})_{max.past}$ = maximum past vertical effective overburden pressure

(σ'_{vo}) = present effective vertical overburden pressure.

For a normally consolidated soil, $(\sigma'_{vo})_{max.past} = (\sigma'_{vo})_{present}$ and OCR = 1, while an overconsolidated soil has an OCR > 1.

OCR calculations for the MFFF site were based on a publication by Mayne (Ref. 5) where OCR is directly correlated to excess pore pressure. As determined from a linear regression of published data, this equation is:

$$OCR = 0.33 \left[\frac{u_{meas} \bullet u_o}{\sigma_{v'o}} \right]^{1.42} \qquad (3.7)$$

COEFFICIENT OF LATERAL CONSOLIDATION (C_H)

Horizontal coefficients of consolidation can be calculated from the pore pressure dissipation tests using a theoretical model developed by Baligh and Levadoux (Ref. 6) and measured dissipation rates. Calculations are performed at 50% of the excess pore pressure

dissipation, U_{50}. Using the theoretical curves in Figure 3.2, C_H is calculated as:

$$C_H = \frac{T_{50}R^2}{t_{50}} \tag{3.8}$$

where: T_{50} = theoretical time factor at 50% dissipation

R = radius of cone in centimeters

t_{50} = measured time at 50% dissipation in seconds

Pore pressure measurements are made just behind the tip; hence, curve 3 in Figure 3.2 is used to determine a T_{50} of 5.5.

COEFFICIENT OF LATERAL PERMEABILITY (K_H)

This method uses the coefficient of lateral consolidation estimated from the pore pressure dissipation test described above and an estimate of the in situ constrained modulus, M, obtained from measured tip resistance values and soil classification according to:

$$K_H = \frac{C_H \gamma_w}{M} \tag{3.9}$$

where: C_H = coefficient of lateral consolidations

γ_W = unit weight of water

M = constrained modulus

The constrained modulus, M can be estimated using the empirical relationship:

$$M = \alpha q_c = \frac{1}{m_v} \tag{3.10}$$

where: α = empirical factor

q_c = measured tip resistance, not corrected for pore pressure effects

m_V = volumetric compressibility.

The factor α is obtained from Figure 3.3 (Ref. 2) is based on the uncorrected tip resistance and soil type.

TYPICAL P-CPT PROFILE

Location CPT-18R represents a typical piezo-resistivity cone penetrometer sounding profile at the proposed MFFF site site (Figure 2.2). Sounding CPT-18R is located at 80192.1 north by 55405.9 east at elevation 277.0 feet. Typical to this site, sands and gravelly sands are encountered in the first 10 feet of penetration from elevation 277.0 to 267.0 feet, as indicated by tip resistance values in excess of 290 tons per square foot (tsf) and friction ratio values ranging from 2% to 4%. Measured soil resistivity remains relatively constant at approximately 4000 ohm-m from elevation 277.0 to 237.0 feet. At elevation 267.0 feet the probe encounters less resistant and less cohesive soils in the form of sands and sand mixes. With the exception of a slight interruption at elevation 237.0 feet, this layer extends approximately 53 feet to elevation 222.0 feet. Sleeve friction values decrease to 1 to 2 tsf and tip resistance in this zone fluctuates between 100 and 200 tsf. This combination of tip stress and sleeve friction results in low friction ratios. As previously mentioned, a fine-grained lens interrupts this layer 4 feet in thickness extending from elevation 237.0 to 233.0 feet. Tip stress decreases while the sleeve friction increases, indicating an increase in soil cohesion. In this less permeable material, the first measurable pore pressure readings are recorded. It is important to note that the soils in this lens are more conductive as is evident by the decrease in measured resistivity. A very resistant soil matrix is encountered at elevation 213 feet. The cone penetrometer typically encounters refusal in such stiff soils, however the thin nature of this lens enabled the crew to cycle the probe through. At elevation 208 to 207 feet, several observations are made. Fine-grained soils are again detected as evident by decreased penetration resistance, elevated penetration pore pressures, and a decrease in soil resistivity. The water table is also encountered at this elevation which is supported by the magnitude of the decrease in soil resistivity. Due to the presence of water below elevation 207 feet, resistivity remains relatively low for the remainder of the sounding. This layer continues to elevation 198 feet where a more resistant, less permeable soil matrix is encountered. Note the dramatic decrease in penetration pore pressure. Dissipation tests were conducted at this location at elevations 194.1 and 179.8 feet. In situ soils at elevation 194.1 feet are best described as fine-grained sands as noted by the elevated tip resistance measurements. The dissipation test conducted at this elevation reveals negative pore pressures for the first 30 seconds of the test, indicating a dilated condition which is consistent with the negative penetration pore pressures measured. At elevation 182 to 171 feet, the soils become

finer and less permeable, resulting in elevated penetration pore pressures. A dissipation test was conducted in this layer and a classic pore pressure profile was obtained supporting the observation of a fine clayey layer. The in situ soils begin to stiffen below elevation 171 feet until penetration refusal is encountered at elevation 156.7 feet.

SEISMIC MEASUREMENTS AND RESULTS

Seismic downhole data of shear and compressional waves were conducted every five feet from the bottom of the pre-augered utility clearance hole to the final depth at six of the CPT locations. The seismic signals were typically recorded at a rate of 10,000 samples per second with the acquisition system set to record a total of 2,500 data points per seismic trace.

The seismic shear wave time histories in Figure 2.4 show several cycles of motion beyond the first peak motion. Any analysis of these late motions should consider the gage frequency response. Geophones are non-linear devices and the amplitude and phase angle are a function of frequency. The data plotted in Figure 2.4 and in Appendix B are presented as the voltage output (vertical scale of each time history trace) of the transducer and have not been corrected for non-linear transducer response. The Geospace transducers (GS-14-L9) used on this project have an undamped natural frequency of 28 Hz, with the transducer sensitivity greatly reduced below 28 Hz. The transducer sensitivity at the natural frequency can be a factor of two greater than the nominal sensitivity below 28 Hz. In addition, there is a phase distortion in the raw data. For the uncorrected seismic time history data presented in this report, the shape of the time histories are qualitatively correct, but the late time motions are exaggerated. The data can be corrected using two methods, the first being a high frequency filter. A second method is to apply a transducer transform function to the data that accounts for the non-linear behavior of the transducer. These corrections were not applied to the data, as only arrival times and wavespeeds were desired.

When the support beam beneath the penetrometer truck is struck on one end, traction between the steel beam and the soil generates a horizontal shear wave. Also generated is a small compressive wave as the energy propagates across the beam. The bulk of the mechanical energy is transferred into shear wave energy at the steel-soil interface. However, the small amount of compressive wave generated will arrive at the velocity transducer first due to its higher wave velocity. This is the source of the small amplitude motion observed in Figure 2.4. The

compression wave contamination is of a very small amplitude when compared to the shear signal, and attenuates rapidly with depth. At greater depths, this compression wave contamination arrives much earlier than the shear wave. The hydraulic shear wave source used by ARA is rich in shear wave energy, and the ability to separate the compression wave from the shear wave is enhanced with the use of polarized shear waves.

The shear wave is identified as the first large out-of-phase motion in Figure 2.4. For shallow locations, the exact arrival time of the shear wave can be difficult to pick. Selection of the first shear wave peak is much easier to accomplish, especially with polarized shear waves. These times are typically more consistent and contain less scatter than the selection of arrival times. The shear wave initial peaks are identified in Figure 2.4 by the small arrows. The times are used in the subsequent analysis to determine the shear wave velocities.

Two methods were used to determine the shear wave velocities. The first method used to determine the wave velocities consisted of visually fitting linear line segments to the travel time data over depth intervals that were interpreted to have the same wave velocity. The second method used least square regression algorithms to determine the peak arrival time data within ±6 ft of a given test depth. A minimum of three data points were required in the ±6 ft zone to determine a wave velocity.

TYPICAL SEISMIC-CPT PROFILE

Location CPT-08S (Figure 3.4) presents in situ conditions and seismic wave velocities typical of the site. Sounding CPT-08S is located at 80393.7 north by 55329.1 east at elevation 273.0. Shear wavespeeds at this location range from 1000 feet per second (fps) to 1530 fps (Figure 3.5). Elevated wavespeeds of 1530 fps are measured in top 5 feet of surface material from elevation 263 to 258 feet. Soil properties change at elevation 258 feet to sands and sand mixes. This layer extends 45 feet to elevation 213 feet where shear wavespeeds range from 1120 fps to 1220 fps. Compression wavespeeds of 2090 fps to 2590 fps are determined is these soils. A less permeable clay lens encountered from elevation 213 to 203 feet slows wavespeeds to 1000 fps. The CPT profile for this location indicates a sand mix layer from elevation 203 feet to 186 feet bgs with an interbedded clay lens at elevation 198 feet, approximately 4 feet in thickness. Seismic tests were conducted on 5-foot intervals making it difficult to disseminate thin layers. As a result, an average shear wavespeed of 1100 fps is measured from elevation 203

to 188 feet. Compression wavespeeds are estimated to be 2870 fps in this layer. The water table is encountered below elevation 198 feet so compression wave generation was discontinued. Shear wavespeed increases slightly to 1180 fps from elevation 188 to 168 feet as more resistant and less permeable soils are encountered. From elevation 168 to 163 feet, shear wavespeeds decrease to 1060 fps. No seismic traces could be recorded at test intervals 115 feet and 120 feet bgs resulting in a gap in the calculated shear wavespeeds from elevation 163 to 148 feet. In situ materials stiffen dramatically as the probe nears refusal, resulting in shear wavespeeds of 1320 fps from elevation 148 feet to sounding termination at elevation 133 feet.

CPT Soil Classification Legend

Zone		Q_t/N	Description
1		2	Sensitive, Fine Grained
2		1	Organic Soils-Peats
3		1.5	Clays-Clay to Silty Clay
4		2	Silt Mixtures-Clayey Silt to Silty Clay
5		3	Sand Mixtures-Silty Sand to Sandy Silt
6		4.5	Sands-Clean Sand to Silty Sand
7		6	Gravelly Sand to Sand
8		1	Very Stiff Sand to Clayey Sand *
9		2	Very Stiff, Fine Grained *

(*) *Heavily Overconsolidated or Cemented*

Normalized Friction Ratio Classification Chart

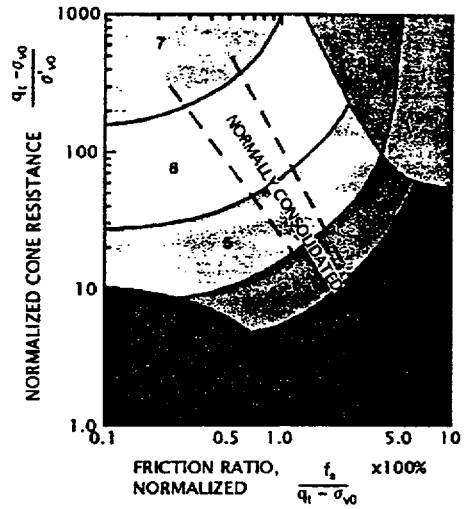

(Ref. Robertson, 1990)

Coefficient of Permeability (cm/s)

Zone	Description	Permeability
1	Sensitive Fines	10^{-5}
2	Organic Soils-Peats	10^{-5}
3	Clays	10^{-7}
4	Silt Mixtures	10^{-6}
5	Sand Mixtures	10^{-4}
6	Sands	10^{-2}
7	Gravelly Sands	10^{-1}
8	Very Stiff Sands	10^{-5}
9	Very Stiff Fines	10^{-6}

Applied Research Associates, Inc., South Royalton, Vermont 05068
(802) 763-8348, cpt@ara.com, http://www.ara.com

Figure 3.1 Friction ratio soil classification chart

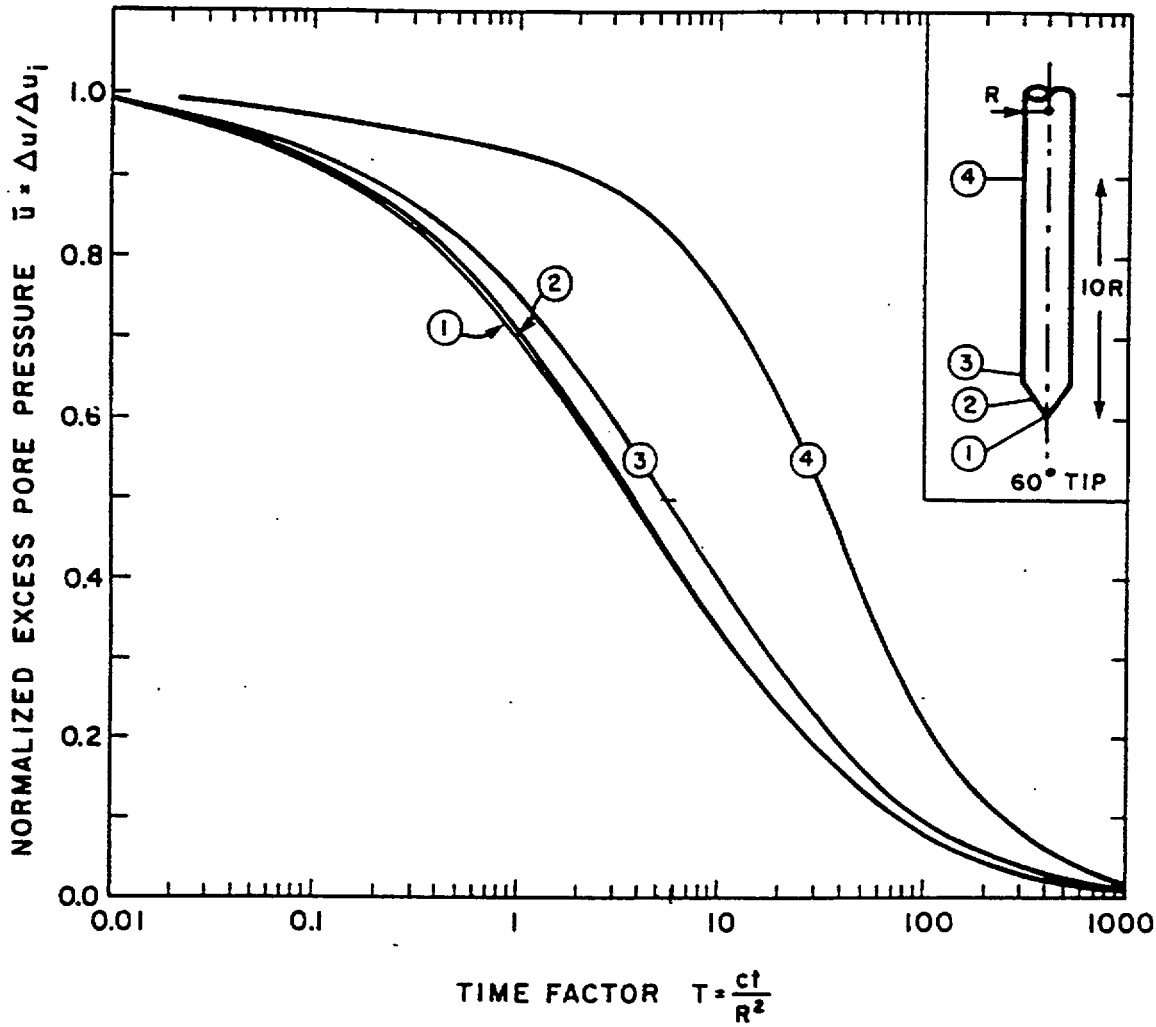

Figure 3.2 Dissipation curves for a 60° cone according to linear isotropic uncoupled solution (after Raligh and Levadoux, 1980)

$$M = \frac{1}{m_v} = \alpha \cdot q_c$$

q_c < 7 bar	3 < α < 8	
7 < q_c < 20 bar	2 < α < 5	Clay of low plasticity (CL)
q_c > 20 bar	1 < α < 2.5	
q_c > 20 bar	3 < α < 6	Silts of low plasticity (ML)
q_c < 20 bar	1 < α < 3	
q_c < 20 bar	2 < α < 6	Highly plastic silts & clays (MH, CH)
q_c < 12 bar	2 < α < 8	Organic silts (OL)
q_c < 7 bar:		
50 < w < 100	1.5 < α < 4	Peat and organic clay (P_t, OH)
100 < w < 200	1 < α < 1.5	
w > 200	0.4 < α < 1	

Figure 3.3 Estimation of the constrained modulus, M, for clays (after Robertson and Campanella, 1988)

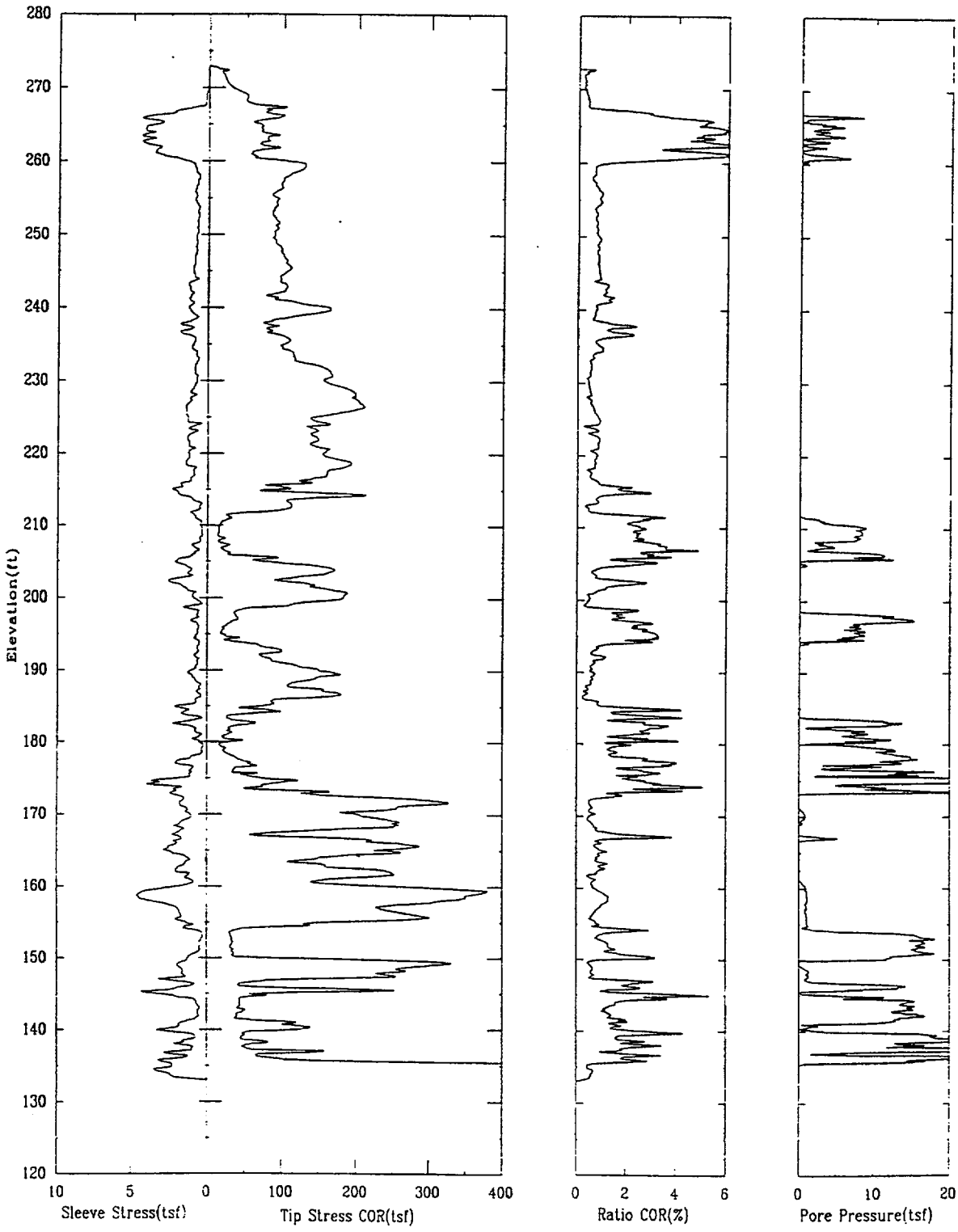

Figure 3.4 CPT profile from location CPT-08S

File 402u004.ECP

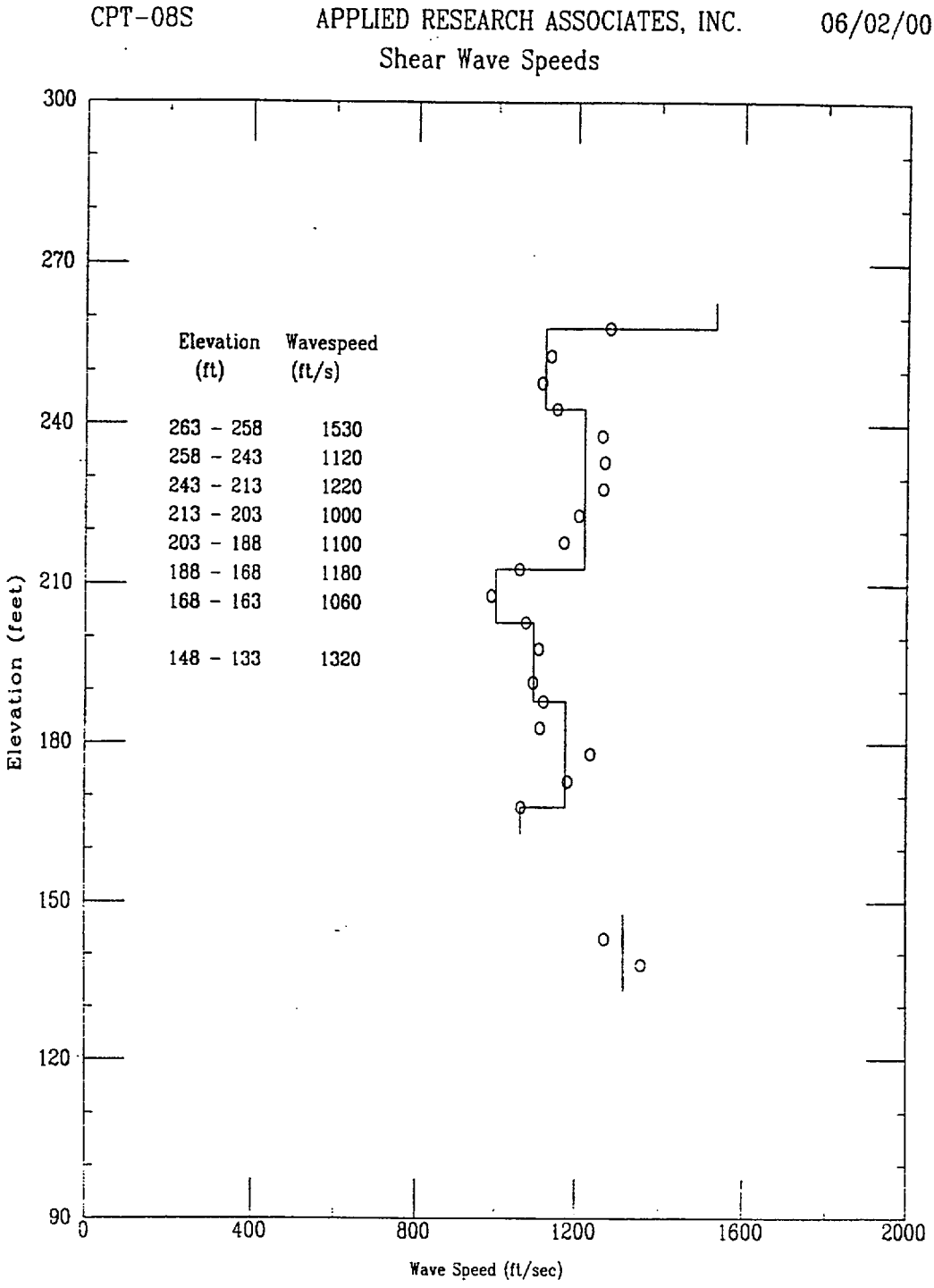

File 402u004S Figure 3.5 Shear wavespeeds from location CPT-08S

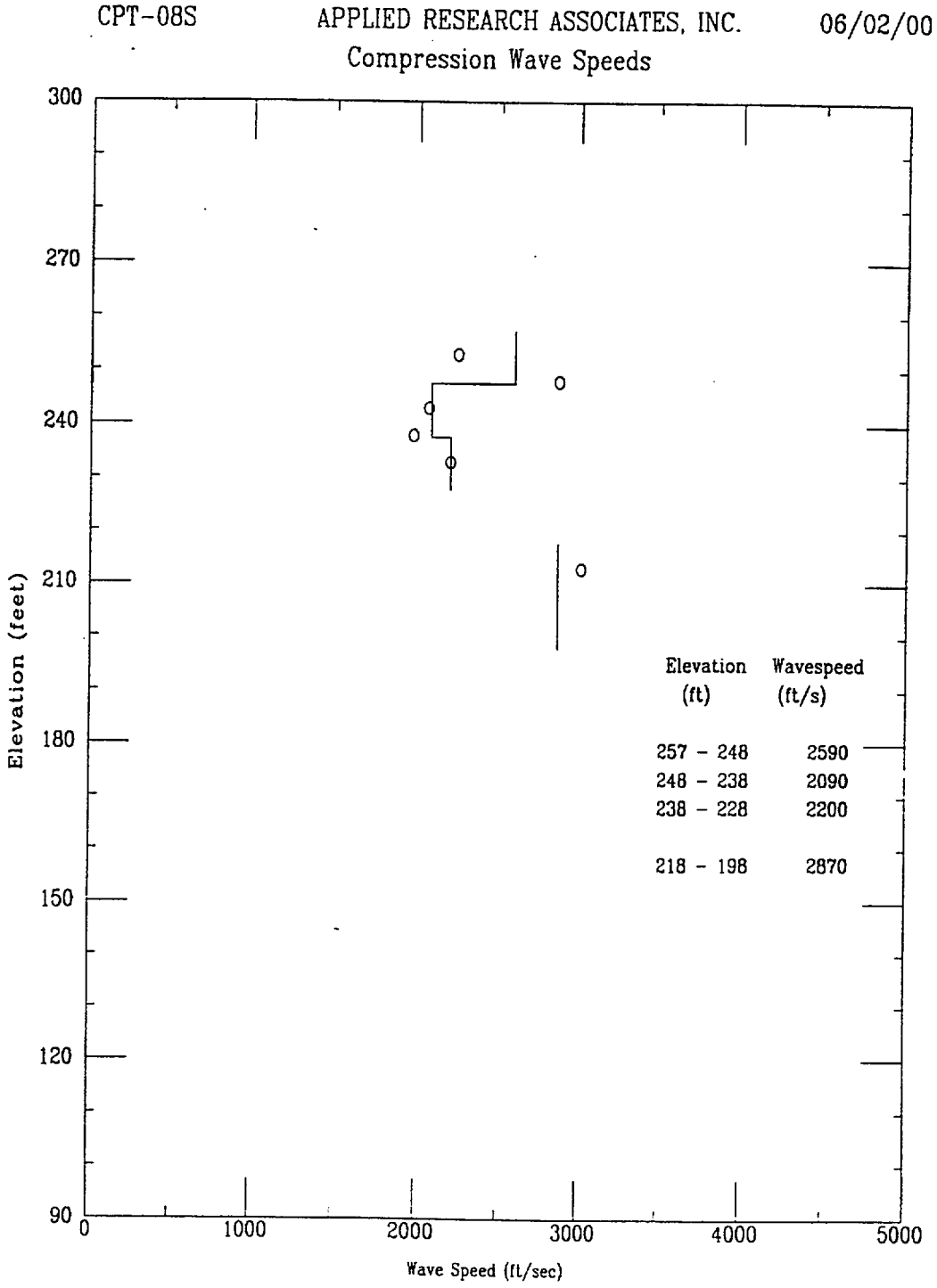

File 408p004S Figure 3.5 Shear wavespeeds from location CPT-08S (concluded)

SECTION 4

LIST OF REFERENCES

1. American Society for Testing Materials, "Standard Test Method for Performing Electric Friction Cone and Piezocone Penetration Testing of Soil," ASTM Designation: D5778, 1995.

2. Robertson, P. K. and R. G. Campanella, *Guidelines for Using the CPT, CPTU and Marchetti DMT for Geotechnical Design*, Vol. II, University of British Columbia, Vancouver, BC, Canada, March 1988.

3. Shinn, J. D. and A. F. Rauch, "Resistivity Surveys with the Electric Cone Penetration Technique," Applied Research Associates, Inc., March 1990.

4. Schmertmann, J. H., *Guidelines for Using the CPT, CPTU, and Marchetti DMT for Geotechnical Design*, Volume III, University of British Columbia, Vancouver, BC, Canada, March 1988.

5. *Use of In Situ Test in Geotechnical Engineering*, S. P. Clemence, ed., Geotechnical Special Publications No. 6, proceedings of In Situ '86 Conference, sponsored by Geotechnical Engineering Division of the American Society of Civil Engineers, Blacksburg, VA, June 1986.

6. Raligh, M. M. and J. N. Levadoux, Pore Pressure Dissipation After Cone Penetration, Massachusetts Institute of Technology, Cambridge, MA, April 1980.

APPENDIX A

PIEZOCONE PROFILES

CPT-01S APPLIED RESEARCH ASSOCIATES, INC. 06/09/00

North 80784.9 East 55554.0 Elevation 258.2

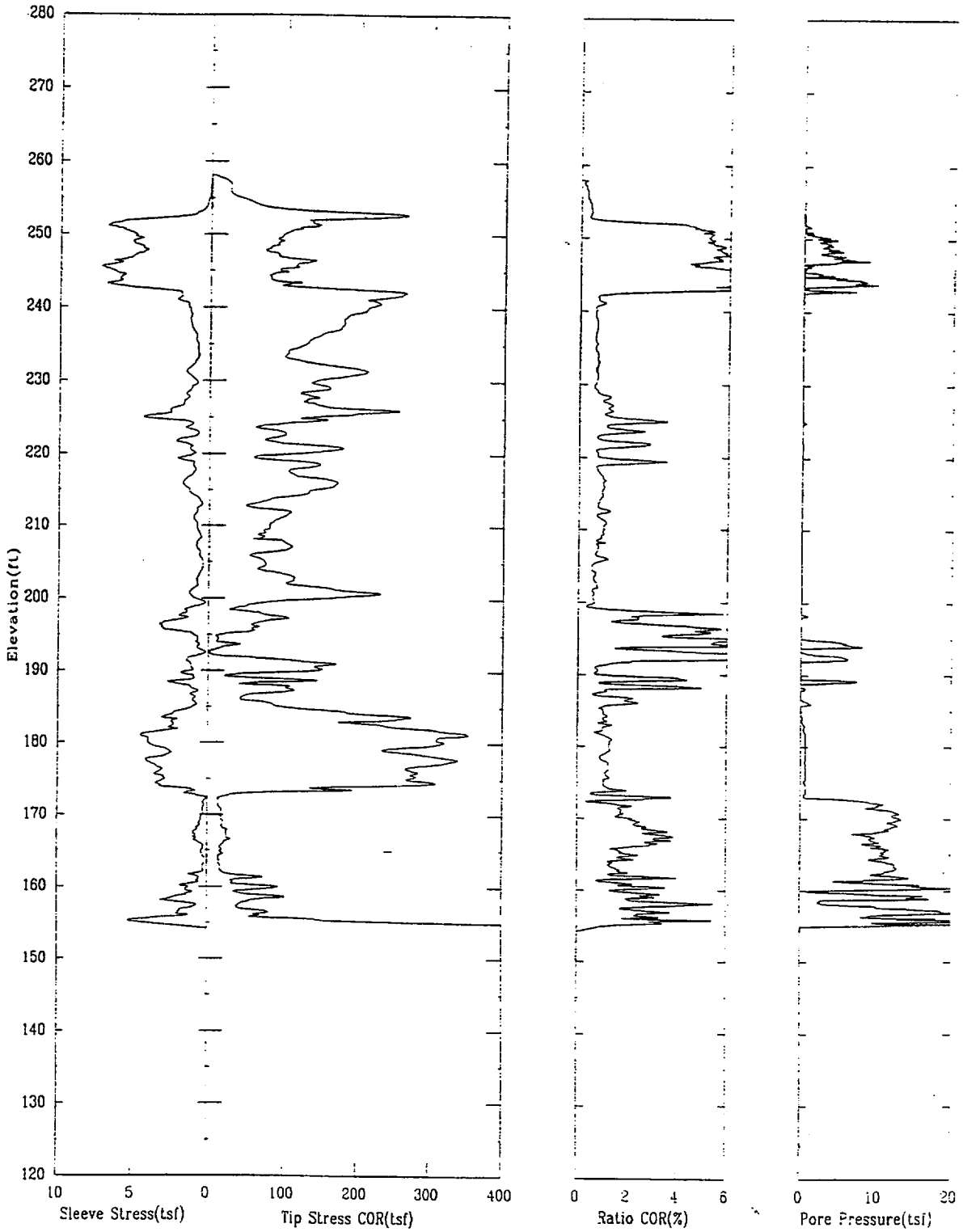

File 409u008.ECP

CPT-01S APPLIED RESEARCH ASSOCIATES, INC. 06/09/00

North 80784.9 East 55554.0 Elevation 258.2

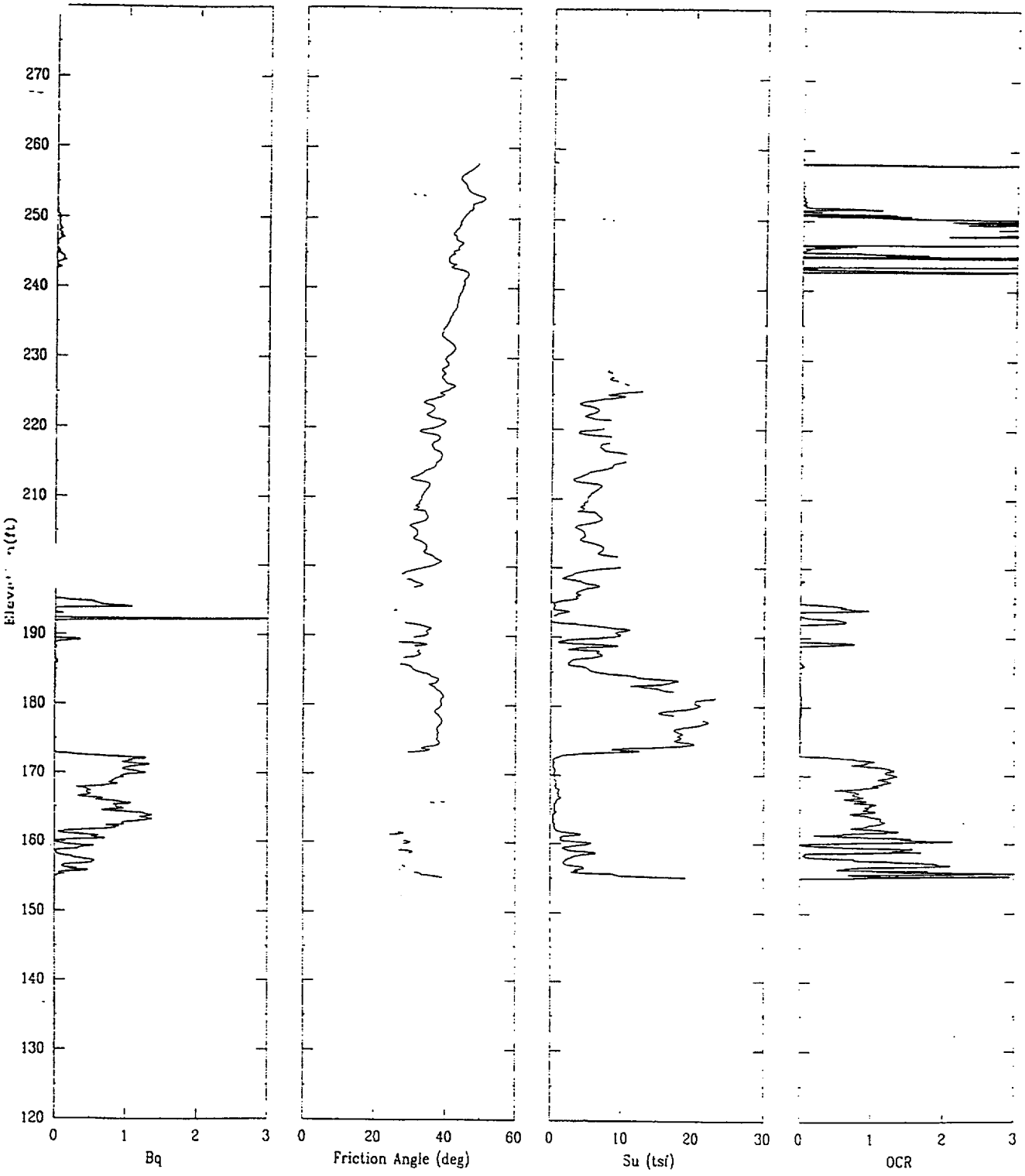

File 409u008.ECP

CPT-01S APPLIED RESEARCH ASSOCIATES, INC. 06/09/00

North 80784.9 East 55554.0 Elevation 258.2

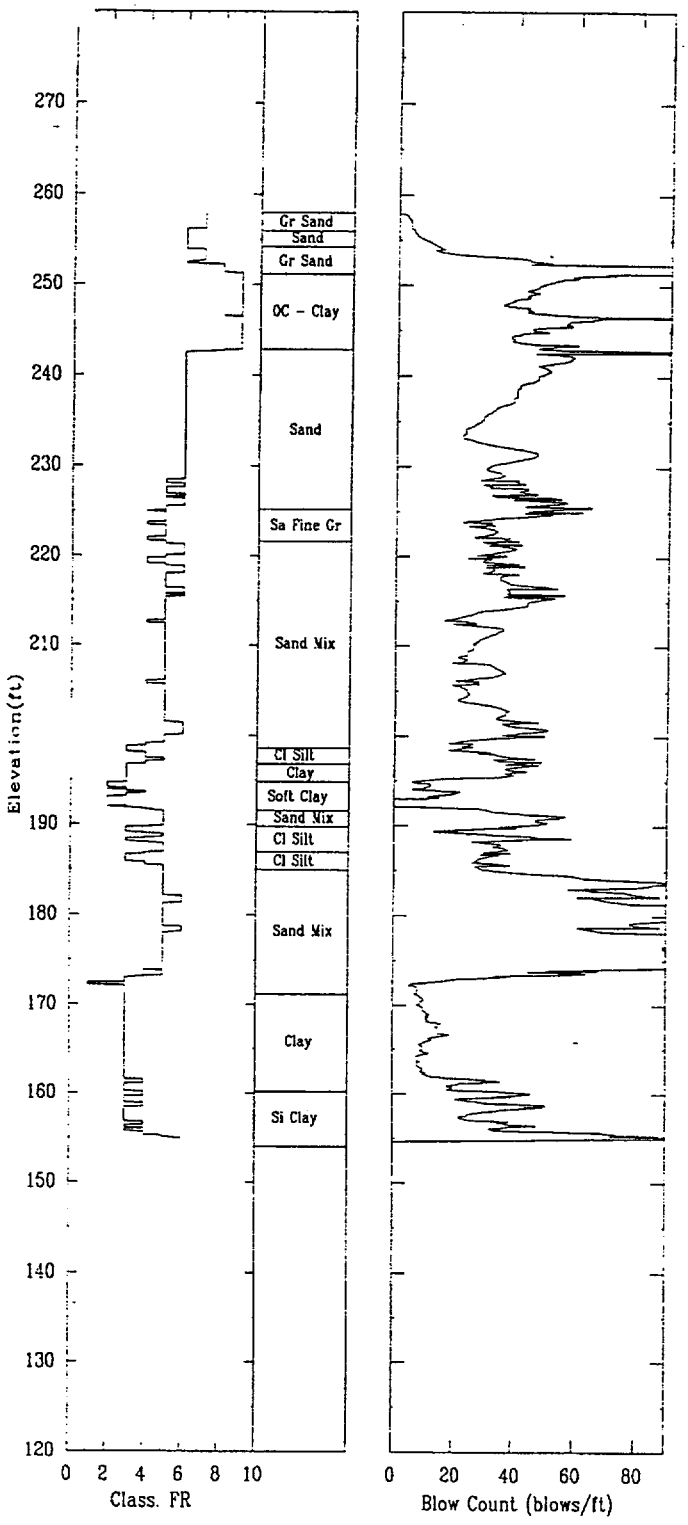

File 409u008.ECP

CPT-02R APPLIED RESEARCH ASSOCIATES, INC. 06/14/00

North 80635.0 East 55616.4 Elevation 257.8

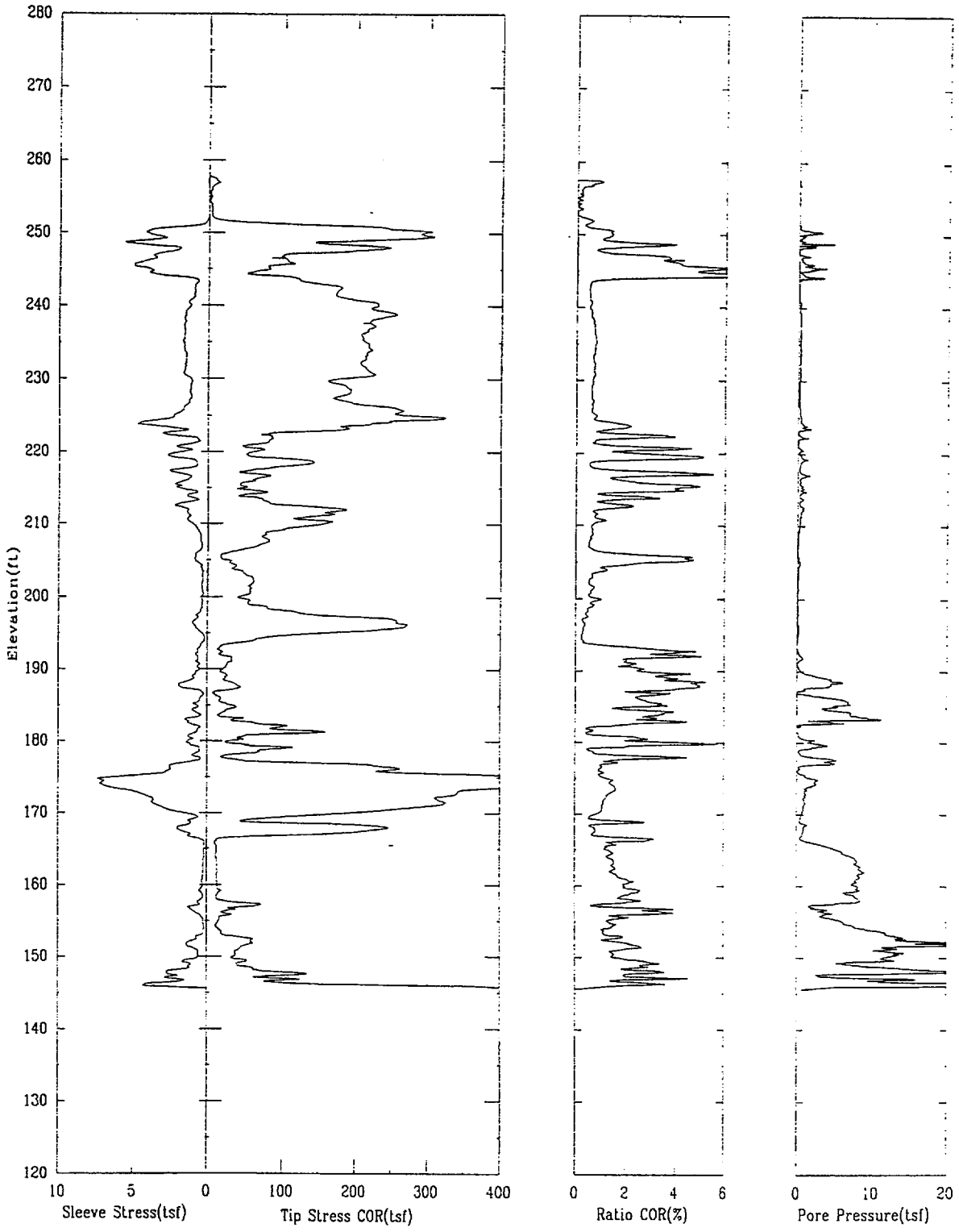

File 414u003.ECP

DCS, MFFF Project No. 08716

CPT-02R APPLIED RESEARCH ASSOCIATES, INC. 06/14/00

North 80635.0 East 55616.4 Elevation 257.8

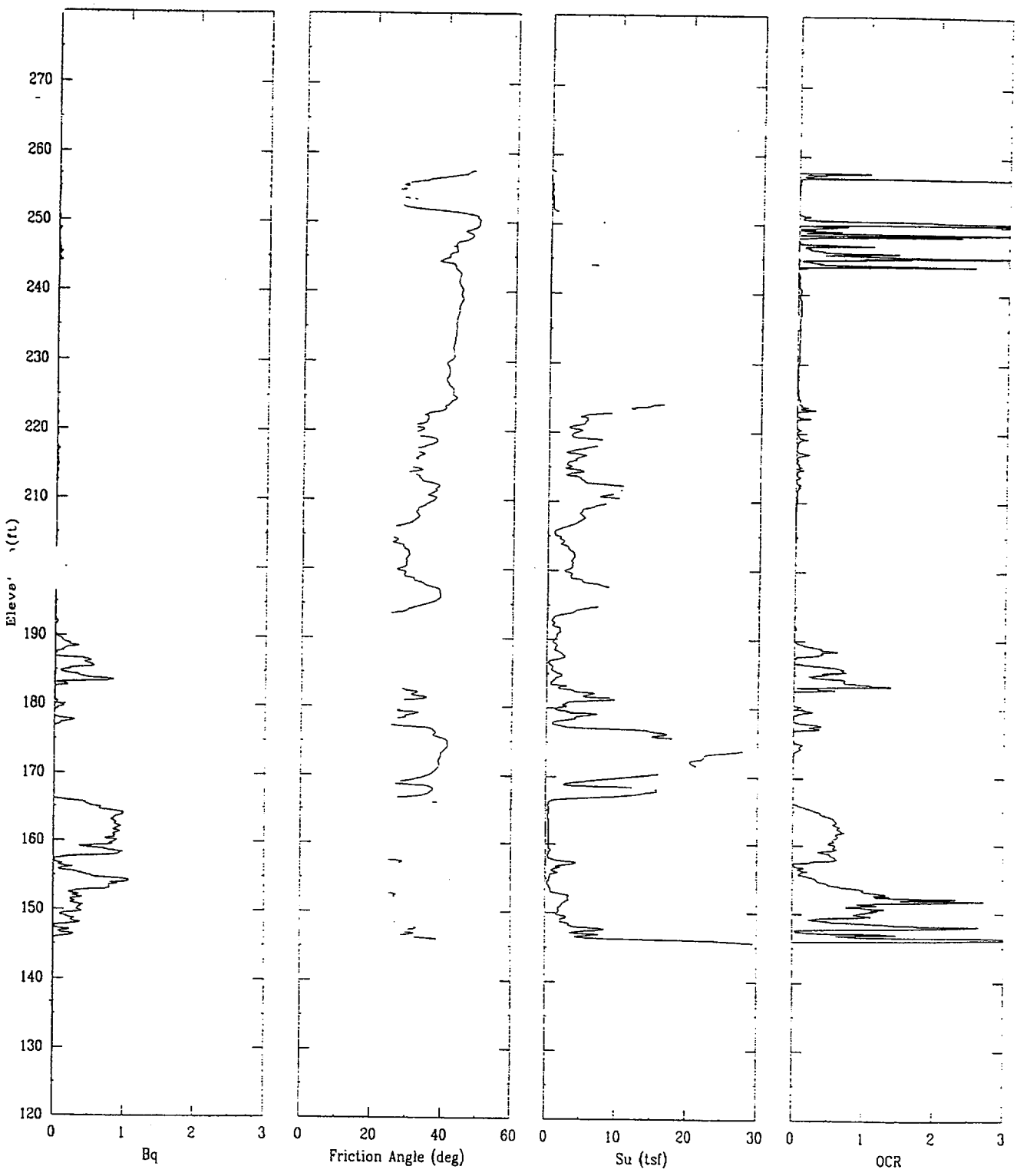

File 414u003.ECP

CPT-02R APPLIED RESEARCH ASSOCIATES, INC. 06/14/00

North 80635.0 East 55616.4 Elevation 257.8

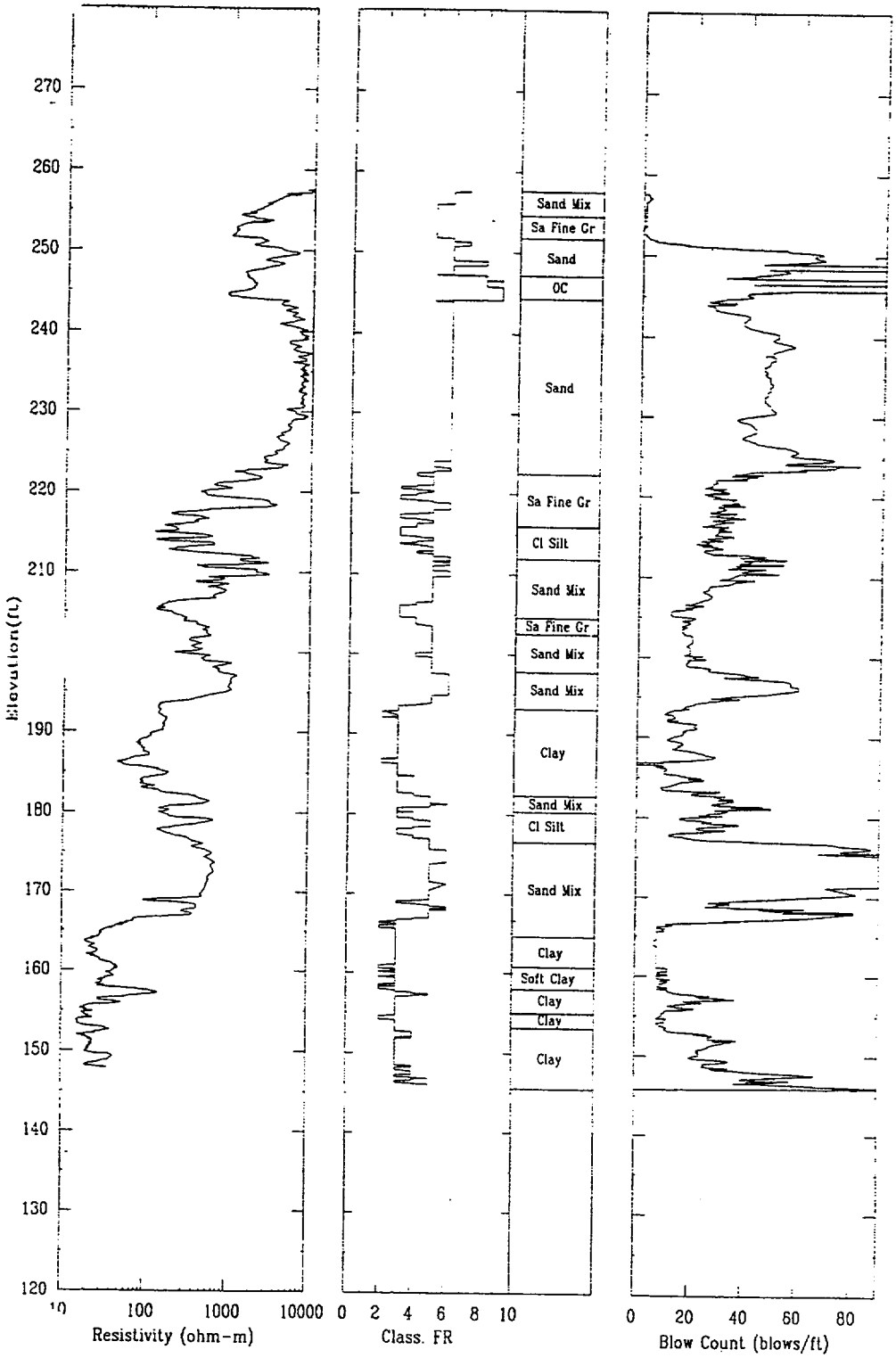

File 414u003.ECP

CPT-03S APPLIED RESEARCH ASSOCIATES, INC. 06/08/00

North 80551.4 East 55700.8 Elevation 253.2

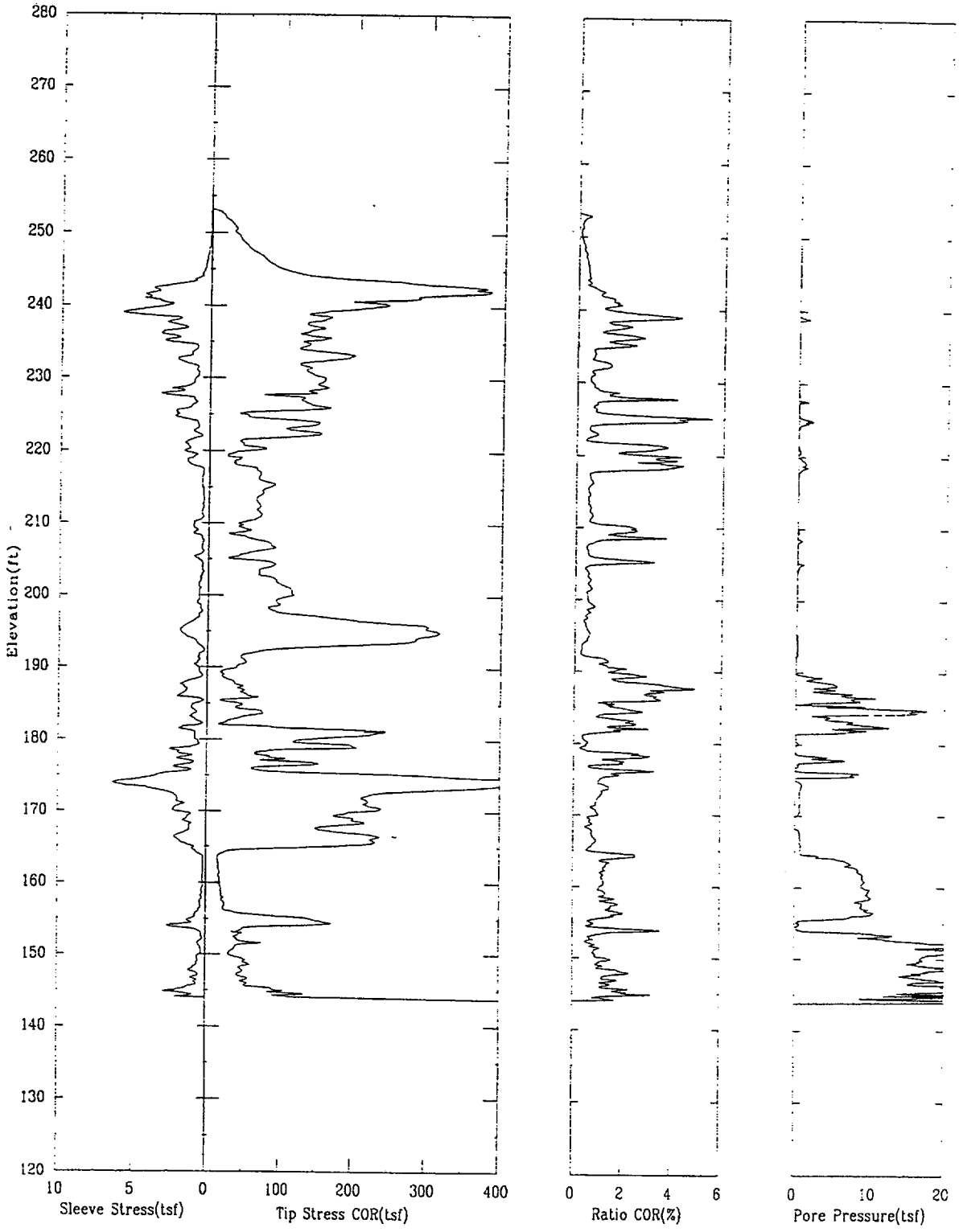

File 408u007.ECP

CPT-03S APPLIED RESEARCH ASSOCIATES, INC. 06/08/00

North 80551.4 East 55700.8 Elevation 253.2

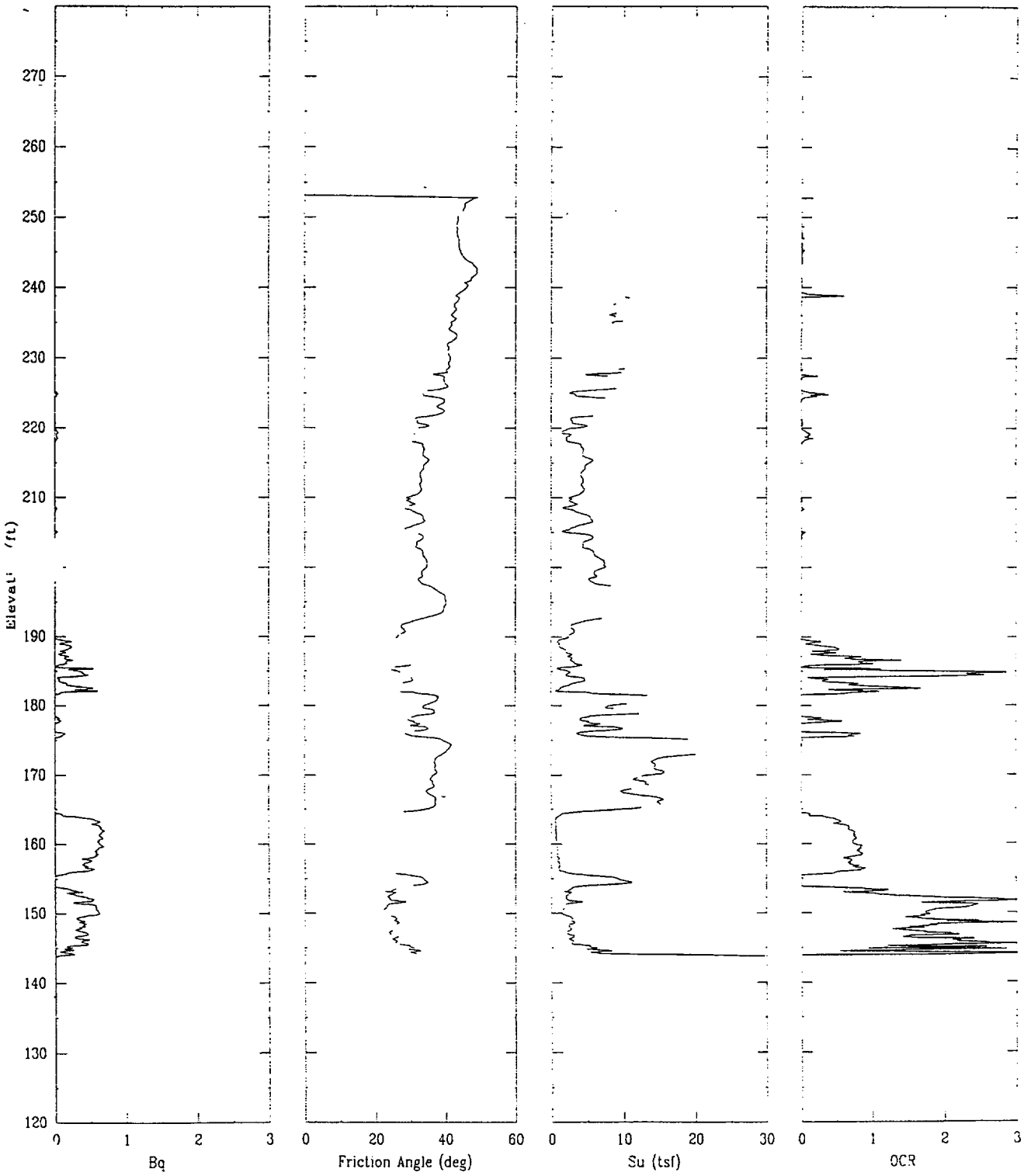

File 408u007.ECP

CPT-03S APPLIED RESEARCH ASSOCIATES, INC. 06/08/00

North 80551.4 East 55700.8 Elevation 253.2

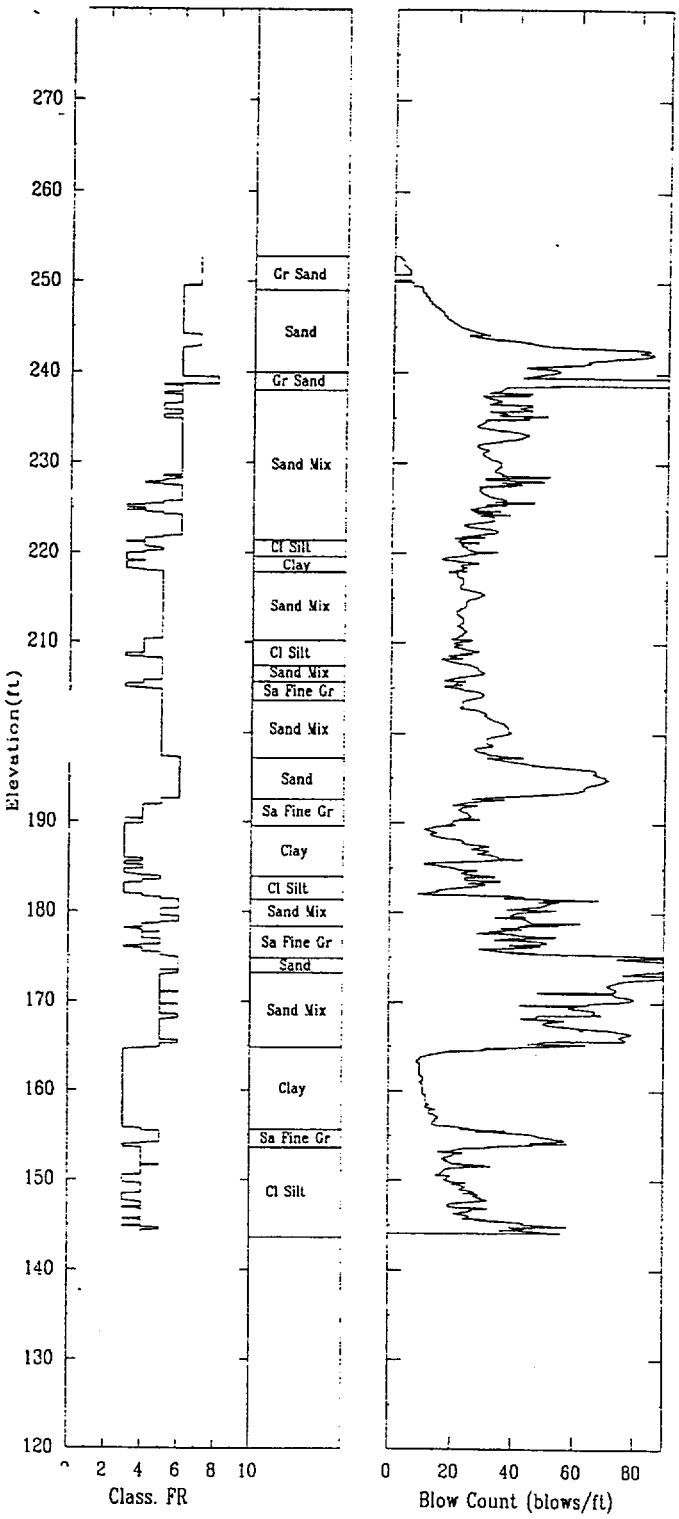

File 408u007.ECP

CPT-04R APPLIED RESEARCH ASSOCIATES, INC. 06/17/00

North 80465.4 East 55320.8 Elevation 272.6

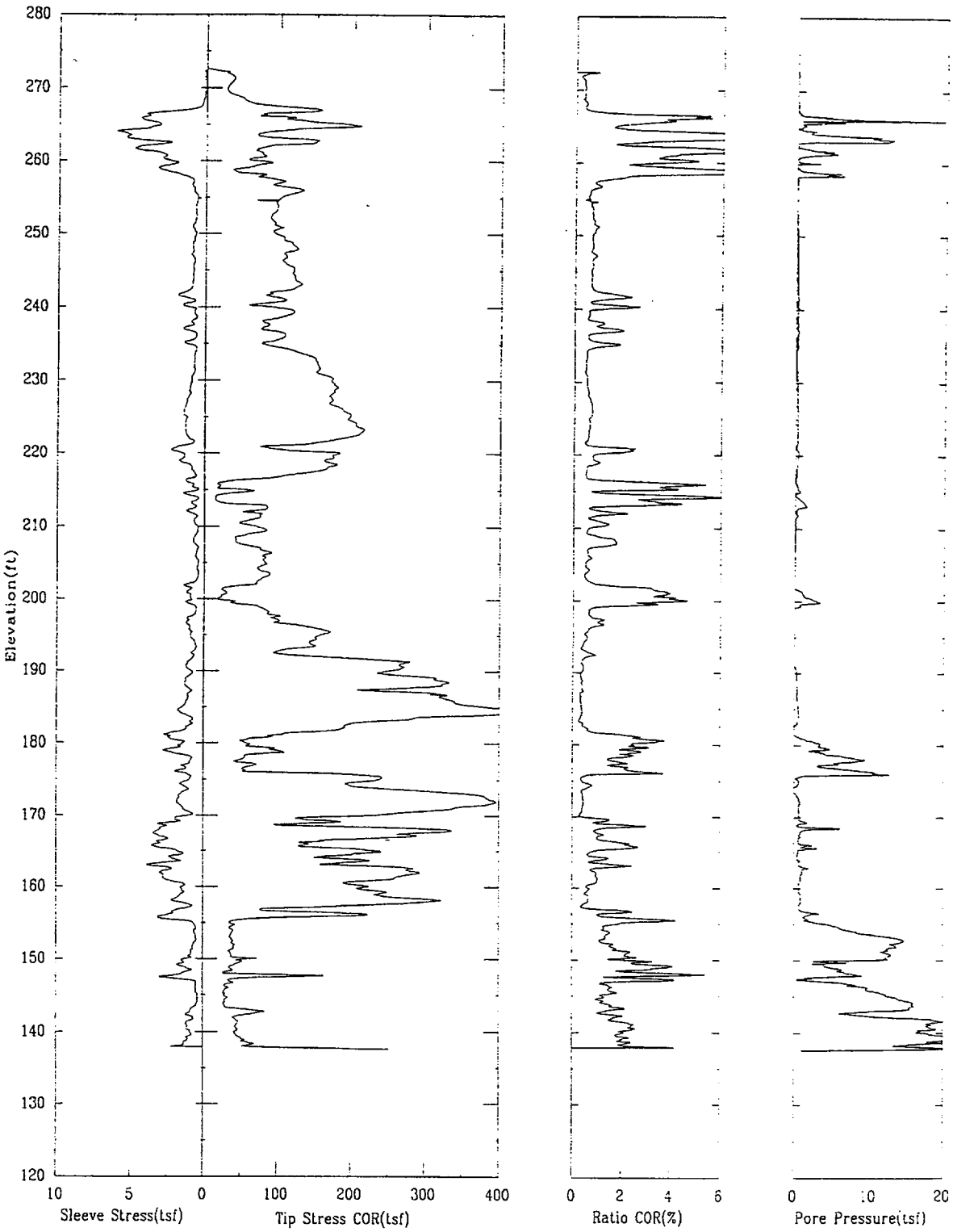

File 417u002B.ECP

CPT-04R APPLIED RESEARCH ASSOCIATES, INC. 06/17/00

North 80465.4 East 55320.8 Elevation 272.6

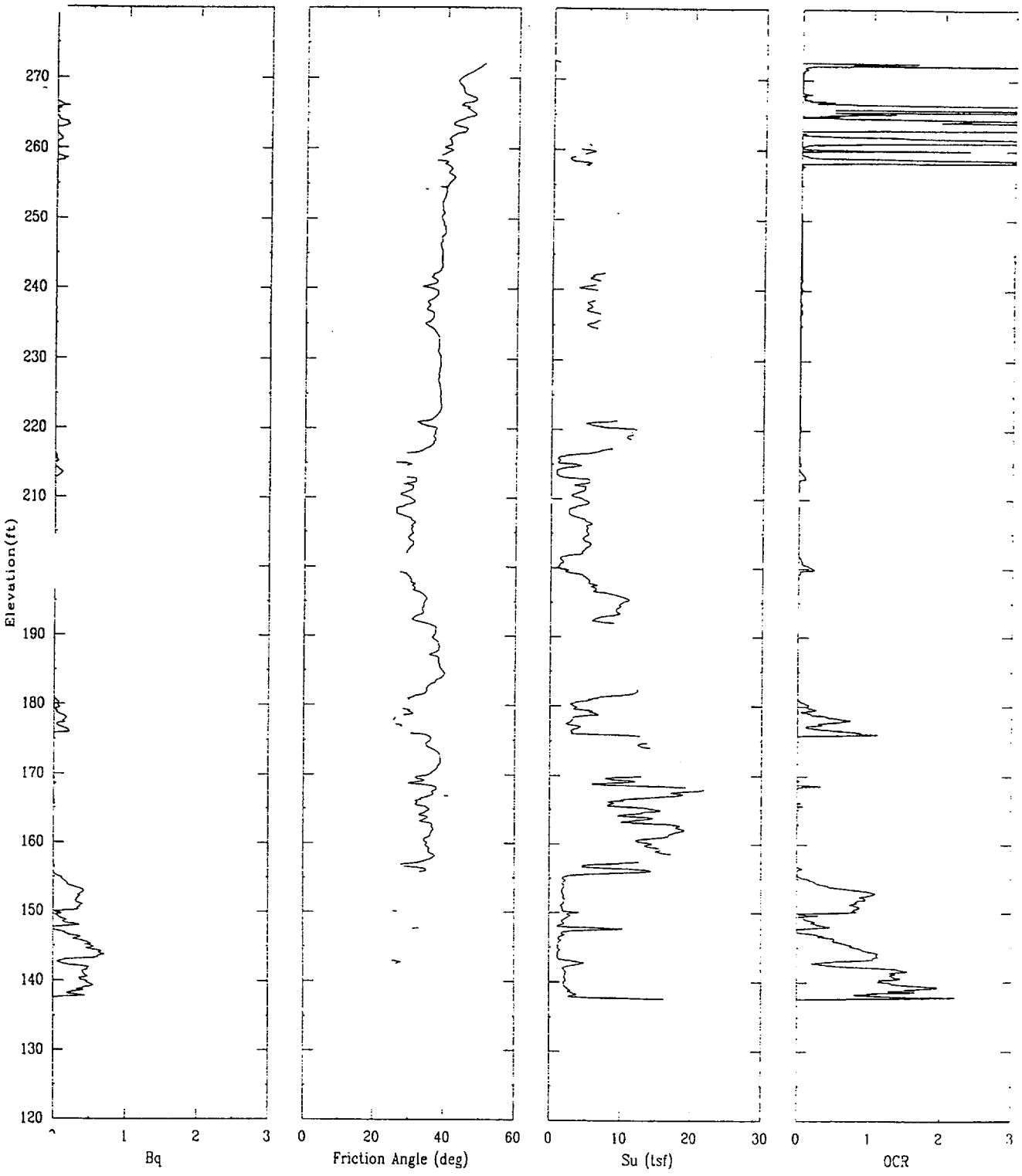

File 417u002B.ECP

CPT-04R APPLIED RESEARCH ASSOCIATES, INC. 06/17/00

North 80465.4 East 55320.8 Elevation 272.6

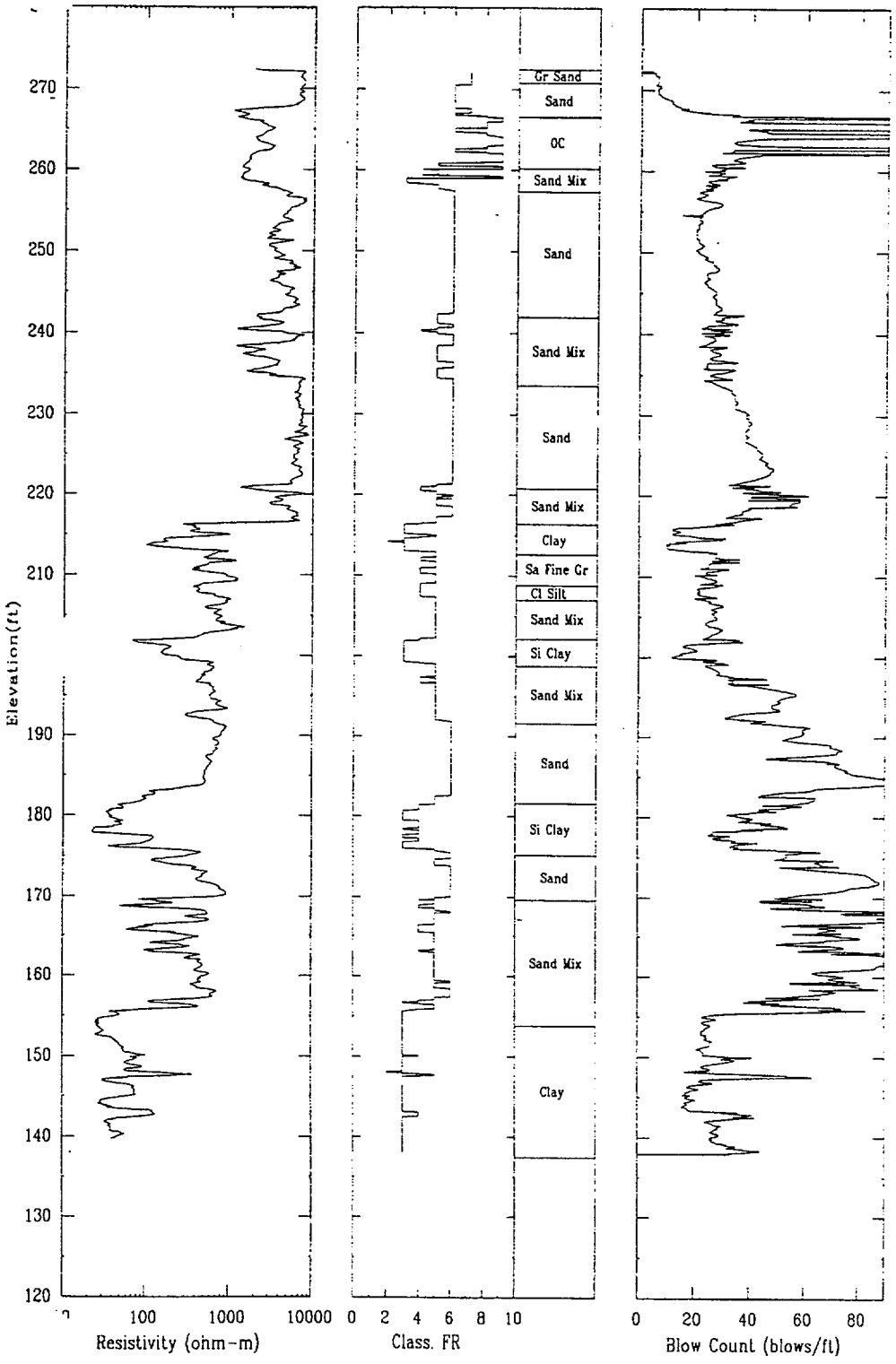

File 417u002B.ECP

DCS, MFFF Project No. 08716

CPT-05S APPLIED RESEARCH ASSOCIATES, INC. 06/08/00

North 80499.7 East 55478.5 Elevation 264.5

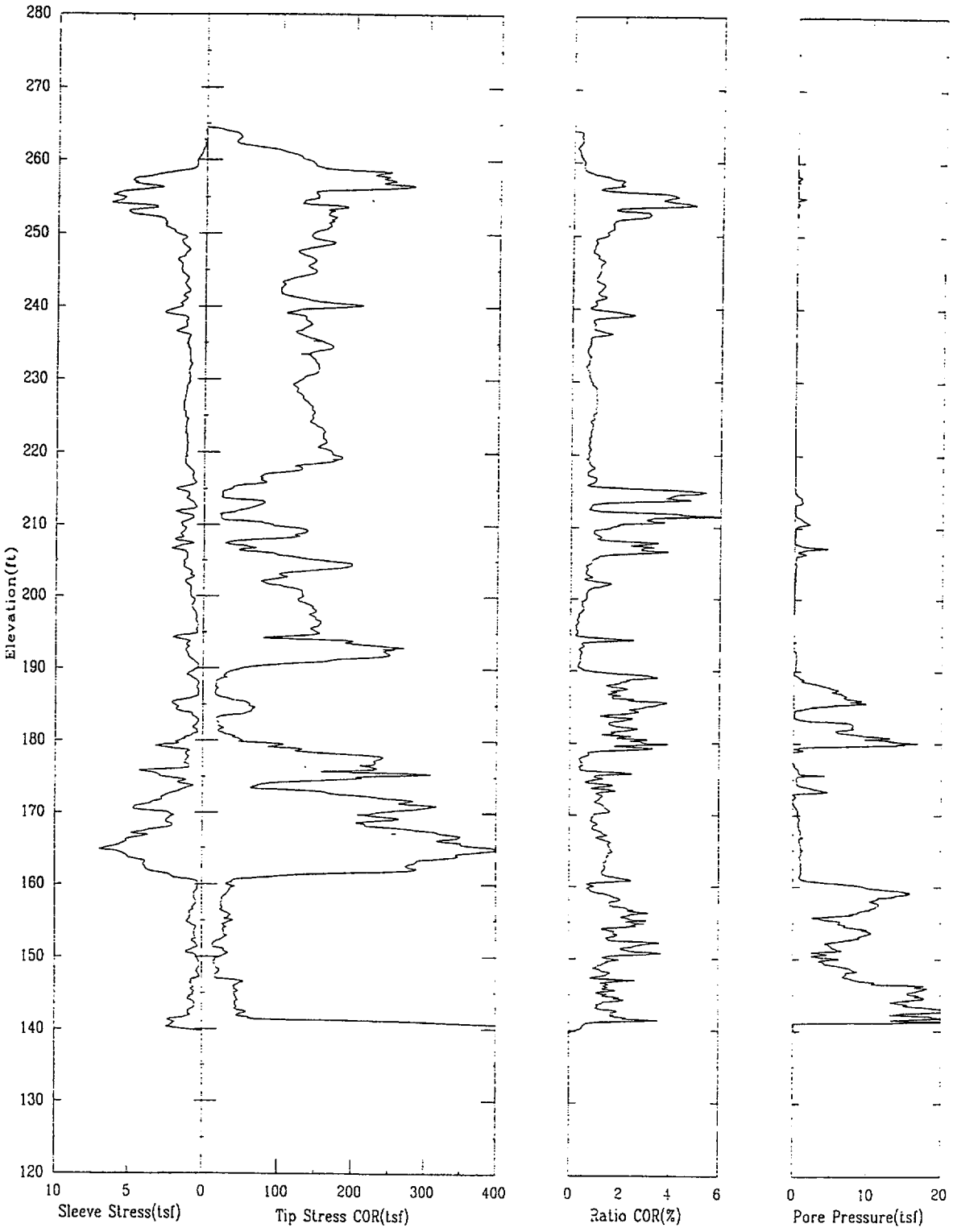

File 408u004.ECP

DCS, MFFF Project No. 08716

CPT-05S APPLIED RESEARCH ASSOCIATES, INC. 06/08/00

North 80499.7 East 55478.5 Elevation 264.5

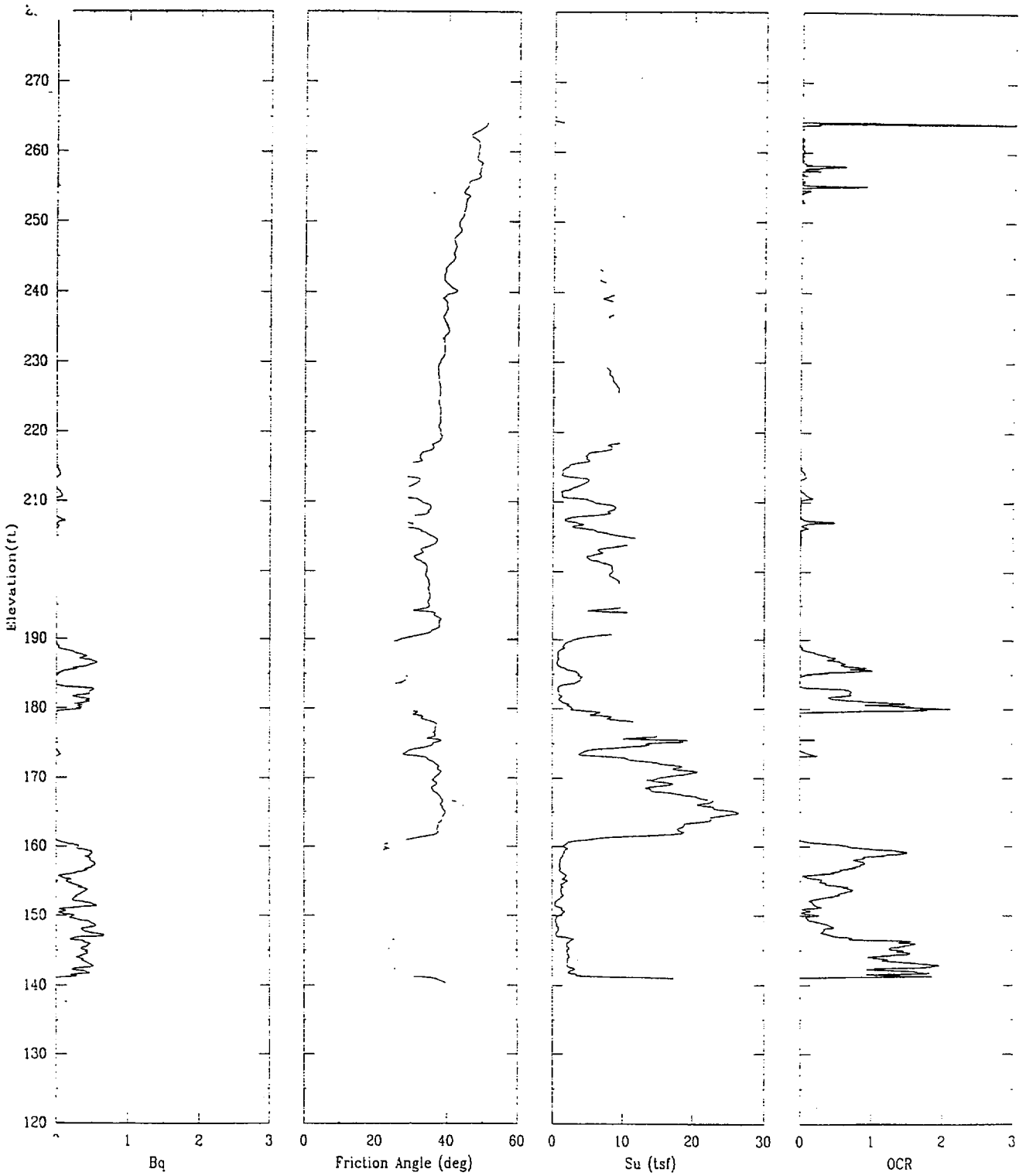

File 408u004.ECP

CPT-05S APPLIED RESEARCH ASSOCIATES, INC. 06/08/00

North 80499.7 East 55478.5 Elevation 264.5

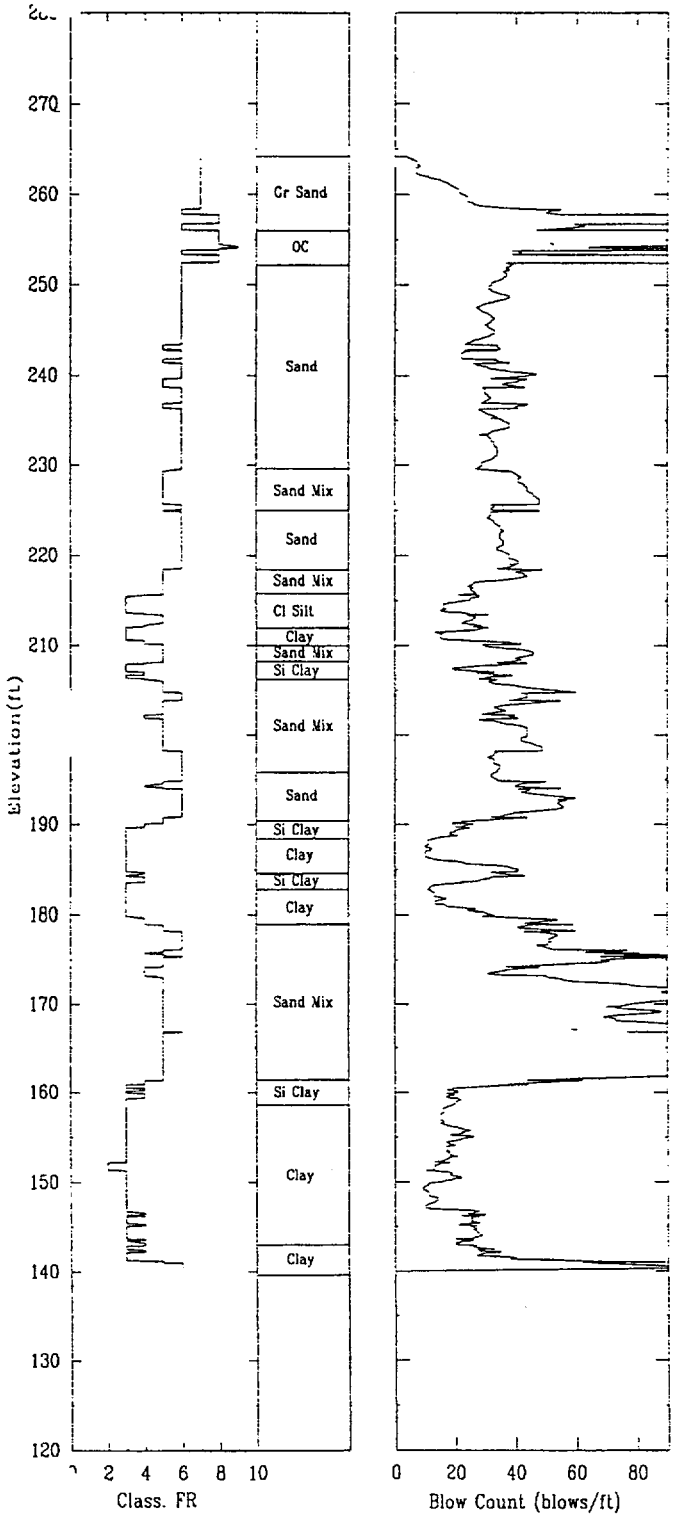

File 408u004.ECP

DCS, MFFF Project No. 08716

CPT-06R APPLIED RESEARCH ASSOCIATES, INC. 06/15/00

North 80470.7 East 55633.2 Elevation 256.9

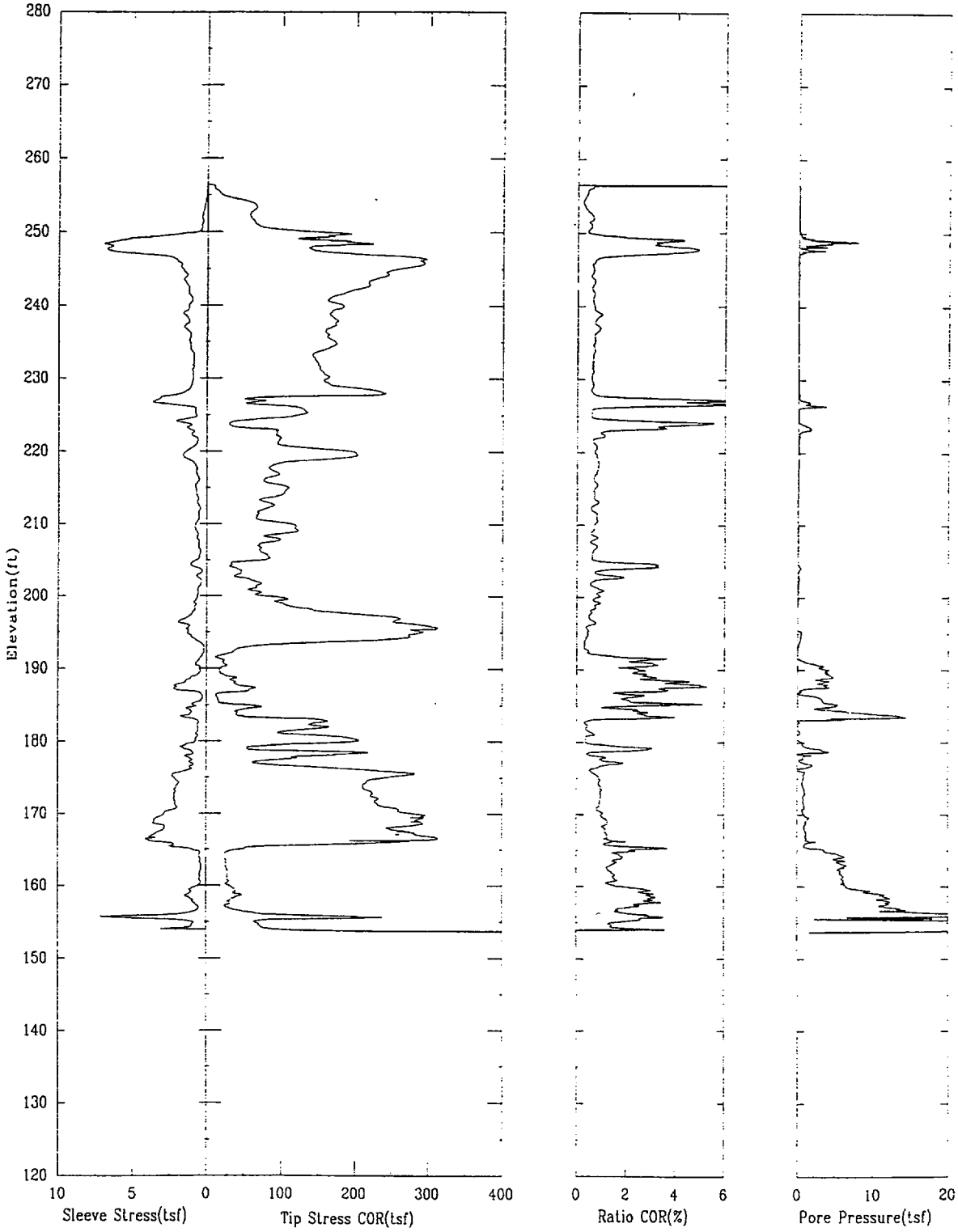

File 415u002.ECP

CPT-06R APPLIED RESEARCH ASSOCIATES, INC. 06/15/00

North 80470.7 East 55633.2 Elevation 256.9

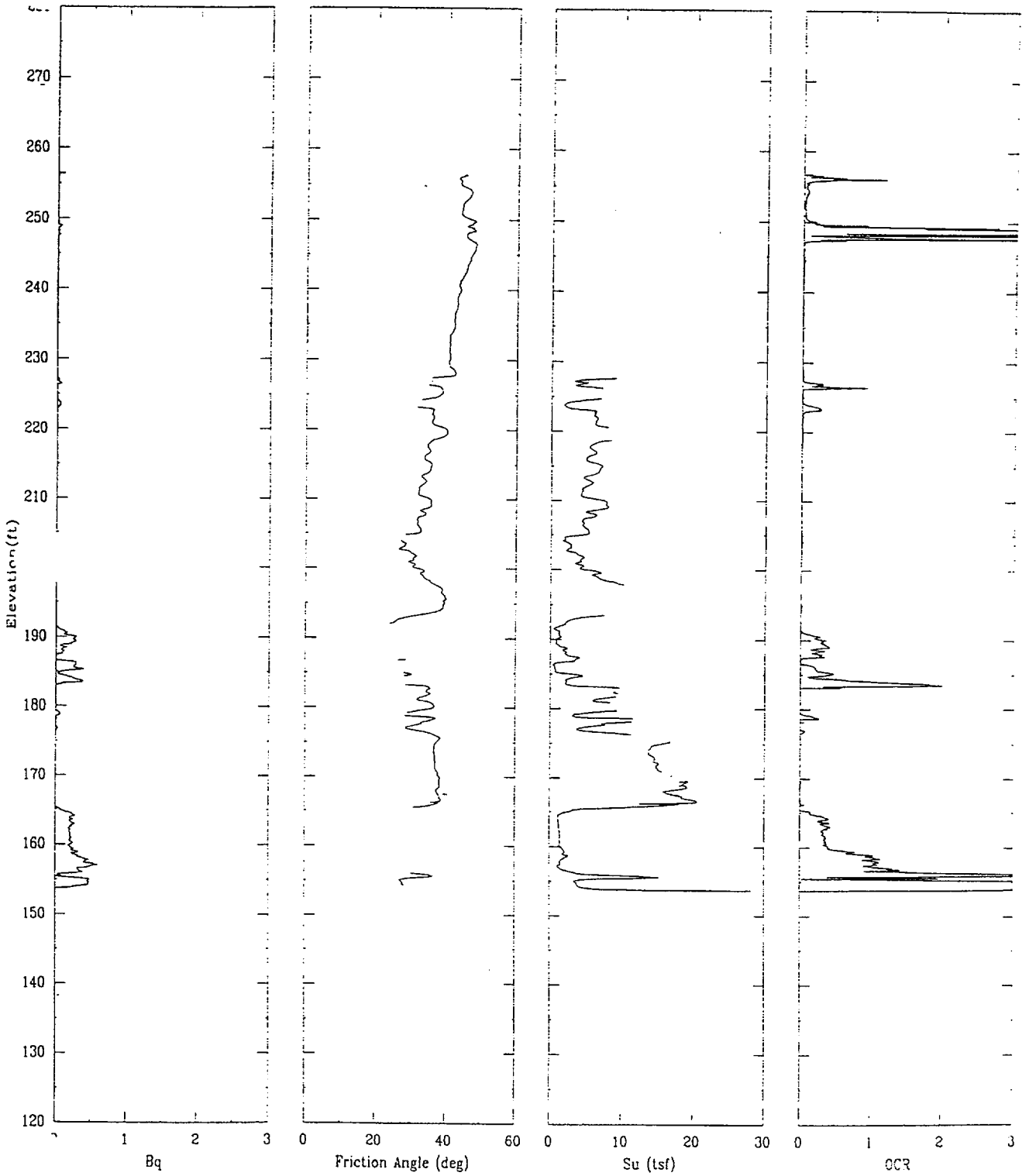

File 415u002.ECP

CPT-06R APPLIED RESEARCH ASSOCIATES, INC. 06/15/00

North 80470.7 East 55633.2 Elevation 256.9

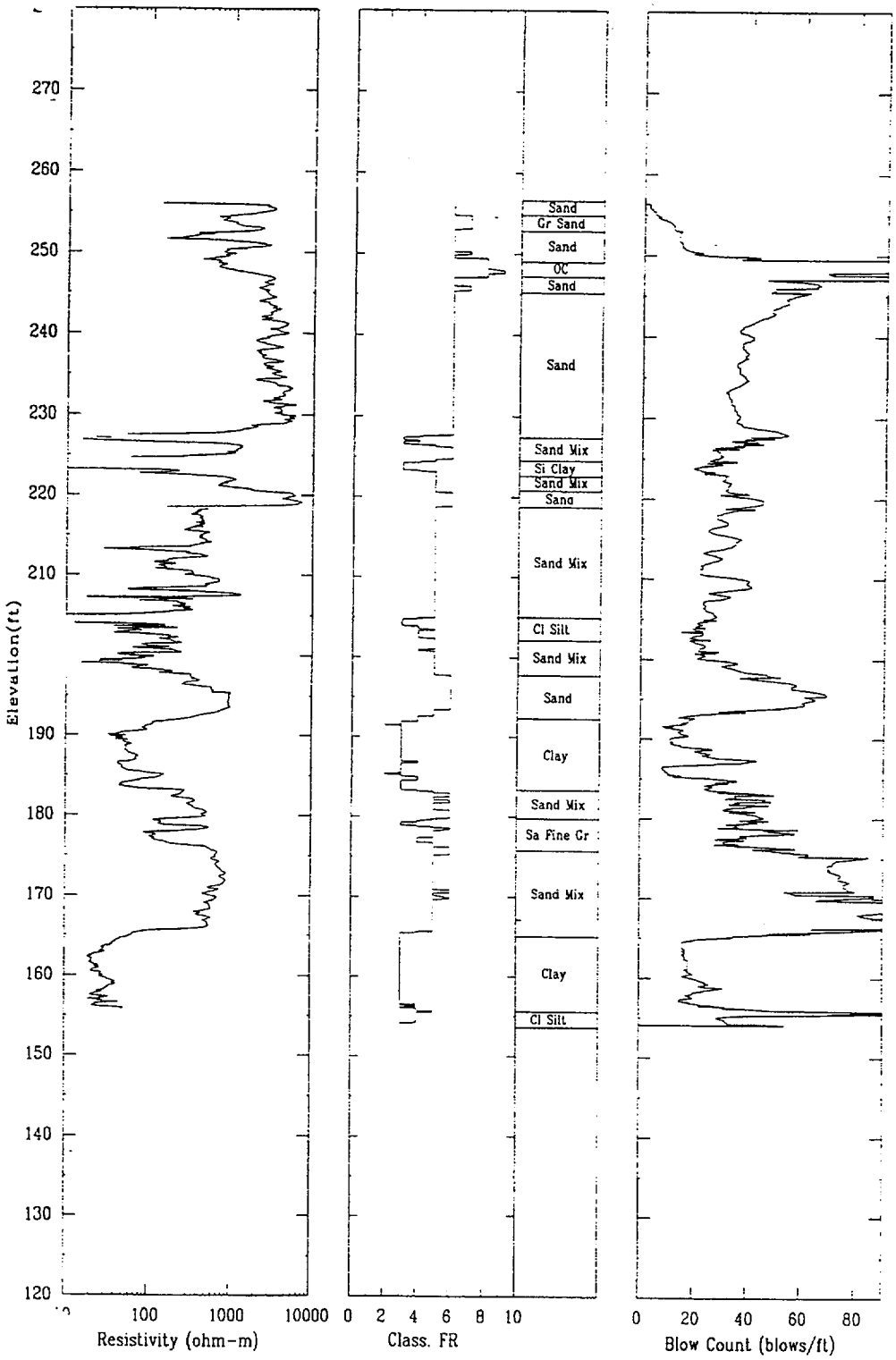

File 415u002.ECP

DCS, MFFF Project No. 08716

CPT-07R APPLIED RESEARCH ASSOCIATES, INC. 06/19/00

North 80438.0 East 55228.2 Elevation 280.2

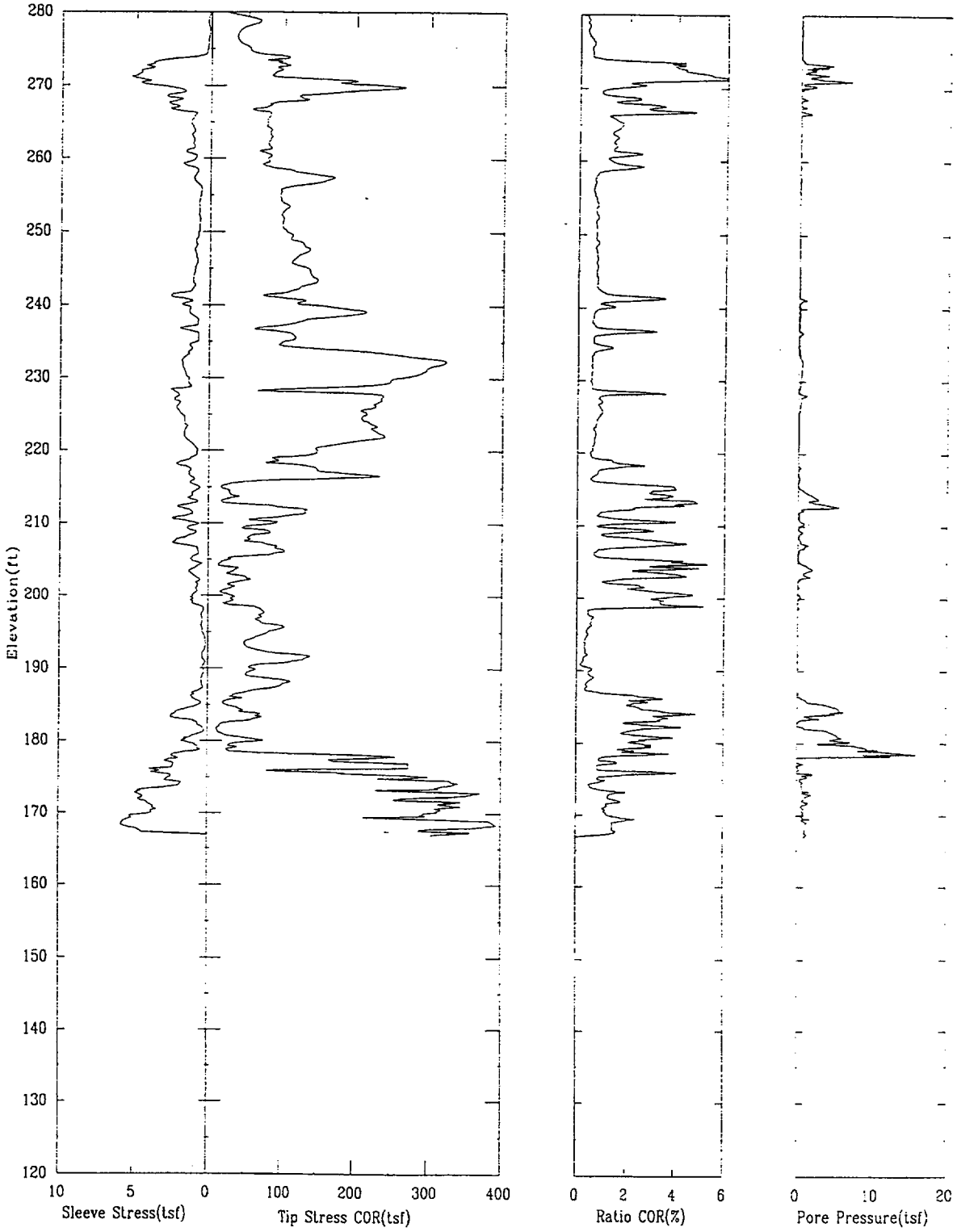

File 419u001.ECP

DCS, MFFF Project No. 08716

CPT-07R APPLIED RESEARCH ASSOCIATES, INC. 06/19/00

North 80438.0 East 55228.2 Elevation 280.2

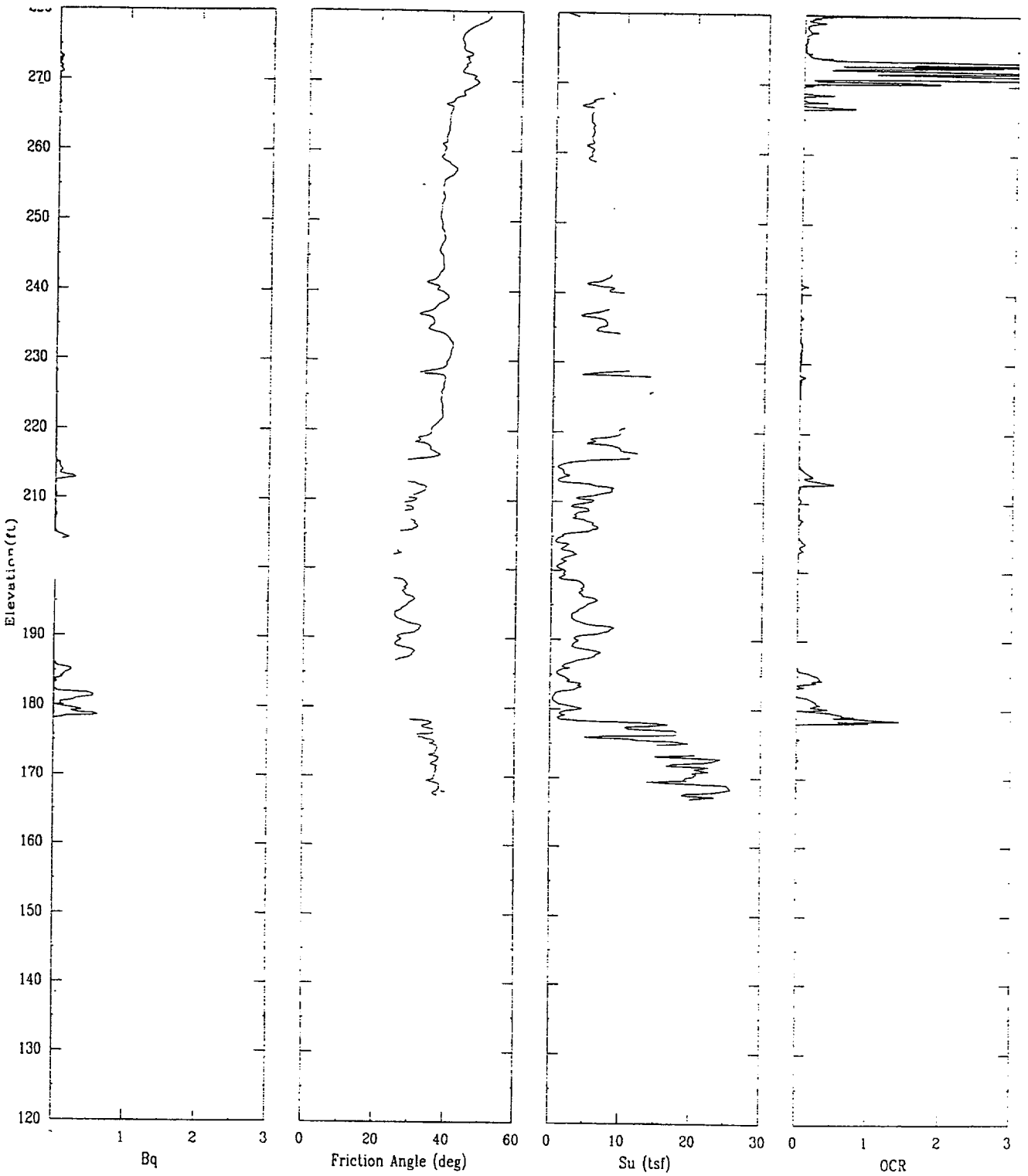

File 419u001.ECP

CPT-07R APPLIED RESEARCH ASSOCIATES, INC. 06/19/00

North 80438.0 East 55228.2 Elevation 280.2

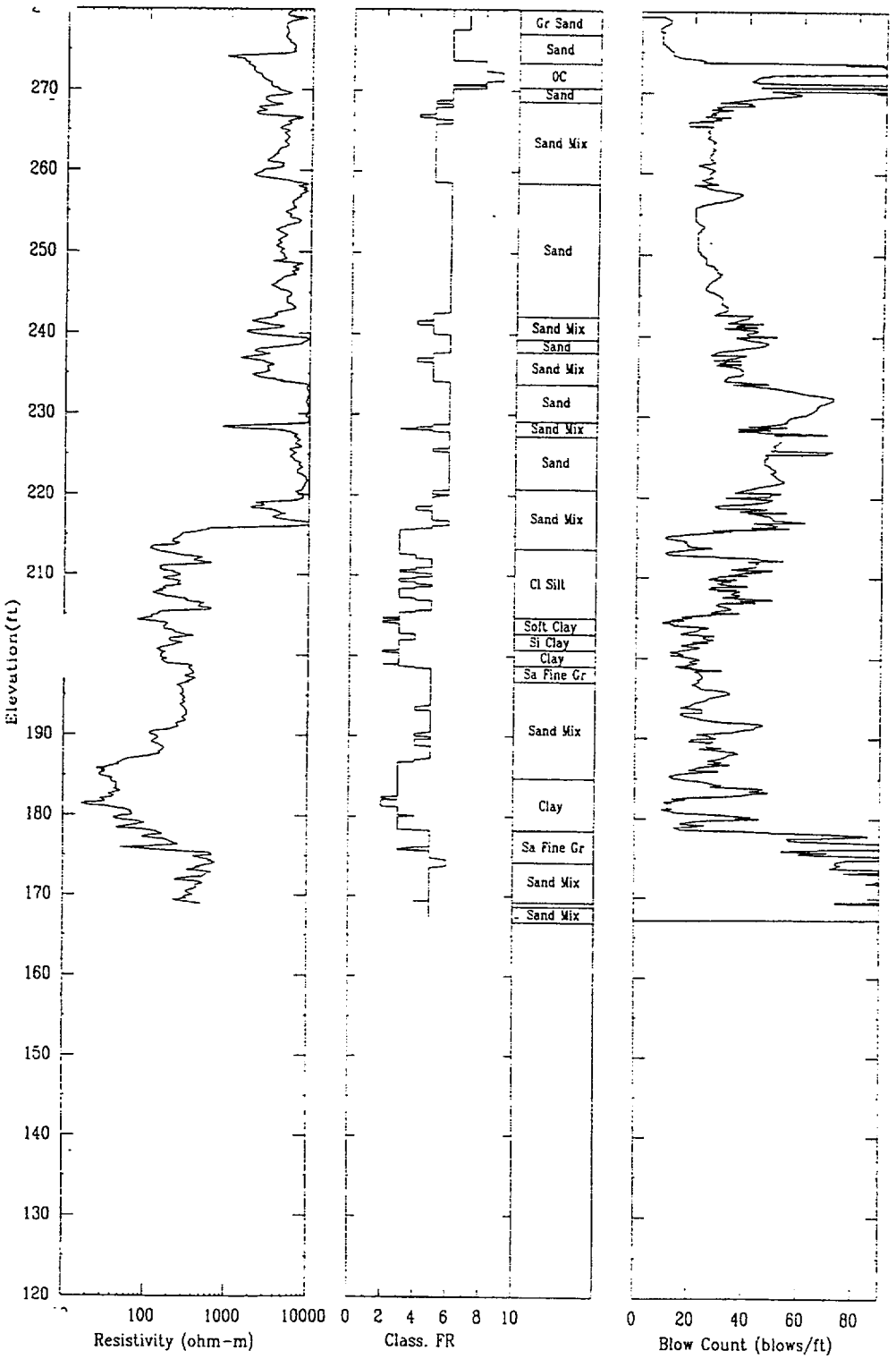

File 419u001.ECP

DCS, MFFF Project No. 08716

CPT-08S APPLIED RESEARCH ASSOCIATES, INC. 06/02/00

North 80393.7 East 55329.1 Elevation 273.0

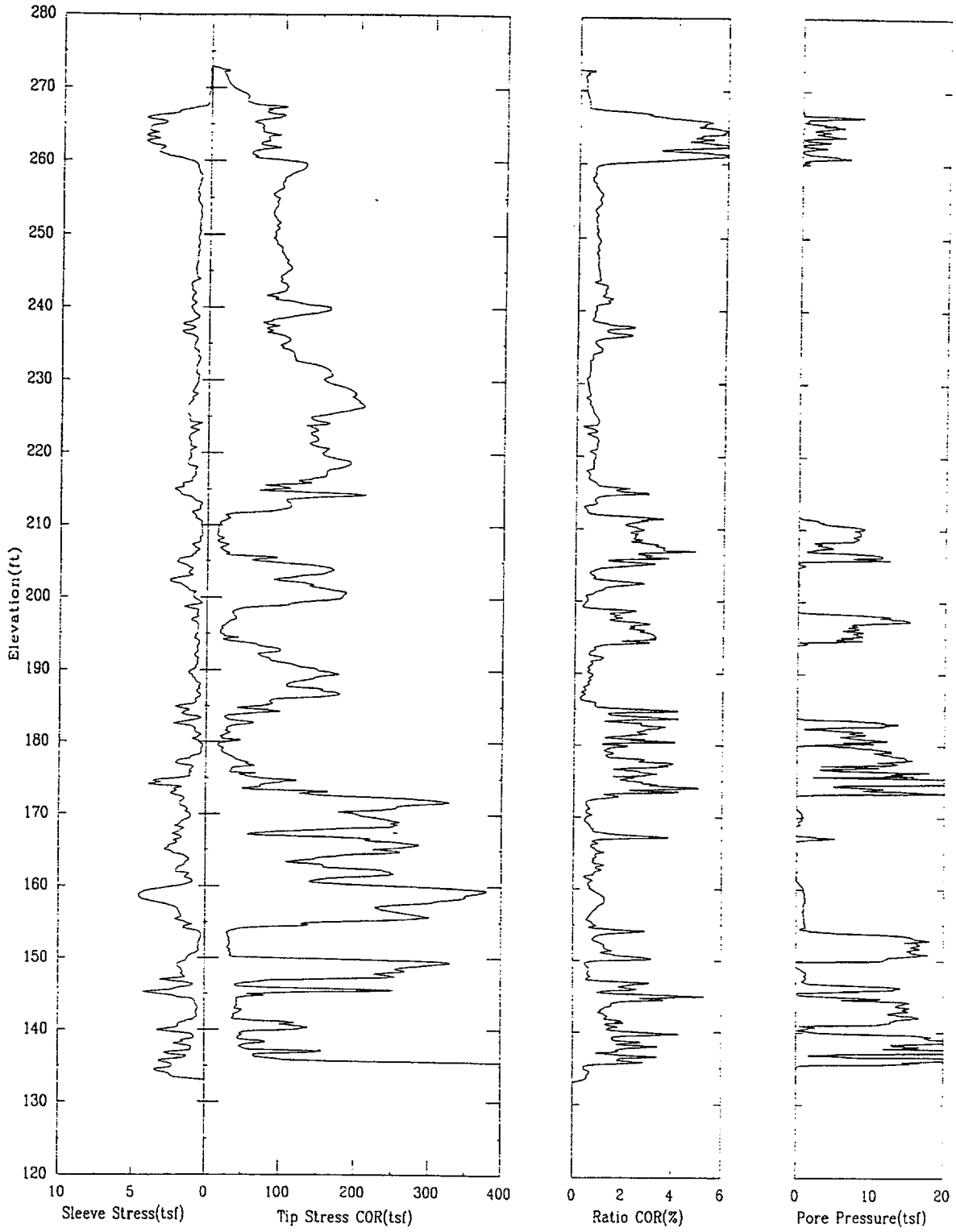

File 402u004.ECP

DCS, MFFF Project No. 08716

CPT-08S APPLIED RESEARCH ASSOCIATES, INC. 06/02/00

North 80393.7 East 55329.1 Elevation 273.0

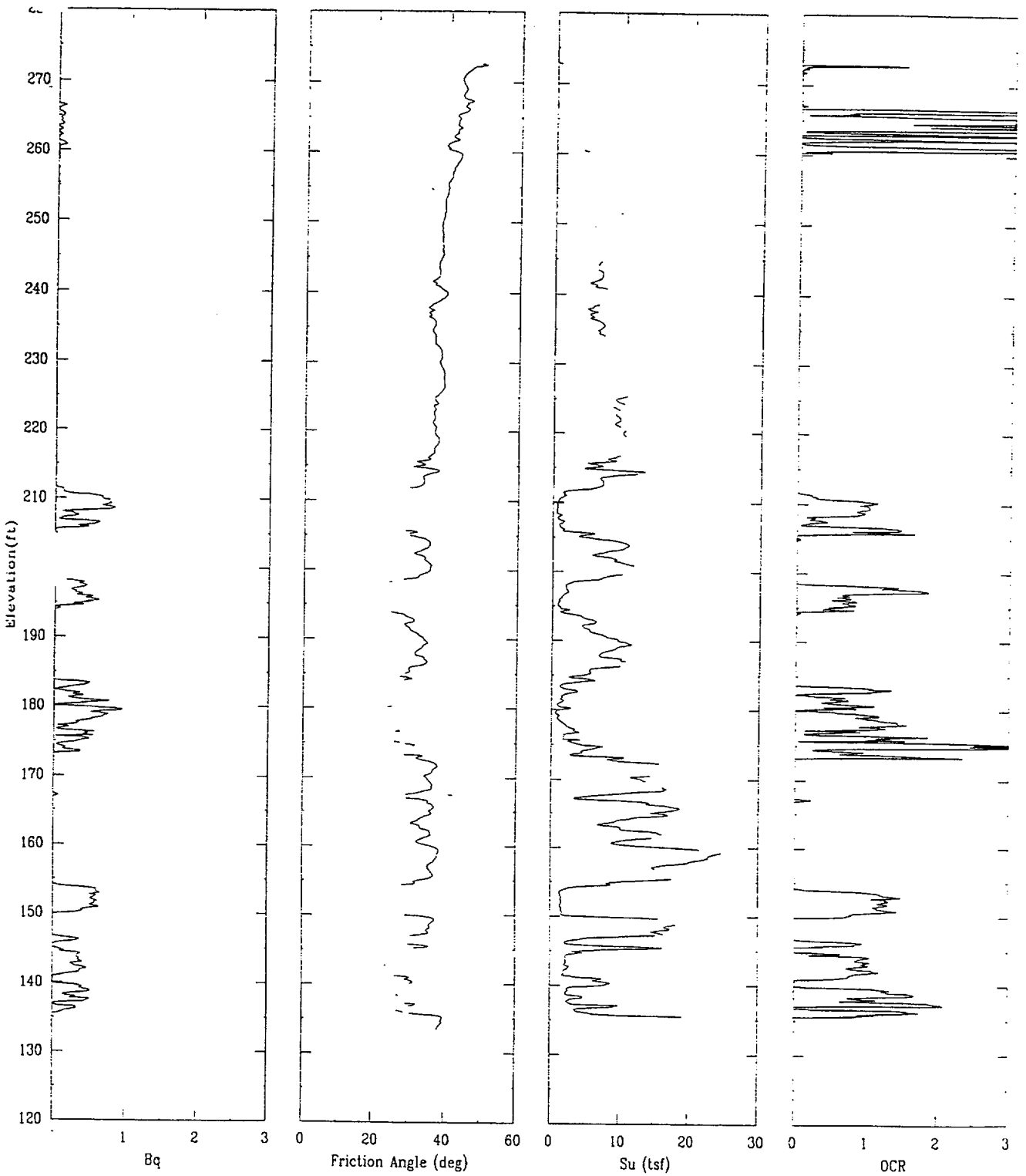

File 402u004.ECP

CPT-08S APPLIED RESEARCH ASSOCIATES, INC. 06/02/00

North 80393.7 East 55329.1 Elevation 273.0

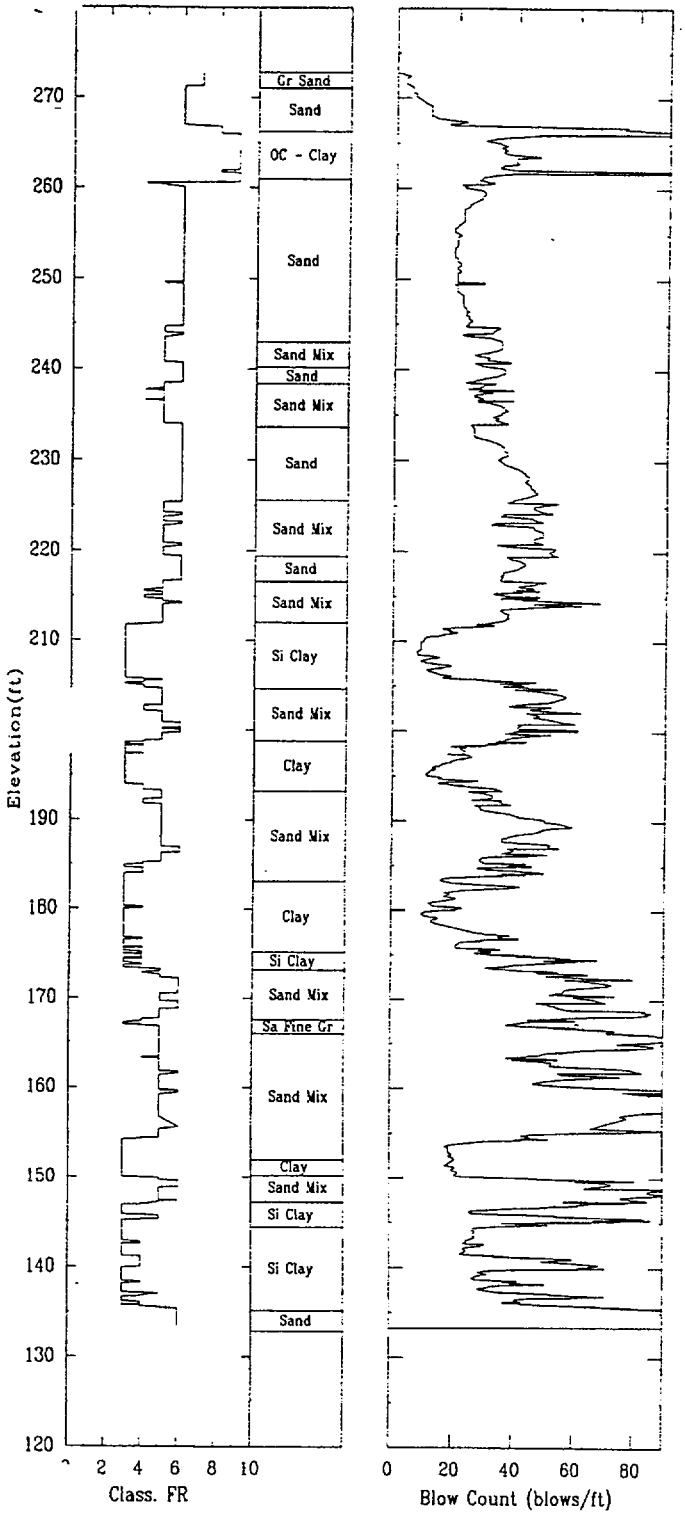

File 402u004.ECP

CPT-09R APPLIED RESEARCH ASSOCIATES, INC. 06/20/00

North 80394.0 East 55445.7 Elevation 266.2

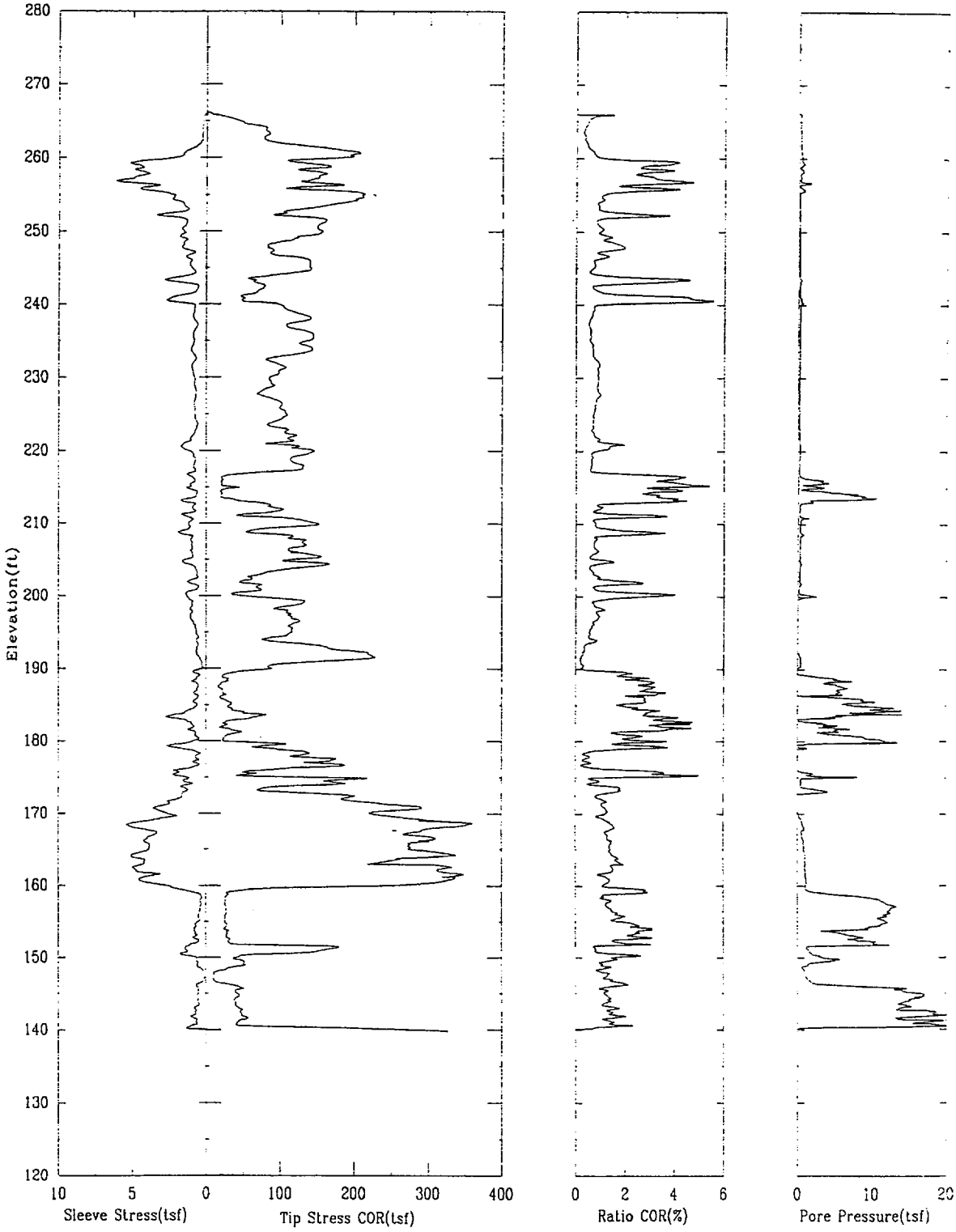

File 420u005.ECP

CPT-09R APPLIED RESEARCH ASSOCIATES, INC. 06/20/00

North 80394.0 East 55445.7 Elevation 266.2

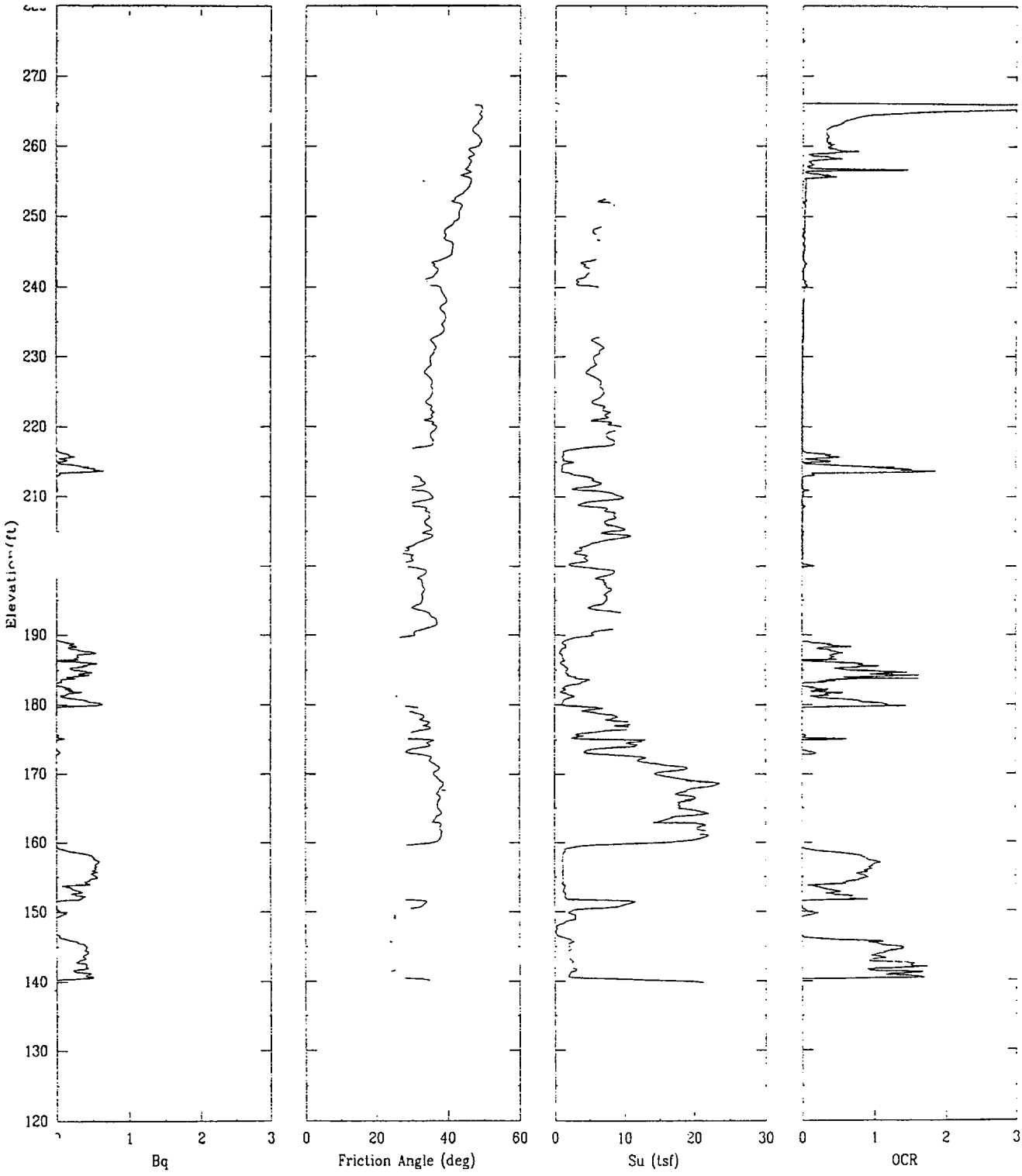

File 420u005.ECP

CPT-09R APPLIED RESEARCH ASSOCIATES, INC. 06/20/00

North 80394.0 East 55445.7 Elevation 266.2

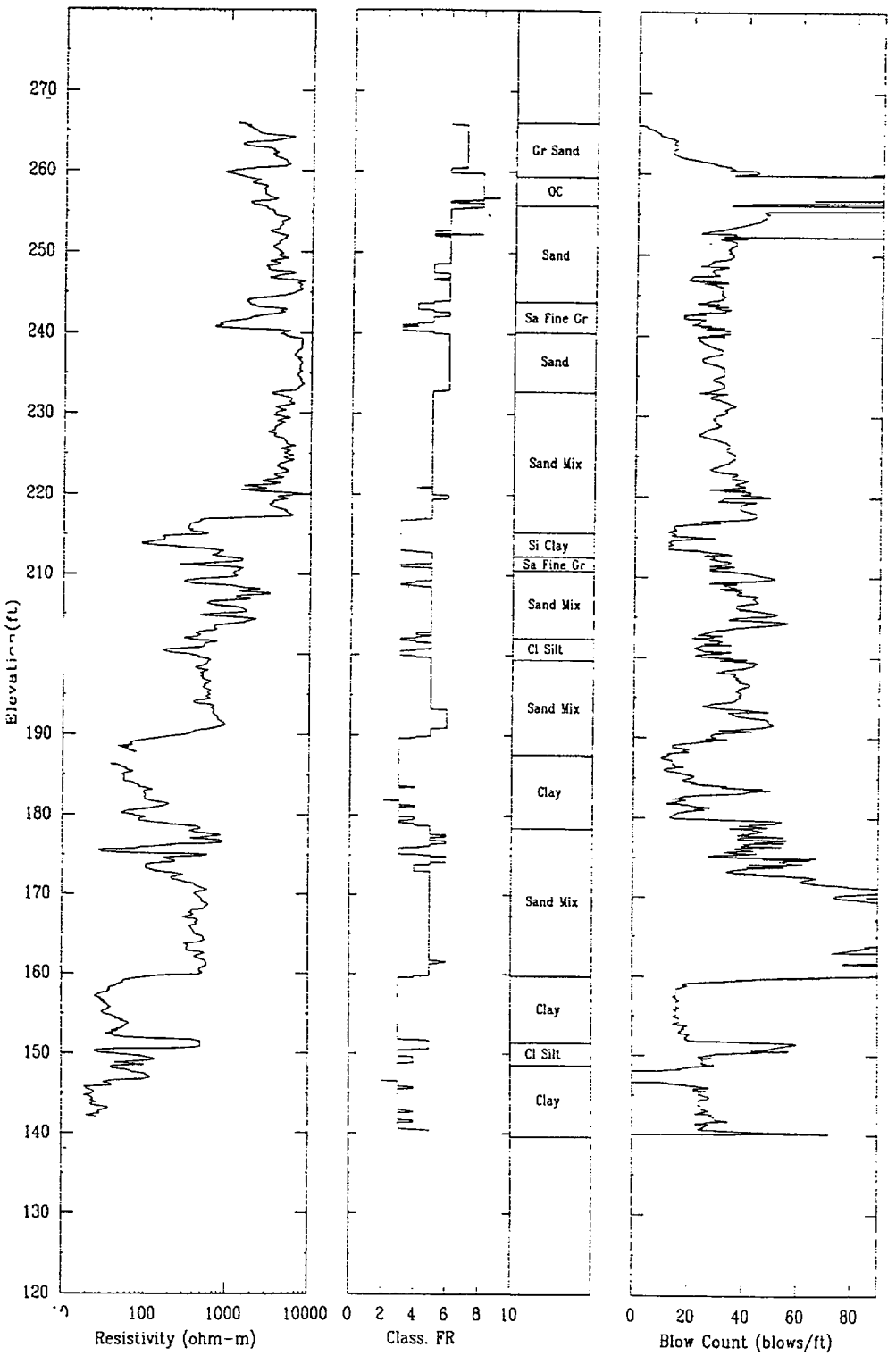

File 420u005.ECP

DCS, MFFF Project No. 08716

CPT-10R APPLIED RESEARCH ASSOCIATES, INC. 06/20/00

North 80406.7 East 55527.1 Elevation 261.9

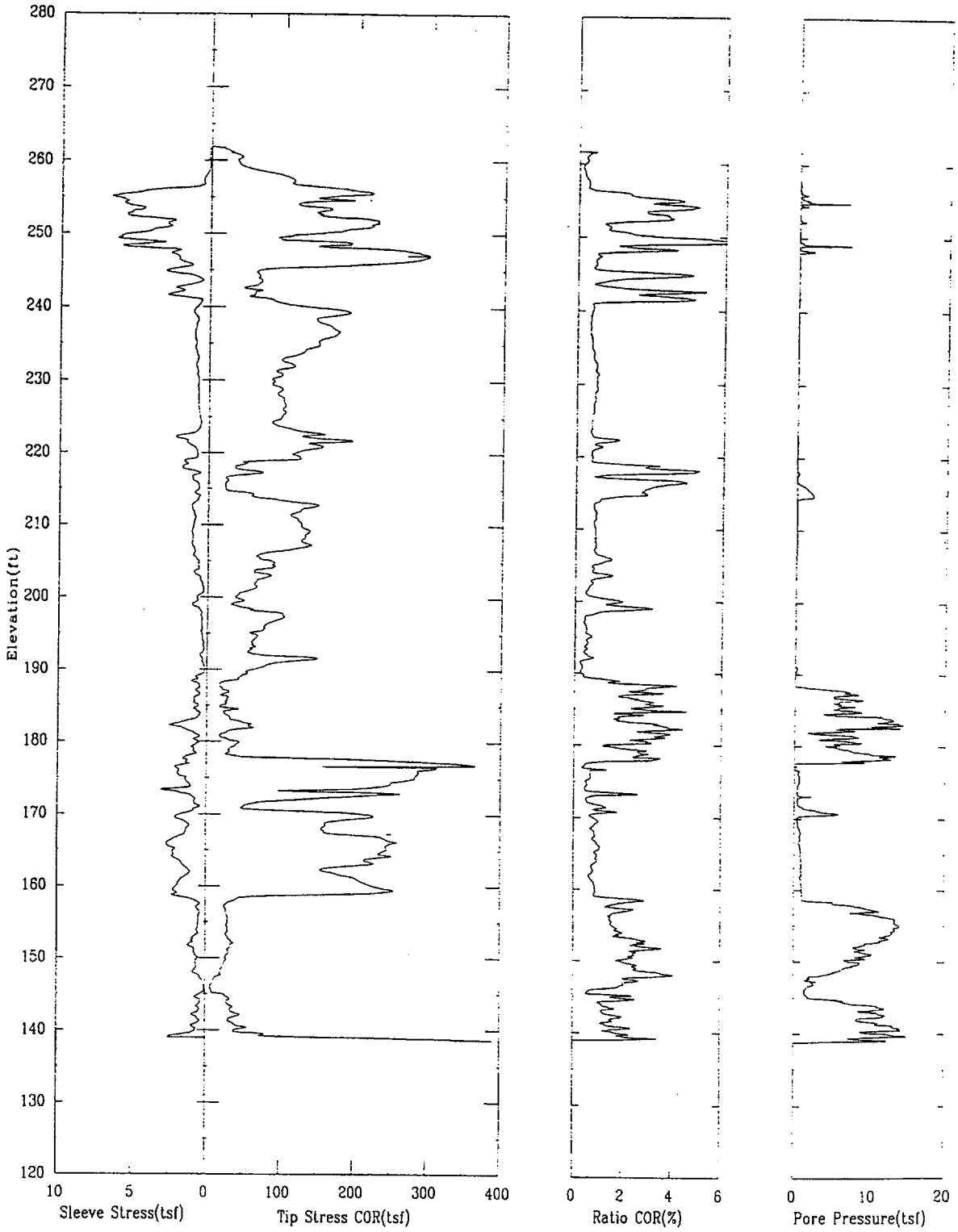

File 420u001.ECP

CPT-10R APPLIED RESEARCH ASSOCIATES, INC. 06/20/00

North 80406.7 East 55527.1 Elevation 261.9

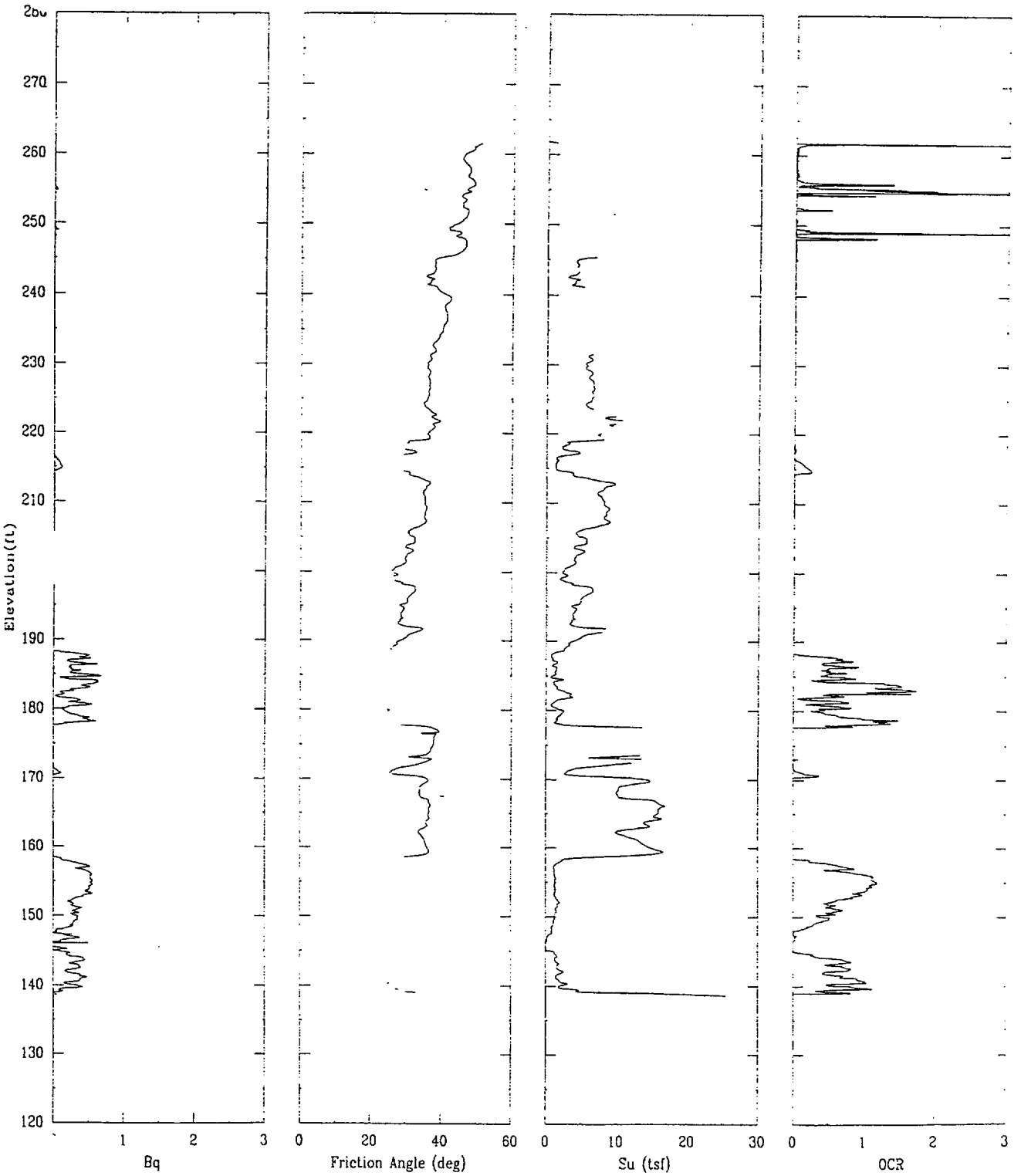

File 420u001.ECP

DCS, MFFF Project No. 08716

CPT-10R APPLIED RESEARCH ASSOCIATES, INC. 06/20/00

North 80406.7 East 55527.1 Elevation 261.9

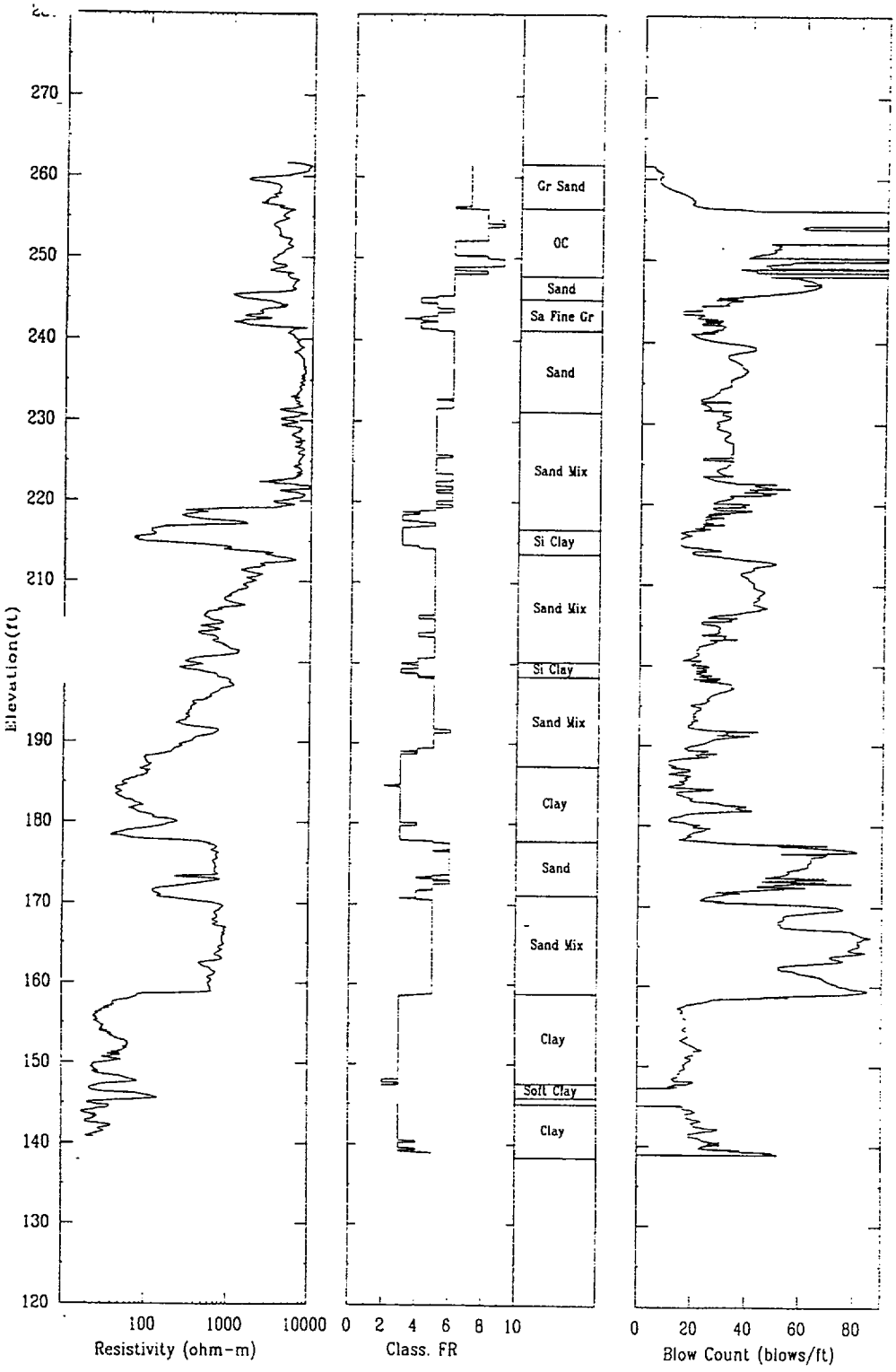

File 420u001.ECP

DCS, MFFF Project No. 08716

CPT-11S APPLIED RESEARCH ASSOCIATES, INC. 06/02/00

North 80394.0 East 55624.1 Elevation 258.5

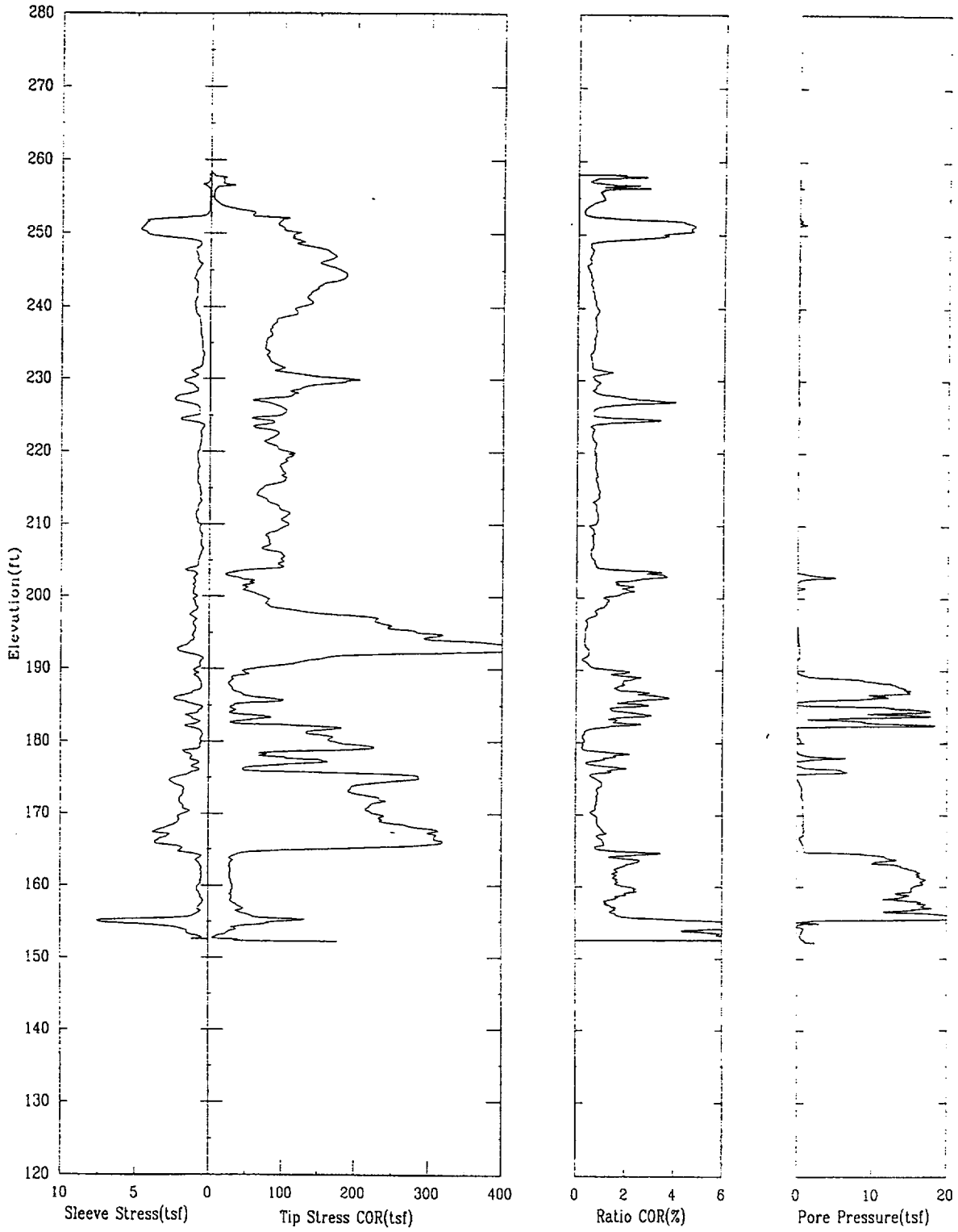

File 402u001.ECP

CPT-11S APPLIED RESEARCH ASSOCIATES, INC. 06/02/00

North 80394.0 East 55624.1 Elevation 258.5

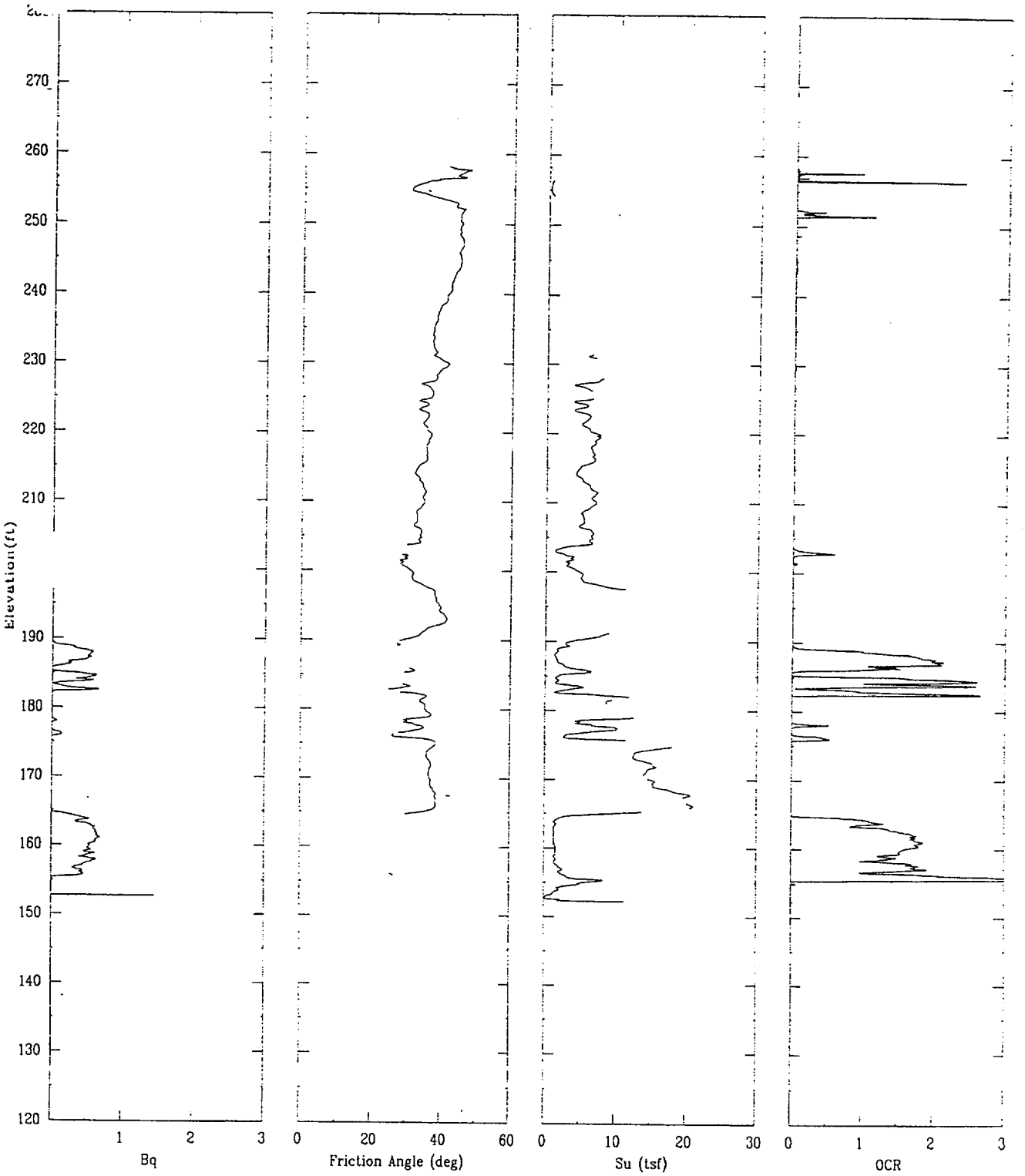

File 402u001.ECP

CPT-11S APPLIED RESEARCH ASSOCIATES, INC. 06/02/00

North 80394.0 East 55624.1 Elevation 258.5

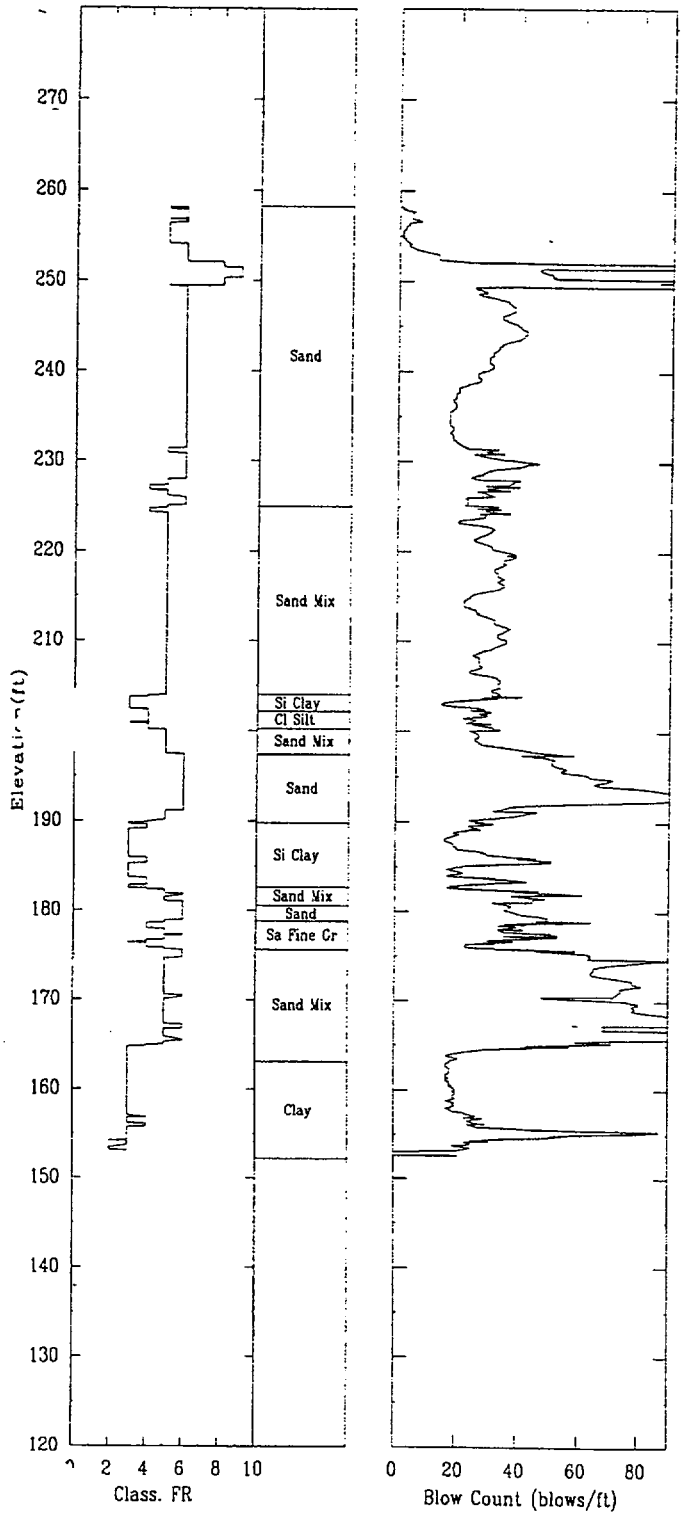

File 402u001.ECP

CPT-12R APPLIED RESEARCH ASSOCIATES, INC. 06/23/00

North 80373.1 East 55747.5 Elevation 254.5

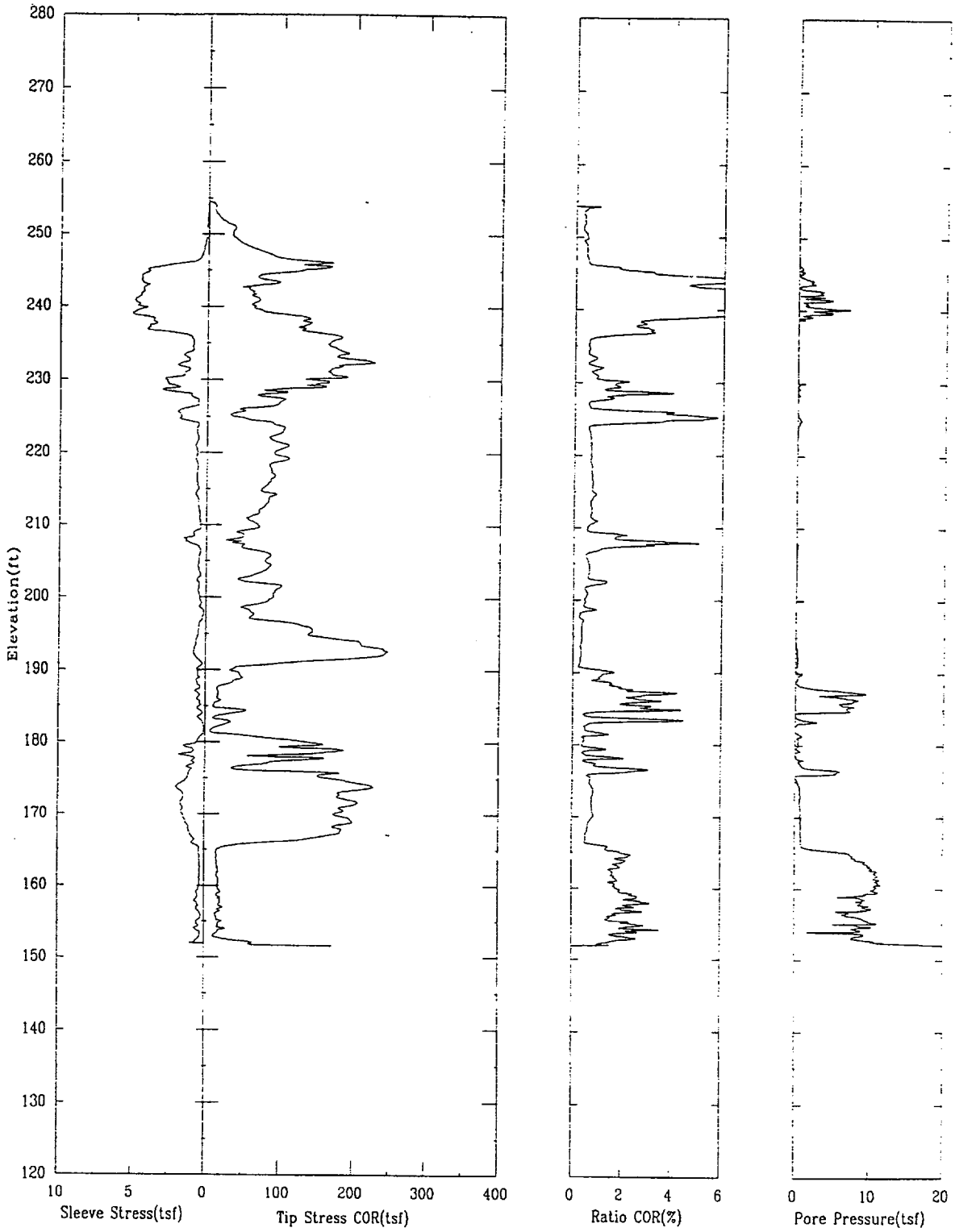

File 323u003.ECP

CPT-12R APPLIED RESEARCH ASSOCIATES, INC. 06/23/00

North 80373.1 East 55747.5 Elevation 254.5

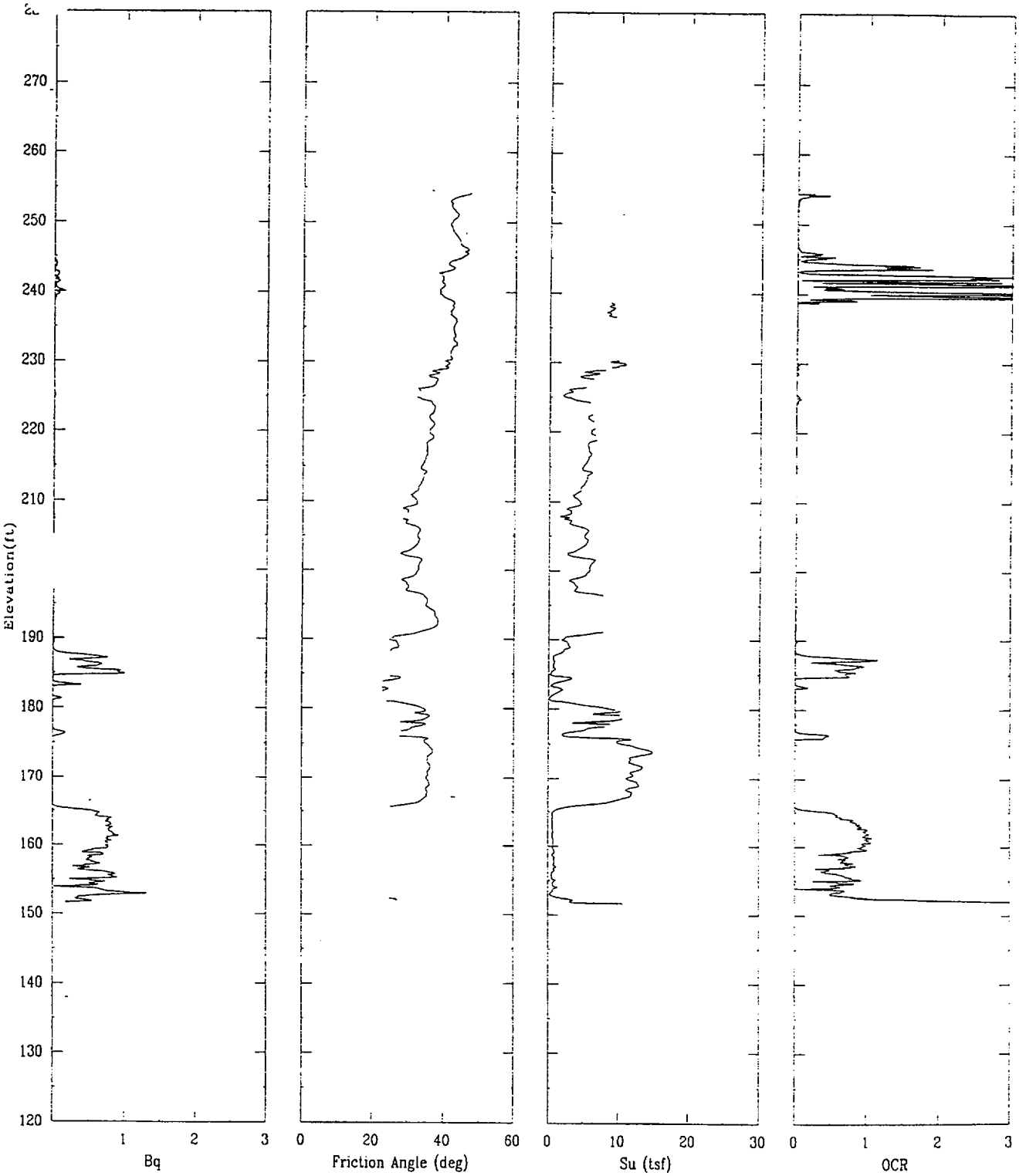

File 323u003.ECP

CPT-12R APPLIED RESEARCH ASSOCIATES, INC. 06/23/00

North 80373.1 East 55747.5 Elevation 254.5

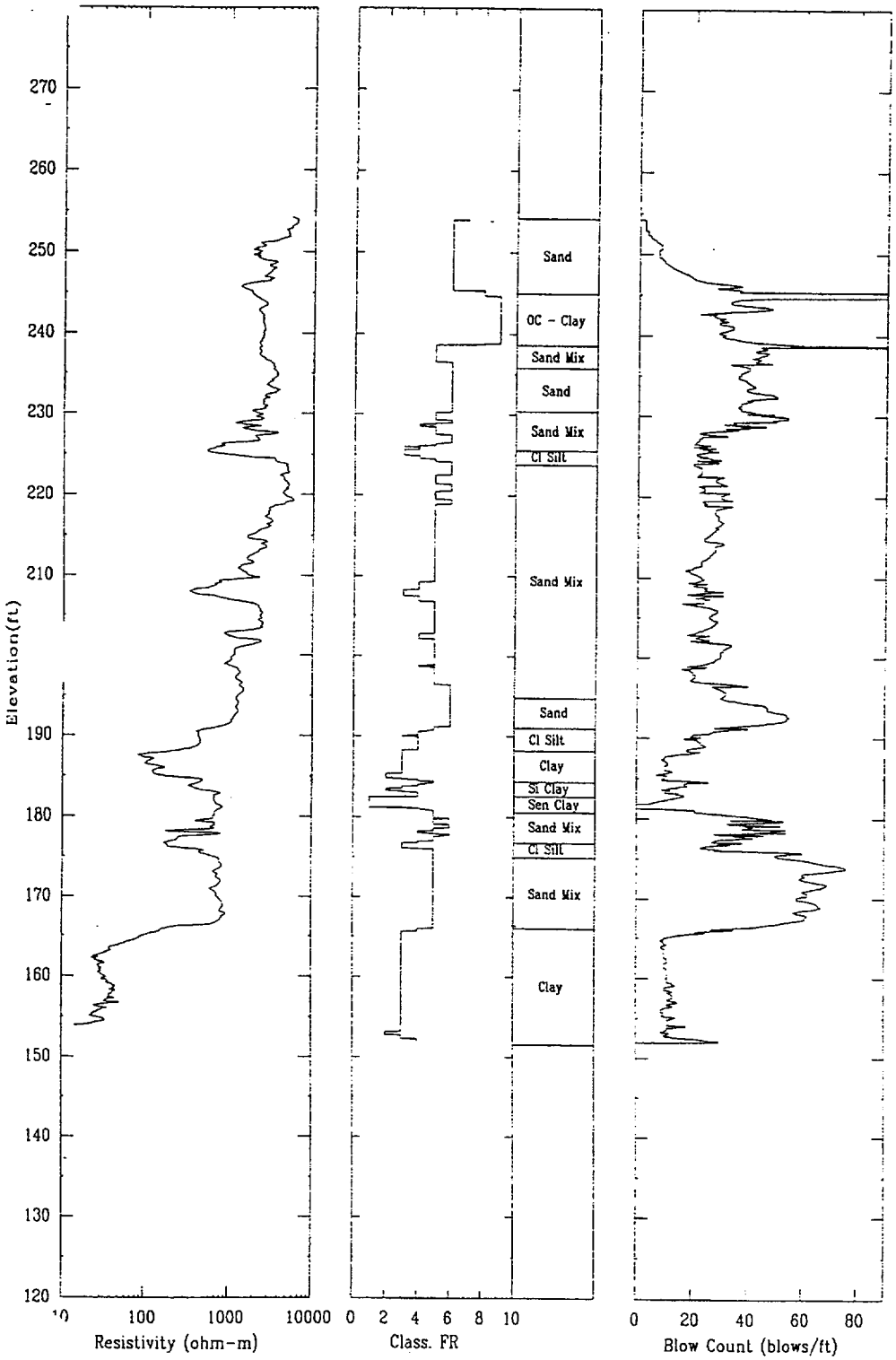

File 323u003.ECP

DCS, MFFF Project No. 08716

CPT-13S APPLIED RESEARCH ASSOCIATES, INC. 06/05/00

North 80262.2 East 55233.6 Elevation 296.7

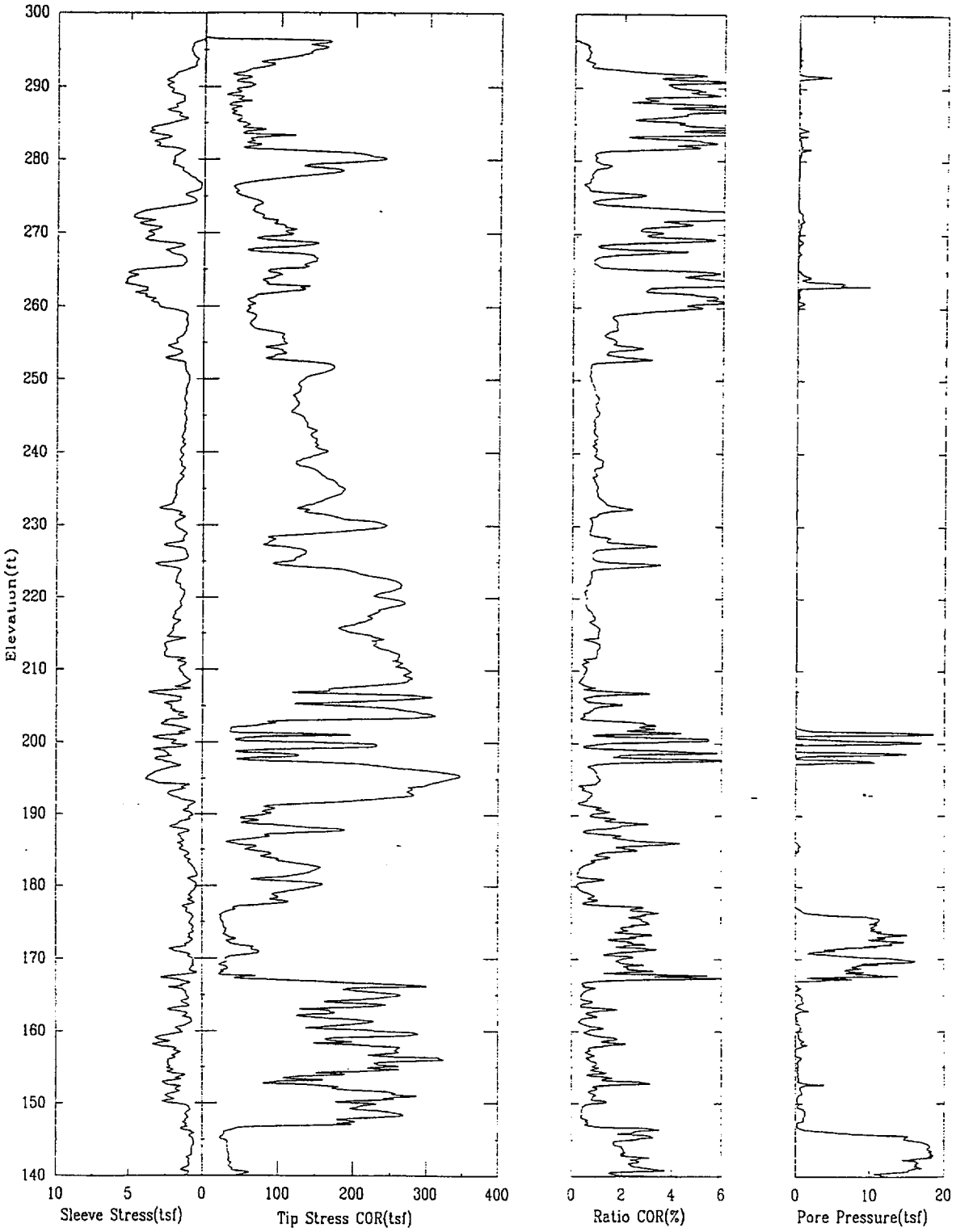

File 405u005.ECP

CPT-13S APPLIED RESEARCH ASSOCIATES, INC. 06/05/00

North 80262.2 East 55233.6 Elevation 296.7

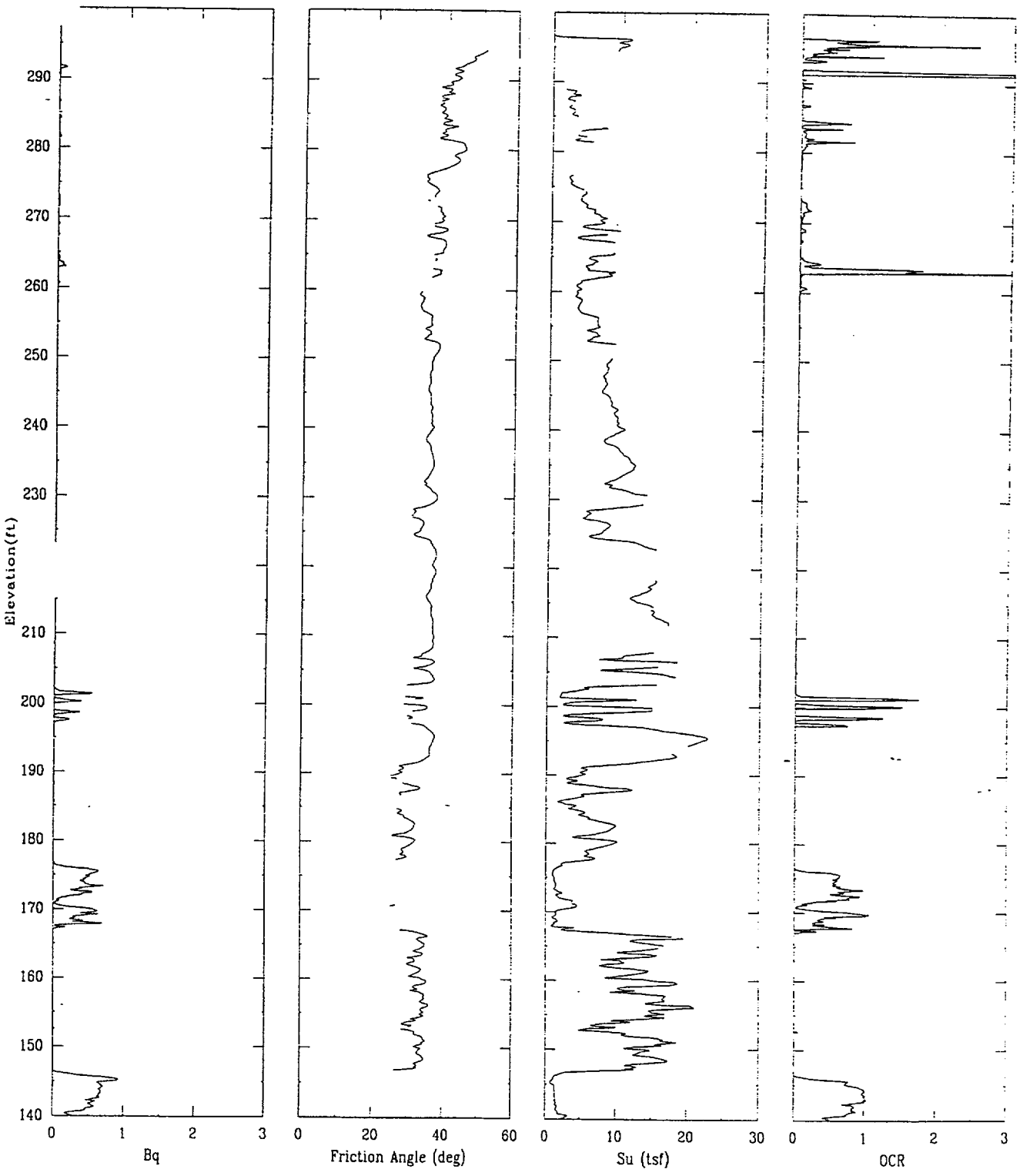

File 405u005.ECP

DCS, MFFF Project No. 08716

CPT-13S APPLIED RESEARCH ASSOCIATES, INC. 06/05/00

North 80262.2 East 55233.6 Elevation 296.7

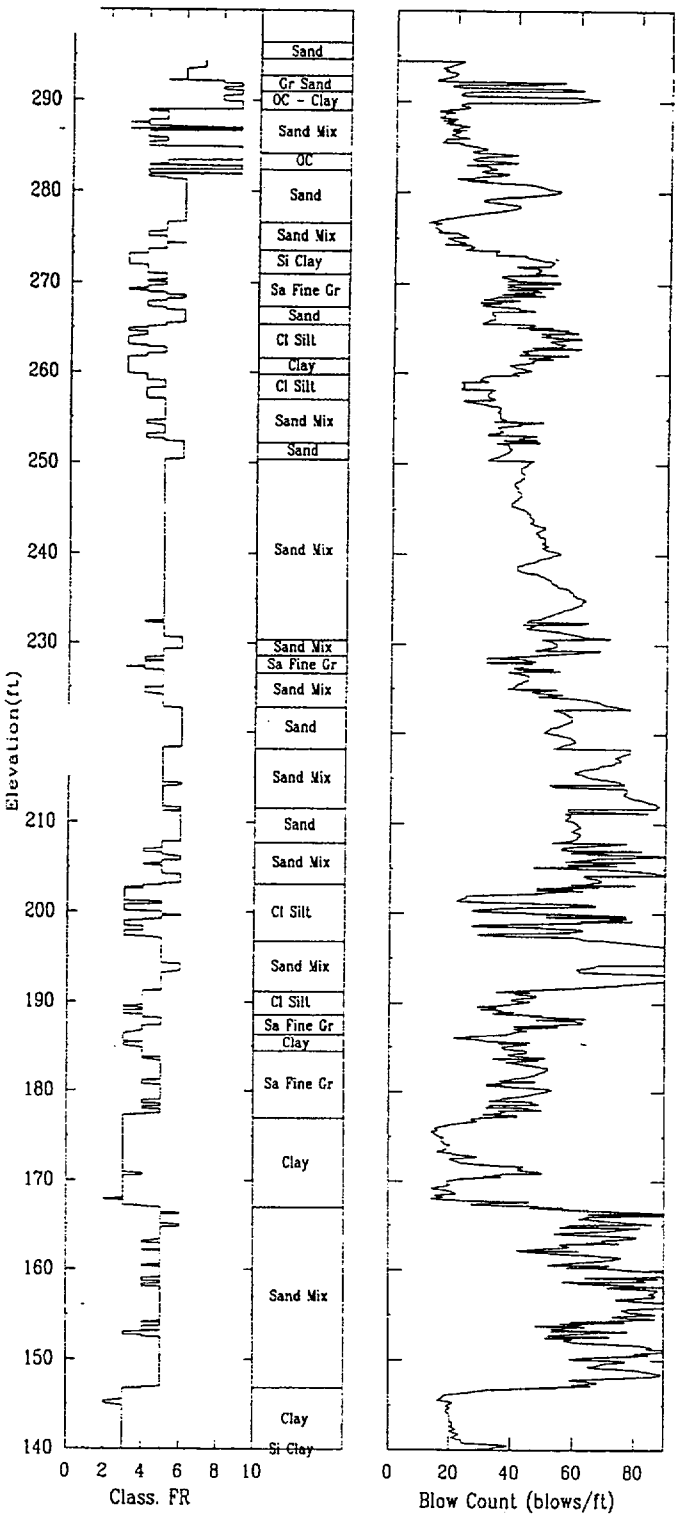

File 405u005.ECP

DCS, MFFF Project No. 08716

CPT-14R APPLIED RESEARCH ASSOCIATES, INC. 06/19/00

North 80292.7 East 55330.8 Elevation 276.0

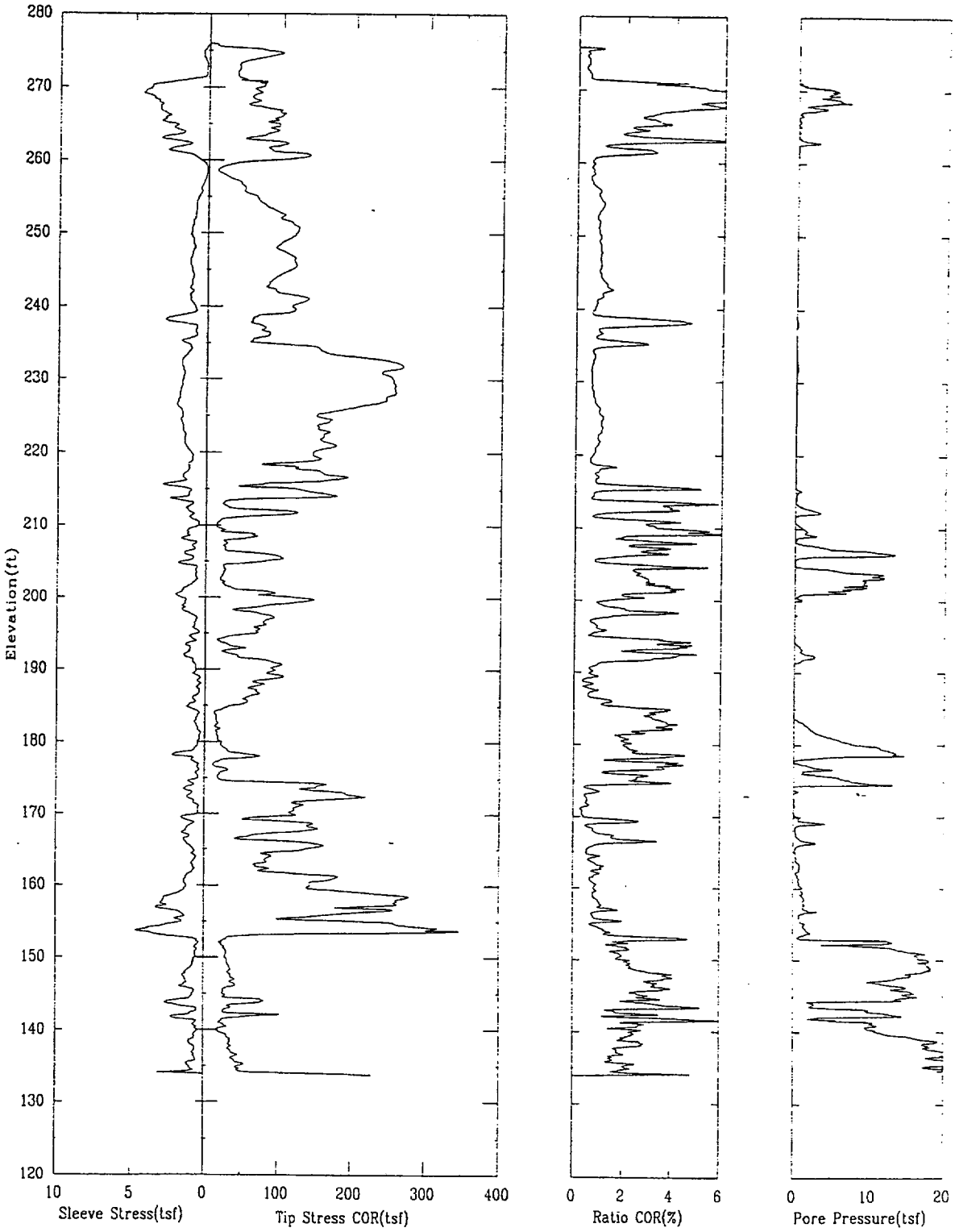

File 419u008.ECP

CPT-14R APPLIED RESEARCH ASSOCIATES, INC. 06/19/00

North 80292.7 East 55330.8 Elevation 276.0

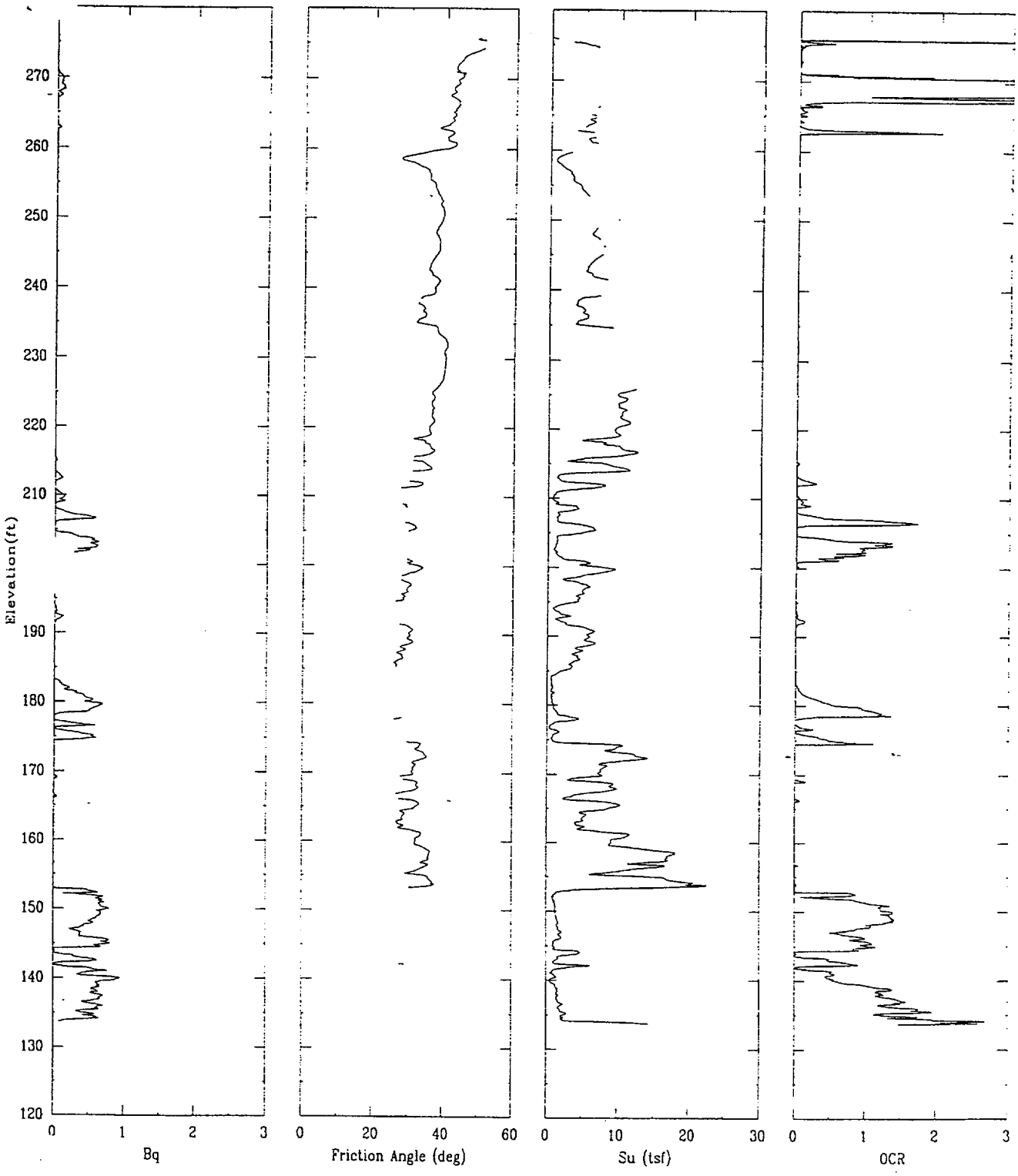

File 419u008.ECP

CPT-14R APPLIED RESEARCH ASSOCIATES, INC. 06/19/00

North 80292.7 East 55330.8 Elevation 276.0

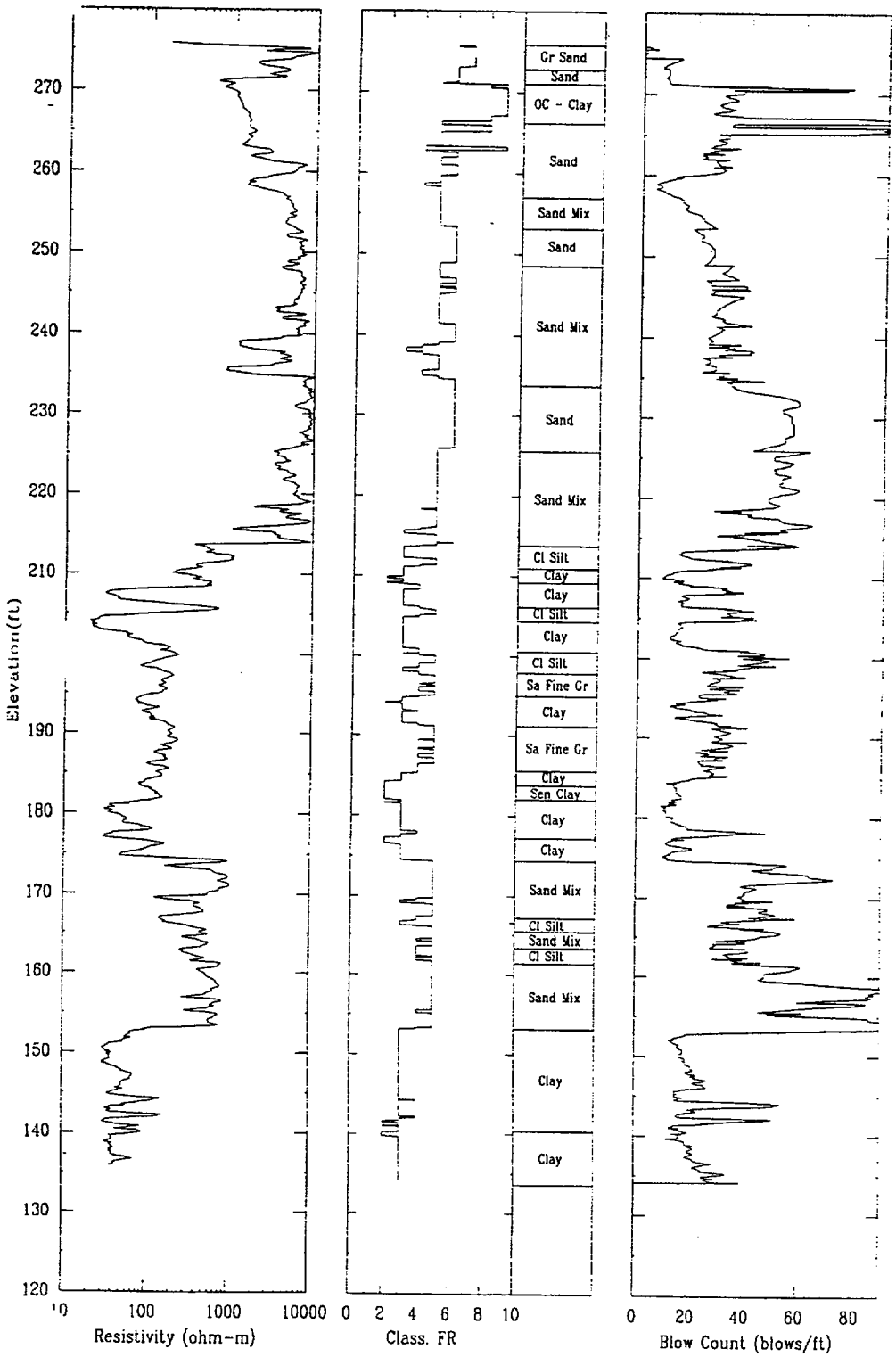

File 419u008.ECP

CPT-15R APPLIED RESEARCH ASSOCIATES, INC. 06/22/00

North 80295.0 East 55462.7 Elevation 269.1

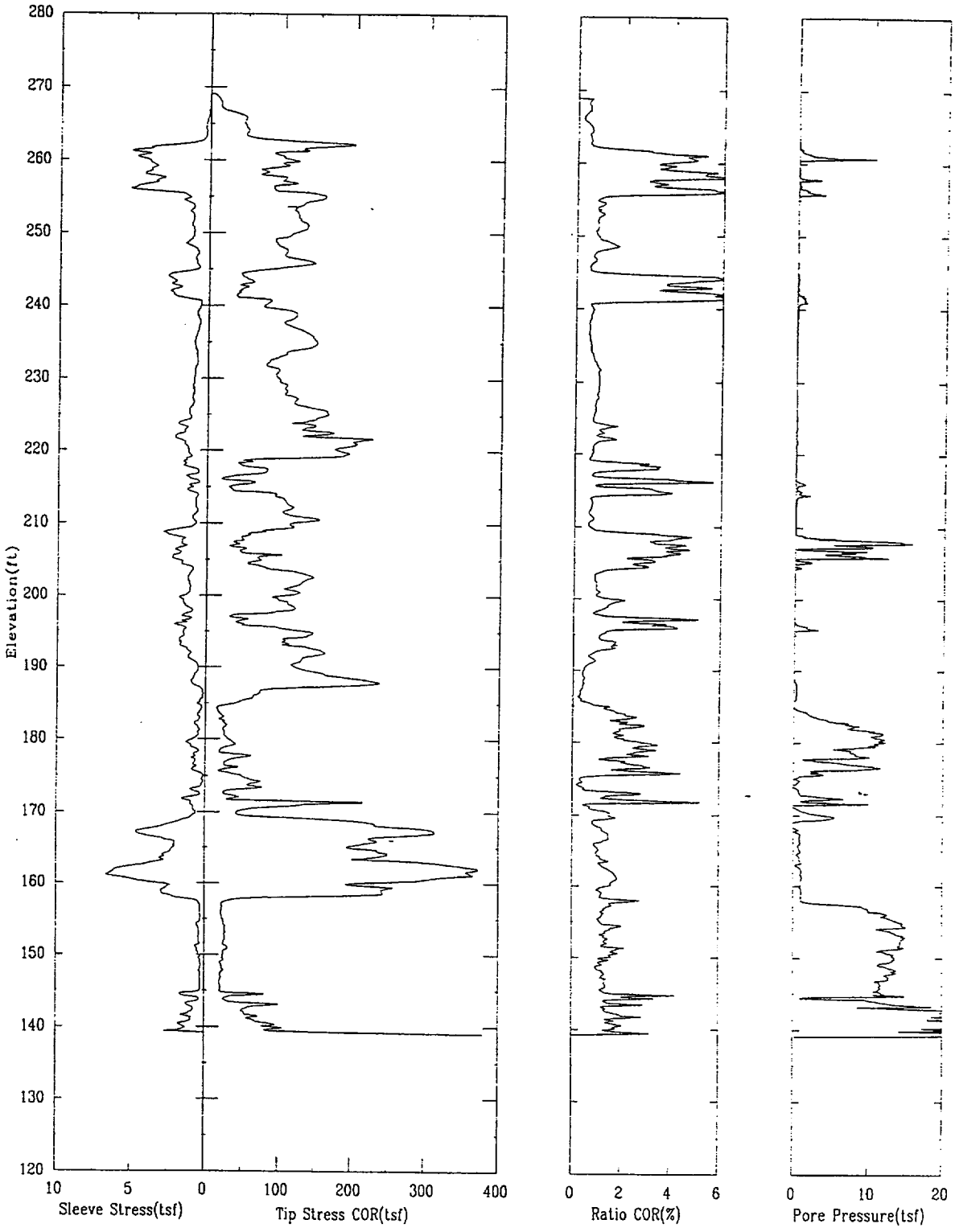

File 322u001.ECP

DCS, MFFF Project No. 08716

CPT-15R APPLIED RESEARCH ASSOCIATES, INC. 06/22/00

North 80295.0 East 55462.7 Elevation 269.1

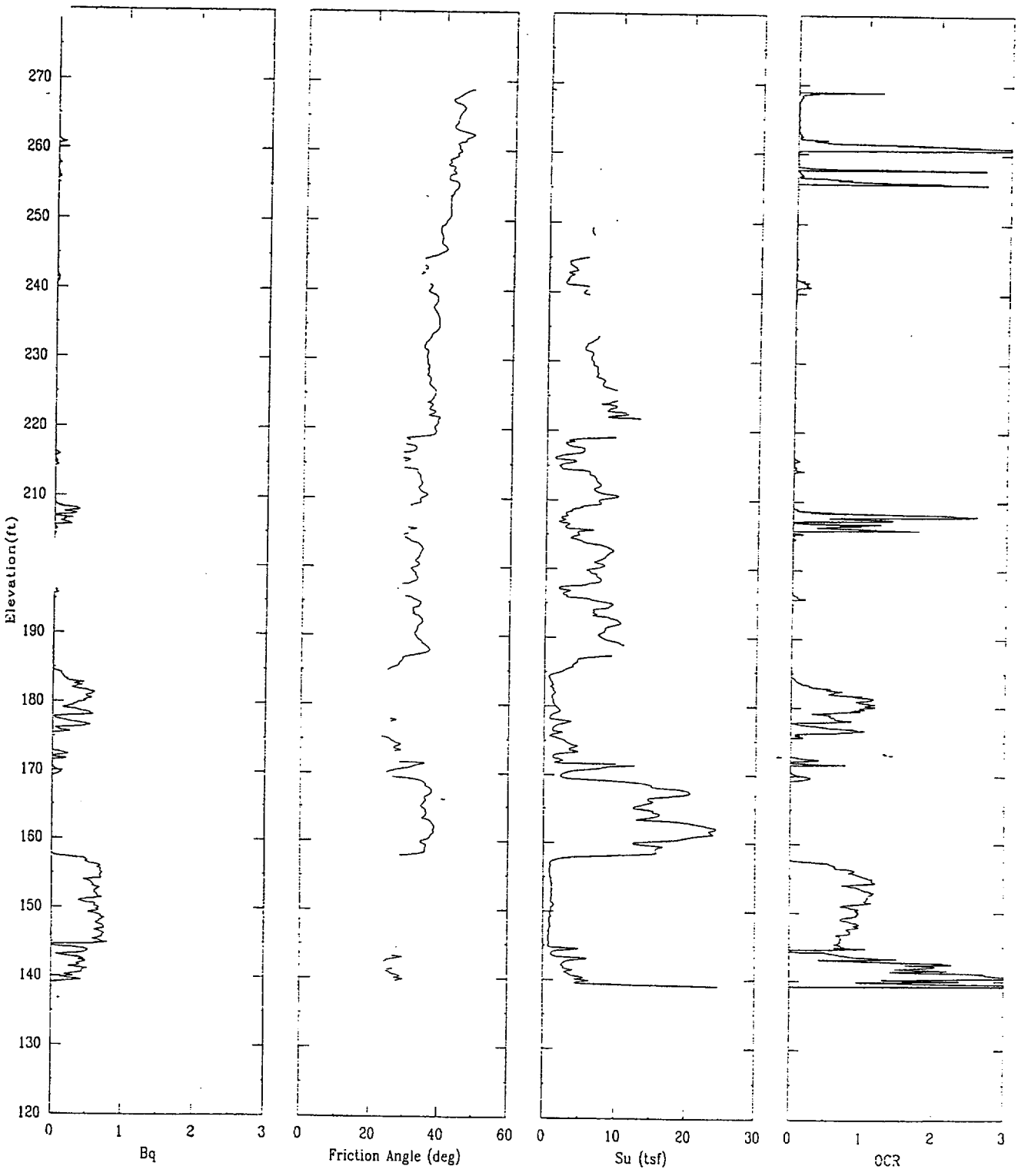

File 322u001.ECP

CPT-15R APPLIED RESEARCH ASSOCIATES, INC. 06/22/00

North 80295.0 East 55462.7 Elevation 269.1

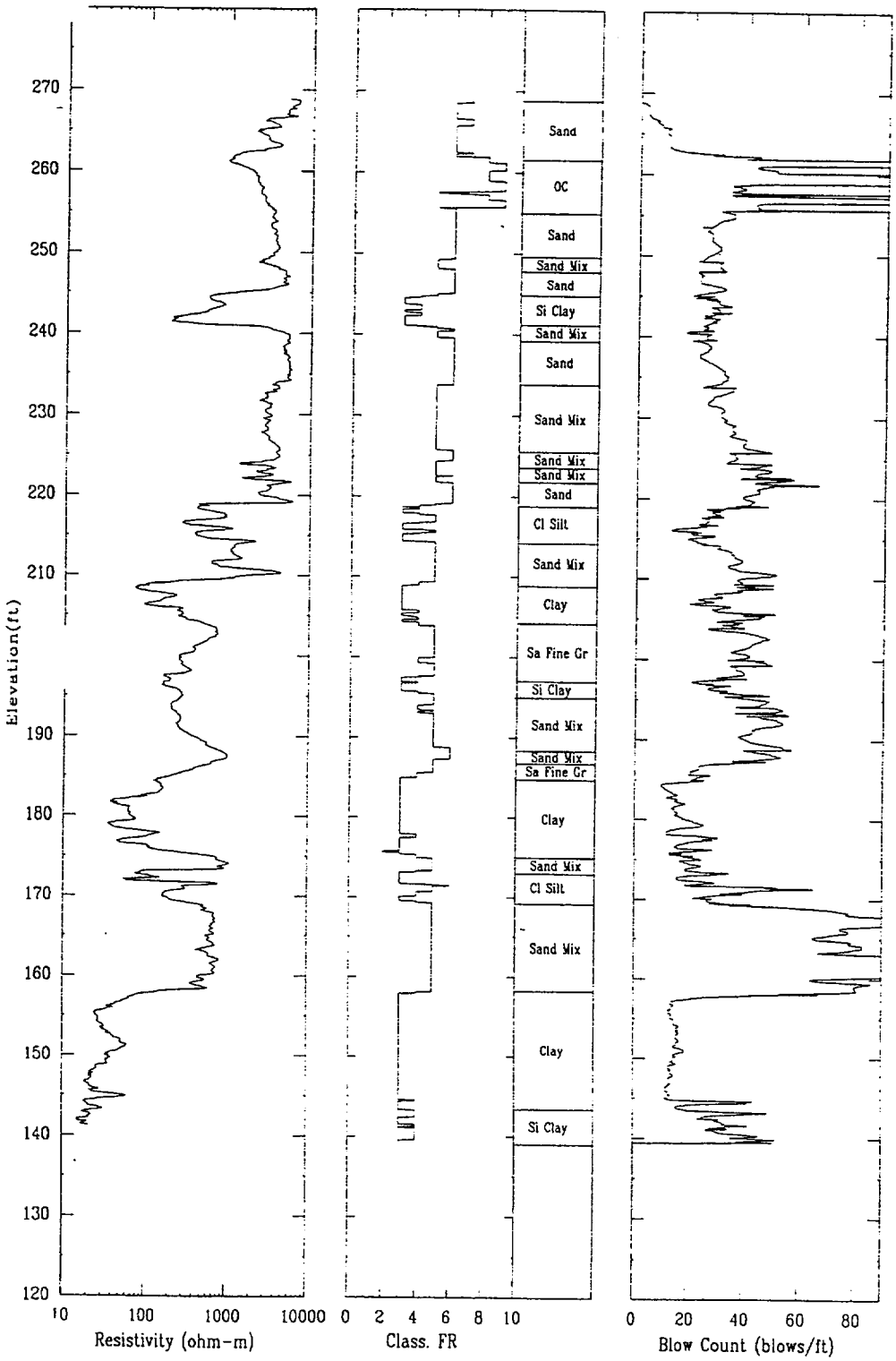

File 322u001.ECP

CPT-16S APPLIED RESEARCH ASSOCIATES, INC. 06/08/00

North 80281.0 East 55628.6 Elevation 260.5

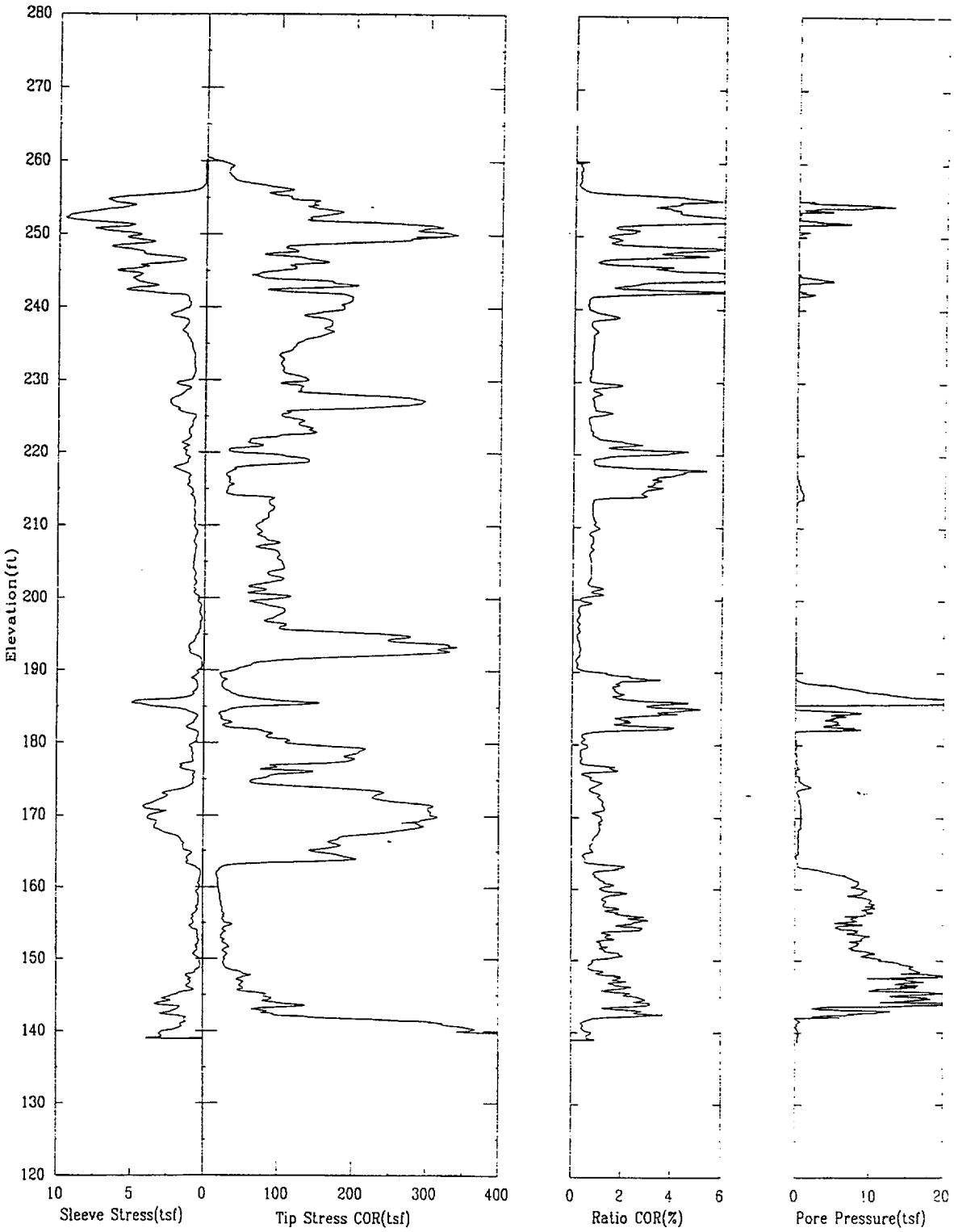

File 408u001B.ECP

CPT-16S APPLIED RESEARCH ASSOCIATES, INC. 06/08/00

North 80281.0 East 55628.6 Elevation 260.5

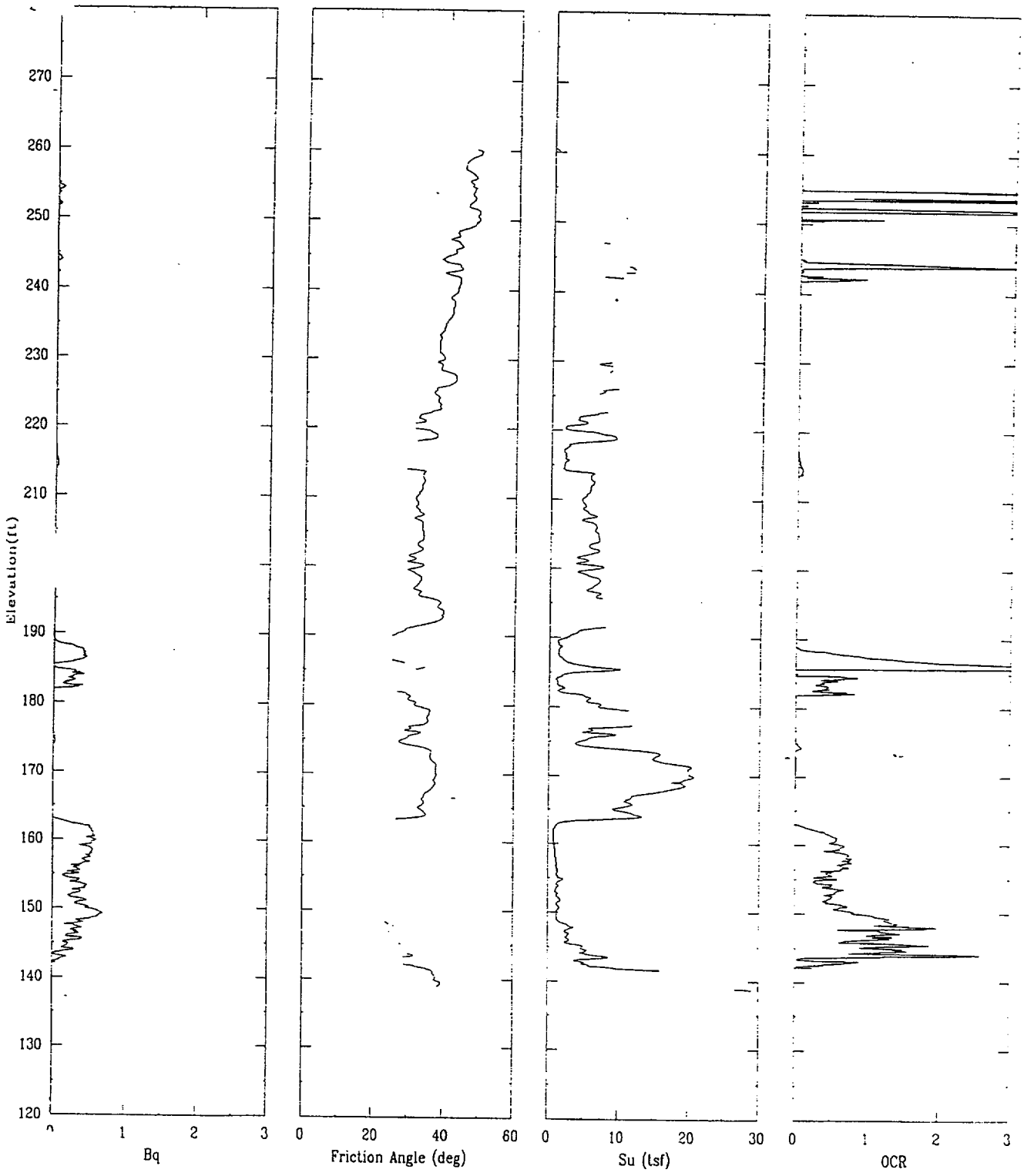

File 408u001B.ECP

CPT-16S APPLIED RESEARCH ASSOCIATES, INC. 06/08/00

North 80281.0 East 55628.6 Elevation 260.5

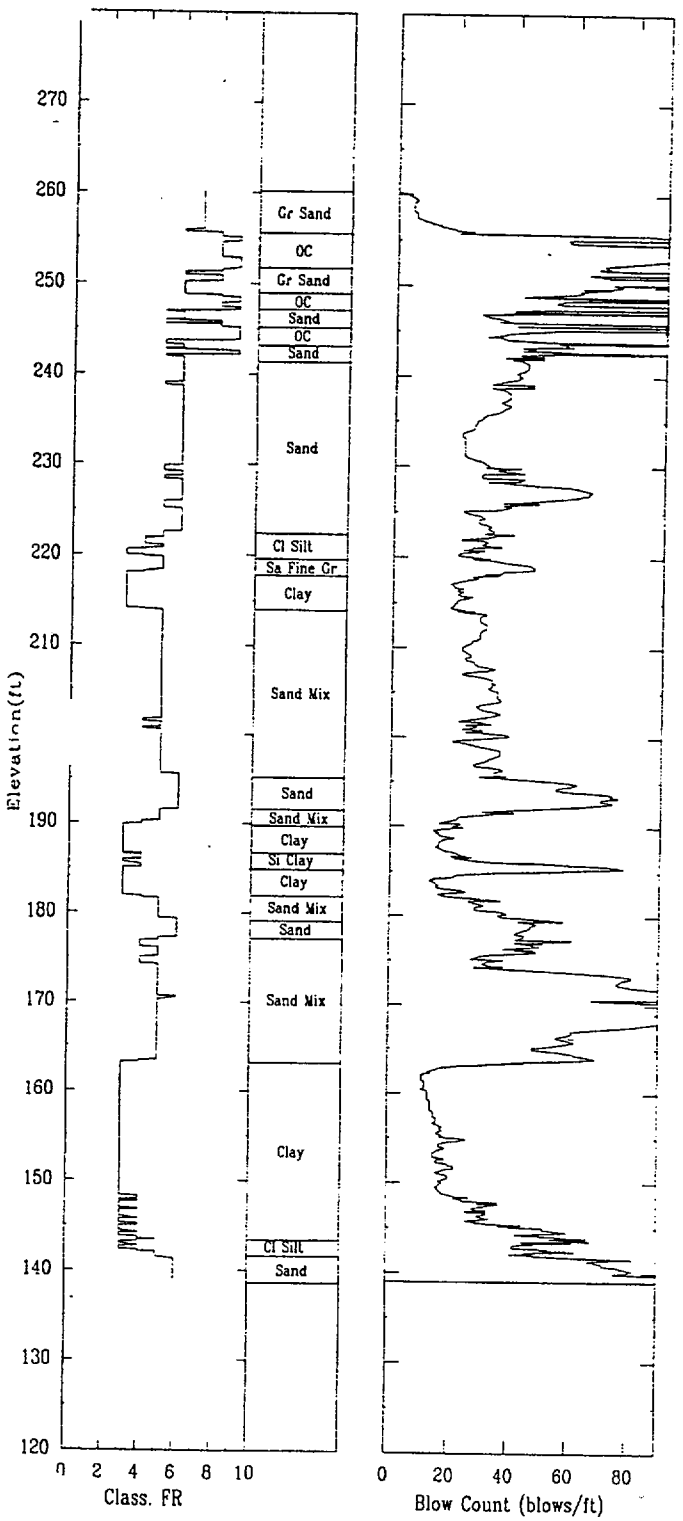

File 408a001B.ECP

CPT-17 APPLIED RESEARCH ASSOCIATES, INC. 06/10/00

North 80259.4 East 55747.7 Elevation 255.9

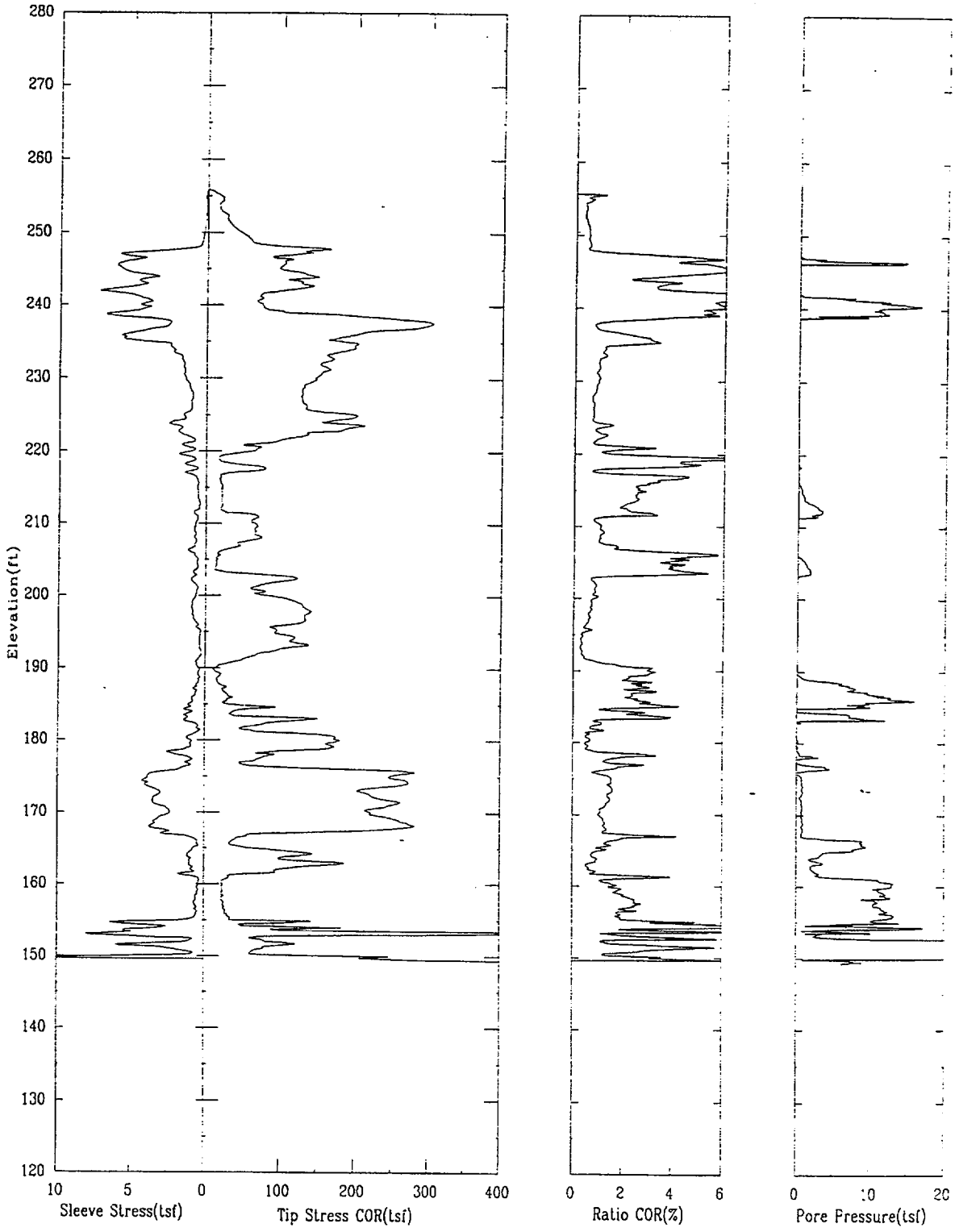

File 410u001B.ECP

DCS, MFFF Project No. 08716

CPT-17 APPLIED RESEARCH ASSOCIATES, INC. 06/10/00

North 80259.4 East 55747.7 Elevation 255.9

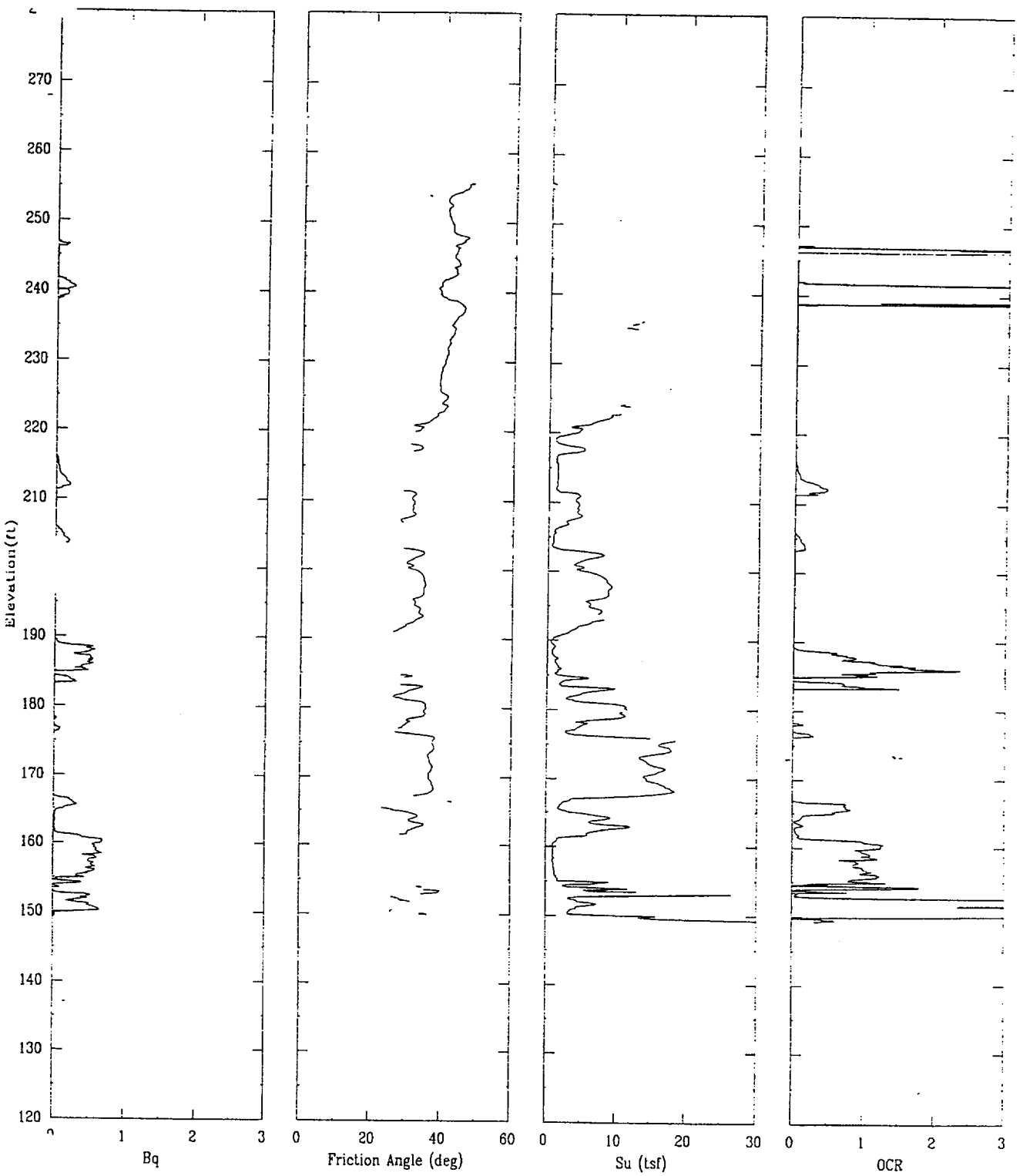

File 410u001B.ECP

DCS, MFFF Project No. 08716

CPT-17 APPLIED RESEARCH ASSOCIATES, INC. 06/10/00

North 80259.4 East 55747.7 Elevation 255.9

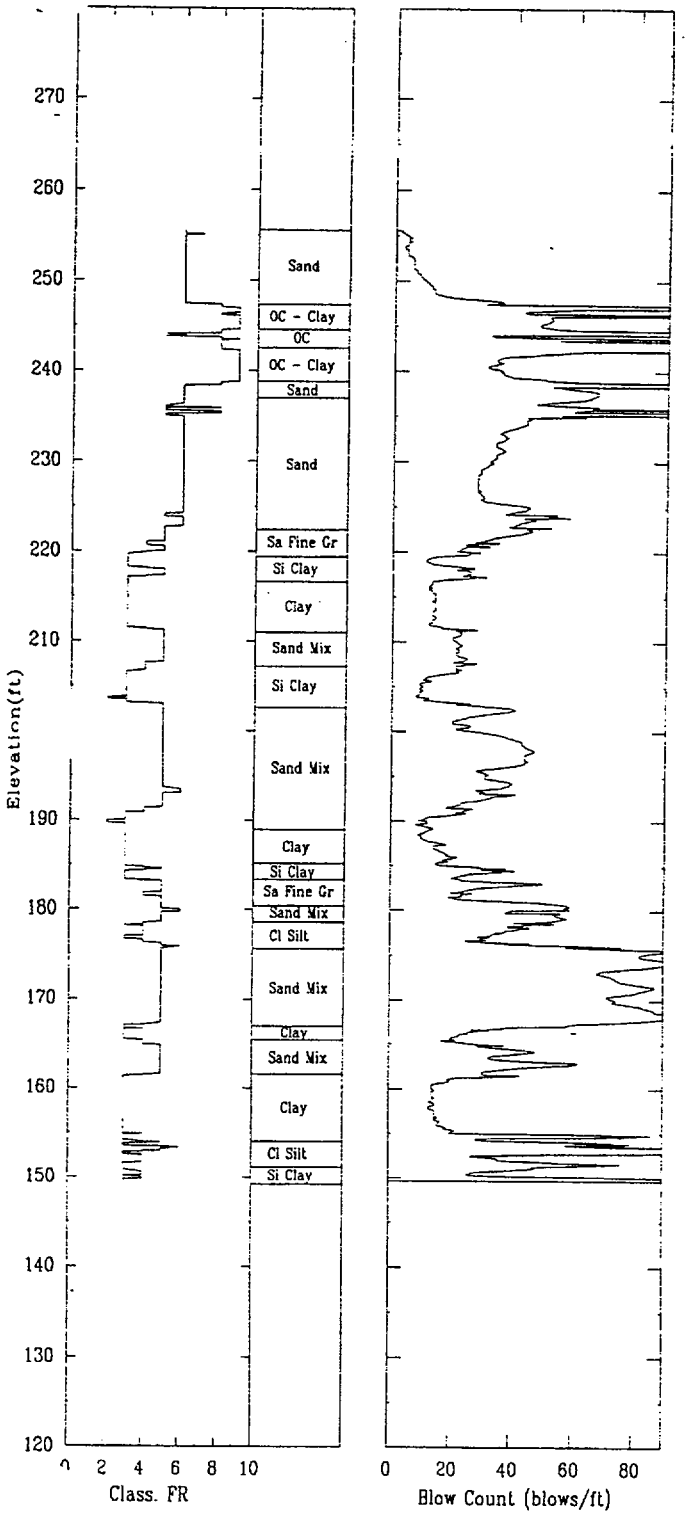

File 410u001B.ECP

CPT-18R APPLIED RESEARCH ASSOCIATES, INC. 06/22/00

North 80192.1 East 55405.9 Elevation 277.0

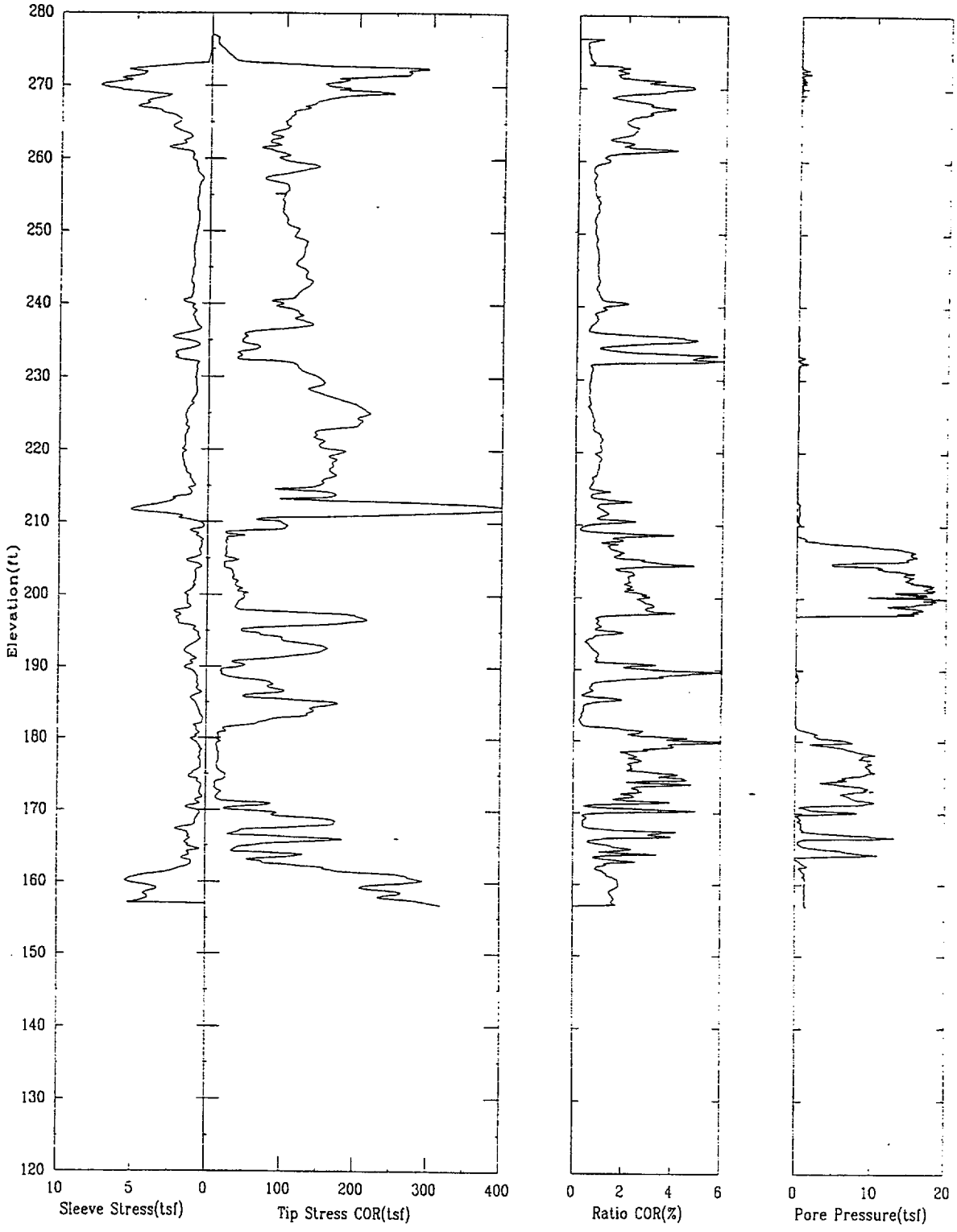

File 322u005.ECP

CPT-18R APPLIED RESEARCH ASSOCIATES, INC. 06/22/00

North 80192.1 East 55405.9 Elevation 277.0

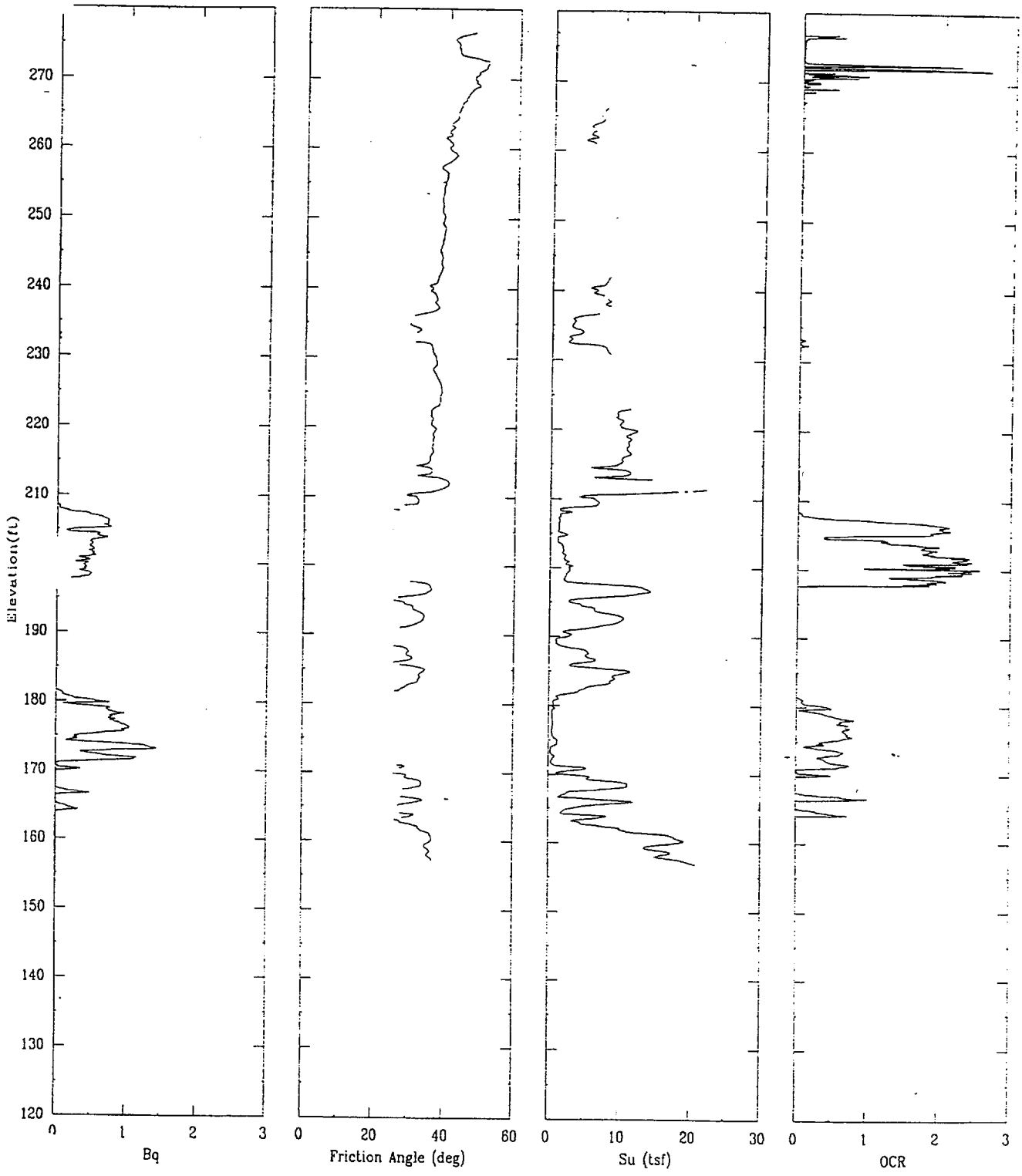

File 322u005.ECP

CPT-18R APPLIED RESEARCH ASSOCIATES, INC. 06/22/00

North 80192.1 East 55405.9 Elevation 277.0

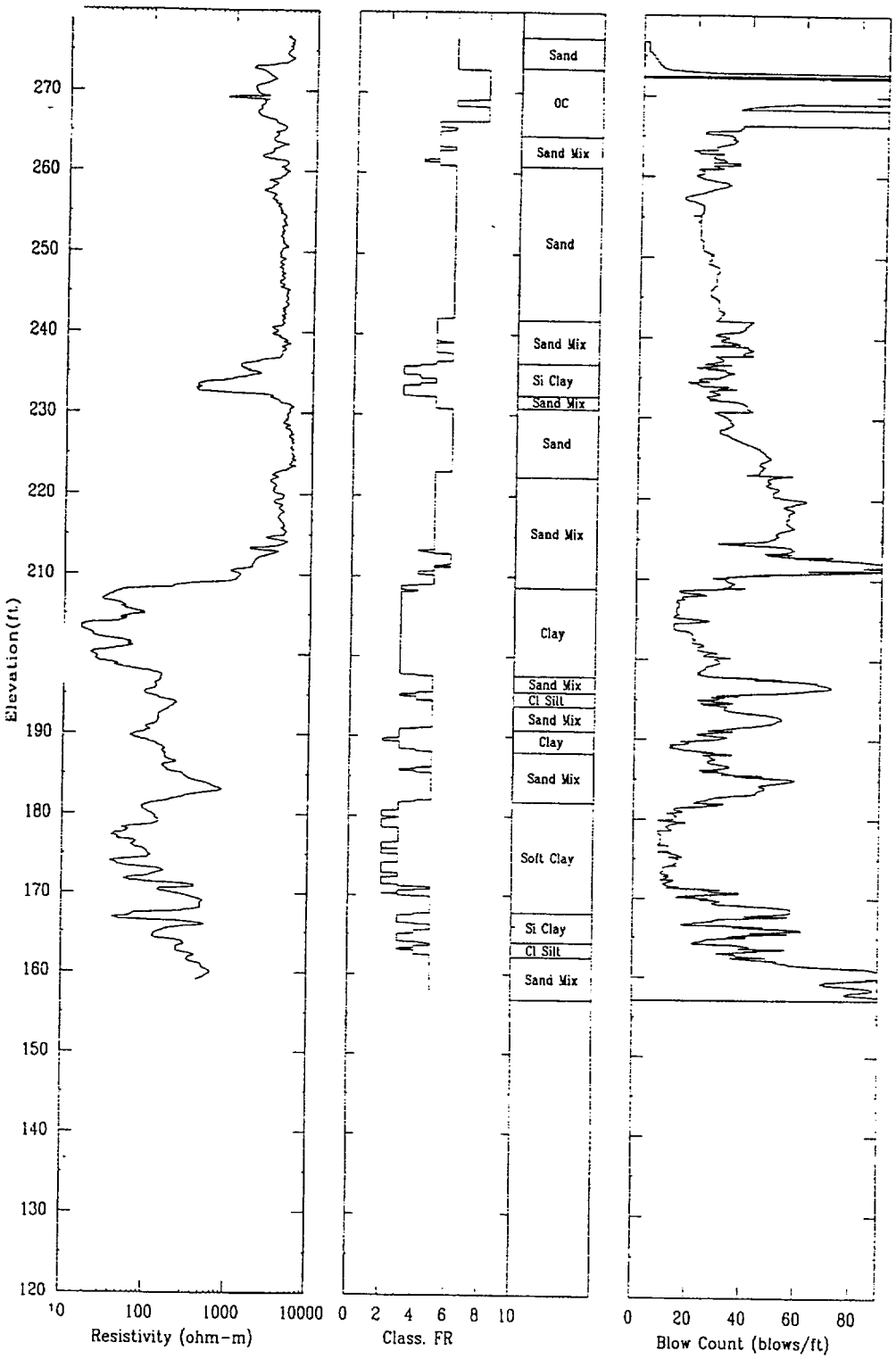

File 322u005.ECP

CPT-19S APPLIED RESEARCH ASSOCIATES, INC. 06/03/00

North 80177.3 East 55467.5 Elevation 274.8

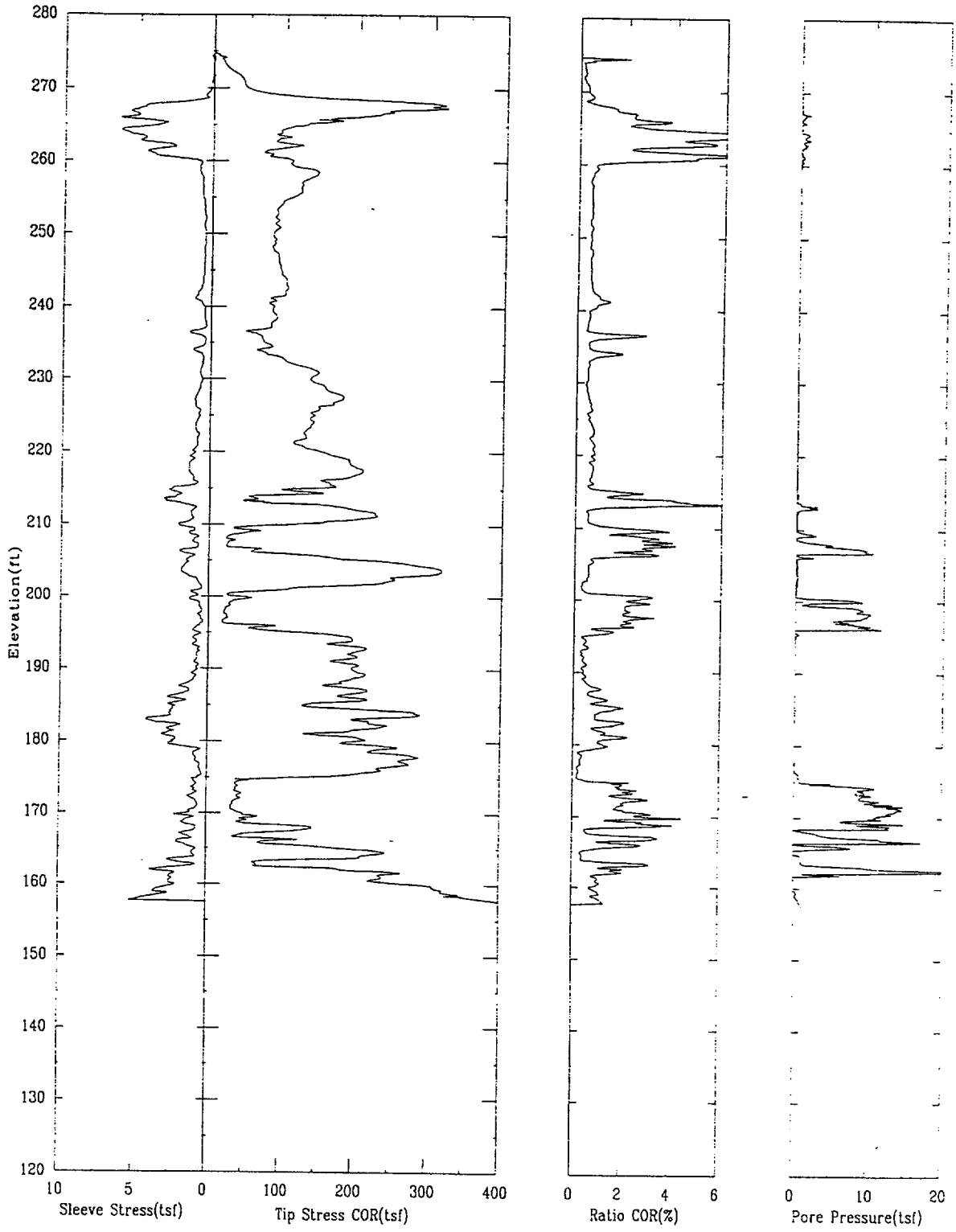

File 403u002.ECP

DCS, MFFF Project No. 08716

CPT-19S APPLIED RESEARCH ASSOCIATES, INC. 06/03/00

North 80177.3 East 55467.5 Elevation 274.8

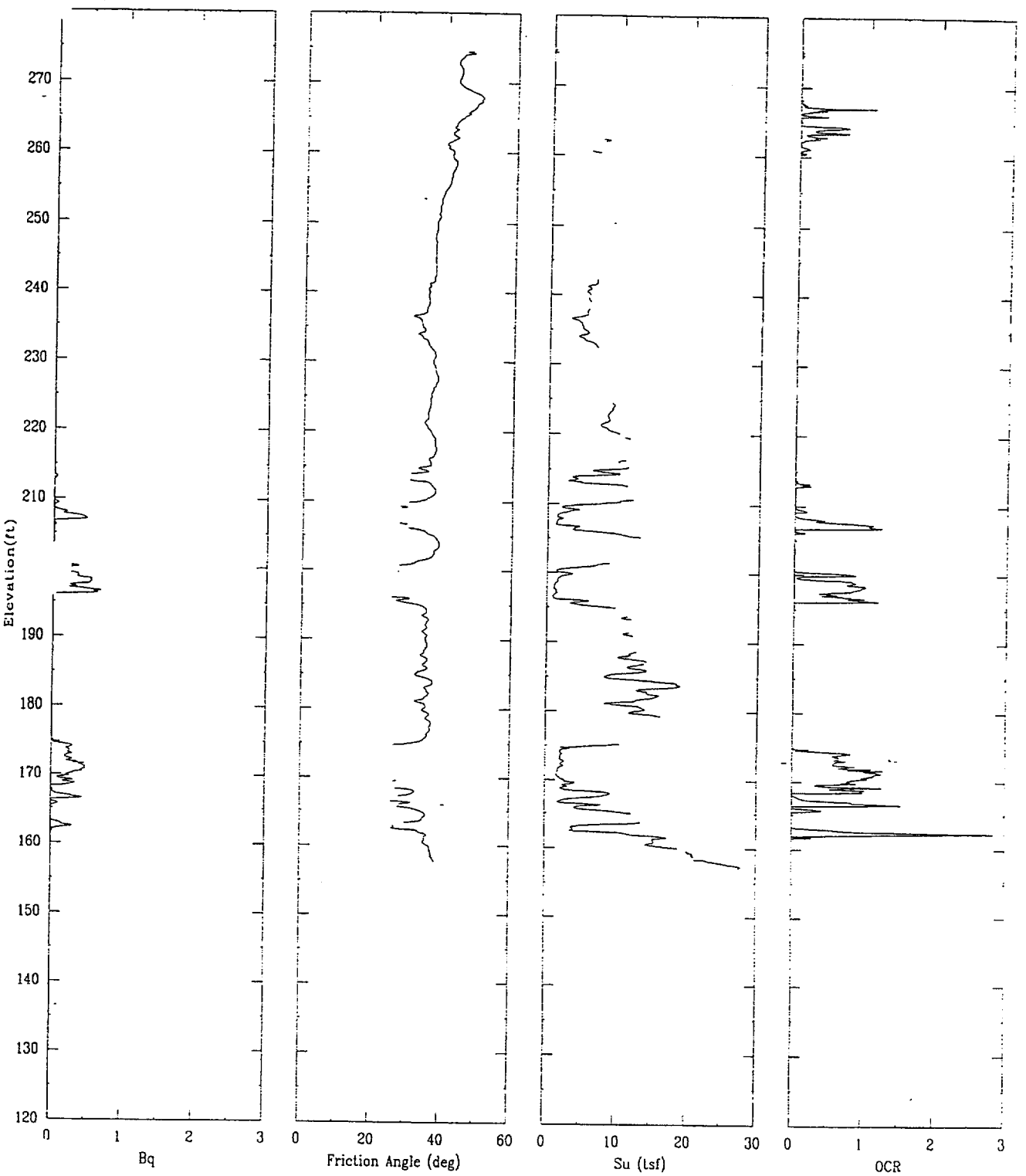

File 403u002.ECP

CPT-19S APPLIED RESEARCH ASSOCIATES, INC. 06/03/00

North 80177.3 East 55467.5 Elevation 274.8

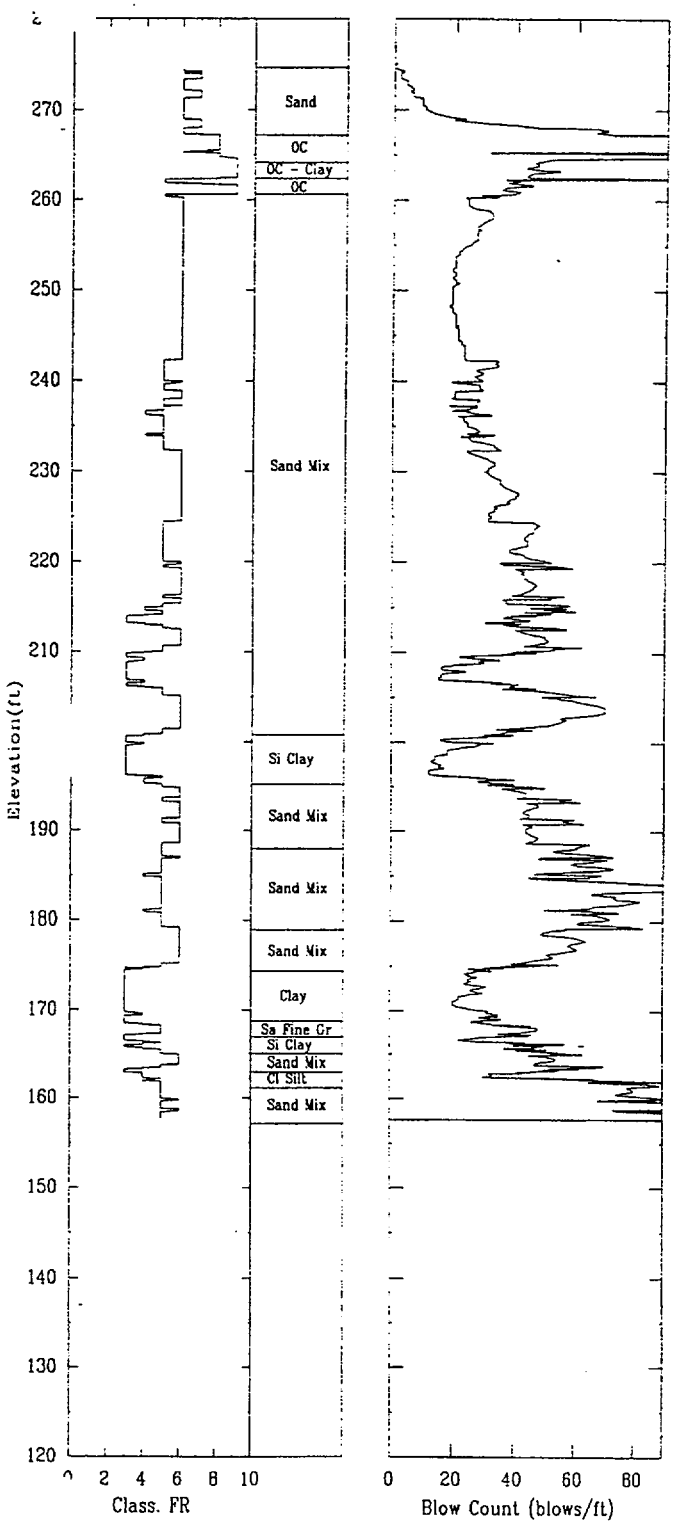

File 403u002.ECP

CPT-20R APPLIED RESEARCH ASSOCIATES, INC. 06/22/00

North 80211.3 East 55570.4 Elevation 266.9

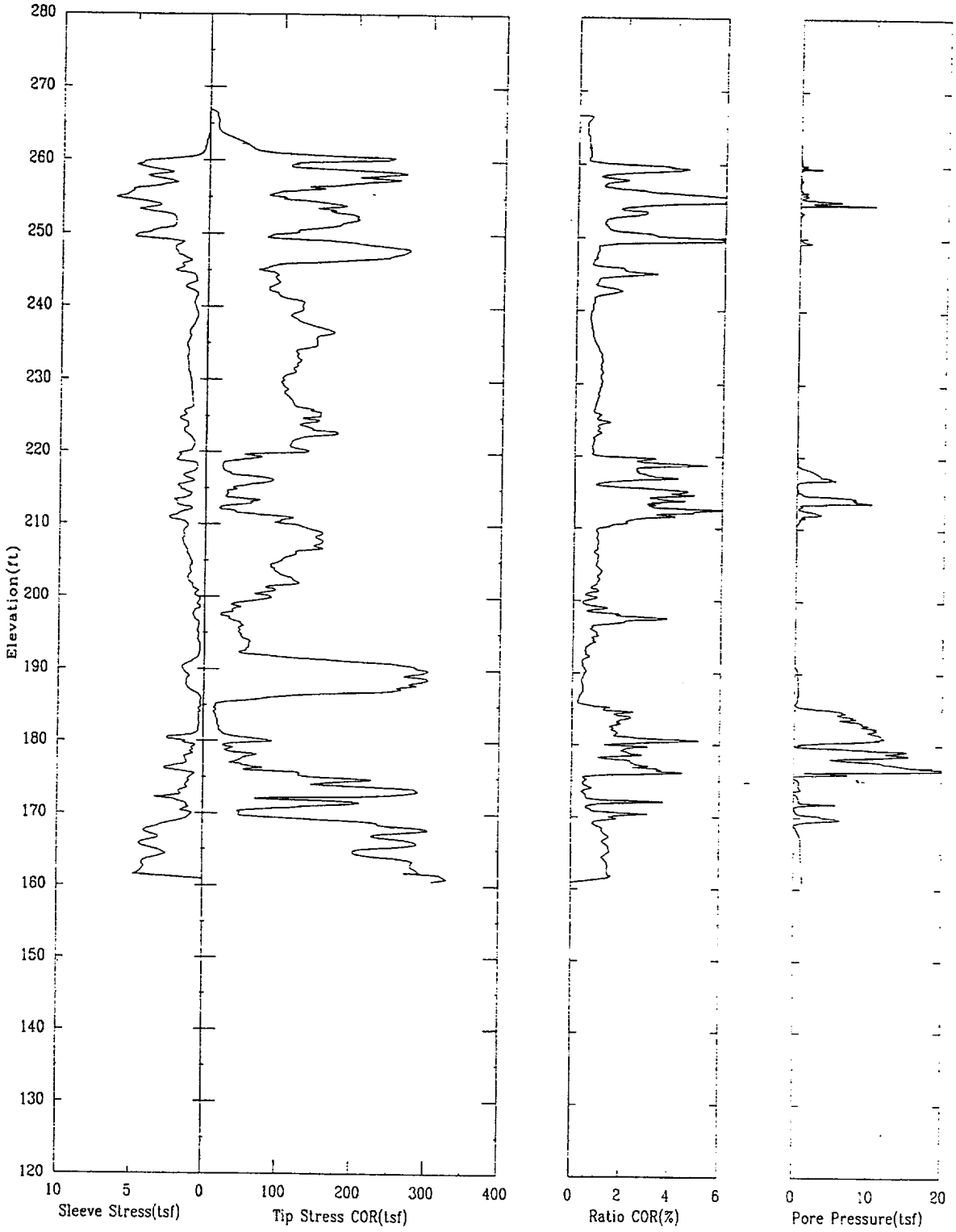

File 322u003.ECP

DCS, MFFF Project No. 08716

CPT-20R APPLIED RESEARCH ASSOCIATES, INC. 06/22/00

North 80211.3 East 55570.4 Elevation 266.9

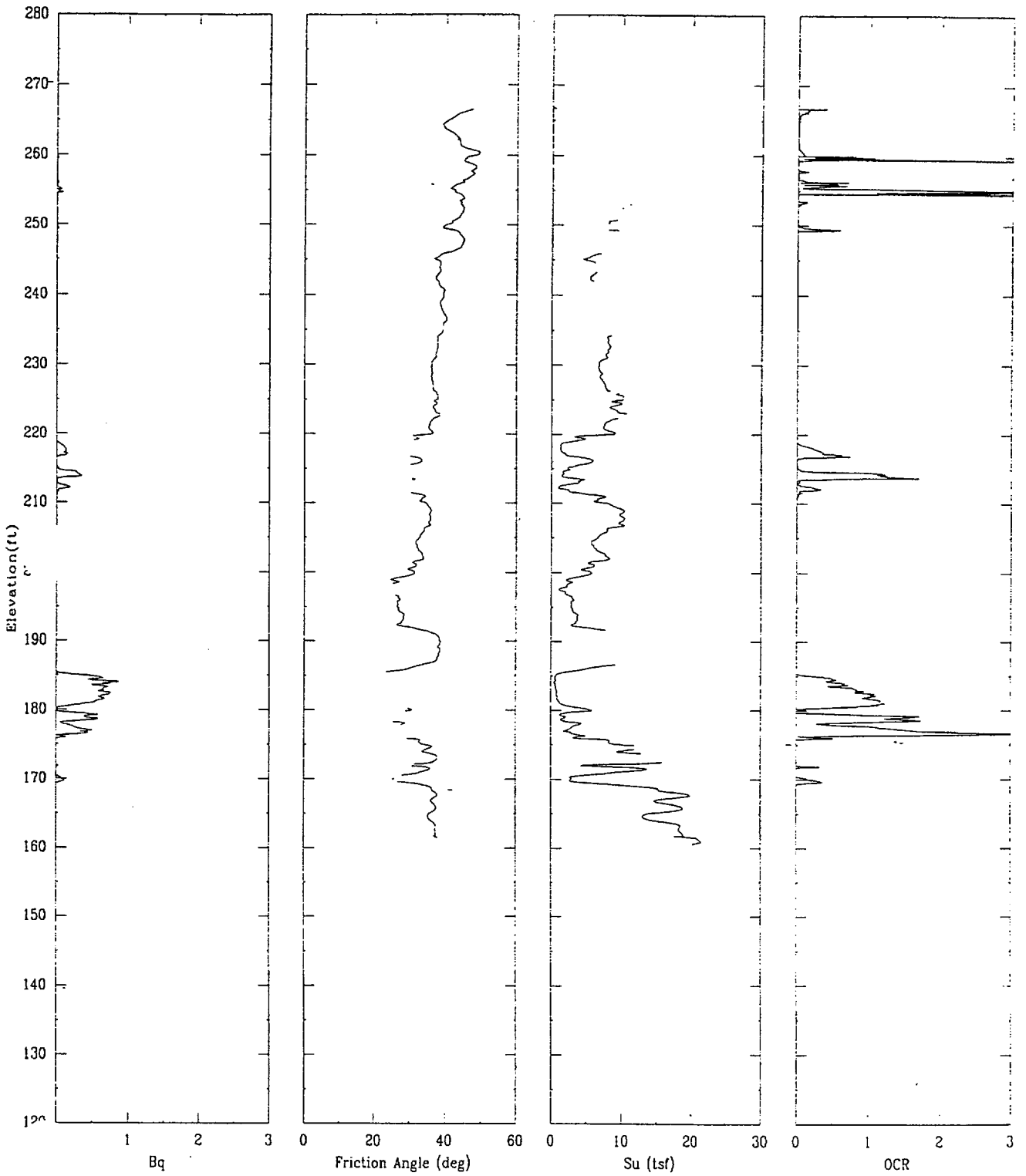

File 322u003.ECP

CPT-20R APPLIED RESEARCH ASSOCIATES, INC. 06/22/00

North 80211.3 East 55570.4 Elevation 266.9

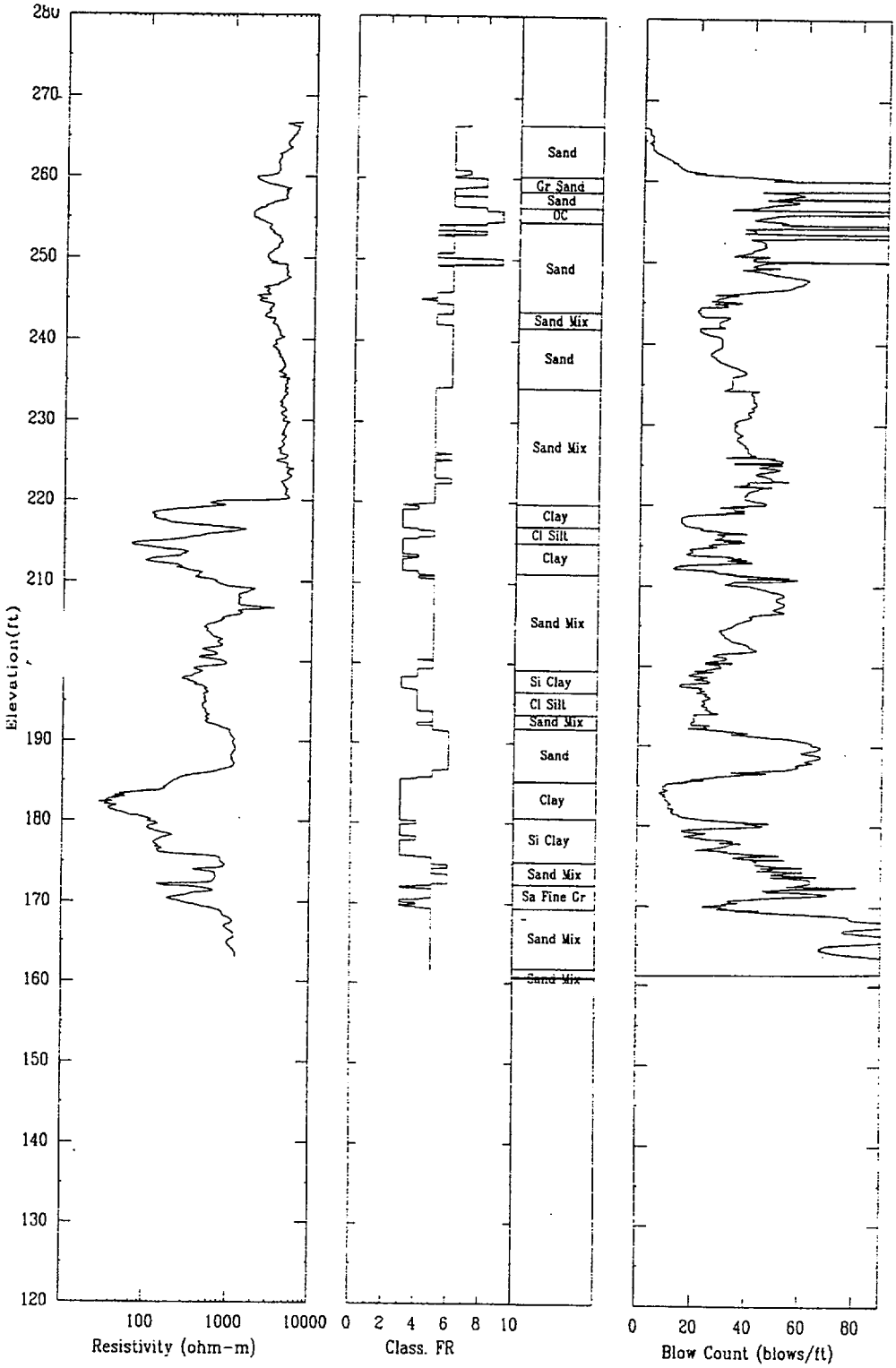

File 322u003.ECP

DCS, MFFF Project No. 08716

102

CPT-21 APPLIED RESEARCH ASSOCIATES, INC. 06/12/00

North 80148.4 East 55060.1 Elevation 295.4

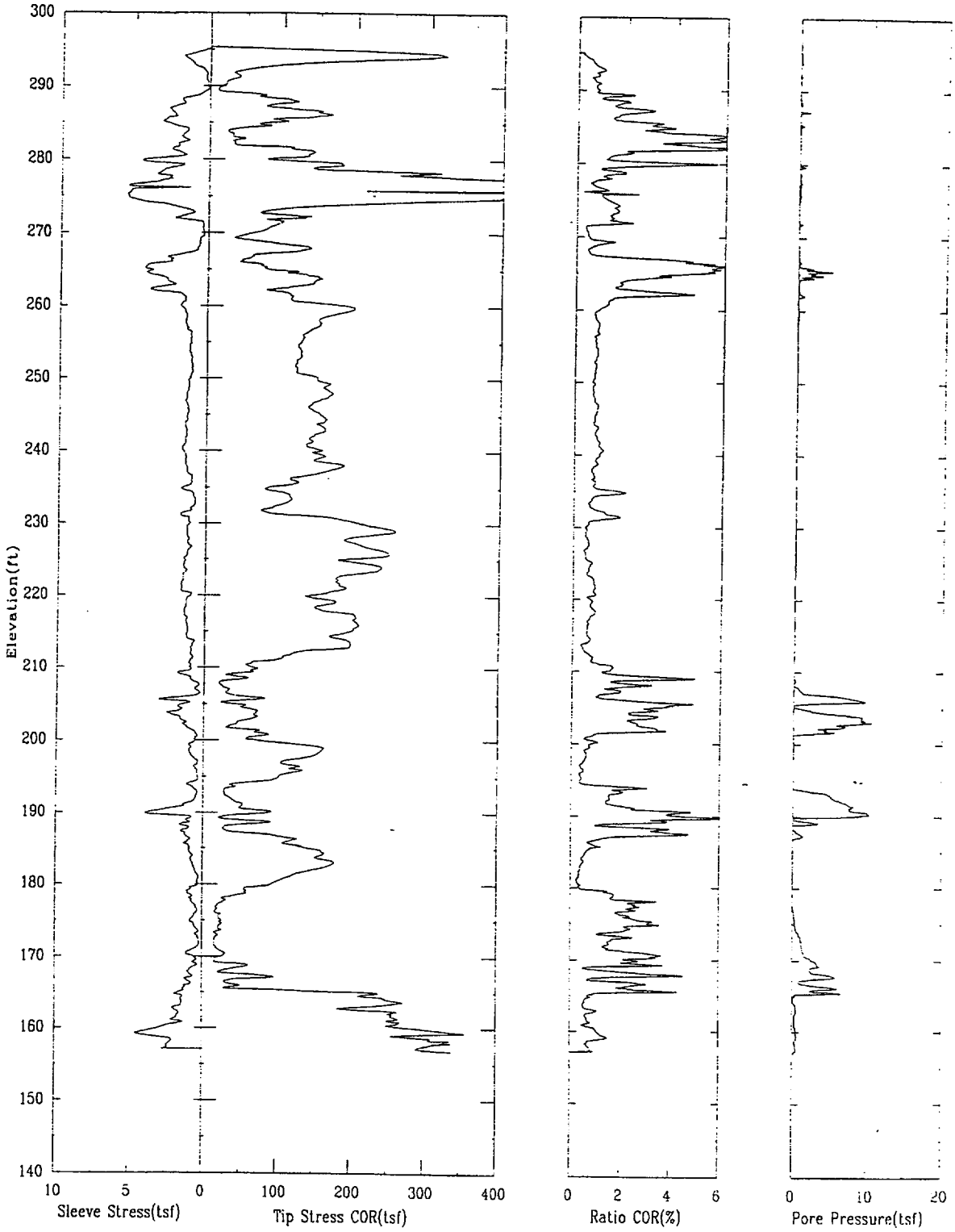

File 412u004.ECP

DCS, MFFF Project No. 08716

CPT-21 APPLIED RESEARCH ASSOCIATES, INC. 06/12/00

North 80148.4 East 55060.1 Elevation 295.4

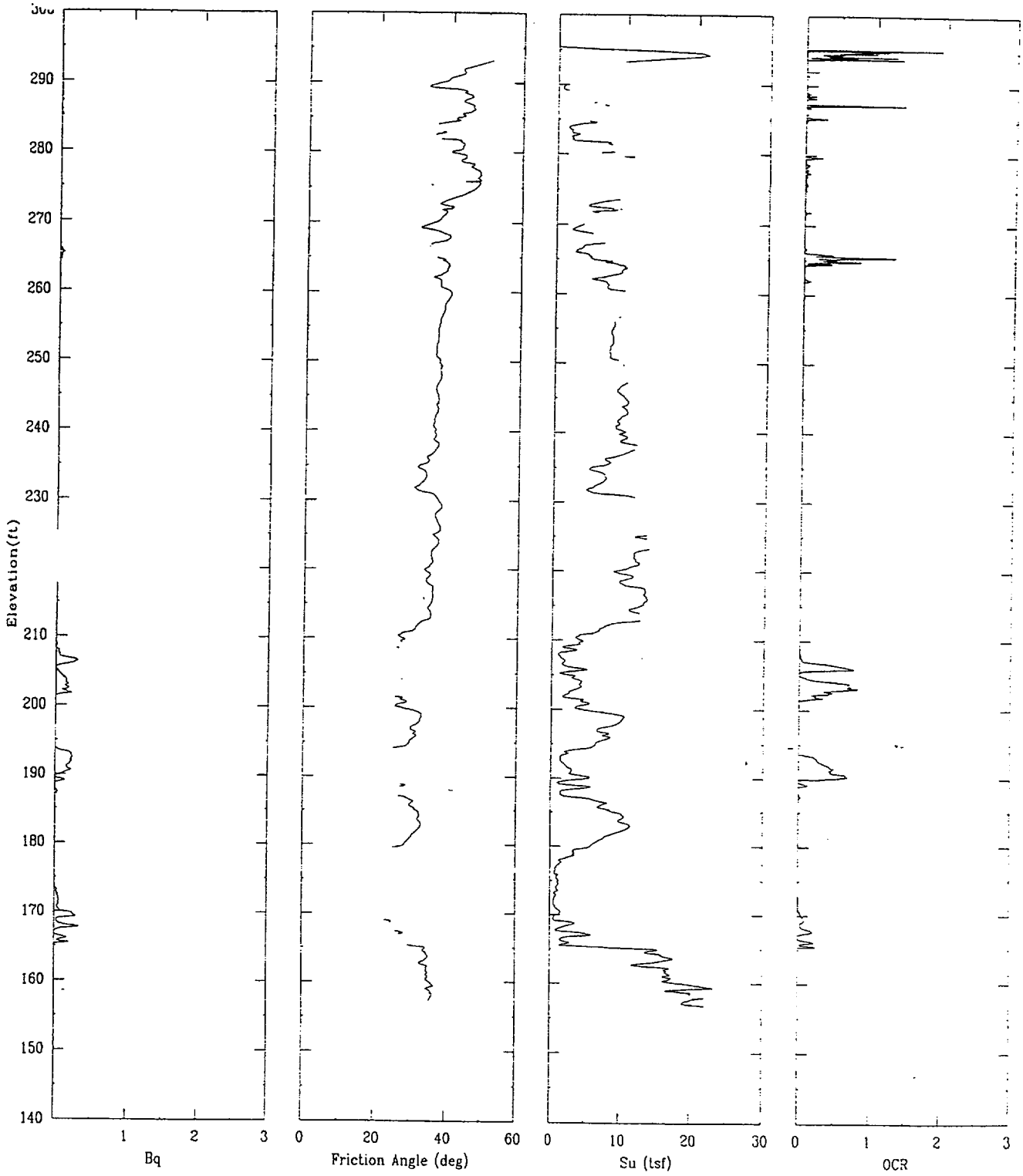

File 412u004.ECP

DCS, MFFF Project No. 08716

CPT-21 APPLIED RESEARCH ASSOCIATES, INC. 06/12/00

North 80148.4 East 55060.1 Elevation 295.4

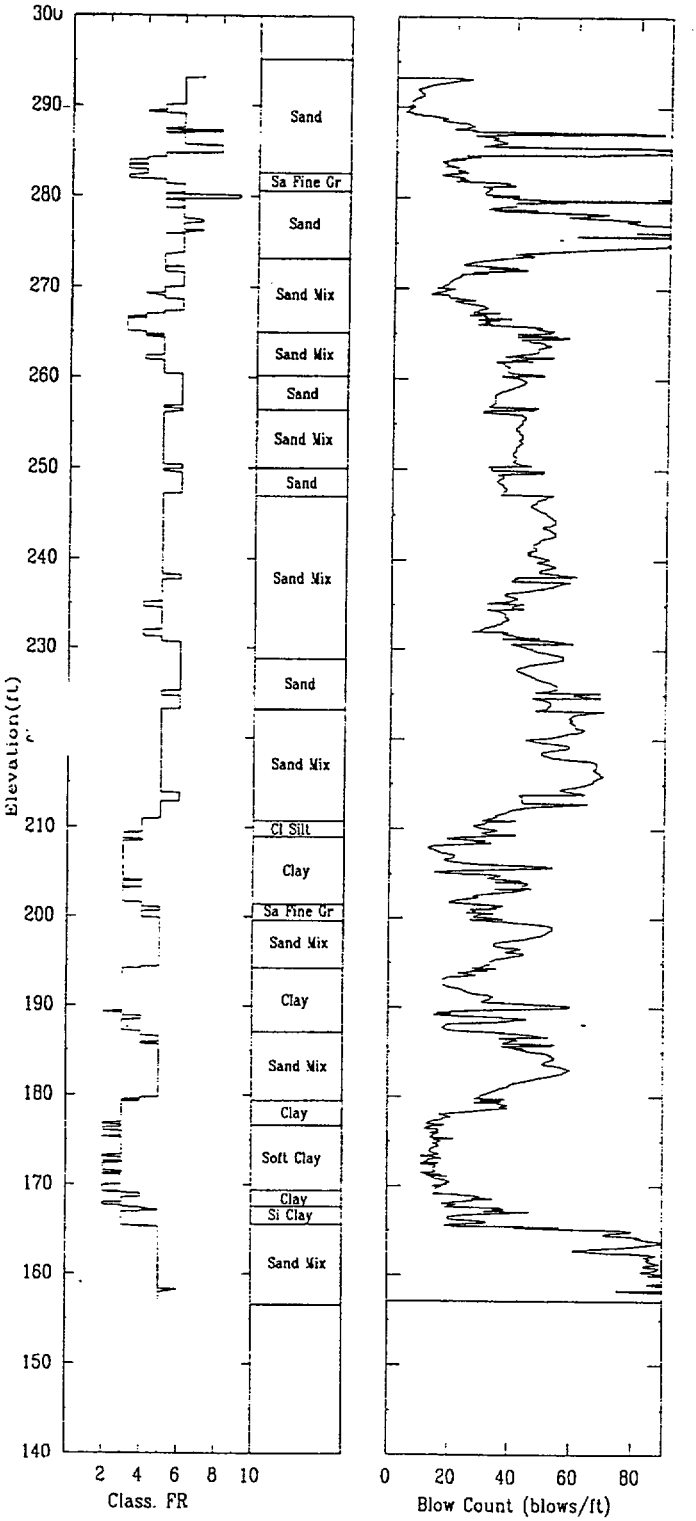

File 412u004.ECP

DCS, MFFF Project No. 08716

CPT-22 APPLIED RESEARCH ASSOCIATES, INC. 06/12/00

North 80143.8 East 55221.9 Elevation 297.3

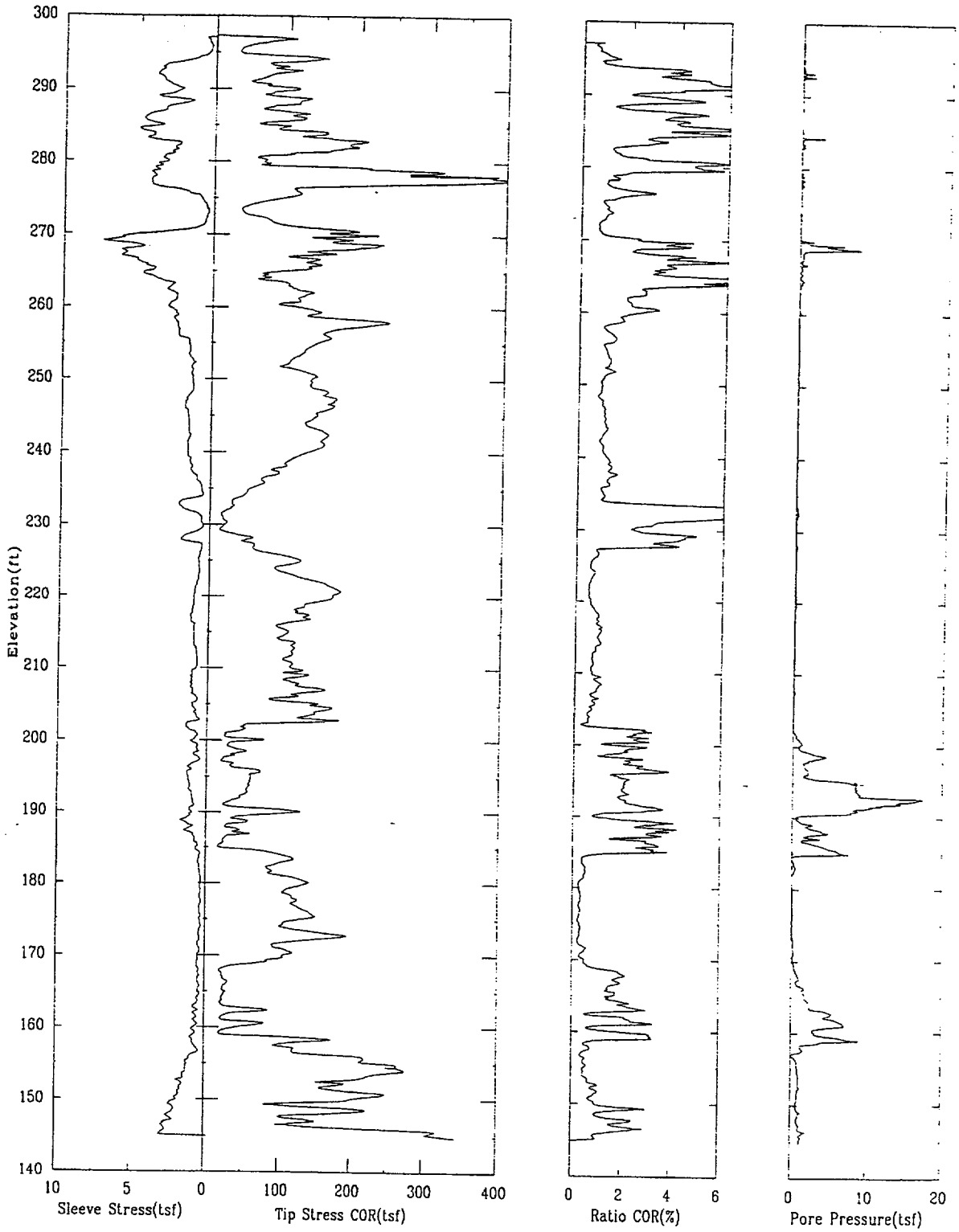

File 412u007.ECP

CPT-22 APPLIED RESEARCH ASSOCIATES, INC. 06/12/00

North 80143.8 East 55221.9 Elevation 297.3

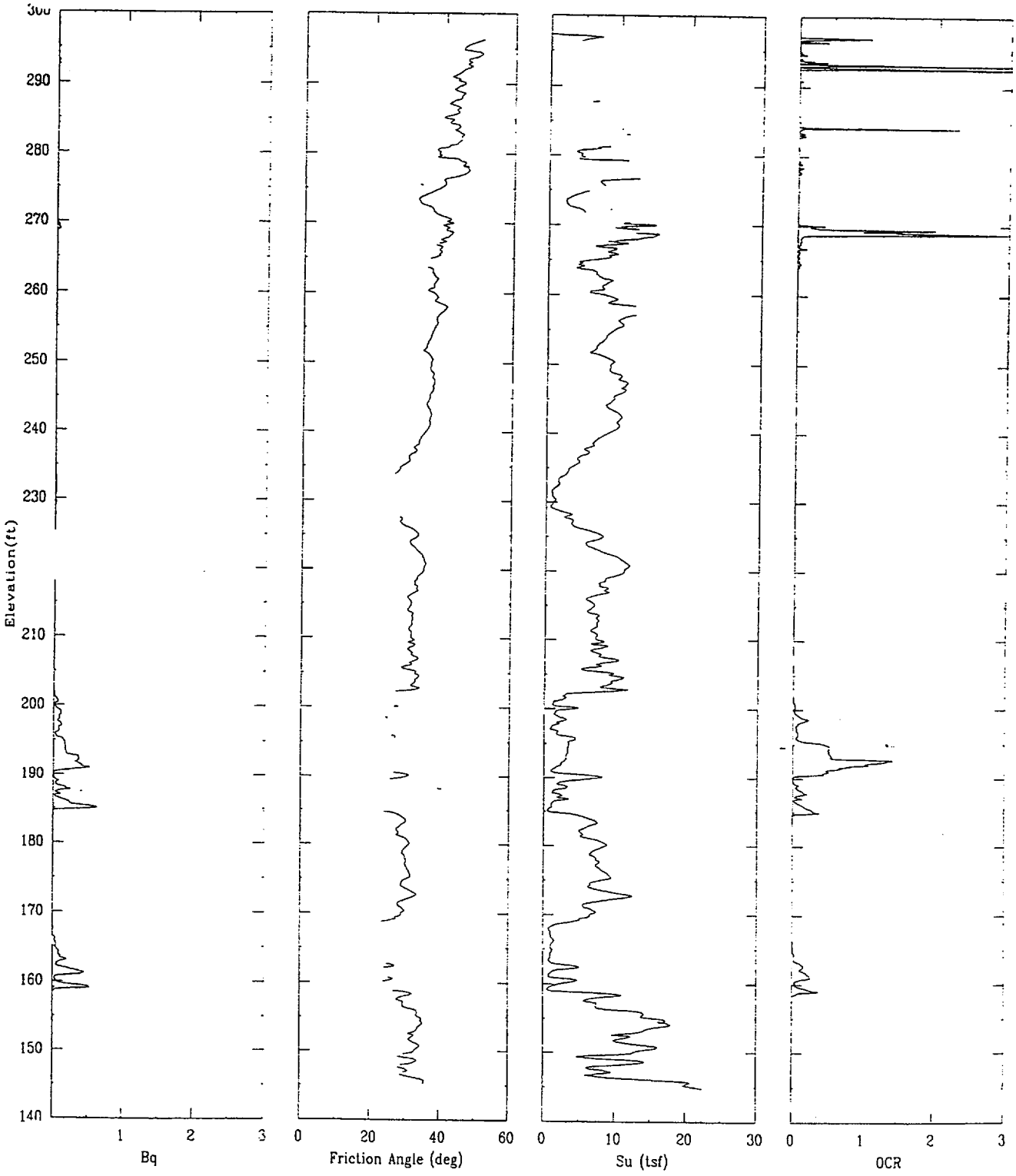

File 412u007.ECP

DCS, MFFF Project No. 08716

CPT-22 APPLIED RESEARCH ASSOCIATES, INC. 06/12/00

North 80143.8 East 55221.9 Elevation 297.3

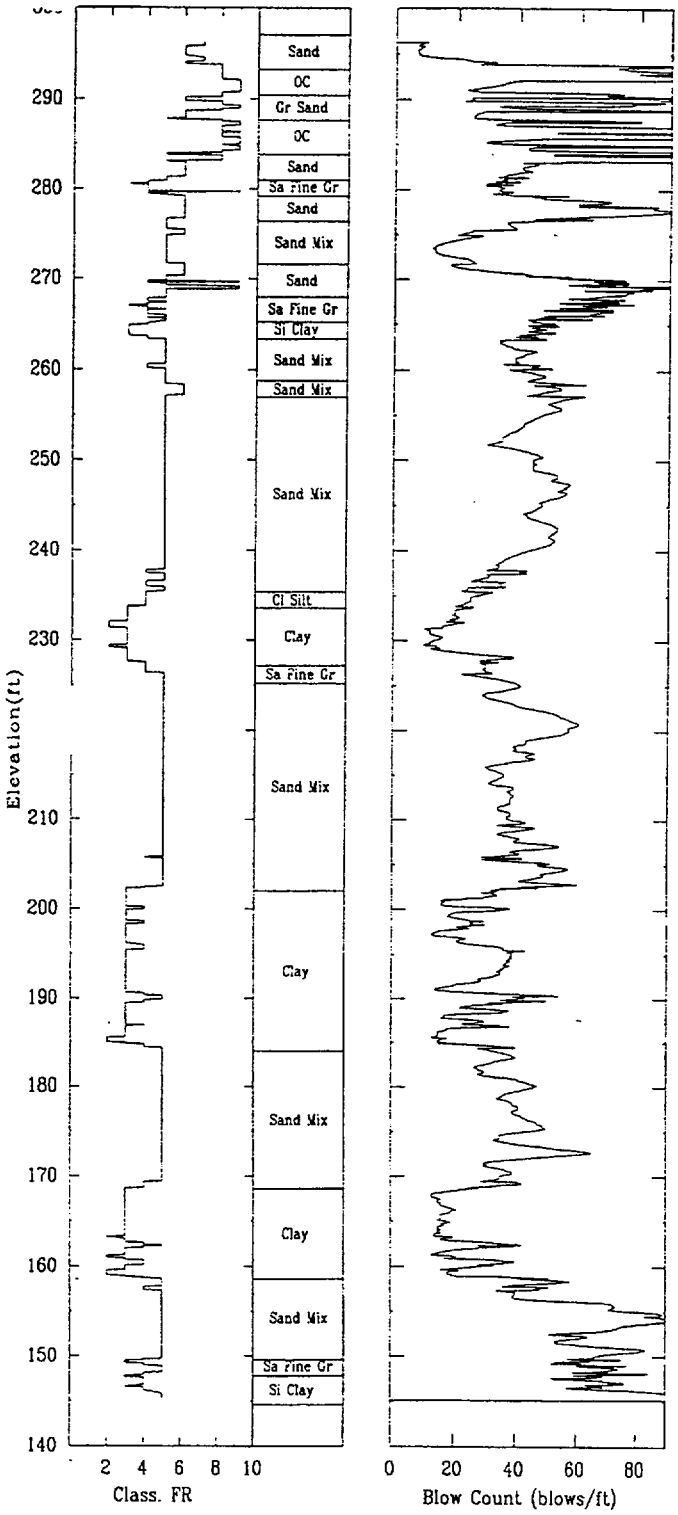

File 412u007.ECP

DCS, MFFF Project No. 08716

CPT-23S APPLIED RESEARCH ASSOCIATES, INC. 06/06/00

North 80088.9 East 55379.4 Elevation 277.3

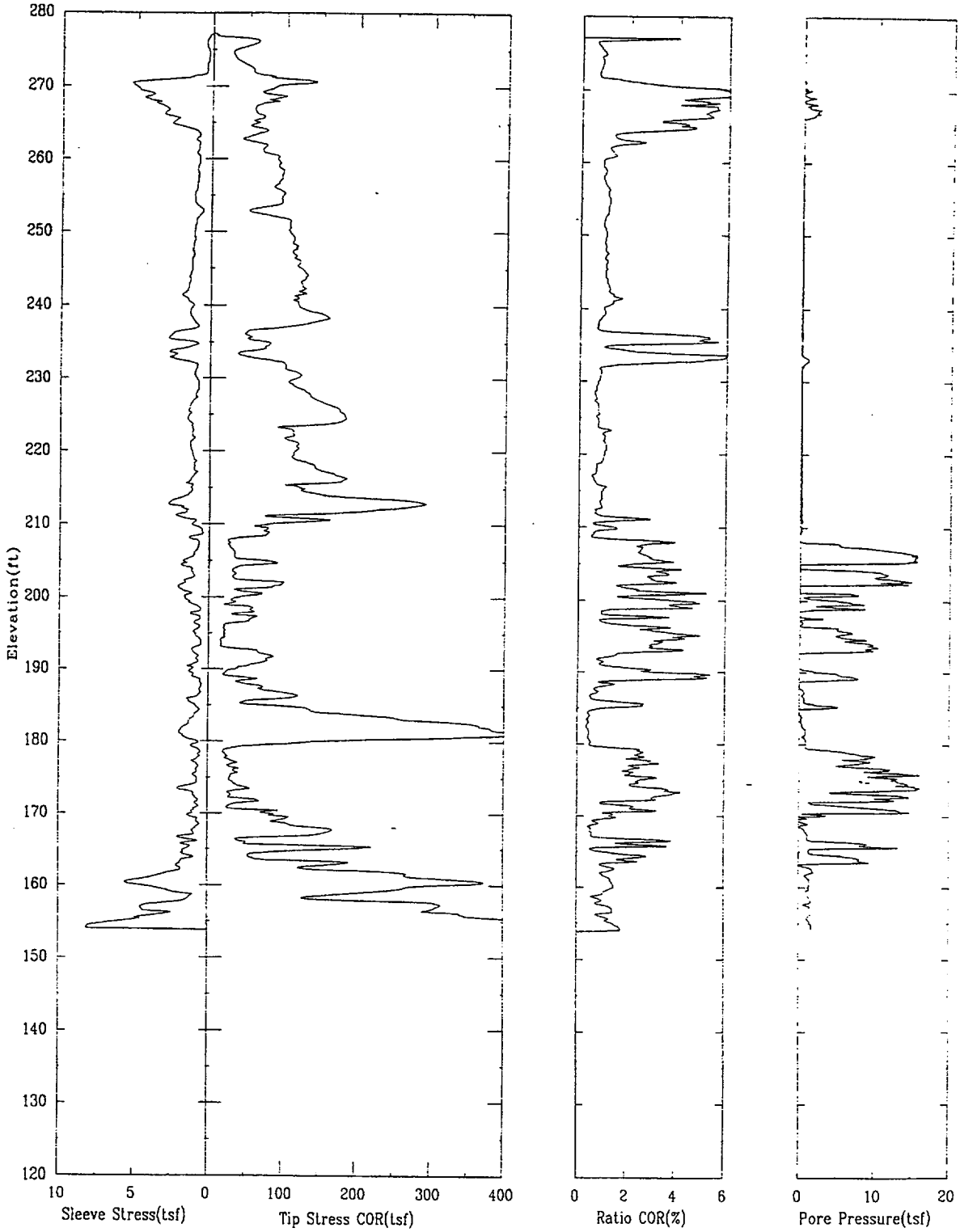

File 406u003.ECP

DCS, MFFF Project No. 08716

CPT-23S APPLIED RESEARCH ASSOCIATES, INC. 06/06/00

North 80088.9 East 55379.4 Elevation 277.3

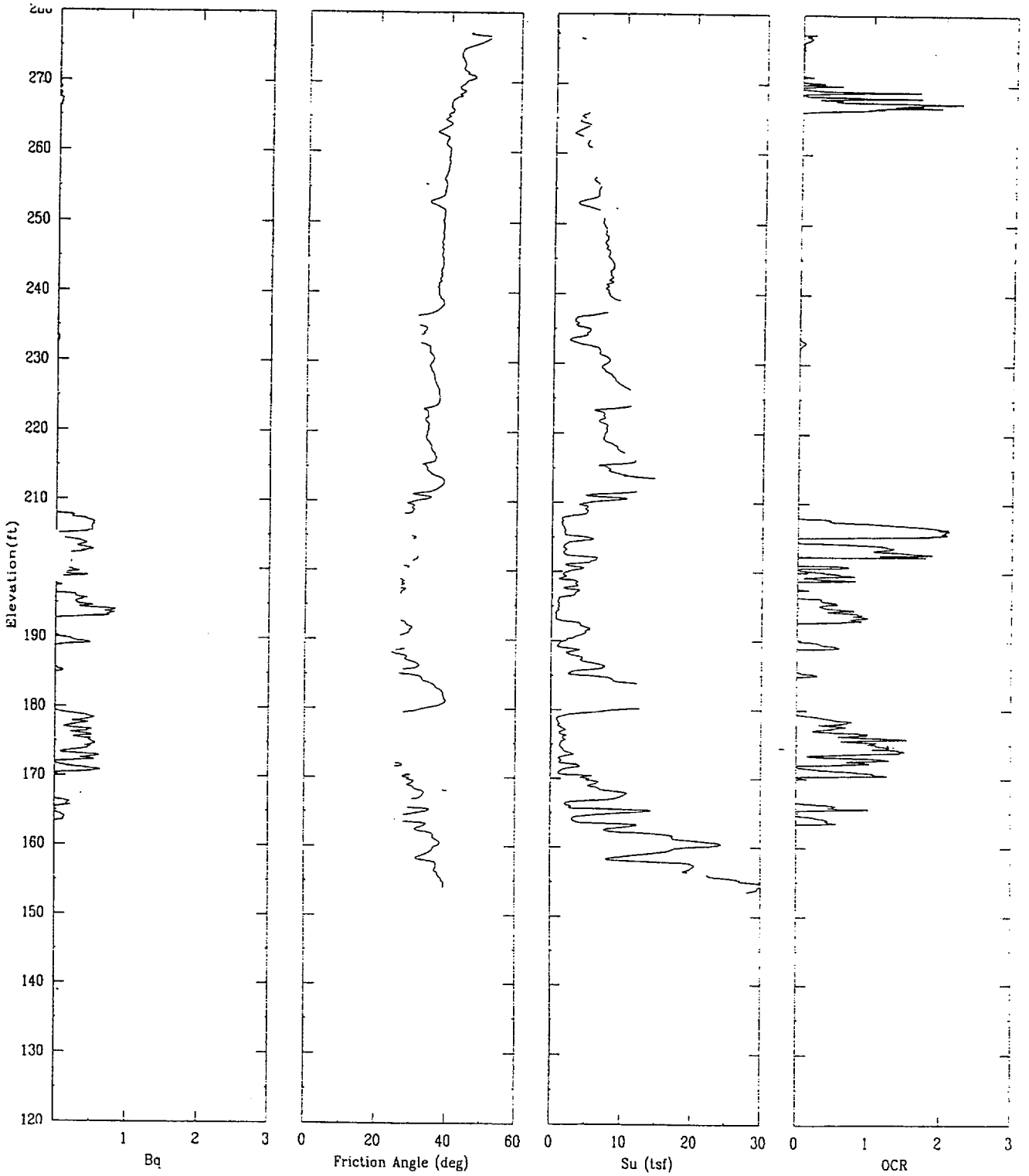

File 406u003.ECP

DCS, MFFF Project No. 08716

CPT-23S APPLIED RESEARCH ASSOCIATES, INC. 06/06/00

North 80088.9 East 55379.4 Elevation 277.3

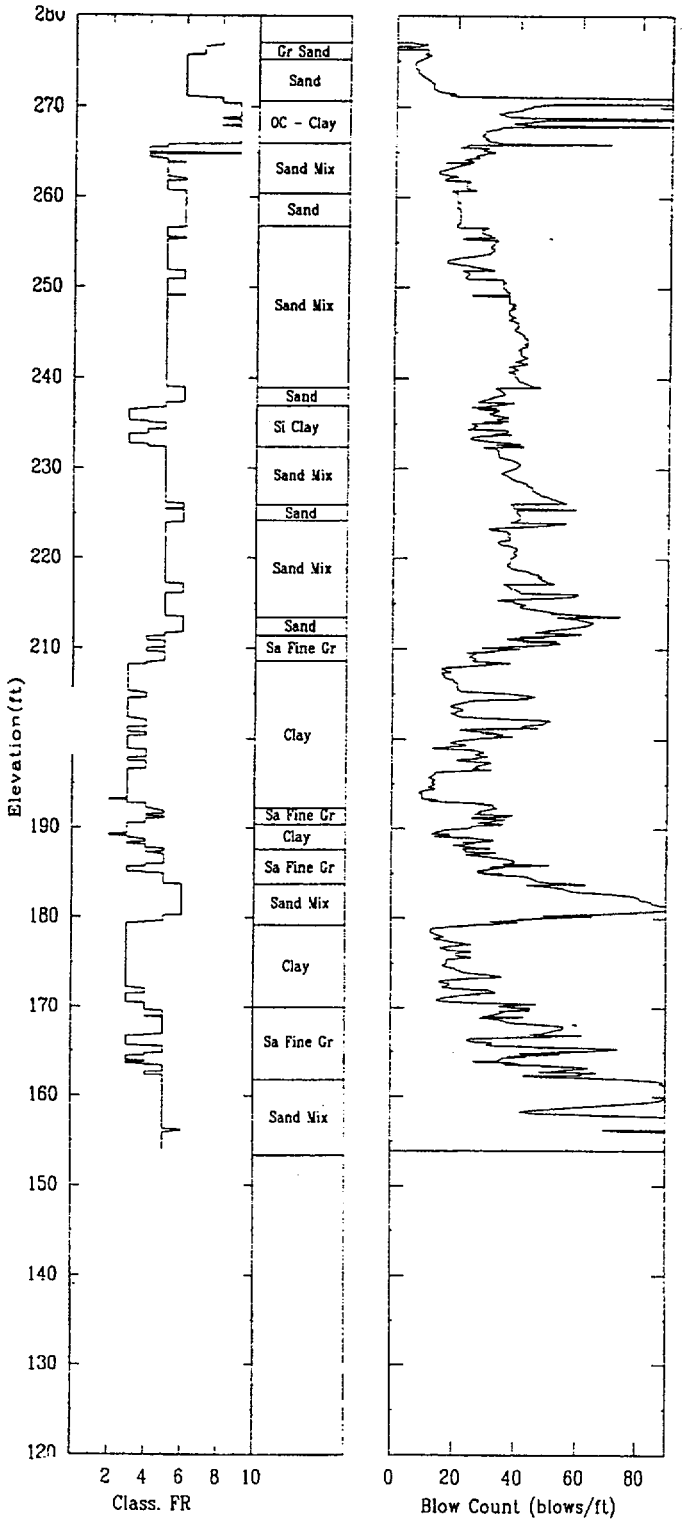

File 406u003.ECP

DCS, MFFF Project No. 08716

CPT-24 APPLIED RESEARCH ASSOCIATES, INC. 06/10/00

North 80115.0 East 55548.5 Elevation 272.6

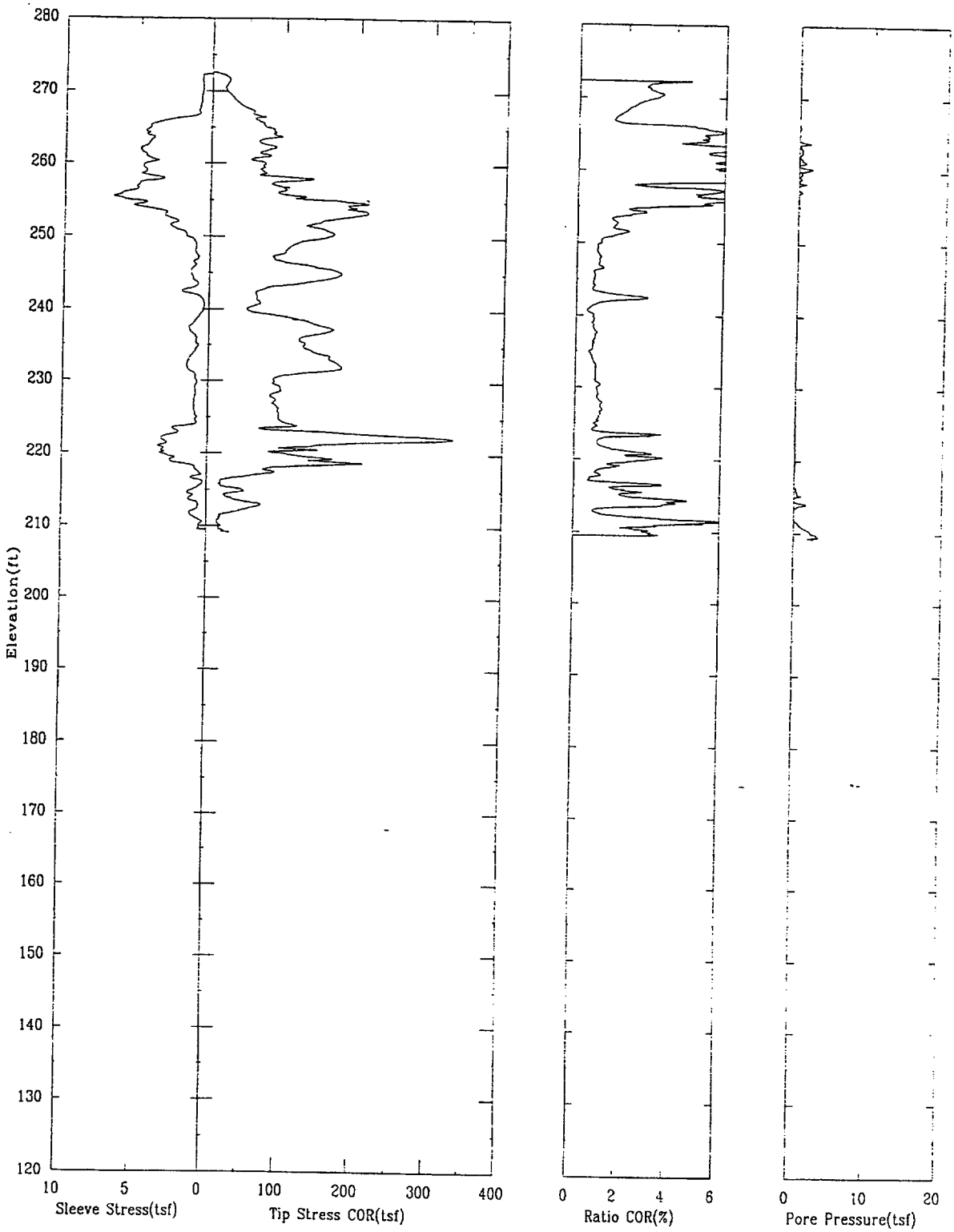

File 410u003B.ECP

CPT-24 APPLIED RESEARCH ASSOCIATES, INC. 06/10/00

North 80115.0 East 55548.5 Elevation 272.6

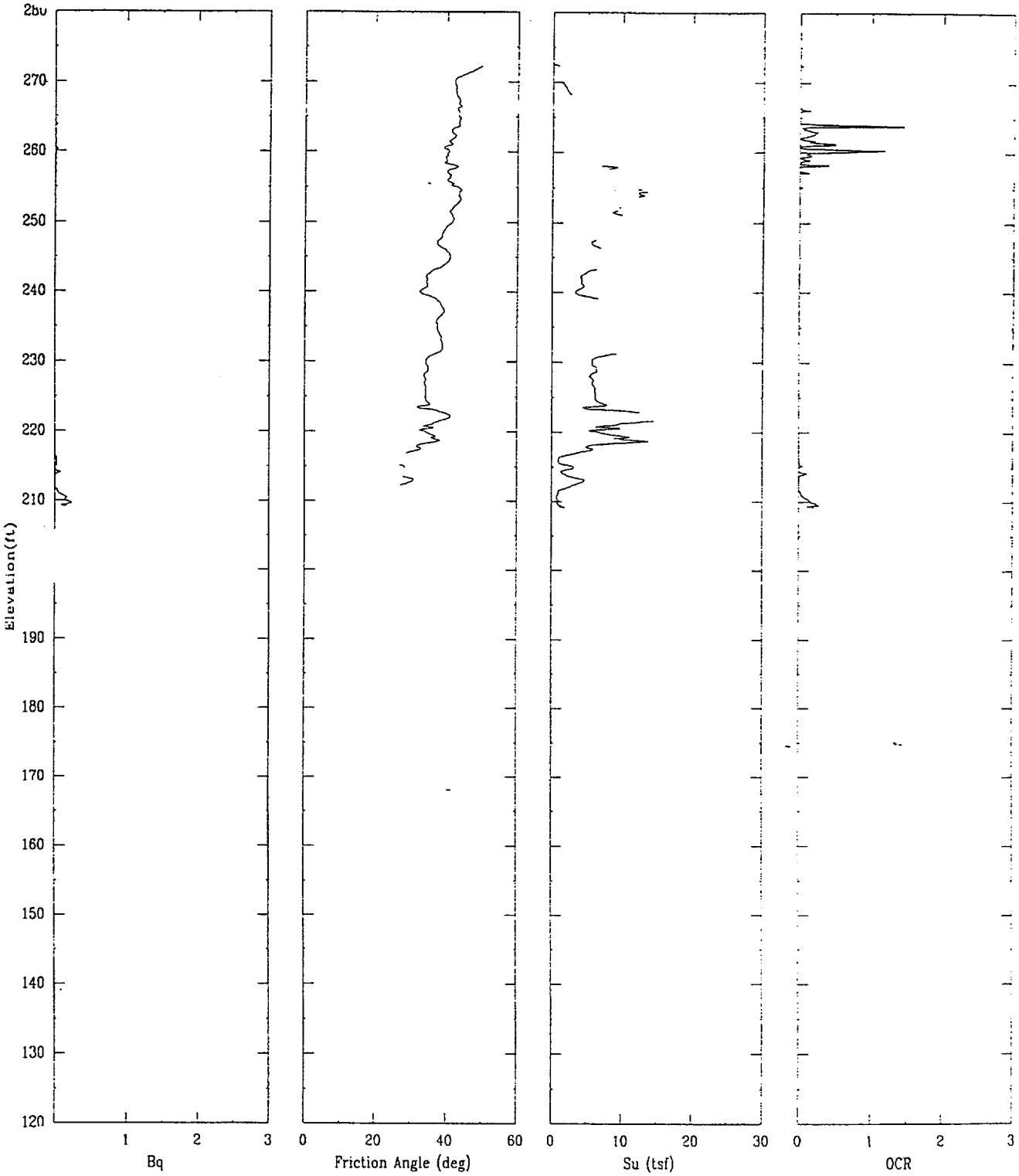

File 410u003B.ECP

DCS, MFFF Project No. 08716

CPT-24 APPLIED RESEARCH ASSOCIATES, INC. 06/10/00

North 80115.0 East 55548.5 Elevation 272.6

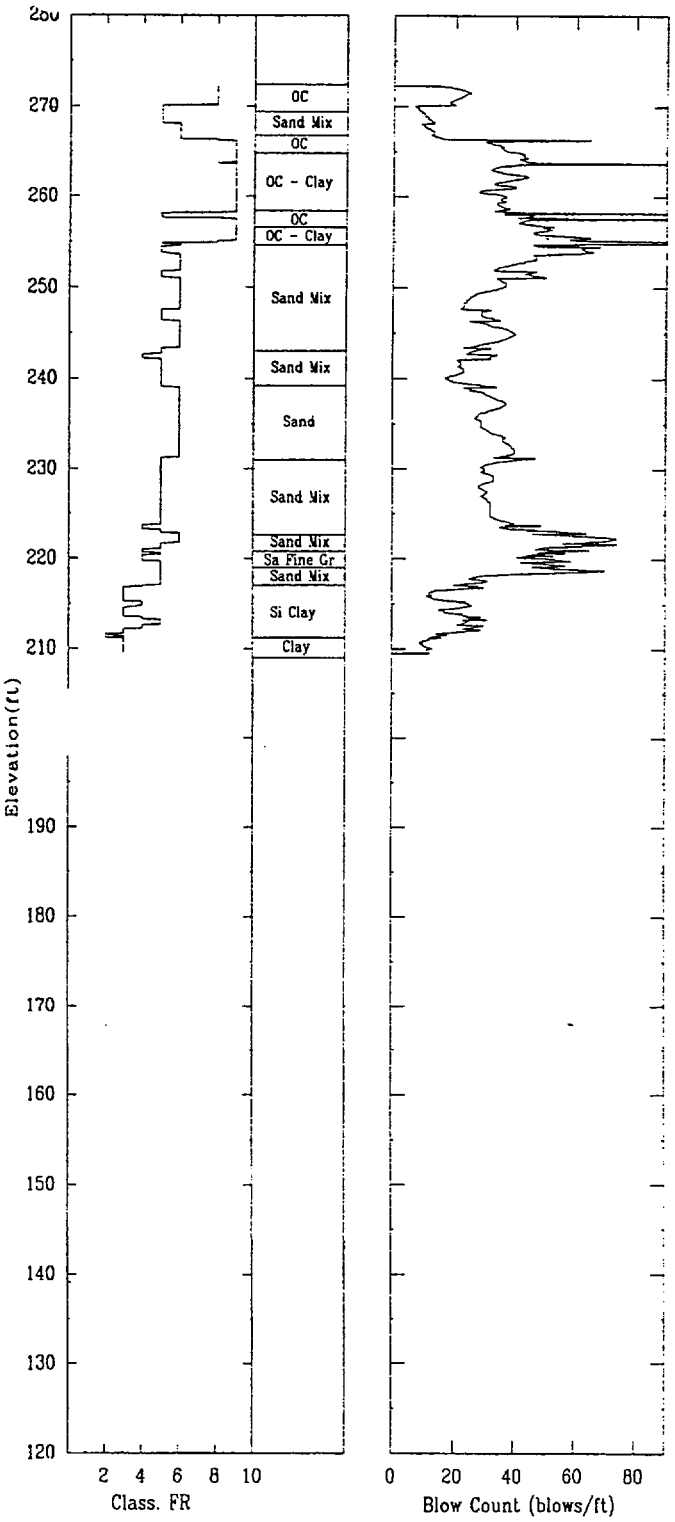

File 410u003B.ECP

DCS, MFFF Project No. 08716

CPT-24A APPLIED RESEARCH ASSOCIATES, INC. 06/10/00

North 80115.0 East 55548.5 Elevation 272.6

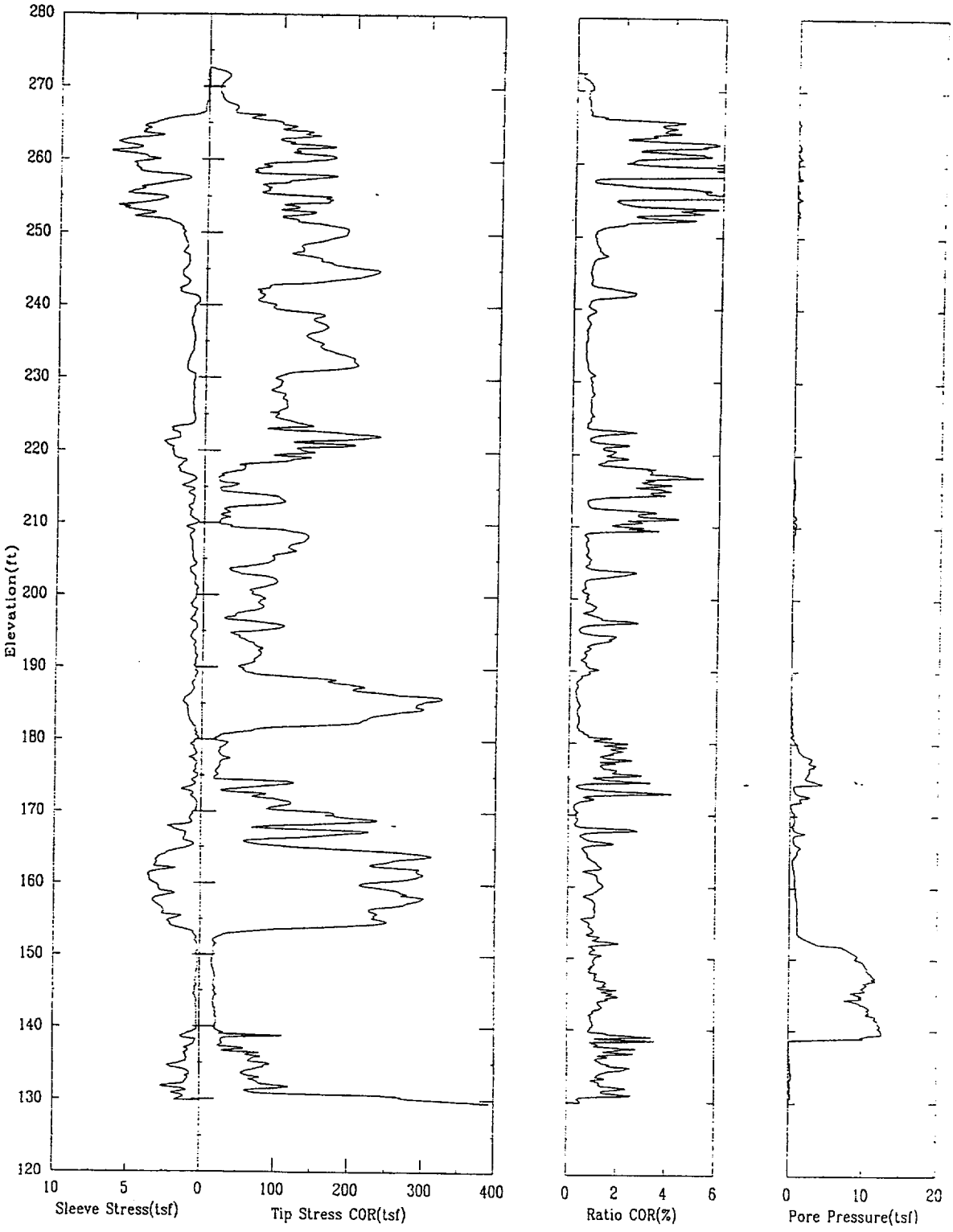

File 410u005.ECP

DCS, MFFF Project No. 08716

CPT-24A APPLIED RESEARCH ASSOCIATES, INC. 06/10/00

North 80115.0 East 55548.5 Elevation 272.6

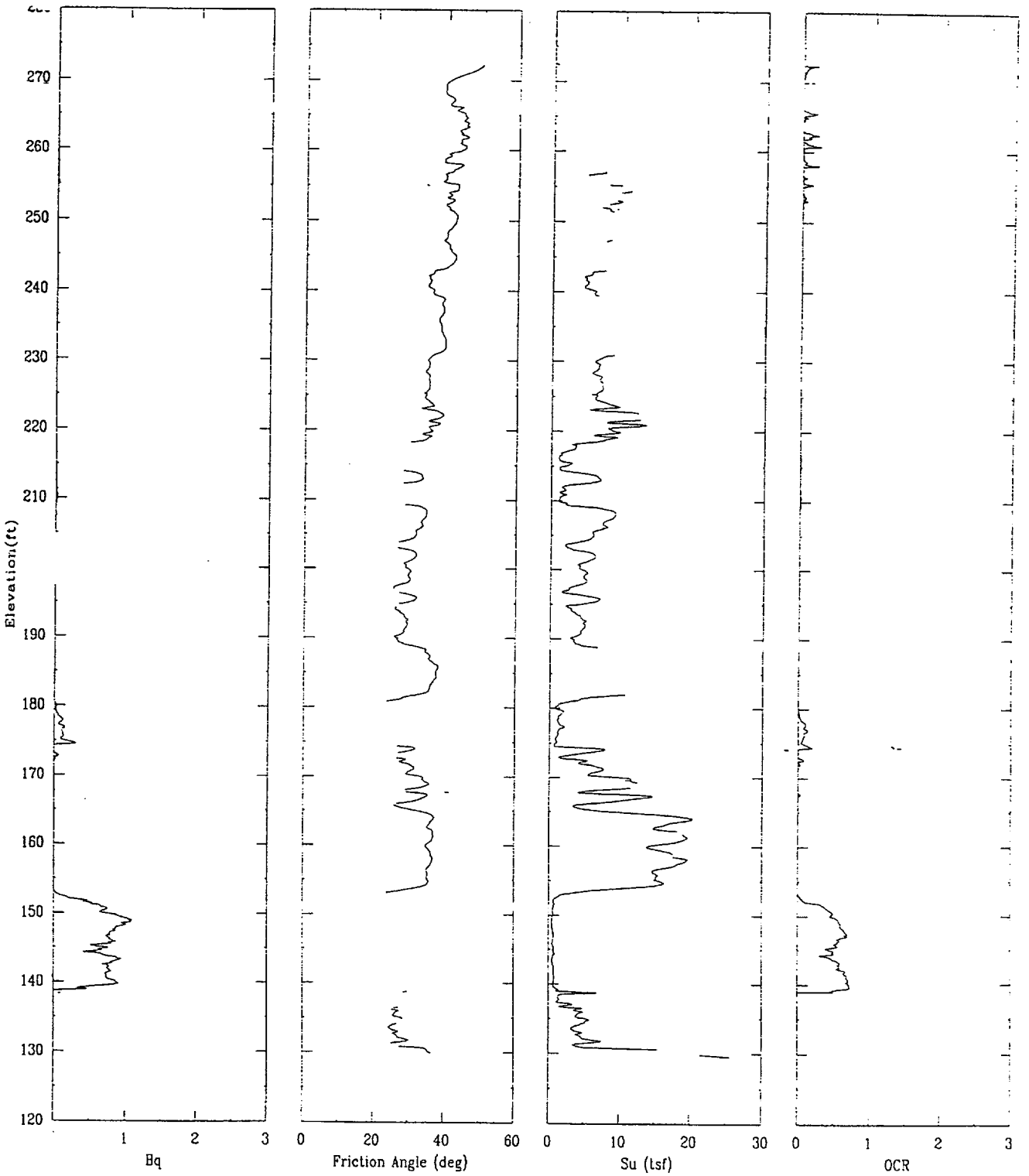

File 410u005.ECP

DCS, MFFF Project No. 08716

CPT-24A APPLIED RESEARCH ASSOCIATES, INC. 06/10/00

North 80115.0 East 55548.5 Elevation 272.6

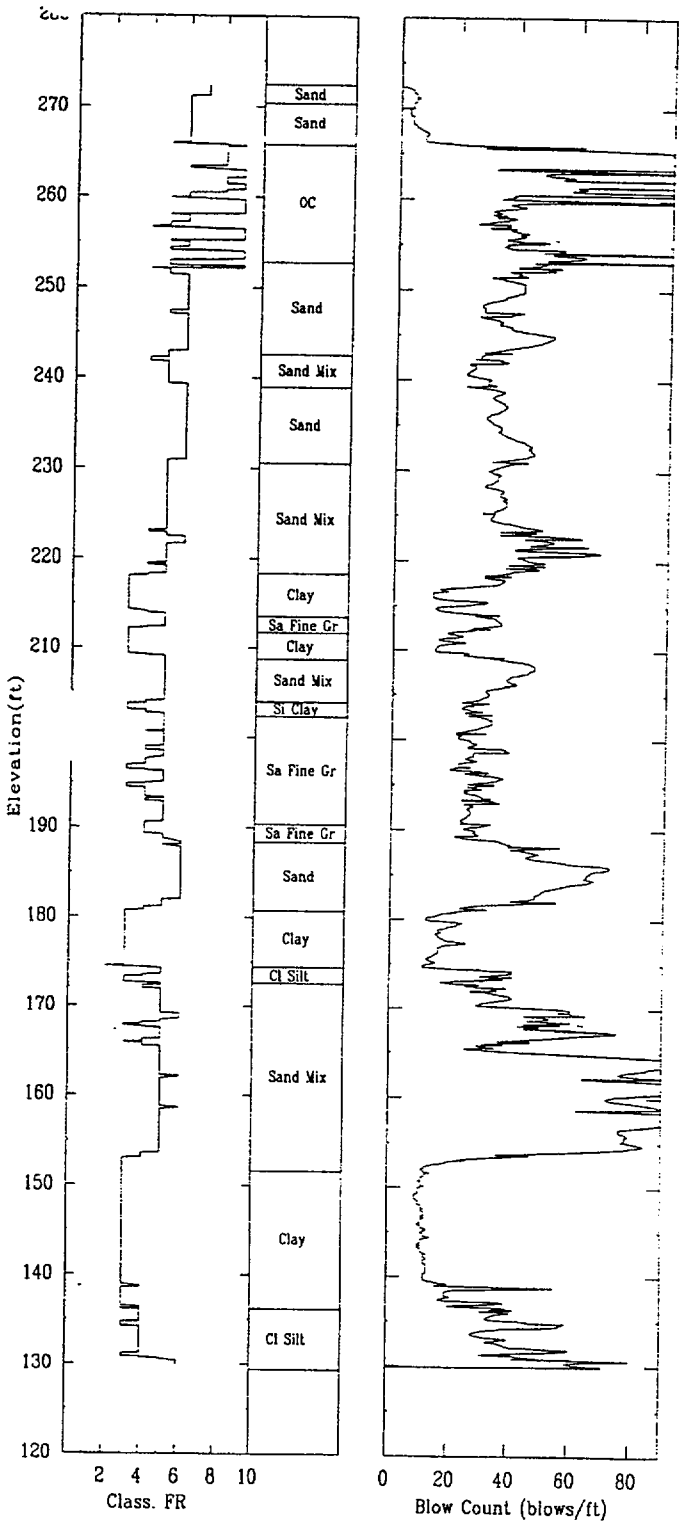

File 410u005.ECP

CPT-25 APPLIED RESEARCH ASSOCIATES, INC. 06/12/00

North 80104.7 East 55621.7 Elevation 268.9

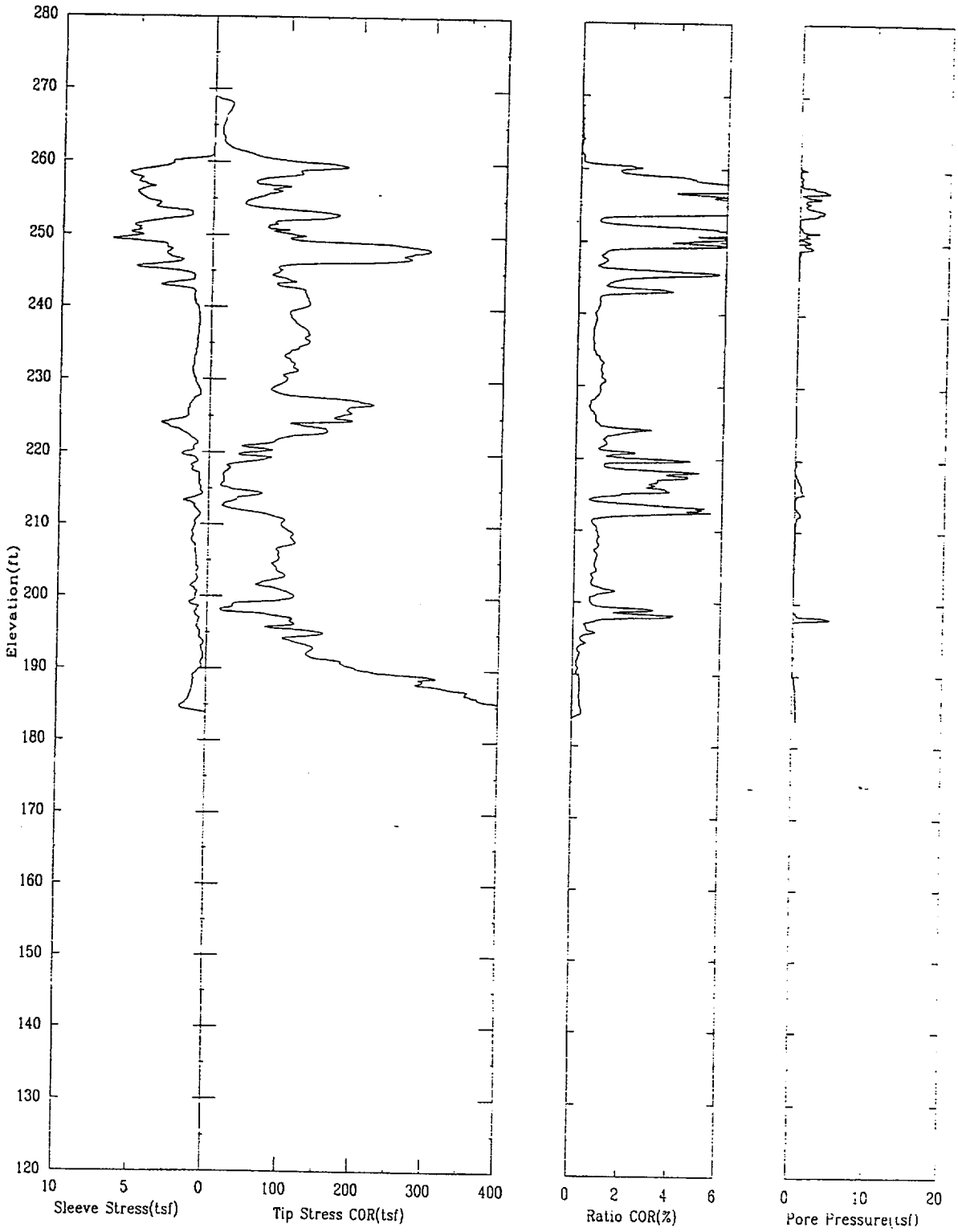

File 412u001.ECP

CPT-25 APPLIED RESEARCH ASSOCIATES, INC. 06/12/00

North 80104.7 East 55621.7 Elevation 268.9

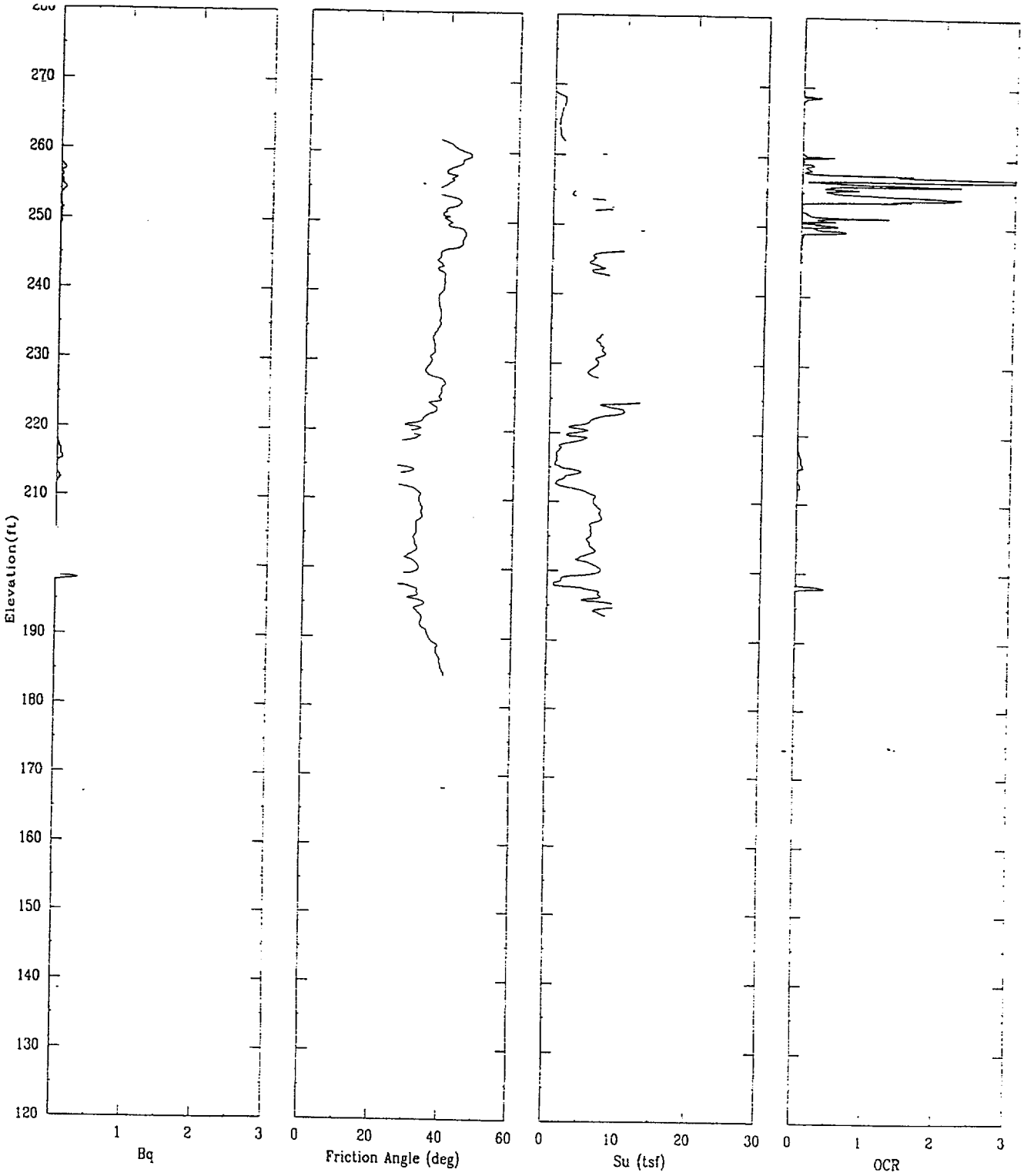

File 412u001.ECP

CPT-25 APPLIED RESEARCH ASSOCIATES, INC. 06/12/00

North 80104.7 East 55621.7 Elevation 268.9

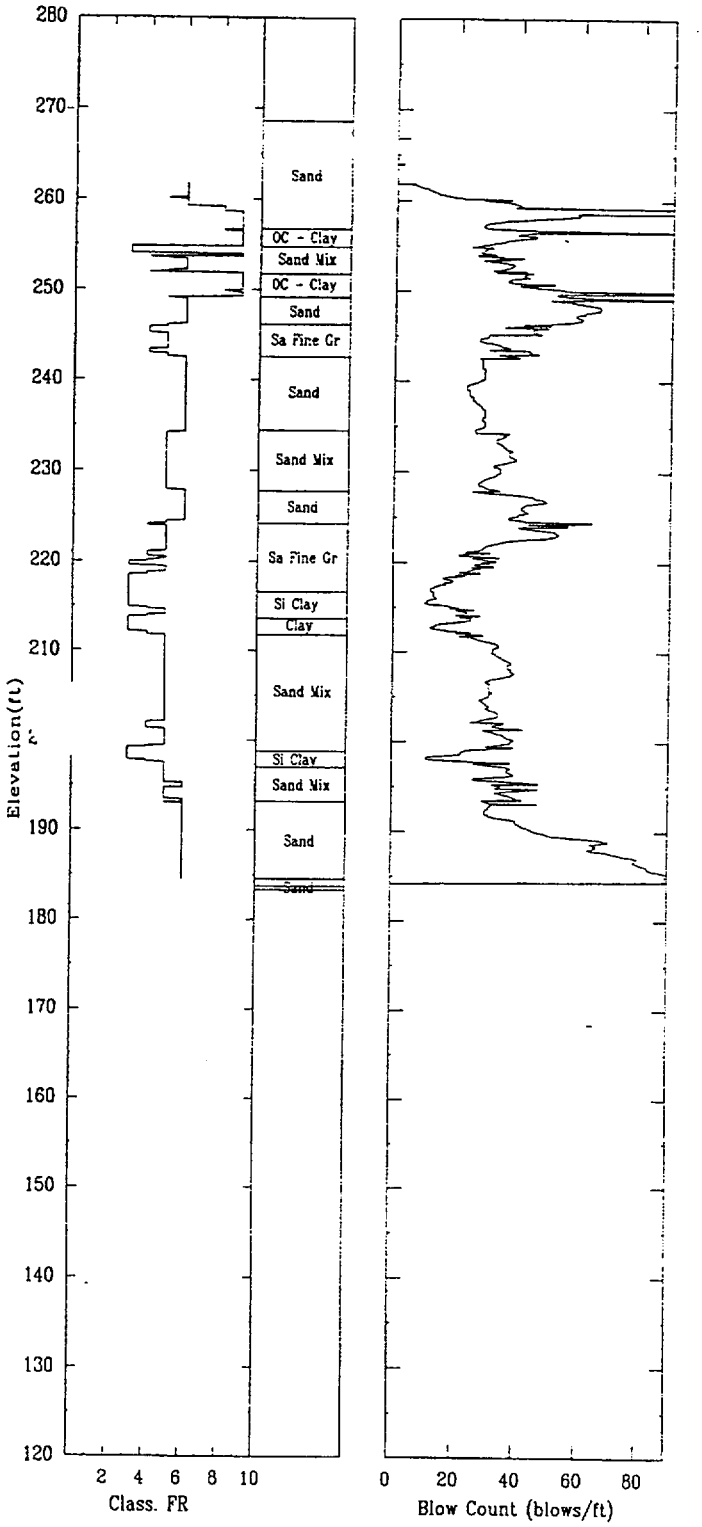

File 412u001.ECP

DCS, MFFF Project No. 08716

CPT-26S APPLIED RESEARCH ASSOCIATES, INC. 06/06/00

North 80116.2 East 55726.7 Elevation 261.9

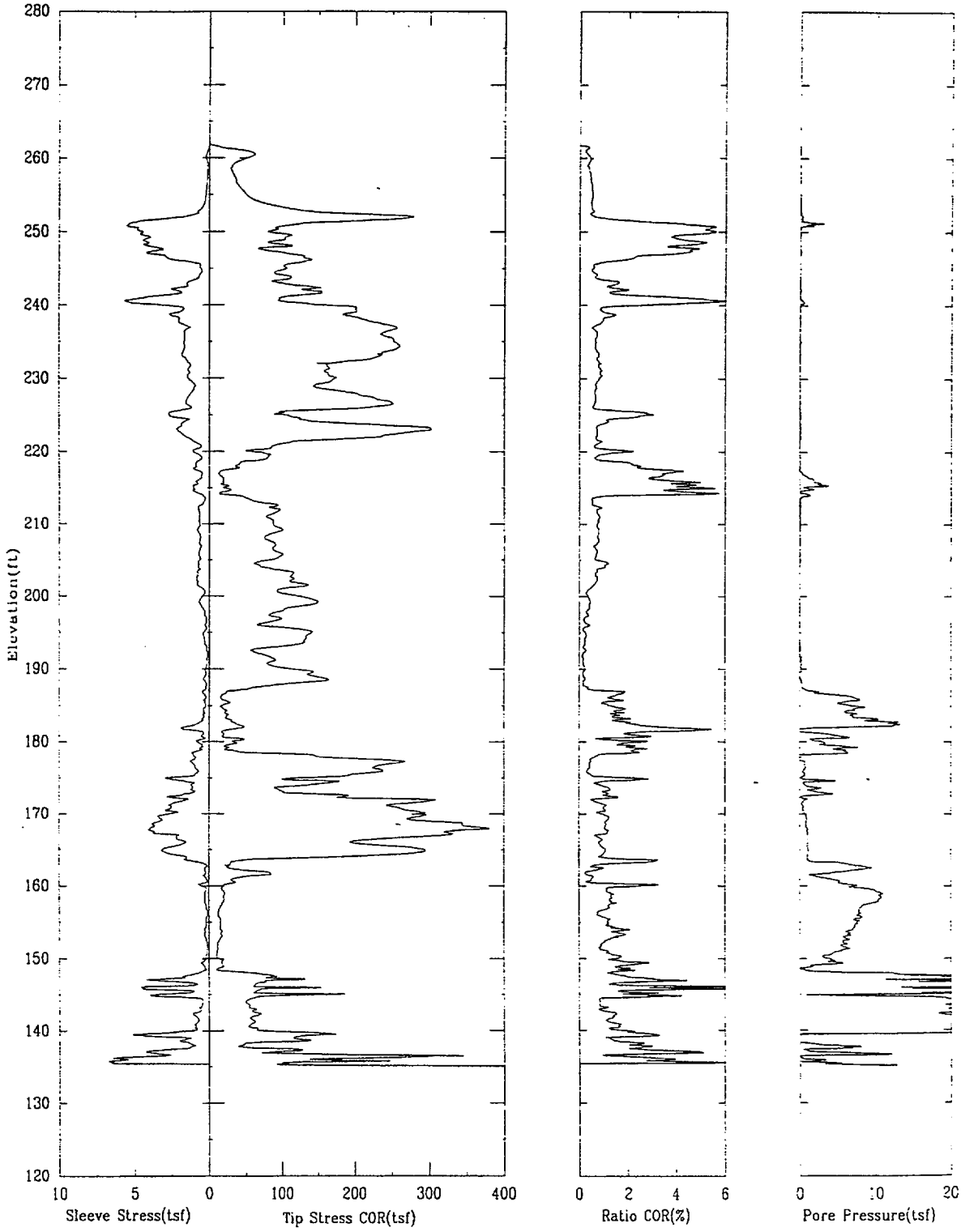

File 406u001.ECP

DCS, MFFF Project No. 08716

CPT-26S APPLIED RESEARCH ASSOCIATES, INC. 06/06/00

North 80116.2 East 55726.7 Elevation 261.9

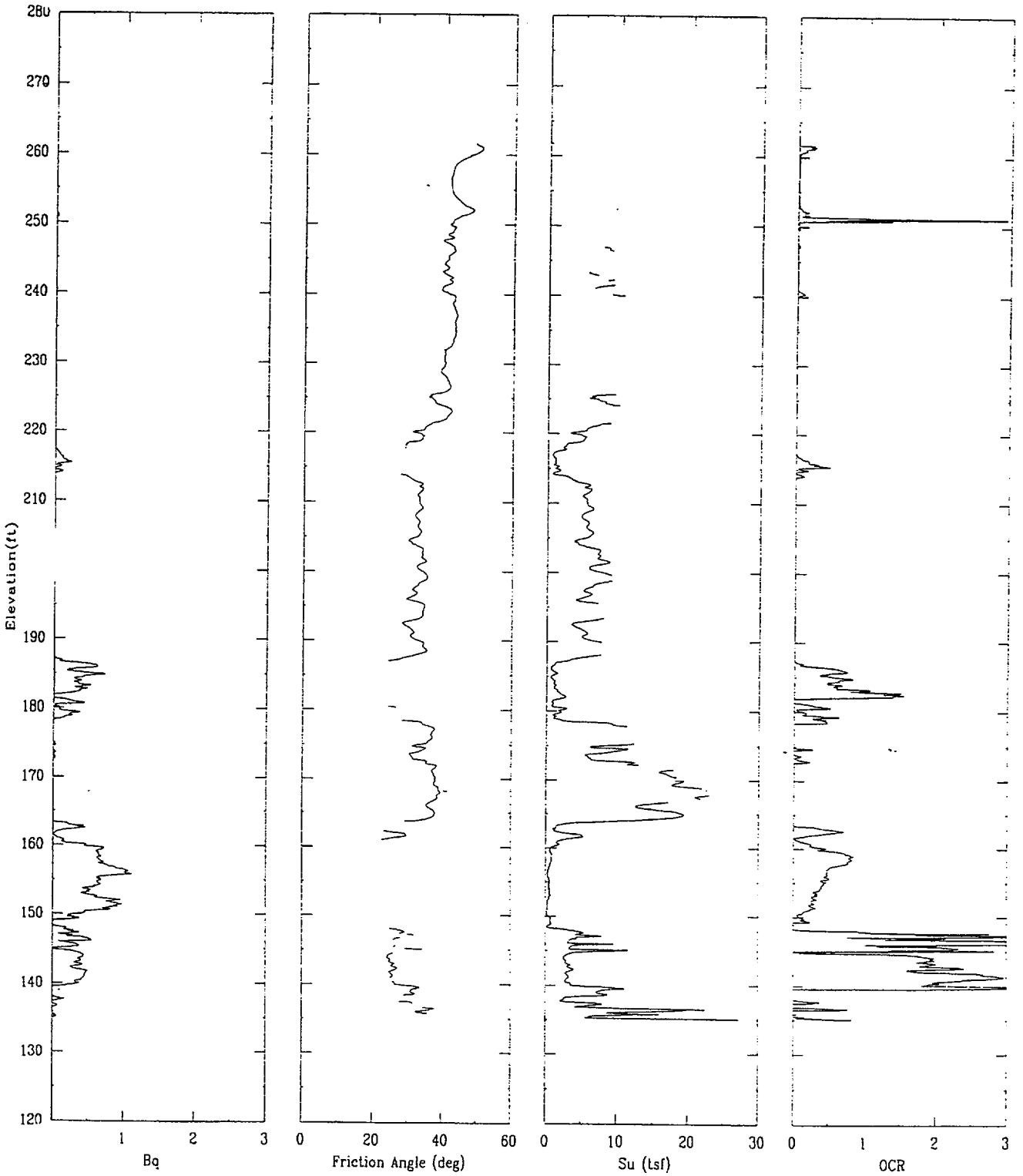

File 406u001.ECP

DCS, MFFF Project No. 08716

CPT-26S APPLIED RESEARCH ASSOCIATES, INC. 06/06/00

North 80116.2 East 55726.7 Elevation 261.9

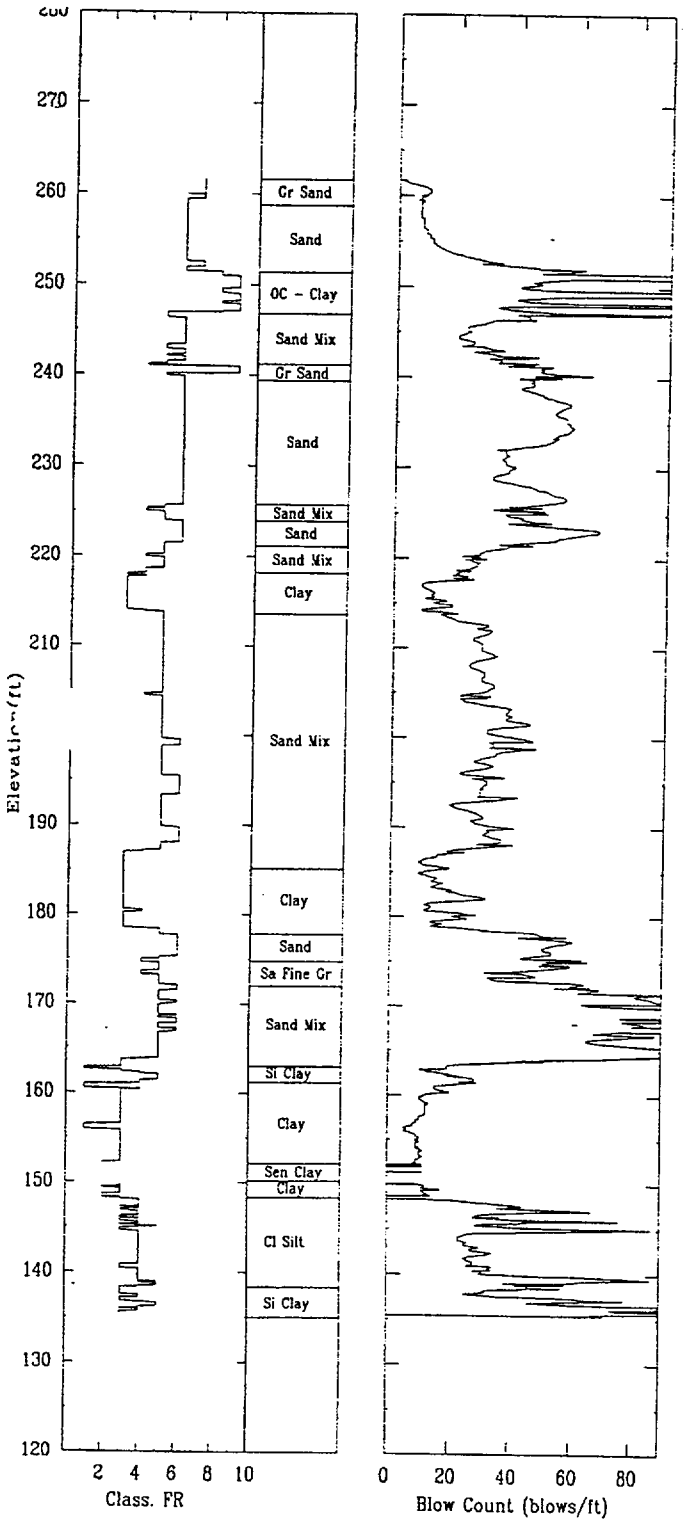

File 406u001.ECP

DCS, MFFF Project No. 08716

CPT-27R APPLIED RESEARCH ASSOCIATES, INC. 06/22/00

North 80001.4 East 55254.2 Elevation 277.5

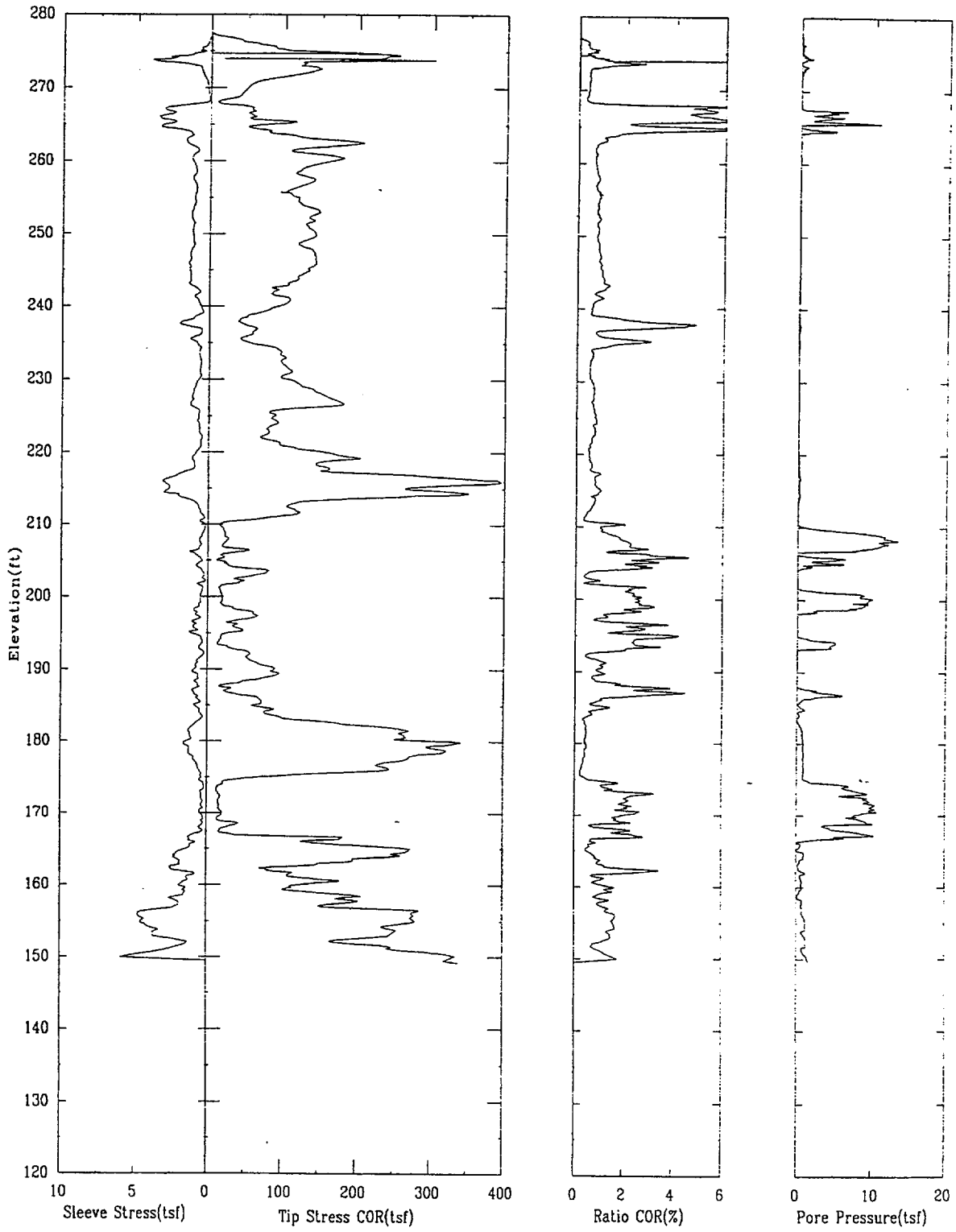

File 322u008.ECP

CPT-27R APPLIED RESEARCH ASSOCIATES, INC. 06/22/00

North 80001.4 East 55254.2 Elevation 277.5

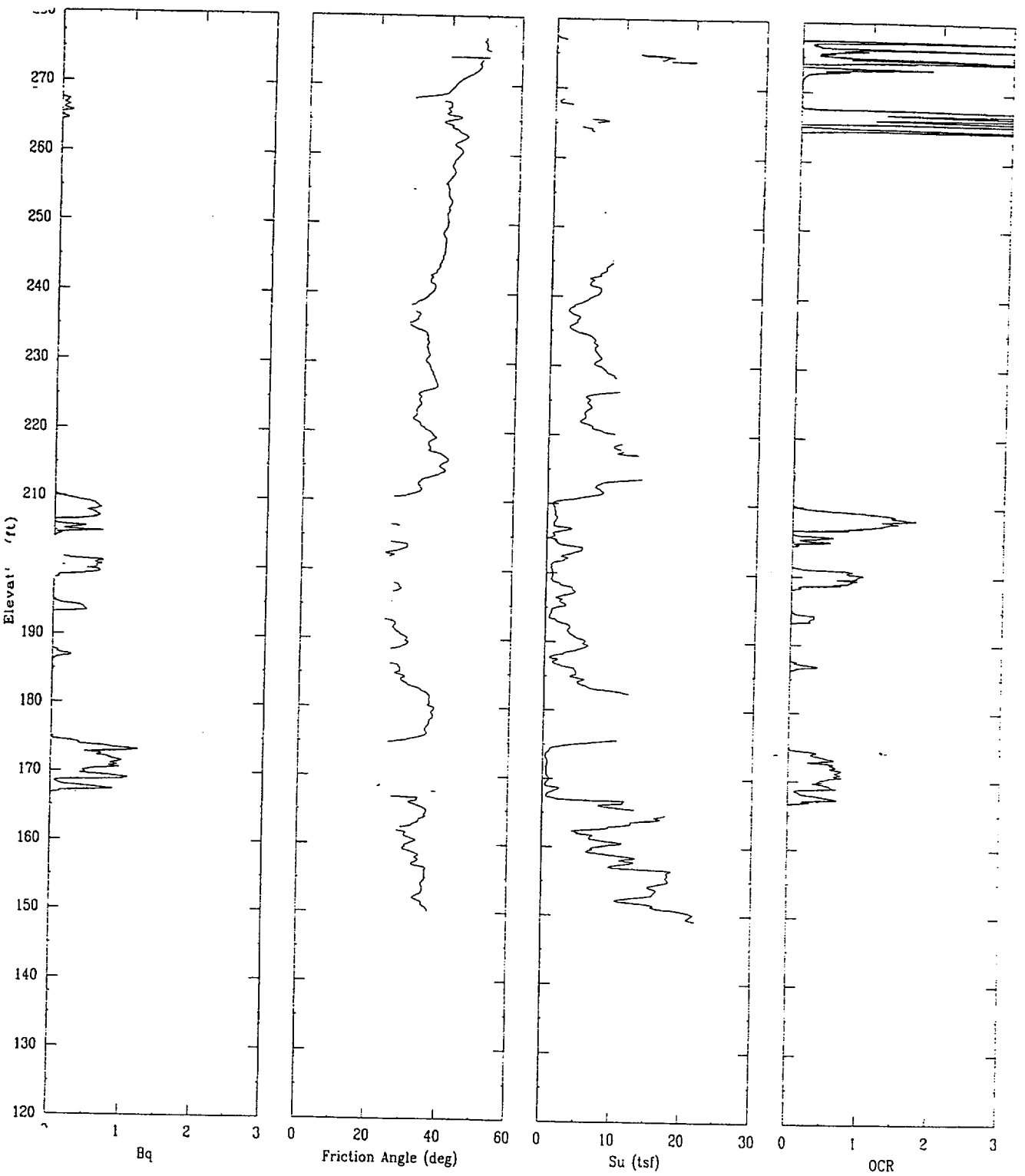

File 322u008.ECP

CPT-27R APPLIED RESEARCH ASSOCIATES, INC. 06/22/00

North 80001.4 East 55254.2 Elevation 277.5

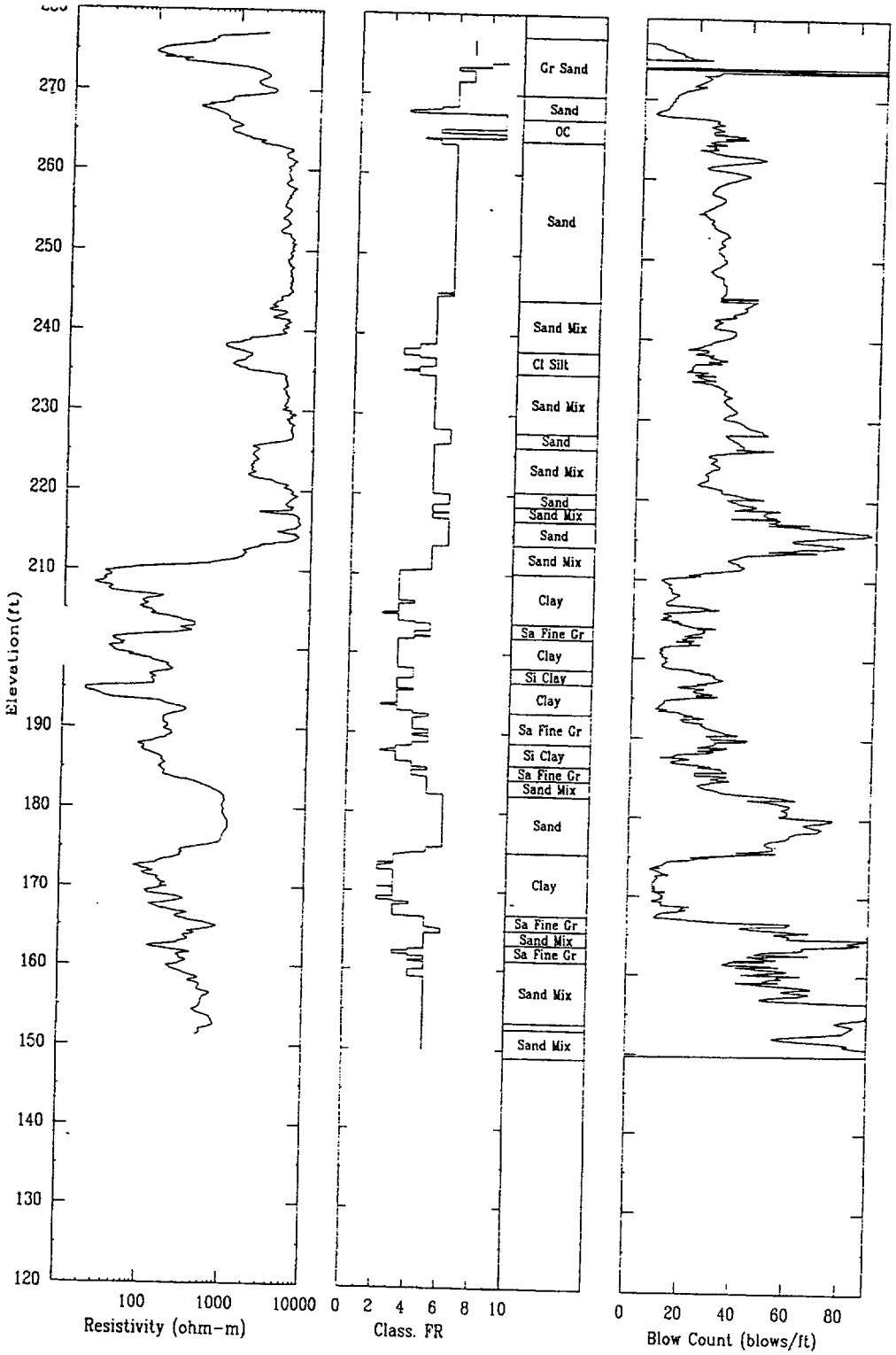

File 322u008.ECP

DCS, MFFF Project No. 08716

CPT-28S APPLIED RESEARCH ASSOCIATES, INC. 05/31/00

North 80001.8 East 55332.0 Elevation 279.2

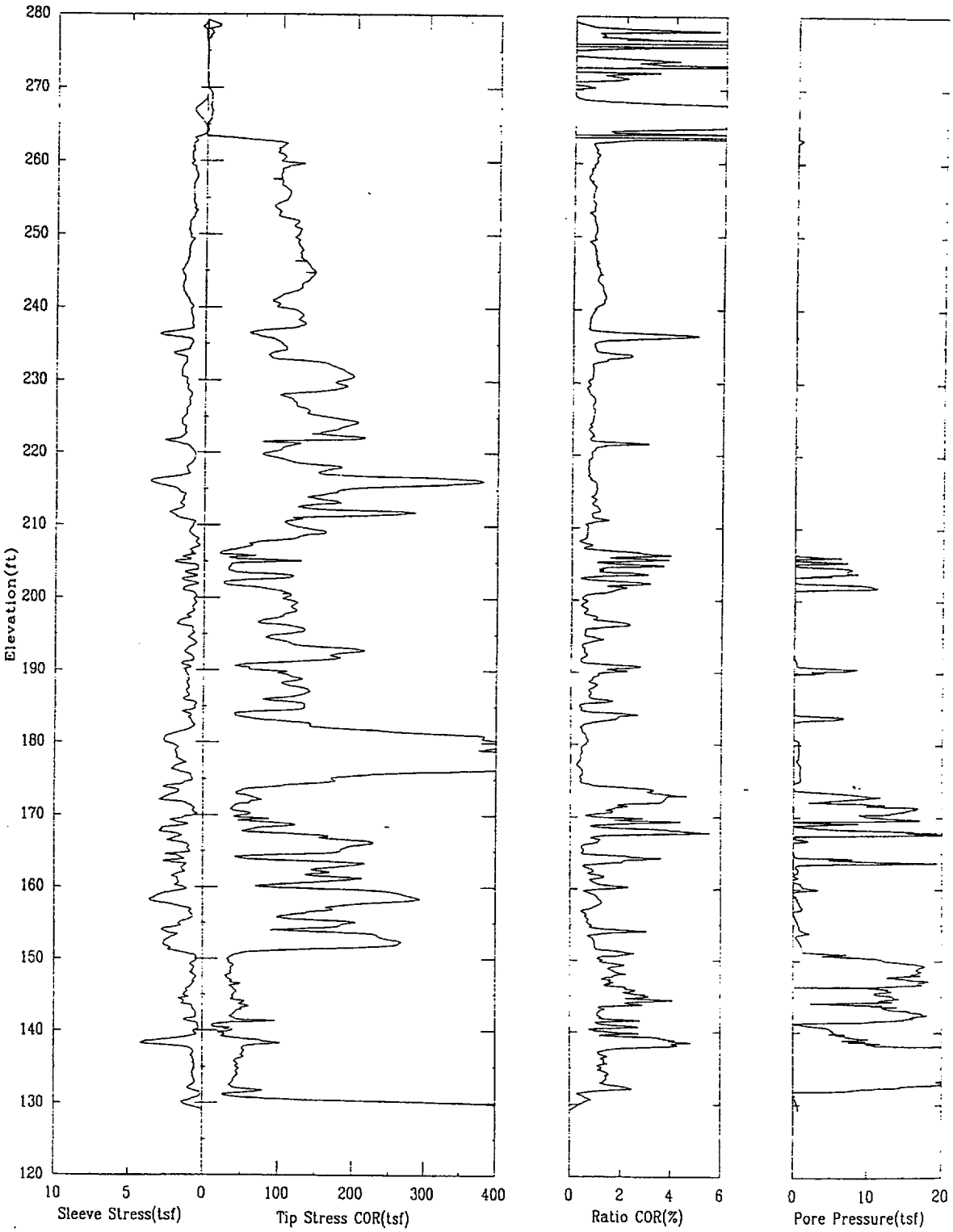

File 431y006.ECP

DCS, MFFF Project No. 08716

CPT-28S APPLIED RESEARCH ASSOCIATES, INC. 05/31/00

North 80001.8 East 55332.0 Elevation 279.2

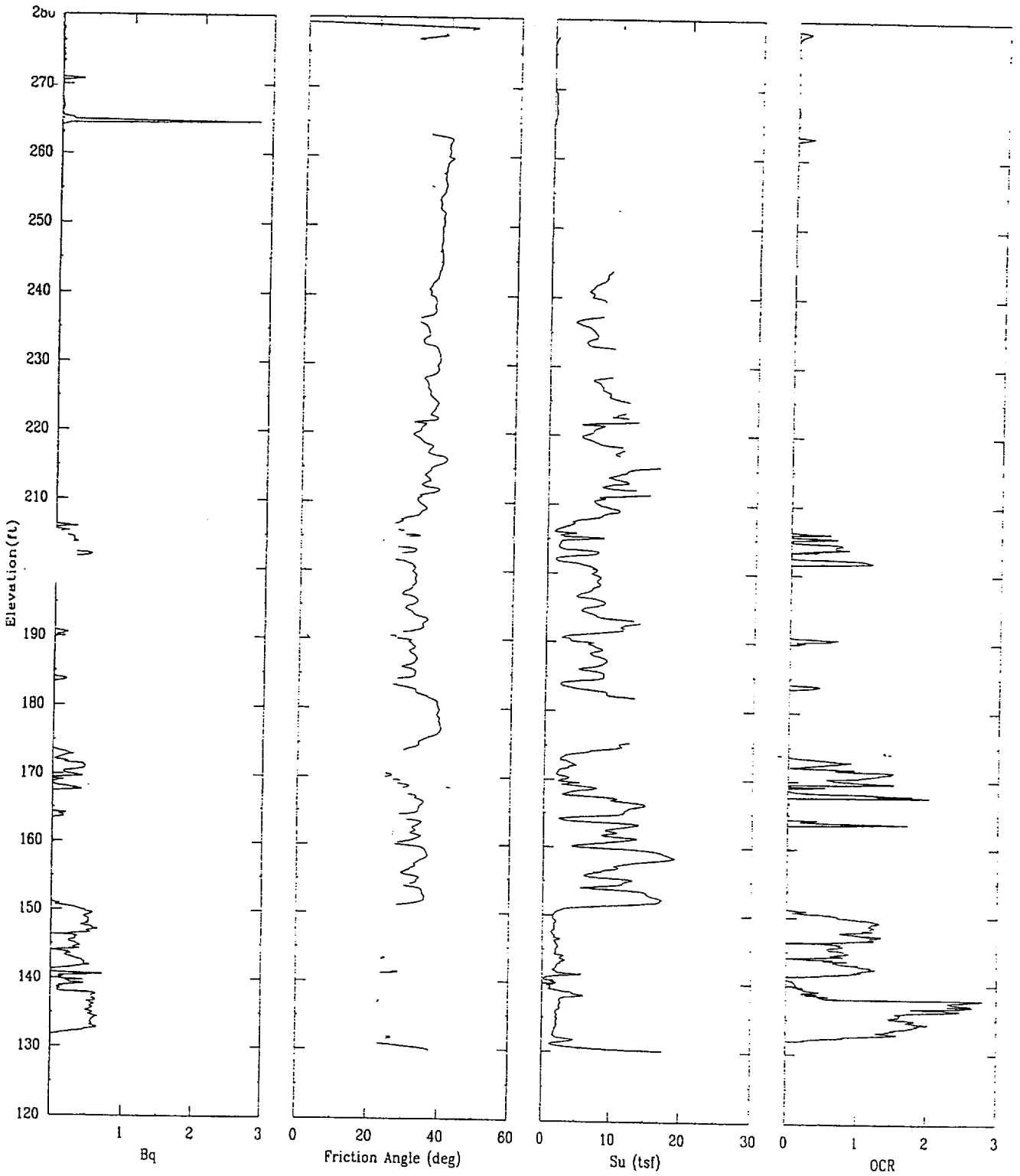

File 431y006.ECP

CPT-28S APPLIED RESEARCH ASSOCIATES, INC. 05/31/00

North 80001.8 East 55332.0 Elevation 279.2

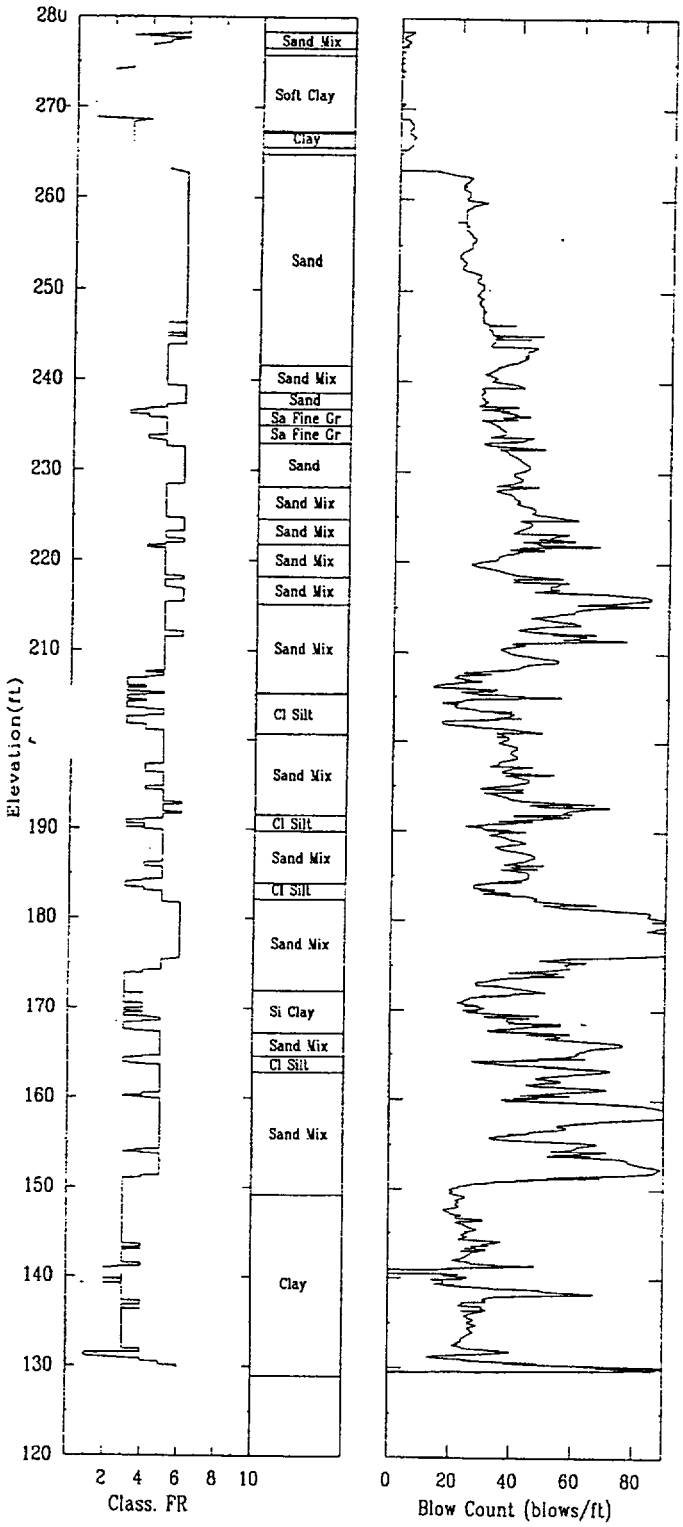

File 431y006.ECP

DCS, MFFF Project No. 08716

CPT-29R APPLIED RESEARCH ASSOCIATES, INC. 06/13/00

North 79985.8 East 55422.4 Elevation 276.4

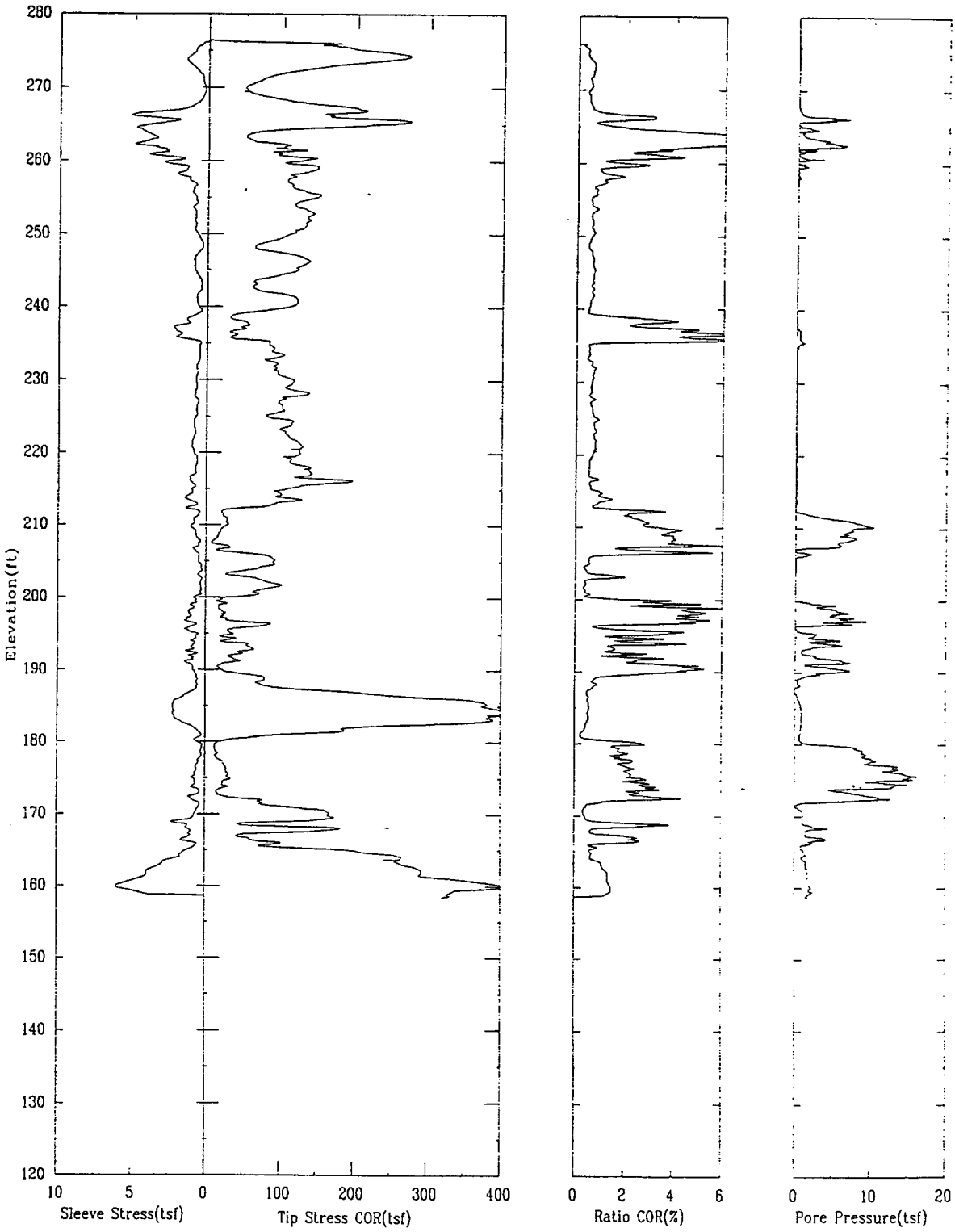

File 413u009.ECP

CPT-29R APPLIED RESEARCH ASSOCIATES, INC. 06/13/00

North 79985.8 East 55422.4 Elevation 276.4

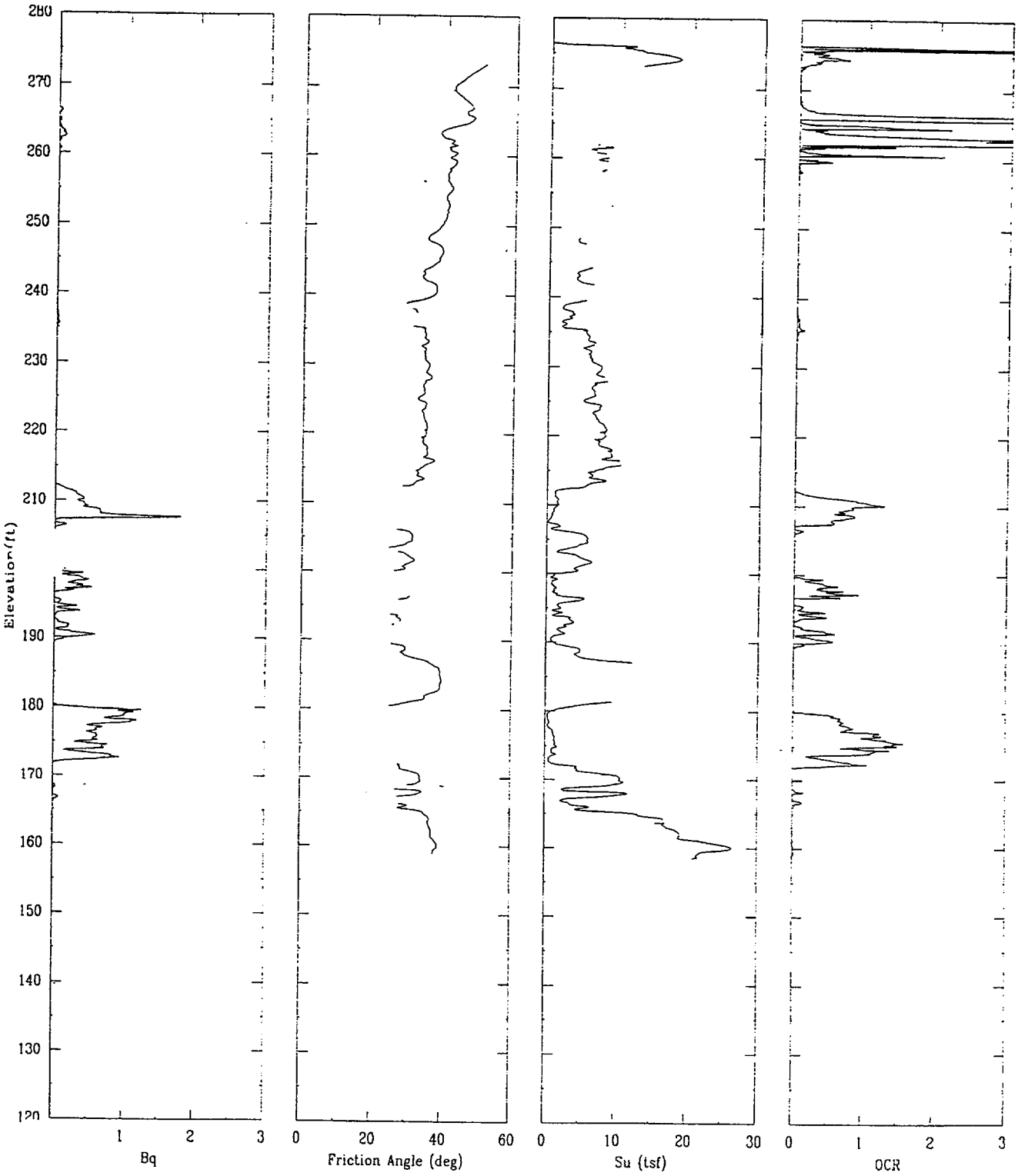

CPT-29R APPLIED RESEARCH ASSOCIATES, INC. 06/13/00

North 79985.8 East 55422.4 Elevation 276.4

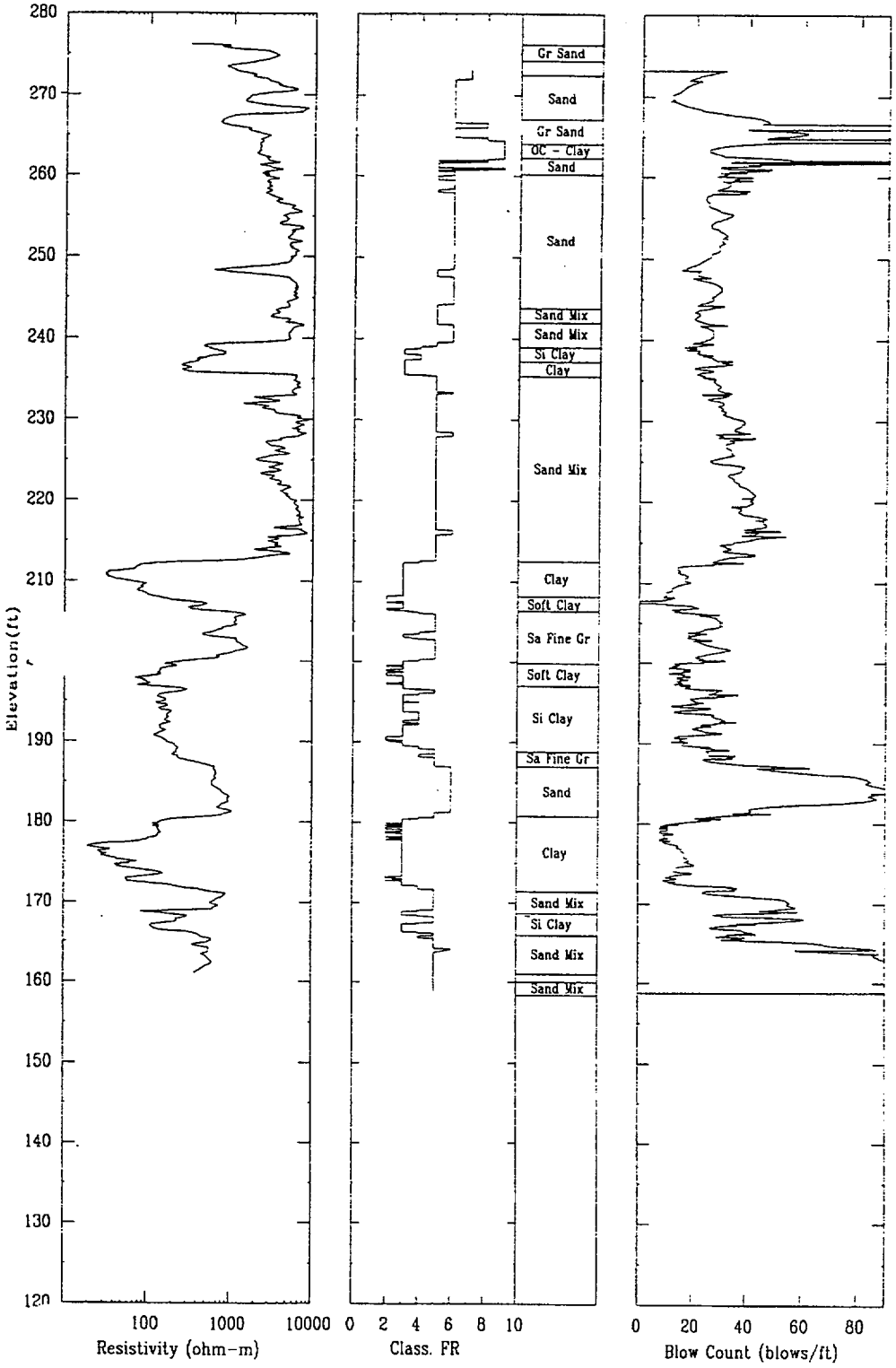

File 413u009.ECP

DCS, MFFF Project No. 08716

CPT-30R APPLIED RESEARCH ASSOCIATES, INC. 06/14/00

North 79973.4 East 55538.3 Elevation 274.2

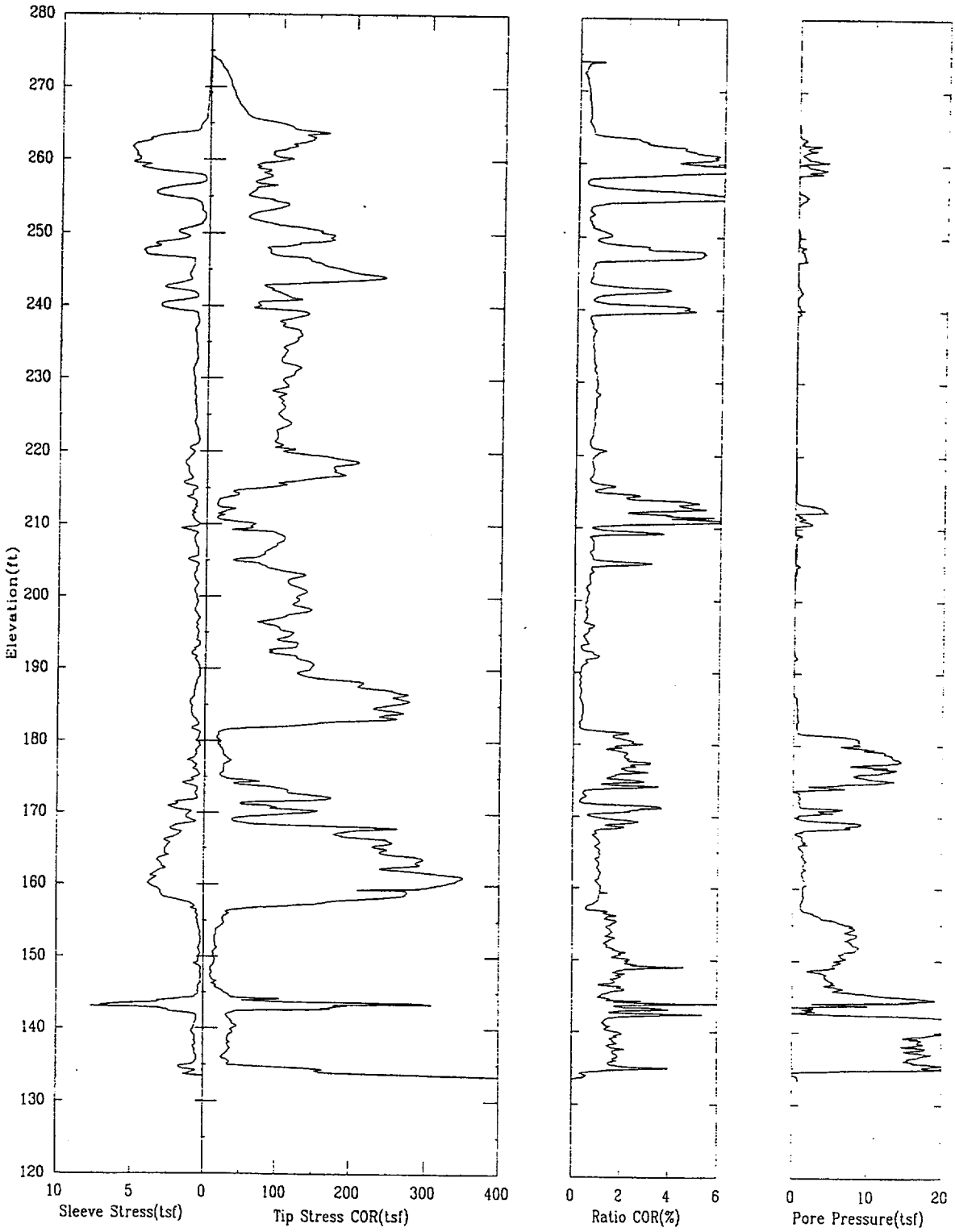

File 414u001.ECP

CPT-30R APPLIED RESEARCH ASSOCIATES, INC. 06/14/00

North 79973.4 East 55538.3 Elevation 274.2

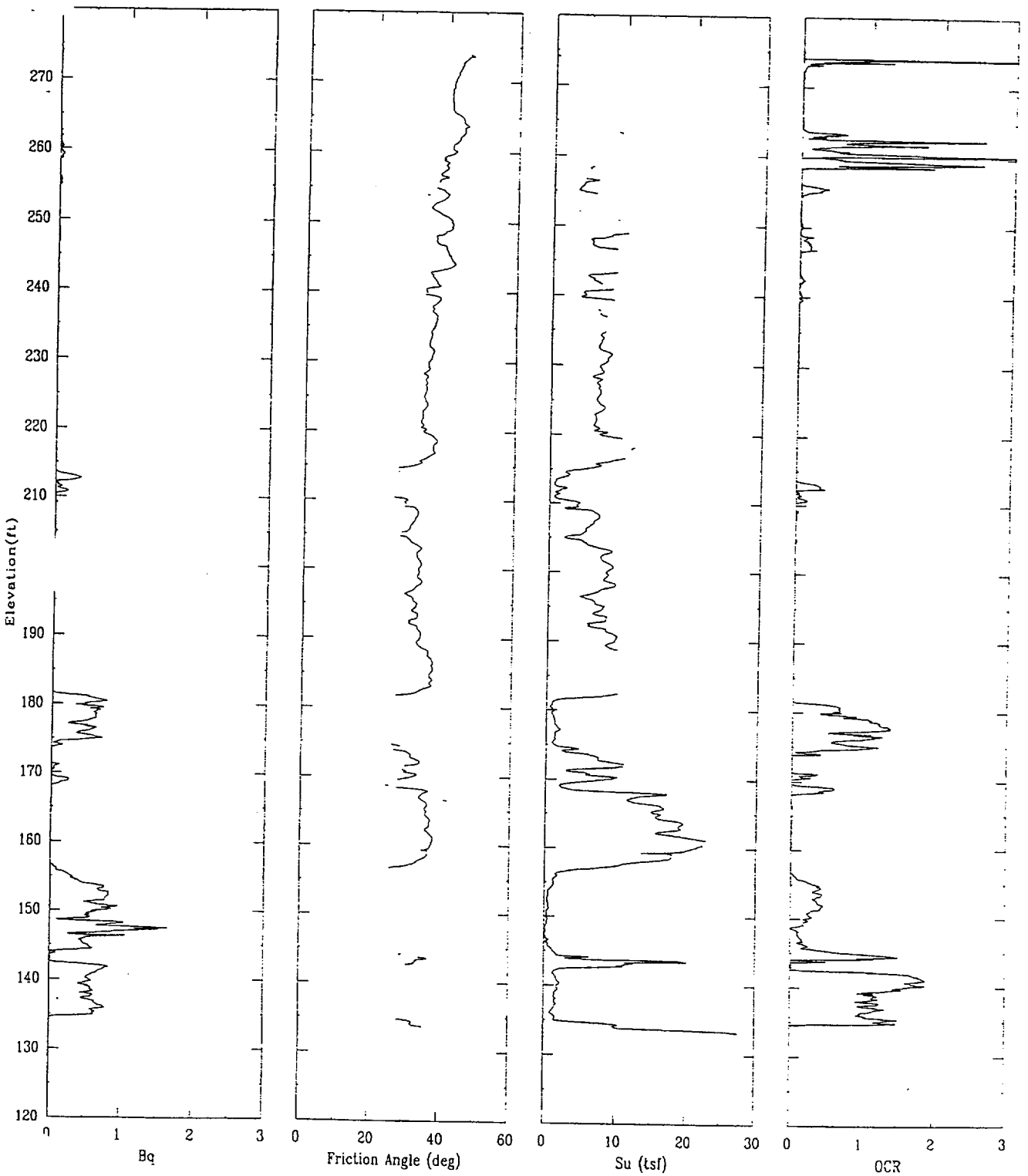

File 414u001.ECP

CPT-30R APPLIED RESEARCH ASSOCIATES, INC. 06/14/00

North 79973.4 East 55538.3 Elevation 274.2

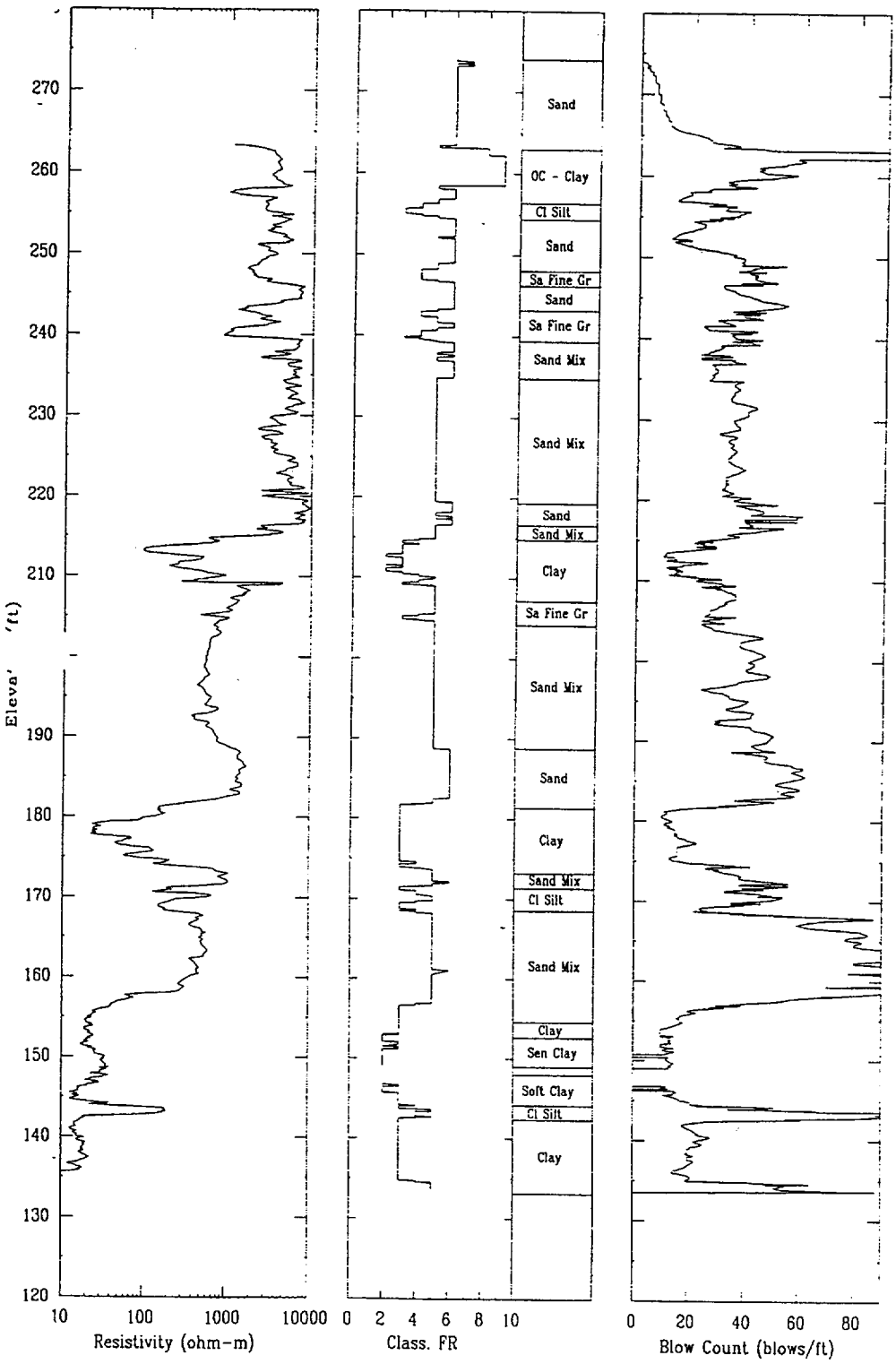

File 414u001.ECP

CPT-31S APPLIED RESEARCH ASSOCIATES, INC. 06/01/00

North 79977.3 East 55610.3 Elevation 271.7

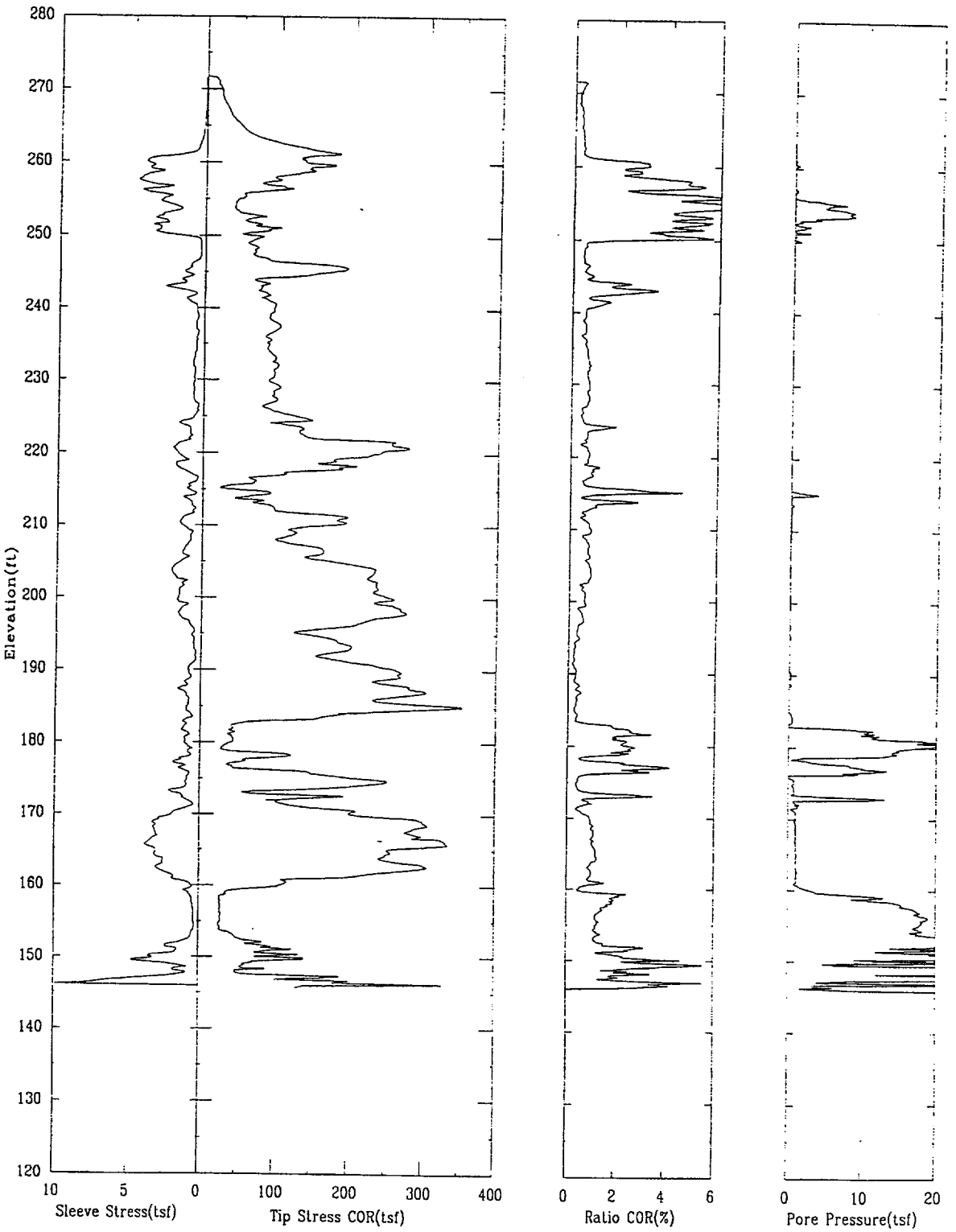

File 401u002.ECP

CPT-31S APPLIED RESEARCH ASSOCIATES, INC. 06/01/00

North 79977.3 East 55610.3 Elevation 271.7

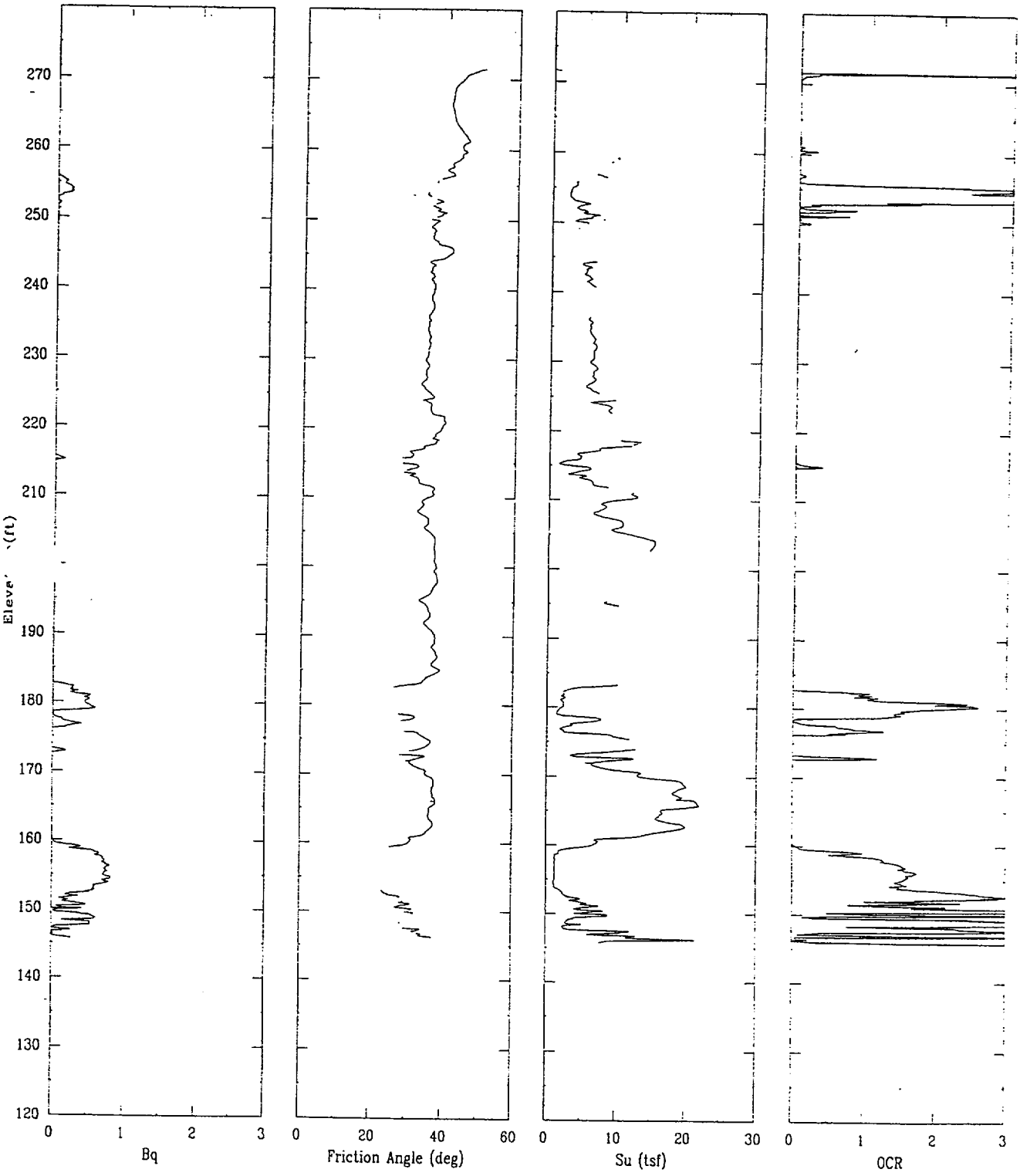

File 401u002.ECP

CPT-31S APPLIED RESEARCH ASSOCIATES, INC. 06/01/00

North 79977.3 East 55610.3 Elevation 271.7

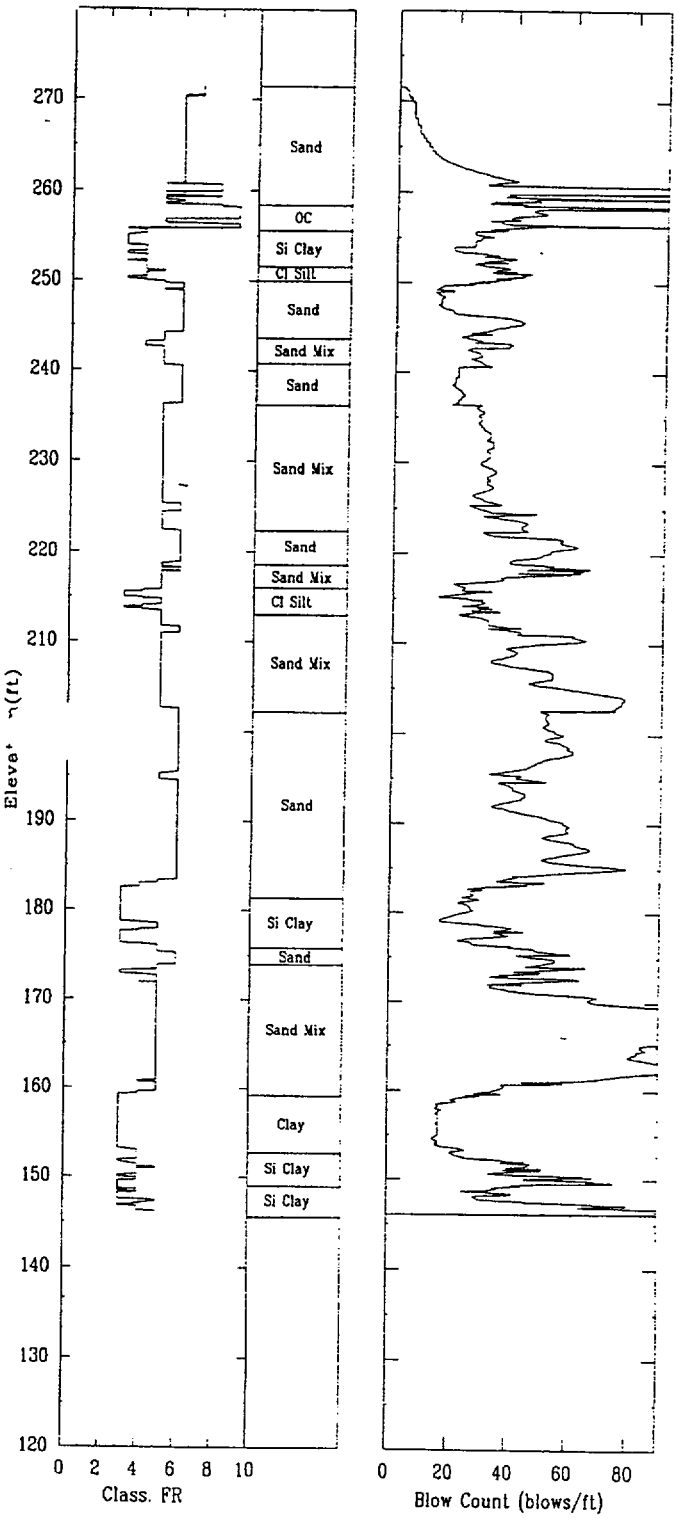

File 401u002.ECP

CPT-32R APPLIED RESEARCH ASSOCIATES, INC. 06/24/00

North 80005.4 East 55755.6 Elevation 264.7

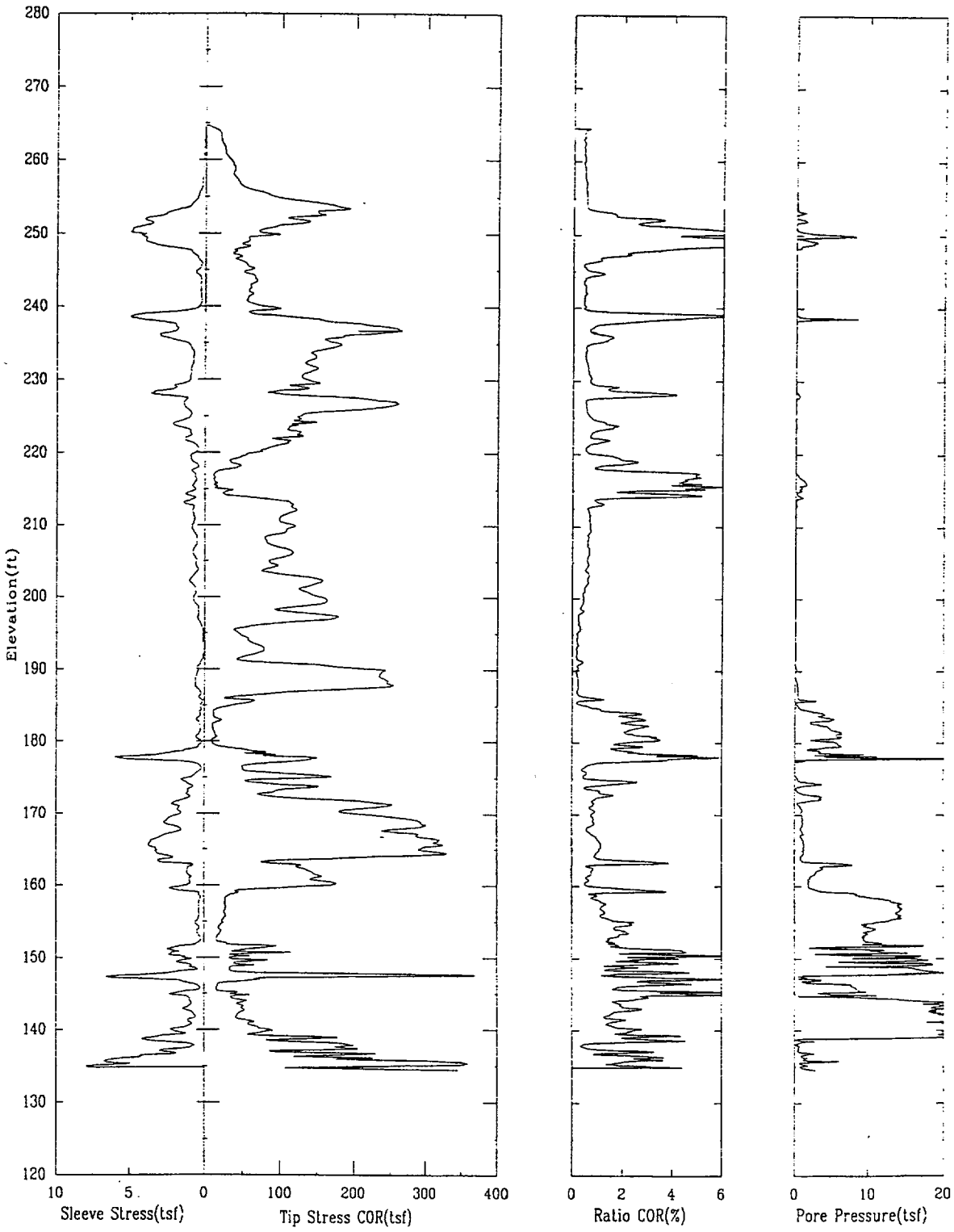

File 324u001.ECP

CPT-32R APPLIED RESEARCH ASSOCIATES, INC. 06/24/00

North 80005.4 East 55755.6 Elevation 264.7

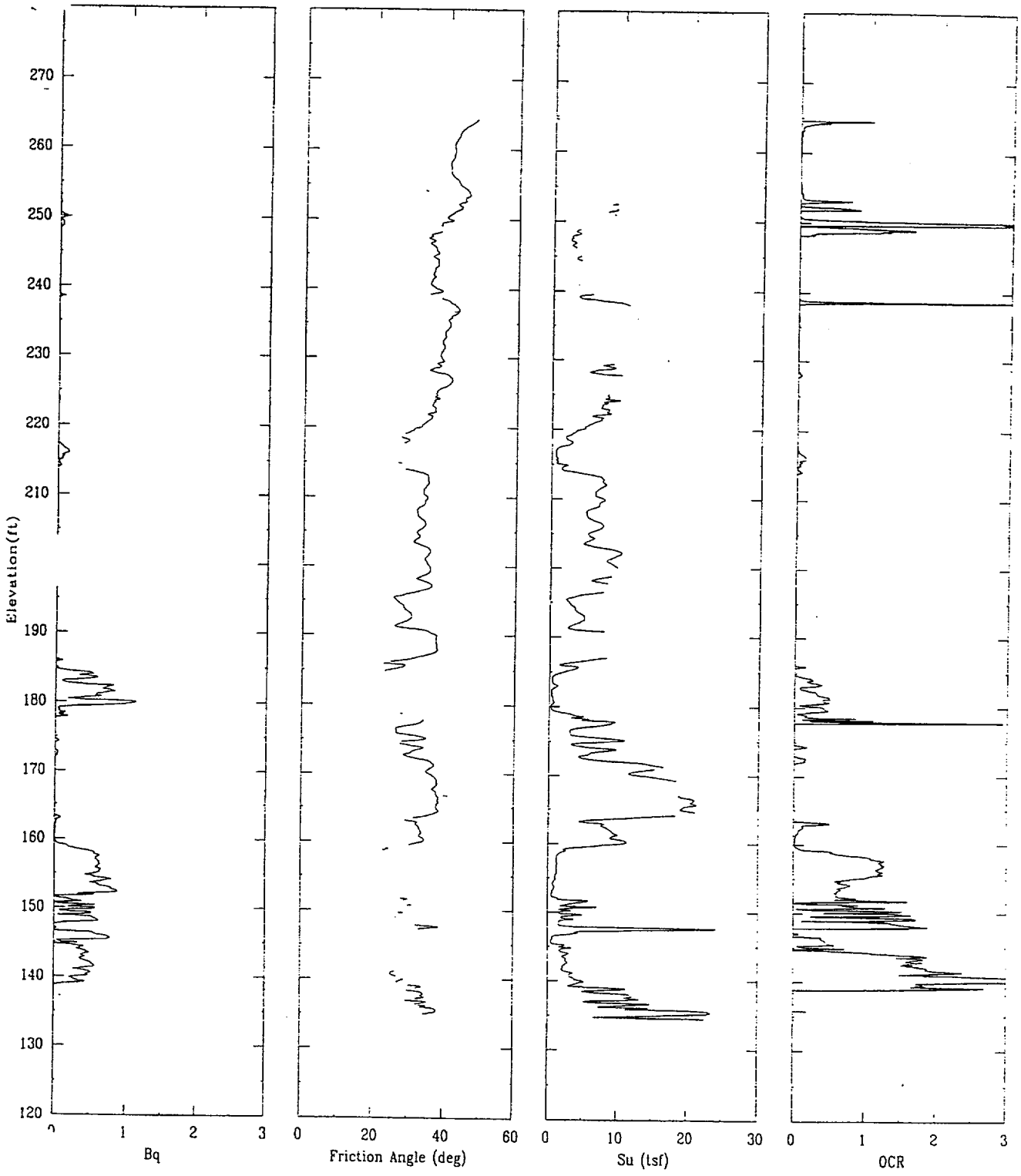

File 324u001.ECP

CPT-32R APPLIED RESEARCH ASSOCIATES, INC. 06/24/00

North 80005.4 East 55755.6 Elevation 264.7

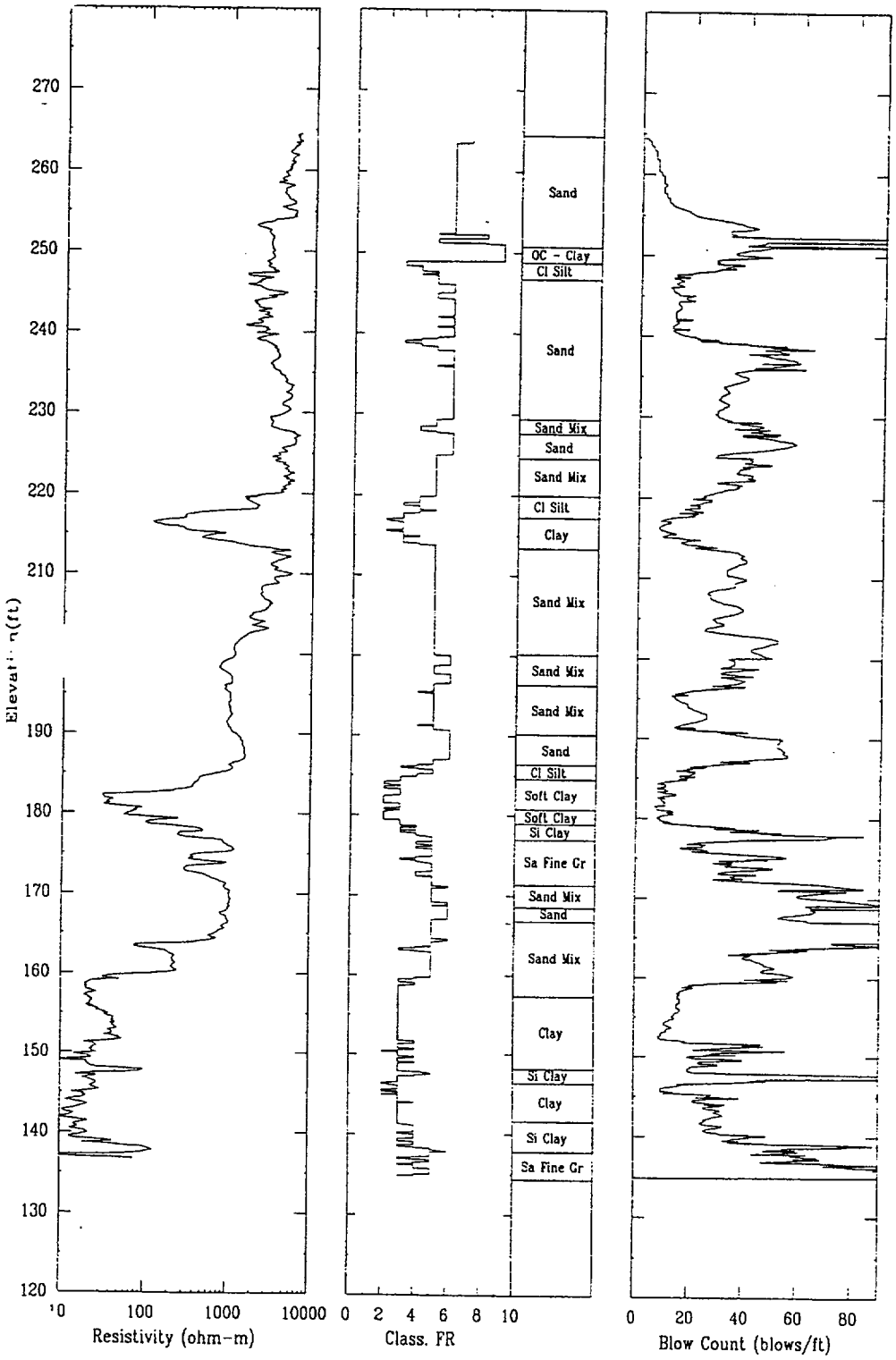

File 324u001.ECP

CPT-33R APPLIED RESEARCH ASSOCIATES, INC. 06/13/00

North 79842.0 East 54922.7 Elevation 274.6

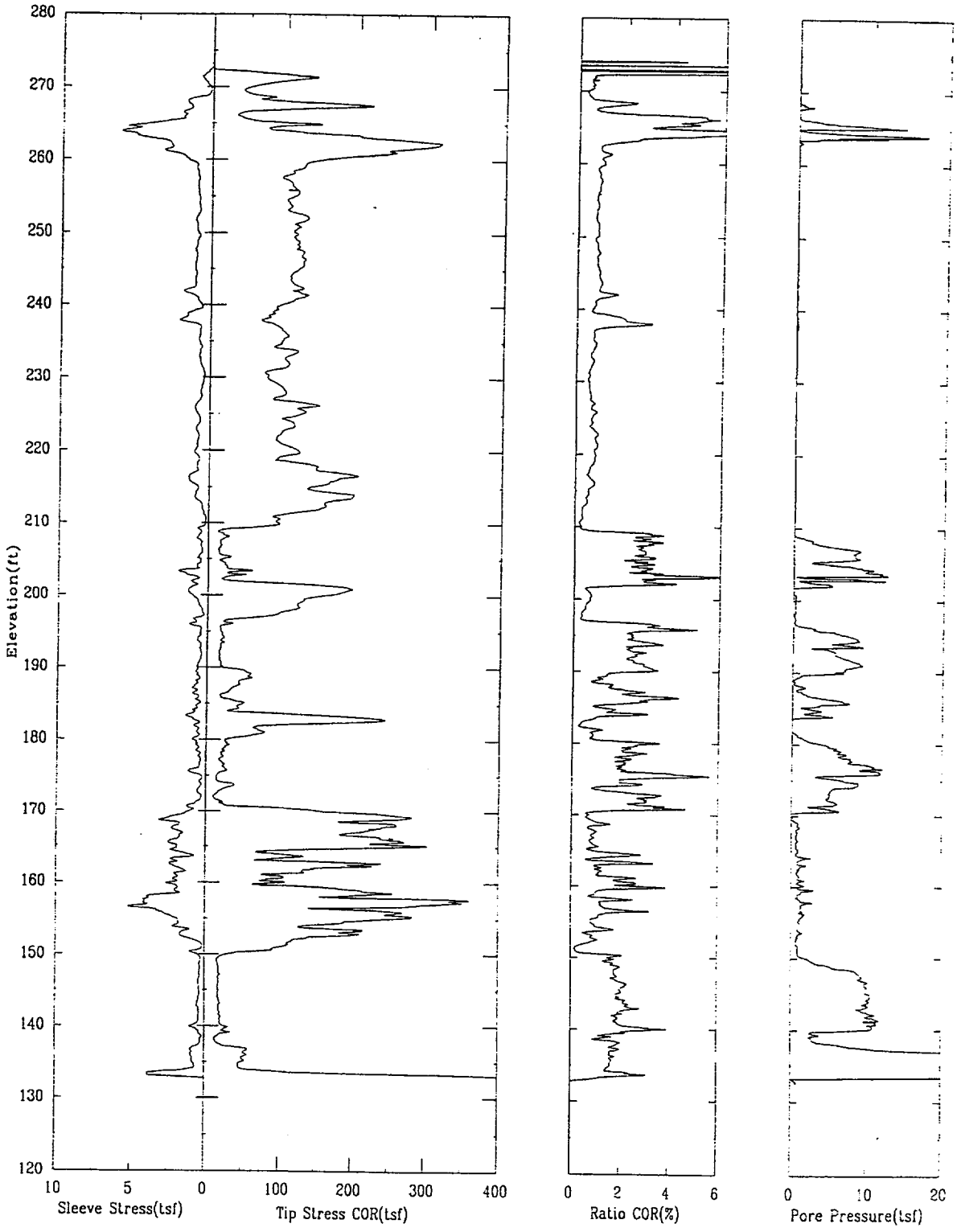

File 413u003B.ECP

CPT-33R APPLIED RESEARCH ASSOCIATES, INC. 06/13/00

North 79842.0 East 54922.7 Elevation 274.6

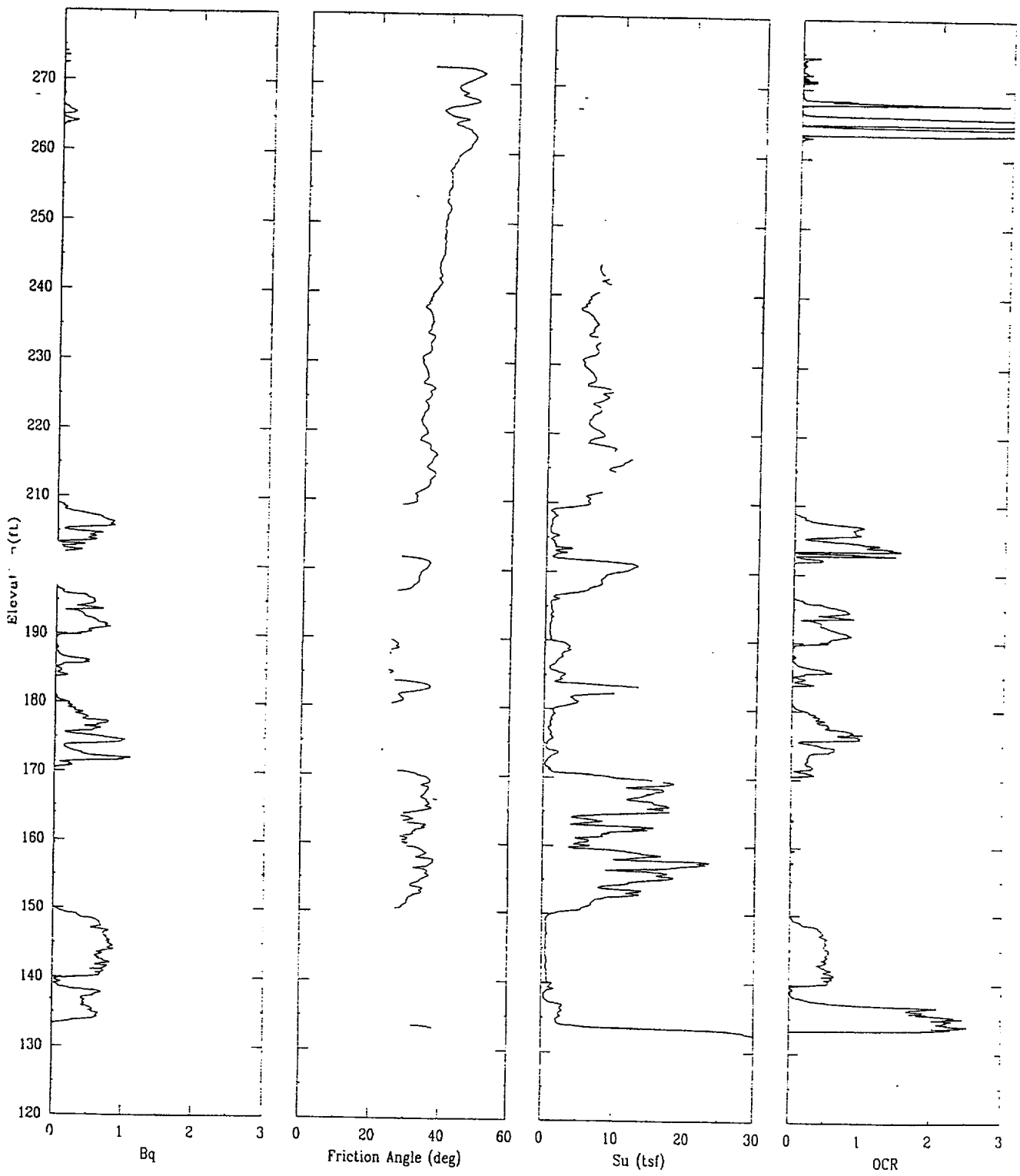

File 413u003B.ECP

DCS, MFFF Project No. 08716

CPT-33R APPLIED RESEARCH ASSOCIATES, INC. 06/13/00

North 79842.0 East 54922.7 Elevation 274.6

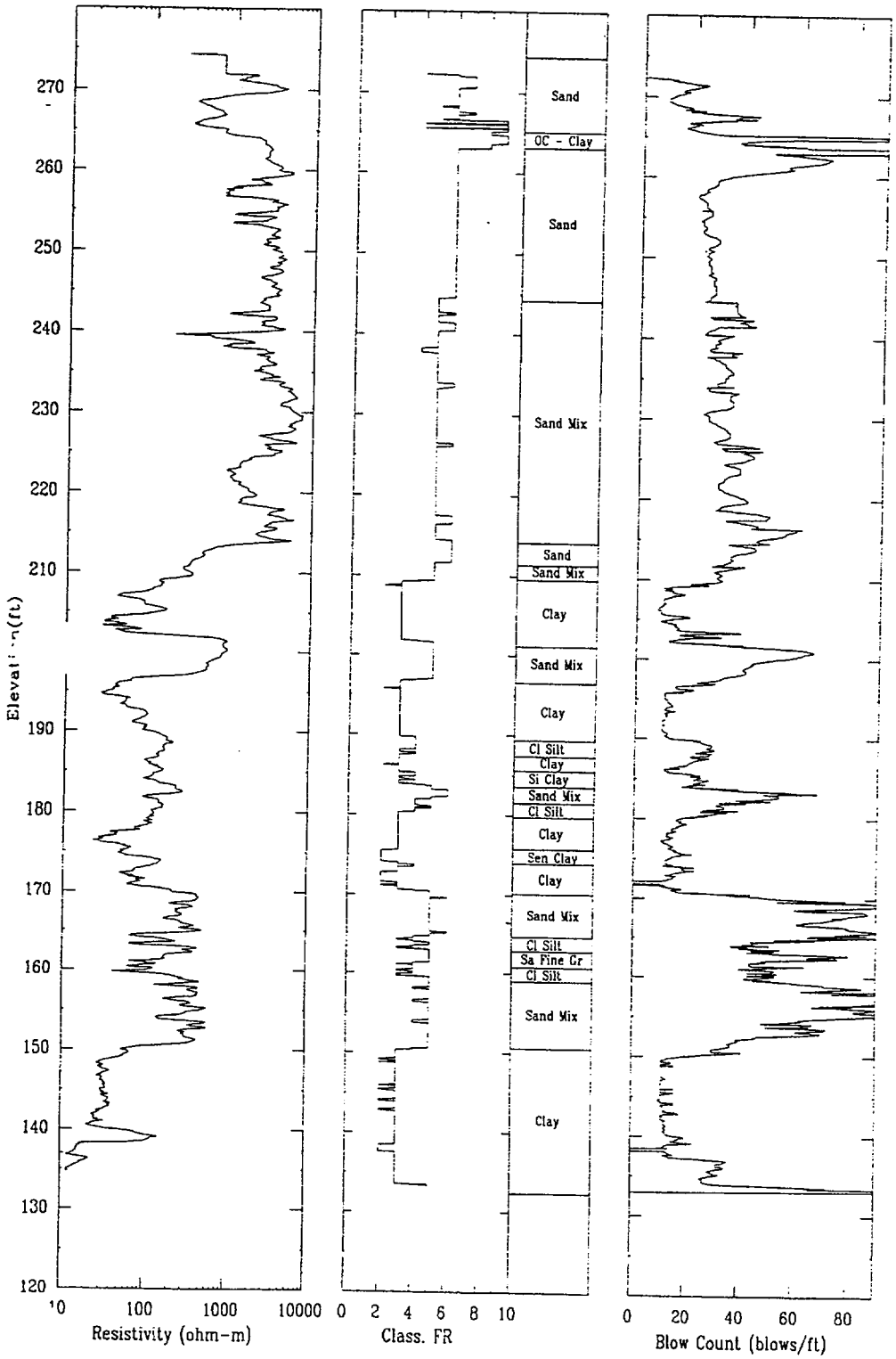

File 413u003B.ECP

CPT-34S APPLIED RESEARCH ASSOCIATES, INC. 06/07/00

North 79826.9 East 55323.2 Elevation 270.8

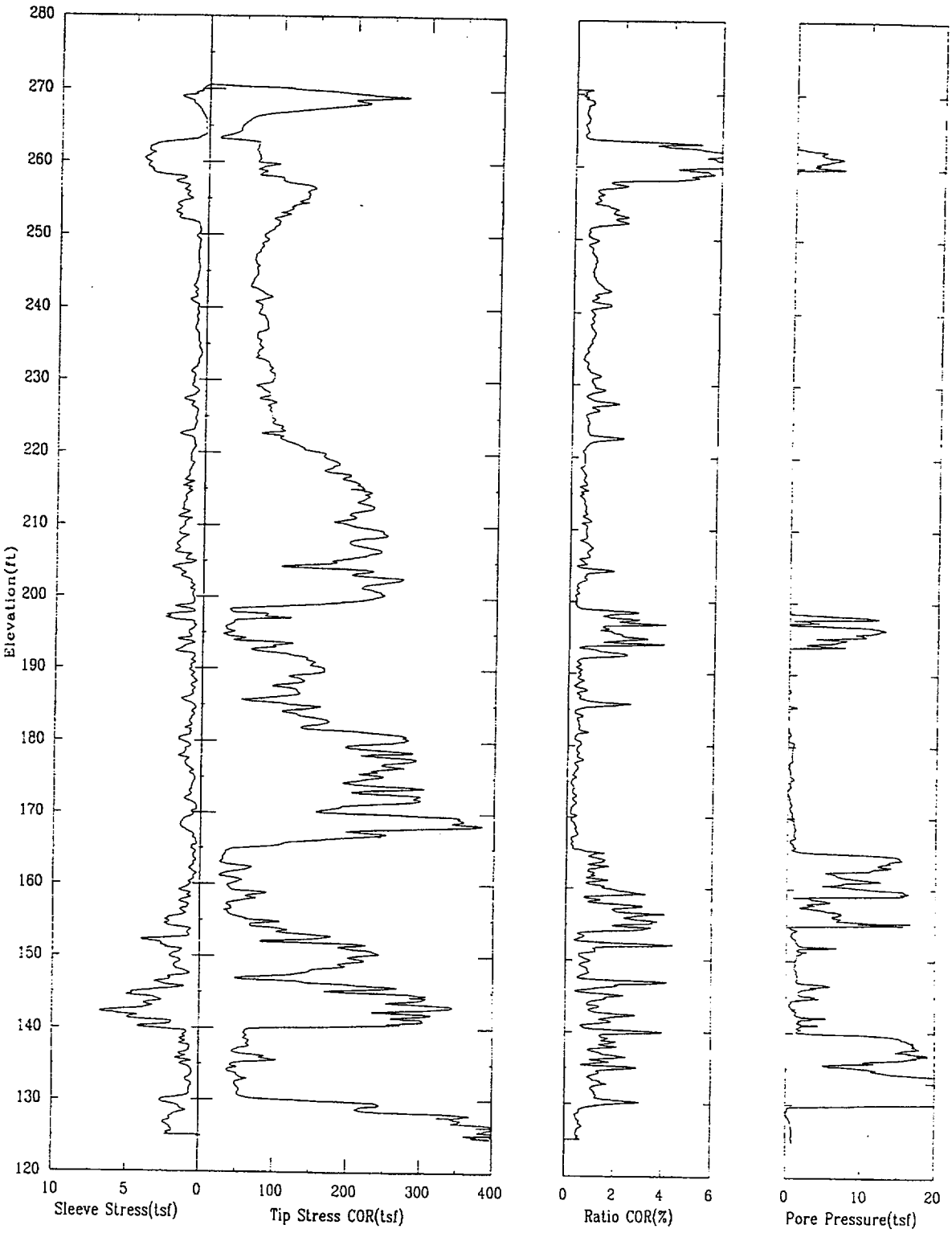

File 407u001B.ECP

CPT-34S APPLIED RESEARCH ASSOCIATES, INC. 06/07/00

North 79826.9 East 55323.2 Elevation 270.8

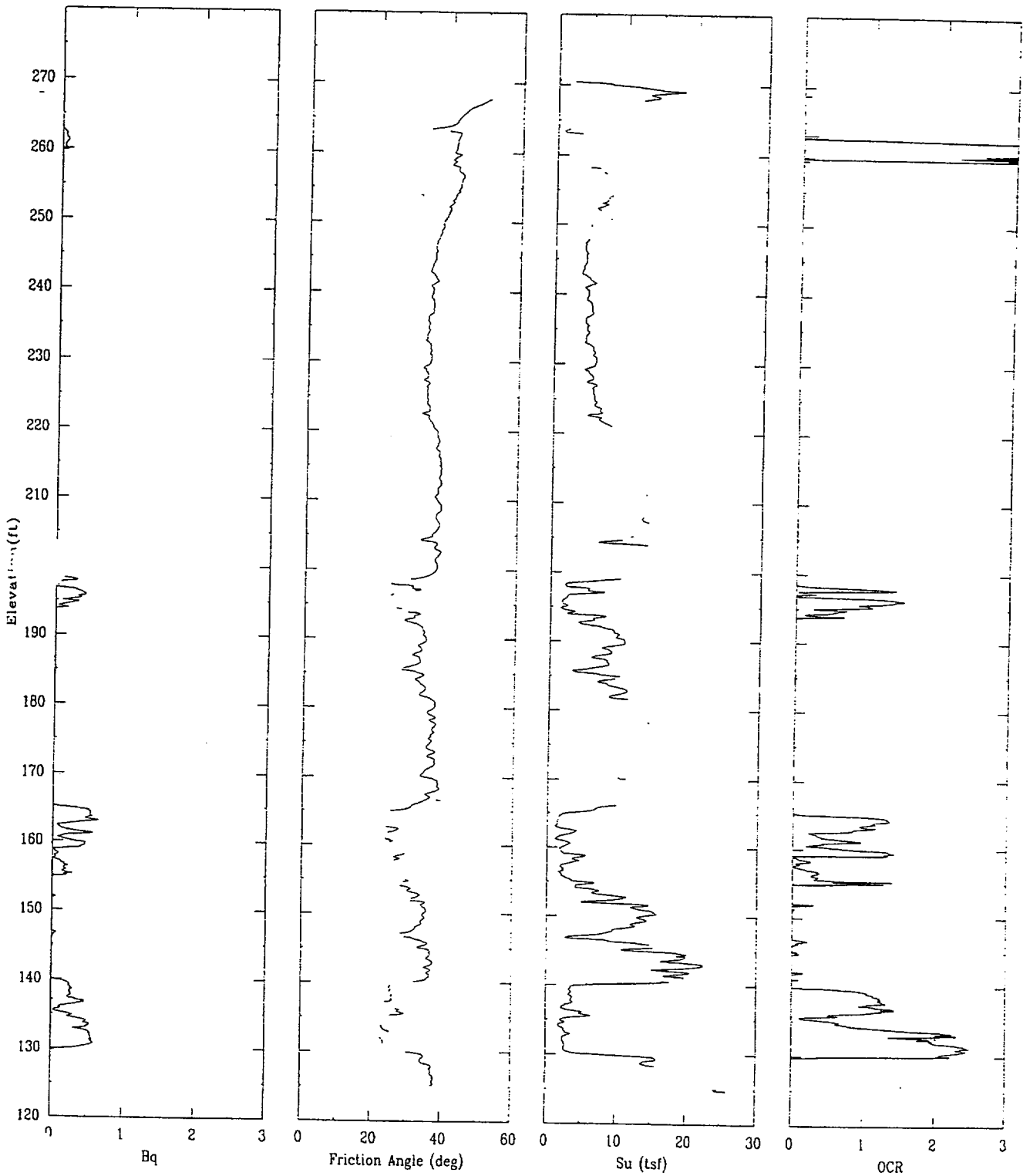

File 407u001B.ECP

CPT-34S APPLIED RESEARCH ASSOCIATES, INC. 06/07/00

North 79826.9 East 55323.2 Elevation 270.8

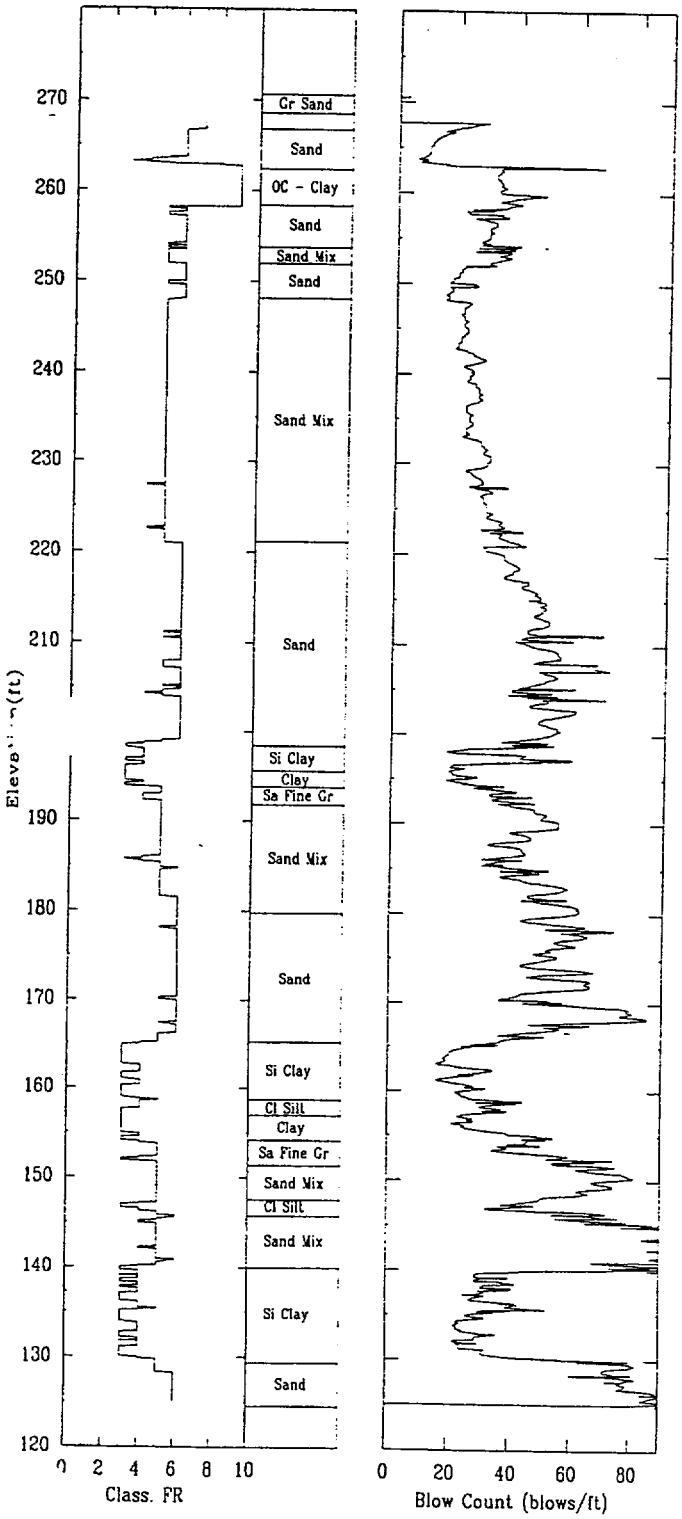

File 407u001B.ECP

CPT-35S APPLIED RESEARCH ASSOCIATES, INC. 06/03/00

North 79888.6 East 55389.0 Elevation 272.6

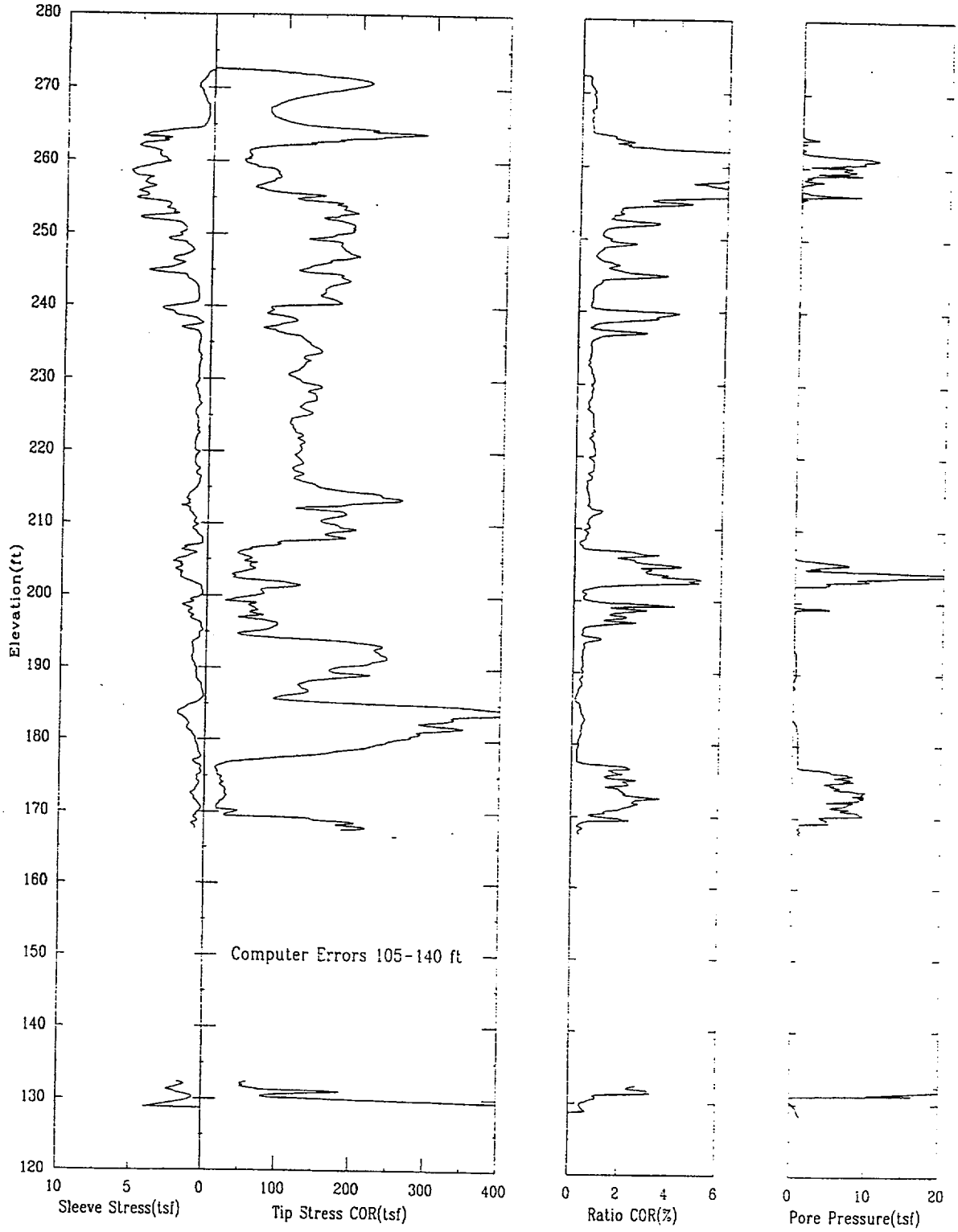

File 403u005.ECP

DCS, MFFF Project No. 08716

CPT-35S APPLIED RESEARCH ASSOCIATES, INC. 06/03/00

North 79888.6 East 55389.0 Elevation 272.6

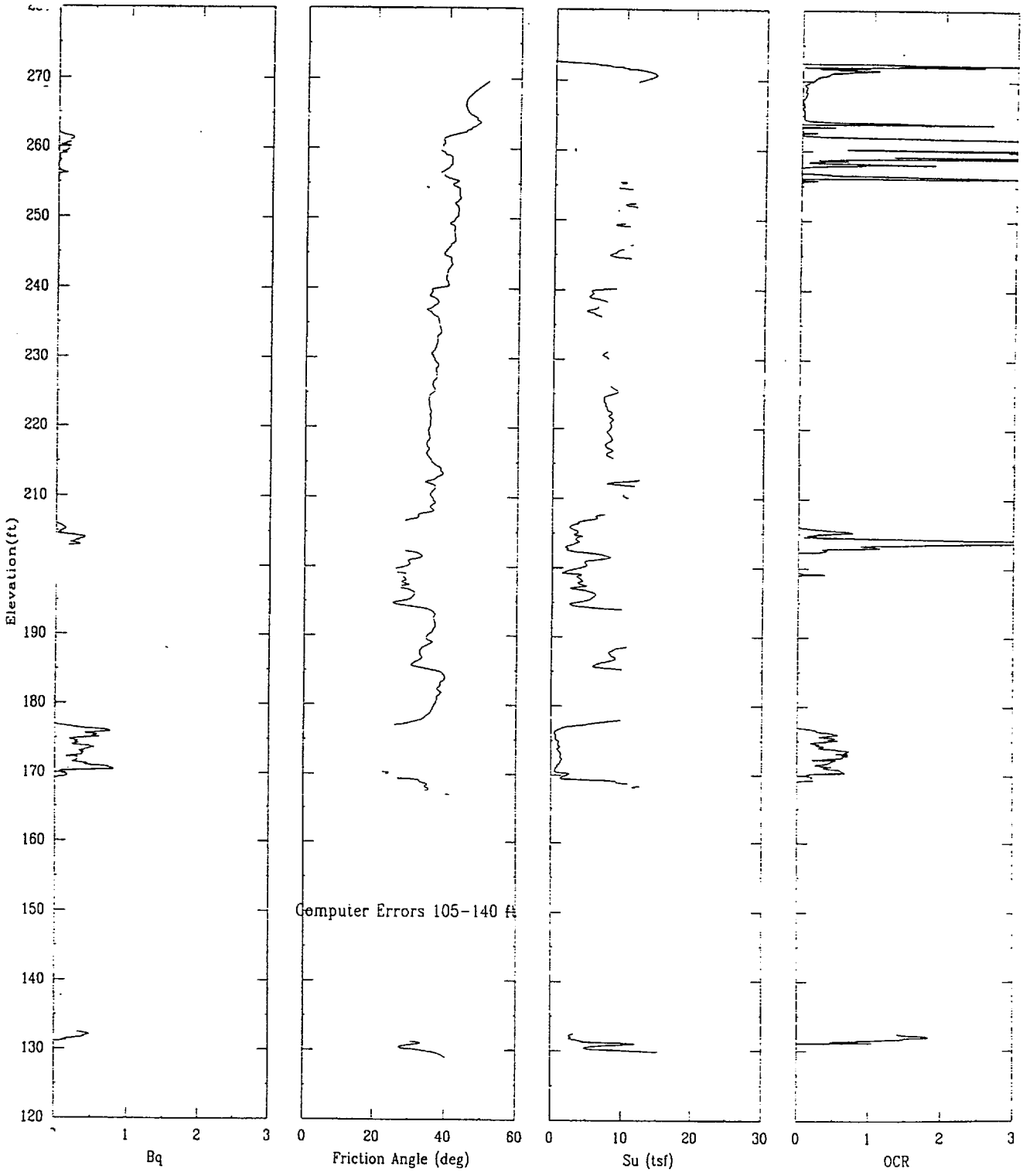

File 403u005.ECP

CPT-35S APPLIED RESEARCH ASSOCIATES, INC. 06/03/00

North 79888.6 East 55389.0 Elevation 272.6

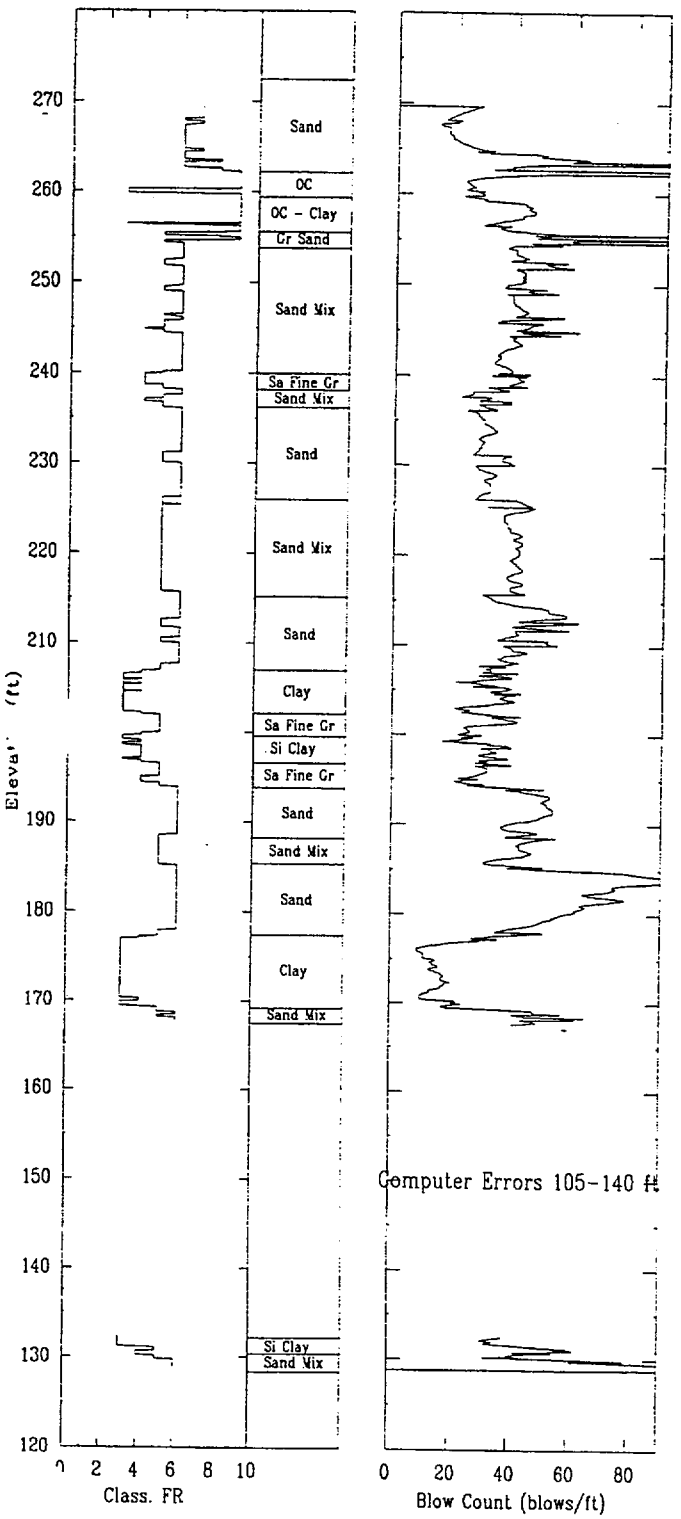

File 403u005.ECP

CPT-36R APPLIED RESEARCH ASSOCIATES, INC. 06/13/00

North 79898.9 East 55478.3 Elevation 273.4

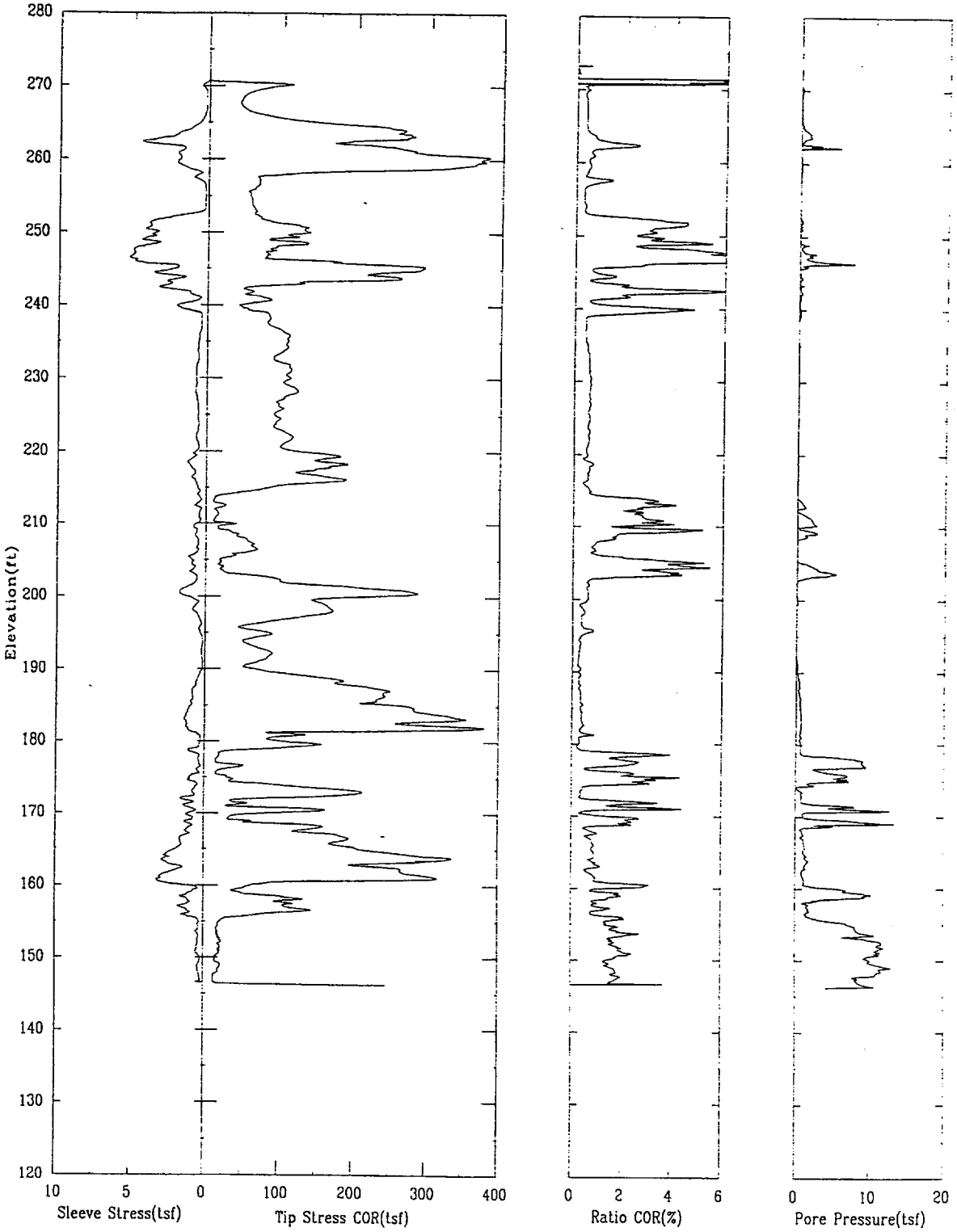

File 413u007.ECP

CPT-36R APPLIED RESEARCH ASSOCIATES, INC. 06/13/00

North 79898.9 East 55478.3 Elevation 273.4

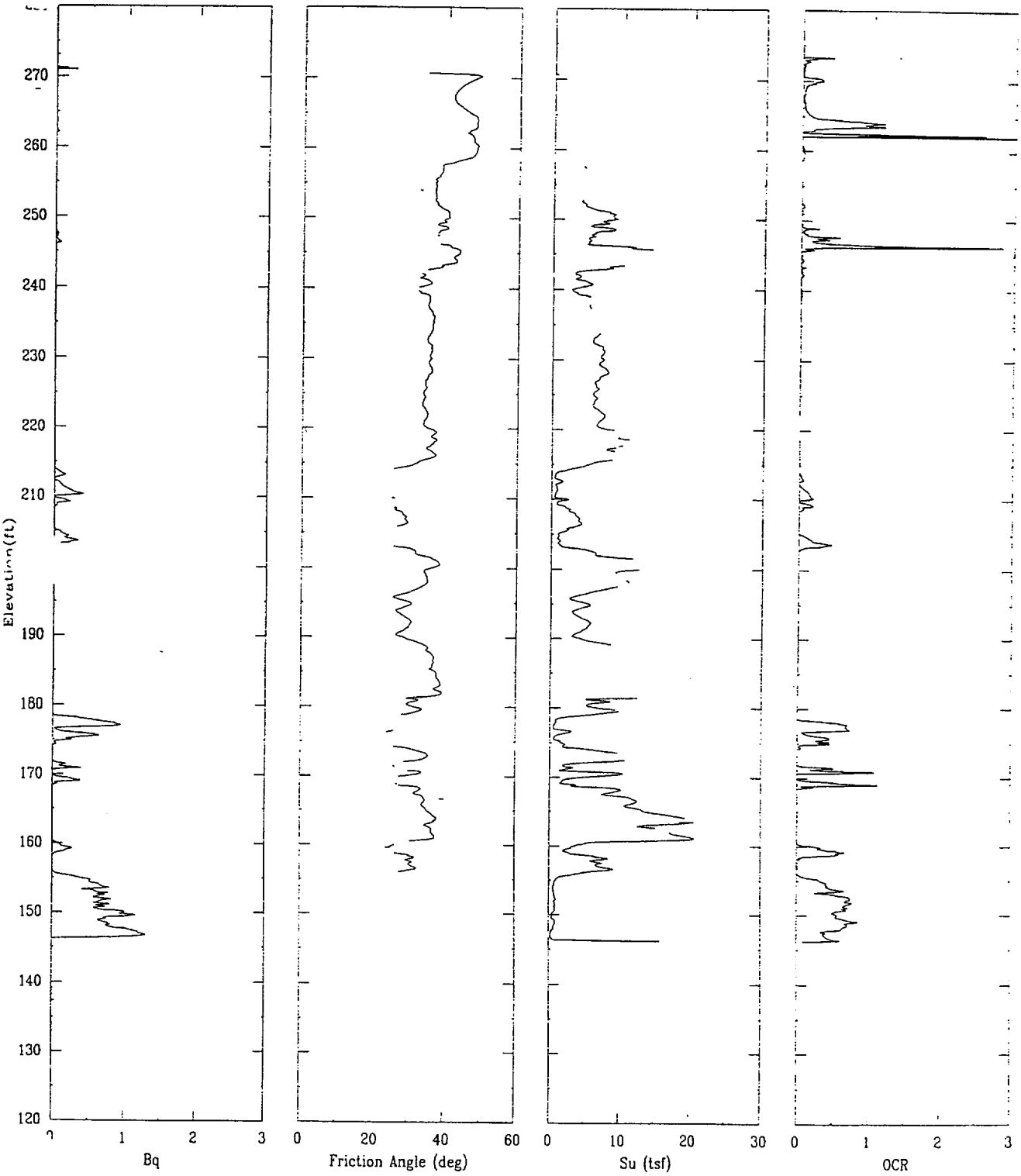

File 413u007.ECP

CPT-36R APPLIED RESEARCH ASSOCIATES, INC. 06/13/00

North 79898.9 East 55478.3 Elevation 273.4

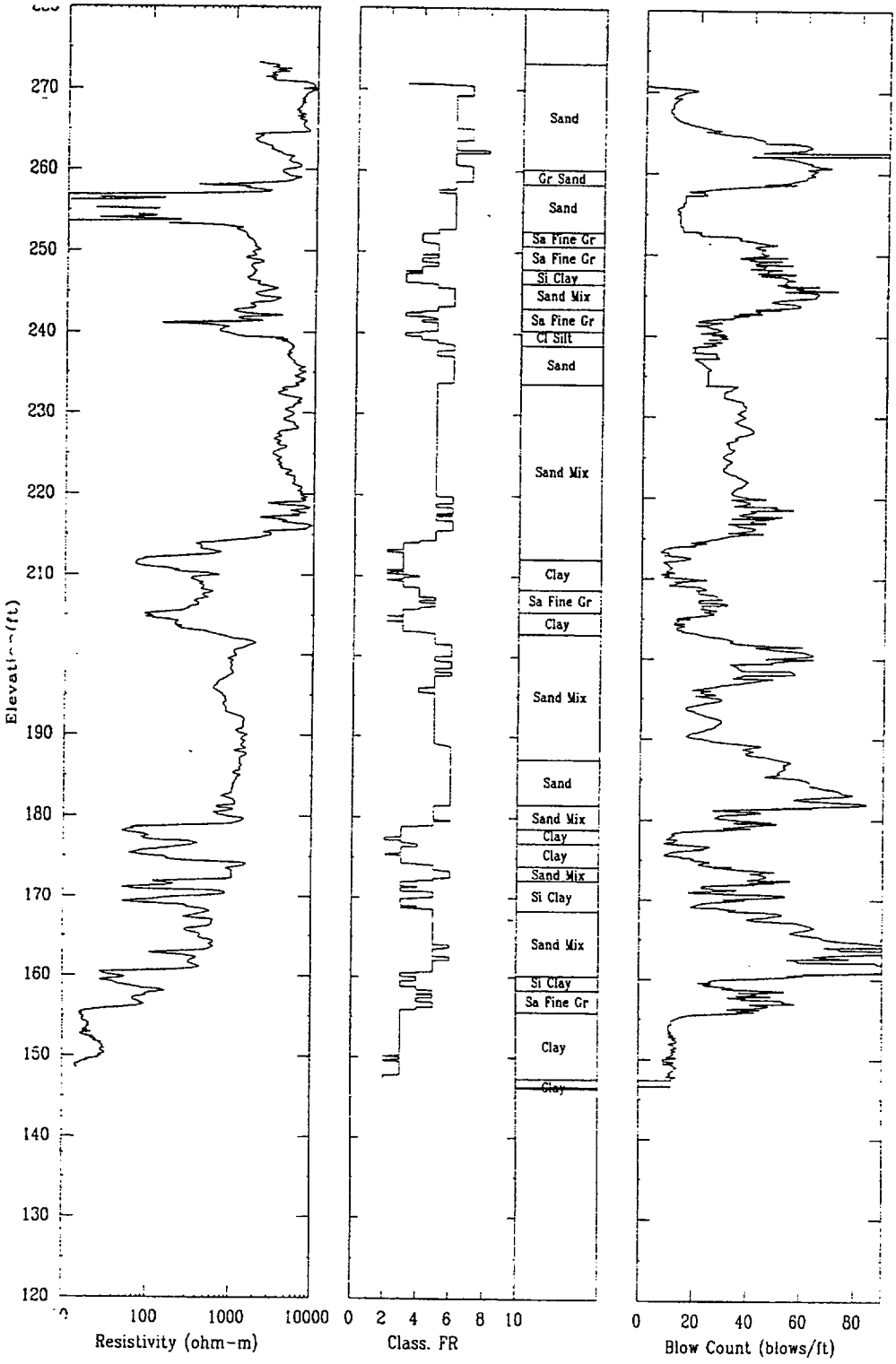

File 413u007.ECP

CPT-37S APPLIED RESEARCH ASSOCIATES, INC. 06/05/00

North 79886.1 East 55629.4 Elevation 268.4

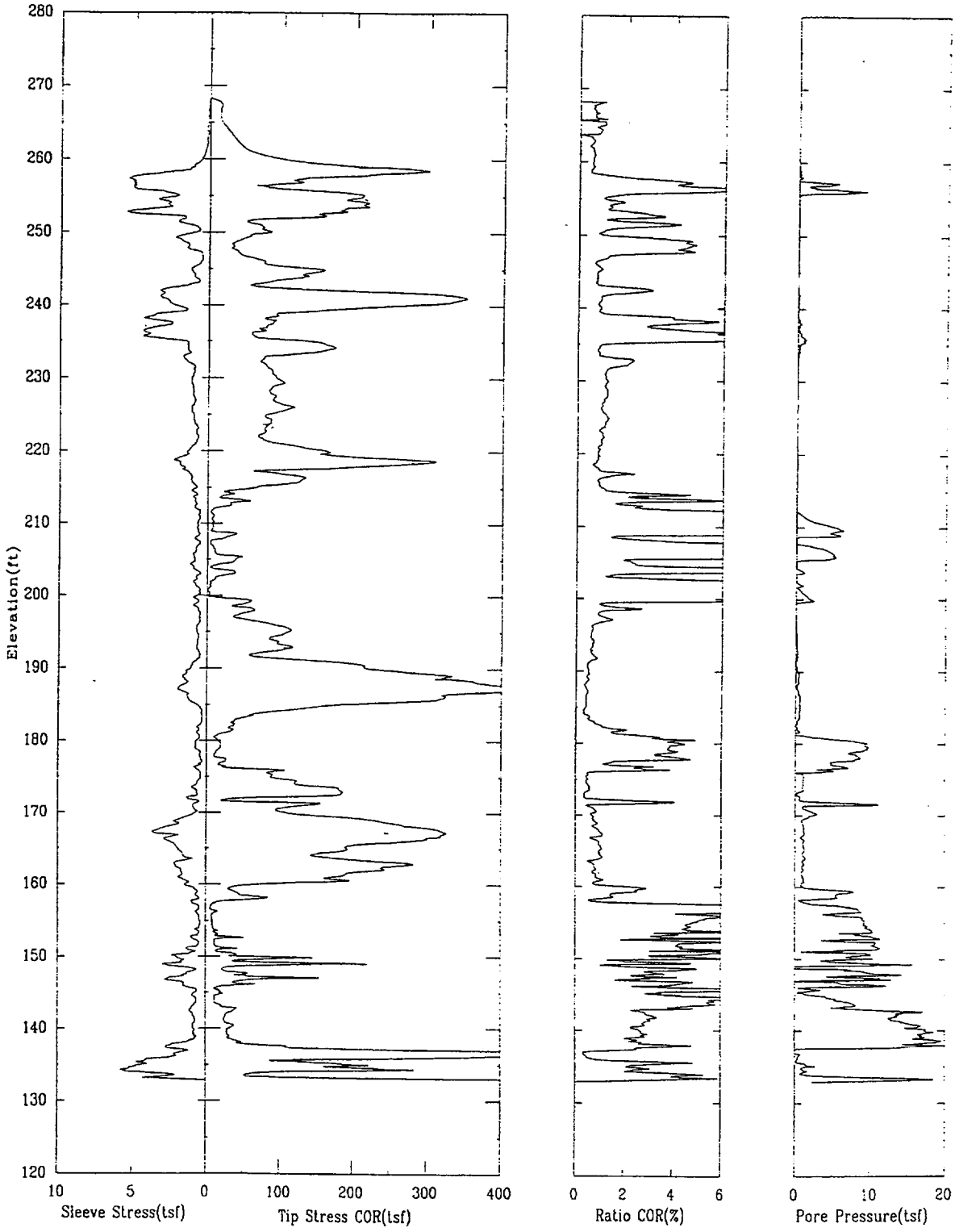

File 405u001.ECP

CPT-37S APPLIED RESEARCH ASSOCIATES, INC. 06/05/00

North 79886.1 East 55629.4 Elevation 268.4

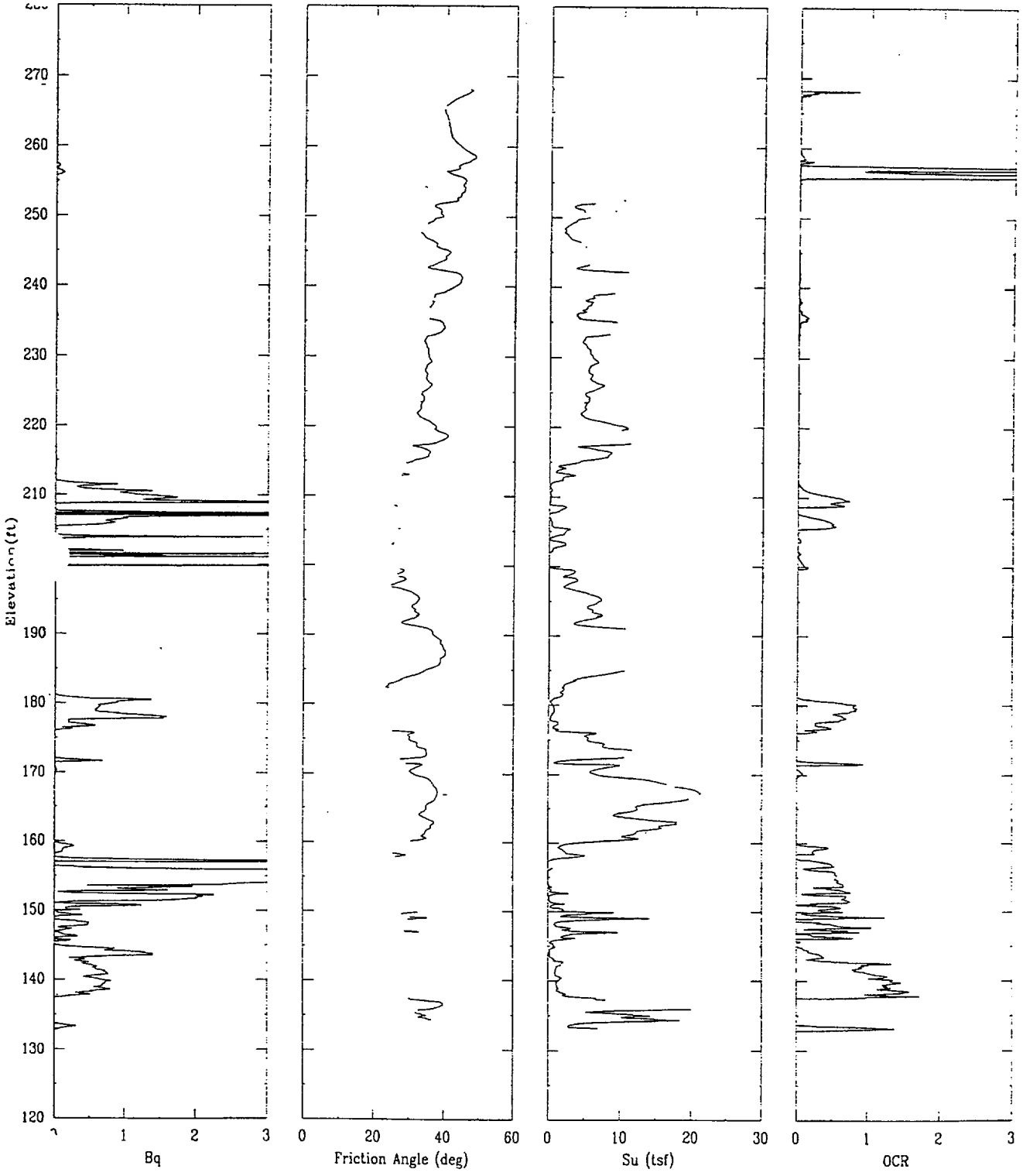

File 405u001.ECP

CPT-37S APPLIED RESEARCH ASSOCIATES, INC. 06/05/00

North 79886.1 East 55629.4 Elevation 268.4

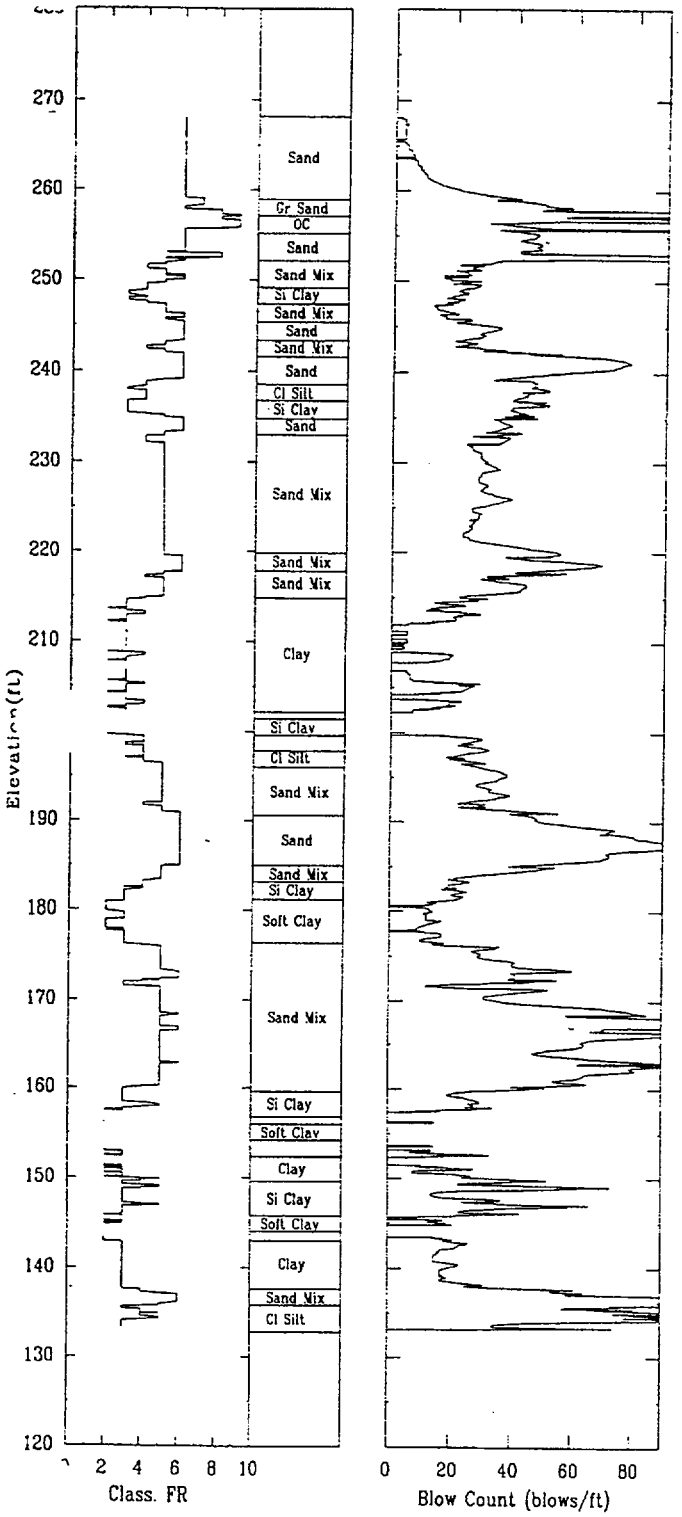

File 405u001.ECP

CPT-38R APPLIED RESEARCH ASSOCIATES, INC. 06/23/00

North 79899.9 East 55568.6 Elevation 271.3

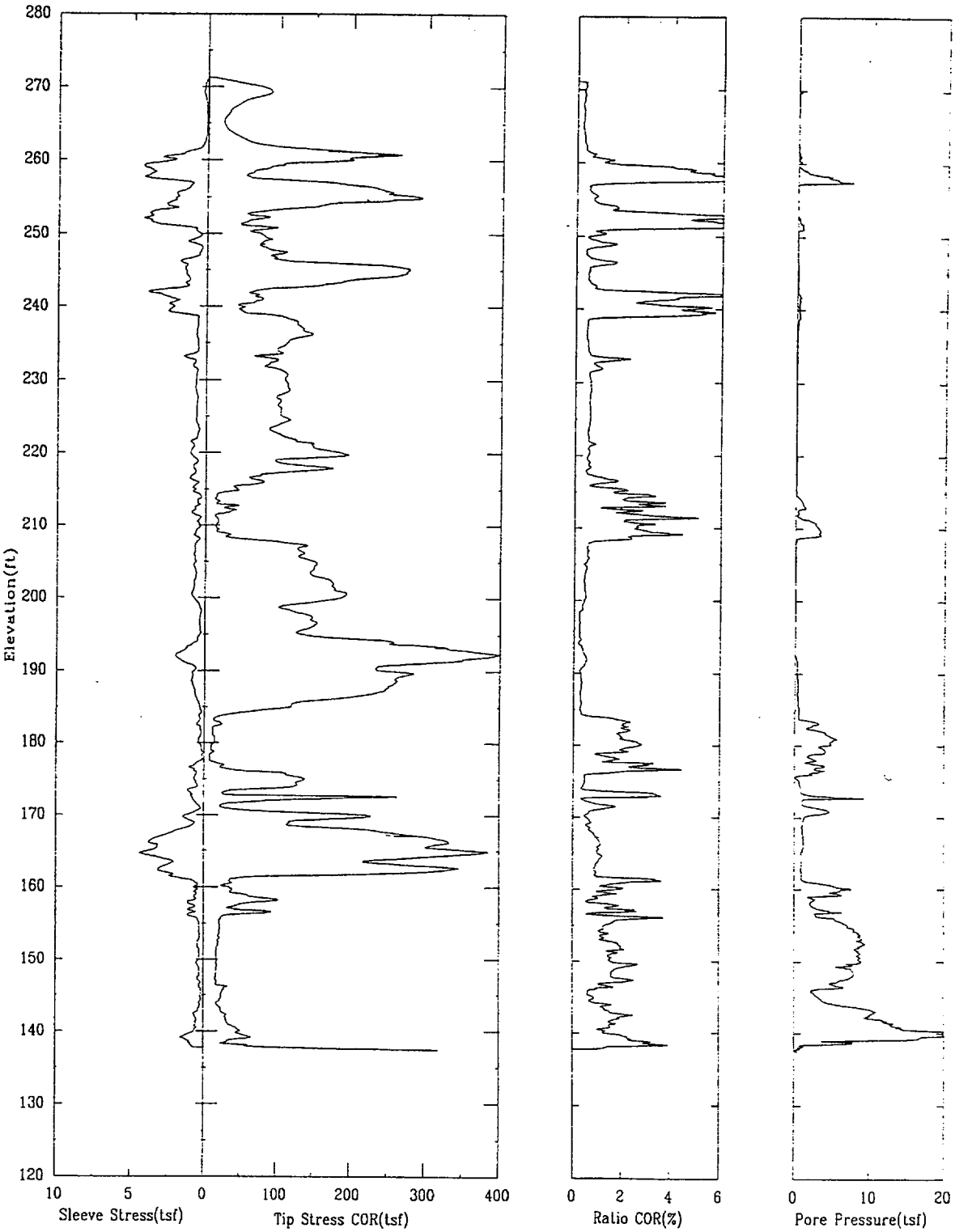

File 323u001.ECP

CPT-38R APPLIED RESEARCH ASSOCIATES, INC. 06/23/00

North 79899.9 East 55568.6 Elevation 271.3

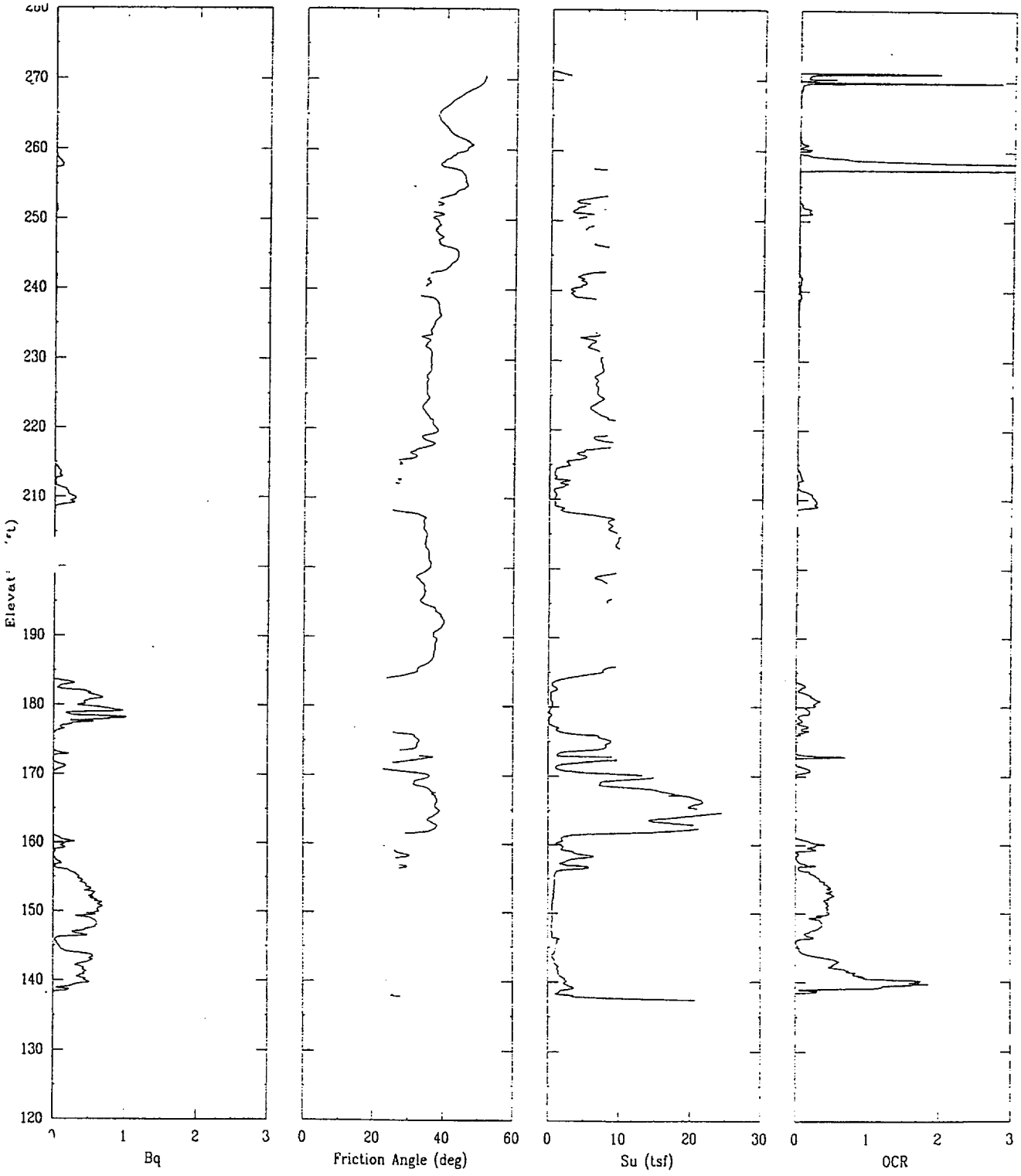

File 323u001.ECP

CPT-38R APPLIED RESEARCH ASSOCIATES, INC. 06/23/00

North 79899.9 East 55568.6 Elevation 271.3

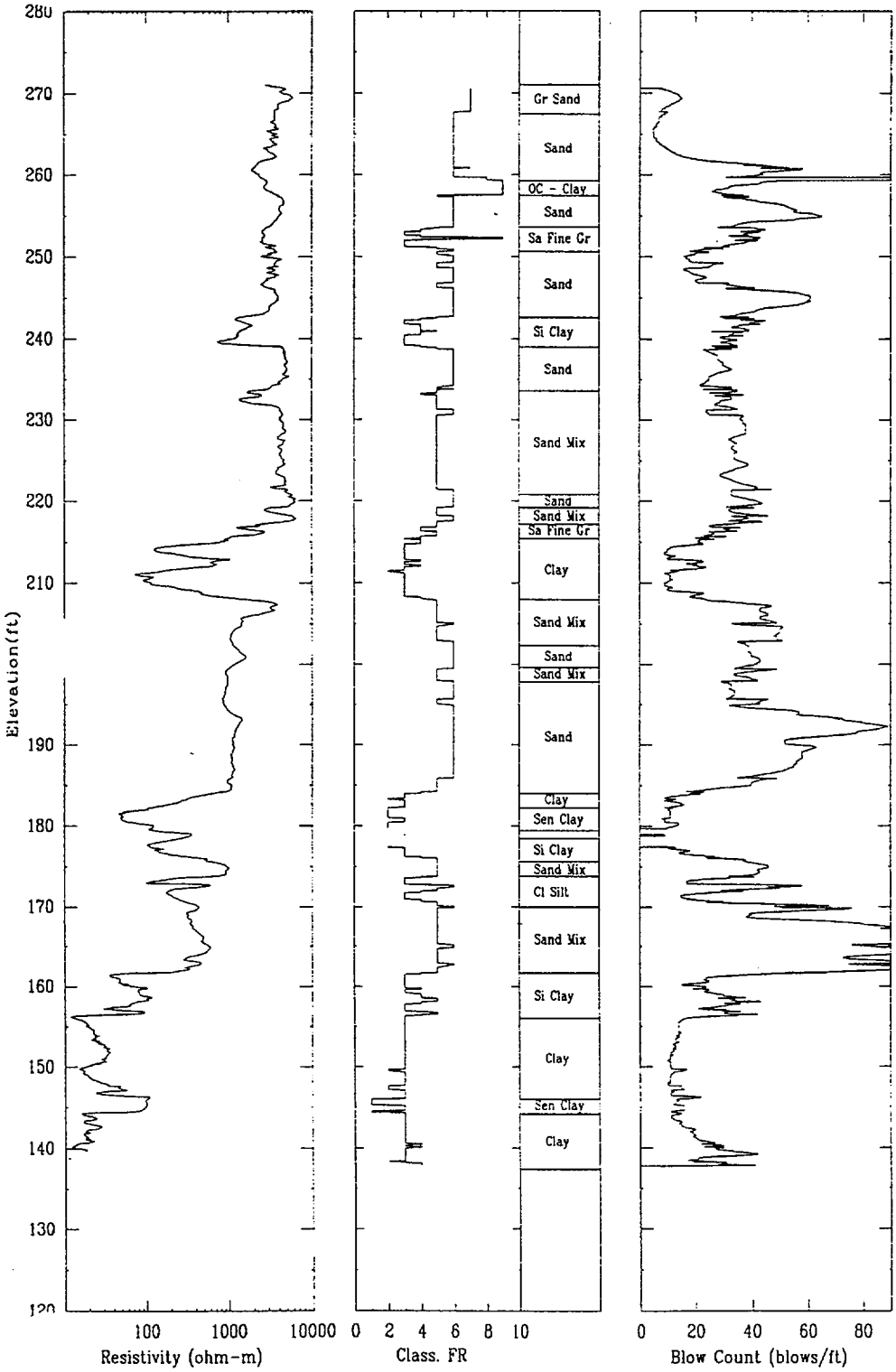

File 323u001.ECP

DCS, MFFF Project No. 08716

CPT-39R APPLIED RESEARCH ASSOCIATES, INC. 06/24/00

North 60206.6 East 55646.9 Elevation 262.1

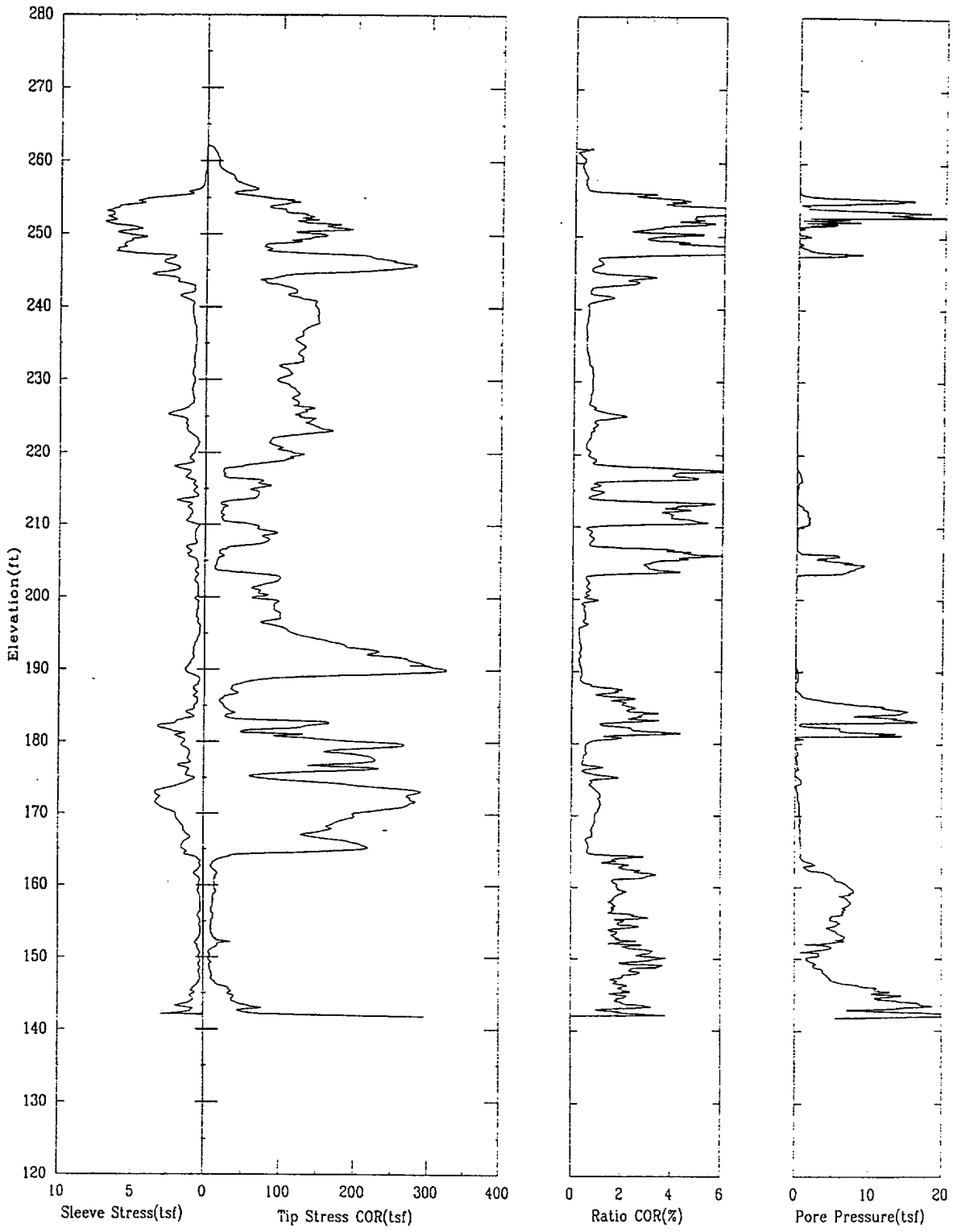

File 324u005.ECP

CPT-39R APPLIED RESEARCH ASSOCIATES, INC. 06/24/00

North 80206.6 East 55646.9 Elevation 262.1

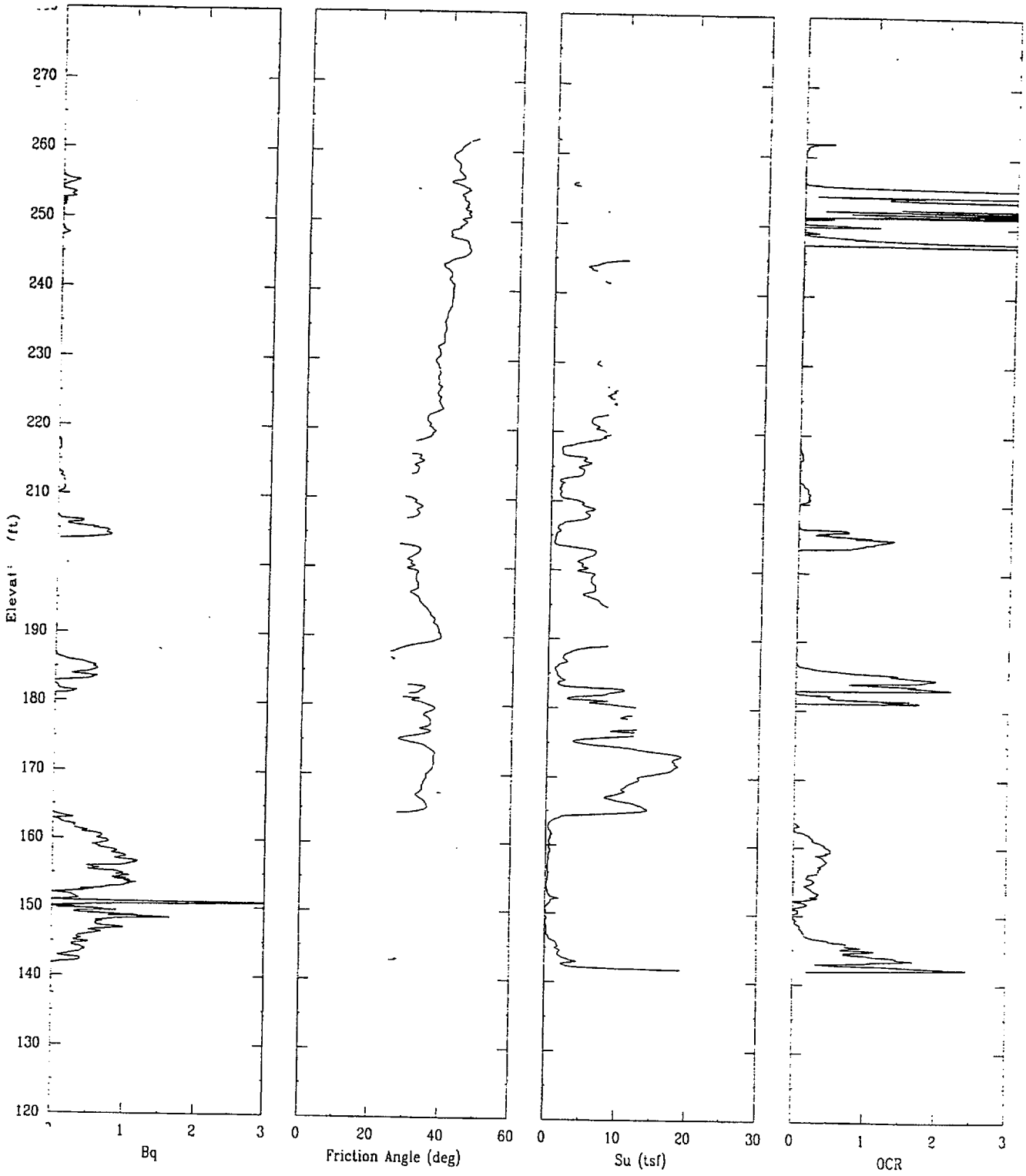

File 324u005.ECP

CPT-39R APPLIED RESEARCH ASSOCIATES, INC. 06/24/00

North 80206.6 East 55646.9 Elevation 262.1

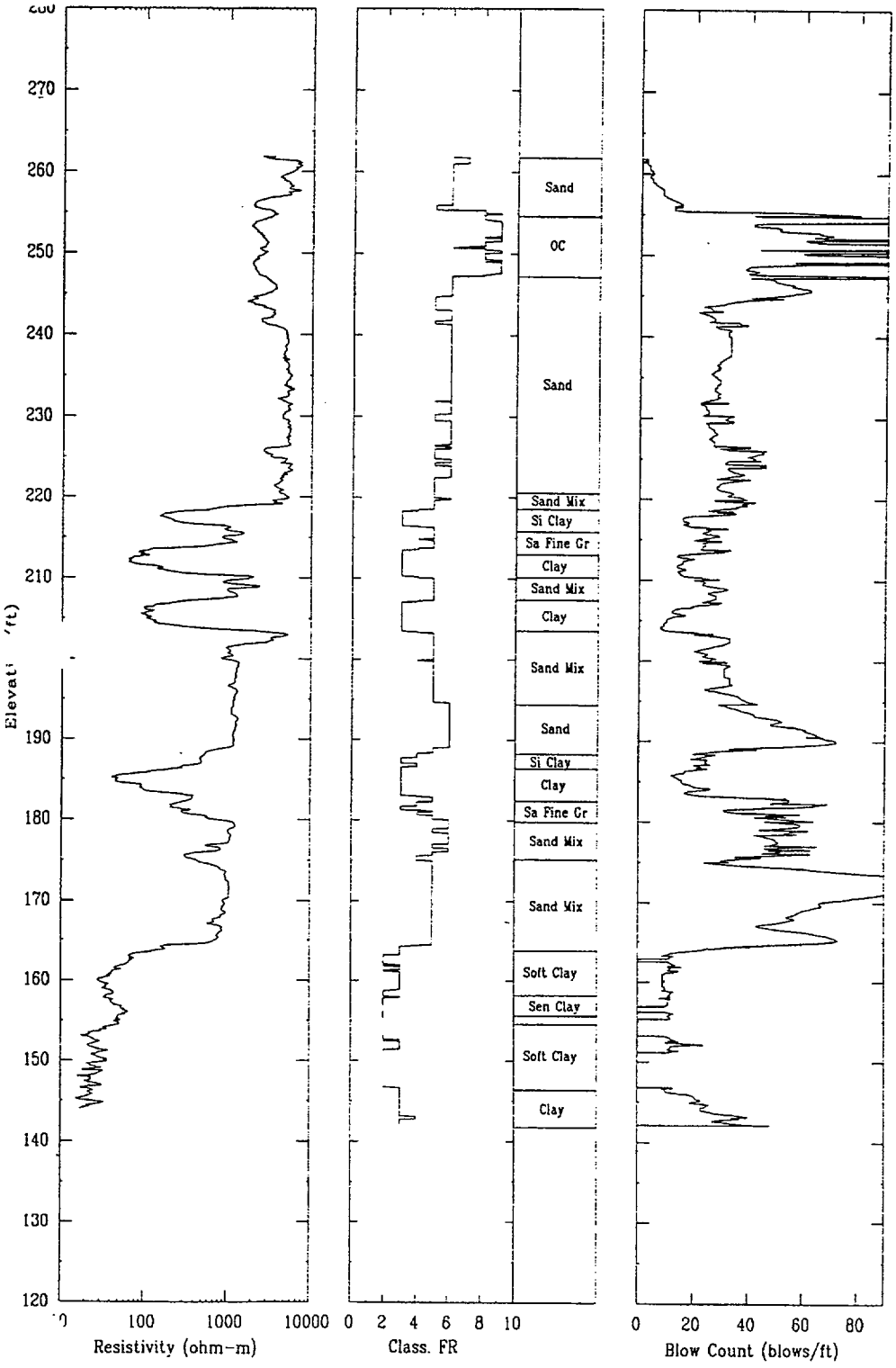

File 324u005.ECP

DCS, MFFF Project No. 08716

CPT-40R APPLIED RESEARCH ASSOCIATES, INC. 06/24/00

North 79941.1 East 55448.0 Elevation 275.0

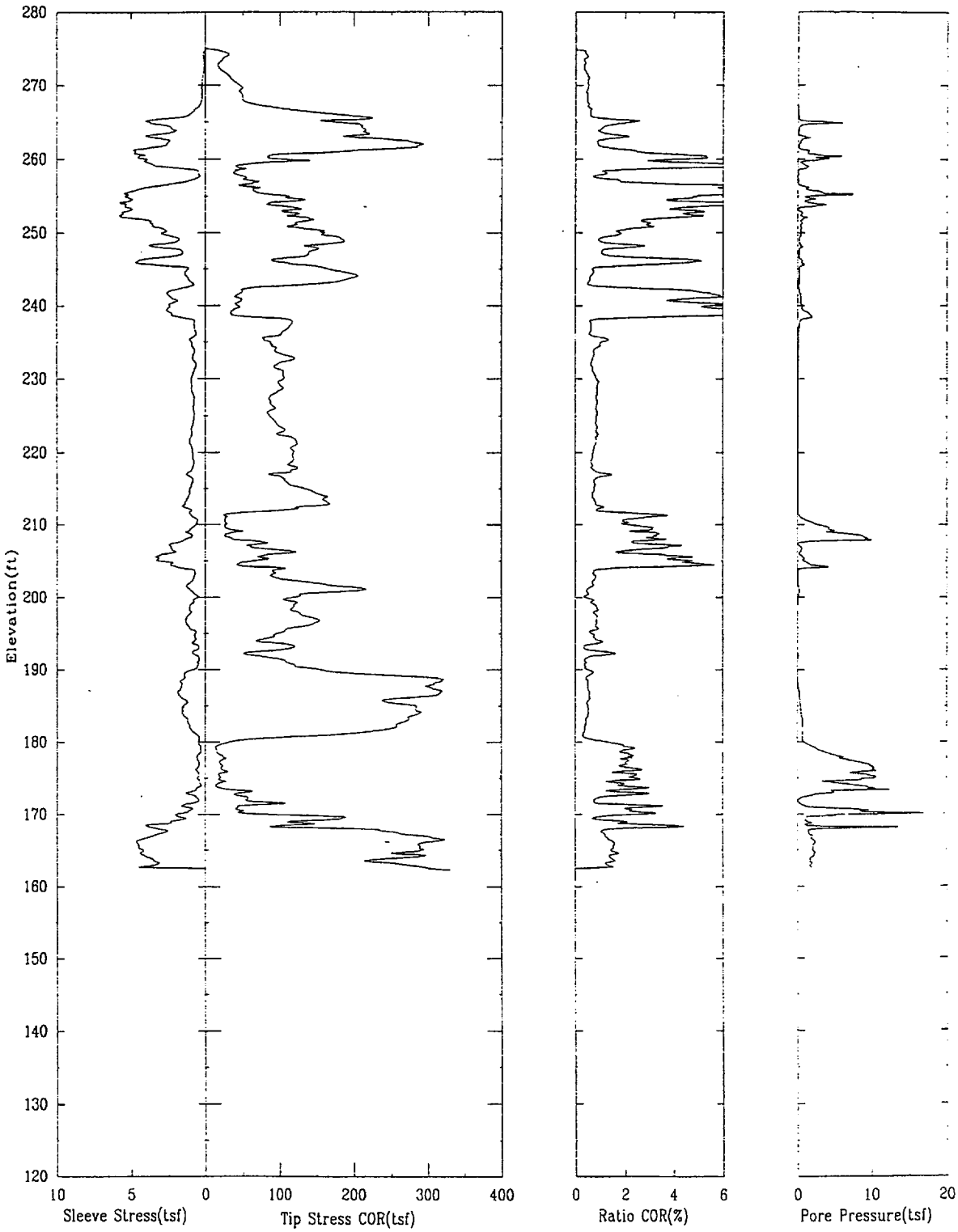

File 324u007.ECP

DCS, MFFF Project No. 08716

CPT-40R APPLIED RESEARCH ASSOCIATES, INC. 06/24/00

North 79941.1 East 55448.0 Elevation 275.0

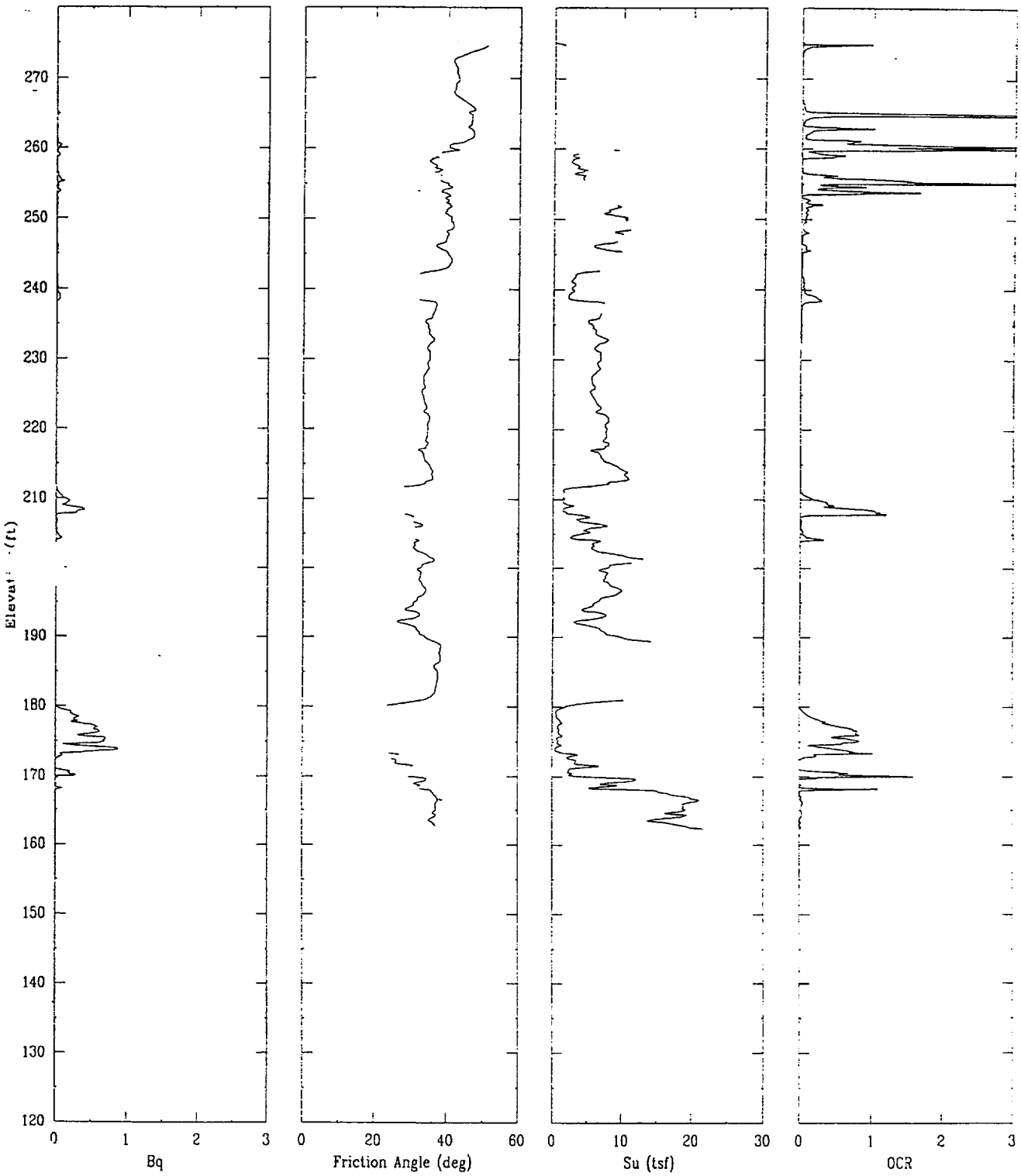

File 324u007.ECP

DCS, MFFF Project No. 08716

CPT-40R APPLIED RESEARCH ASSOCIATES, INC. 06/24/00

North 79941.1 East 55448.0 Elevation 275.0

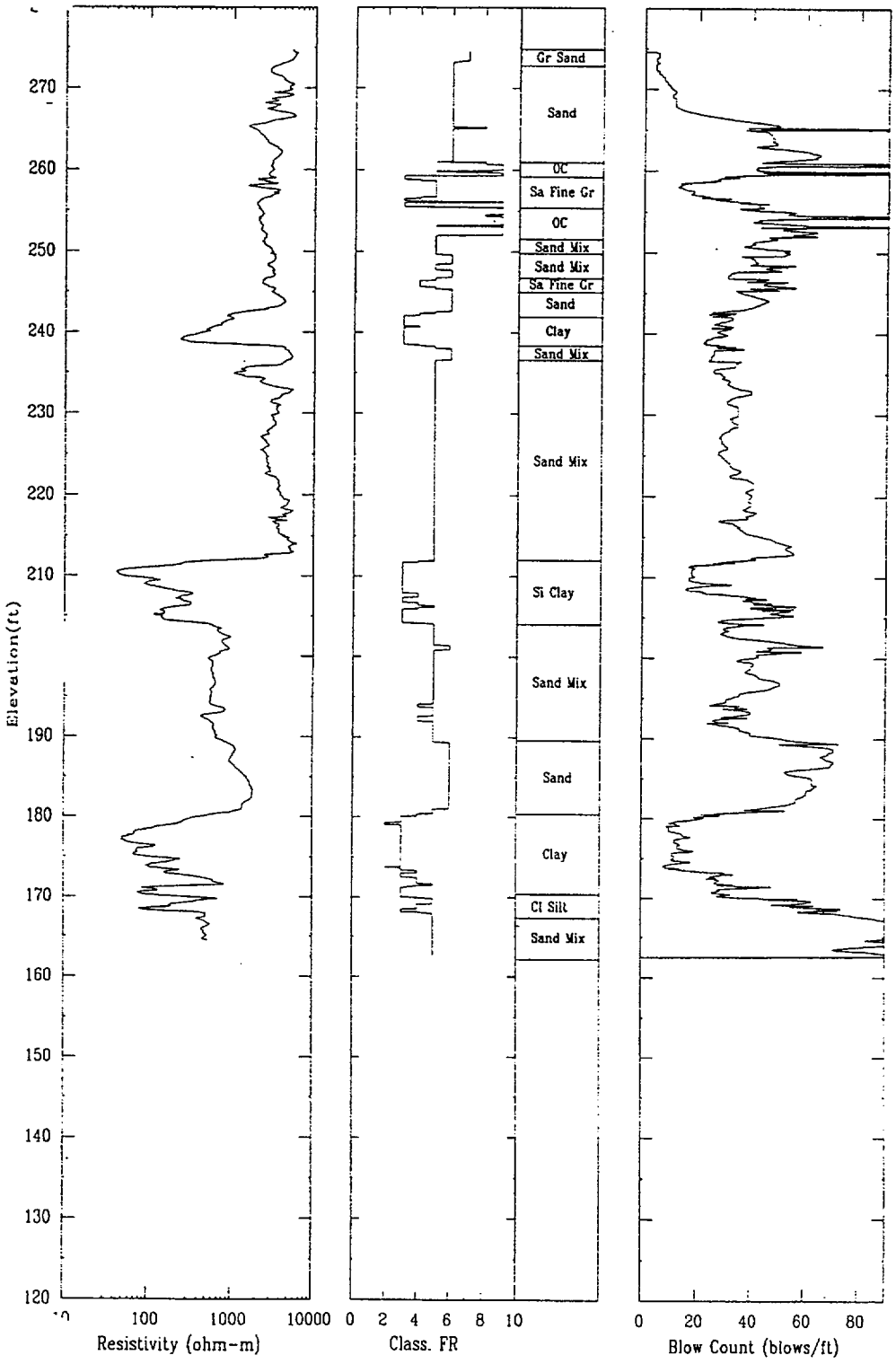

File 324u007.ECP

CPT-42 APPLIED RESEARCH ASSOCIATES, INC. 07/08/00

North 80169.8 East 55591.7 Elevation 267.5

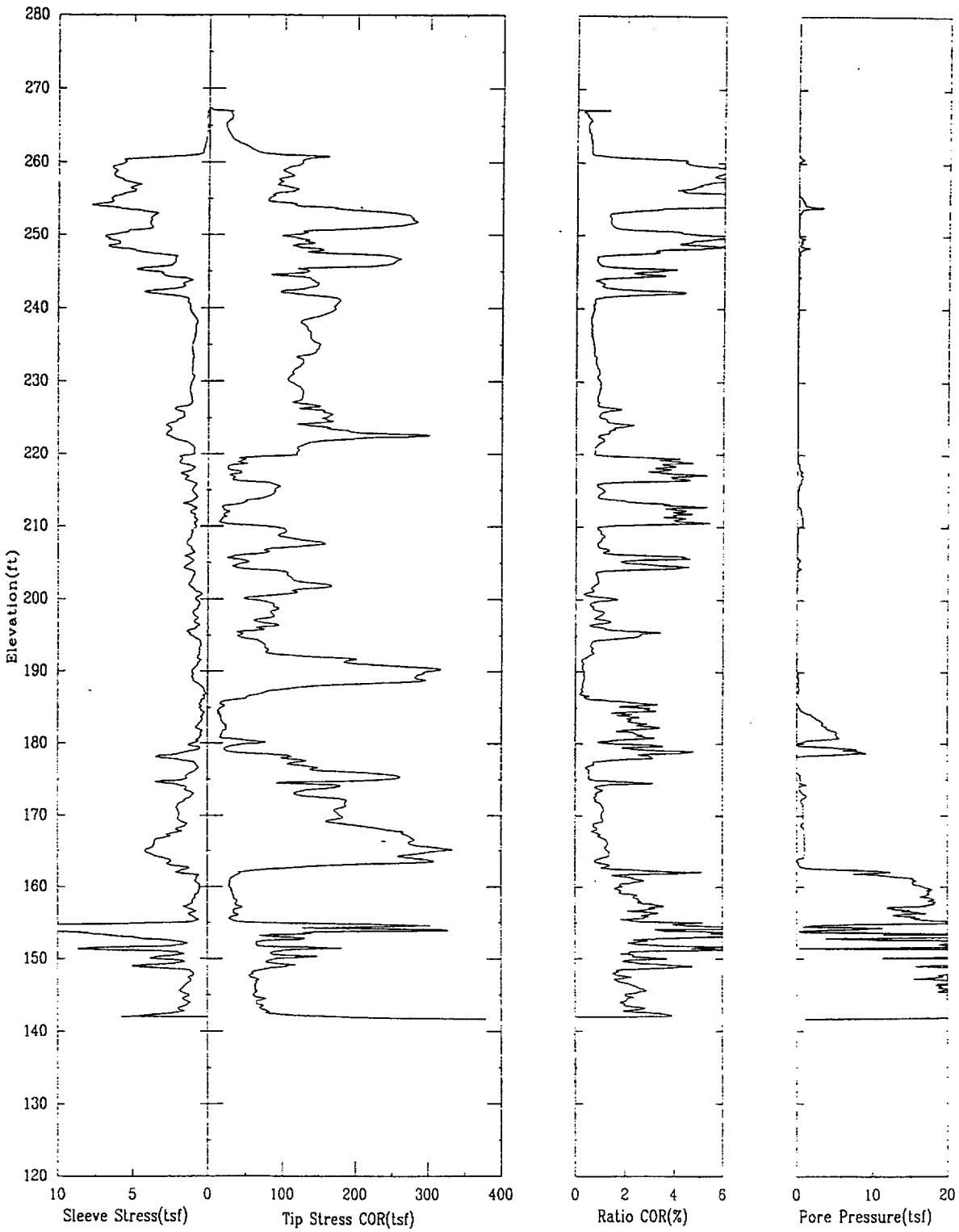

File 408L001.ECP

CPT-42 APPLIED RESEARCH ASSOCIATES, INC. 07/08/00

North 80169.8 East 55591.7 Elevation 267.5

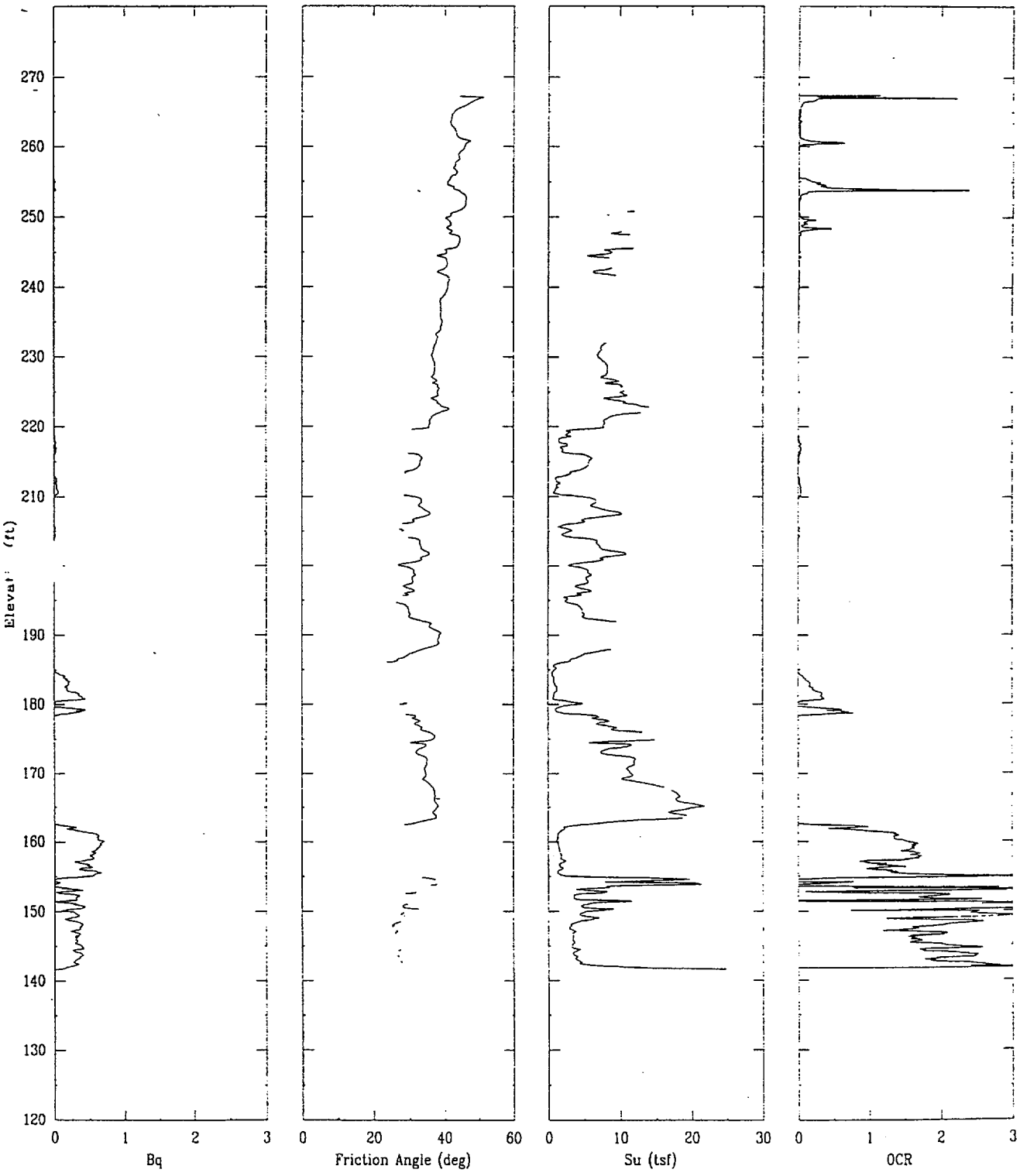

File 408L001.ECP

DCS, MFFF Project No. 08716

CPT-42 APPLIED RESEARCH ASSOCIATES, INC. 07/08/00

North 80169.8 East 55591.7 Elevation 267.5

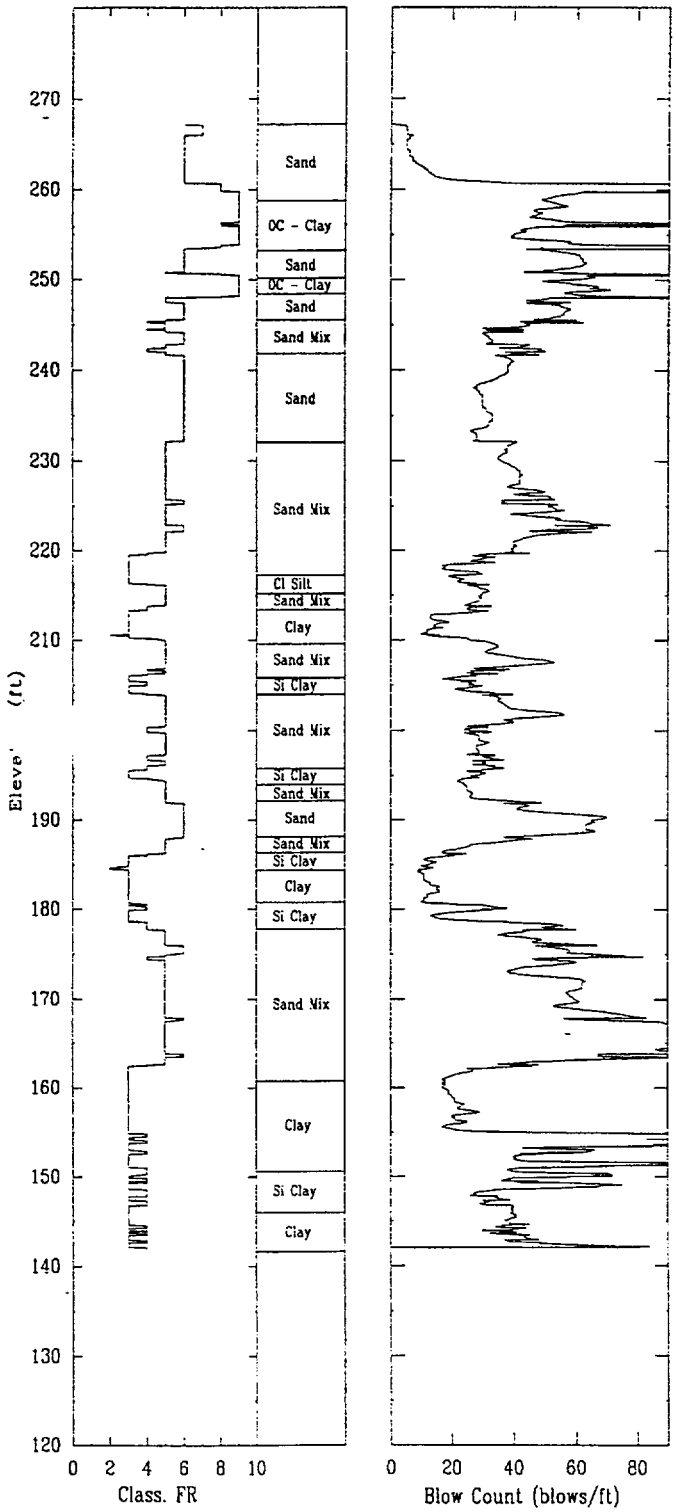

File 408L001.ECP

CPT-43 APPLIED RESEARCH ASSOCIATES, INC. 07/15/00

North 80257.7 East 55585.0 Elevation 264.0

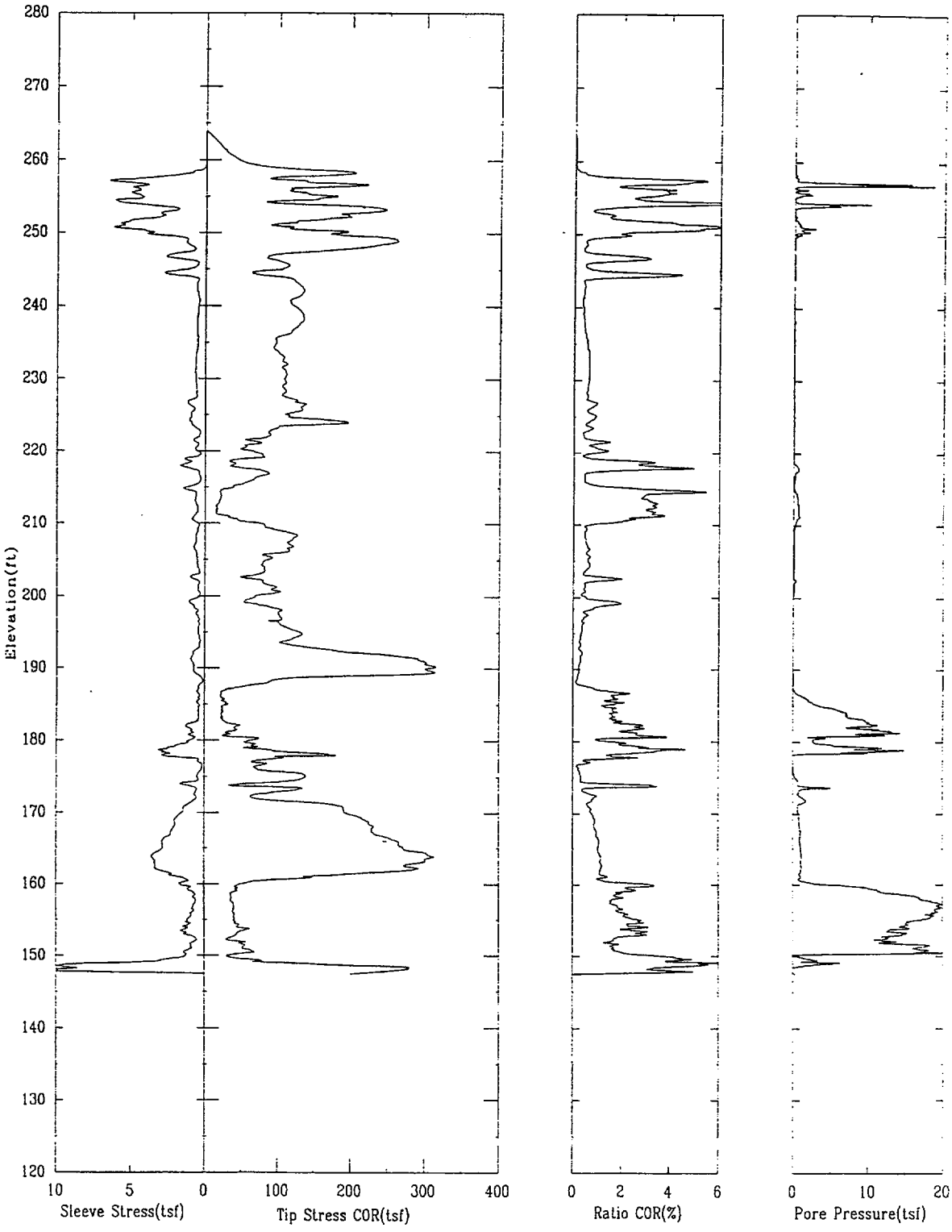

File 3151055.ECP

DCS, MFFF Project No. 08716

CPT-43 APPLIED RESEARCH ASSOCIATES, INC. 07/15/00

North 80257.7 East 55585.0 Elevation 264.0

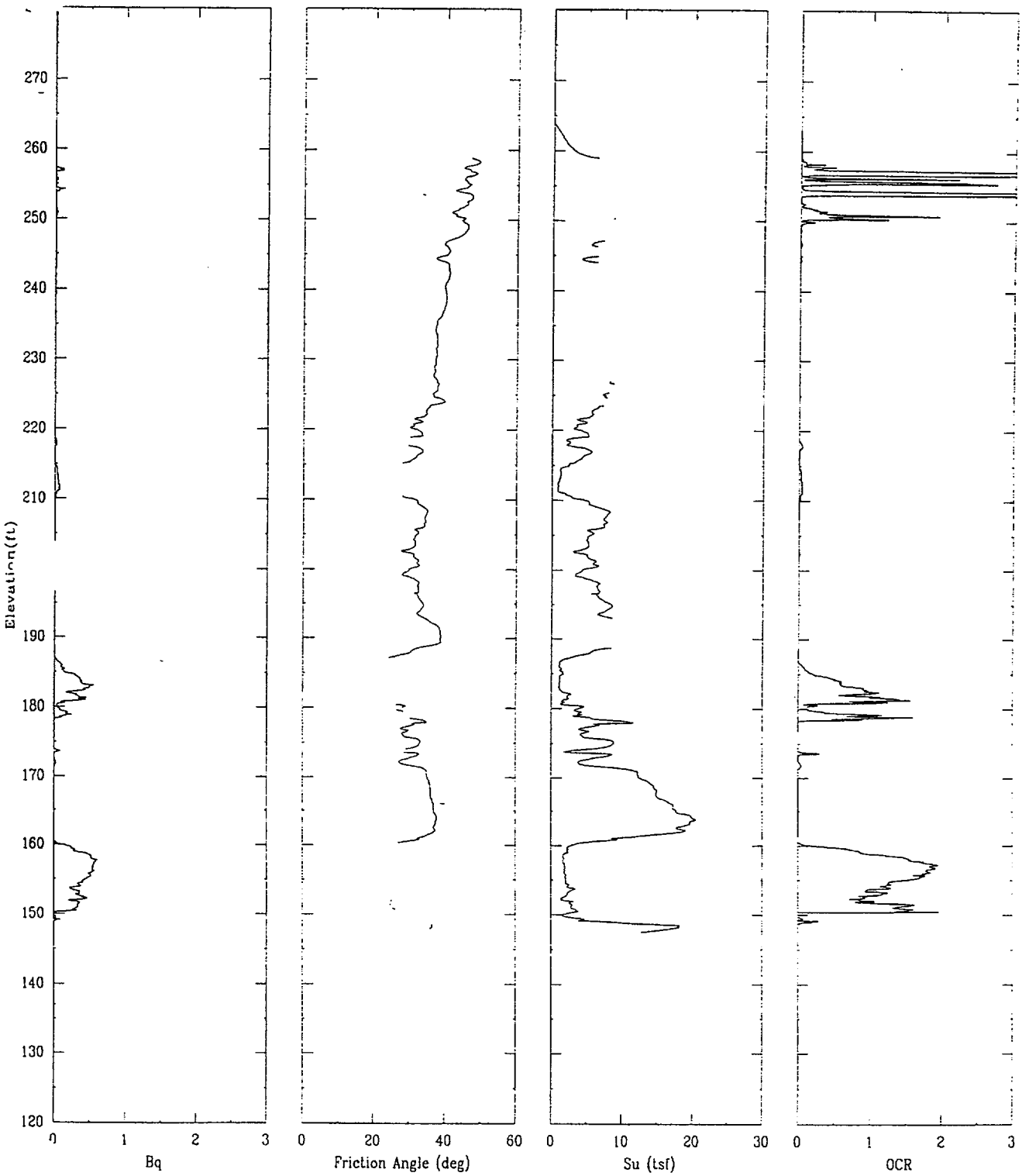

File 315L055.ECP

DCS, MFFF Project No. 08716

CPT-43 APPLIED RESEARCH ASSOCIATES, INC. 07/15/00

North 80257.7 East 55585.0 Elevation 264.0

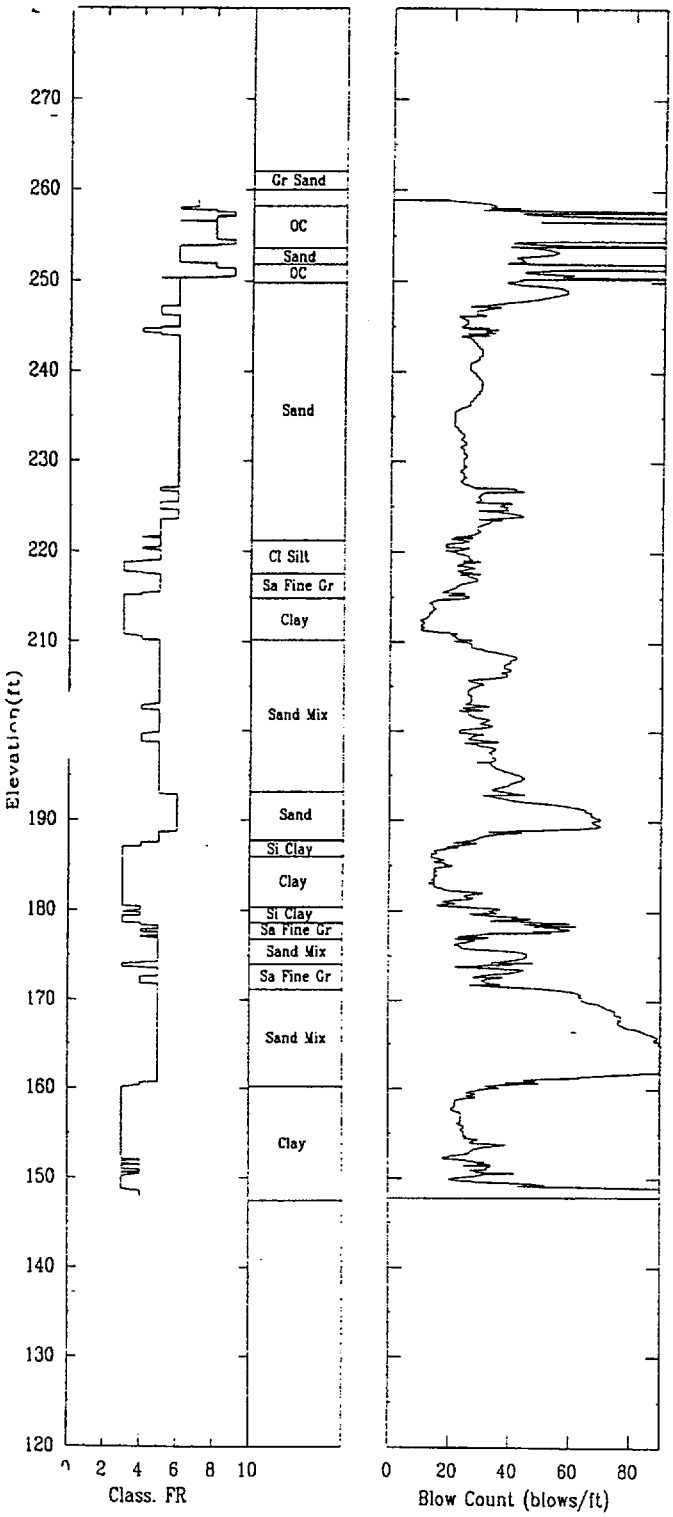

File 315L055.ECP

CPT-44 APPLIED RESEARCH ASSOCIATES, INC. 07/20/00

North 60530.3 East 55109.3 Elevation 284.7

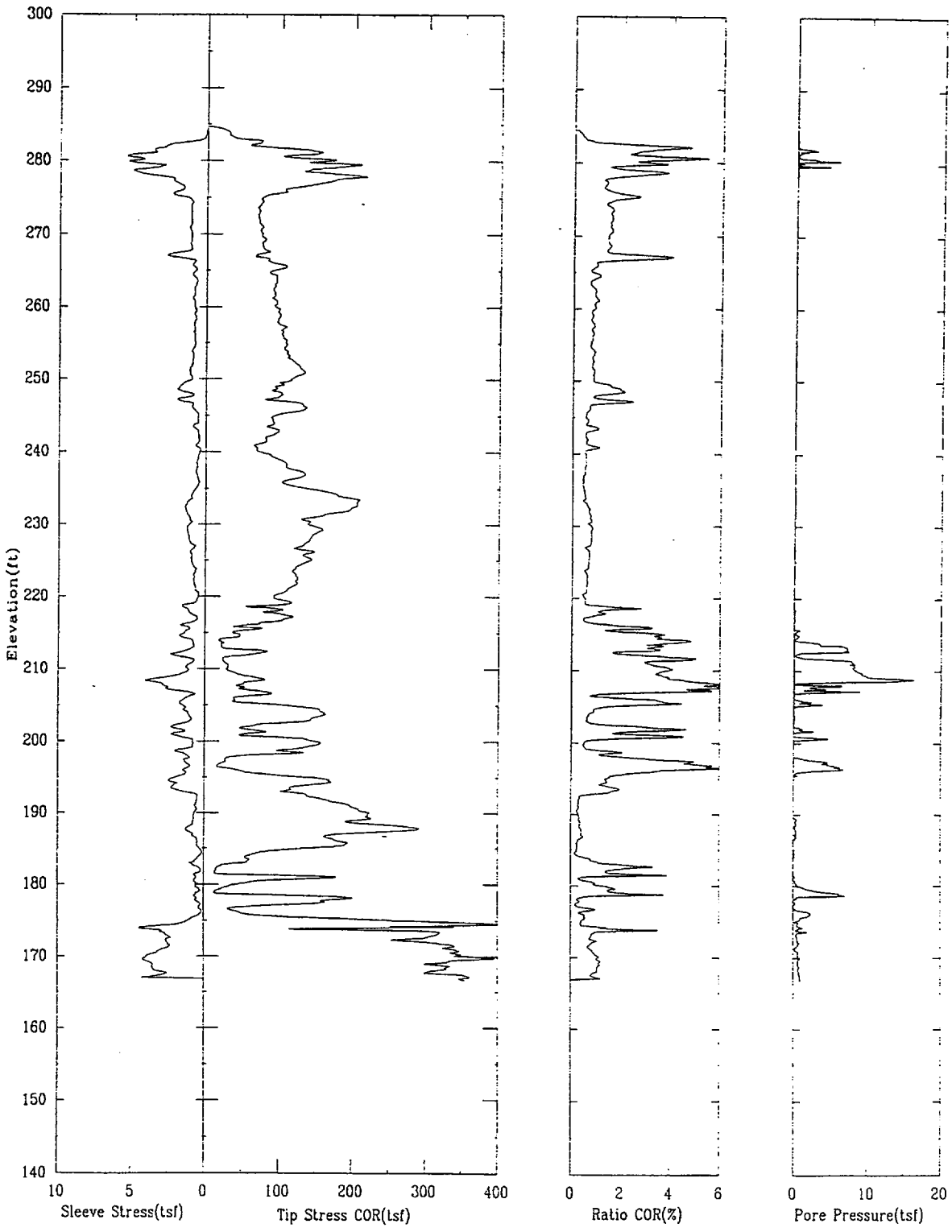

File 320L005.ECP

CPT-44 APPLIED RESEARCH ASSOCIATES, INC. 07/20/00

North 80530.3 East 55109.3 Elevation 284.7

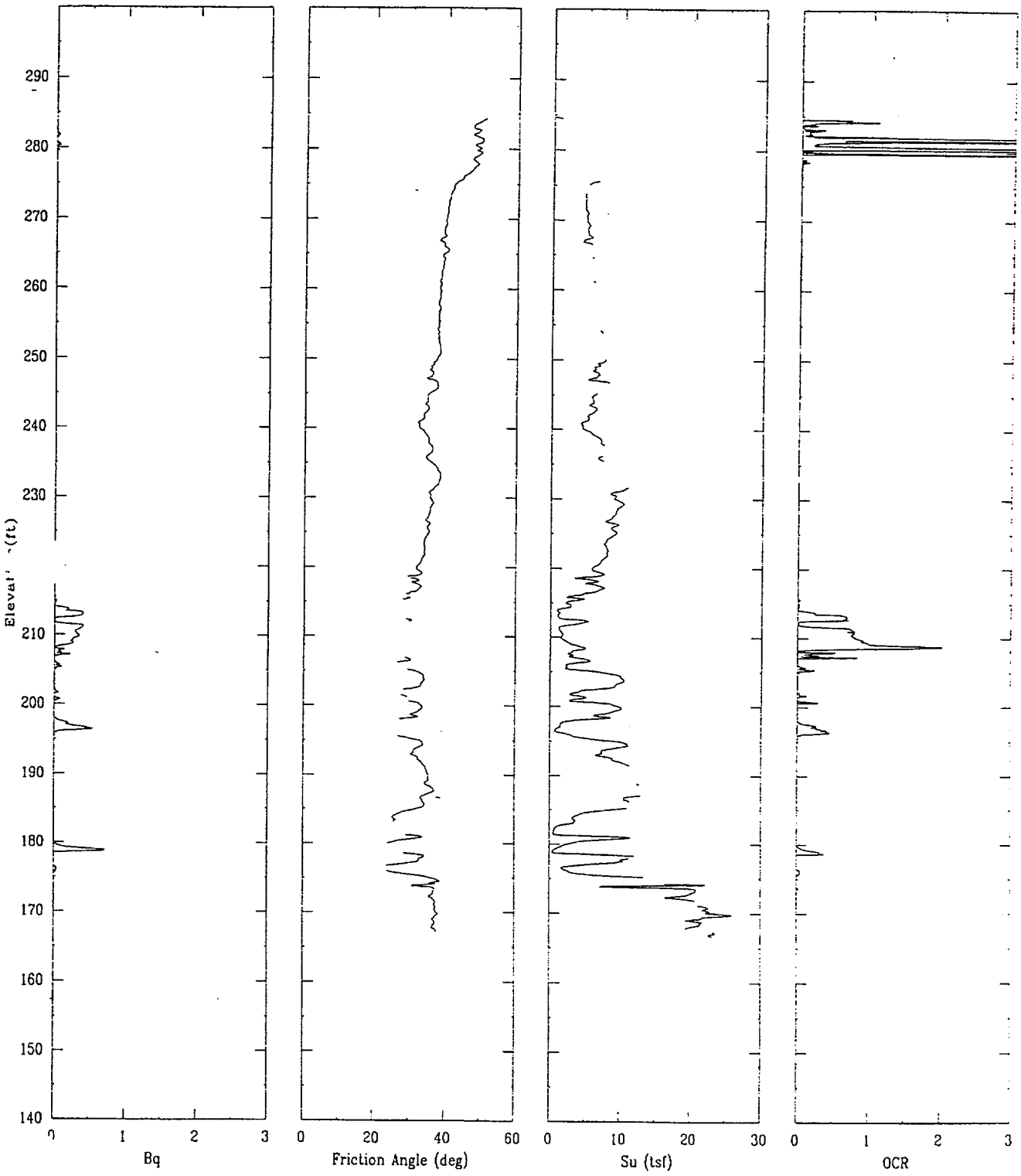

File 320L005.ECP

CPT-44 APPLIED RESEARCH ASSOCIATES, INC. 07/20/00

North 80530.3 East 55109.3 Elevation 284.7

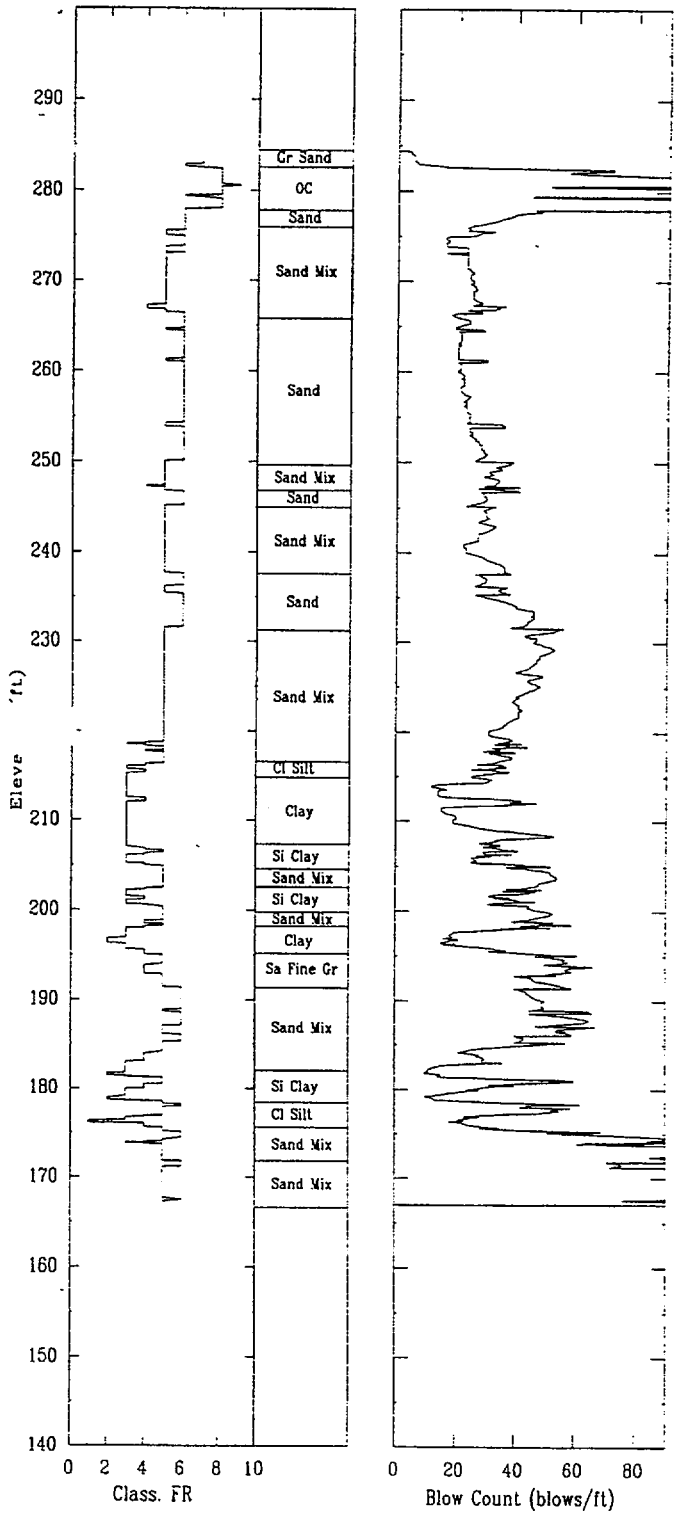

File 320L005.ECP

DCS, MFFF Project No. 08716

CPT-45 APPLIED RESEARCH ASSOCIATES, INC. 07/21/00

North 80531.1 East 55194.0 Elevation 280.5

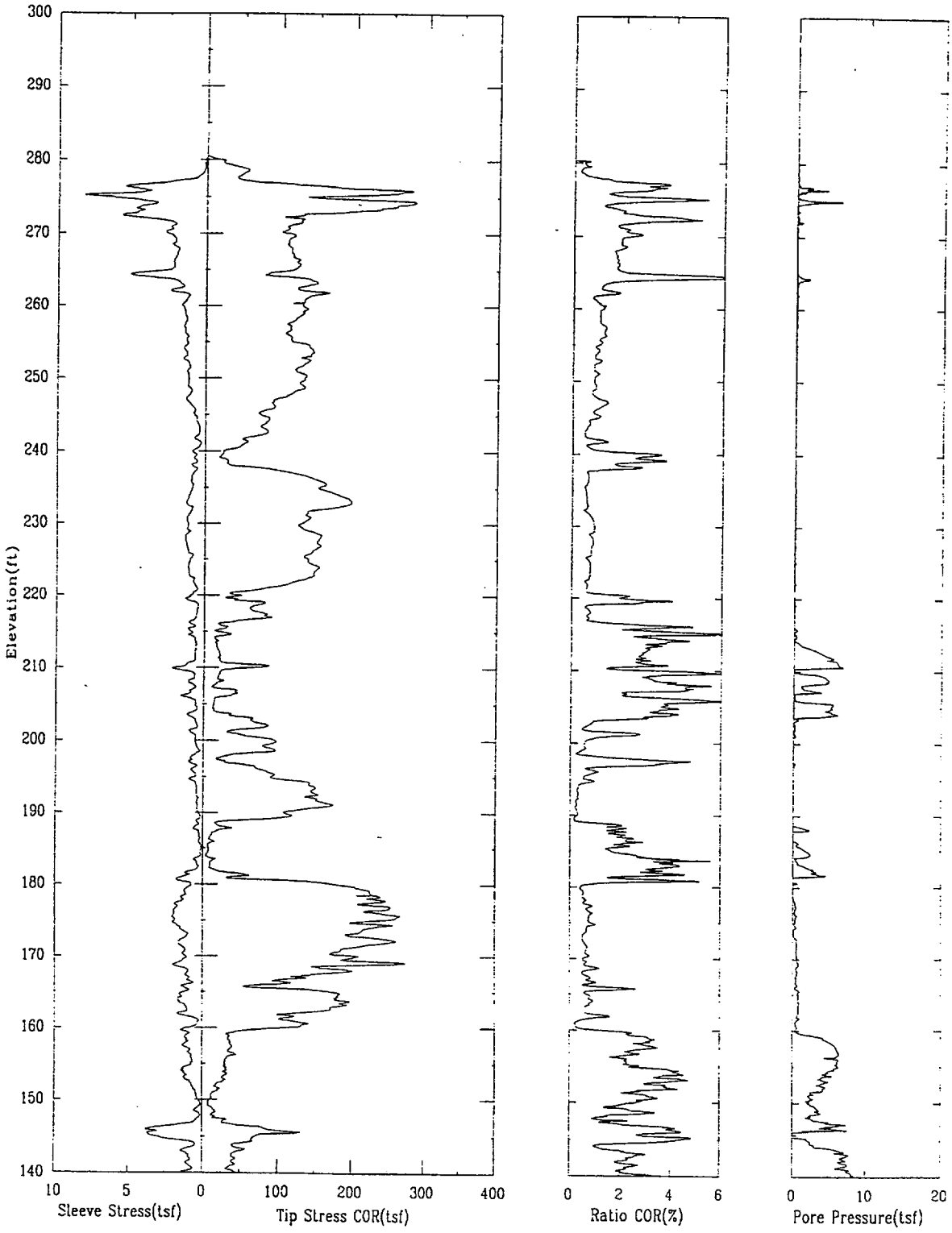

File 321L001.ECP

CPT-45 APPLIED RESEARCH ASSOCIATES, INC. 07/21/00

North 80531.1 East 55194.0 Elevation 280.5

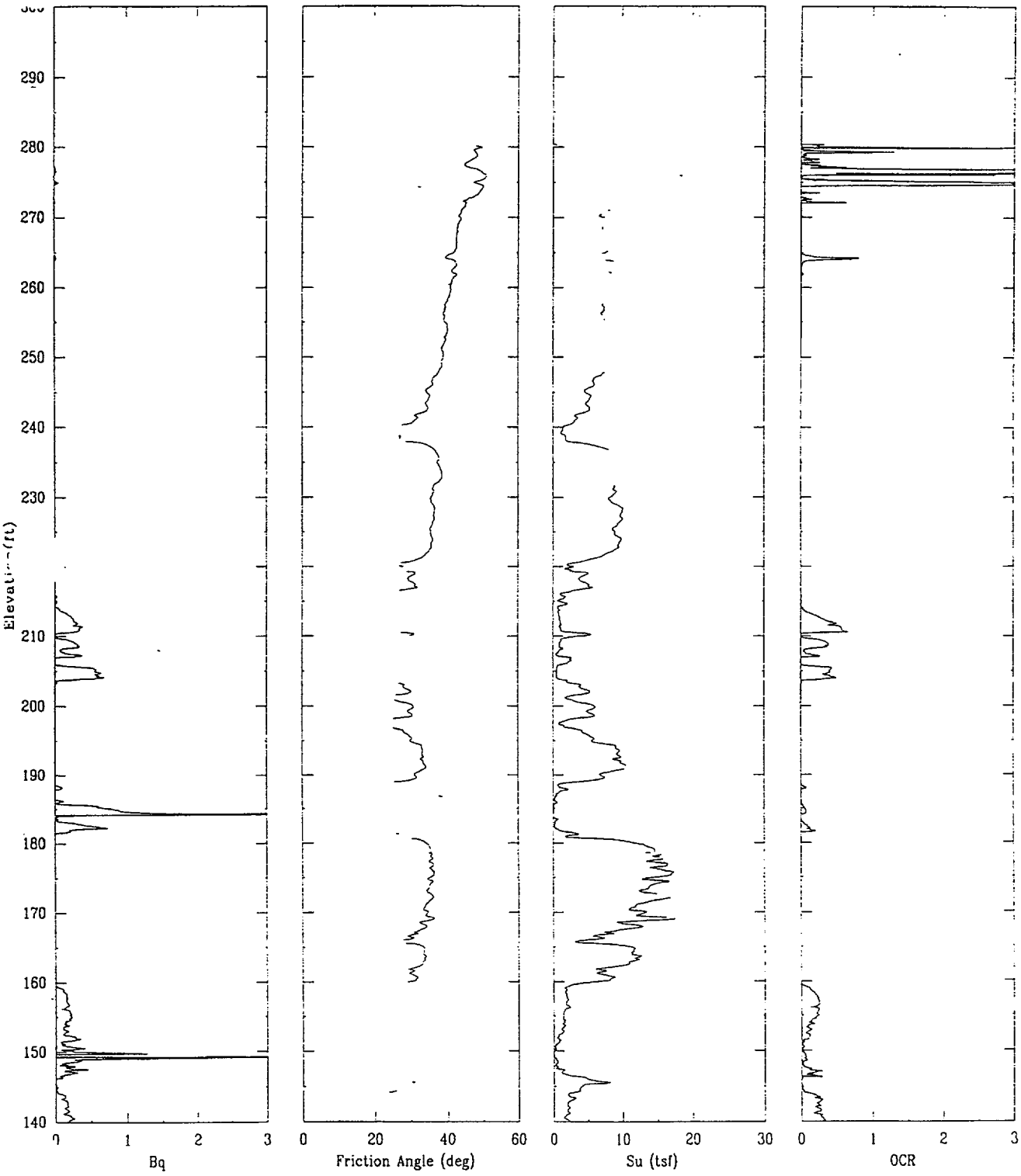

File 321L001.ECP

CPT-45 APPLIED RESEARCH ASSOCIATES, INC. 07/21/00

North 80531.1 East 55194.0 Elevation 280.5

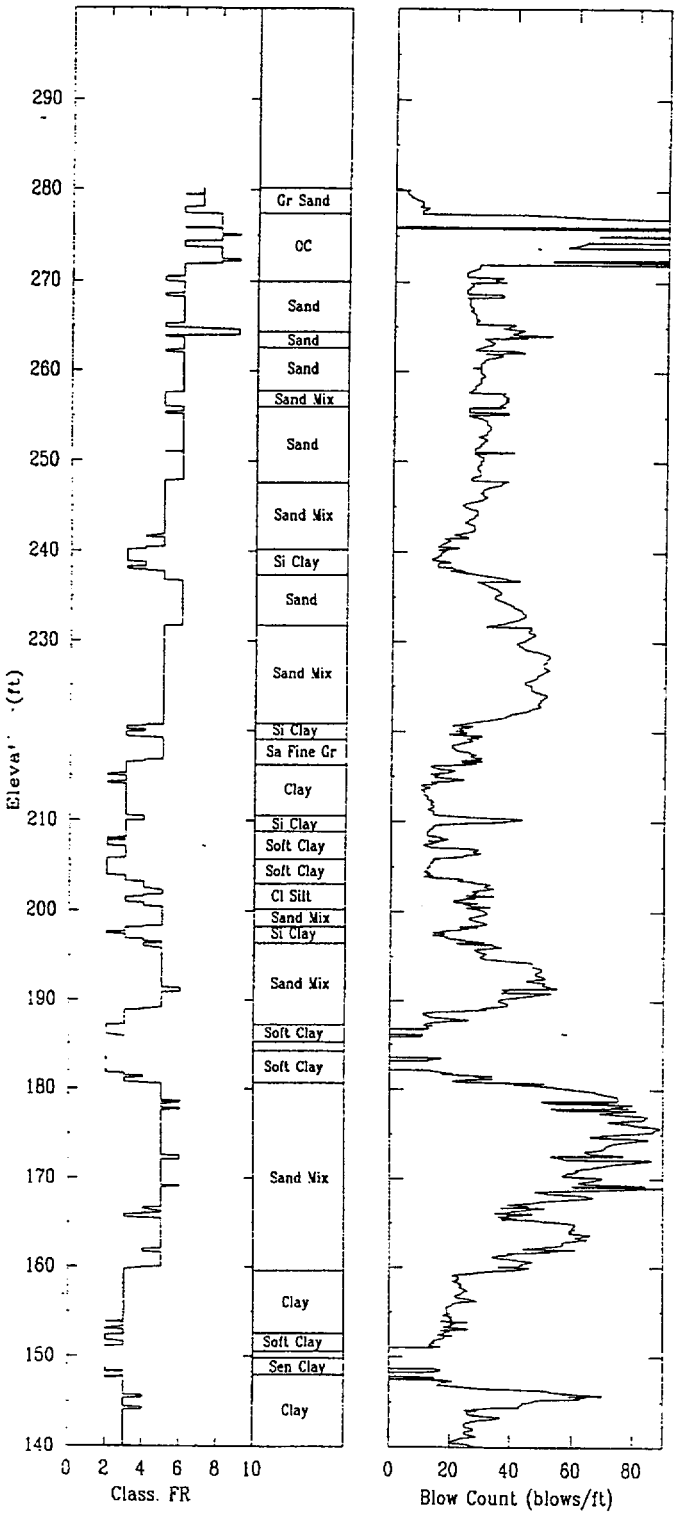

File 321L001.ECP

CPT-46 APPLIED RESEARCH ASSOCIATES, INC. 07/20/00

North 80482.0 East 55032.8 Elevation 284.5

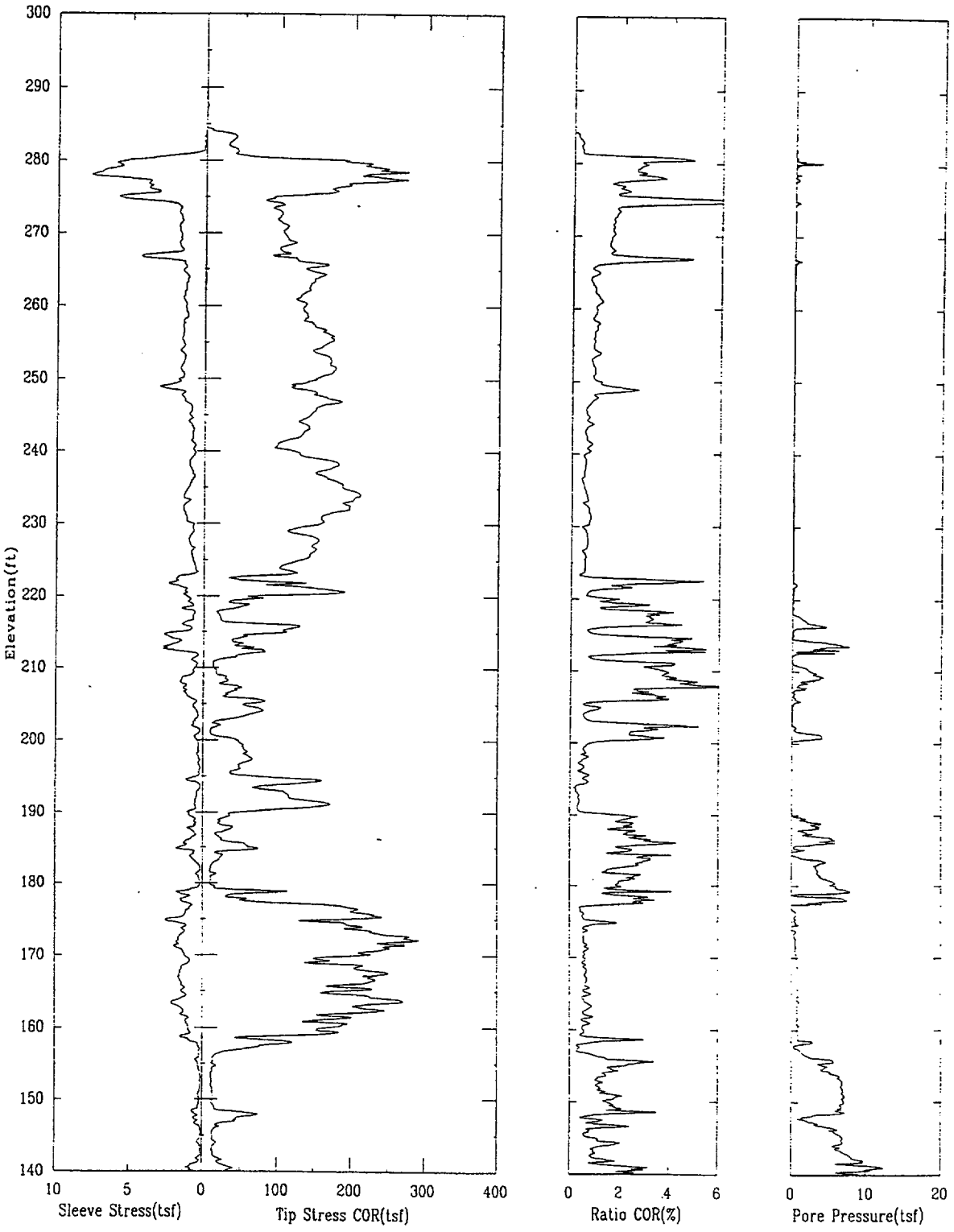

File 320L003.ECP

CPT-46 APPLIED RESEARCH ASSOCIATES, INC. 07/20/00

North 80482.0 East 55032.8 Elevation 284.5

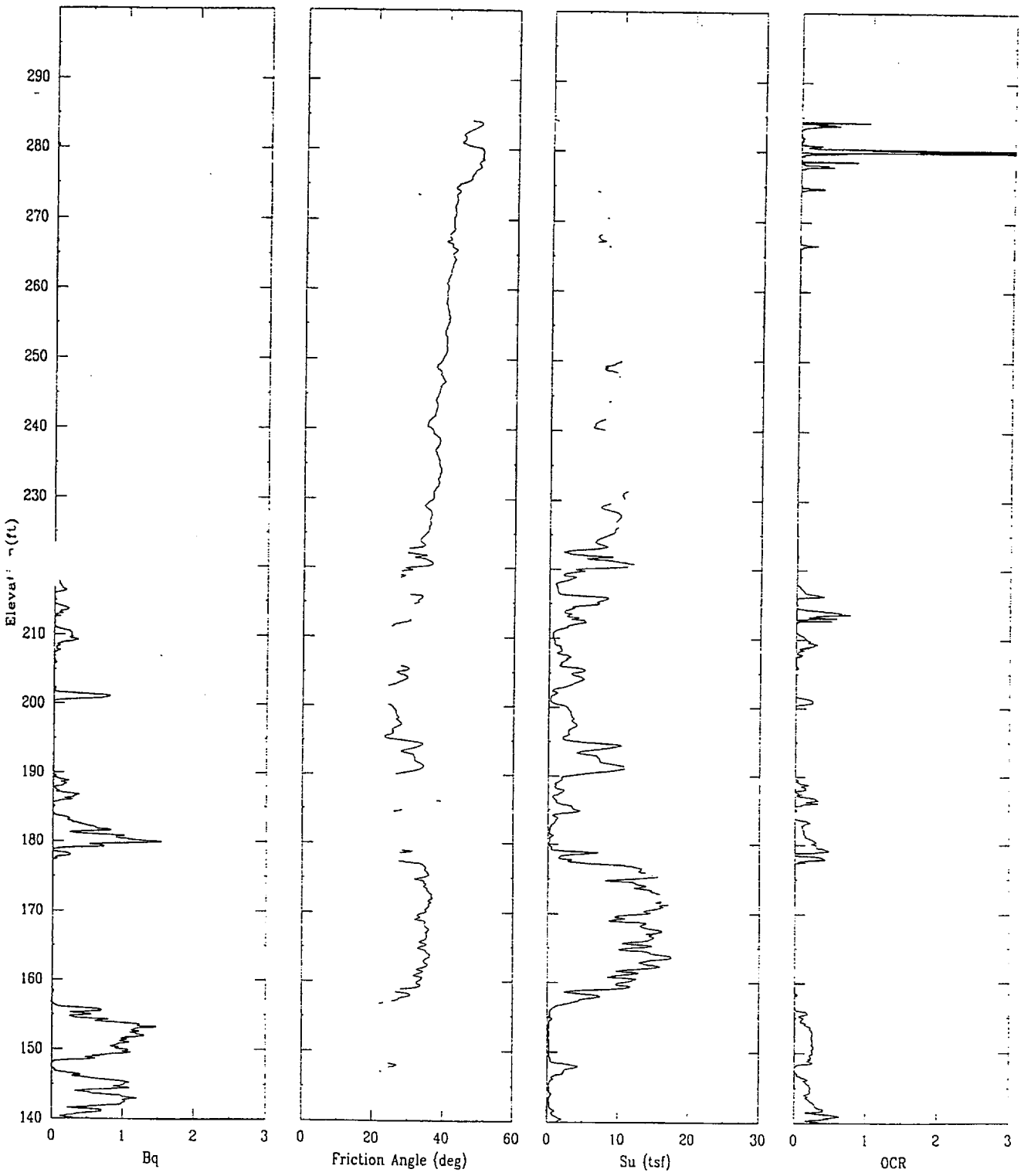

File 320L003.ECP

DCS, MFFF Project No. 08716

CPT-46 APPLIED RESEARCH ASSOCIATES, INC. 07/20/00

North 80482.0 East 55032.8 Elevation 284.5

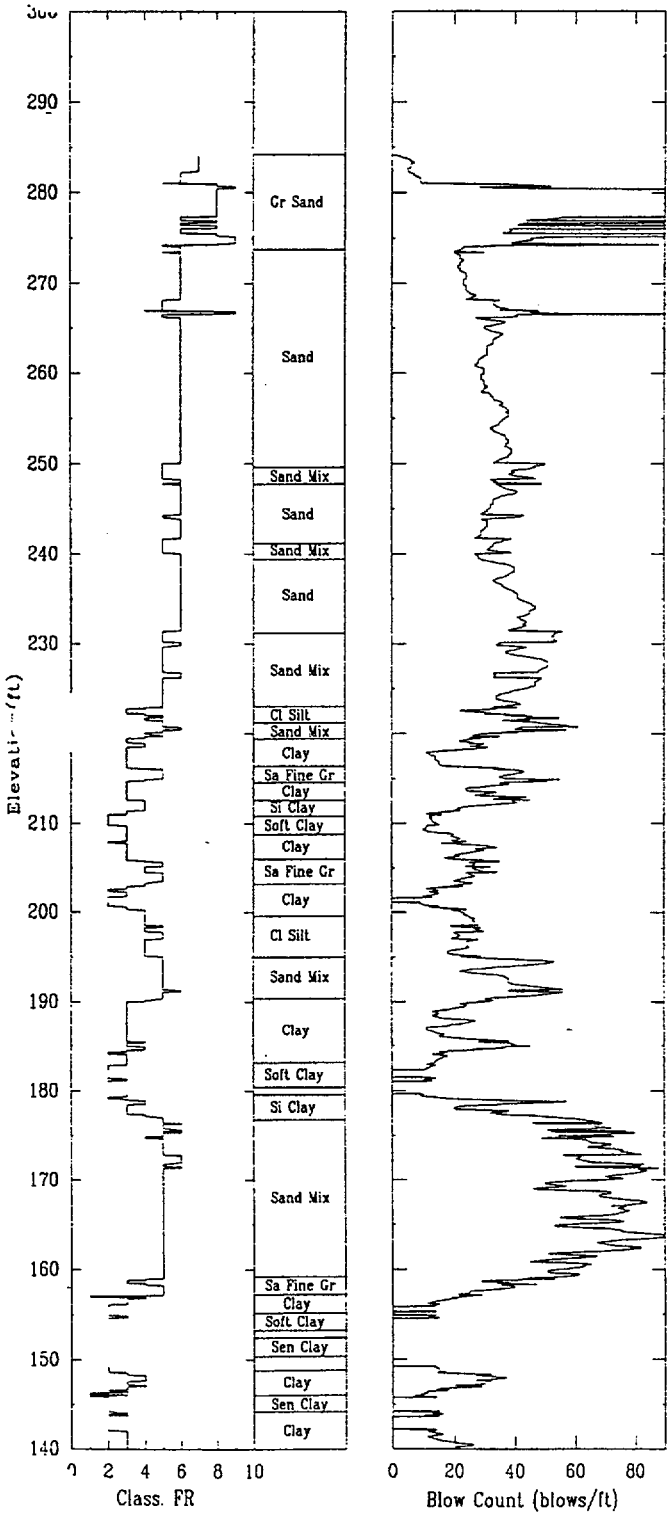

File 320L003.ECP

CPT-47 APPLIED RESEARCH ASSOCIATES, INC. 07/20/00

North 80456.7 East 55146.5 Elevation 284.1

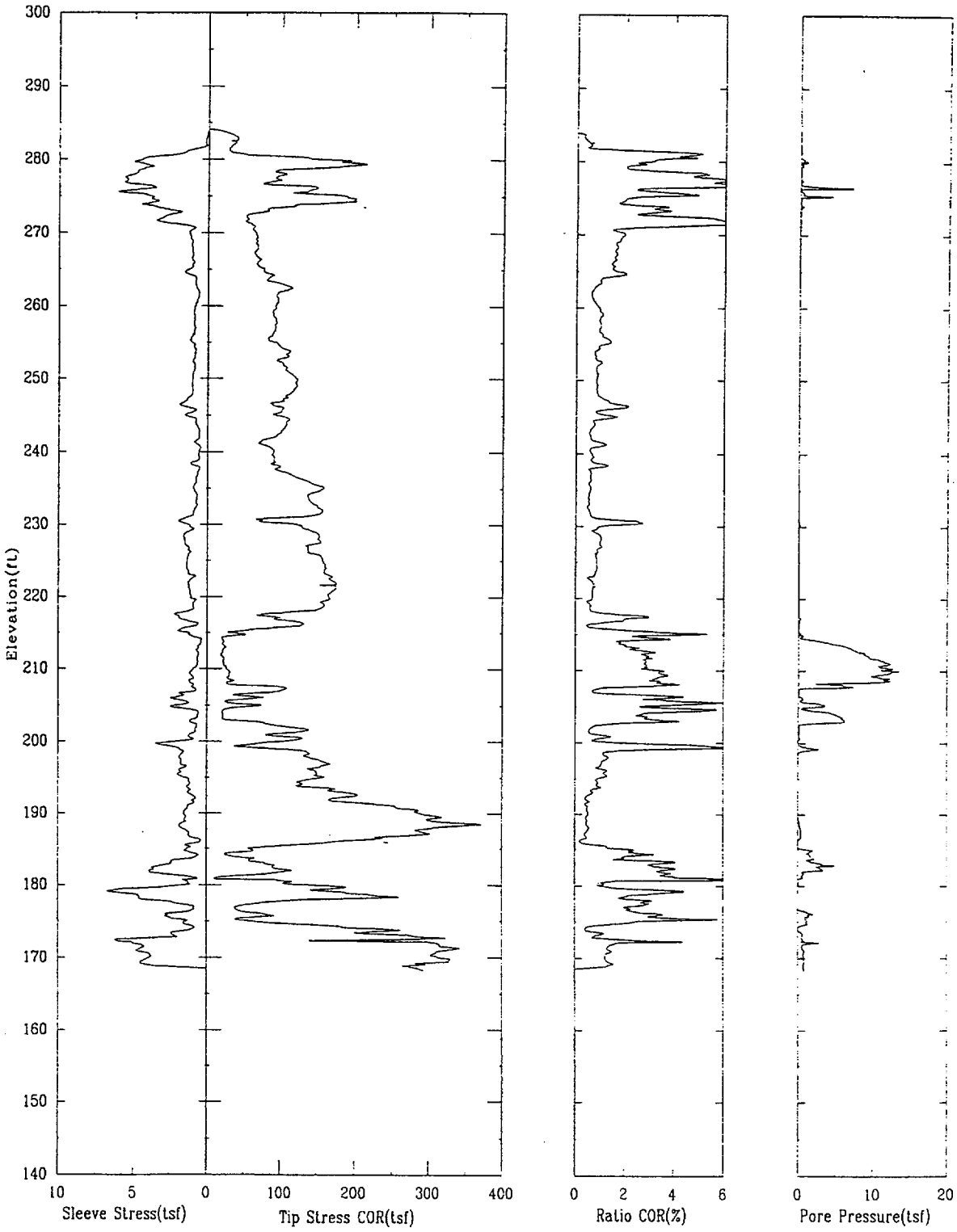

File 320L007.ECP

DCS, MFFF Project No. 08716

CPT-47 APPLIED RESEARCH ASSOCIATES, INC. 07/20/00

North 80456.7 East 55146.5 Elevation 284.1

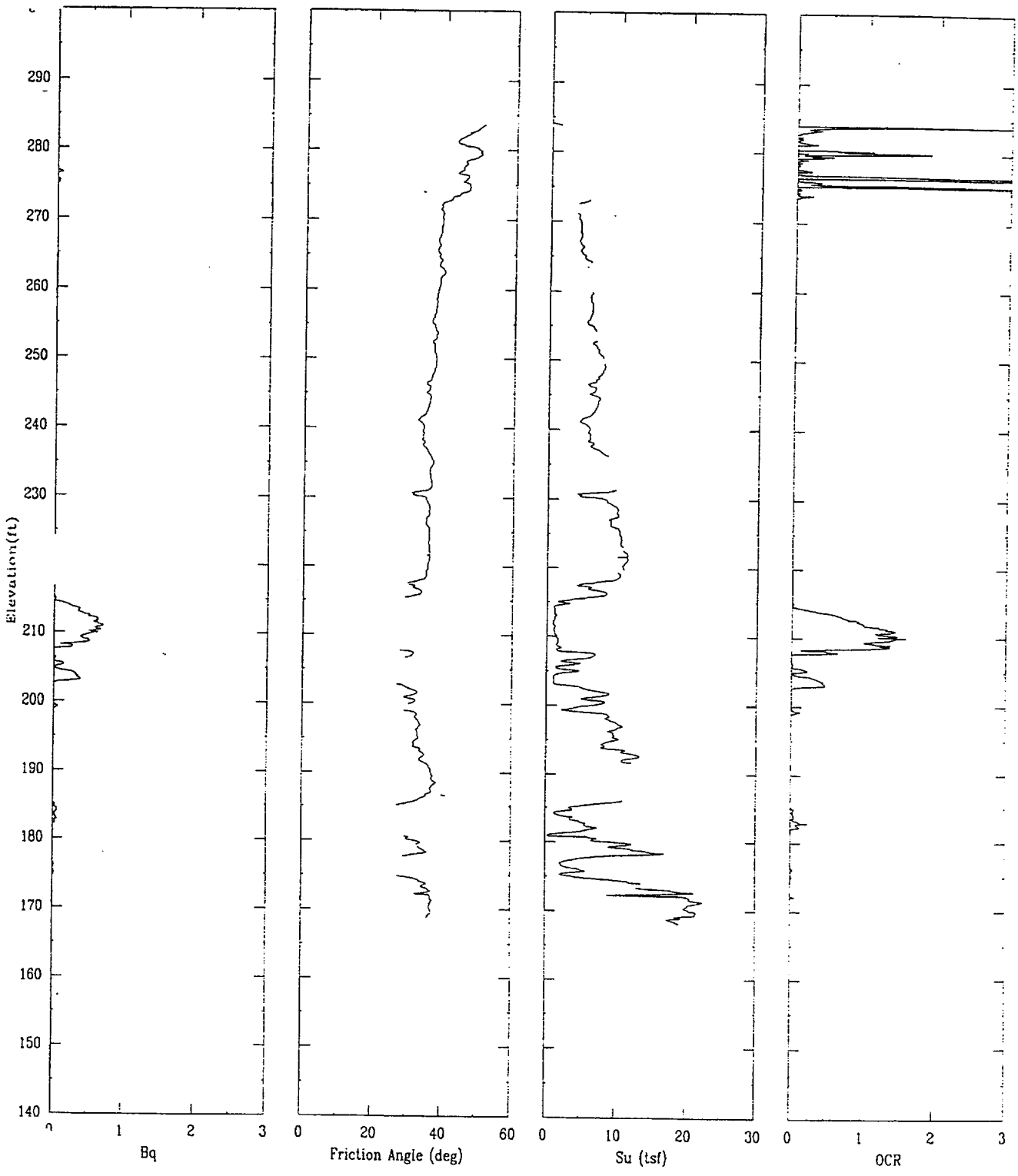

File 320L007.ECP

CPT-47 APPLIED RESEARCH ASSOCIATES, INC. 07/20/00

North 80456.7 East 55146.5 Elevation 284.1

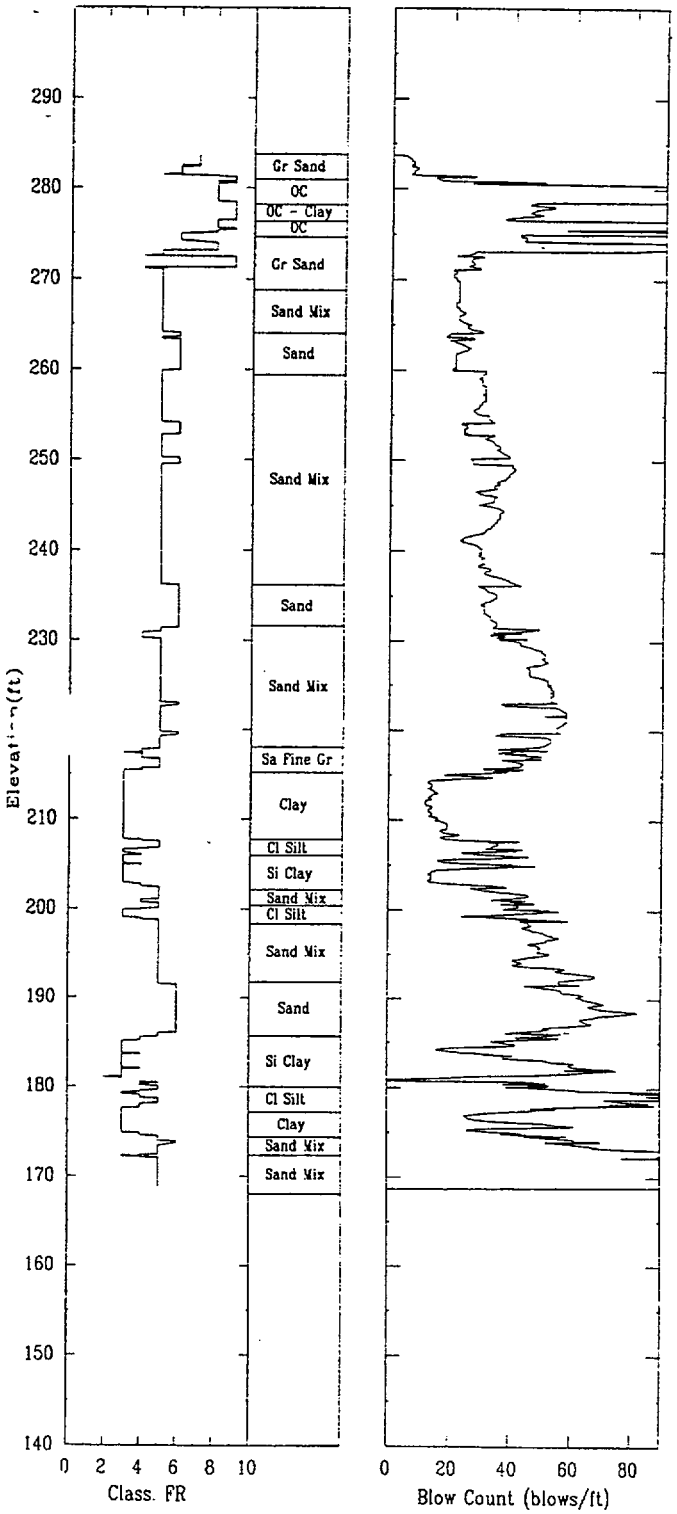

File 320L007.ECP

CPT-48 APPLIED RESEARCH ASSOCIATES, INC. 07/22/00

North 80463.6 East 54964.1 Elevation 281.2

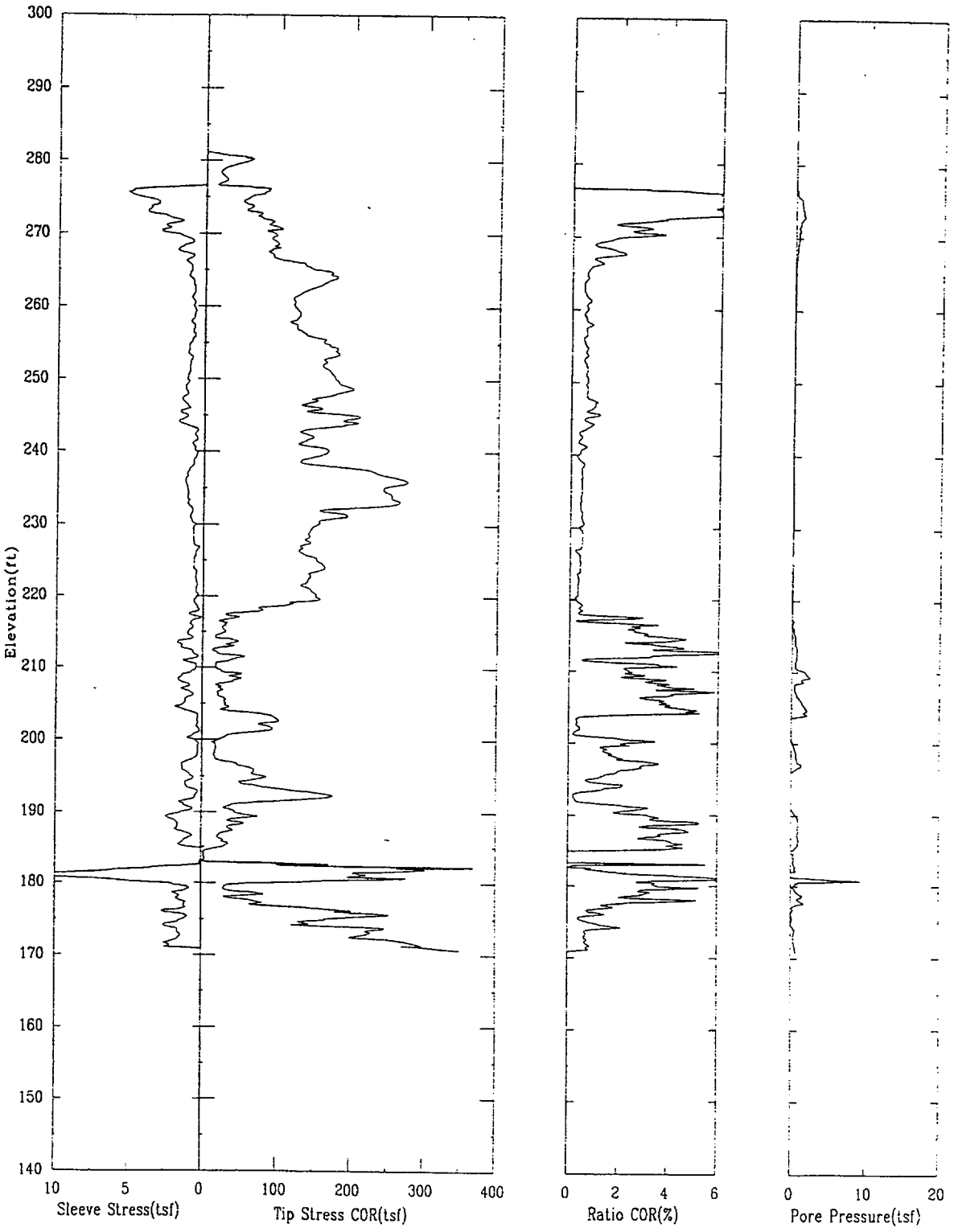

File 322L005.ECP

DCS, MFFF Project No. 08716

CPT-48 APPLIED RESEARCH ASSOCIATES, INC. 07/22/00

North 80463.6 East 54964.1 Elevation 281.2

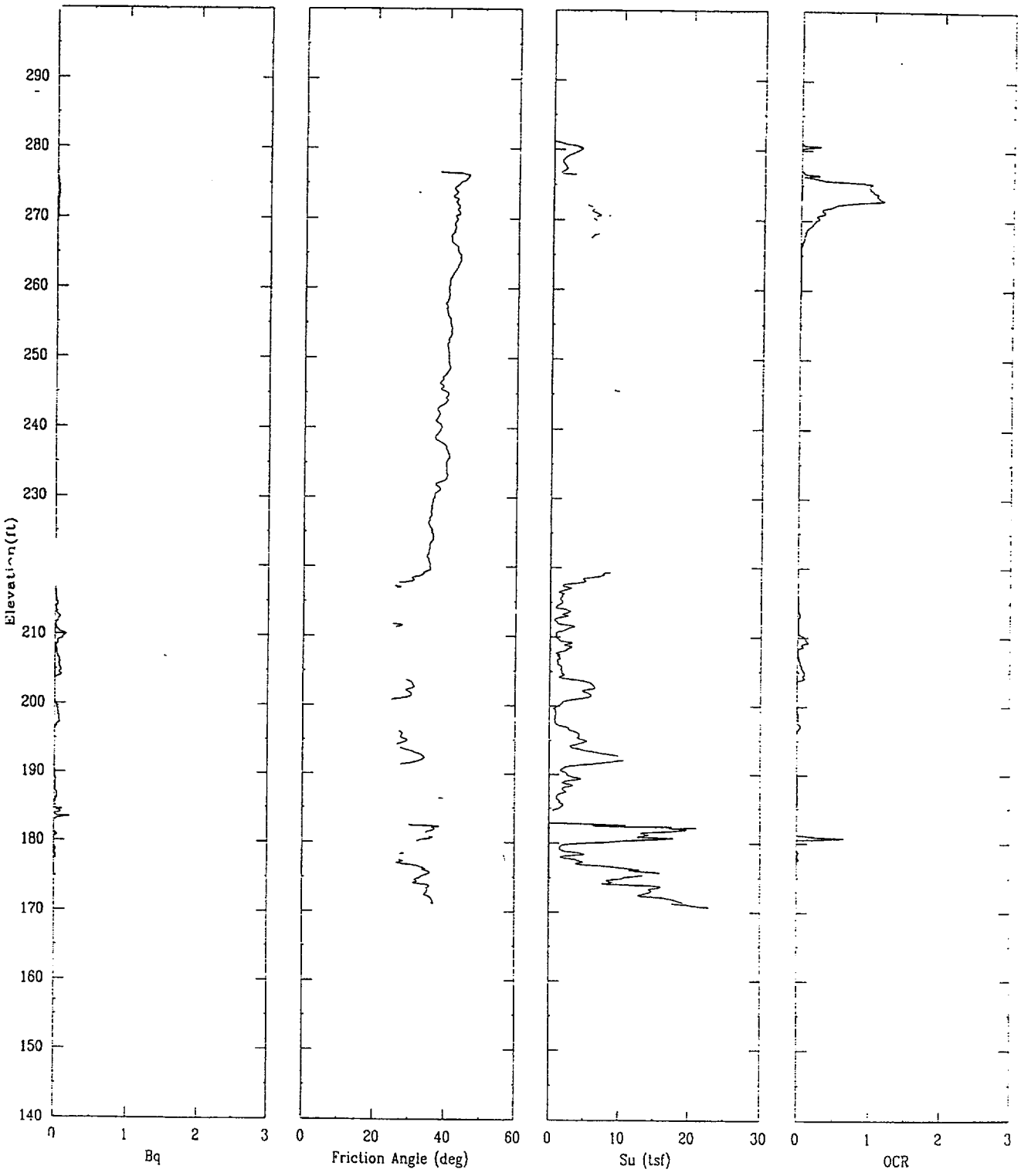

File 322L005.ECP

CPT-48 APPLIED RESEARCH ASSOCIATES, INC. 07/22/00

North 80463.6 East 54964.1 Elevation 281.2

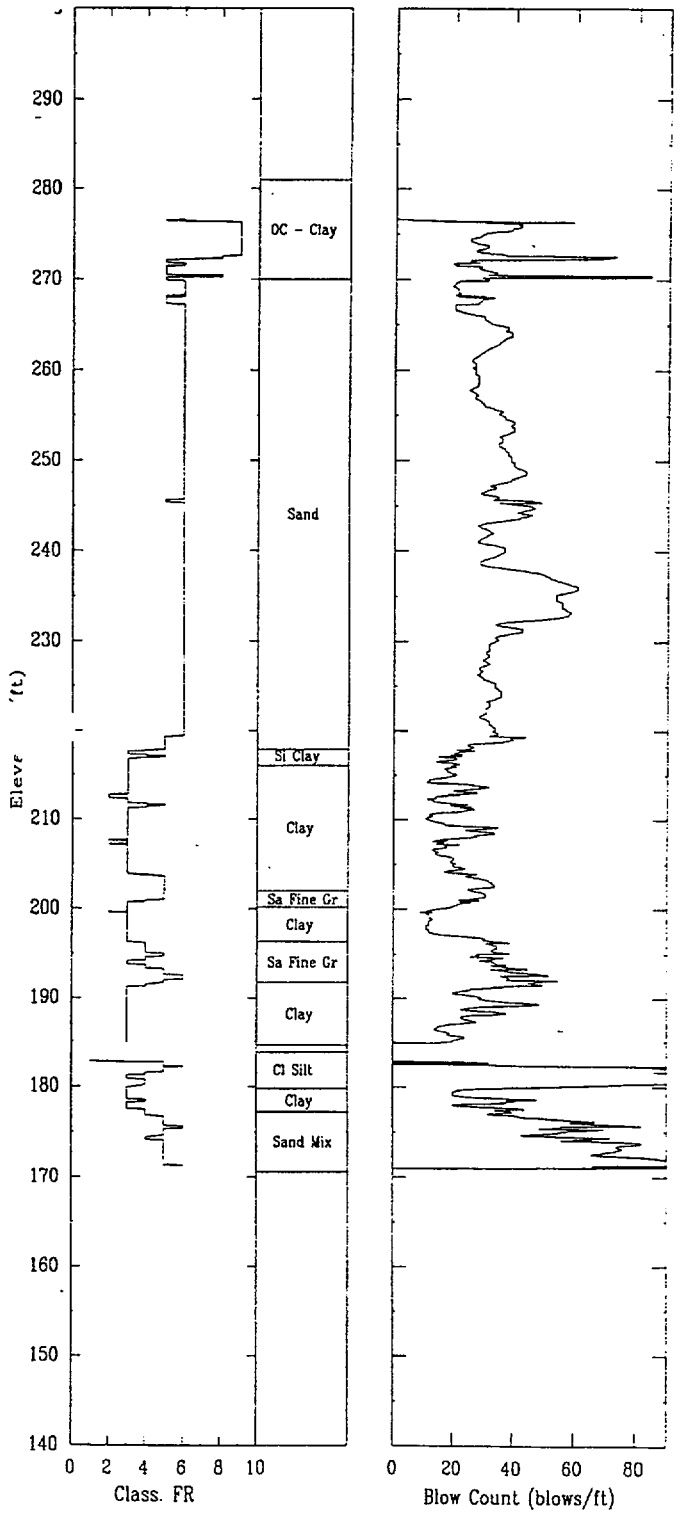

File 322L005.ECP

CPT-49 APPLIED RESEARCH ASSOCIATES, INC. 07/19/00

North 80332.7 East 54931.1 Elevation 292.4

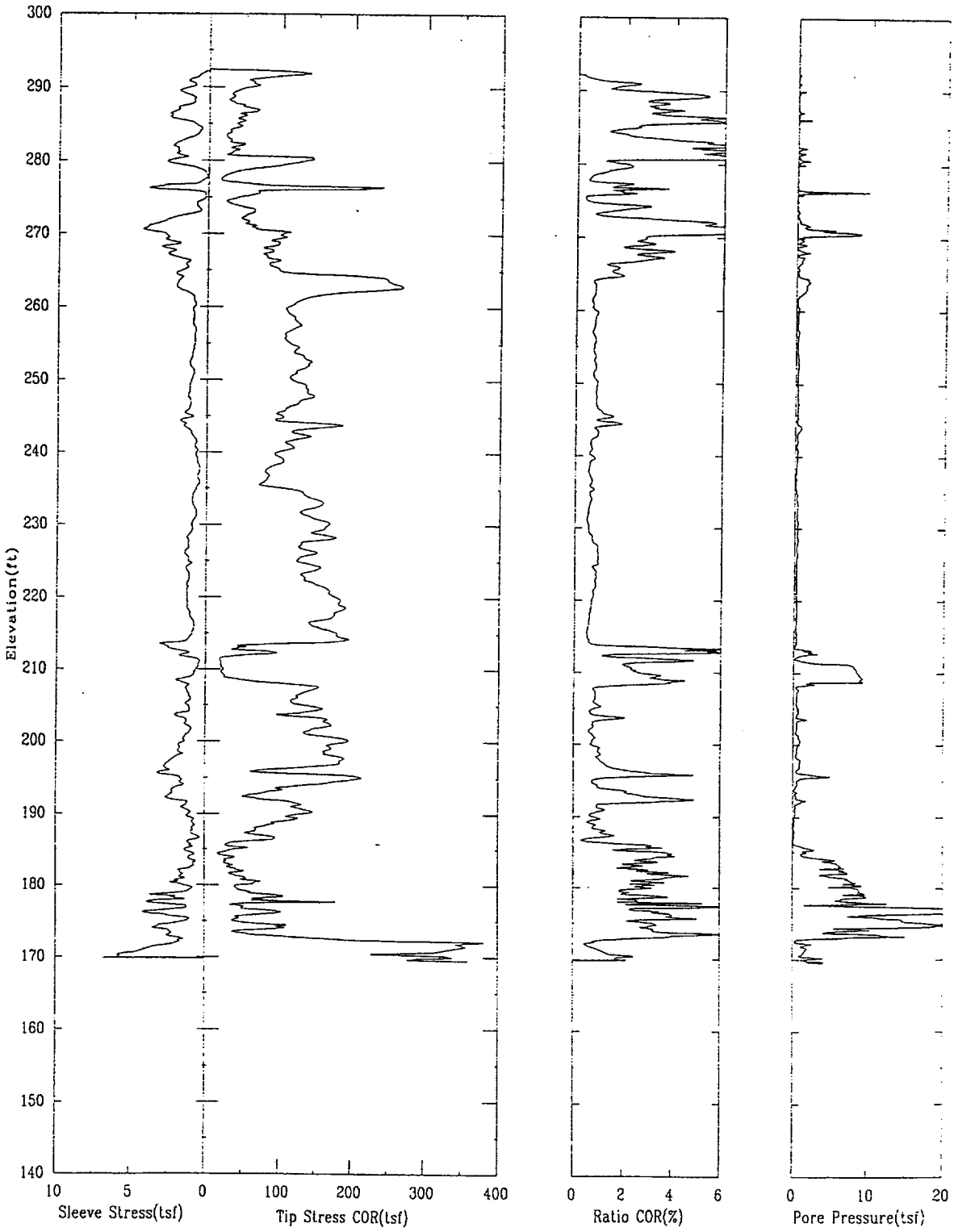

File 319L003.ECP

CPT-49 APPLIED RESEARCH ASSOCIATES, INC. 07/19/00

North 80332.7 East 54931.1 Elevation 292.4

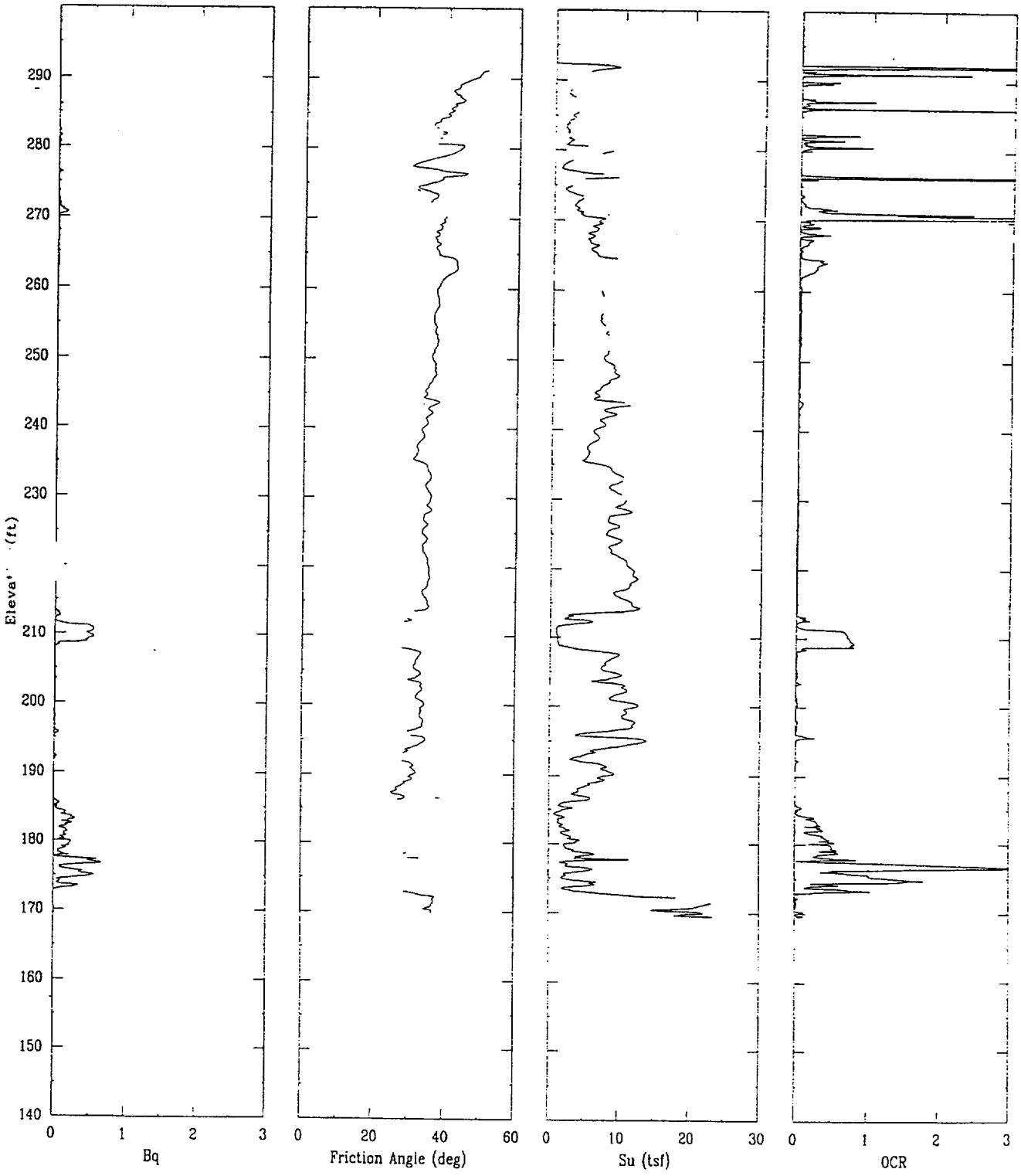

File 319L003.ECP

CPT-49 APPLIED RESEARCH ASSOCIATES, INC. 07/19/00

North 80332.7 East 54931.1 Elevation 292.4

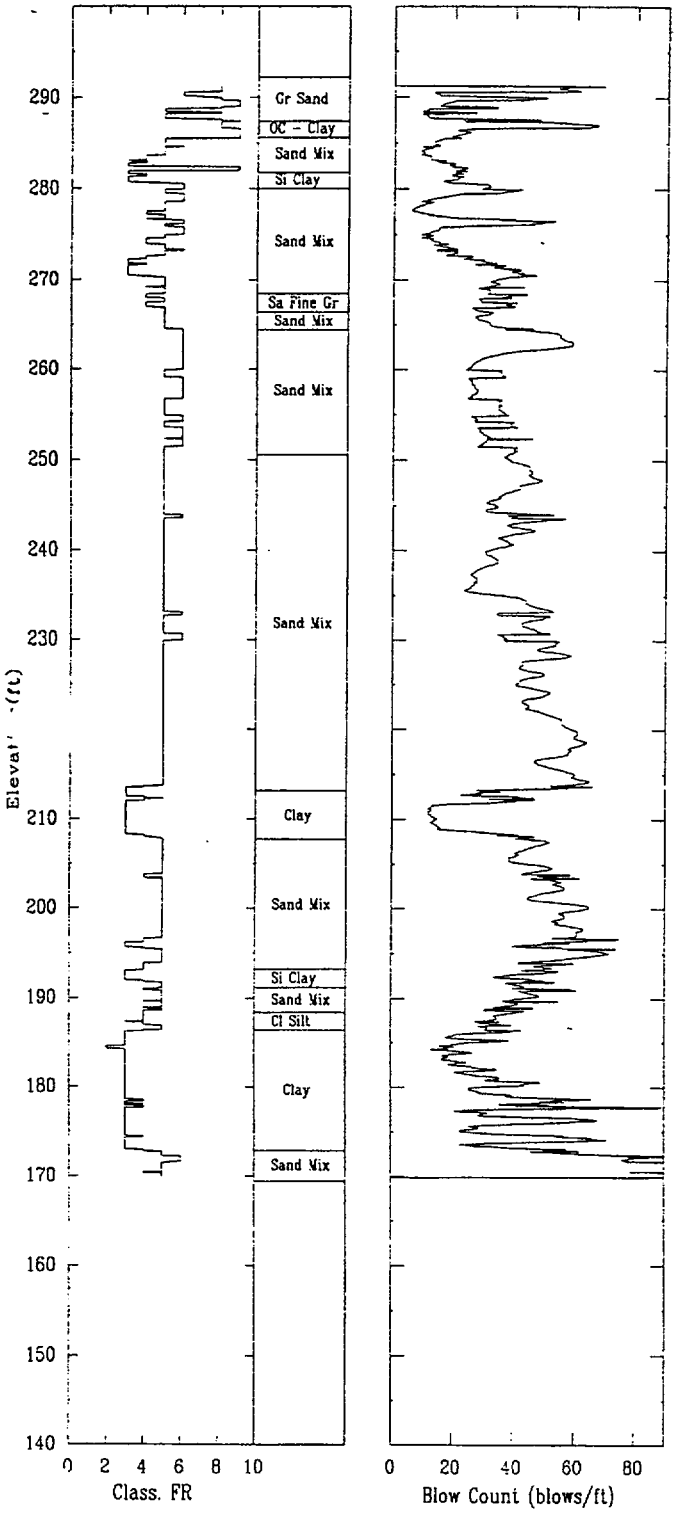

File 319L003.ECP

CPT-50 APPLIED RESEARCH ASSOCIATES, INC. 07/19/00

North 80370.9 East 55140.0 Elevation 294.4

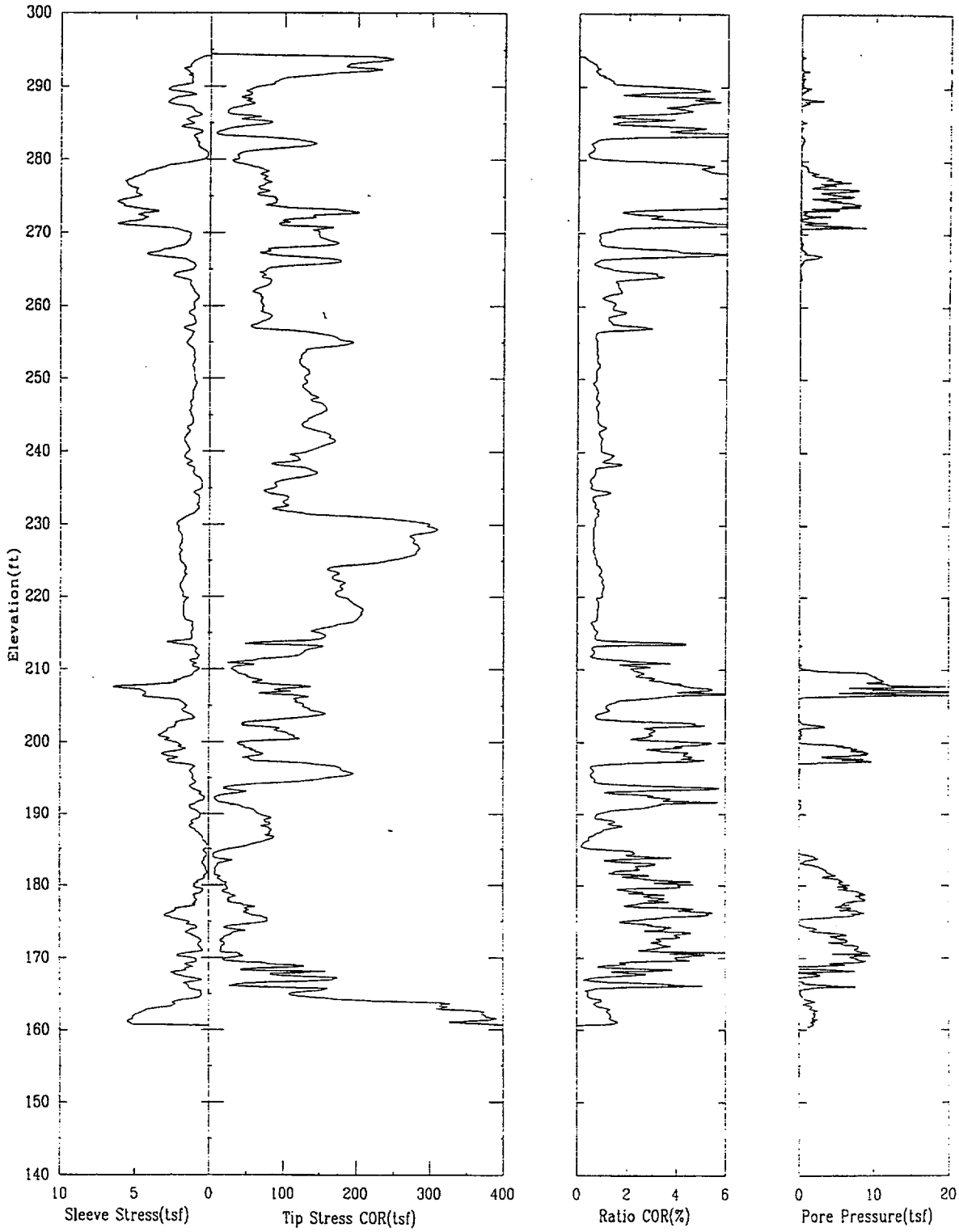

File 319L001.ECP

CPT-50 APPLIED RESEARCH ASSOCIATES, INC. 07/19/00

North 80370.9 East 55140.0 Elevation 294.4

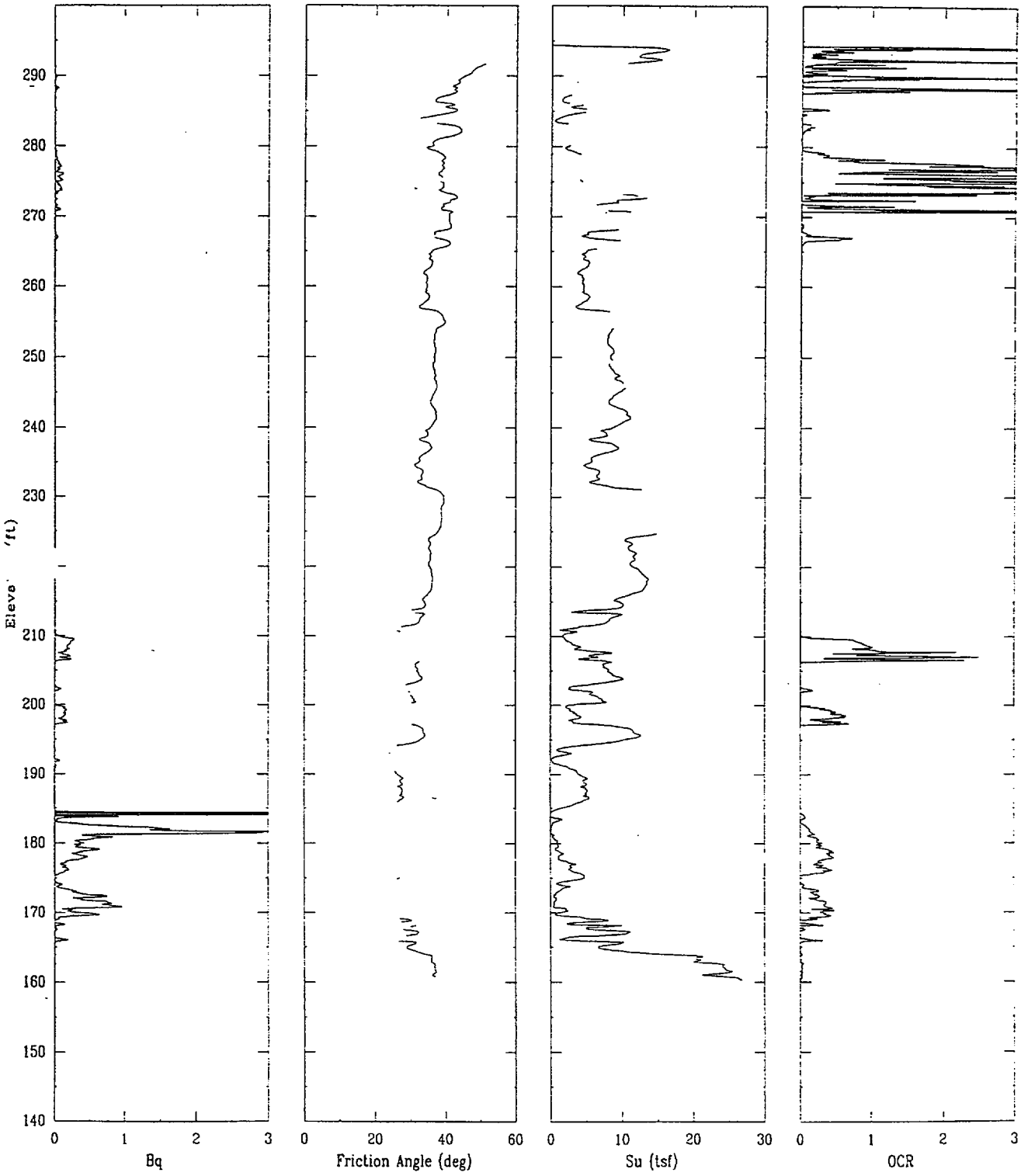

File 3191001.ECP

CPT-50 APPLIED RESEARCH ASSOCIATES, INC. 07/19/00

North 80370.9 East 55140.0 Elevation 294.4

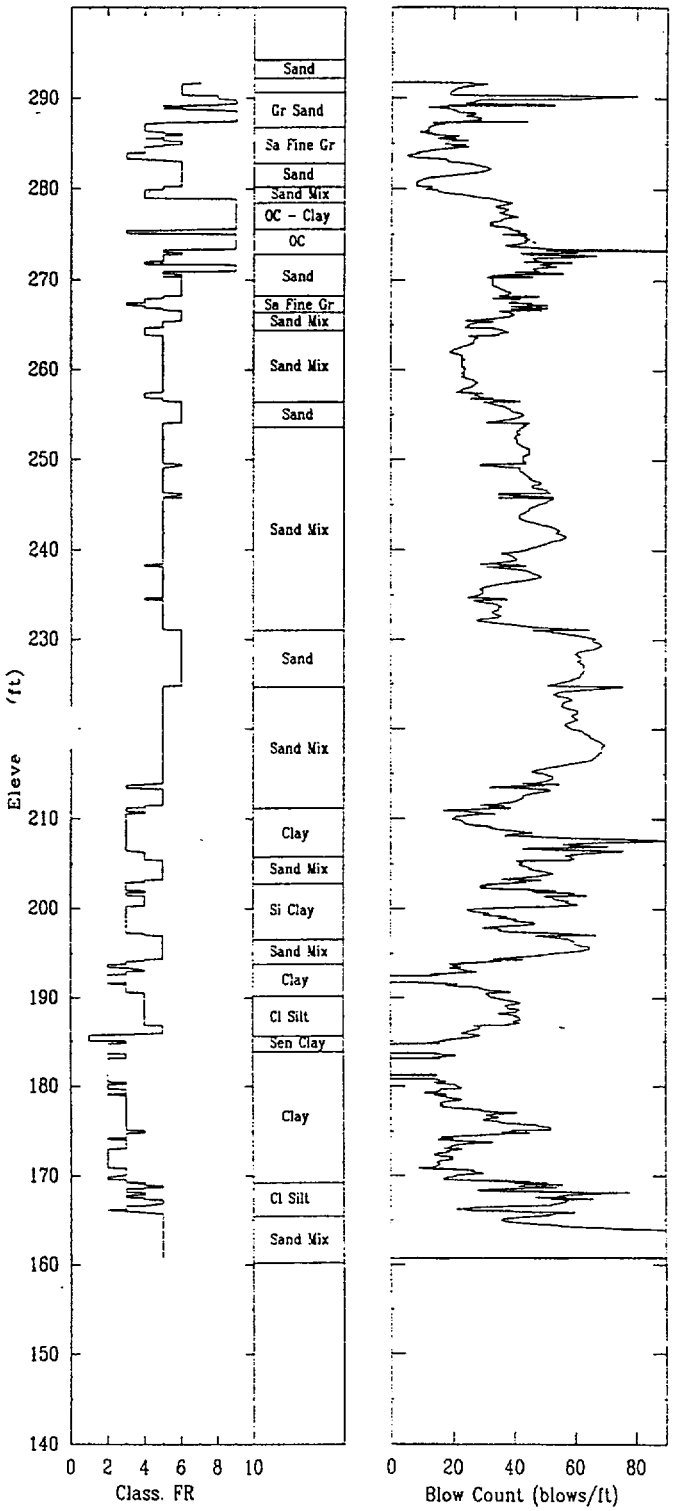

File 319L001.ECP

CPT-51 APPLIED RESEARCH ASSOCIATES, INC. 07/18/00

North 80318.7 East 55198.3 Elevation 295.5

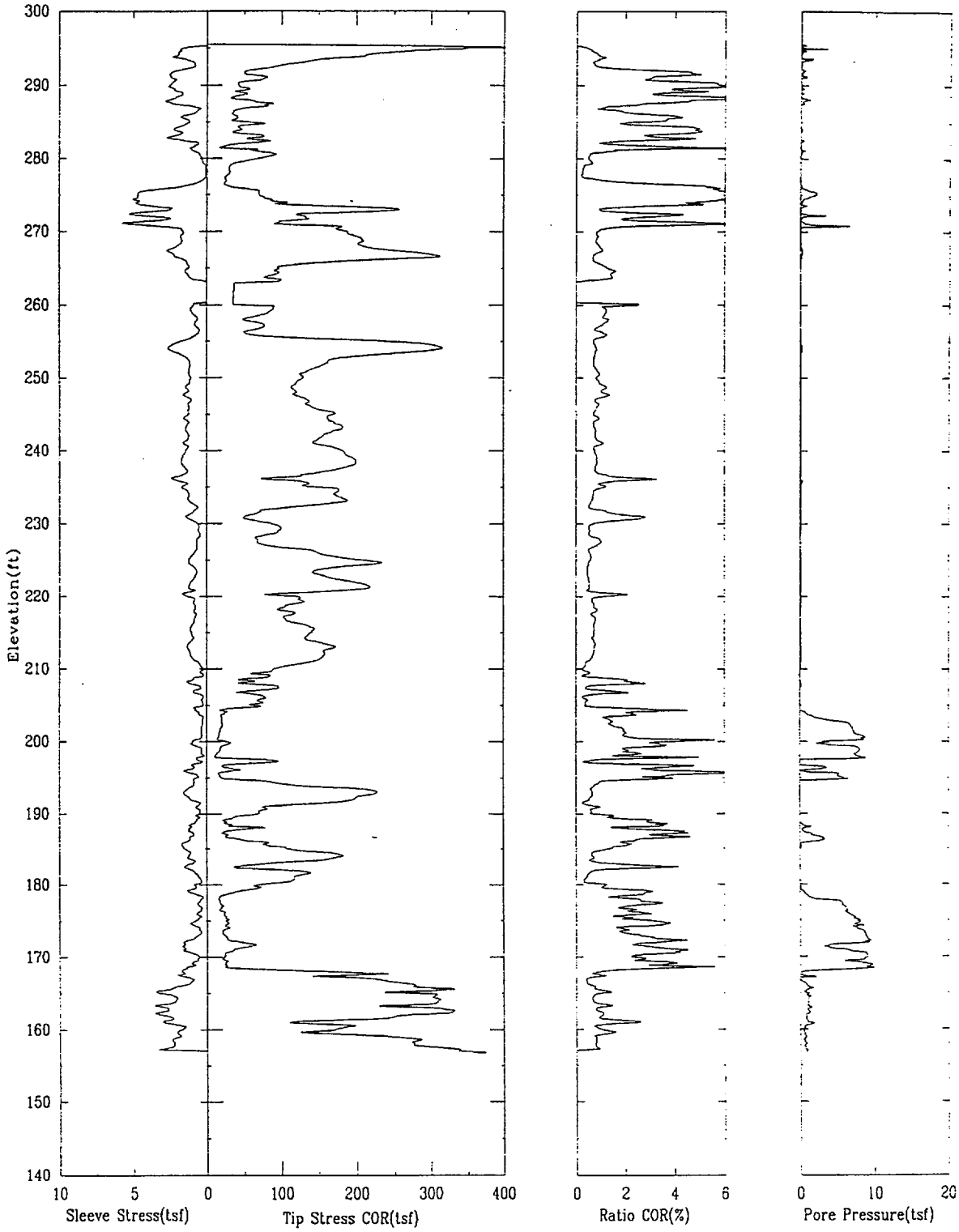

File 318L008.ECP

CPT-51 APPLIED RESEARCH ASSOCIATES, INC. 07/18/00

North 80318.7 East 55198.3 Elevation 295.5

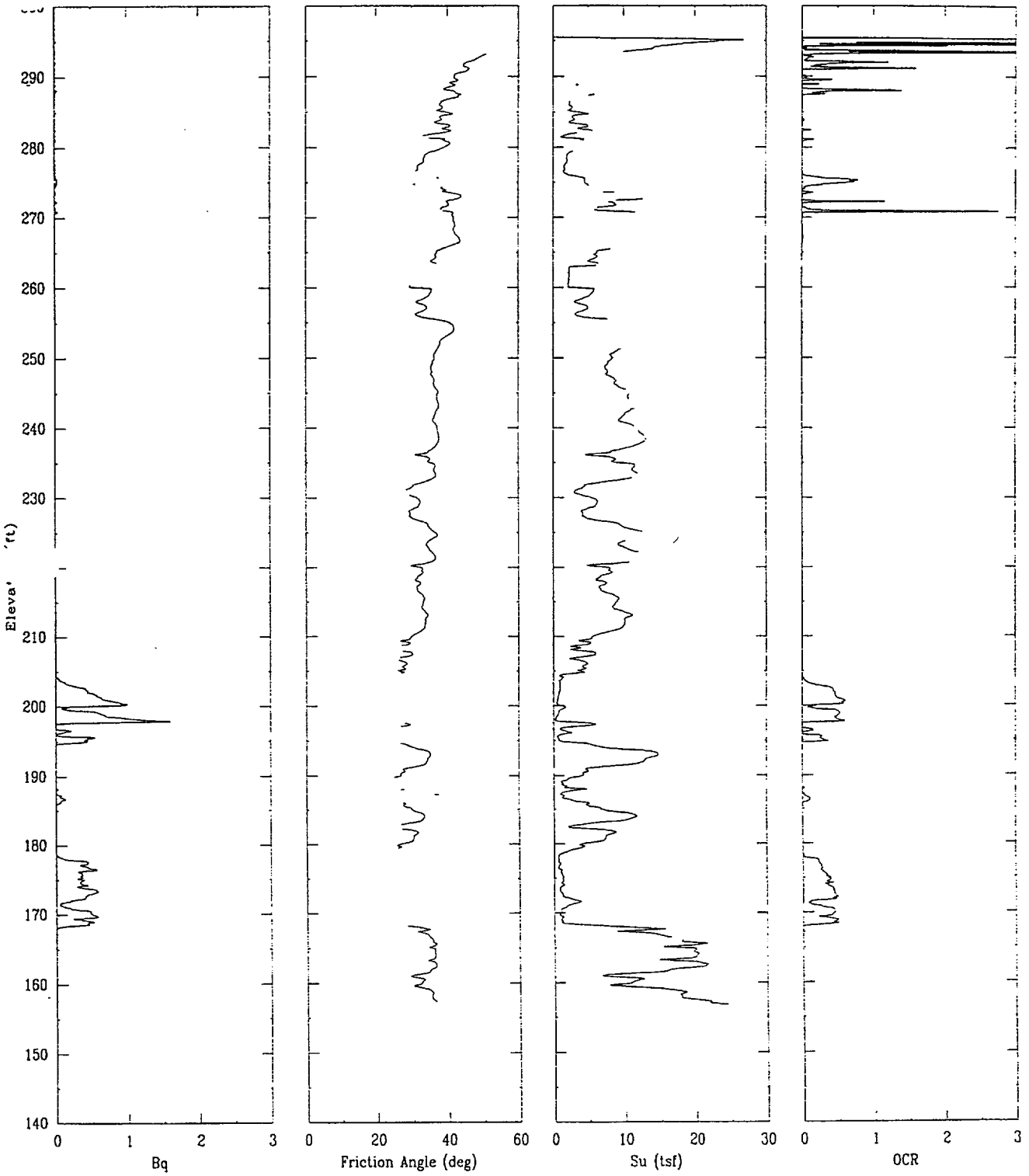

File 318L008.ECP

CPT-51 APPLIED RESEARCH ASSOCIATES, INC. 07/18/00

North 80318.7 East 55198.3 Elevation 295.5

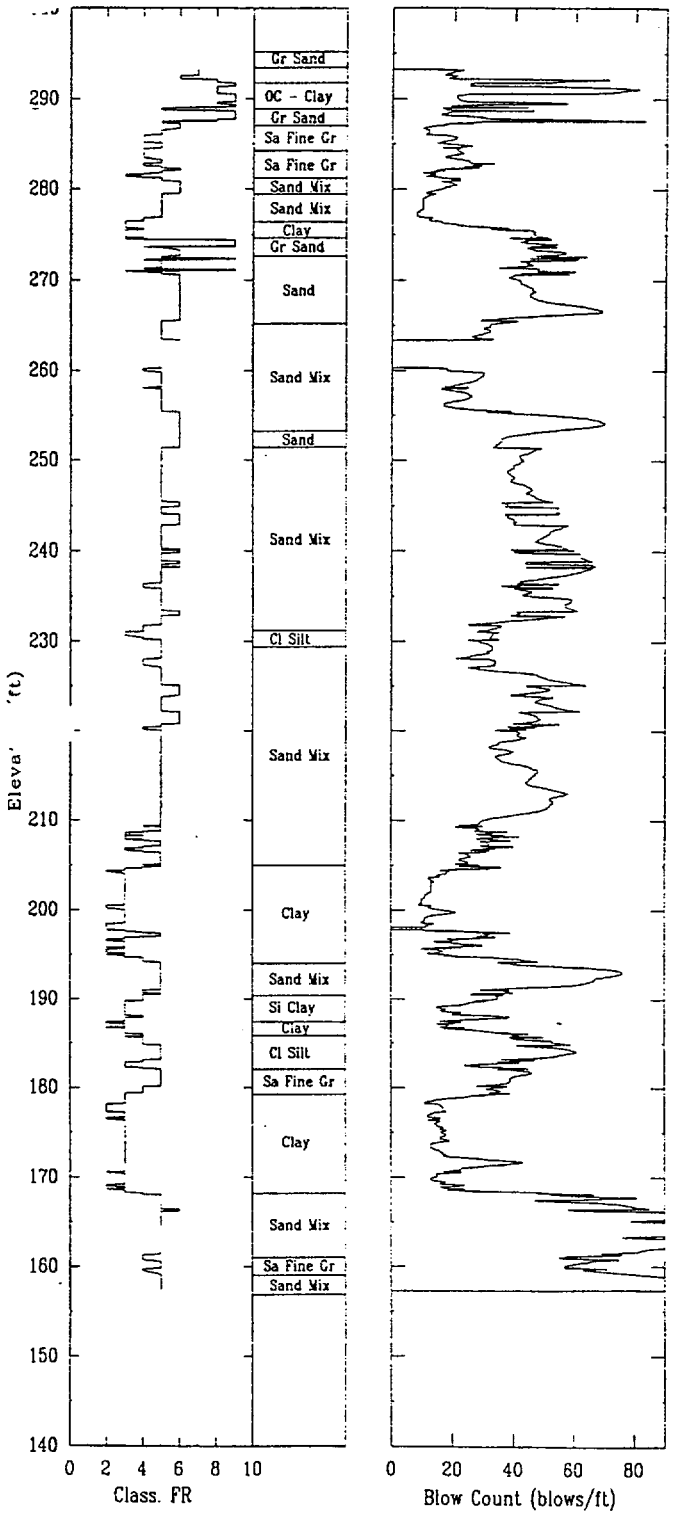

File 318L008.ECP

CPT-52 APPLIED RESEARCH ASSOCIATES, INC. 07/19/00

North 60277.0 East 54867.3 Elevation 293.4

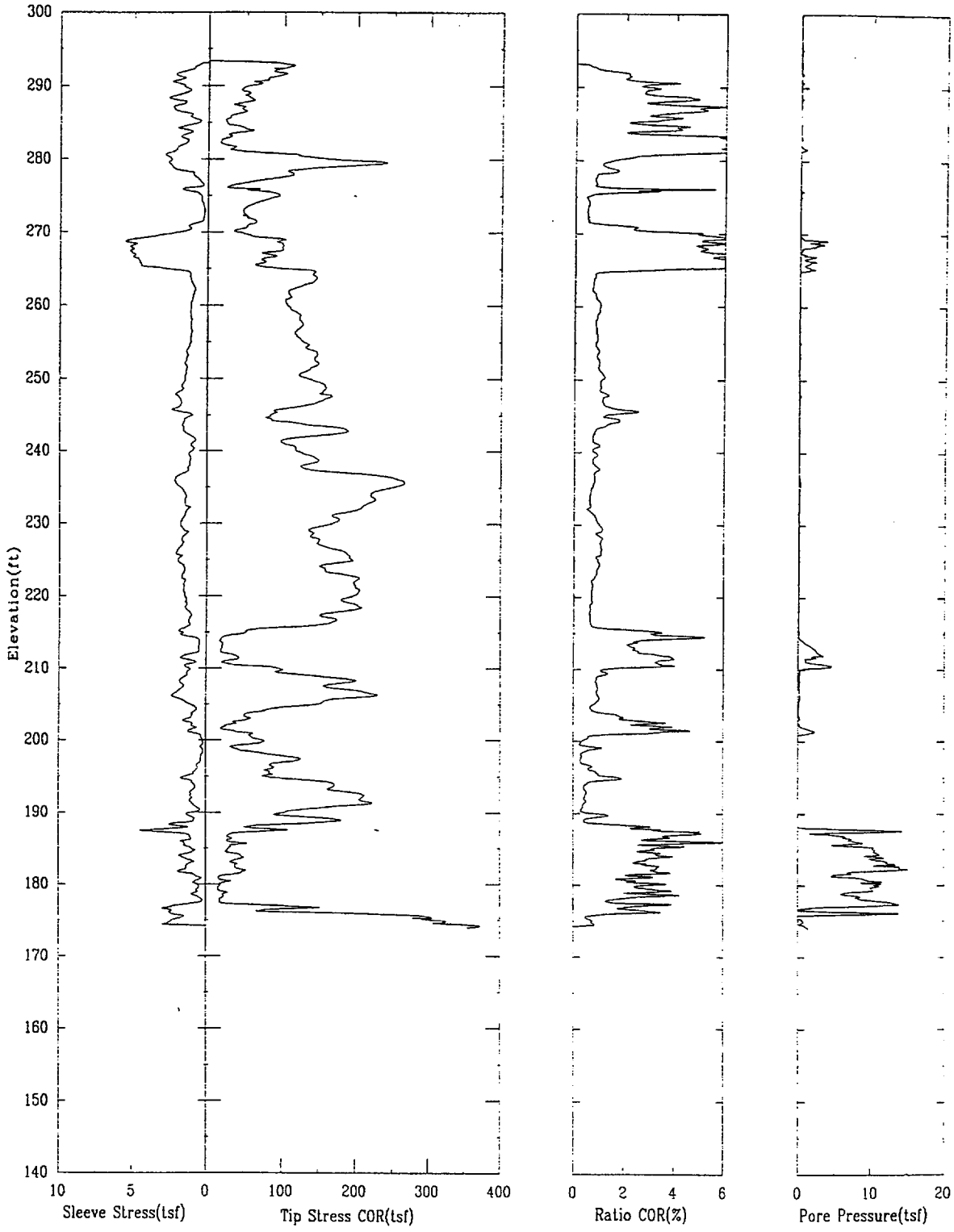

File 319L005.ECP

CPT-52 APPLIED RESEARCH ASSOCIATES, INC. 07/19/00

North 80277.0 East 54867.3 Elevation 293.4

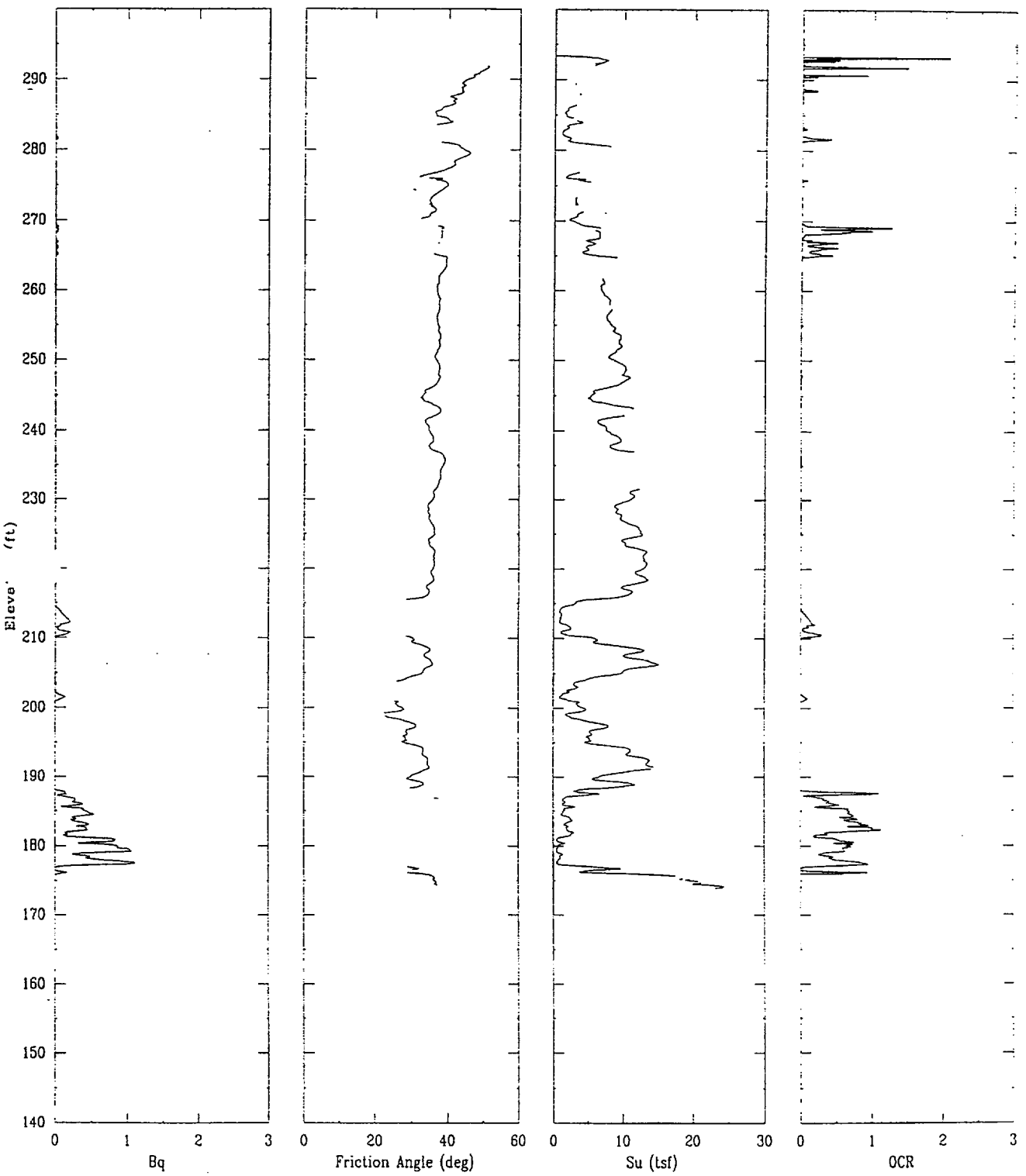

File 319L005.ECP

CPT-52 APPLIED RESEARCH ASSOCIATES, INC. 07/19/00

North 80277.0 East 54867.3 Elevation 293.4

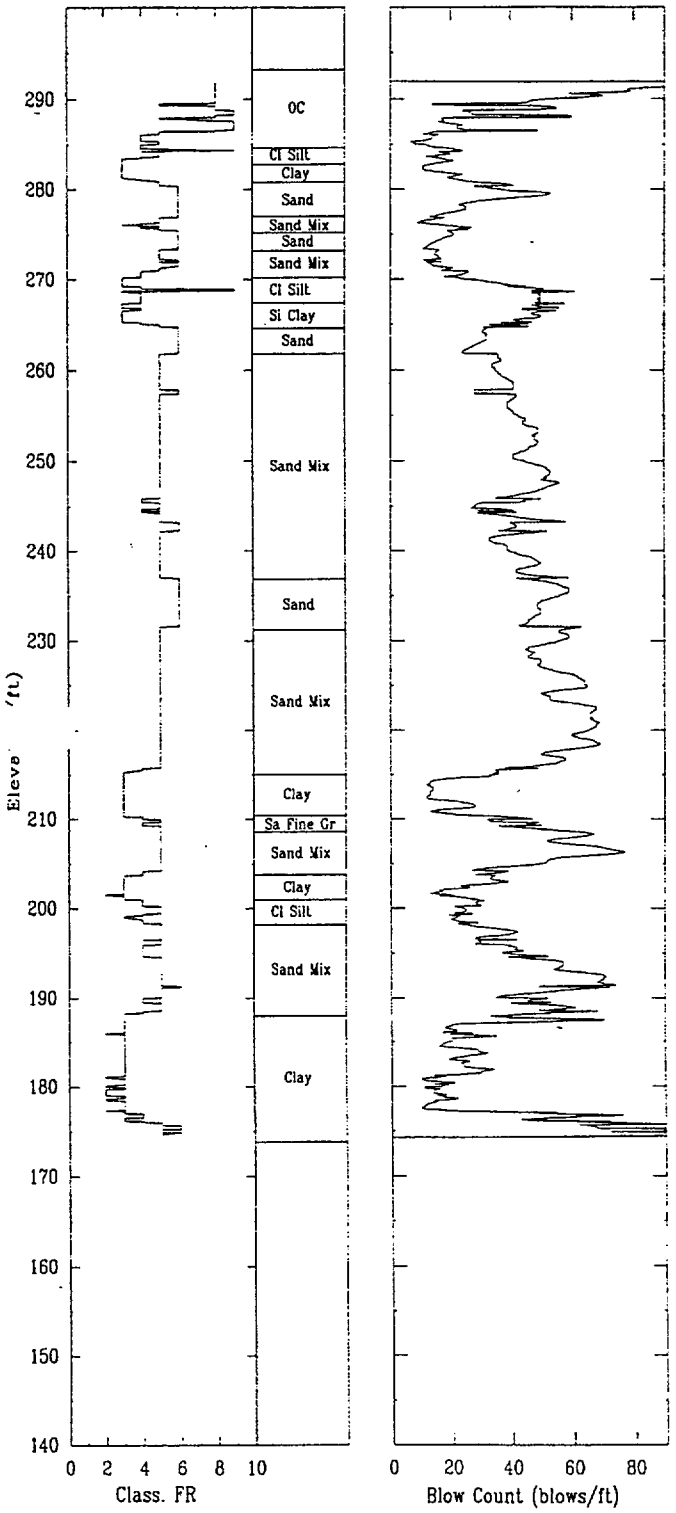

File 319L005.ECP

DCS, MFFF Project No. 08716

CPT-53 APPLIED RESEARCH ASSOCIATES, INC. 07/15/00

North 80309.5 East 55059.9 Elevation 292.8

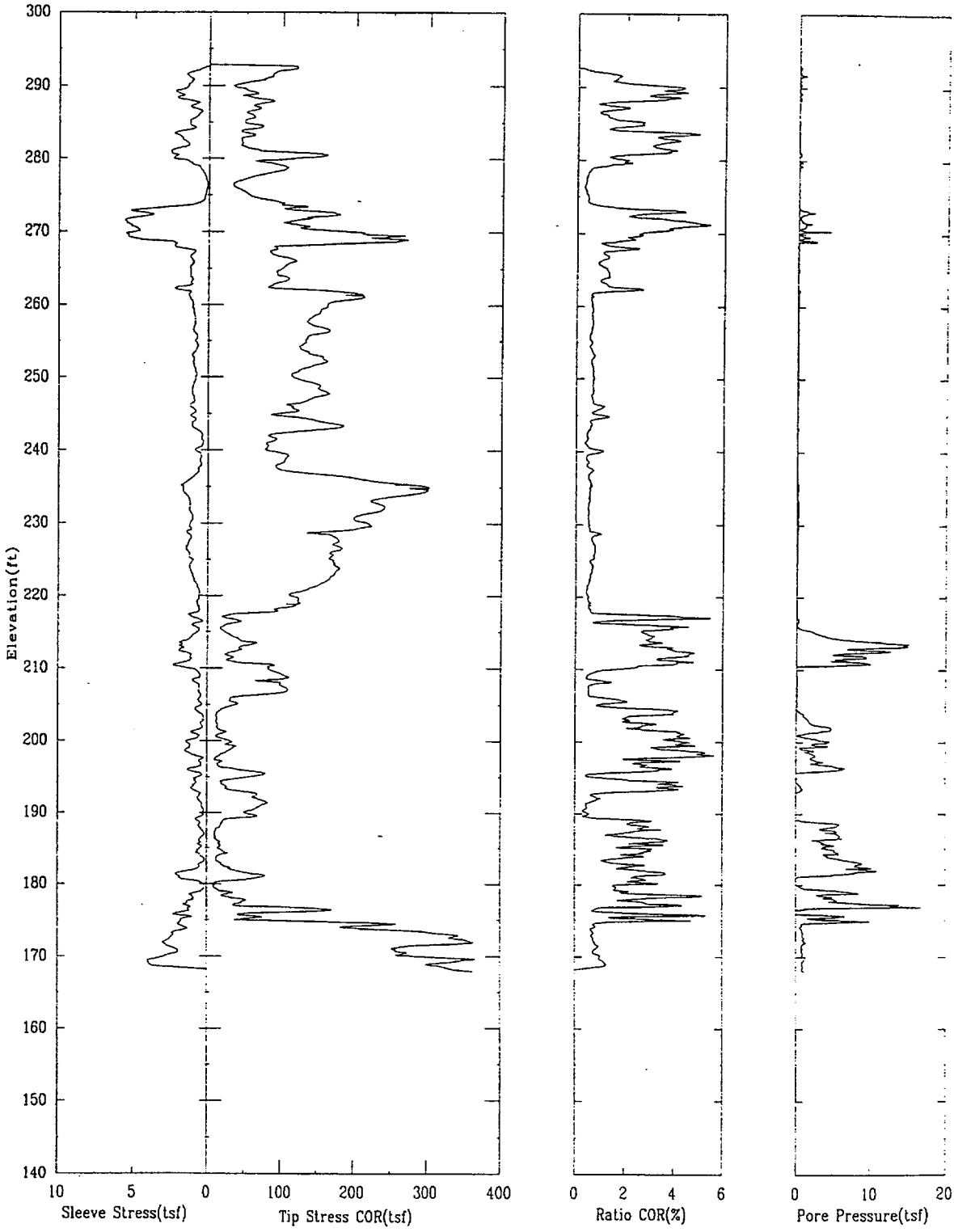

File 315L022.ECP

DCS, MFFF Project No. 08716

CPT-53 APPLIED RESEARCH ASSOCIATES, INC. 07/15/00

North 80309.5 East 55059.9 Elevation 292.8

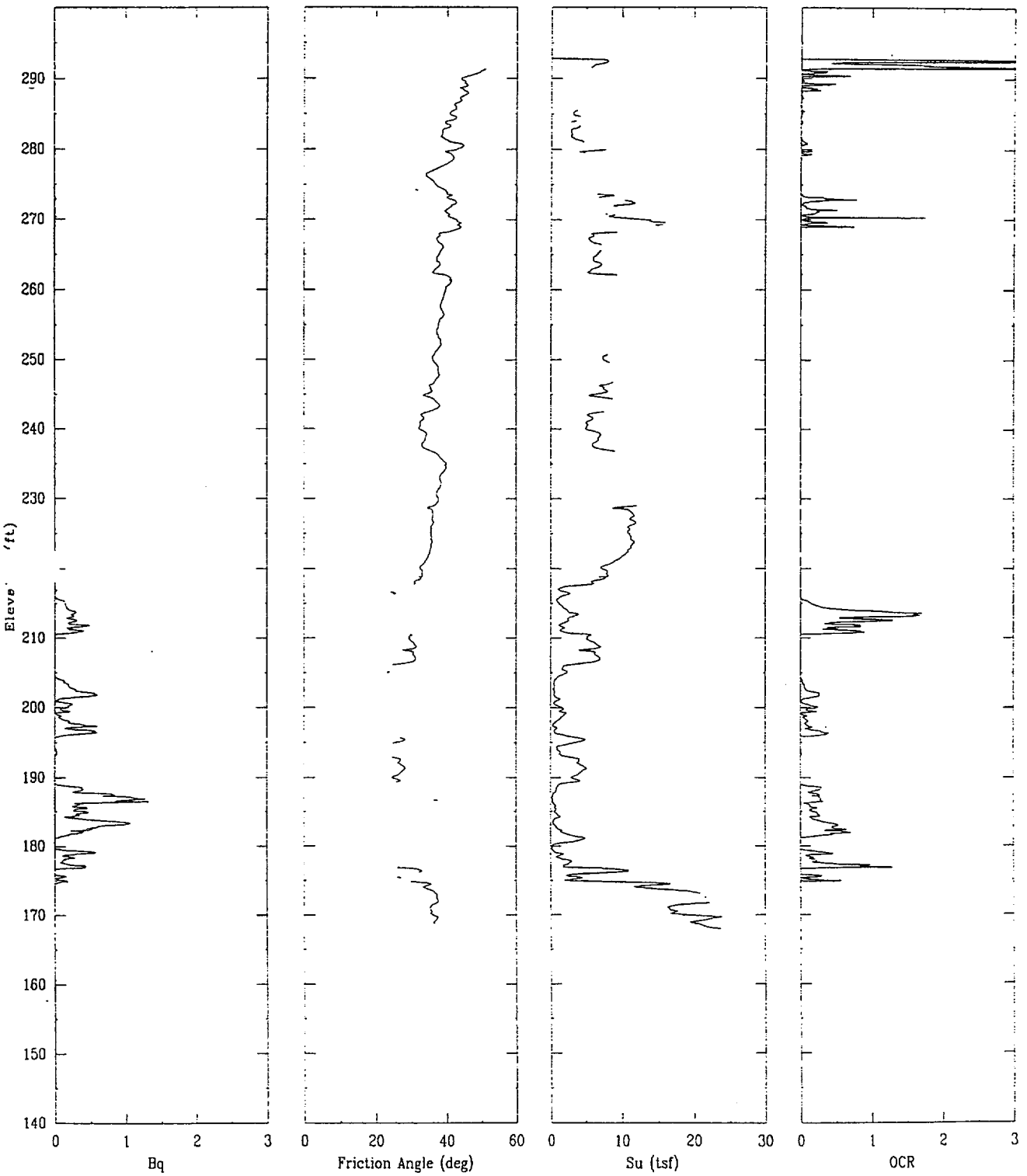

File 315L022.ECP

CPT-53 APPLIED RESEARCH ASSOCIATES, INC. 07/15/00

North 80309.5 East 55059.9 Elevation 292.8

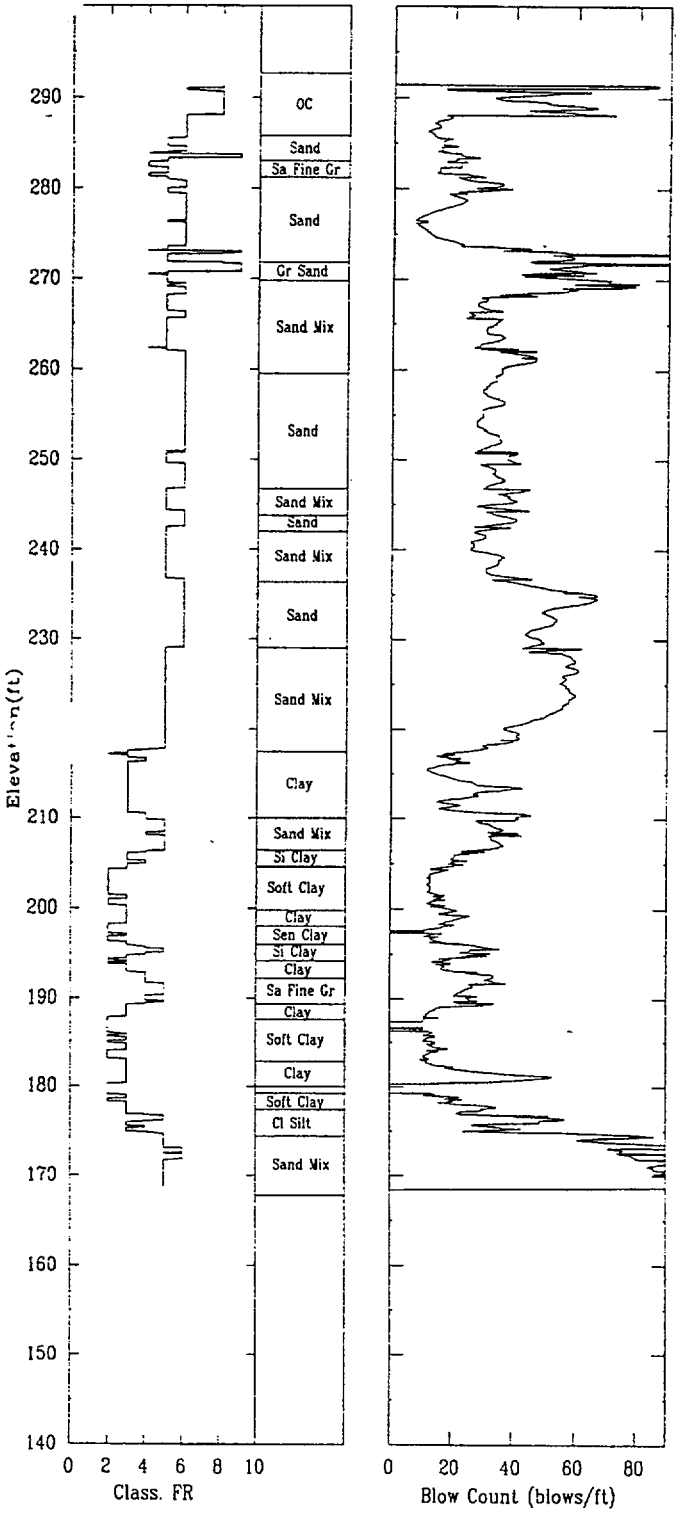

File 315L022.ECP

CPT-54 APPLIED RESEARCH ASSOCIATES, INC. 07/20/00

North 80243.1 East 54940.0 Elevation 293.7

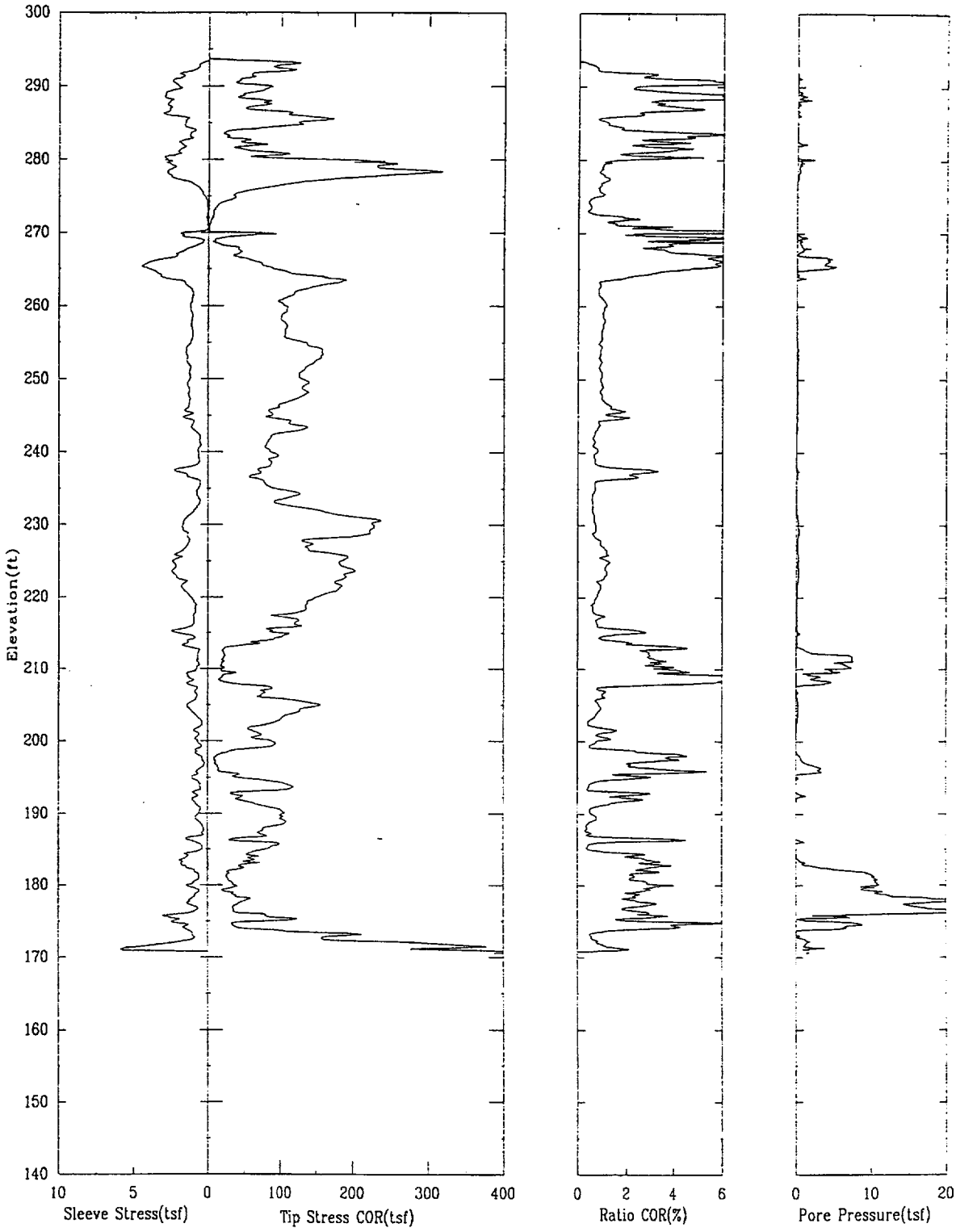

File 320L001.ECP

DCS, MFFF Project No. 08716

CPT-54 APPLIED RESEARCH ASSOCIATES, INC. 07/20/00

North 80243.1 East 54940.0 Elevation 293.7

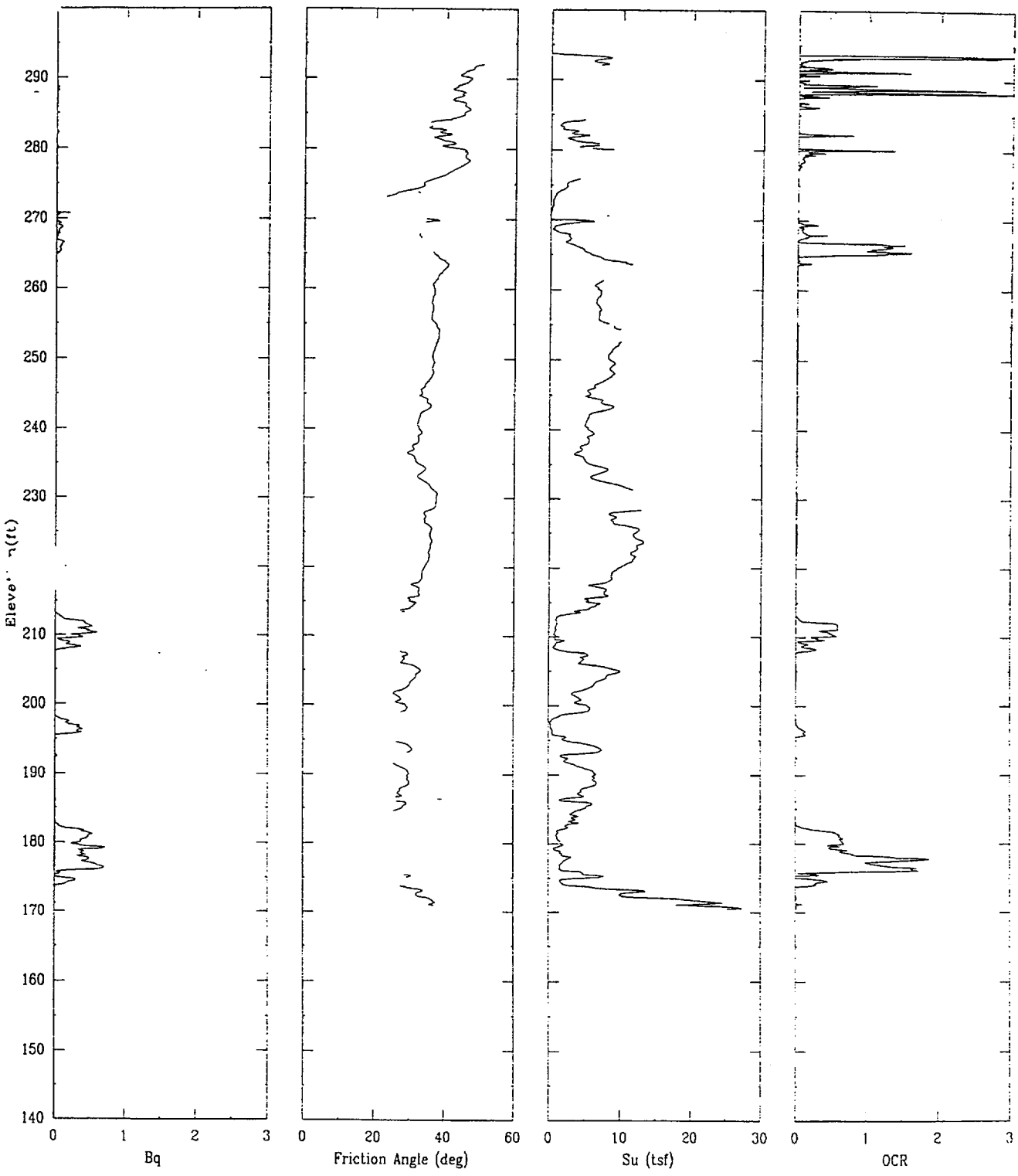

File 320L001.ECP

DCS, MFFF Project No. 08716

CPT-54 APPLIED RESEARCH ASSOCIATES, INC. 07/20/00

North 80243.1 East 54940.0 Elevation 293.7

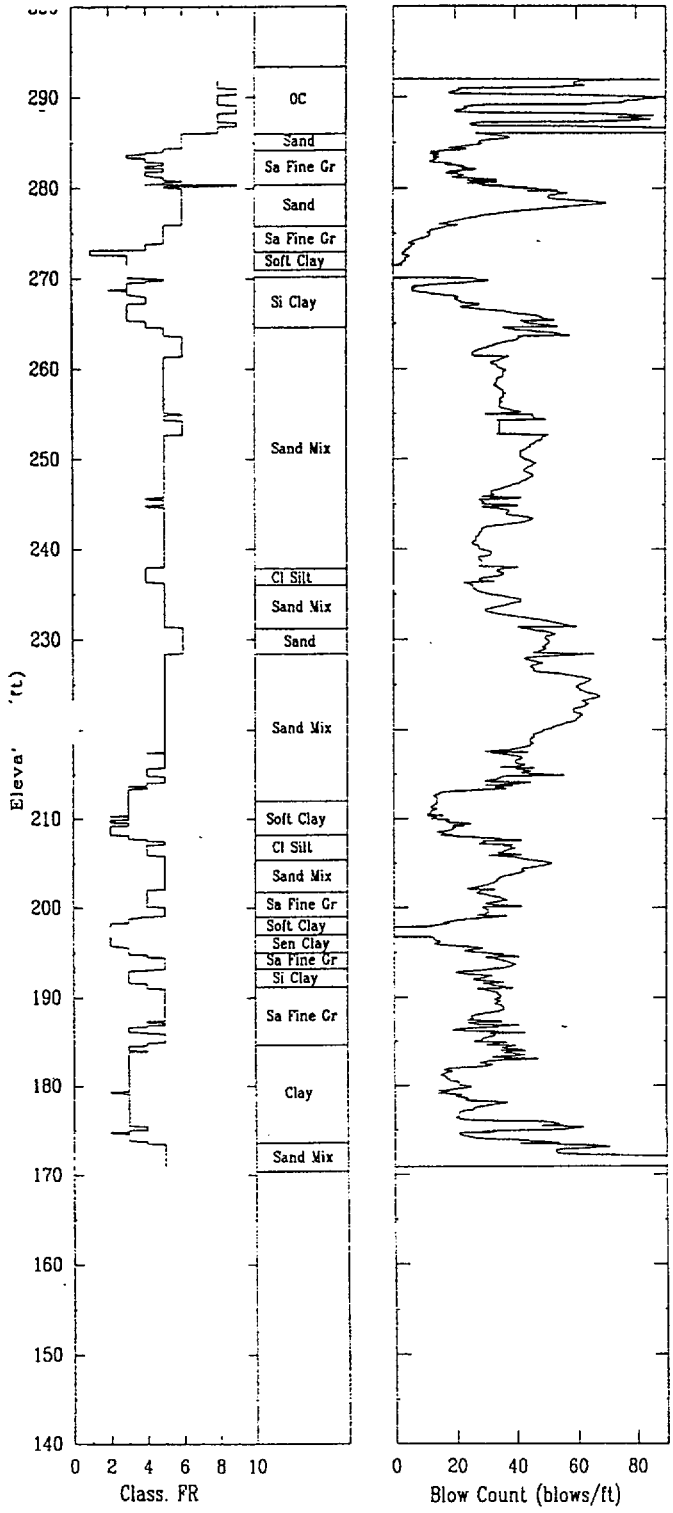

File 320L001.ECP

CPT-55 APPLIED RESEARCH ASSOCIATES, INC. 07/18/00

North 80259.6 East 55141.9 Elevation 294.4

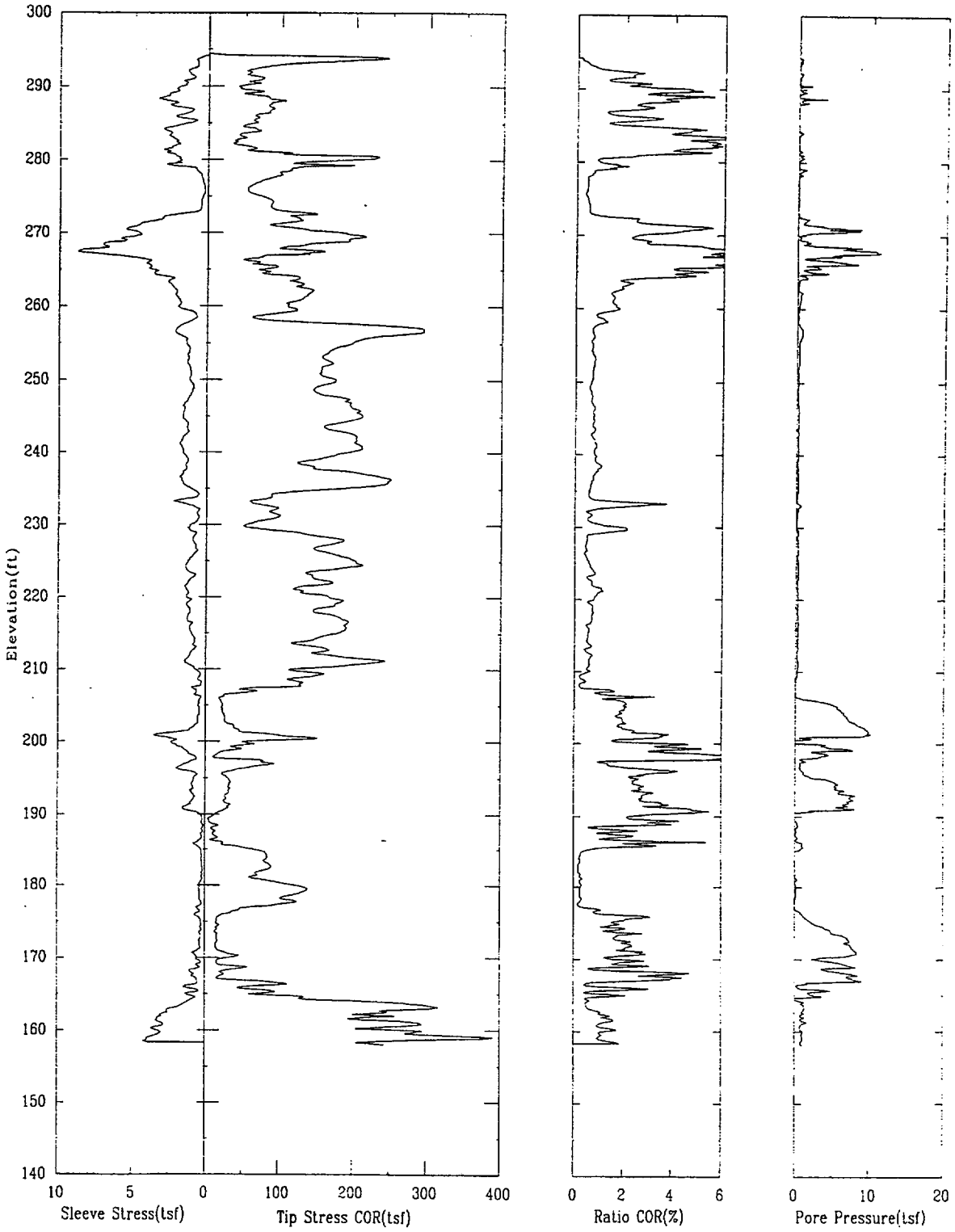

File 318L005.ECP

DCS, MFFF Project No. 08716

CPT-55 APPLIED RESEARCH ASSOCIATES, INC. 07/18/00

North 80259.6 East 55141.9 Elevation 294.4

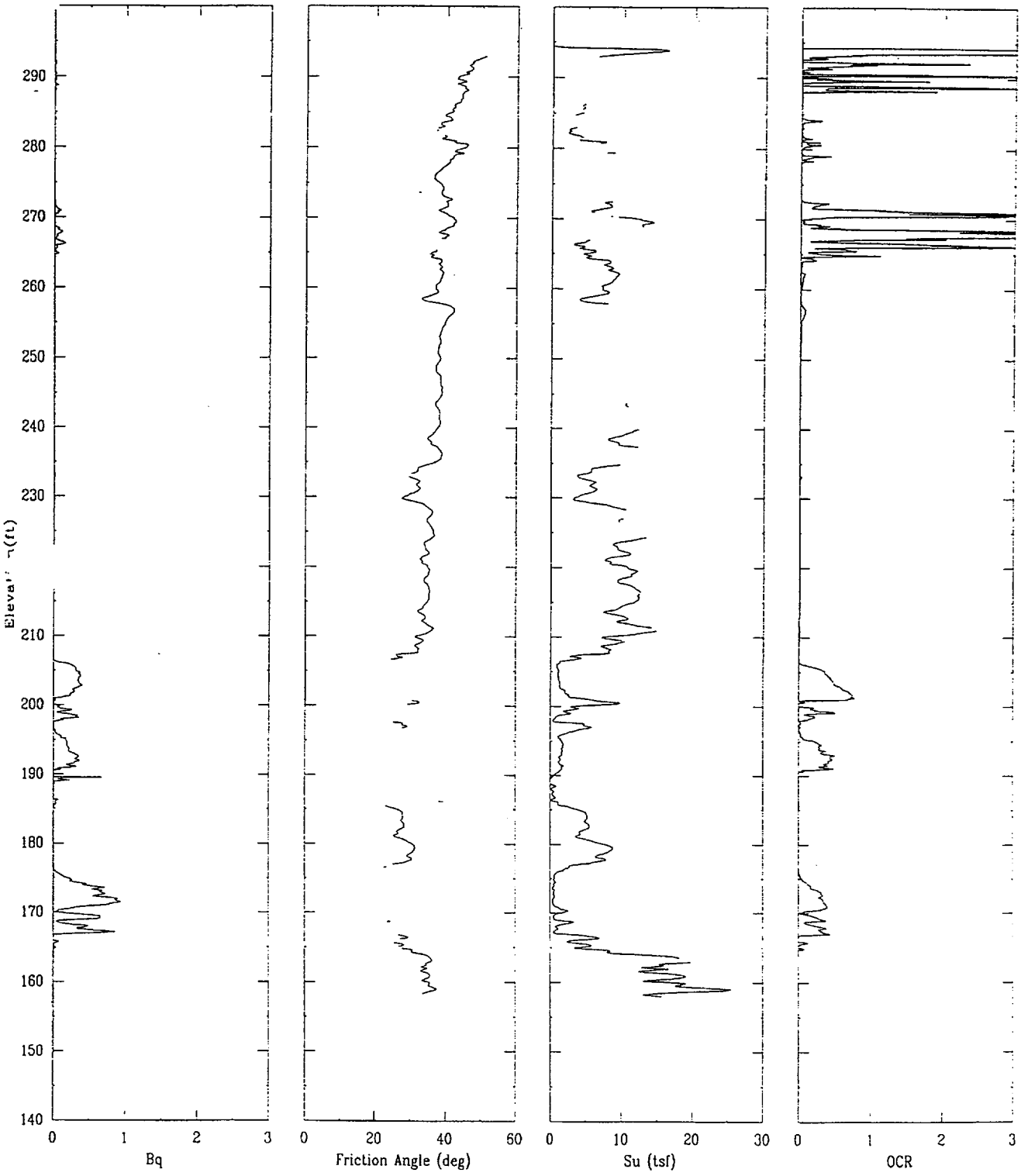

File 318L005.ECP

CPT-55 APPLIED RESEARCH ASSOCIATES, INC. 07/18/00

North 80259.6 East 55141.9 Elevation 294.4

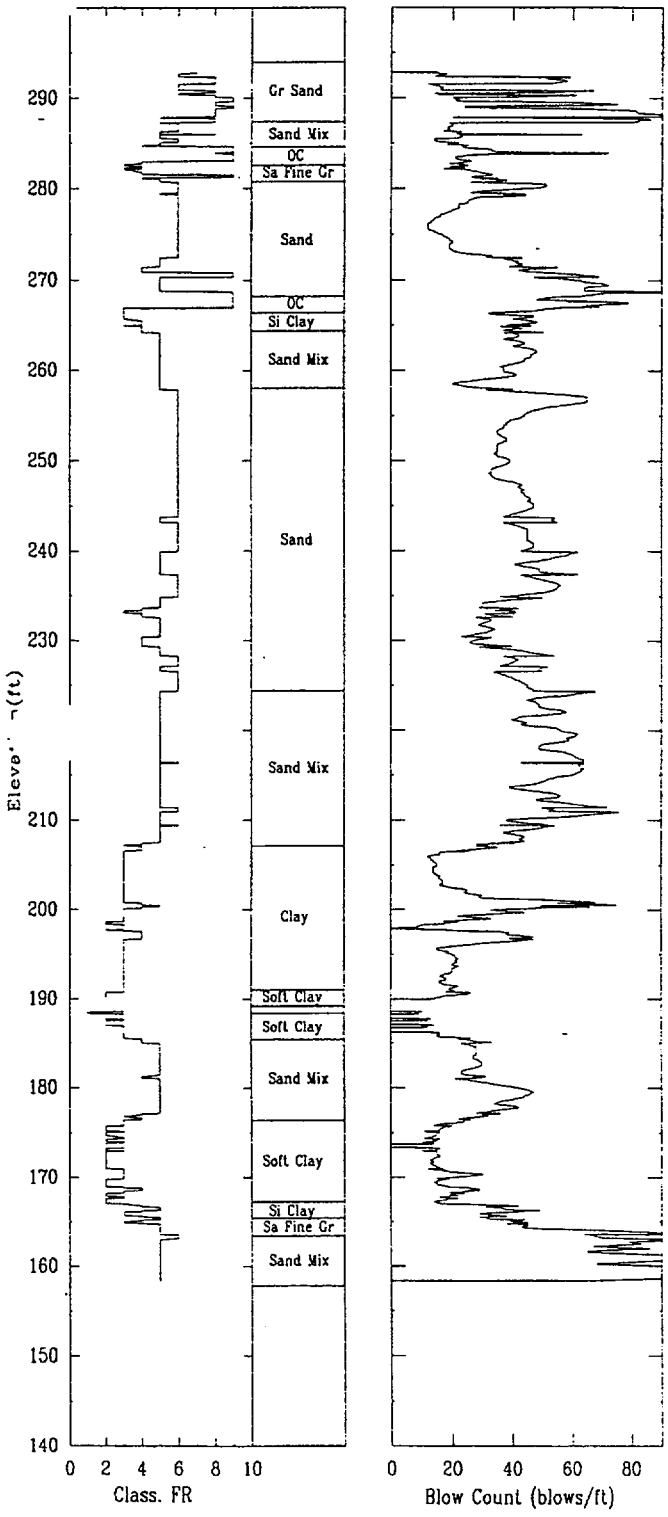

File 3181005.ECP

DCS, MFFF Project No. 08716

CPT-56 APPLIED RESEARCH ASSOCIATES, INC. 07/18/00

North 8J207.0 East 54866.7 Elevation 294.2

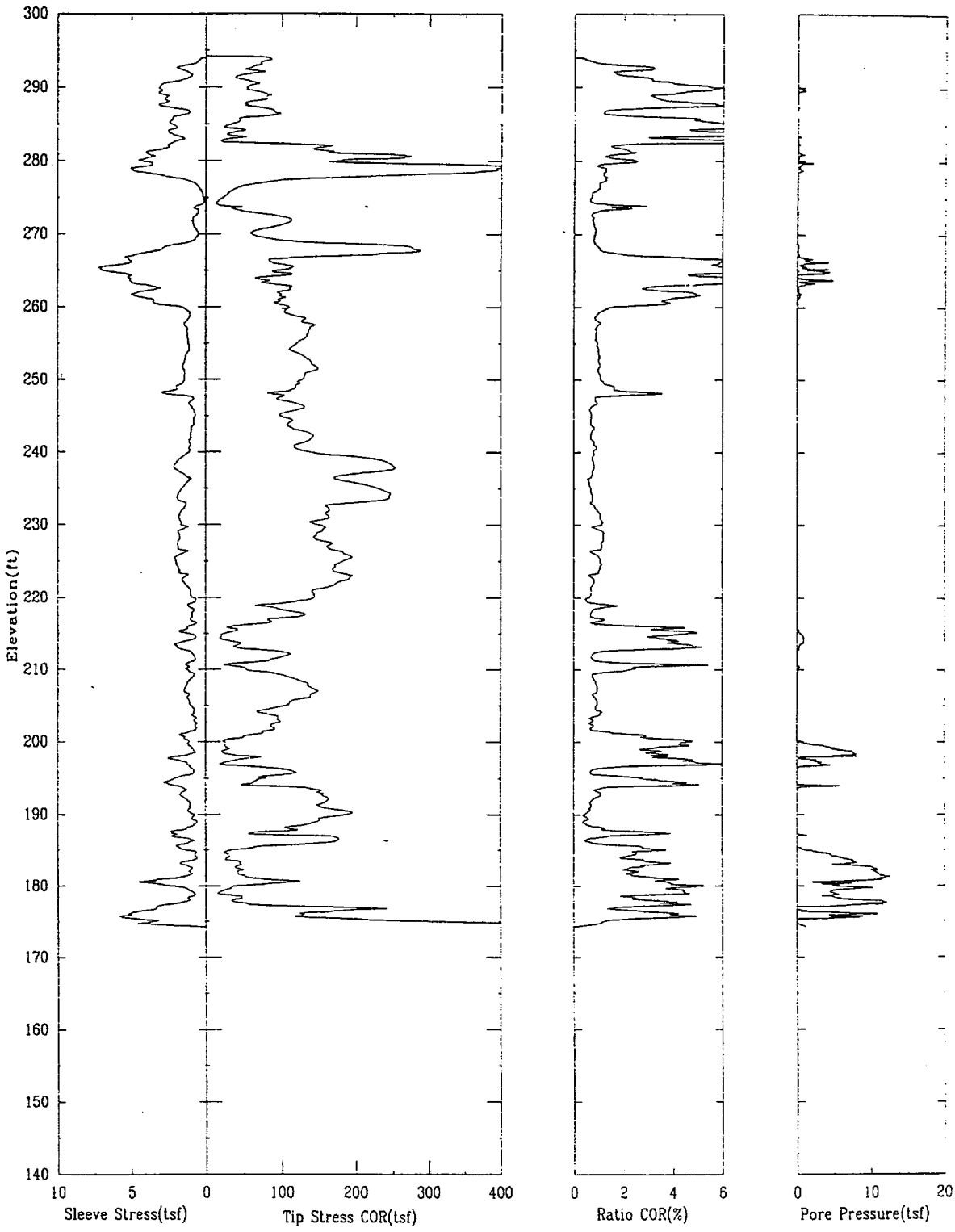

File 318L001.ECP

CPT-56 APPLIED RESEARCH ASSOCIATES, INC. 07/18/00

North 80207.0 East 54866.7 Elevation 294.2

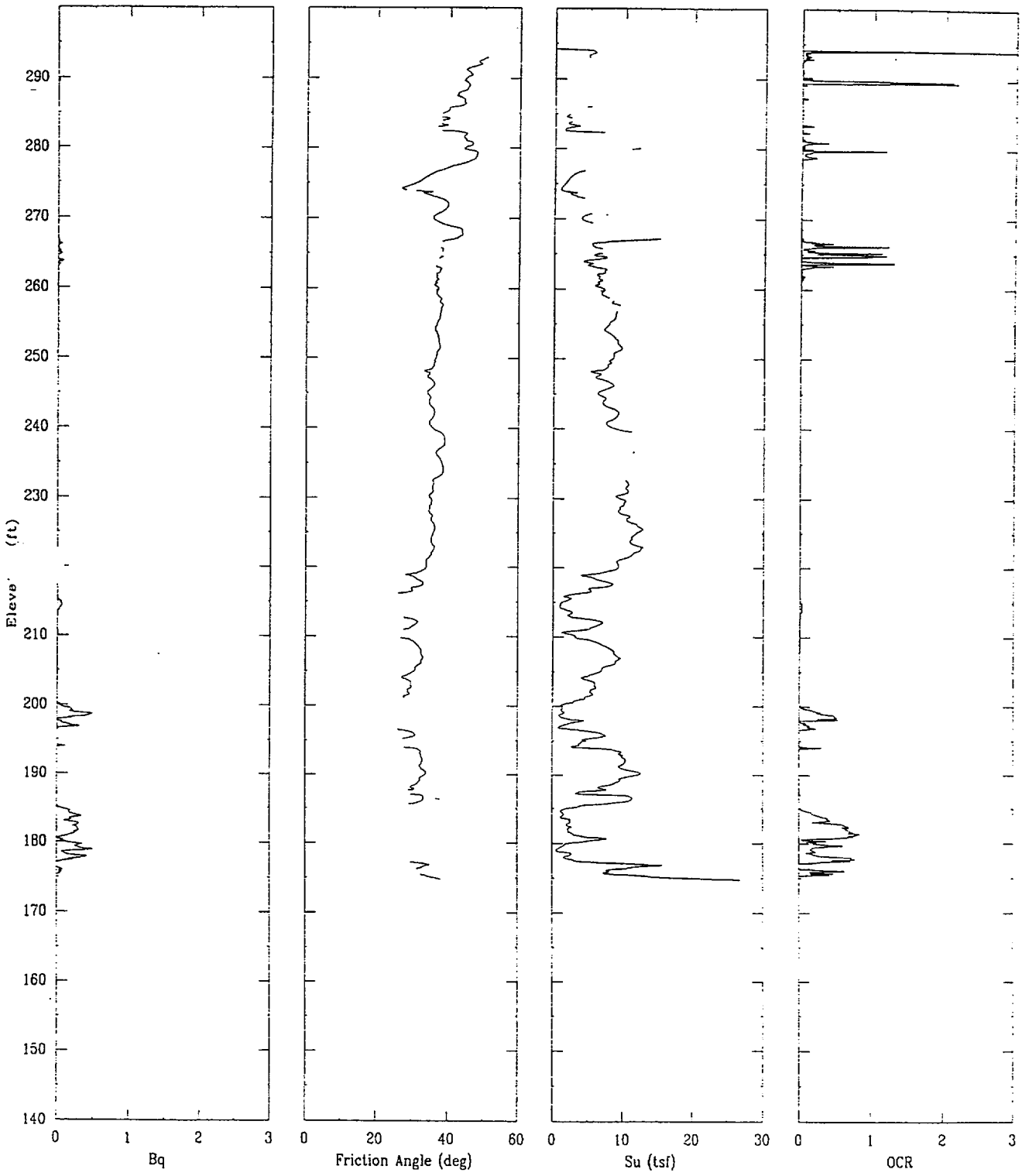

File 318L001.ECP

DCS, MFFF Project No. 08716

CPT-56 APPLIED RESEARCH ASSOCIATES, INC. 07/18/00

North 80207.0 East 54866.7 Elevation 294.2

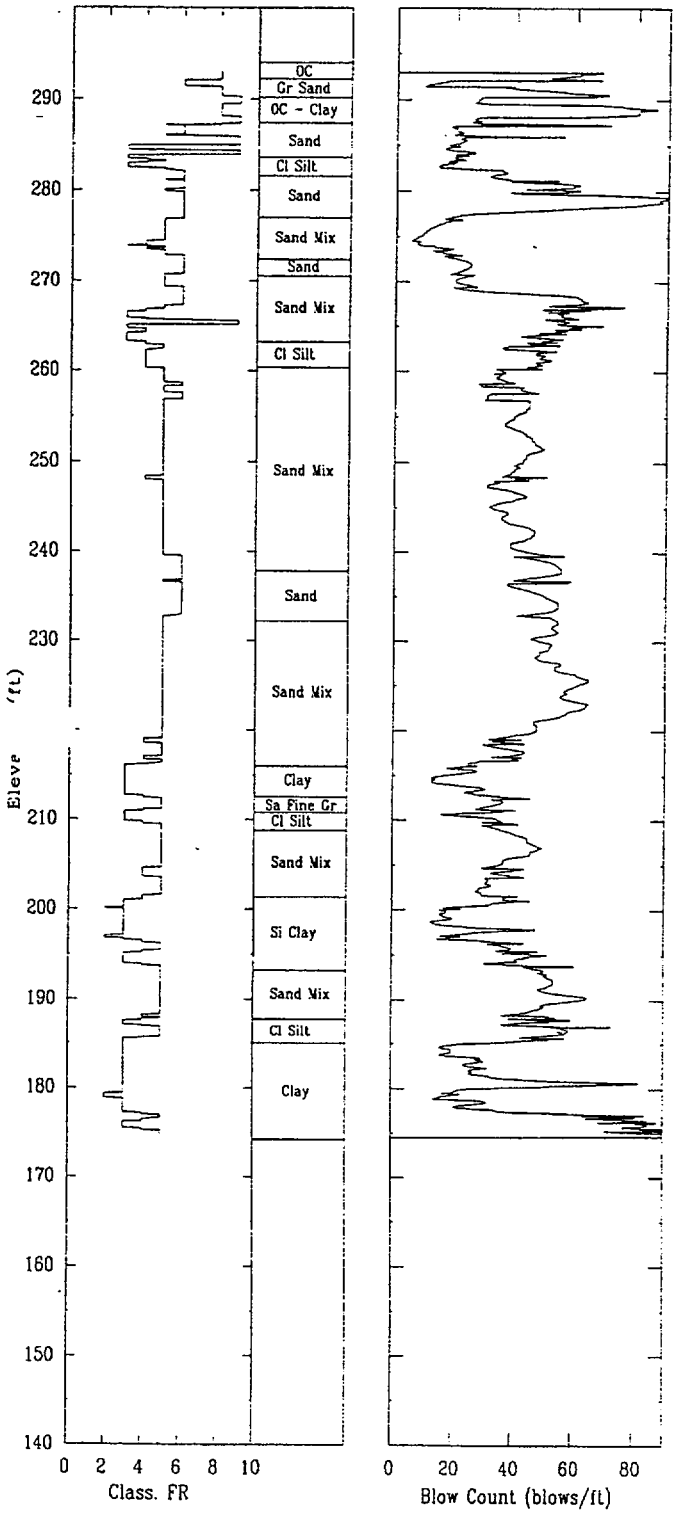

File 318L001.ECP

CPT-57 APPLIED RESEARCH ASSOCIATES, INC. 07/18/00

North 80229.2 East 55058.2 Elevation 293.6

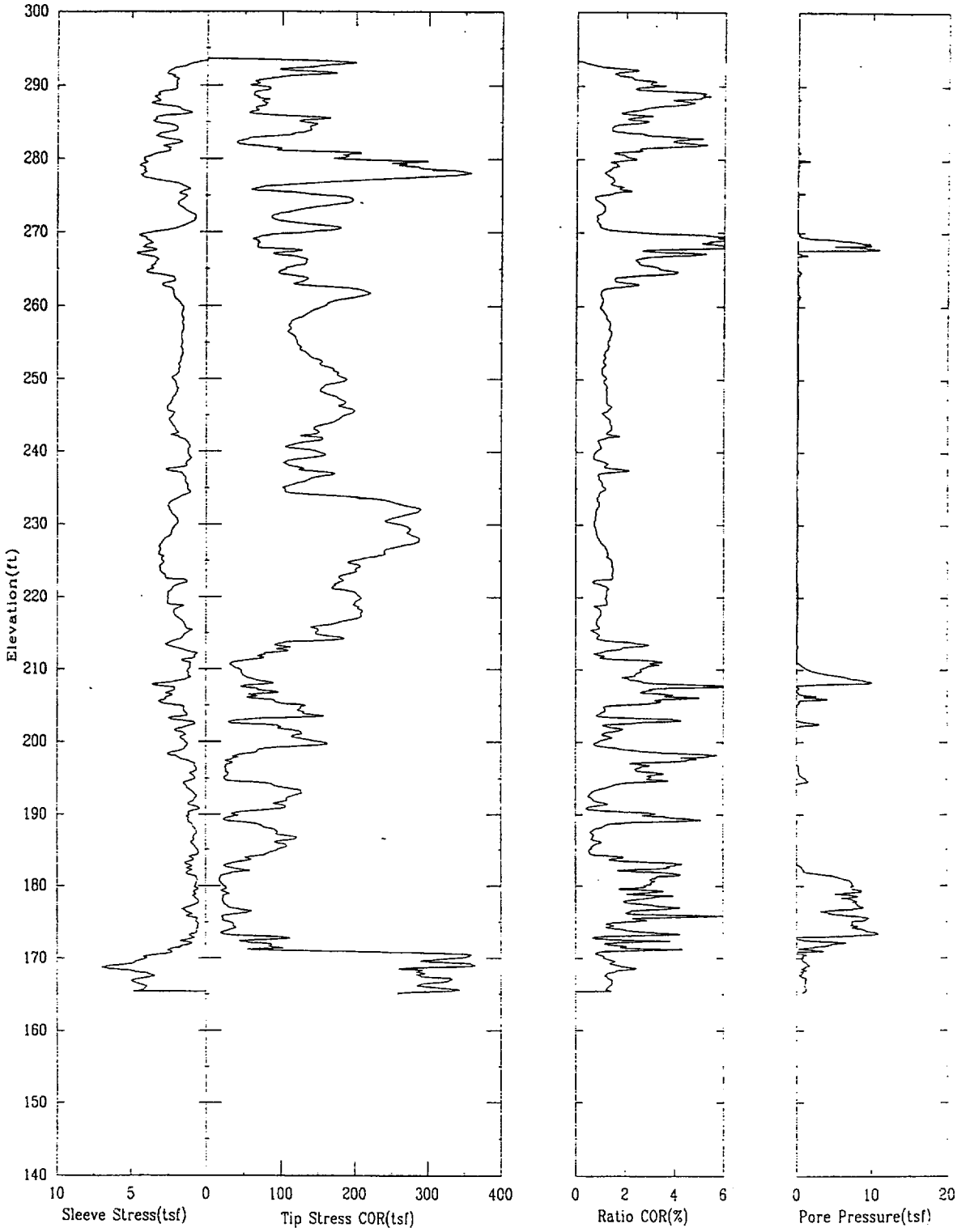

File 318L003.ECP

DCS, MFFF Project No. 08716

CPT-57 APPLIED RESEARCH ASSOCIATES, INC. 07/18/00

North 80229.2 East 55058.2 Elevation 293.6

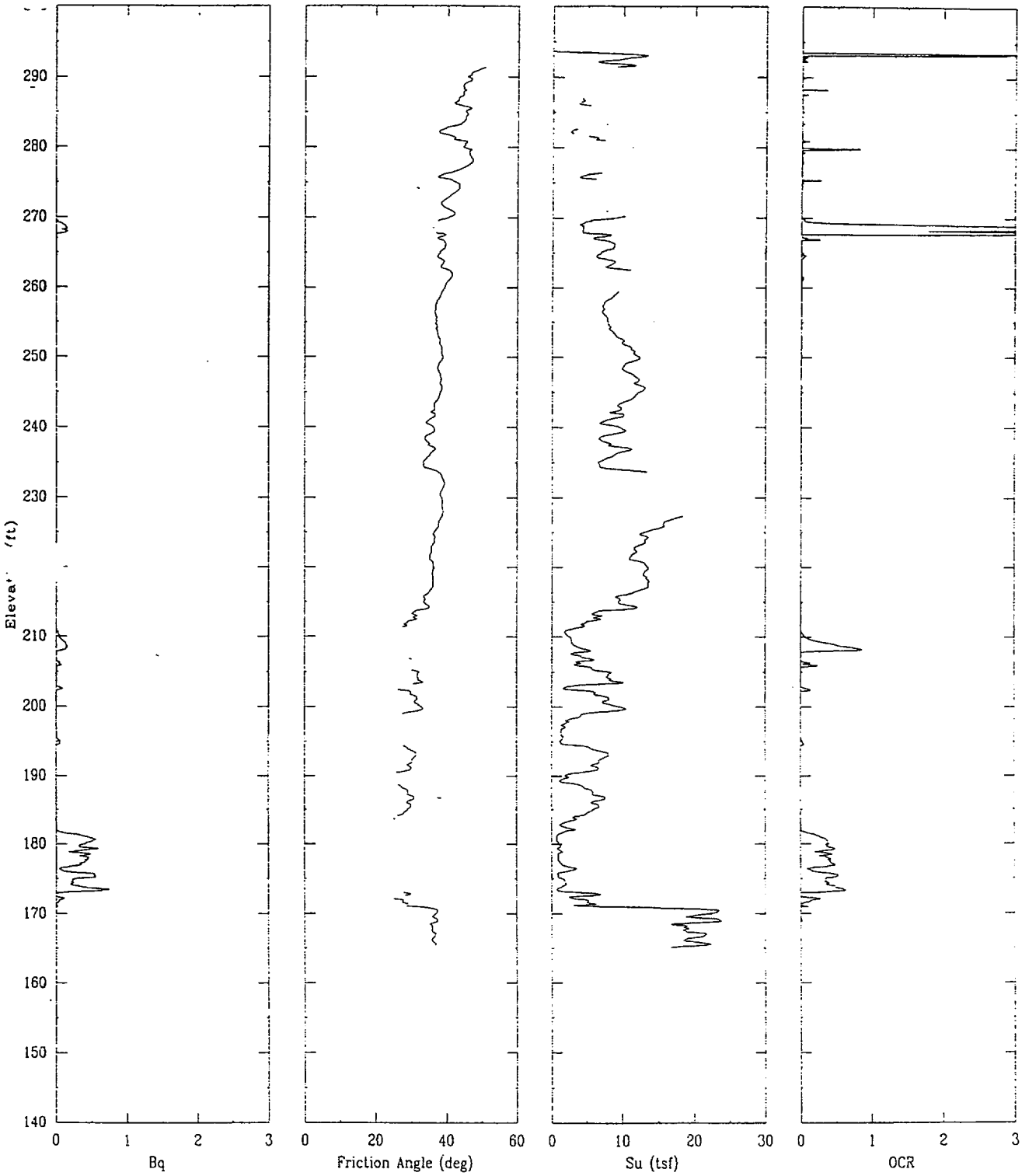

File 3181003.ECP

DCS, MFFF Project No. 08716

CPT-57 APPLIED RESEARCH ASSOCIATES, INC. 07/18/00

North 80229.2 East 55058.2 Elevation 293.6

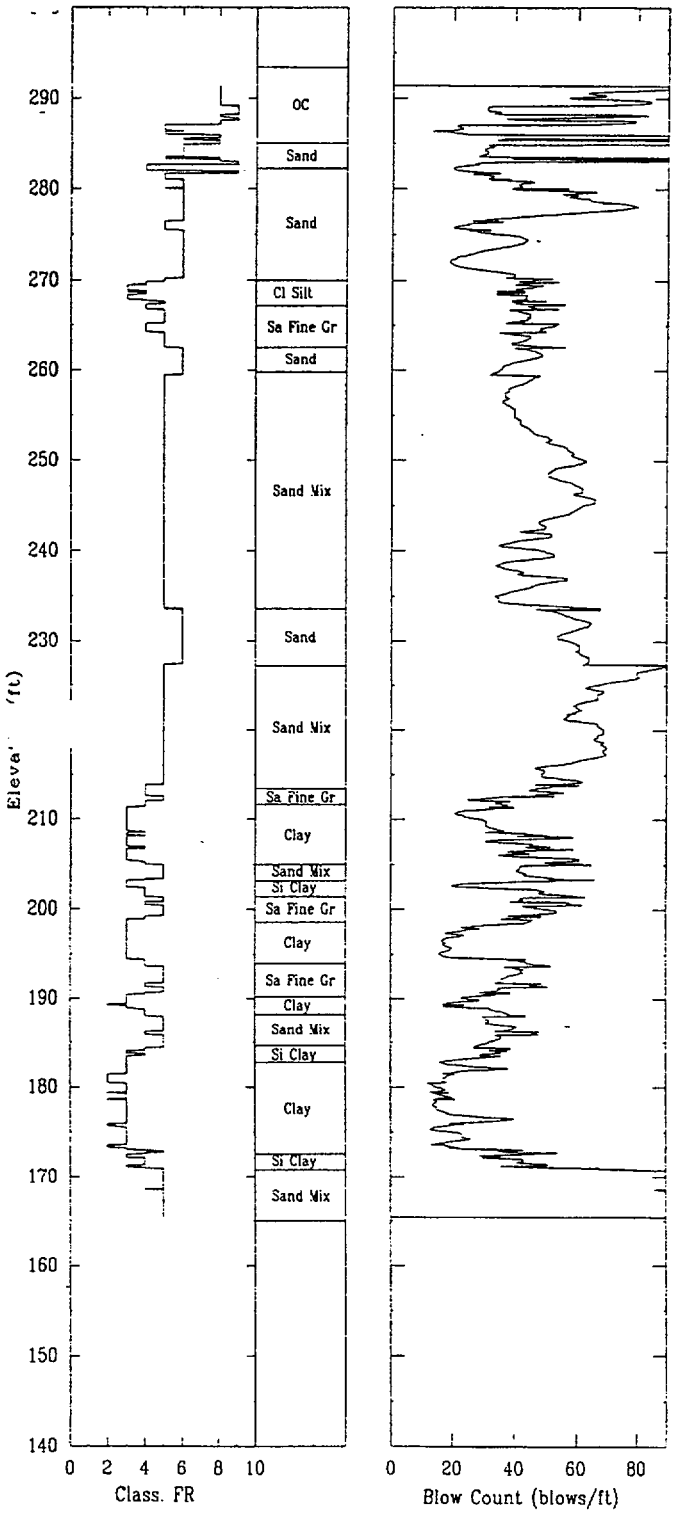

File 318L003.ECP

213

DCS, MFFF Project No. 08716

CPT-58 APPLIED RESEARCH ASSOCIATES, INC. 07/17/00

North 80135.1 East 54866.9 Elevation 295.1

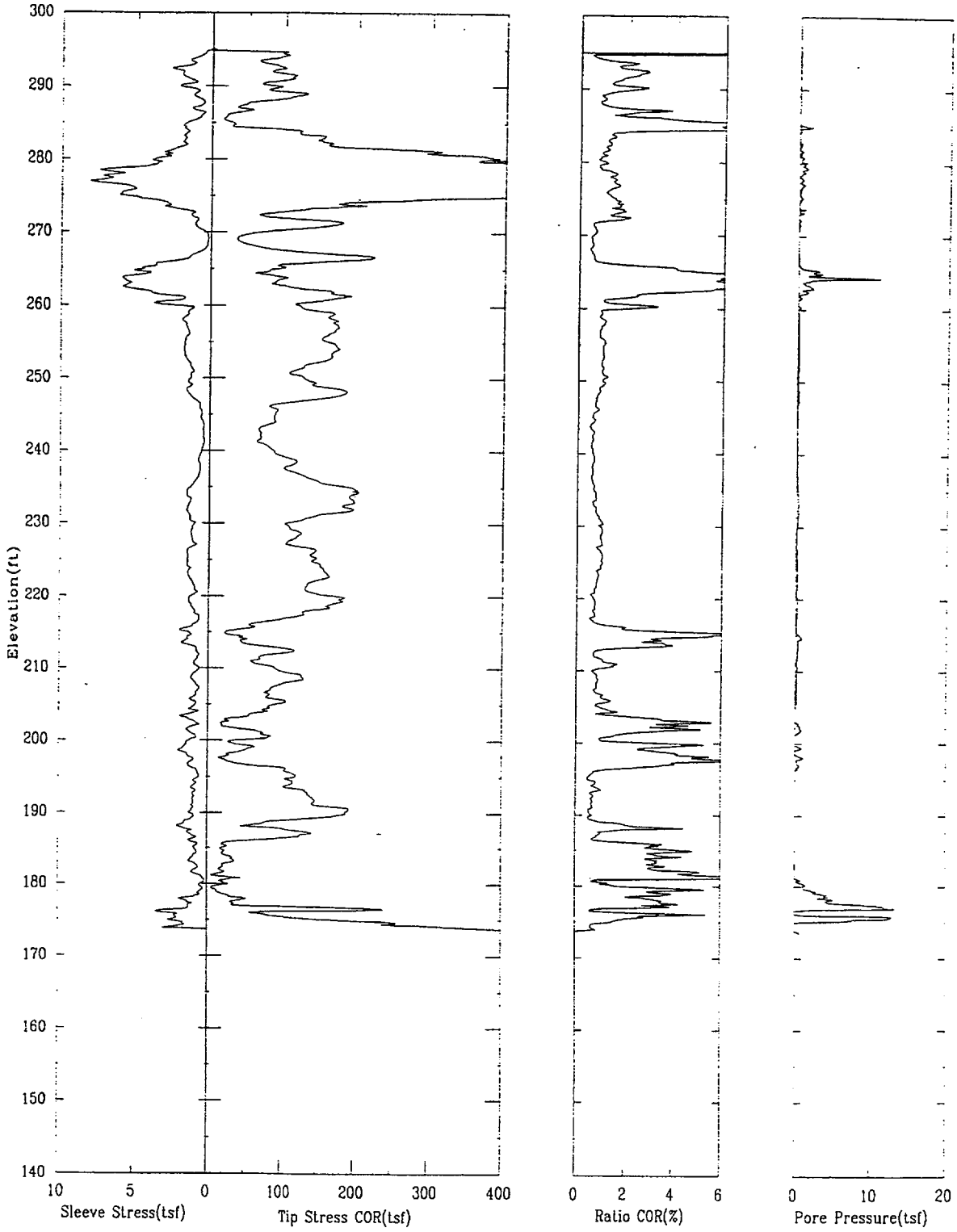

File 317L004.ECP

DCS, MFFF Project No. 08716

CPT-58 APPLIED RESEARCH ASSOCIATES, INC. 07/17/00

North 80135.1 East 54866.9 Elevation 295.1

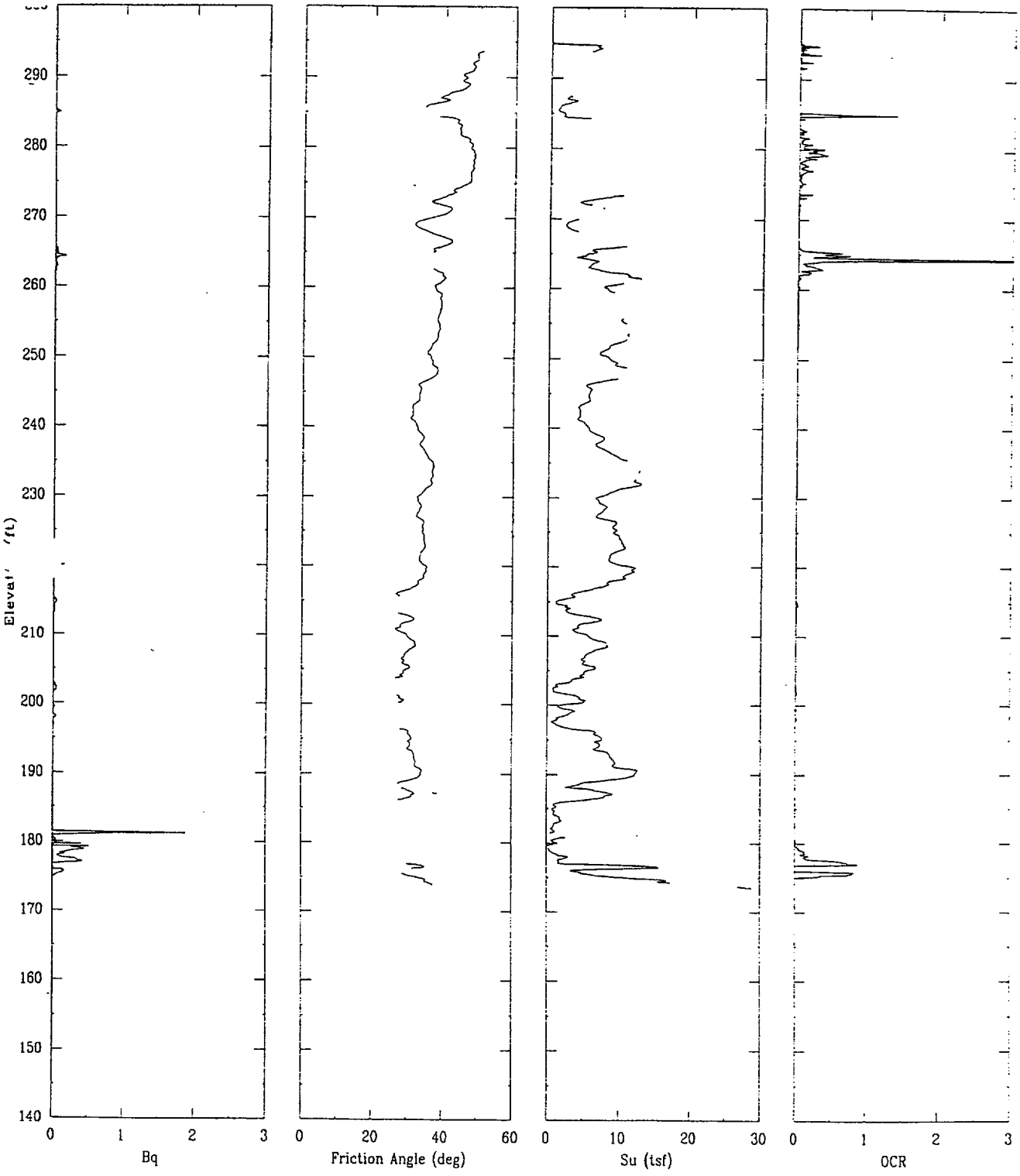

File 317L004.ECP

DCS, MFFF Project No. 08716

CPT-58 APPLIED RESEARCH ASSOCIATES, INC. 07/17/00

North 80135.1 East 54866.9 Elevation 295.1

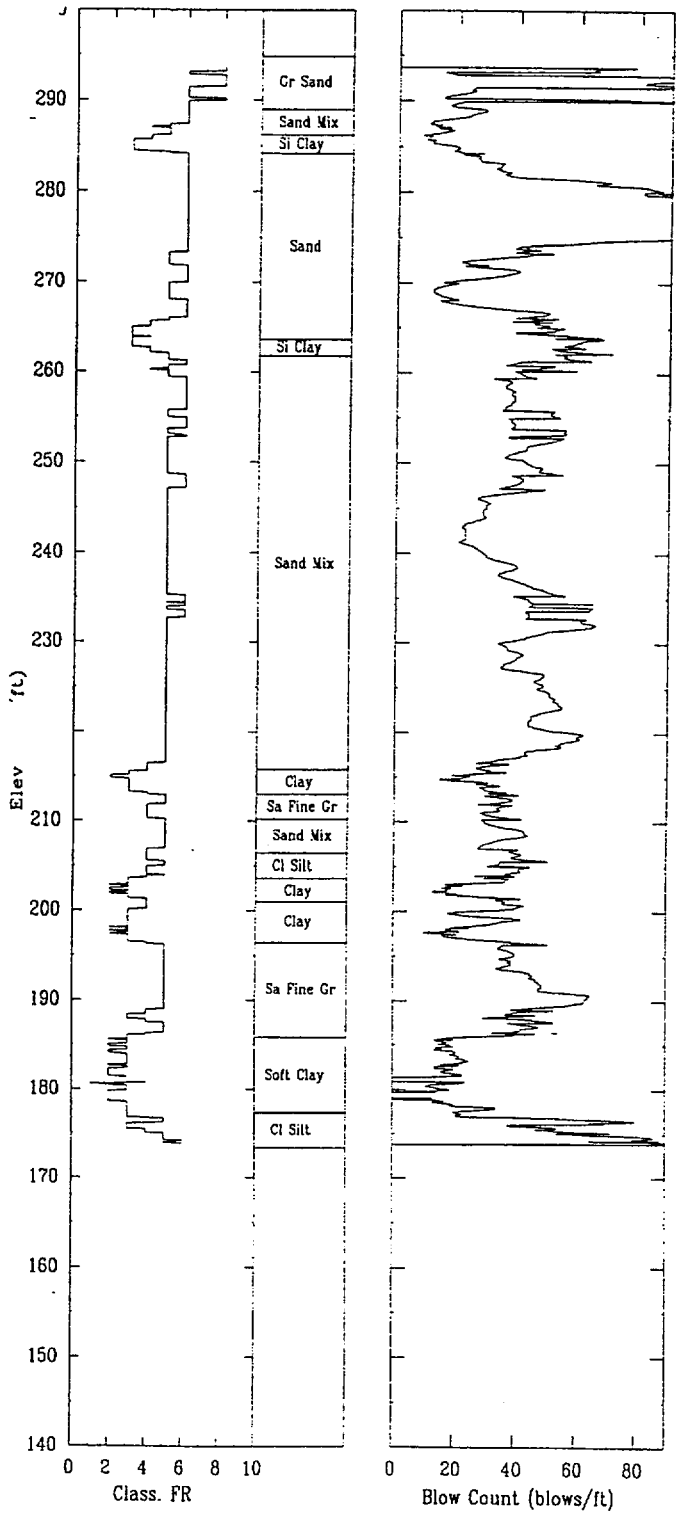

File 317L004.ECP

CPT-59 APPLIED RESEARCH ASSOCIATES, INC. 07/15/00

North 80152.7 East 54956.9 Elevation 295.5

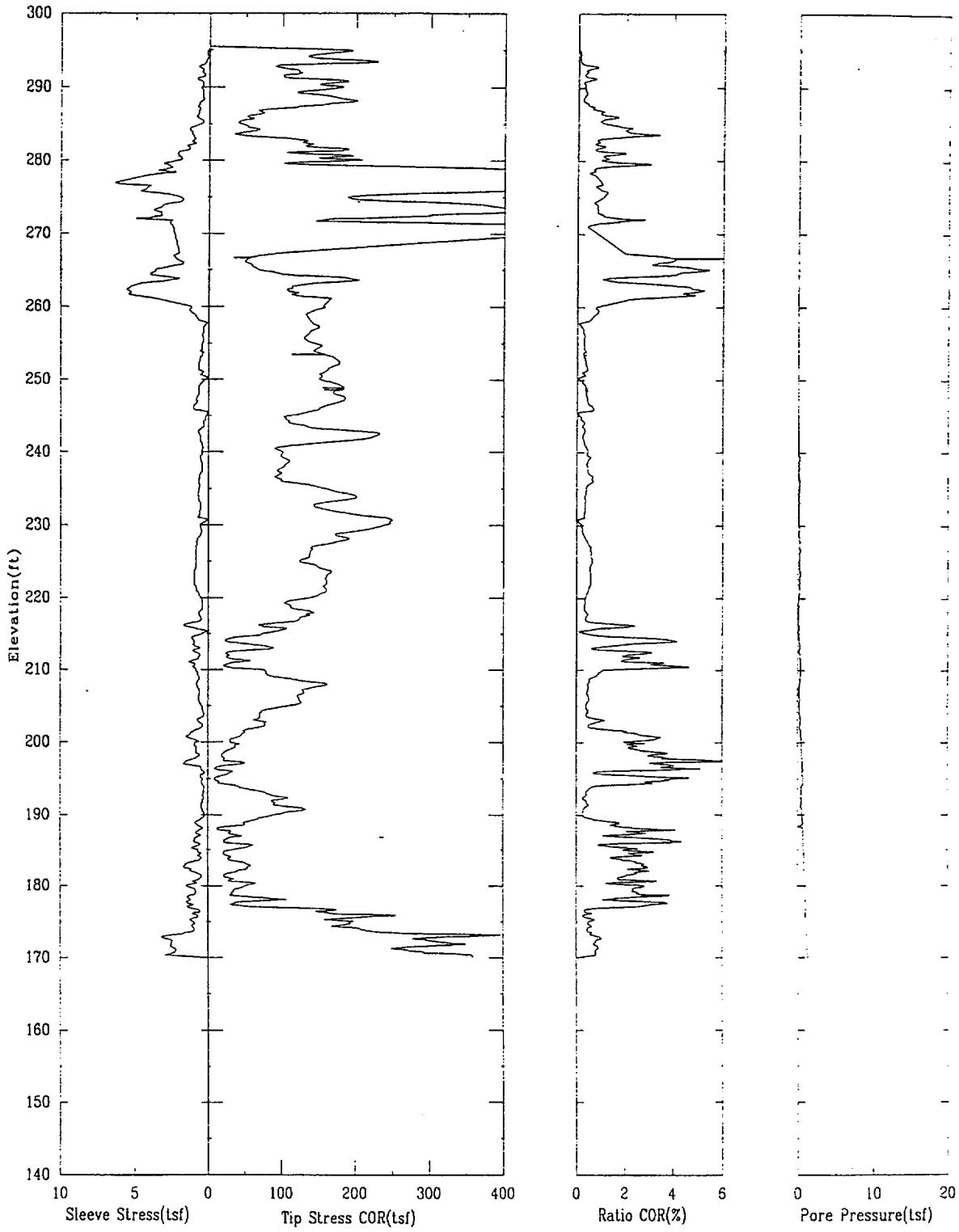

File 415L005.ECP

DCS, MFFF Project No. 08716

CPT-59 APPLIED RESEARCH ASSOCIATES, INC. 07/15/00

North 80152.7 East 54956.9 Elevation 295.5

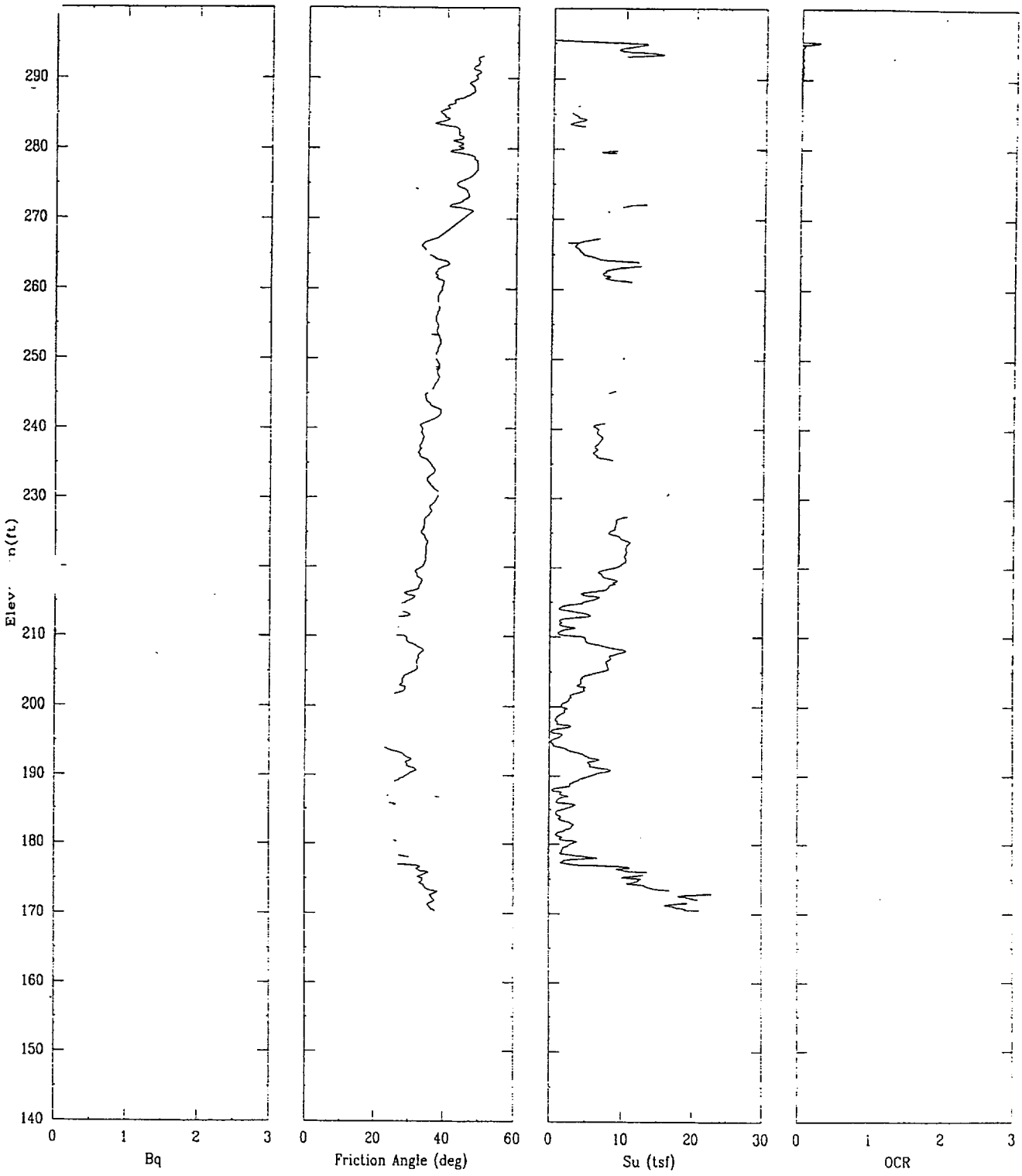

File 415L005.ECP

CPT-59 APPLIED RESEARCH ASSOCIATES, INC. 07/15/00

North 80152.7 East 54956.9 Elevation 295.5

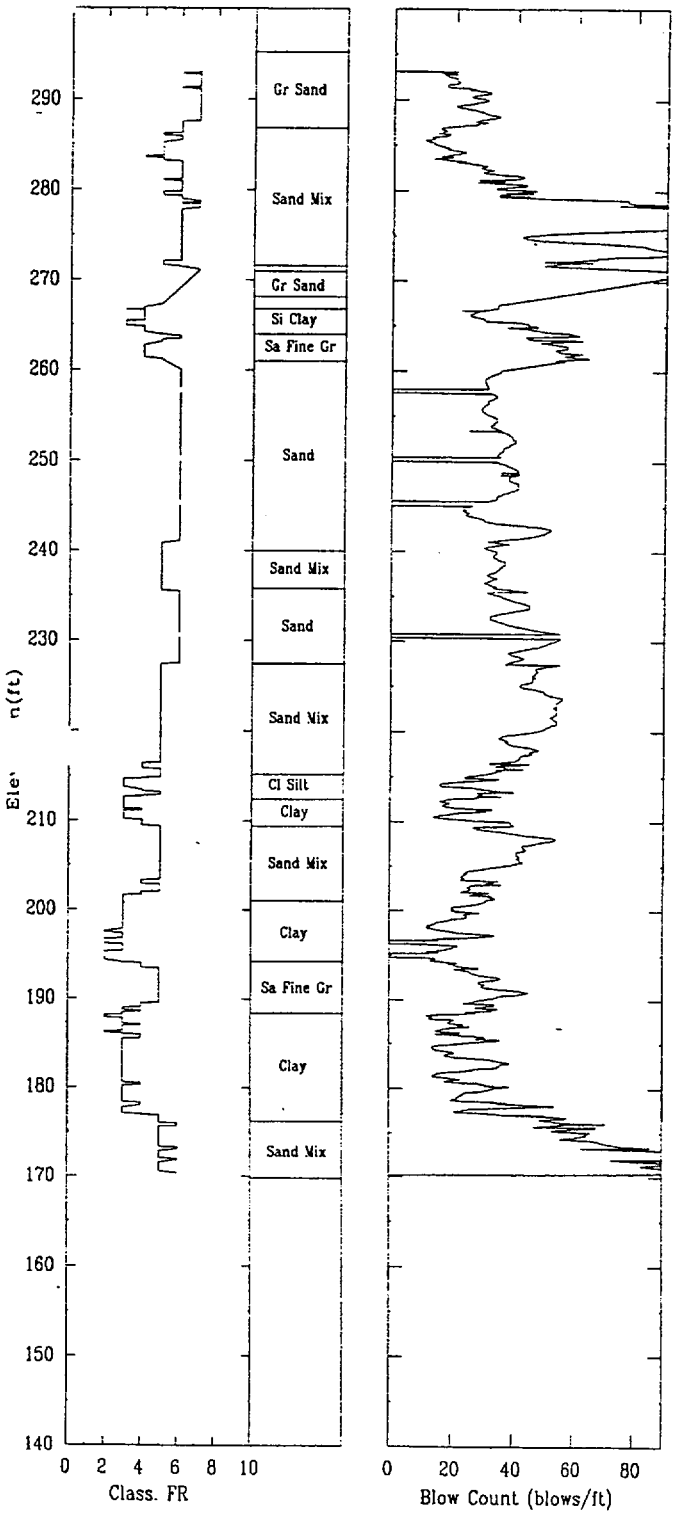

File 415L005.ECP

DCS, MFFF Project No. 08716

CPT-60 APPLIED RESEARCH ASSOCIATES, INC. 07/15/00

North d0142.2 East 55140.6 Elevation 295.7

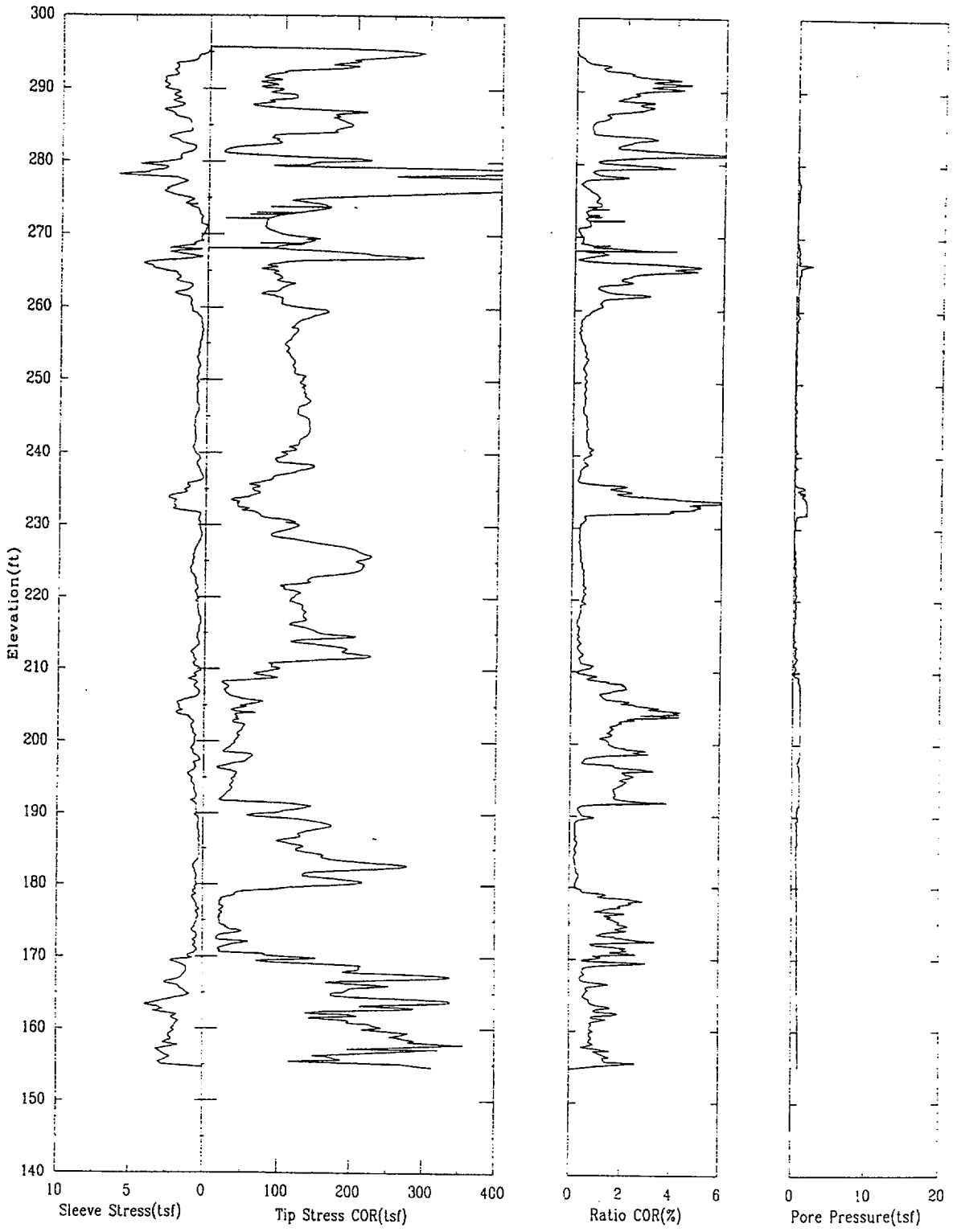

File 415L003.ECP

DCS, MFFF Project No. 08716

CPT-60 APPLIED RESEARCH ASSOCIATES, INC. 07/15/00

North 80142.2 East 55140.6 Elevation 295.7

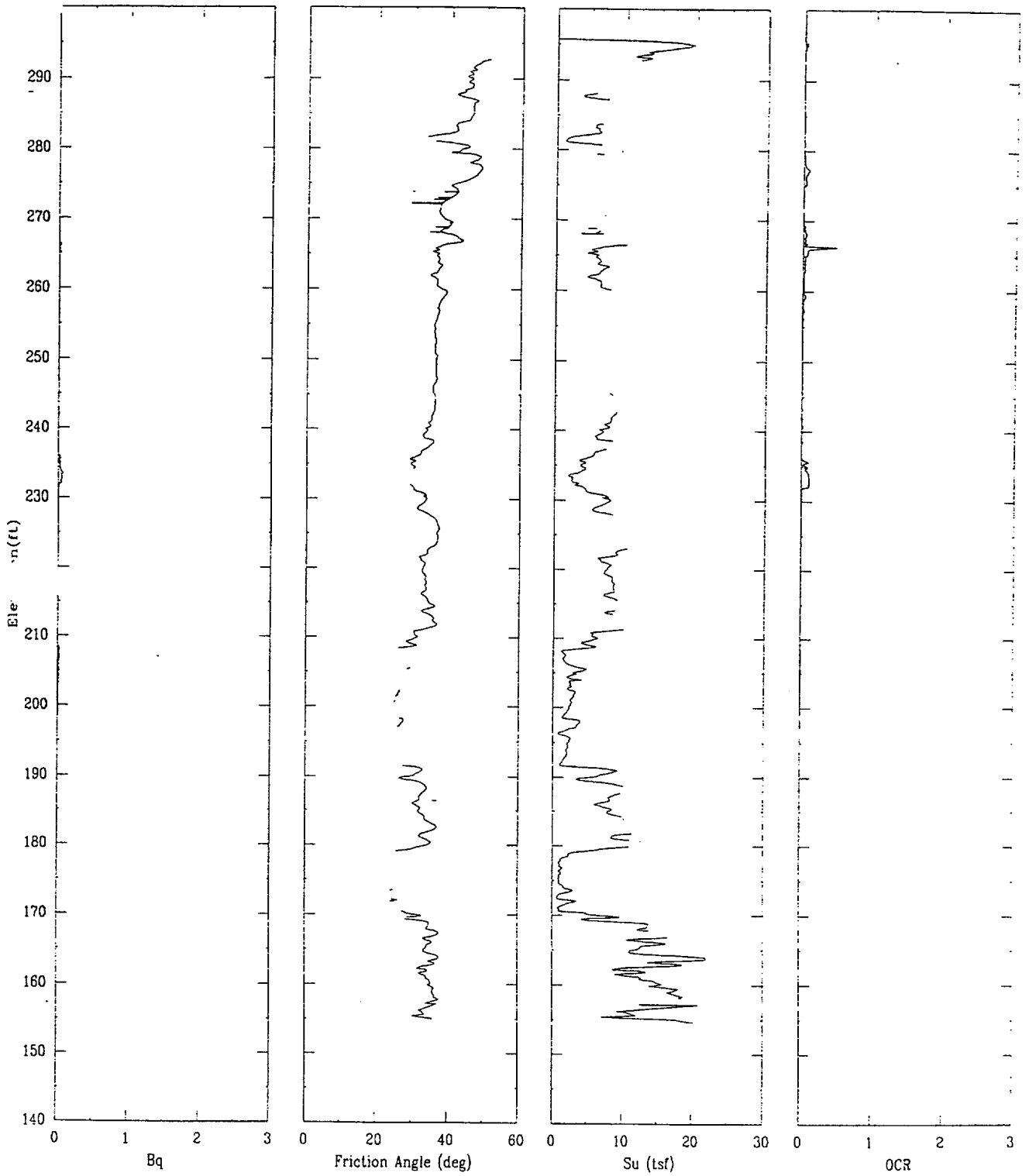

File 415L003.ECP

CPT-60 APPLIED RESEARCH ASSOCIATES, INC. 07/15/00

North 80142.2 East 55140.6 Elevation 295.7

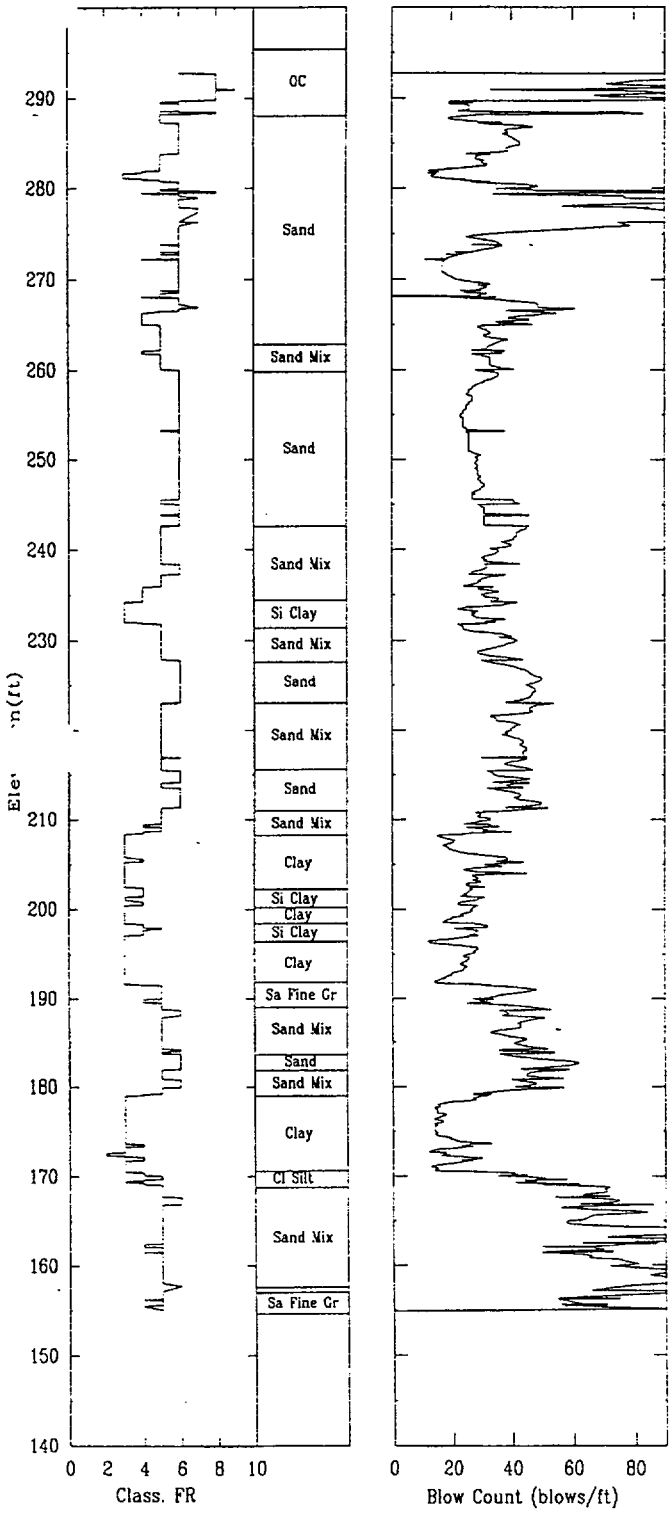

File 415L003.ECP

DCS, MFFF Project No. 08716

CPT-61 APPLIED RESEARCH ASSOCIATES, INC. 07/21/00

North 80037.6 East 54869.6 Elevation 279.3

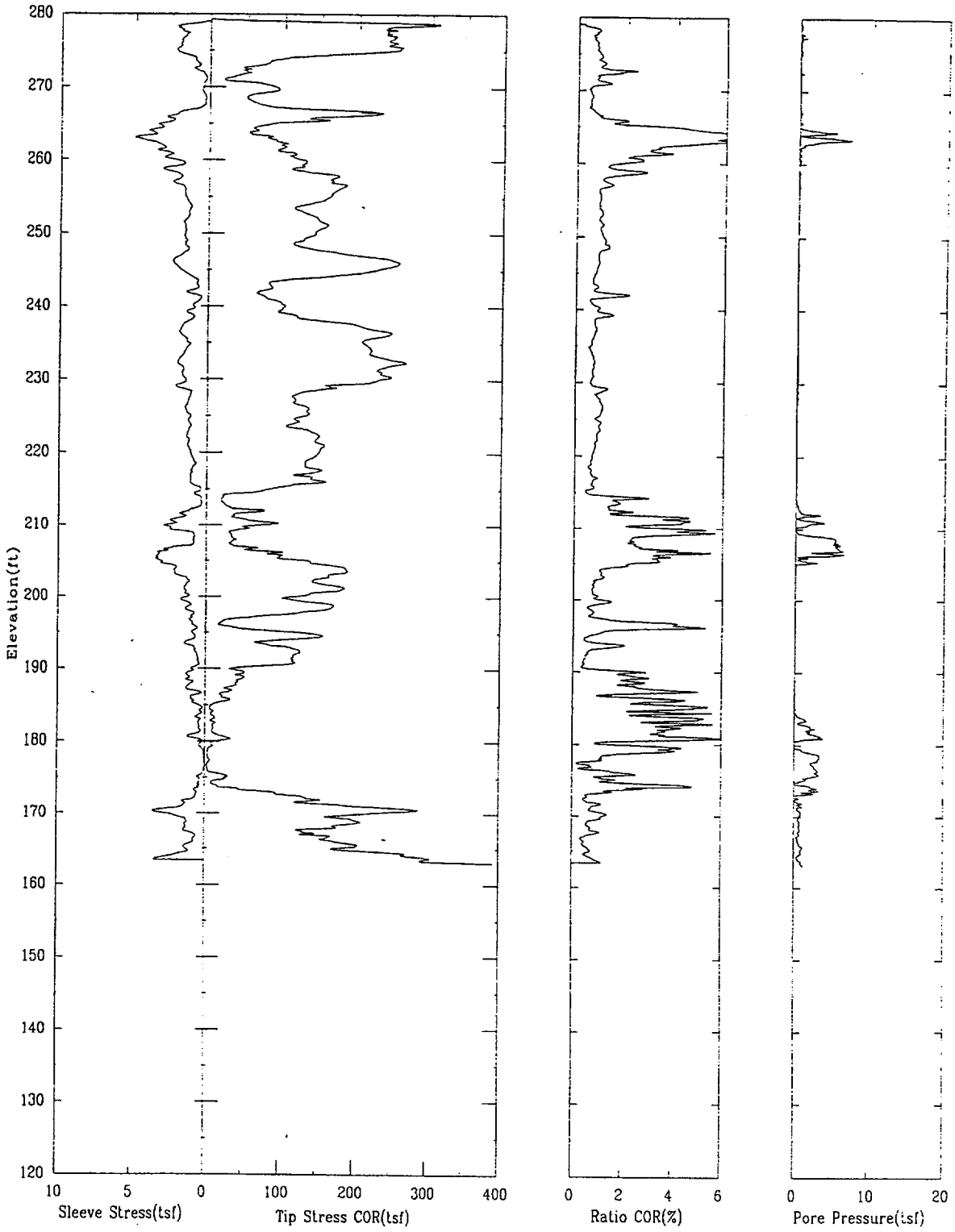

File 321L003.ECP

DCS, MFFF Project No. 08716

CPT-61 APPLIED RESEARCH ASSOCIATES, INC. 07/21/00

North 60037.6 East 54869.6 Elevation 279.3

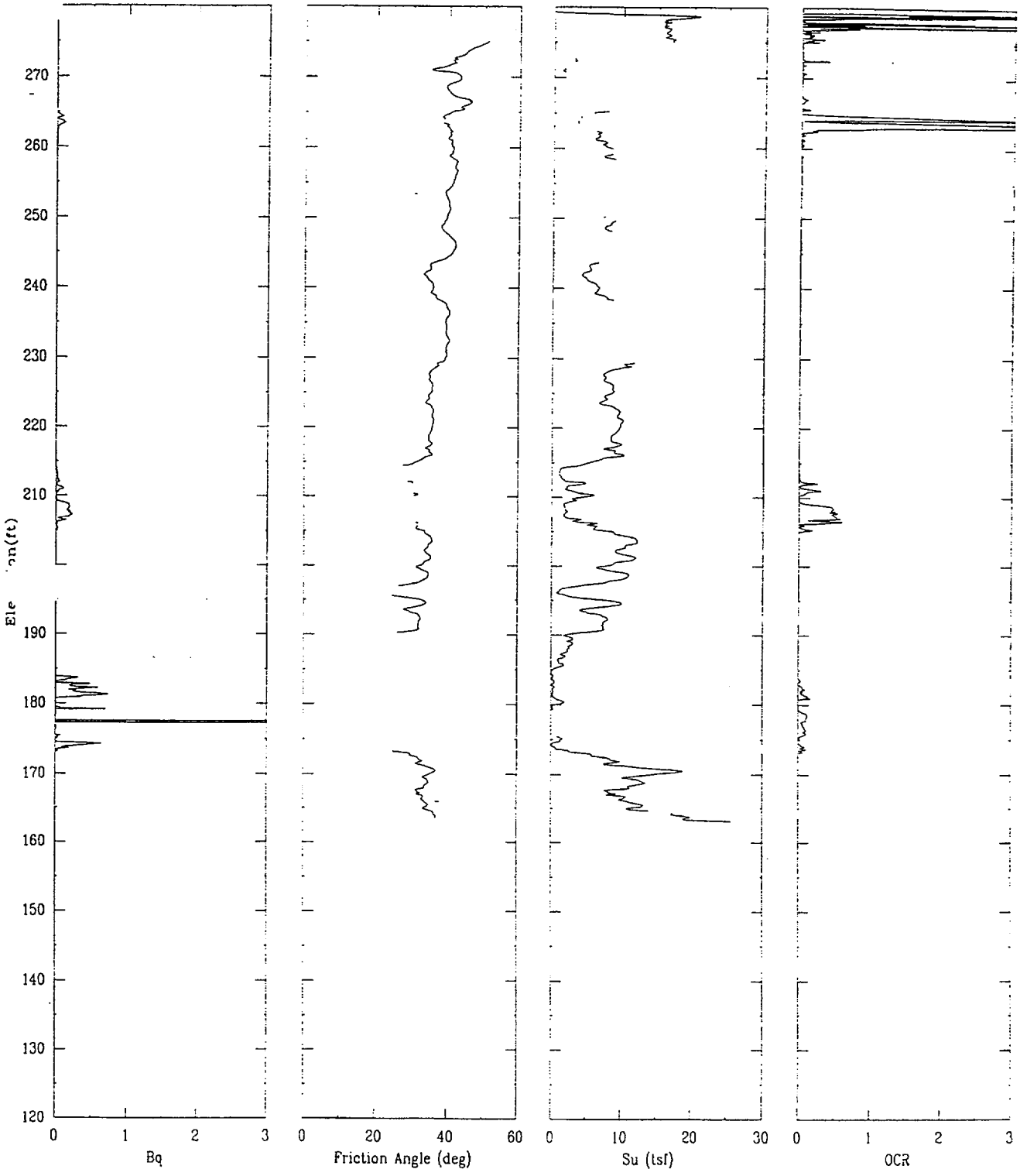

File 321L003.ECP

DCS, MFFF Project No. 08716

CPT-61 APPLIED RESEARCH ASSOCIATES, INC. 07/21/00

North 80037.6 East 54869.6 Elevation 279.3

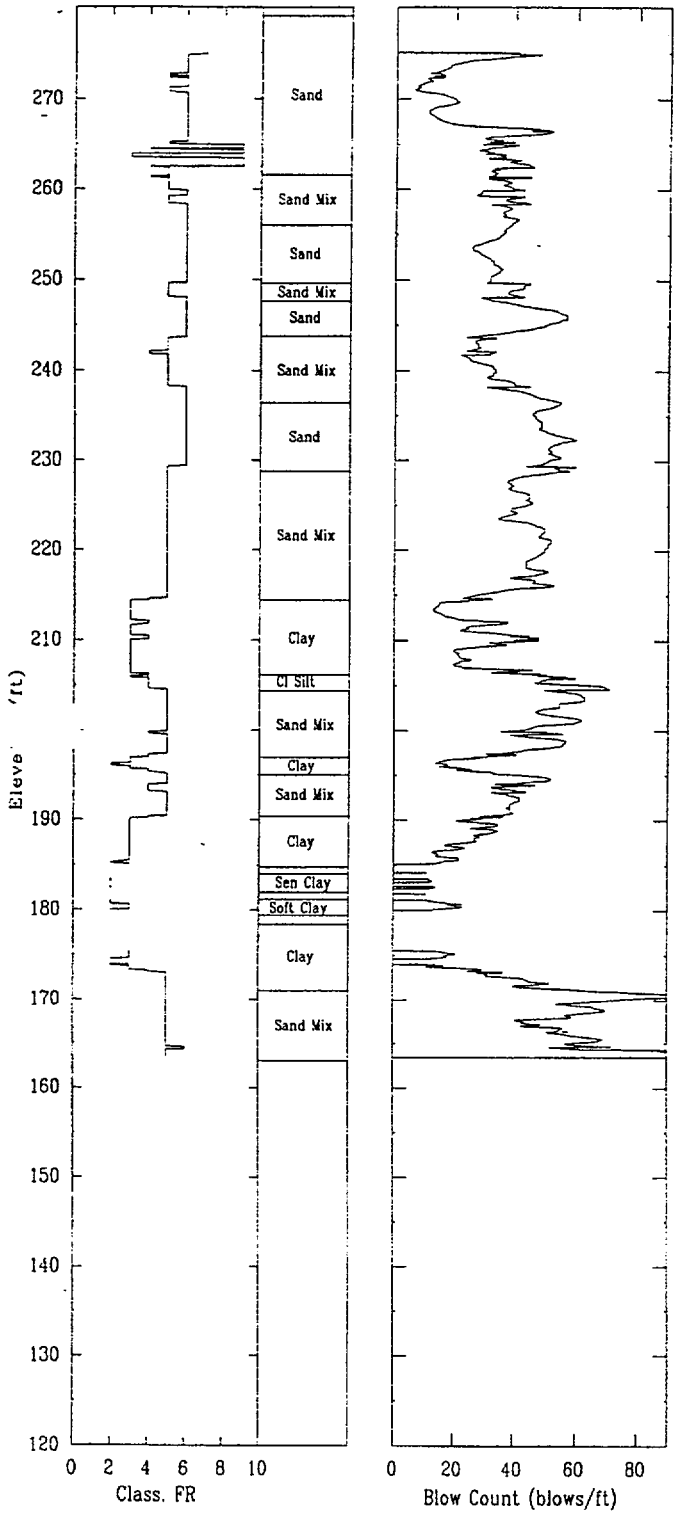

File 321L003.ECP

CPT-62 APPLIED RESEARCH ASSOCIATES, INC. 07/22/00

North 80055.6 East 54956.3 Elevation 278.5

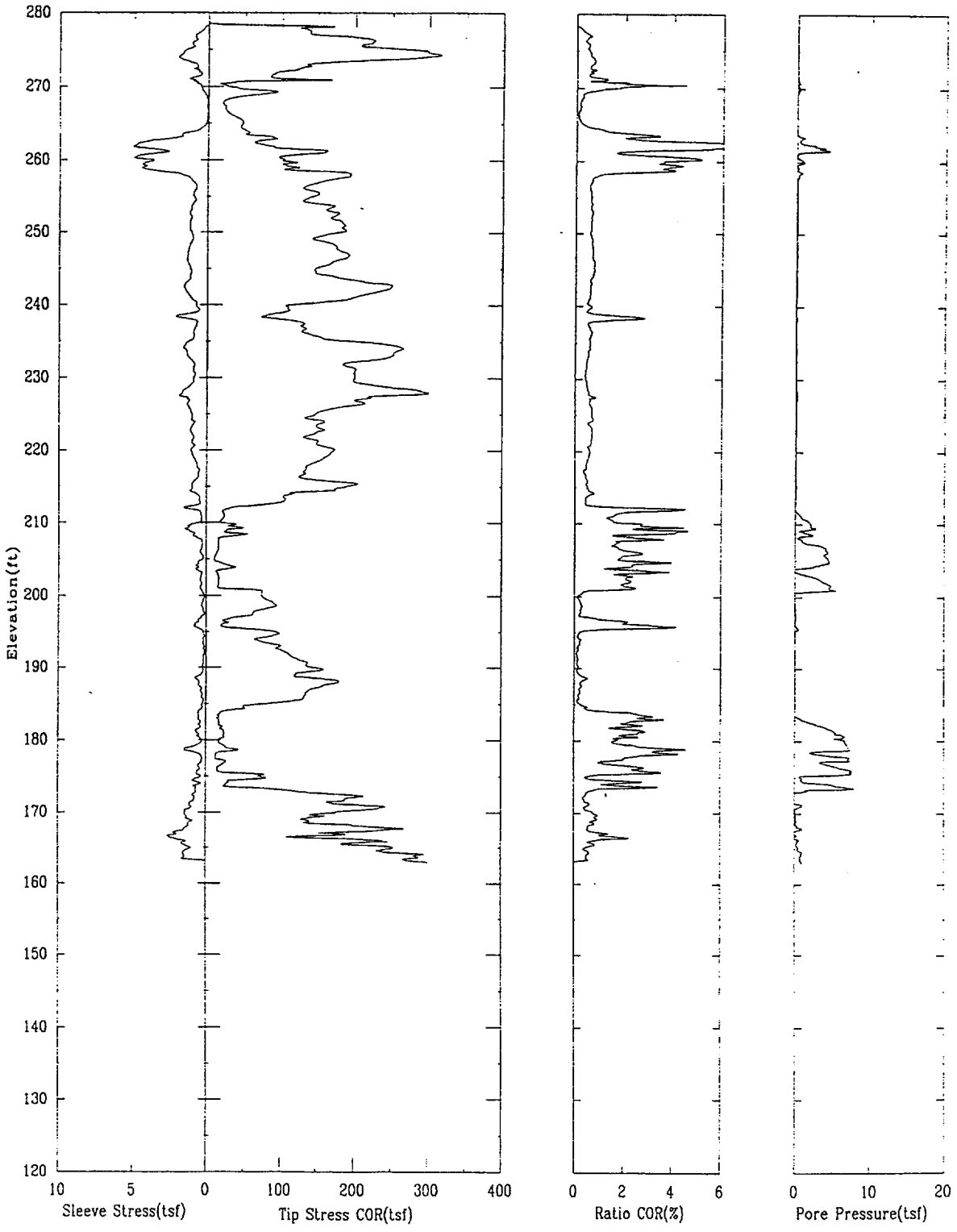

File 322L001.ECP

CPT-62 APPLIED RESEARCH ASSOCIATES, INC. 07/22/00

North 80055.6 East 54956.3 Elevation 278.5

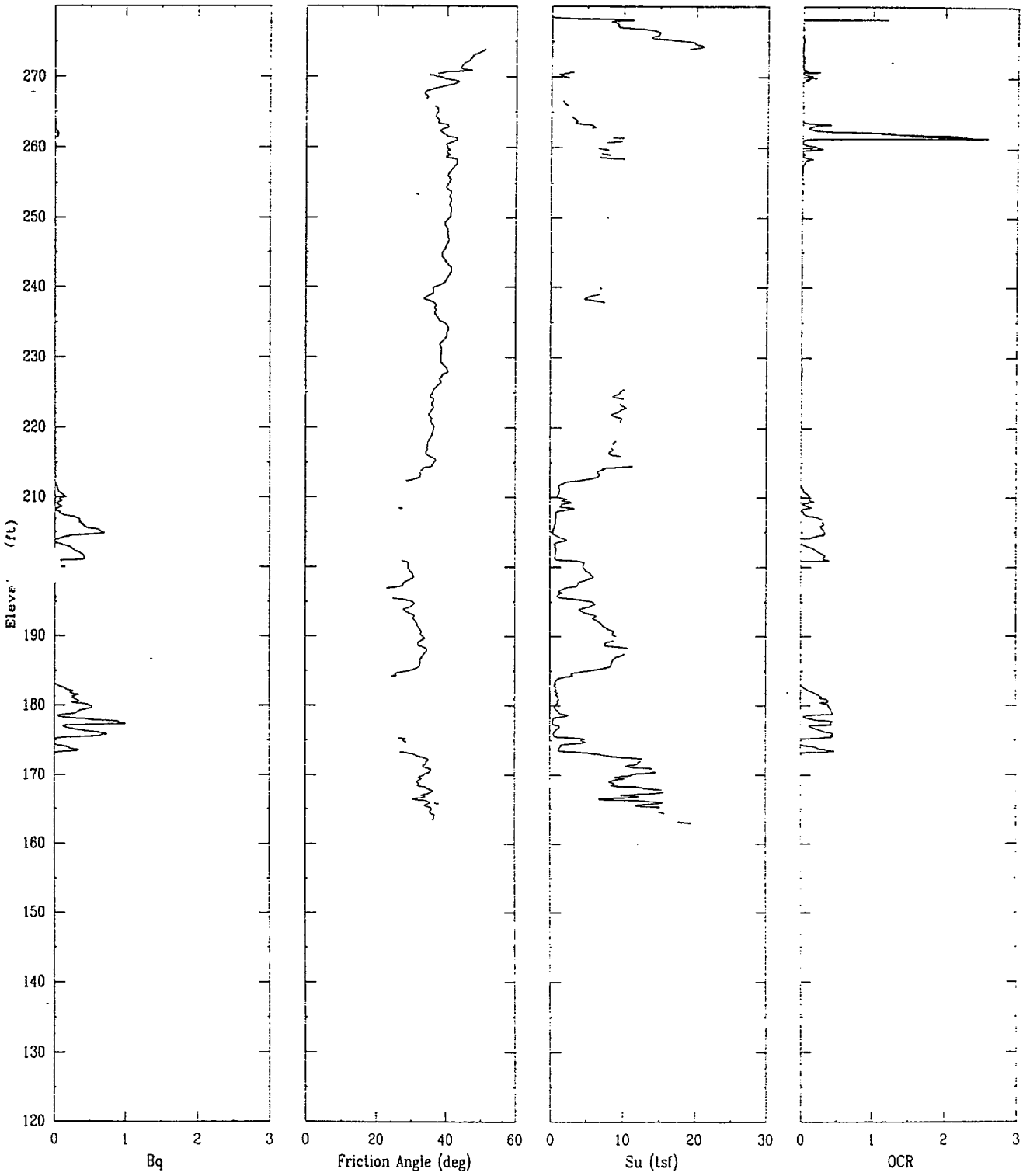

File 322L001.ECP

DCS, MFFF Project No. 08716

CPT-62 APPLIED RESEARCH ASSOCIATES, INC. 07/22/00

North 80055.6 East 54956.3 Elevation 278.5

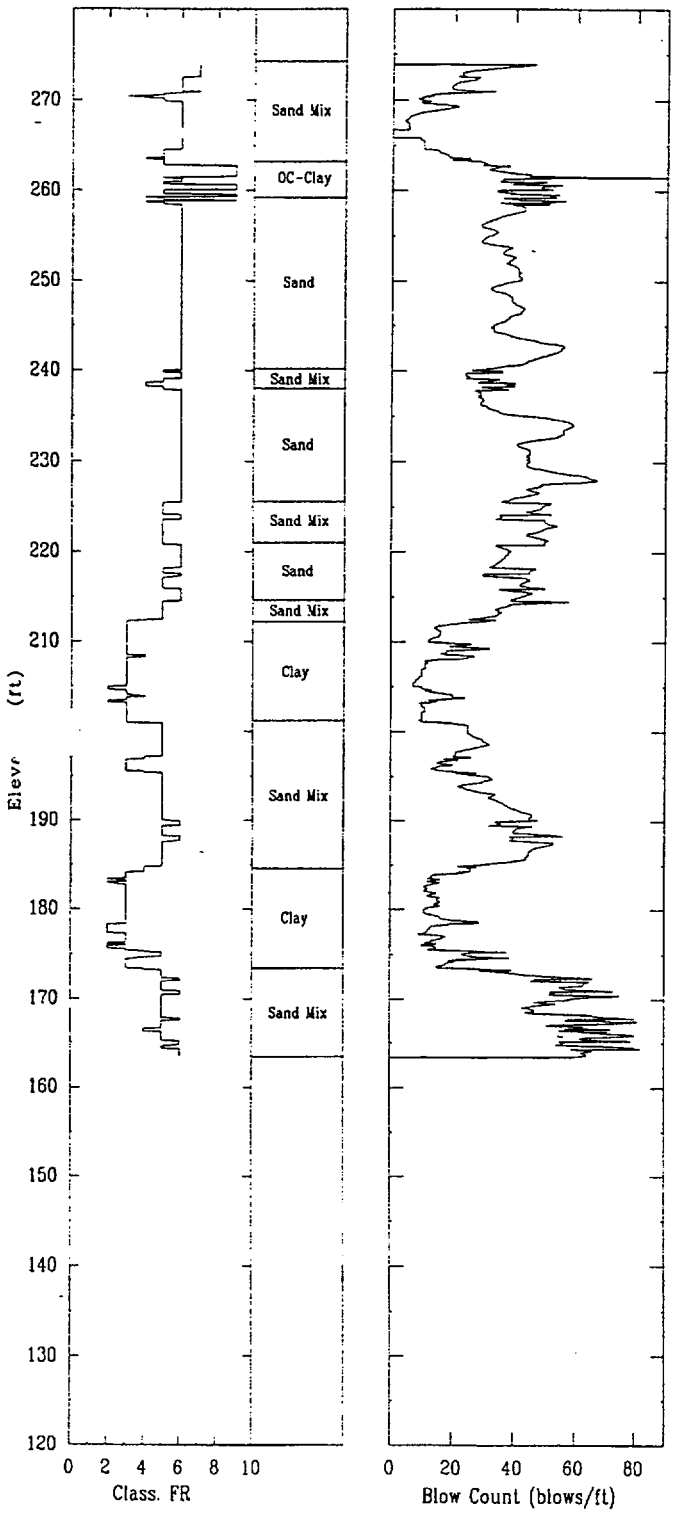

File 322L001.ECP

CPT-63 APPLIED RESEARCH ASSOCIATES, INC. 07/22/00

North 80066.0 East 55055.5 Elevation 279.4

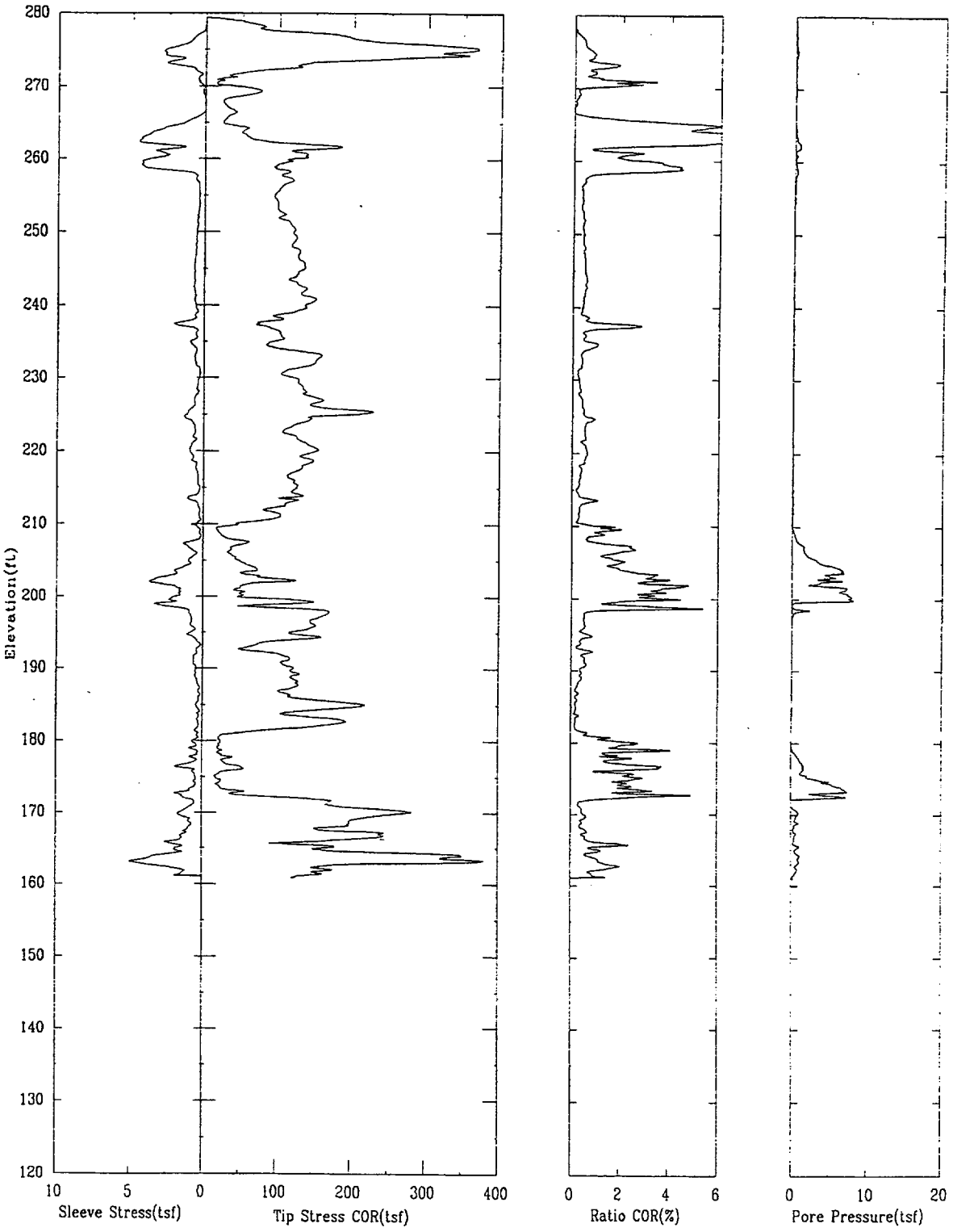

File 322L003.ECP

DCS, MFFF Project No. 08716

CPT-63 APPLIED RESEARCH ASSOCIATES, INC. 07/22/00

North 80066.0 East 55055.5 Elevation 279.4

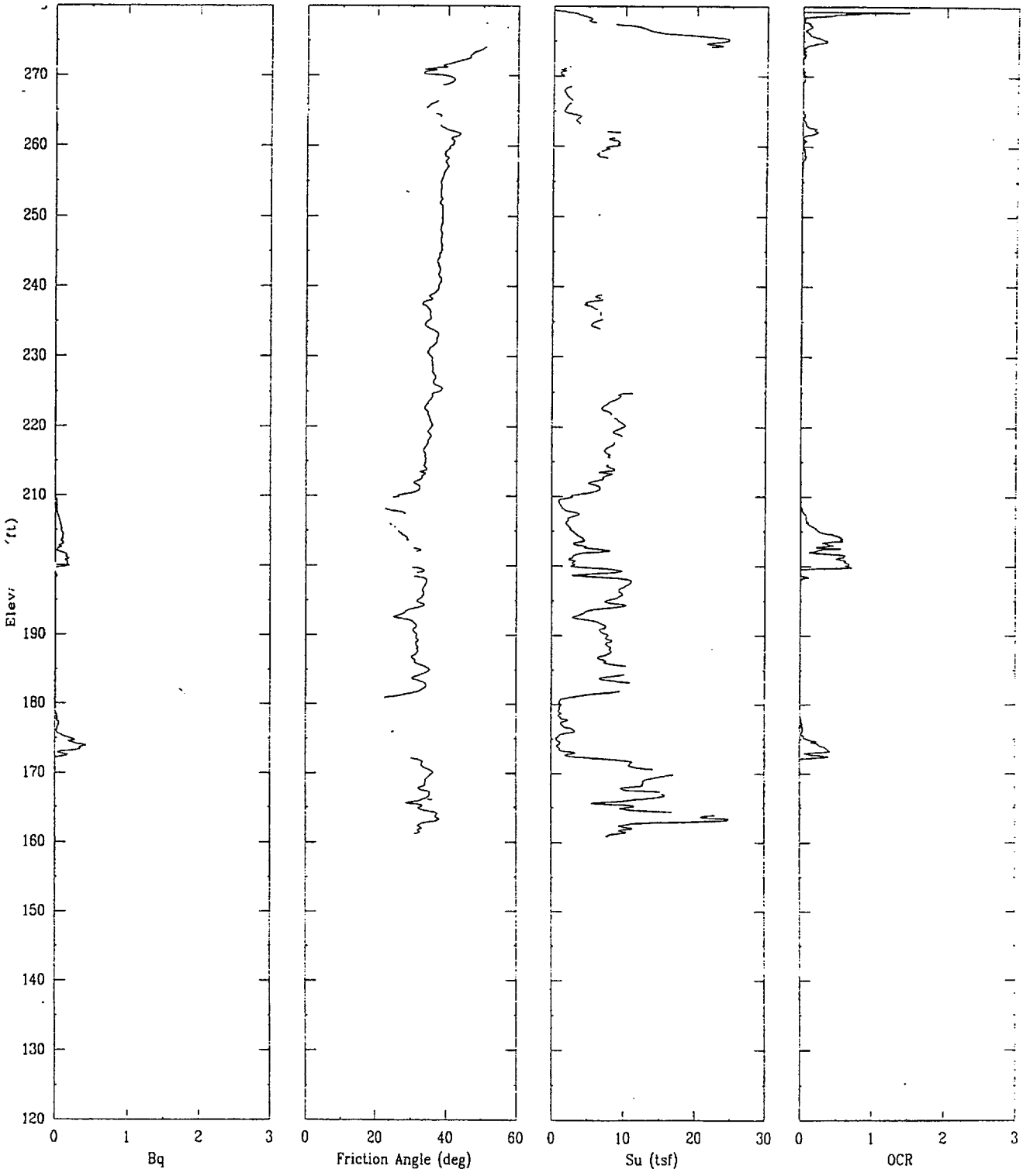

File 322L003.ECP

CPT-63 APPLIED RESEARCH ASSOCIATES, INC. 07/22/00

North 80066.0 East 55055.5 Elevation 279.4

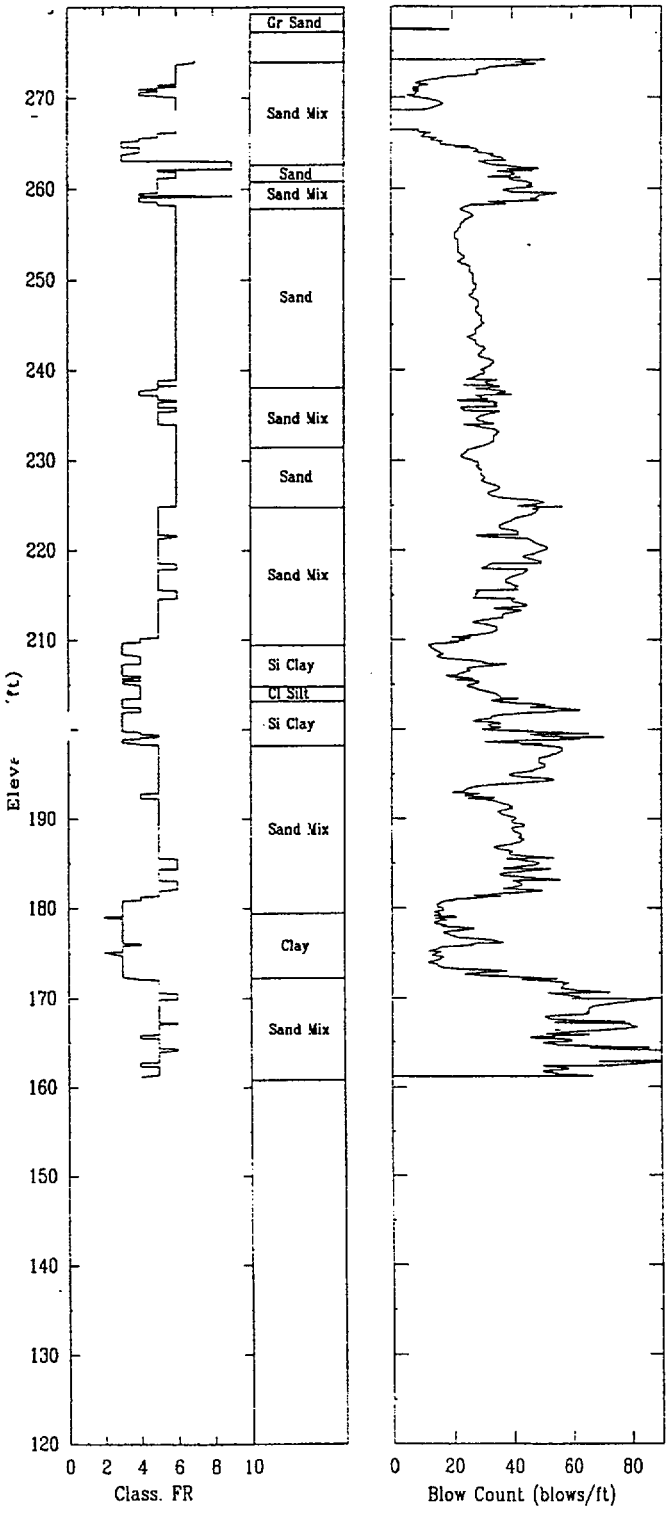

File 322L003.ECP

DCS, MFFF Project No. 08716

CPT-64 APPLIED RESEARCH ASSOCIATES, INC. 07/15/00

North 80034.9 East 55165.3 Elevation 279.8

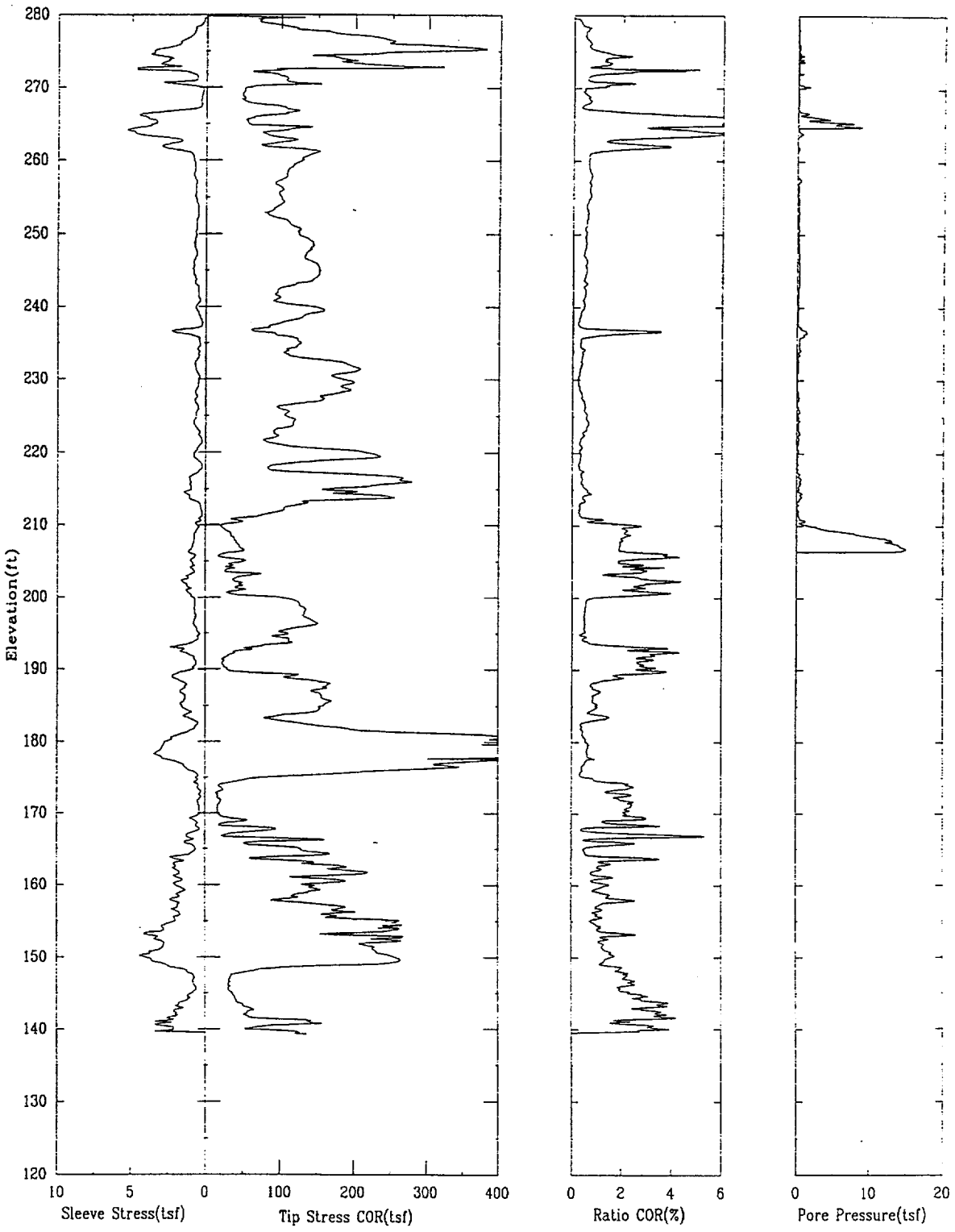

File 415L001.ECP

CPT-64 APPLIED RESEARCH ASSOCIATES, INC. 07/15/00

North 80034.9 East 55165.3 Elevation 279.8

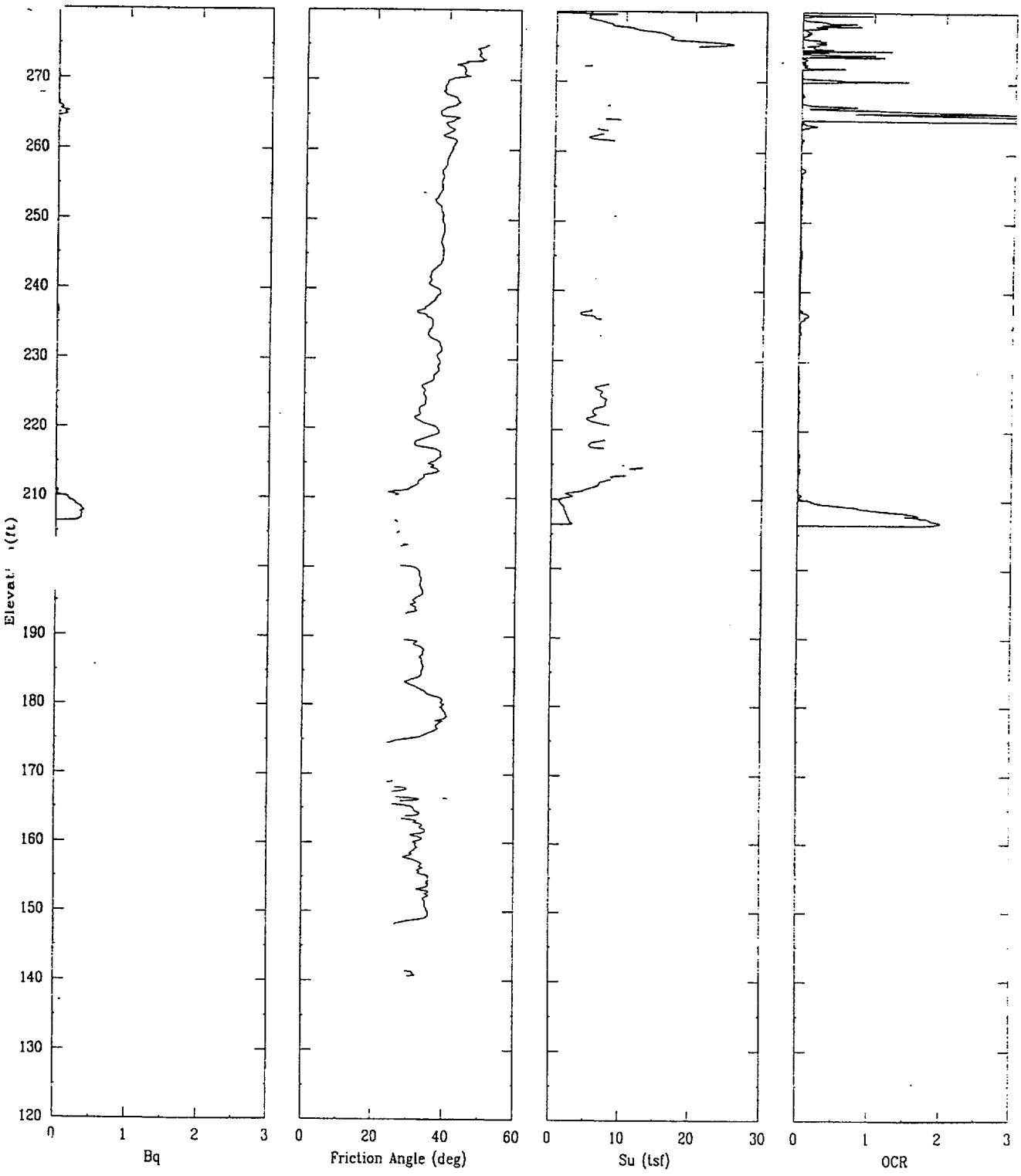

File 415L001.ECP

APPENDIX B

INTENTIONALLY LEFT BLANK

APPENDIX C

SEISMIC DATA

CPT-37S APPLIED RESEARCH ASSOCIATES, INC. 06/05/00

Compression Wave Speeds

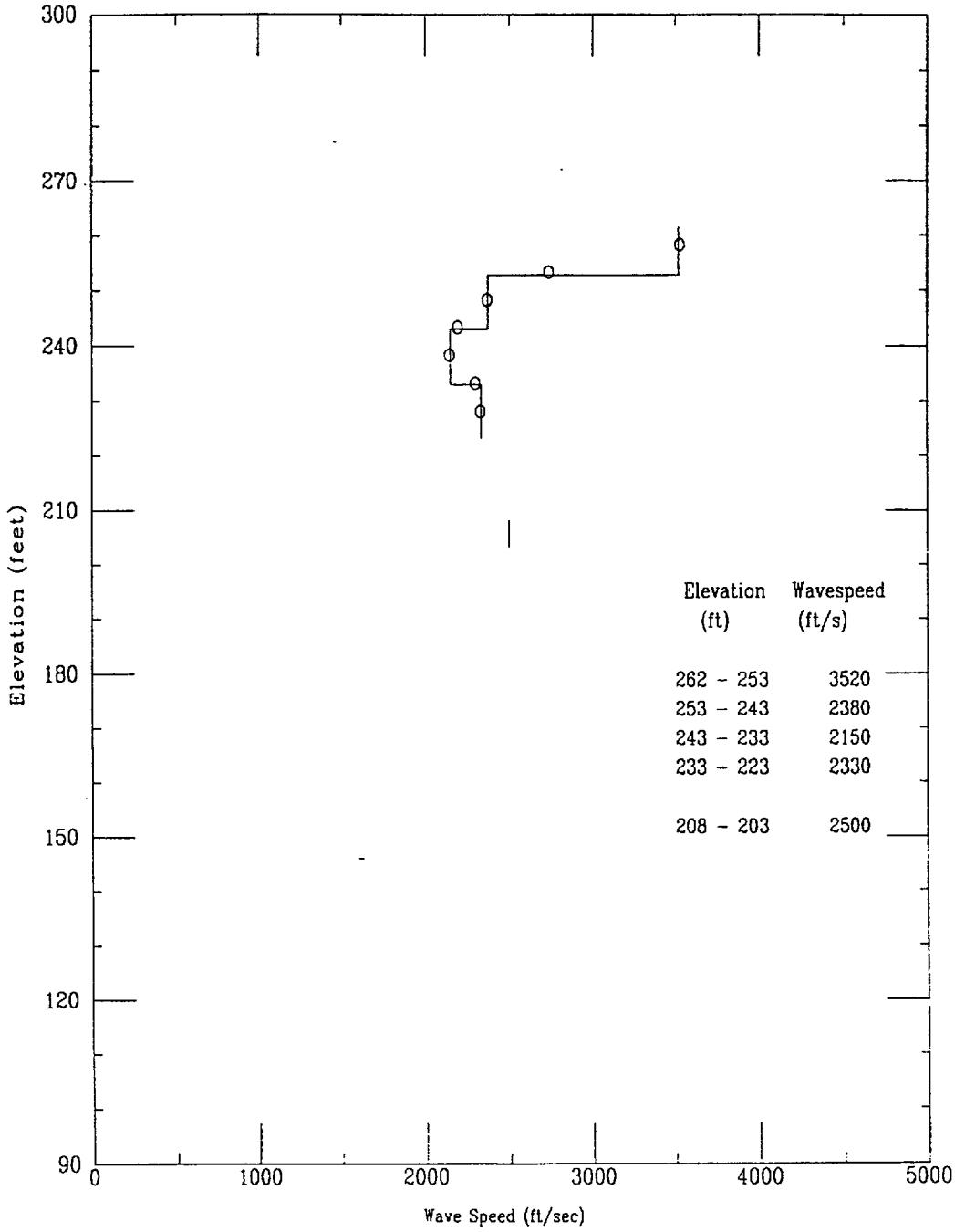

File 405u001S

CPT-37S APPLIED RESEARCH ASSOCIATES, INC. 06/05/00

Compression Wave Time of Peak

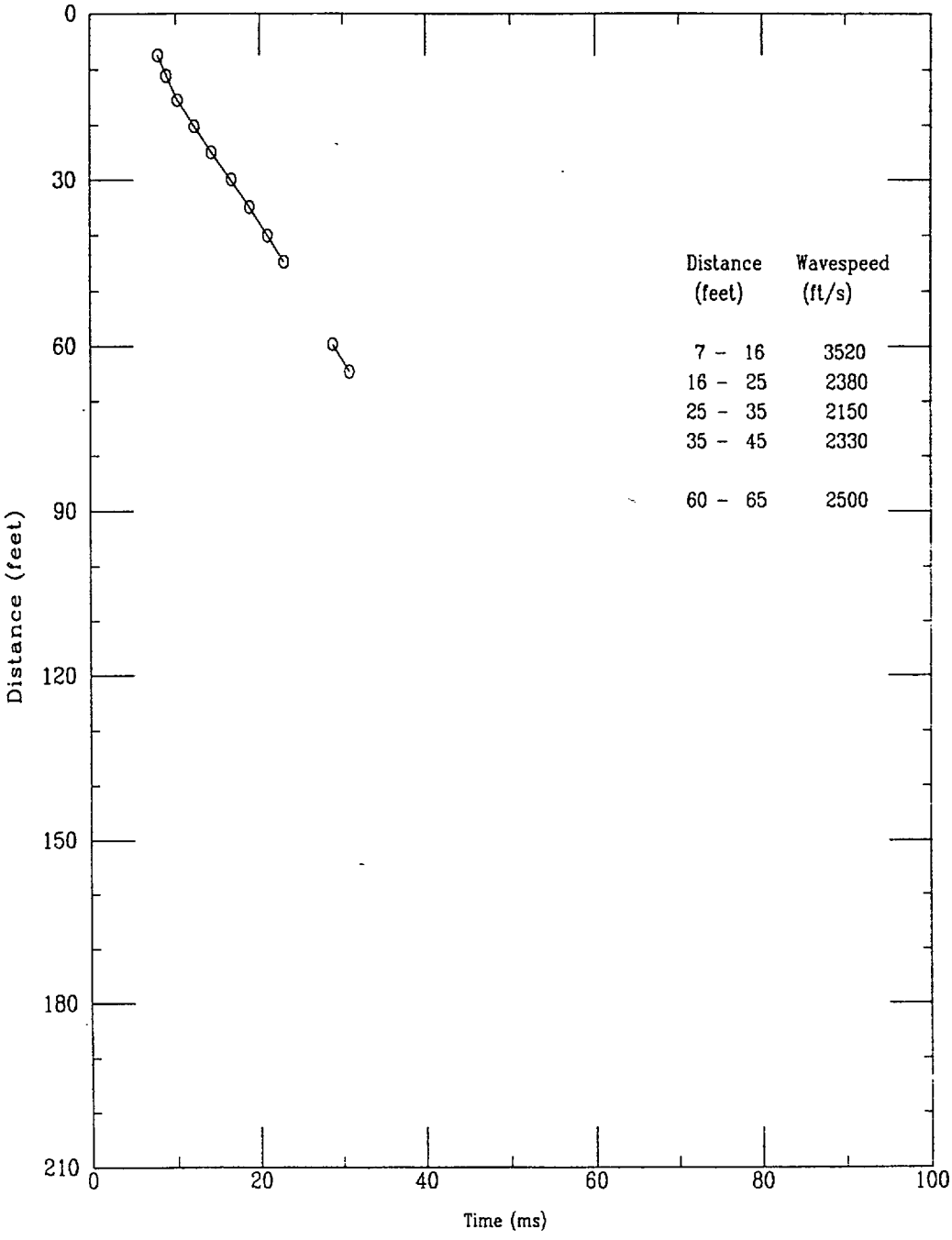

File 405u001S

CPT-37S APPLIED RESEARCH ASSOCIATES, INC. 06/05/00

Shear Wave Speeds

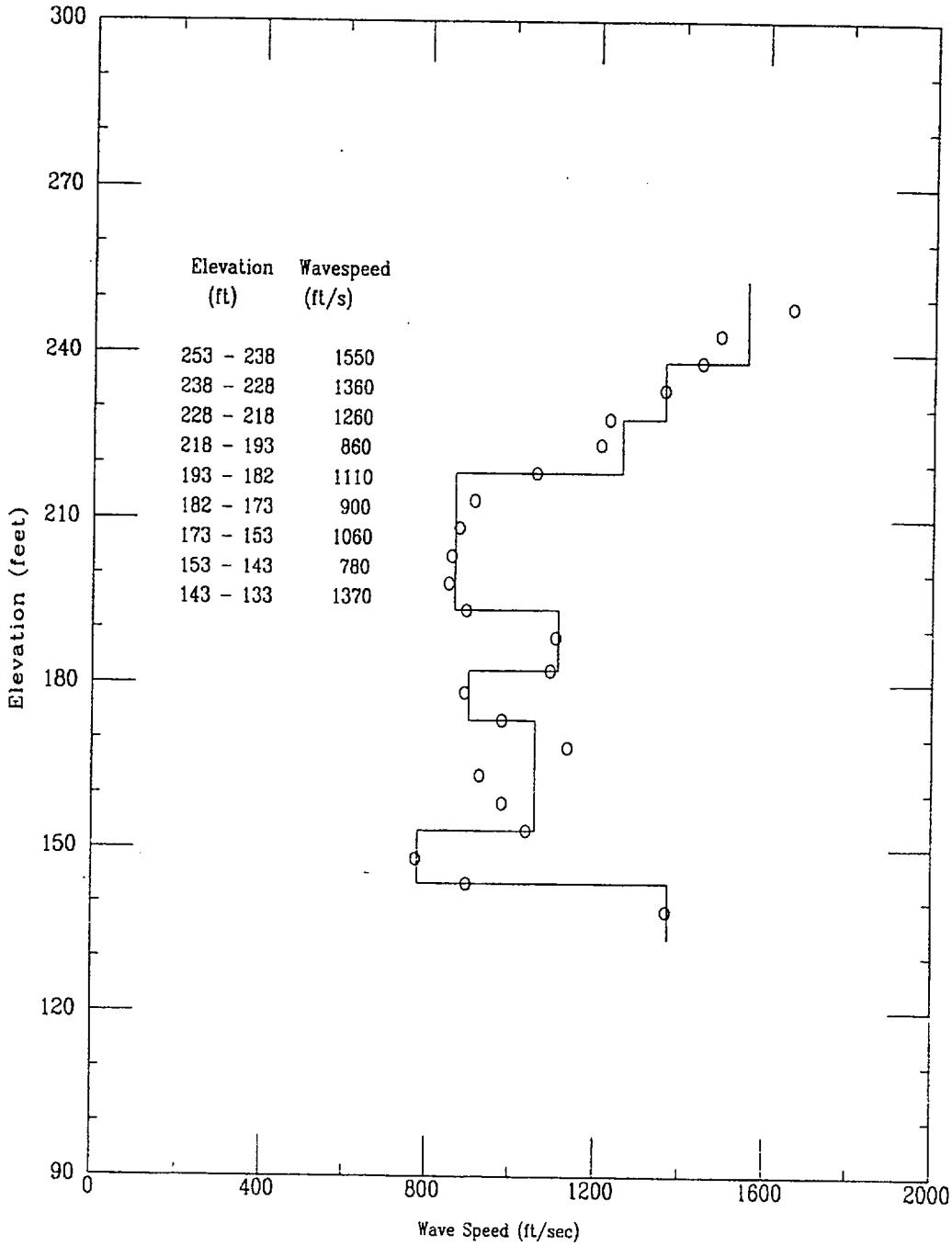

File 405u001S

CPT-37S APPLIED RESEARCH ASSOCIATES, INC. 06/05/00

Shear Wave Time of Peak

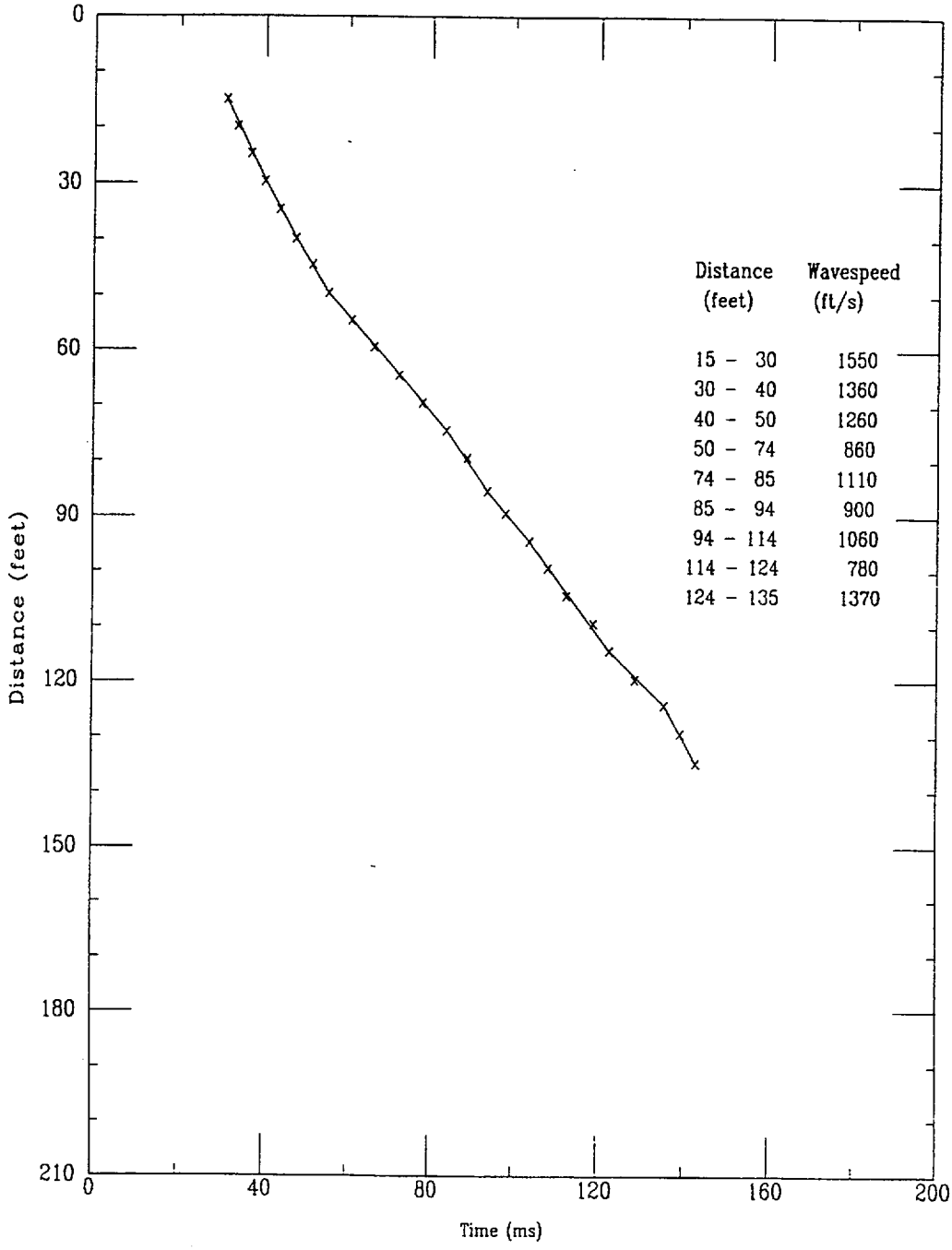

File 405u001S

CPT-35S APPLIED RESEARCH ASSOCIATES, INC. 06/03/00

Compression Wave Speeds

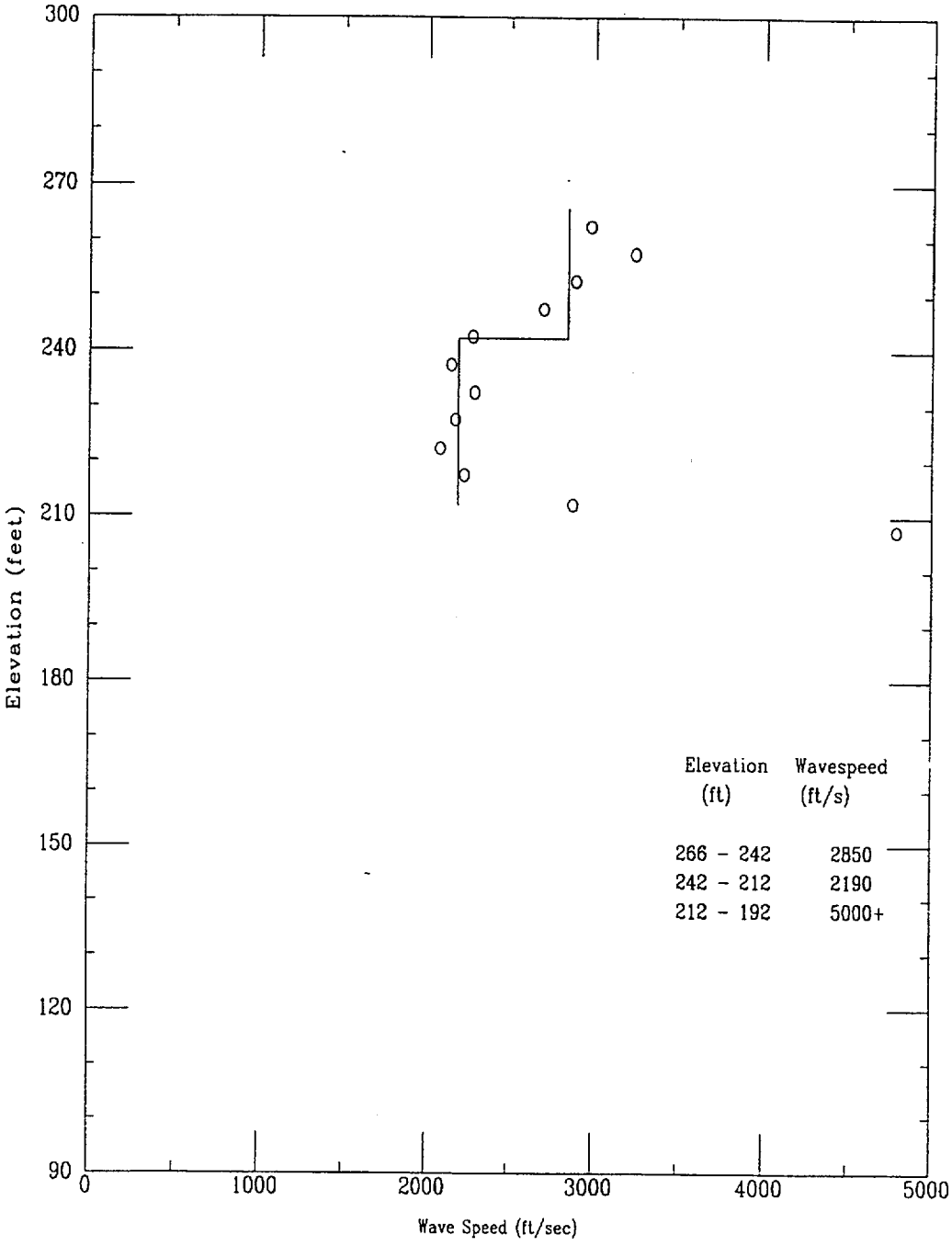

File 403U005S

CPT-35S APPLIED RESEARCH ASSOCIATES, INC. 06/03/00

Compression Wave Time of Peak

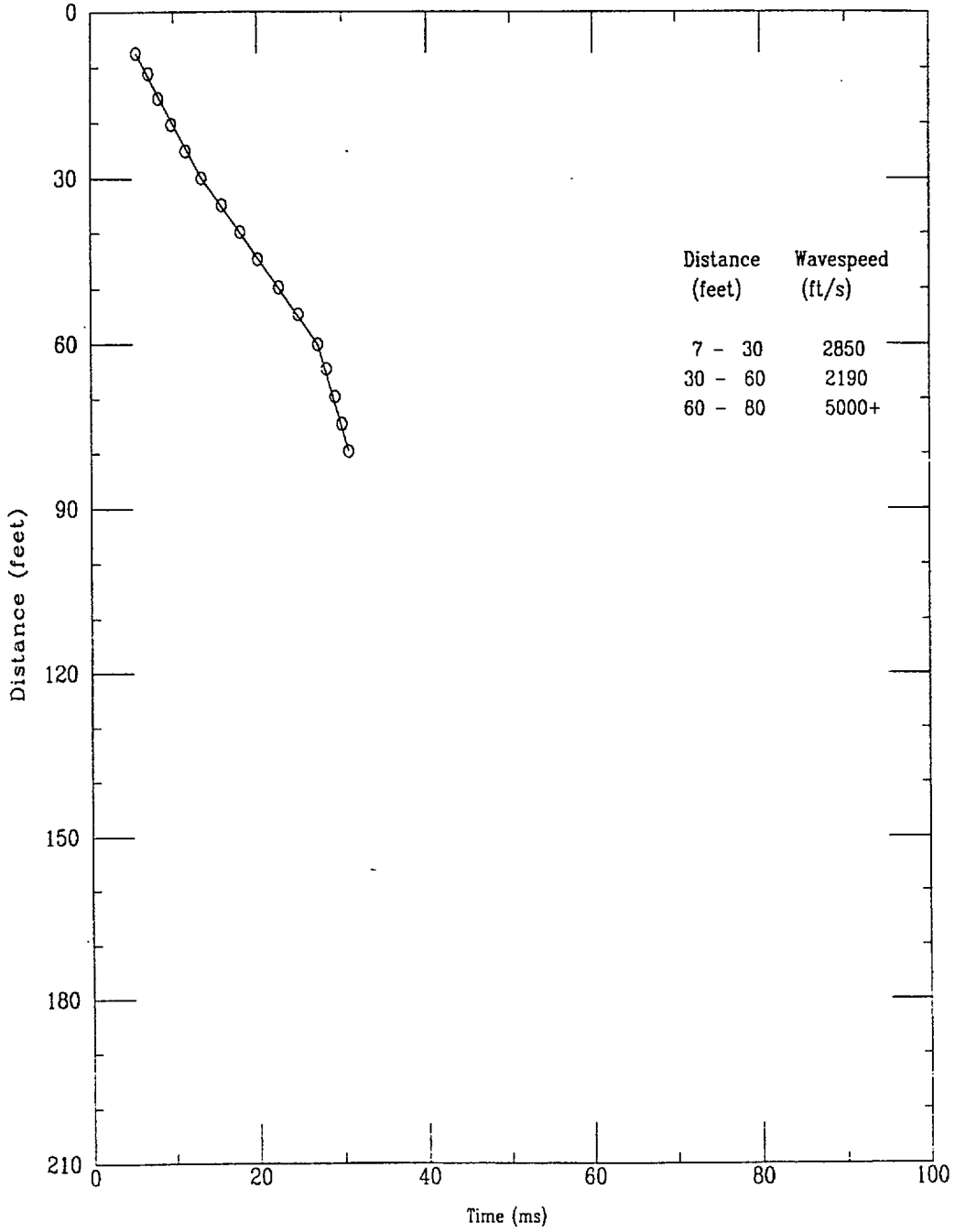

File 403U005S

CPT-35S APPLIED RESEARCH ASSOCIATES, INC. 06/03/00

Shear Wave Speeds

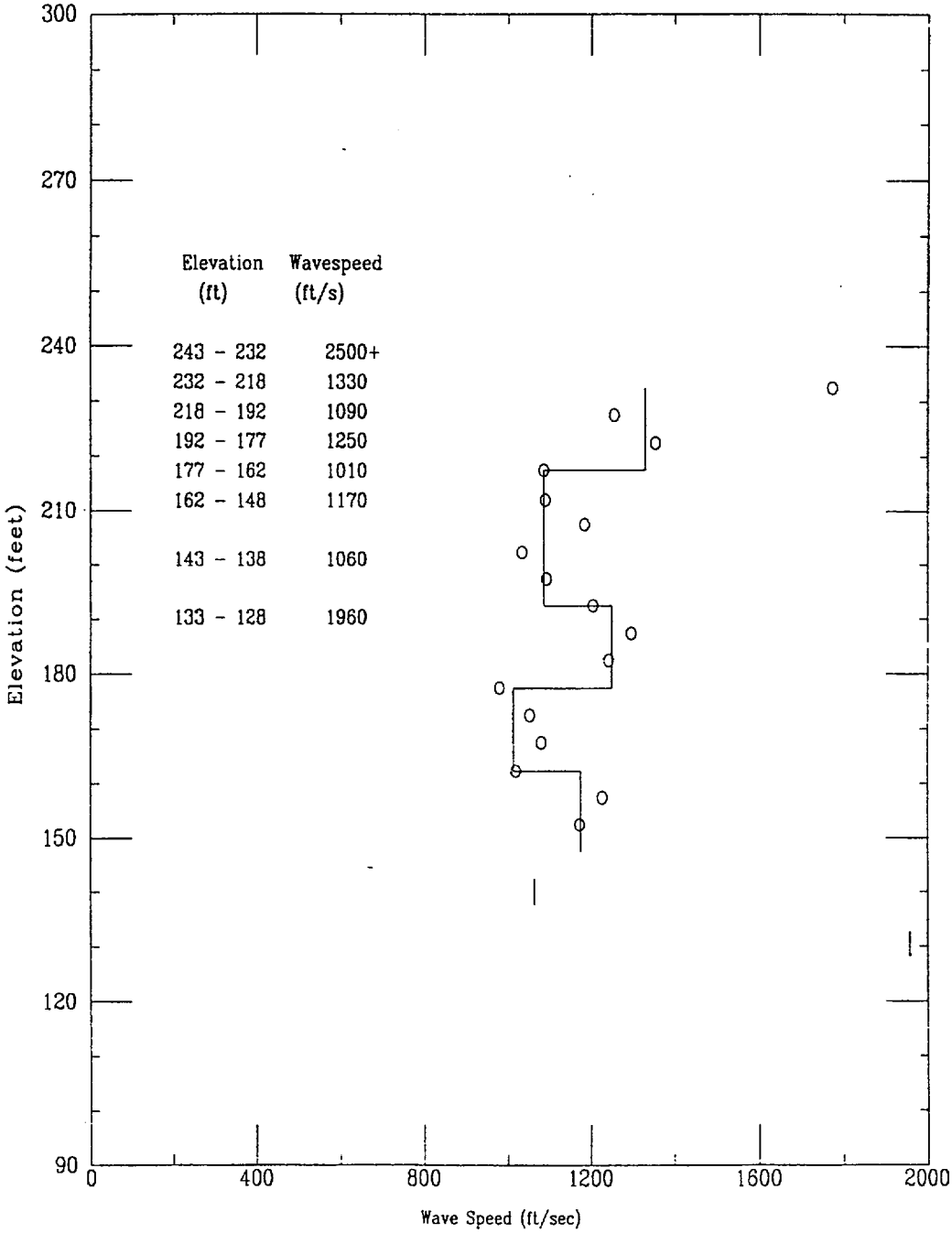

File 403u005S

CPT-35S APPLIED RESEARCH ASSOCIATES, INC. 06/03/00

Shear Wave Time of Peak

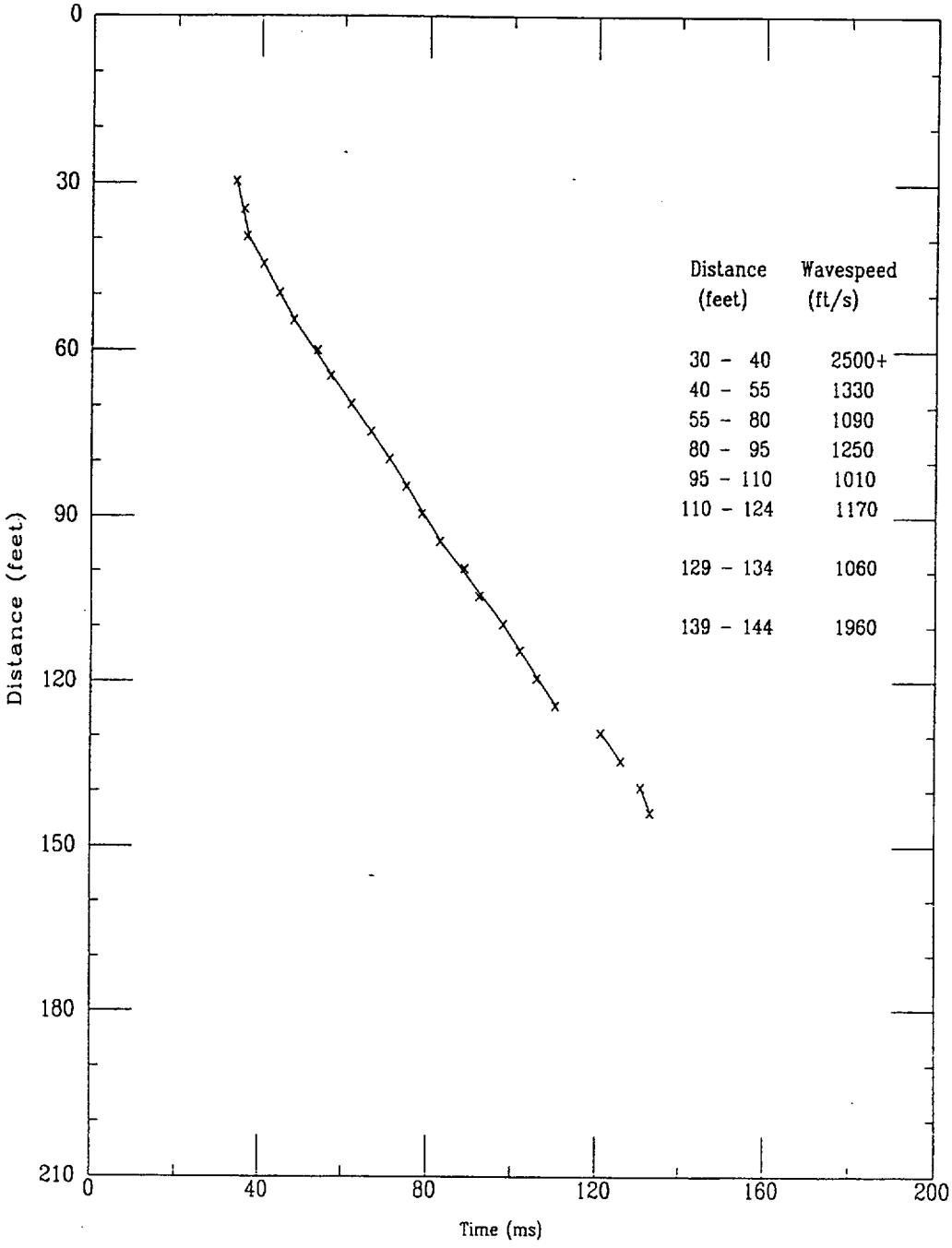

File 403u005S

CPT-34S APPLIED RESEARCH ASSOCIATES, INC. 06/07/00

Compression Wave Speeds

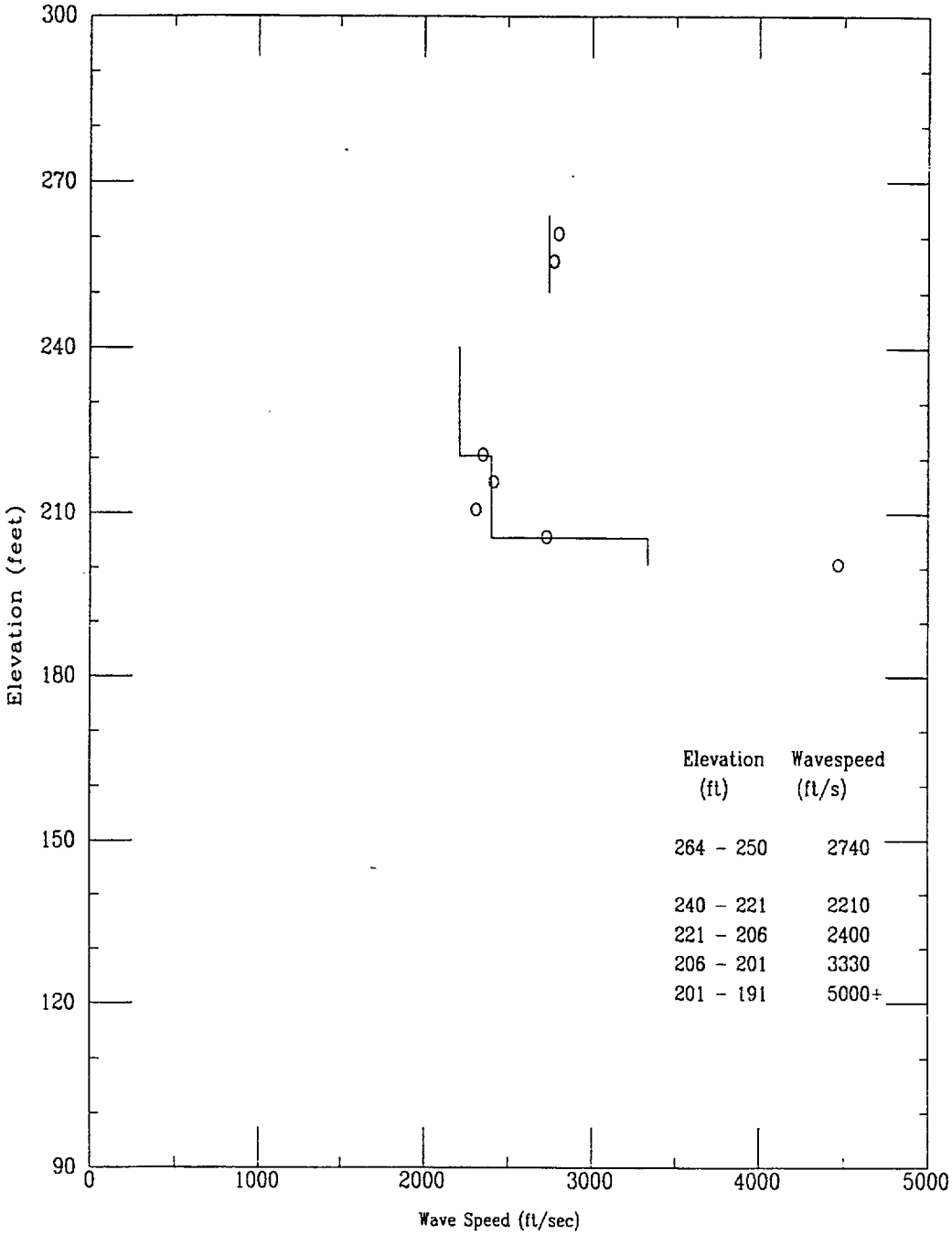

File 407u001S

CPT-34S APPLIED RESEARCH ASSOCIATES, INC. 06/07/00

Compression Wave Time of Peak

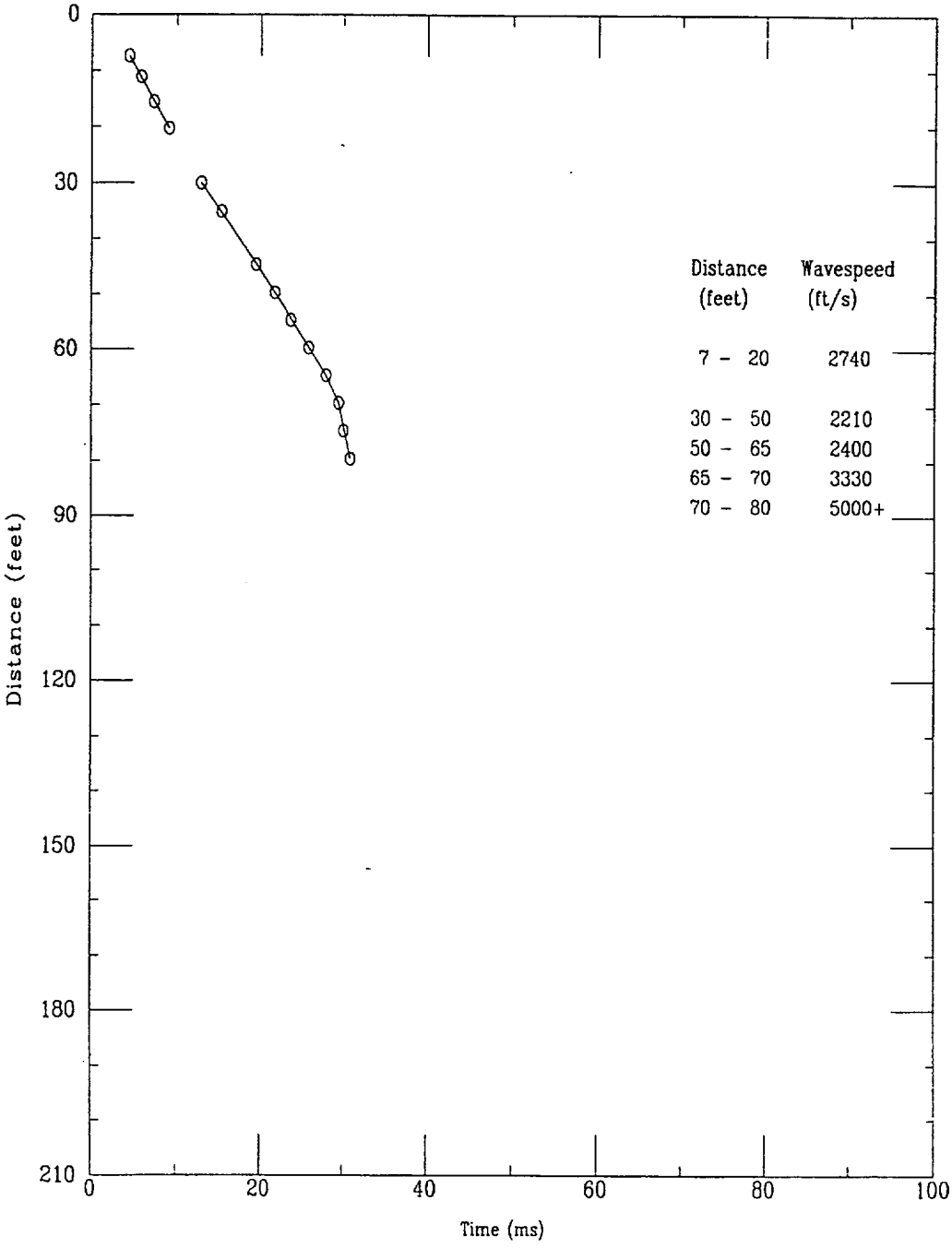

File 407u001S

CPT-34S APPLIED RESEARCH ASSOCIATES, INC. 06/07/00

Shear Wave Speeds

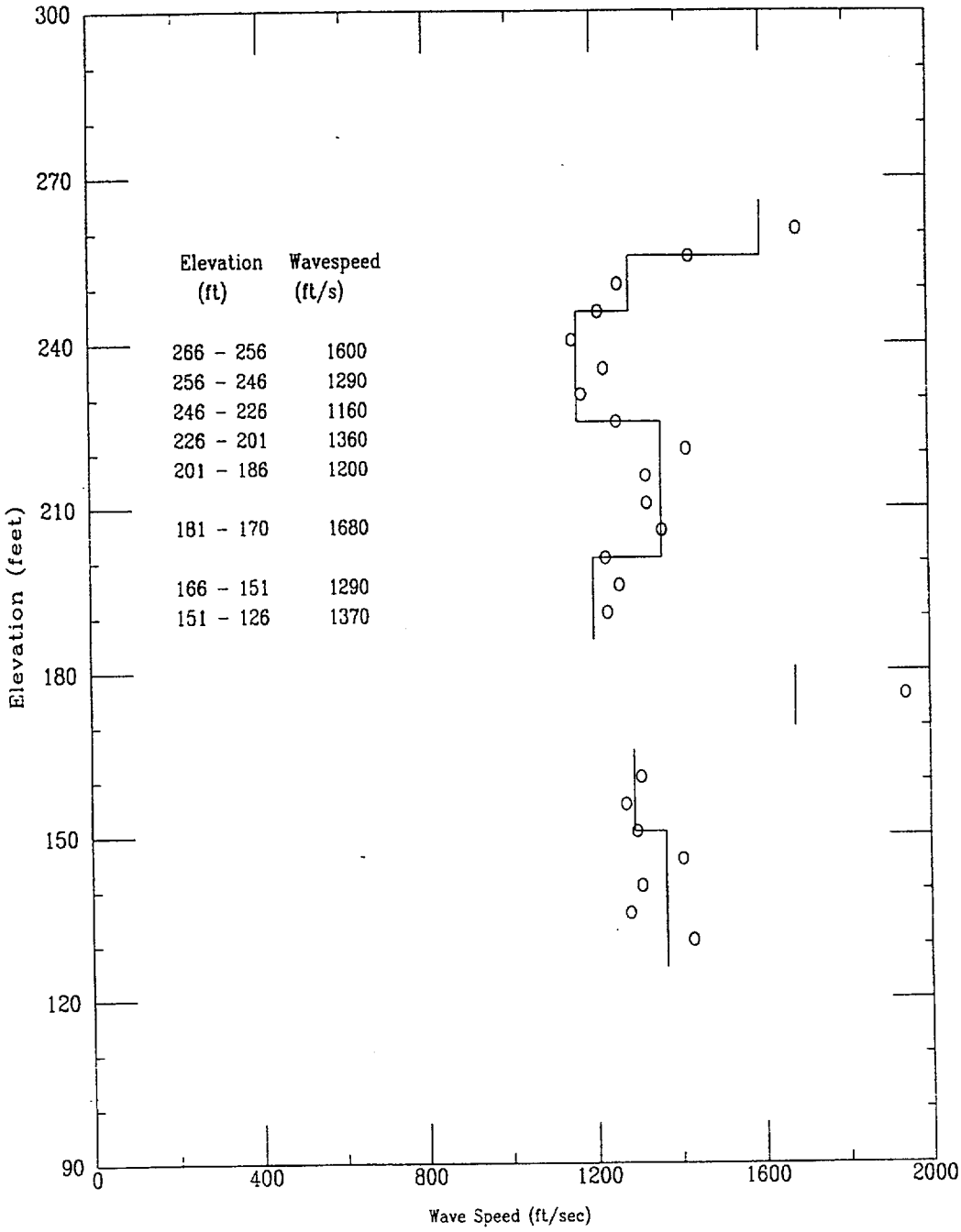

Elevation (ft)	Wavespeed (ft/s)
266 - 256	1600
256 - 246	1290
246 - 226	1160
226 - 201	1360
201 - 186	1200
181 - 170	1680
166 - 151	1290
151 - 126	1370

File 407U001S

CPT-34S APPLIED RESEARCH ASSOCIATES, INC. 06/07/00

Shear Wave Time of Peak

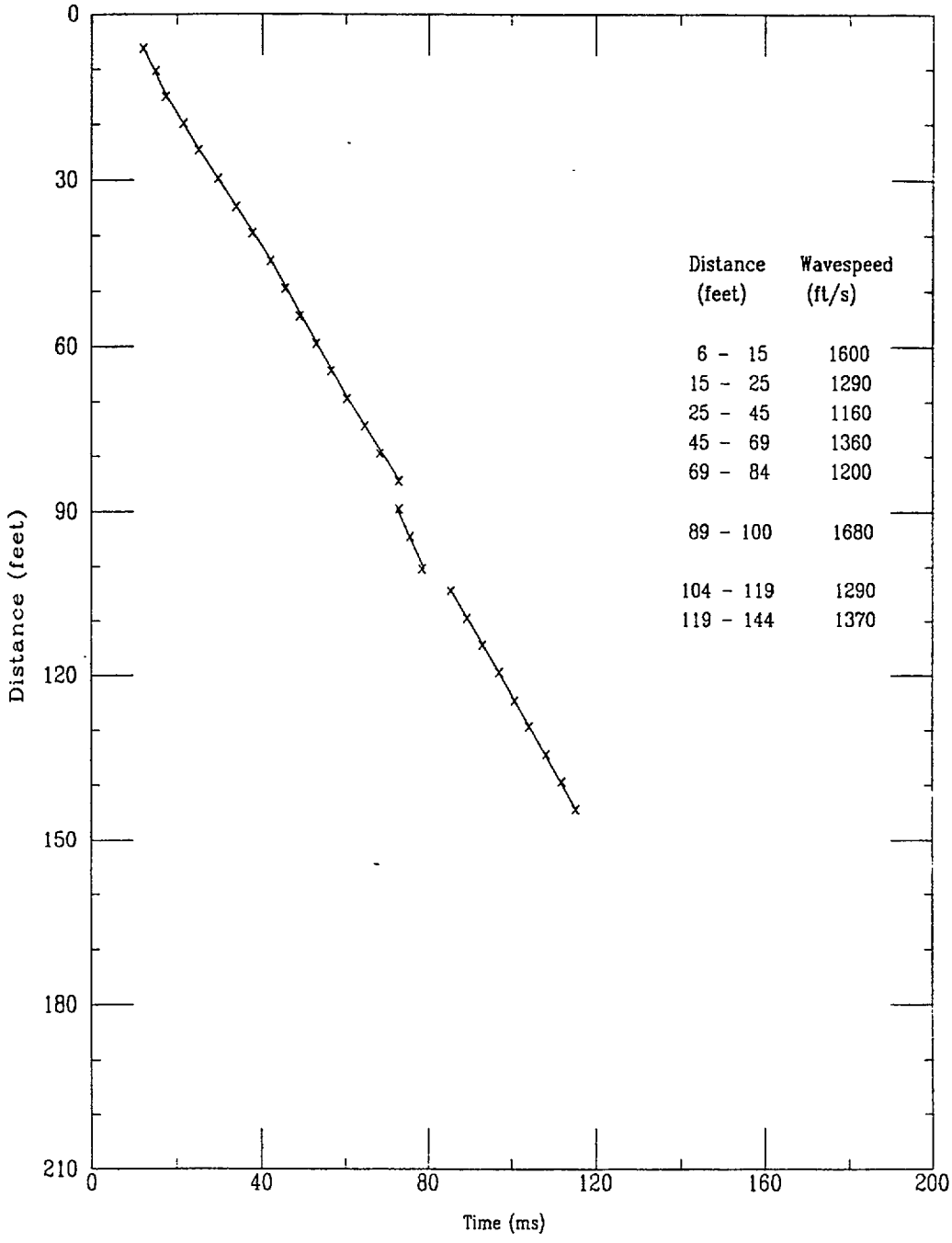

FILE 407U001S

CPT-31S APPLIED RESEARCH ASSOCIATES, INC. 06/01/00

Compression Wave Speeds

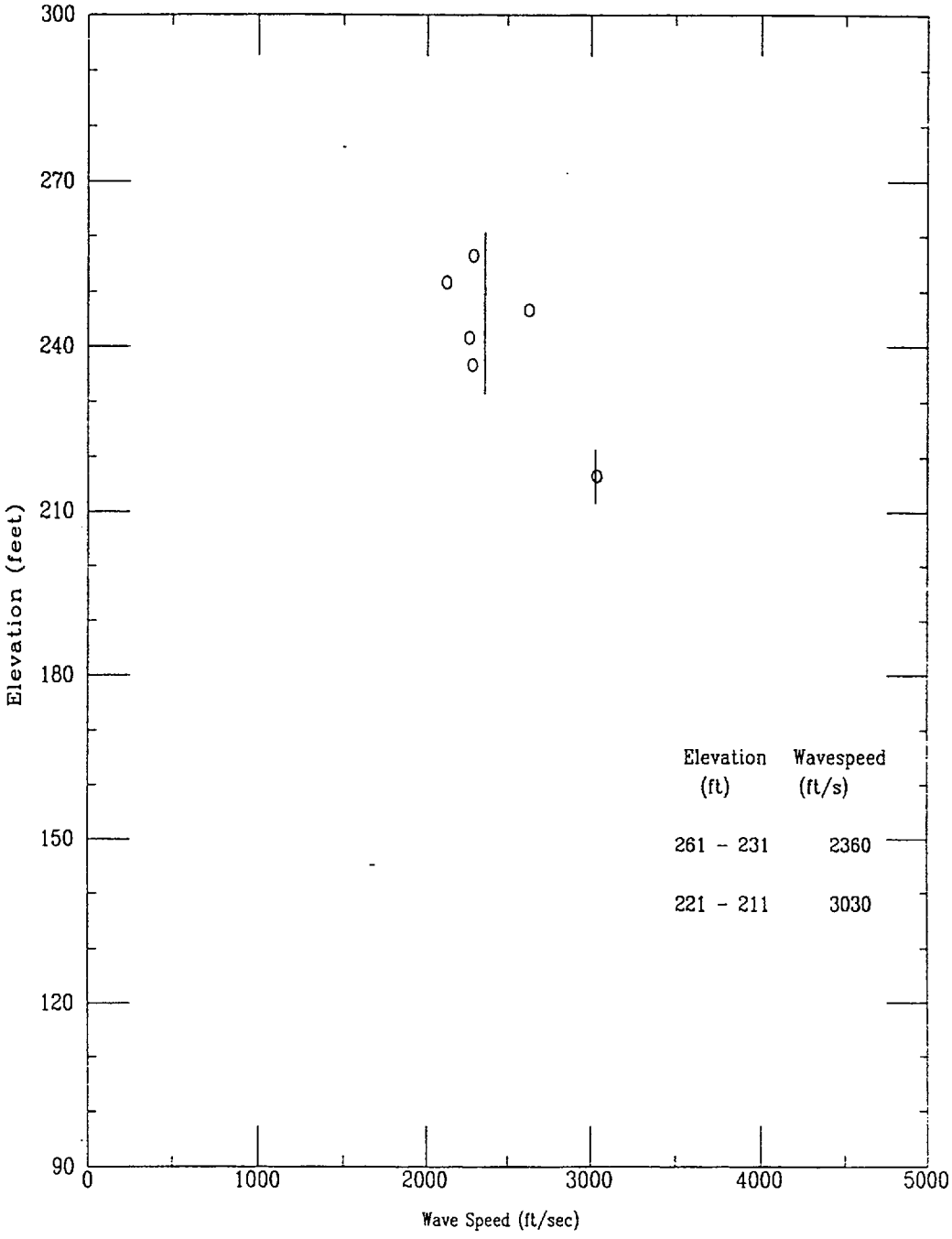

File 401u002S

CPT-31S APPLIED RESEARCH ASSOCIATES, INC. 06/01/00

Compression Wave Time of Peak

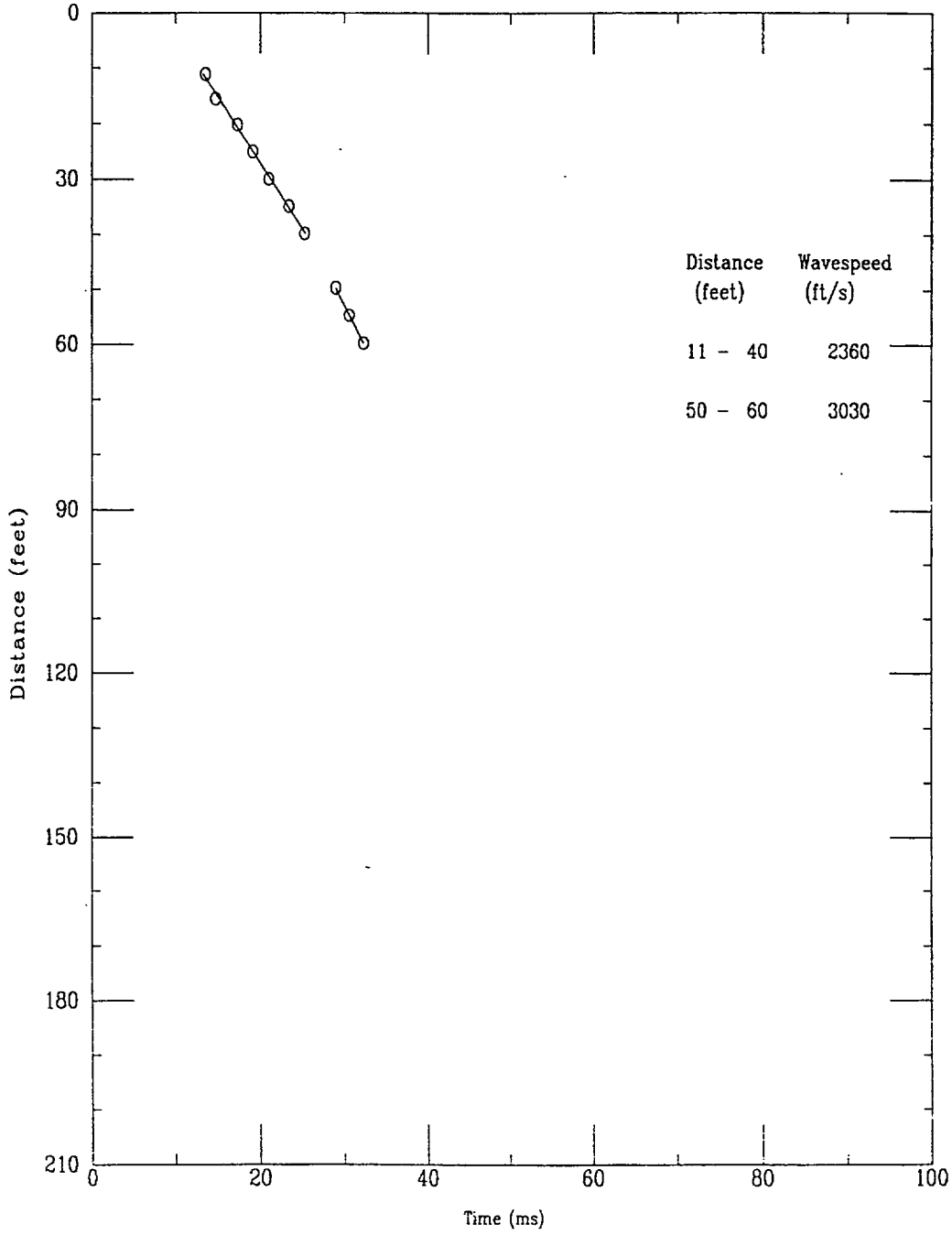

File 401u002S

CPT-31S APPLIED RESEARCH ASSOCIATES, INC. 06/01/00

Shear Wave Speeds

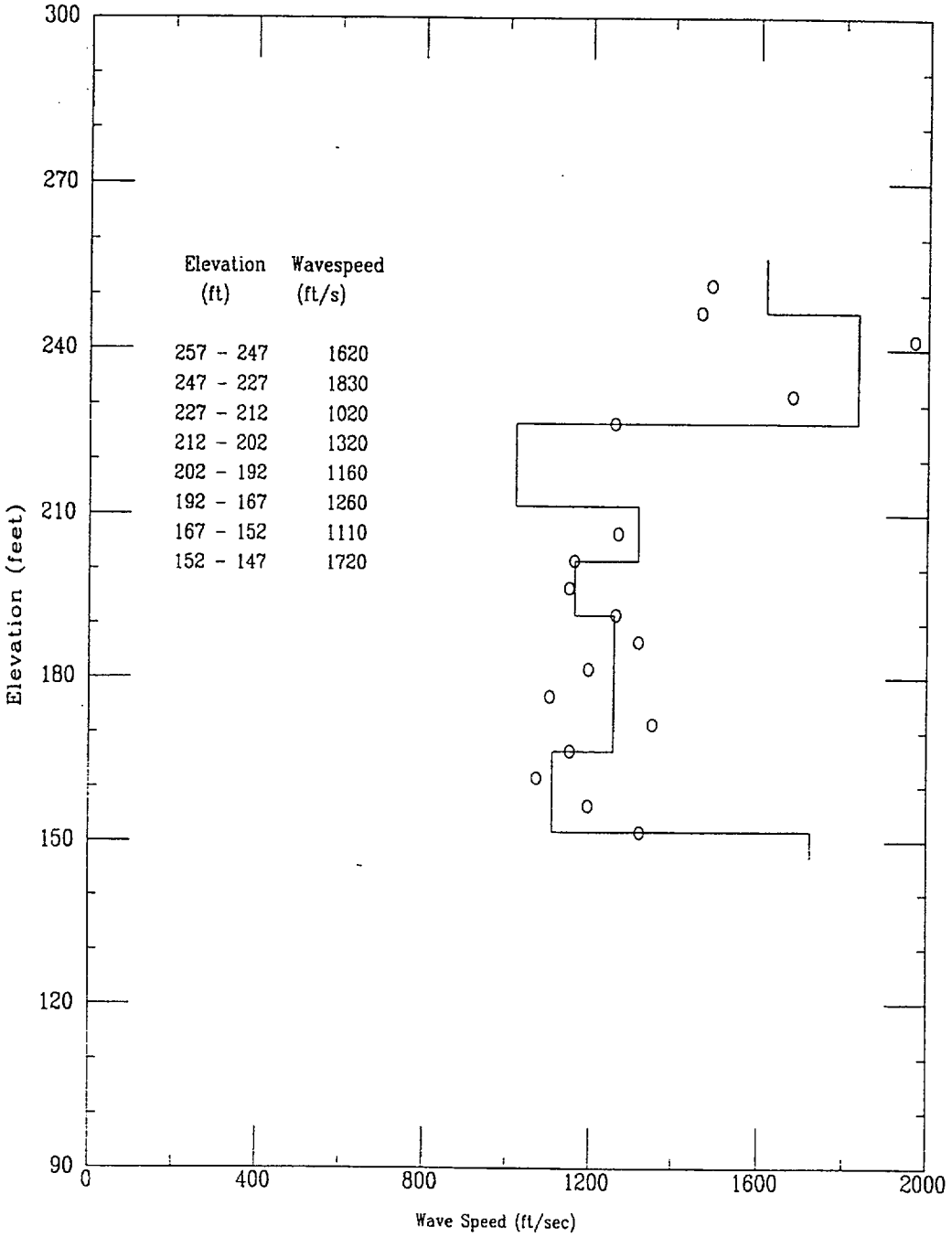

File 401u002S